NASA/TP-20240004259

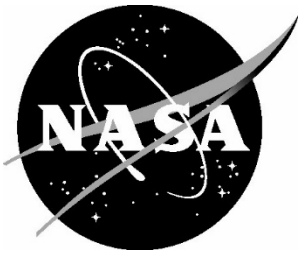

Goddard Enhanced Onboard Navigation System (GEONS) Mathematical Specifications

Anne C. Long
Goddard Space Flight Center, Greenbelt, Maryland

March 2024

NASA STI Program Report Series

Since its founding, NASA has been dedicated to the advancement of aeronautics and space science. The NASA scientific and technical information (STI) program plays a key part in helping NASA maintain this important role.

The NASA STI program operates under the auspices of the Agency Chief Information Officer. It collects, organizes, provides for archiving, and disseminates NASA's STI. The NASA STI program provides access to the NTRS Registered and its public interface, the NASA Technical Reports Server, thus providing one of the largest collections of aeronautical and space science STI in the world. Results are published in both non-NASA channels and by NASA in the NASA STI Report Series, which includes the following report types:

- TECHNICAL PUBLICATION. Reports of completed research or a major significant phase of research that present the results of NASA Programs and include extensive data or theoretical analysis. Includes compilations of significant scientific and technical data and information deemed to be of continuing reference value. NASA counterpart of peer-reviewed formal professional papers but has less stringent limitations on manuscript length and extent of graphic presentations.

- TECHNICAL MEMORANDUM. Scientific and technical findings that are preliminary or of specialized interest, e.g., quick release reports, working papers, and bibliographies that contain minimal annotation. Does not contain extensive analysis.

- CONTRACTOR REPORT. Scientific and technical findings by NASA-sponsored contractors and grantees.

- CONFERENCE PUBLICATION. Collected papers from scientific and technical conferences, symposia, seminars, or other meetings sponsored or co-sponsored by NASA.

- SPECIAL PUBLICATION. Scientific, technical, or historical information from NASA programs, projects, and missions, often concerned with subjects having substantial public interest.

- TECHNICAL TRANSLATION. English-language translations of foreign scientific and technical material pertinent to NASA's mission.

Specialized services also include organizing and publishing research results, distributing specialized research announcements and feeds, providing information desk and personal search support, and enabling data exchange services.

For more information about the NASA STI program, see the following:

- Access the NASA STI program home page at http://www.sti.nasa.gov

.

NASA/TP-20240004259

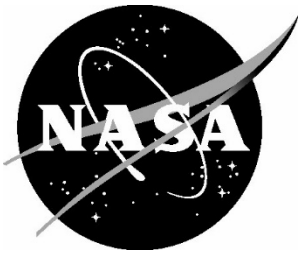

Goddard Enhanced Onboard Navigation System (GEONS) Mathematical Specifications

Anne C. Long
Goddard Space Flight Center, Greenbelt, Maryland

National Aeronautics and
Space Administration

Goddard Space Flight Center
Greenbelt, Maryland

March 2024

Available from:

NASA STI Program / Mail Stop 050
NASA Langley Research Center
Hampton, VA 23681-2199

GODDARD ENHANCED ONBOARD NAVIGATION SYSTEM (GEONS) MATHEMATICAL SPECIFICATIONS

March 2024

Goddard Space Flight Center
Greenbelt, Maryland

National Aeronautics and Space Administration

Goddard Enhanced Onboard Navigation System (GEONS) Mathematical Specifications Release 3.0

Prepared by:

Anne C. Long
a. i. solutions, Inc,
4500 Forbes Blvd.
Lanham, MD 20706

Date

Approved by:

David Gaylor
Code 595
Goddard Spaceflight Center
Greenbelt, Maryland

Date

Nathan Stacey
Code 595
Goddard Spaceflight Center
Greenbelt, Maryland

Date

Preface

This document defines the mathematical specifications for the Goddard Enhanced Onboard Navigation System (GEONS), which was previously known as the GPS Enhanced Onboard Navigation System. This document is a revision of the document FDSS-23-0035, issued November 28, 2012 (Reference 4). It has been updated to include all capabilities implemented in GEONS Flight Software Release 3.0.

Proposed changes to this document should be submitted to the signatories along with supportive material justifying the proposed change. Changes to this document shall be made by complete revision.

Comments or questions concerning this document and proposed changes shall be addressed to:

David Gaylor
Code 595
Goddard Spaceflight Center
Greenbelt, Maryland

Change Information Page

List of Effective Pages		
Page Number	**Release**	**Version**
Title	Release 3.0	Original
ii through xvi	Release 3.0	Original
1-1 through 1-6	Release 3.0	Original
2-1 through 2-42	Release 3.0	Original
3-1 through 3-58	Release 3.0	Original
4-1 through 4-88	Release 3.0	Original
5-1 through 5-154	Release 3.0	Original
6-1 through 6-4	Release 3.0	Original
7-1 through 7-7	Release 3.0	Original
8-1 through 8-10	Release 3.0	Original
9-1 through 9-10	Release 3.0	Original
10-1 through 10-10	Release 3.0	Original
11-1 through 11-20	Release 3.0	Original
12-1 through 12-17	Release 3.0	Original
A-1 and A-2	Release 3.0	Original
R-1 through R-5	Release 3.0	Original
Document History		
Document Number	**Release/Issue**	**Issue Date**
CSC-5506-02R0UD0	Original	August 2001
CSC-5506-02R0UD1	Release 1.1, Update 1	November 2001
CSC-5506-02R1UD0	Release 1.2	February 2002
CSC-5547-02R0UD0	Release 1.2, Update 1	July 2002
CSC-5547-09R0UD0	Release 1.3	November 2002
CSC-5547-09R1UD0	Release 1.4	December 2002
CSC-5547-09R1UD1	Release 1.4, Update 1	January 2003
CSC-5570-01R0UD0	Release 2.0	February 2003
CSC-5570-01R0UD1	Release 2.0, Update 1	June 2003
CSC-5570-14R0UD0	Release 2.1	December 2003
FDF-59-001	Release 2.2	March 2004
FDF-59-001	Release 2.2, Revision 1	August 2004
FDF-59-002	Release 2.3	June 2004
FDF-59-002	Release 2.3, Revision 1	April 2005
FDF-59-003	Release 2.4	May 2005
FDF-59-005	Release 2.5	December 2005
FDF-59-009	Release 2.6	February 2006
FDF-59-010	Release 2.7	September 2006
Document Number	**Release/Issue**	**Issue Date**

FDF-59-012	Release 2.8	January 2007
FDF-59-014	Release 2.9	September 2007
FDF-59-016	Release 2.10	December 2007
FDF-59-017	Release 2.11	September 2008
FDF-59-018	Release 2.12	February 2009
FDF-59-019	Release 2.13	November 2009
FDSS-14-0002	Release 2.14	November 2010
FDSS-14-0006	Release 2.15	April 2011
FDSS-14-0010	Release 2.16	November 2011
FDSS-23-0035	Release 2.17	November 2012
GEONS-MS-2024	Release 3.0	March 2024

Contents

Section 5. Measurement Models

List of Figures

List of Tables

Section 1. Introduction

The National Aeronautics and Space Administration (NASA) Goddard Space Flight Center (GSFC) has developed the capability to provide high-accuracy attitude, orbit, and time autonomously onboard NASA spacecraft. The GSFC Mission Engineering and Systems Analysis Division has implemented NASA-developed navigation algorithms for high-accuracy real-time onboard orbit determination in the Global Positioning System (GPS) Enhanced Orbit Determination (GEODE) flight software. The Goddard Enhanced Onboard Navigation System (GEONS) extends the capabilities of the GEODE flight software to include additional measurement types and additional navigation algorithms.

1.1 Purpose and Scope

This document presents the mathematical algorithms implemented in the GEONS Software Library (or GEONS). Reference 1 defines the GEONS flight software requirements. These algorithms were initially developed based on prototype flight software developed to support the Explorer Platform (EP)/Extreme Ultraviolet Explorer (EUVE) Tracking and Data Relay Satellite System (TDRSS) Onboard Navigation System (TONS) experiment (Reference 2) and the TONS flight software implemented for the Earth Observing System (EOS) Terra mission (Reference 3).

The GEONS Software Design Document (Reference 76) describes the software architecture and design of the GEONS Computer Software Configuration Items (CSCIs). The GEONS Software Library consists of four CSCIs: GEONS Flight, GEONS Ground Tools, GEONS Analysis Tools, and GEONS Beta, shown in Figure 1-1. This document includes mathematical specifications for all capabilities implemented in Release 3.0 of the GEONS Software Library. In addition, an indication is provided for algorithms that are implemented in the Beta and Ground CSCIs or planned for implementation in future versions of GEONS.

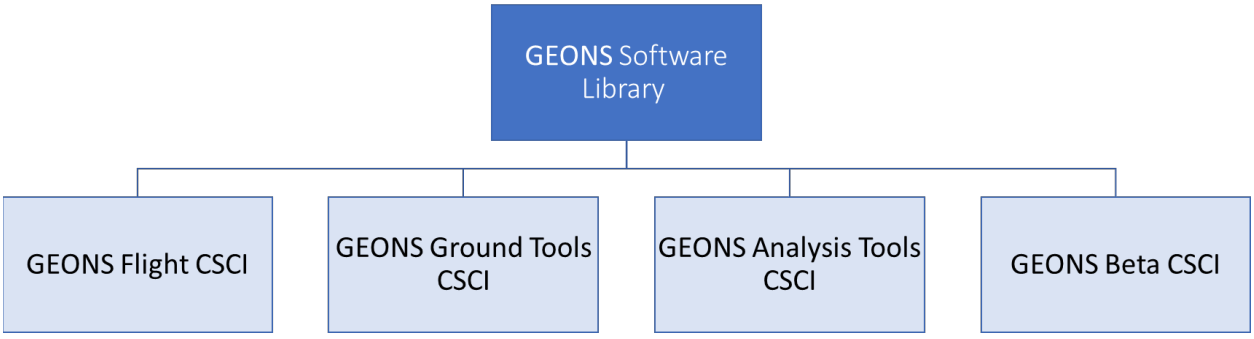

Figure *1-1 GEONS Software Library*

1.2 Document Organization

Section 1.3 provides an overview of the algorithms implemented in GEONS. Sections 2 through 12 define the explicit algorithms implemented and provide associated mathematical background useful in understanding these algorithms. To distinguish the flight software

algorithms from the background discussion, each equation number associated with an explicit flight software algorithm is followed by an asterisk (*).

Section 2 provides a high-level description of the orbit estimation algorithms. The estimation state is defined, and the extended Kalman filter (EKF) processing flow is described. Section 3 describes the coordinate systems, transformations, and time systems used in GEONS. In addition, the algorithm used in the calculation of the Greenwich hour angle is provided.

Section 4 describes the single-step Runge-Kutta numerical integration algorithm and force models used in the propagation of the spacecraft equations of motion. Algorithms for propagation of nonspacecraft state variables and ground-based receivers are given. State error covariance propagation algorithms are also presented.

Section 5 defines the Global Navigation Satellite Systems (GNSS)/Wide Area Augmentation System (WAAS) and cross-link measurement models and measurement partial derivatives. Algorithms for computing the GNSS space vehicle (SV) position and velocity are provided. This section also includes the point solution, ground-station-to–satellite range and Doppler, celestial object, and TDRSS forward-link Doppler measurement models and measurement partial derivatives.

Section 6 provides the algorithms used to propagate the user state vector to real time. Section 7 provides an algorithm for Doppler compensation prediction. Section 8 provides a backup ephemeris computation algorithm. Section 9 describes the generic maneuver targeting algorithm based on Lambert's method. Section 10 provides a cold start initialization algorithm that uses range and Doppler measurements. Section 11 provides attitude estimation algorithms that may be implemented in a future version of GEONS. Section 12 provides algorithms that are used to simulate GNSS measurements.

A list defining the abbreviations and acronyms used and a list of the references cited throughout this document follows Section 12.

1.3 Overview of the GEONS Navigation Algorithms

Table 1-1 summarizes the GEONS navigation algorithms defined in this document. Algorithms supported in Release 3.0 of the GEONS Flight CSCI (referred to as GEONS 3.0 throughout this document) are indicated as well as algorithms currently included in the GEONS Beta or Ground CSCI or future if not currently available in a GEONS CSCI. A ground receiver propagation model is also provided to support prelaunch testing of spacecraft receivers and vehicles on the surface of the Moon, planet, or asteroid. These algorithms are defined in detail in Sections 2 through 12 of this document.

GEONS navigation processing consists of two primary activities:

- State vector estimation based on the processing of GNSS SV, WAAS GEO, cross-link range and Doppler, cross-link line-of-sight, Ground-Station-to-satellite range and Doppler, celestial object, TDRSS forward-link Doppler, and/or point solution position measurements
- Real-time state vector propagation

In addition, Doppler compensation prediction, backup ephemeris computation, maneuver targeting, and cold start initialization are also implemented in Beta versions of GEONS. Figure 1-2 provides an overview of the GEONS navigation processing scenario. In this figure, dt is the time interval between state vector updates by the estimator, nominally equal to 30 to 60 seconds.

During the same time intervals, measurement, GEONS state estimation, and real-time propagation processing are performed for different time periods. For example, the GPS/WAAS measurement process and real-time propagation could occur once per second. GEONS state vector estimation could be performed at regular intervals, e.g., every 30 or 60 seconds, with intermediate propagation of the filter state vector if required to maintain prediction accuracy.

Table 1-1 Summary of GEONS Flight Software Algorithms

Algorithm Type	Algorithm (Section #)	GEONS 3.0 CSCI
Primary coordinate system	• Mean equator and equinox of J2000.0 with analytic coordinate transformations (3.2)	• Flight
	• Options for Moon-centered and asteroid-centered trajectory propagation (4.1.1)	• Beta
	• Option for to Geocentric Celestial Reference Frame (GCRF) and International Terrestrial Reference Frame (ITRF) reference frames (3.2.15)	• Beta
Primary time system	• Coordinated universal time (UTC) (3.3)	• Flight
Numerical integrator	• Runge-Kutta 4th-and 8th order (4.2)	• Flight
Filter spacecraft orbit acceleration model	• Joint Gravity Model-2 (JGM-2) geopotential up to degree and order 30 (4.1.2.2)	• Flight
	• Earth Gravity Model 96 (EGM96) geopotential up to degree and order 360 (4.1.2.2)	• Beta
	• LP100K non-spherical lunar potential model (4.1.2.2)	• Beta
	• GRGM900C non-spherical lunar potential model (4.1.2.2)	• Beta
	• Other planetary non-spherical potential models (4.1.2.2)	• Beta
	• Earth, solar, and lunar point masses with low precision analytic ephemeris or Earth, solar, lunar, and planetary point masses with high precision analytic ephemeris or JPL Developmental Ephemeris (DExxx) (4.1.1)	• Flight
	• Analytic representation of Harris-Priester atmospheric density (4.1.3)	• Flight
	• Solar radiation pressure with spherical area model (4.1.4)	• Flight
	• Measured accelerations in RIC, VBN, Spacecraft body, or Mean of J2000.0 frames (4.1.5)	• Flight
	• Impulsive delta-V maneuver model (4.1.5)	• Flight
Estimation state	• Position and velocity vectors for local and remote satellites or ground-based receiver (2.1 and 4.6)	• Flight
	• Moon-based receiver (4.7)	• Beta
	• Atmospheric drag coefficient correction for local and remote satellites (4.3)	• Flight
	• Solar radiation pressure coefficient correction for local and remote satellites (4.3)	• Flight
	• GPS receiver time bias, time bias rate, and time bias acceleration for local and remote satellites modeled as random walk, FOGM drift, or FOGM bias and SOGM drift processes. A relativistic clock bias correction can be included in the random walk model. (4.3)	• Flight
	• Pseudorange and Doppler biases for each GPS SV (4.3)	• Flight
	• GPS Ionospheric delay scale factor (4.3 and 5.3.5)	• Beta
	• Ground-station-to-satellite range and Doppler biases for each Ground Station (4.3)	• Beta
	• Pseudorange and Doppler biases for each cross-link transmitter (4.3)	• Beta
	• Unmodeled acceleration biases in the RIC, VBN, or spacecraft body frame (4.3)	• Beta
	• Accelerometer measurement biases (4.3)	• Future
	• Integrated carrier phase biases for each GPS SV and GPS receiver (4.3)	• Beta
	• Singly-differenced carrier phase biases for each GPS SV and remote GPS receiver with respect to the local receiver (4.3)	• Beta
	• Celestial object sensor biases (4.3)	• Beta
	• Cross-link line-of-sight sensor biases (4.3)	• Beta
	• TDRSS forward-link Doppler bias for each TDRSS satellite (4.3)	• Beta
	• Hierarchical relative navigation capability (2.4)	• Future

Algorithm Type	Algorithm (Section #)	GEONS 3.0 CSCI
Estimator	• Extended Kalman filter with physically realistic process noise models and factored covariance matrix (2.3)	• Flight
	• Scalar and hybrid batch measurement update options (2.3.2)	• Flight
	• Measurement underweighting option (2.3.2)	• Flight
	• Consider parameter option (2.3.2)	• Flight
Measurement model	• GPS pseudorange with GPS receiver time and time bias corrections (5.3)	• Flight
	• Camera range and bearing angles to spacecraft or landmarks on celestial bodies (5.8.2.3 and 5.8.2.4)	• Flight
	• TDRSS Differenced One-Way Doppler (DOWD) (5.9.4)	• Ground
	• TDRSS forward-link Doppler (5.9.3)	• Beta
	• Point solution position and time bias (5.7)	• Ground
	• Ground-station-to-satellite range and Doppler (5.6)	• Beta
	• Intersatellite one-way and two-way cross-link pseudorange and Doppler with option to propagate transmitting satellite states if not being estimated (5.5)	• Beta
	• GNSS pseudorange, Doppler, and integrated carrier phase with GNSS receiver time and time bias corrections, single-frequency and dual-frequency ionospheric delay corrections (5.3)	• Beta
	• GPS TASS Differential Corrections, and ICE Differential Correction parameters (5.2.4 and 5.2.5)	• Beta
	• GPS-to-relay-to-ground two-leg pseudorange (5.11)	• Beta
	• GPS signal-to-noise ratio and double-difference carrier phase for attitude estimation (11.5)	• Future
	• Standard and singly differenced WAAS GEO pseudorange and Doppler with receiver time and time bias corrections (5.3)	• Beta
	• Line-of-sight vector to a celestial object (3-axis stabilized spacecraft) (5.8.2)	• Beta
	• Intersatellite bearing to another satellite (3-axis stabilized spacecraft) (5.8.2.2)	• Beta
	• Bearing to a landmark or celestial object (5.8.2.3)	• Beta
	• Sun sensor elevation angle (spinning spacecraft) (5.8.3)	• Beta
	• Earth horizon crossing times (spinning spacecraft) (5.8.3)	• Beta
	• Near-to-far-body and Near-to-near-body pseudoangle (5.8.4)	• Beta
	• X-ray Pulsar phase and frequency (5.10)	• Beta
Spacecraft orbit state transition matrix	• Semianalytic formulation including J2 and Earth and planetary point mass gravity, atmospheric drag, and solar radiation pressure acceleration partial derivatives (4.4.1)	• Flight
	• Second-order Gauss-Markov orbital covariance artificial damping (4.4.1)	• Beta
Attitude estimation state	• Attitude error, angular rate or gyro bias error, and antenna gain calibration coefficient states for each satellite (11.1)	• Future
Filter spacecraft attitude acceleration model	• Gravity gradient and measured torques (11.4)	• Future
Real-time spacecraft acceleration model	• Earth point mass and J2 (6)	• Beta
Backup Ephemeris	• Averaged equinoctial element ephemeris (8)	• Beta
Maneuver targeting	• Lambert's method for Earth and planetary orbits (9)	• Beta
Cold Start Initialization	• Search for initial mean longitude (10)	• Beta
Measurement Simulation	• GNSS measurement simulation (12)	• Analysis

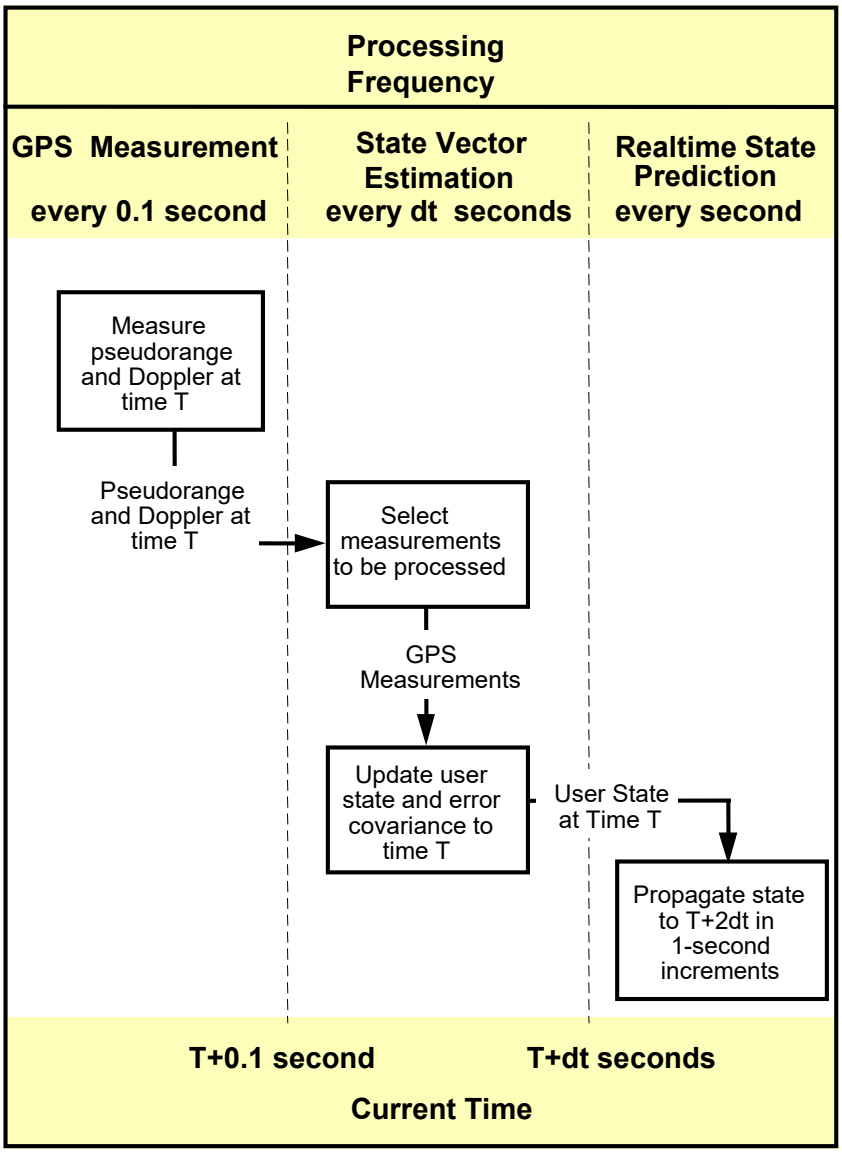

Figure *1-2 GEONS Navigation Processing Scenario*

Section 2. State Estimation Algorithms

The state estimation algorithm for GEONS consists of an extended Kalman filter (EKF) that uses physically connected process noise covariance models to account for force model and measurement errors.

This section provides a high-level description of the state estimation algorithms. Section 2.1 defines the estimation state, Section 2.2 defines the state error covariance, and Section 2.3 describes the state estimation processing flow, with appropriate references made to the more detailed algorithms provided in Sections 3 through 5.

2.1 Estimation State Vector

The GEONS estimation algorithm estimates a state vector, $\overline{X}$, which consists of one or more satellite state vectors, $\overline{X}^i$, a vector of tracking-system-dependent measurement biases, $\overline{B}$, and the ionospheric delay scale factor, γ_I. Each satellite state vector consists of the satellite's position and velocity vectors and optionally the receiver time bias, the receiver time bias drift, the receiver time bias acceleration, the atmospheric drag coefficient correction, the solar radiation pressure coefficient correction, and/or acceleration biases. The estimator models the drag coefficient correction, solar radiation pressure coefficient correction, the receiver time bias corrections, acceleration biases, accelerometer sensor biases, and tracking-sensor-dependent measurement biases as random variables. Alternatively, the state vector can include the position and velocity vectors of a surface receiver located on the Earth, Moon or planet. In the case of a surface receiver, the drag coefficient correction and solar radiation pressure coefficient correction cannot be estimated.

Optionally, any parameter in the estimation state vector except for the satellite position and velocity can be processed as a consider parameter. However, GEONS 3.0 only supports the inclusion of the atmospheric drag coefficient correction and sensor and global biases as consider parameters. The value and covariance of a consider parameter is not updated by the filter measurement update process but the effects of consider parameter uncertainties are included in the calculation of corrections to and covariance of estimated parameters and in the error cross-covariance of estimated and consider parameters. In addition, GEONS provides the capability to configure the estimation state vector to estimate a subset of the total estimation state vector. This capability can be used to reduce the state vector when different state vector components are estimated for multiple vehicles.

The total estimation state vector with dimension $(\sum_{n=1}^{N_S} n_S^n + N_B + 1)$, where n_s is the size of each receiver's state vector, N_s is the number of satellite/receiver state vectors being estimated, and N_B is the number of measurement biases being estimated, has the following form:

$$\overline{X} = \begin{bmatrix} \overline{X}^1 \\ \vdots \\ \overline{X}^{N_S} \\ \overline{B} \\ \gamma_I \end{bmatrix} \tag{2.1-1a}*$$

Each receiver state vector with dimension ≤ 11 has the following form:

$$\overline{X}^n = \begin{bmatrix} \overline{R} \\ \dot{\overline{R}} \\ \Delta C_D \\ \Delta C_R \\ \overline{b}_R \\ \overline{a}_U \end{bmatrix}^n \tag{2.1-1b}*$$

where

$\overline{R}$ = satellite/receiver position vector in Earth-centered J2000.0 coordinates (meters)

$\dot{\overline{R}}$ = satellite/receiver velocity vector in Earth-centered J2000.0 coordinates (meters per second)

$\Delta C_D, \Delta C_R$ = atmospheric drag and solar radiation pressure coefficient corrections (unitless)

$\overline{b}_R$ = vector of receiver-dependent bias parameters, given by

$$\overline{b}_R = \begin{bmatrix} b_R \\ d_R \\ \dot{d}_R \end{bmatrix} \tag{2.1-2a}*$$

where

b_R = receiver time bias from onboard reference time (defined in Section 4.3) (meters)

d_R = receiver time bias rate (defined in Section 4.3) (meters per second)

$\dot{d}_R$ = optional receiver time bias acceleration (defined in Section 4.3) (meters per second^2)

and $\overline{a}_U$ = unmodeled acceleration biases in radial-intrack-crosstrack (RIC), velocity-binormal-normal (VBN), or spacecraft body frame (defined in Section 4.3) (meters per second^2)

Optionally, the state vector can include the relative state vector of each nonlocal satellite with respect to the local satellite (n=1) can be estimated, rather than its absolute state vector:

$$\overline{X}_{rel} = \begin{bmatrix} \overline{X}^1 \\ \overline{X}^2_{rel} \\ \vdots \\ \overline{X}^{N_S}_{rel} \\ \overline{B} \\ \gamma_I \end{bmatrix} \tag{2.1-1c}$$

where

$$\overline{X}^n_{rel} = \overline{X}^n - \overline{X}^1 = \begin{bmatrix} \overline{R}^n - \overline{R}^1 \\ \dot{\overline{R}}^n - \dot{\overline{R}}^1 \\ \Delta C^n_D - \Delta C^1_D \\ \Delta C^n_R - \Delta C^1_R \\ \overline{b}^n_R - \overline{b}^1_R \\ \overline{a}^n_U - \overline{a}^1_U \end{bmatrix} = \begin{bmatrix} \overline{R}^n_{rel} \\ \dot{\overline{R}}^n_{rel} \\ \left(\Delta C^n_D\right)_{rel} \\ \left(\Delta C^n_R\right)_{rel} \\ \left(\overline{b}^n_R\right)_{rel} \\ \left(a^n_U\right)_{rel} \end{bmatrix}; n \neq 1 \tag{2.1-1d}*$$

The N_B–dimension vector of tracking-sensor-dependent biases can include 32 GPS + 36 Galileo + 8 WAAS GEO pseudorange biases, 32 GPS + 36 Galileo + 8 WAAS GEO Doppler biases, N_s cross-link pseudorange and Doppler biases, measurement biases for each celestial object sensor on each of the N_s satellite/receivers being estimated, n_{GS} Ground Station (GS) range and Doppler biases, n_{TDRS} Tracking and Data Relay Satellite System (TDRSS) Doppler biases, 40 GPS/WAAS + 36 Galileo carrier phase biases for each of the N_s satellite/receivers being estimated, 40 GPS/WAAS + 36 Galileo singly differenced carrier phase biases between the local satellite/receiver and each of the N_s-1 remote satellite/receivers being estimated, and 3 accelerometer sensor measurement biases for each accelerometer:

$$\overline{B} = \begin{bmatrix} \overline{b}_{\rho}^{G/W} \\ \overline{b}_{d}^{G/W} \\ \overline{b}_{\rho}^{CL} \\ \overline{b}_{d}^{CL} \\ \overline{b}^{CO} \\ \overline{b}_{\rho}^{GS} \\ \overline{b}_{d}^{GS} \\ \overline{b}_{d}^{TDRS} \\ \overline{b}_{\phi}^{G/W} \\ \overline{b}_{\Delta\phi}^{G/W} \\ \overline{b}_{IMU}^{A} \end{bmatrix} \tag{2.1-2b}$$

where

$\overline{b}_{\rho}^{G/W}$ = vector of 32 GPS + 36 Galileo + 8 WAAS GEO pseudorange biases (defined in Section 4.3) (meters)

$\overline{b}_{d}^{G/W}$ = vector of 32 GPS + 36 Galileo + 8 WAAS GEO Doppler biases (defined in Section 4.3) (Hertz)

$\overline{b}_{\rho}^{CL}$ = vector of N_s cross-link pseudorange biases (defined in Section 4.3) (meters)

$\overline{b}_{d}^{CL}$ = vector of N_s cross-link Doppler biases (defined in Section 4.3) (Hertz)

$\overline{b}^{CO}$ = vector of biases for n_s celestial object sensors on N_s satellites (defined in Section 4.3)

$\overline{b}_{\rho}^{GS}$ = vector of n_{GS} GS range biases (defined in Section 4.3) (meters)

$\overline{b}_{d}^{GS}$ = vector of n_{GS} GS Doppler biases (defined in Section 4.3) (Hertz)

$\overline{b}_{d}^{TDRS}$ = vector of n_{TDRS} TDRS Doppler biases (defined in Section 4.3) (Hertz)

$\overline{b}_{\phi}^{G/W}$ = vector of carrier phase biases between each of 32 GPS + 36 Galileo + 8 WAAS GEO transmitters and the receiver on each of the N_s satellites being estimated (defined in Section 4.3) (meters)

$\overline{b}_{\Delta\phi}^{G/W}$ = vector of singly differenced carrier phase biases for each of 32 GPS + 36 Galileo + 8 WAAS GEO transmitters between the local satellite/receiver and each of the N_s -1 remote satellite/receivers being estimated (defined in Section 4.3) (meters)

$\overline{b}_{IMU}^{A}$ = vector of accelerometer sensor measurement biases in the IMU frame (defined in Section 4.3) (meters/second^2).

The system equations are given by

$$\dot{\overline{X}} = \begin{bmatrix} \dot{\overline{X}}^1(t) \\ \vdots \\ \dot{\overline{X}}^{N_S}(t) \\ \dot{\overline{B}}(t) \\ \dot{\gamma}_I \end{bmatrix} \tag{2.1-3}$$

where

$$\dot{\overline{X}}^n = \begin{bmatrix} \dot{\overline{R}} \\ \ddot{\overline{R}} \\ \Delta\dot{C}_D \\ \Delta\dot{C}_R \\ \dot{\overline{b}}_R \\ \dot{\overline{a}}_U \end{bmatrix}^n + \begin{bmatrix} \overline{w}_R(t) \\ \overline{w}_{\dot{R}}(t) \\ w_{C_D}(t) \\ w_{C_R}(t) \\ \overline{w}_b(t) \\ \overline{w}_a(t) \end{bmatrix}^n \tag{2.1-3a}$$

$$\dot{\overline{B}} = \begin{bmatrix} \dot{\overline{b}}_\rho^{G/W} \\ \dot{\overline{b}}_d^{G/W} \\ \dot{\overline{b}}_\rho^{CL} \\ \dot{\overline{b}}_d^{CL} \\ \dot{\overline{b}}^{CO} \\ \dot{\overline{b}}_\rho^{GS} \\ \dot{\overline{b}}_d^{GS} \\ \dot{\overline{b}}_d^{TDRS} \\ \dot{\overline{b}}_\phi^{G/W} \\ \dot{\overline{b}}_{\Delta\phi}^{G/W} \\ \dot{\overline{b}}_{IMU}^{A} \end{bmatrix} + \begin{bmatrix} \overline{w}_\rho^{G/W} \\ \overline{w}_d^{G/W} \\ \overline{w}_\rho^{CL} \\ \overline{w}_d^{CL} \\ \overline{w}^{CO} \\ \overline{w}_\rho^{GS} \\ \overline{w}_d^{GS} \\ \overline{w}_d^{TDRS} \\ \overline{w}_\phi^{G/W} \\ \overline{w}_{\Delta\phi}^{G/W} \\ \overline{w}_{IMU}^{A} \end{bmatrix} \tag{2.1-4}$$

$$\dot{\gamma}_I = w_I \tag{2.1-4a}$$

where

$\overline{w}_R(t)$ =noise process that models random disturbance on $\overline{R}$

$\overline{w}_{\dot{R}}(t)$ =noise process that models random disturbances on $\dot{\overline{R}}$

$w_{C_D}(t)$ =white noise process that models random disturbances on ΔC_D

$w_{C_R}(t)$ =white noise process that models random disturbances on ΔC_R

$\overline{w}_b(t)$ =noise process that models random disturbance on $\overline{b}_R$

$\overline{w}_a(t)$ =noise process that models random disturbance on $\overline{a}_U$

$\overline{w}_\rho^{G/W}(t)$ =noise process that models random disturbance on $\overline{b}_\rho^{G/W}$

$\overline{w}_d^{G/W}(t)$ =noise process that models random disturbance on $\overline{b}_d^{G/W}$

$\overline{w}_\rho^{CL}(t)$ =noise process that models random disturbance on $\overline{b}_\rho^{CL}$

$\overline{w}_d^{CL}(t)$ =noise process that models random disturbance on $\overline{b}_d^{CL}$

$\overline{w}^{CO}(t)$ =noise process that models random disturbance on $\overline{b}^{CO}$

$\overline{w}_\rho^{GS}(t)$ =noise process that models random disturbance on $\overline{b}_\rho^{GS}$

$\overline{w}_d^{GS}(t)$ =noise process that models random disturbance on $\overline{b}_d^{GS}$

$\overline{w}_d^{TDRS}(t)$ =noise process that models random disturbance on $\overline{b}_d^{TDRS}$

$\overline{w}_\phi^{G/W}(t)$ =noise process that models random disturbance on $\overline{b}_\phi^{G/W}$

$\overline{w}_{\Delta\phi}^{G/W}(t)$ =noise process that models random disturbance on $\overline{b}_{\Delta\phi}^{G/W}$

$\overline{w}_{IMU}^{A}(t)$ =noise process that models random disturbance on $\overline{b}_{IMU}^{A}$

$w_I(t)$ =noise process that models random disturbance on γ_I

The quantity $\overline{w}_b(t)$ is a column vector given by

$$\overline{w}_b(t) = \begin{bmatrix} w_1 \\ w_2 \\ w_3 \end{bmatrix} \tag{2.1-5}$$

where w_1, w_2, and w_3 are white noise processes that model random disturbances on b_R, d_R, and $\dot{d}_R$ respectively.

The satellite acceleration equations, $\ddot{\overline{R}}(t)$, are provided in Section 4.1. The derivatives of ΔC_D, ΔC_R, $\overline{b}_R$, $\overline{a}_U$, $\overline{b}_\rho^{G/W}$, $\overline{b}_d^{G/W}$, $\overline{b}_\rho^{CL}$, $\overline{b}_d^{CL}$, $\overline{b}^{CO}$, $\overline{b}_\rho^{GS}$, $\overline{b}_d^{GS}$, $\overline{b}_d^{TDRS}$, $\overline{b}_\phi^{G/W}$, $\overline{b}_{\Delta\phi}^{G/W}$, $\overline{b}_{IMU}^{A}$, and γ_I are defined in Section 4.3. The ground-based receiver propagation equations are given in Section 4.6.

2.2 State Error Covariance Matrix

The state error covariance at time t_k is defined as the expectation value of the square of the deviation of the estimated state $\left(\hat{\overline{X}}_k\right)$ at time t_k from the true (unknown) state $\left(\overline{X}_k\right)$ at time t_k, i.e.,

$$P_k \equiv E\left(\left[\hat{\overline{X}}_k - \overline{X}_k\right]\left[\hat{\overline{X}}_k - \overline{X}_k\right]^T\right) \tag{2.2-1}$$

In the equations below, a plus sign in parentheses (+) denotes the value of a quantity that has been corrected to include the effects of a measurement; a minus sign in parentheses (–) denotes the value of a quantity before this correction has been implemented.

If the effects of the k^{th} measurement have been included in the state error estimate, then

$$P_k(+) = E\left(\left[\hat{\overline{X}}(+) - \overline{X}_k\right]\left[\hat{\overline{X}}(+) - \overline{X}_k\right]^T\right) \tag{2.2-2}$$

If they have not been included, then

$$P_k(-) = E\left(\left[\hat{\overline{X}}(-) - \overline{X}_k\right]\left[\hat{\overline{X}}(-) - \overline{X}_k\right]^T\right) \tag{2.2-3}$$

The state error covariance matrix represents the filter uncertainty in the estimated state vector. It also accounts for error correlations between estimated state vector elements. For the filter to be accurate and stable, the covariance matrix must represent the actual errors in the estimated state vector. The state error covariance matrix is defined below:

$$[P] = \begin{bmatrix} \sigma_1^2 & C_{1,2}\,\sigma_1\,\sigma_2 & \cdots & C_{1,N}\,\sigma_1\,\sigma_N \\ C_{2,1}\,\sigma_1\,\sigma_2 & \sigma_2^2 & \cdots & \cdot \\ \cdot & \cdot & \cdots & \cdot \\ \cdot & \cdot & \cdots & \cdot \\ \cdot & \cdot & \cdots & \cdot \\ \cdot & \cdot & \cdots & \cdot \\ \cdot & \cdot & \cdots & \cdot \\ \cdot & \cdot & \cdots & \cdot \\ C_{N,1}\,\sigma_1\,\sigma_N & \cdot & \cdots & \sigma_N^2 \end{bmatrix} \tag{2.2-4}$$

where

$[P]$ = [N × N] state error covariance matrix, where N equals $(n_s \times N_s + N_B + 1)$

σ_i = standard deviation in estimate of state vector element i

σ_i^2 = variance in estimate of state vector element i

$C_{i,j} = C_{j,i}$ = correlation coefficient for elements i and j, absolute value < 1

The state error covariance is initialized or reinitialized using command parameters. If the initial state error variances σ_i^2 are provided in Mean of J2000.0 XYZ coordinates, they are used directly in Equation 2.2-4 to form $[P]_{XYZ}$ with $C_{i,i} = 1$ and off-diagonal $C_{i,j} = 0$.

If the state error variances σ_i^2 are provided in instantaneous radial, in-track, cross-track (RIC) coordinates, they are used as follows to form the receiver position and velocity state vector covariance submatrices $[P]_{RIC}^n$, for each of the N_s satellites/receivers. In this case $C_{i,i} = 1$ and all off-diagonal $C_{i,j} = 0$ except for the radial velocity/in-track position correlations, $C_{4,2}$ and $C_{2,4}$, and the radial position/in-track velocity correlations, $C_{1,5}$ and $C_{5,1}$, which are uplinked parameters, nominally equal to –0.95.

$$[P]_{RIC}^n = \begin{bmatrix} \sigma_R^2 & 0 & 0 & 0 & C_{1,5}\sigma_R\sigma_{\dot{I}} & 0 \\ 0 & \sigma_I^2 & 0 & C_{2,4}\sigma_{\dot{R}}\sigma_I & 0 & 0 \\ 0 & 0 & \sigma_C^2 & 0 & 0 & 0 \\ 0 & C_{4,2}\sigma_{\dot{R}}\sigma_I & 0 & \sigma_{\dot{R}}^2 & 0 & 0 \\ C_{5,1}\sigma_R\sigma_{\dot{I}} & 0 & 0 & 0 & \sigma_{\dot{I}}^2 & 0 \\ 0 & 0 & 0 & 0 & 0 & \sigma_{\dot{C}}^2 \end{bmatrix} \quad \text{(2.2-4b)}$$

Each of the resulting RIC covariance submatrices is then transformed to the Earth-centered Mean of J2000.0 frame as defined in Equation (3.2-53) in Section 3.2.5. The initial covariance matrix is then constructed as follows:

$$[P] = \begin{bmatrix} [P]^{11} & \cdots & 0 & 0 & 0 \\ \vdots & \ddots & 0 & 0 & 0 \\ 0 & 0 & [P]^{N_S N_S} & 0 & 0 \\ 0 & 0 & 0 & \sigma(\overline{B})^2 & 0 \\ 0 & 0 & 0 & 0 & \sigma(\gamma_I)^2 \end{bmatrix} \quad \text{(2.2-4c)*}$$

where:

$$\sigma(\overline{B})^2 = \begin{bmatrix} (\overline{\sigma}_\rho^{G/W})^2 & 0 & 0 & 0 & 0 & 0 & 0 & 0 & 0 & 0 & 0 \\ 0 & (\overline{\sigma}_d^{G/W})^2 & 0 & 0 & 0 & 0 & 0 & 0 & 0 & 0 & 0 \\ 0 & 0 & (\overline{\sigma}_\rho^{CL})^2 & 0 & 0 & 0 & 0 & 0 & 0 & 0 & 0 \\ 0 & 0 & 0 & (\overline{\sigma}_d^{CL})^2 & 0 & 0 & 0 & 0 & 0 & 0 & 0 \\ 0 & 0 & 0 & 0 & (\overline{\sigma}^{CO})^2 & 0 & 0 & 0 & 0 & 0 & 0 \\ 0 & 0 & 0 & 0 & 0 & (\overline{\sigma}_\rho^{GS})^2 & 0 & 0 & 0 & 0 & 0 \\ 0 & 0 & 0 & 0 & 0 & 0 & (\overline{\sigma}_d^{GS})^2 & 0 & 0 & 0 & 0 \\ 0 & 0 & 0 & 0 & 0 & 0 & 0 & (\overline{\sigma}_d^{TDRS})^2 & 0 & 0 & 0 \\ 0 & 0 & 0 & 0 & 0 & 0 & 0 & 0 & (\overline{\sigma}_\phi^{G/W})^2 & 0 & 0 \\ 0 & 0 & 0 & 0 & 0 & 0 & 0 & 0 & 0 & (\overline{\sigma}_{\Delta\phi}^{G/W})^2 & 0 \\ 0 & 0 & 0 & 0 & 0 & 0 & 0 & 0 & 0 & 0 & (\overline{\sigma}_{IMU}^{A})^2 \end{bmatrix} \quad \text{(2.2-4d)*}$$

The covariance for individual state vector elements can be reinitialized by resetting the associated diagonal elements in the full covariance matrix to their initial values and the associated off-diagonal elements to zero. Whenever the state error covariance is initialized or reinitialized, it is factored as discussed below.

Similarly, when the relative state vectors of satellite n with respect to satellite 1 are estimated, the initial covariance matrix is given by

$$[P] = \begin{bmatrix} [P]^{11} & \cdots & 0 & 0 & 0 \\ \vdots & \ddots & 0 & 0 & 0 \\ 0 & 0 & [P_{rel}]^{N_S N_S} & 0 & 0 \\ 0 & 0 & 0 & \sigma(\overline{B})^2 & 0 \\ 0 & 0 & 0 & 0 & \sigma(\gamma_I)^2 \end{bmatrix} \quad \text{(2.2-4e)*}$$

where

$$[P_{rel}]^{nn} = E\left(\left[\hat{\overline{X}}^n_{rel}(t_k) - \overline{X}^n_{rel}(t_k) \right] \left[\hat{\overline{X}}^n_{rel}(t_k) - \overline{X}^n_{rel}(t_k) \right]^T \right) \quad \text{(2.2-4f)}$$

The relative covariance matrices are related to the absolute covariance matrices as follows:

$$[P_{rel}]^{nn} = [P_{abs}]^{nn} + [P_{abs}]^{11} - [P_{abs}]^{n1} - [P_{abs}]^{1n} \quad \text{(2.2-4g)}$$

and similarly

$$[P_{abs}]^{nn} = [P_{abs}]^{11} + [P_{rel}]^{nn} + [P_{rel}]^{n1} + [P_{rel}]^{1n} \quad \text{(2.2-4h)}$$

2.2.1 Covariance Factorization

The state error covariance matrix [P] is factored into a unit upper triangular matrix [U] and a diagonal matrix [D] (Reference 5). This factorization guarantees nonnegativity of the computed covariance and is numerically stable and accurate. This factorization also avoids the use of square roots. Subsequent sections define how the $[U]$ and [D] matrices are time propagated and measurement updated directly, rather than the state error covariance matrix [P]. The [U] and [D] matrices are defined as

$$[P] = [U]\,[D]\,[U]^T \tag{2.2-5}$$

where

[P] = [N × N] state error covariance matrix

[U] = [N × N] unit upper triangular matrix

[D] = [N × N] diagonal matrix

and

$$[U] = \begin{bmatrix} 1 & U_{1,2} & \cdot & \cdot & \cdot & \cdot & \cdot & \cdot & U_{1,N} \\ 0 & 1 & \cdot & \cdot & \cdot & \cdot & \cdot & \cdot & \cdot \\ \cdot & \cdot & \cdot & \cdot & \cdot & \cdot & \cdot & \cdot & \cdot \\ \cdot & \cdot & \cdot & \cdot & \cdot & \cdot & \cdot & \cdot & \cdot \\ \cdot & \cdot & \cdot & \cdot & \cdot & \cdot & \cdot & \cdot & \cdot \\ \cdot & \cdot & \cdot & \cdot & \cdot & \cdot & \cdot & \cdot & \cdot \\ \cdot & \cdot & \cdot & \cdot & \cdot & \cdot & \cdot & \cdot & \cdot \\ \cdot & \cdot & \cdot & \cdot & \cdot & \cdot & 1 & U_{N-1,N} \\ 0 & \cdot & \cdot & \cdot & \cdot & \cdot & 0 & 1 \end{bmatrix} \tag{2.2-6}$$

$$[D] = \begin{bmatrix} D_{1,1} & 0 & \cdot & \cdot & \cdot & \cdot & \cdot & \cdot & 0 \\ 0 & D_{2,2} & \cdot & \cdot & \cdot & \cdot & \cdot & \cdot & \cdot \\ \cdot & \cdot & \cdot & \cdot & \cdot & \cdot & \cdot & \cdot & \cdot \\ \cdot & \cdot & \cdot & \cdot & \cdot & \cdot & \cdot & \cdot & \cdot \\ \cdot & \cdot & \cdot & \cdot & \cdot & \cdot & \cdot & \cdot & \cdot \\ \cdot & \cdot & \cdot & \cdot & \cdot & \cdot & \cdot & \cdot & \cdot \\ \cdot & \cdot & \cdot & \cdot & \cdot & \cdot & \cdot & \cdot & \cdot \\ \cdot & \cdot & \cdot & \cdot & \cdot & \cdot & D_{N-1,N-1} & 0 \\ 0 & \cdot & \cdot & \cdot & \cdot & \cdot & 0 & D_{N,N} \end{bmatrix} \tag{2.2-7}$$

The covariance matrix is a symmetric positive definite matrix. A symmetric positive definite matrix has the following properties (see page 34 of Reference 5): (a) all eigenvalues are positive,

(b) all diagonal elements are positive, and (c) all correlation coefficient magnitudes are less than 1. Symmetry and positive definiteness are required for $\left[UDU^T\right]$ covariance factorization (Reference 5). The factorization algorithm given below was taken from Reference 5.

First, for the N^{th} column,

$$D_{N,N} = P_{N,N} \tag{2.2-8}*$$

$$U_{i,N} = \begin{cases} 1 & i = N \\ P_{i,N} / D_{N,N} & i = N-1,\ N-2,\ \ldots,\ 1 \end{cases} \tag{2.2-9}*$$

Then, for the remaining columns, j = N-1, ..., 1, compute

$$D_{j,j} = P_{j,j} - \sum_{k=j+1}^{N} \left[D_{k,k}\ U_{j,k}^2\right] \tag{2.2-10}*$$

$$U_{i,j} = \begin{cases} 0 & i > j \\ 1 & i = j \\ \left[P_{i,j} - \sum_{k=j+1}^{N} D_{k,k}\ U_{i,k}\ U_{j,k}\right] / D_{j,j} & i = j-1,\ j-2, \ldots, 1 \end{cases} \tag{2.2-11}*$$

The state noise covariance matrix [Q] is also factored into a unit upper triangular matrix [G_d] and a diagonal matrix [Q_d] as follows, using the same factorization algorithm as for the state error covariance matrix (the state noise covariance matrix is sometimes referred to as the process noise covariance matrix):

$$[Q] = [G_d]\ [Q_d]\ [G_d]^T \tag{2.2-12}*$$

where

[Q]= [N × N] state error covariance matrix

[G_d]= [N × N] unit upper triangular matrix

[Q_d]= [N × N] diagonal matrix

One result of the positive definiteness requirement for covariance factorization is that the time bias drift estimation cannot be disabled simply by setting its initial variance to zero and setting its state noise to zero.

2.2.2 Semimajor Axis Variance

The absolute semimajor axis standard deviation is used to assess the filter convergence. The absolute semimajor axis standard deviation for satellite n, $\sigma_{\Delta a}^{n}$, is computed from the user satellite position and velocity state error covariance matrix using the following algorithm.

The semimajor axis is computed as follows:

$$a^n = \left[\frac{2}{R^n} - \frac{\left|\dot{\overline{R}}^n\right|^2}{\mu_E} \right]^{-1} \qquad (2.2\text{-}13)^*$$

where

a^n =semimajor axis for satellite n (meters)

μ_E =gravitational constant of the Earth (meters^3/second^2)

R^n = magnitude of the satellite position vector (meters)

$\left|\dot{\overline{R}}^n\right|$ =magnitude of the satellite velocity vector (meters/second)

The absolute semimajor axis variance for satellite n is defined as follows

$$\left(\sigma_{\Delta a}^{n}\right)^2 = E\left(\left[\hat{a}_k^n - a_k^n\right]\left[\hat{a}_k^n - a_k^n\right]^T\right) = \overline{S}^n W_{abs}^{n,n} \overline{S}^{nT} \qquad (2.2\text{-}14a)^*$$

where

$\hat{a}_k^n$ = estimated semimajor axis at time t_k (meters)

a_k^n = true (unknown) semimajor axis (meters)

$\overline{S}^n$ = vector of partial derivatives of the semimajor axis with respect to the position and velocity components of the estimation vector

$$\left[\overline{S}^n\right] = \left[\frac{\partial a^n}{\partial \overline{R}^n} \quad \frac{\partial a^n}{\partial \dot{\overline{R}}^n} \right] = 2\left(a_k^n\right)^2 \left[\frac{X^n}{R^{n^3}} \quad \frac{Y^n}{R^{n^3}} \quad \frac{Z^n}{R^{n^3}} \quad \frac{\dot{X}^n}{\mu_E} \quad \frac{\dot{Y}^n}{\mu_E} \quad \frac{\dot{Z}^n}{\mu_E} \right] \qquad (2.2\text{-}14)^*$$

$W_{abs}^{n,n}$ = 6×6 user satellite position and velocity submatrix of the absolute state error covariance matrix [P] for satellite n defined in Equation (2.2-4c)

The absolute semimajor axis one sigma standard deviation is then computed as follows

$$\sigma_{\Delta a}^{n} = \sqrt{\overline{S}^n W_{abs}^{n,n} \overline{S}^{nT}} \qquad (2.2\text{-}15)^*$$

The relative semimajor axis is defined as

$$a_{rel}^{n} = a^{n} - a^{1} \tag{2.2-16}$$

The relative semimajor axis covariance for satellite n relative to satellite 1 at time t_k is defined as follows

$$\begin{aligned}\left(\sigma_{\Delta a_{rel}}^{n}\right)^2 &= E\left(\left[\left(\hat{a}_k^n - a_k^n\right) - \left(\hat{a}_k^1 - a_k^1\right)\right]\left[\left(\hat{a}_k^n - a_k^n\right) - \left(\hat{a}_k^1 - a_k^1\right)\right]^T\right) \\ &= E\left(\left[\hat{a}_k^n - a_k^n\right]\left[\hat{a}_k^n - a_k^n\right]^T\right) + E\left(\left[\hat{a}_k^1 - a_k^1\right]\left[\hat{a}_k^1 - a_k^1\right]^T\right) \\ &\quad - E\left(\left[\hat{a}_k^n - a_k^n\right]\left[\hat{a}_k^1 - a_k^1\right]^T\right) - E\left(\left[\hat{a}_k^1 - a_k^1\right]\left[\hat{a}_k^n - a_k^n\right]^T\right)\end{aligned} \tag{2.2-17}$$

The relative semimajor axis standard deviation for satellite n relative to satellite 1 is computed as follows

$$\sigma_{\Delta a_{rel}}^{n} = \left(\begin{bmatrix} -\bar{S}^1 & \bar{S}^n \end{bmatrix} \begin{bmatrix} W_{abs}^{1,1} & W_{abs}^{1,n} \\ W_{abs}^{n,1} & W_{abs}^{n,n} \end{bmatrix} \begin{bmatrix} -\bar{S}^{1T} \\ \bar{S}^{nT} \end{bmatrix} \right)^{1/2} \tag{2.2-18)*}$$

where $W_{abs}^{i,j}$ is the 6×6 submatrix of the absolute state error covariance matrix [P_{abs}] associated with the correlation of the position and velocity estimates for satellite i with the estimates for satellite j, defined in Equation (2.2-4c).

If the relative state vector is estimated for nonlocal satellites, the relative semimajor axis standard deviation for satellite n relative to satellite 1 is then computed as follows

$$\sigma_{\Delta a_{rel}}^{n} = \left(\begin{bmatrix} \left(\bar{S}^n - \bar{S}^1\right) & \bar{S}^n \end{bmatrix} \begin{bmatrix} W_{rel}^{1,1} & W_{rel}^{1,n} \\ W_{rel}^{n,1} & W_{rel}^{n,n} \end{bmatrix} \begin{bmatrix} \left(\bar{S}^n - \bar{S}^1\right)^T \\ \bar{S}^{nT} \end{bmatrix} \right)^{1/2} \tag{2.2-18a)*}$$

where $W_{rel}^{n,n}$ is 6×6 submatrix of the relative state error covariance matrix [P_{rel}] associated with the relative state of satellite n with respect to satellite 1.

2.3 Extended Kalman Filter Algorithms

The EKF algorithm consists of the following two major processes:

1. **Time Update**. This process consists of propagating the estimated state and state error covariance factors from the time of the previous $(k-1)^{th}$ filter update [denoted by $\hat{\bar{X}}_{k-1}(+)$, $U_{k-1}(+)$, and $D_{k-1}(+)$, respectively] to the time of the current $(k)^{th}$ filter update [denoted by $\hat{\bar{X}}_k(-)$, $U_k(-)$, and $D_k(-)$].

2. **Measurement Update**. This process consists of correcting $\hat{\bar{X}}_k(-)$, $U_k(-)$, and $D_k(-)$ to include the effects of the current measurement. The corrected state and state error covariance are denoted by $\hat{\bar{X}}_k(+)$, $U_k(+)$ and $D_k(+)$.

These steps are described in the subsections below.

GEONS provides the following three estimation modes for performing the EKF processing where

- toTime is the time passed to EKF process
- measTimeX is one of the measurement times
- outTime is the time when the EKF process outputs the state and covariances

ESTIMATION_TIME_LEGACY=0

- GEONS selects the most recent time for the first sensor type (measTime1) and propagates to that time (propTime=measTime1) or propTime= toTime if no measurements
- All measurement processing is performed at propTime=measTime1
- State and covariance are updated at outTime= propTime= measTime1

ESTIMATION_TIME_TOTIME = 1

- GEONS propagates its state to propTime=toTime
- All measurements are processed at propTime=toTime
- State and covariance are updated at outTime= propTime=toTime

ESTIMATION_TIME_EACHMEAS = 2

- All measurements are sorted based on measTime.
- For each measurement
  - GEONS propagates the state and covariance to propTime= measTimeX
  - Processes the measurement at propTime= measTimeX
  - Updates the state and covariance at propTime= measTimeX
- Output state and covariances are propagated to outTime= toTime

2.3.1 Time Update Process

The time update is performed at either a specified estimation time or a valid measurement time t_k and at the intermediate time t_i if the time between measurements is greater than the maximum integration step size

$$t_k - t_{k-1} > \delta t_{max} \tag{2.3-1}*$$

where δt_{max} is equal to the maximum state vector integration step size.

The estimated total state vector at the previous measurement time (t_{k-1}), $\hat{\bar{X}}_{k-1}(+)$, and the state error covariance matrix factors, $U_{k-1}(+)$ and $D_{k-1}(+)$ are propagated to the time of current measurement update, t_k , using the following procedure.

When there are consider parameters, the state vector is partitioned into estimated states (x) and consider states (p), where n_s=number of estimated parameters and n_p= number of consider parameters. If a consider parameter has a "known" mean value (e.g. based on a prior calibration), the initial value of this consider parameter should be set to this mean value. If the consider parameter has a mean value of zero (e.g. a correction to the SRP coefficient that is not being estimated), the initial consider parameter value should be set to zero and will remain as zero. The consider states are included in the state and covariance propagation.

1. Propagate the state vector to the time t_i. The quantity $\hat{\bar{X}}_i(-)$ is obtained by integrating the following N equations:

$$\dot{\bar{X}} = \begin{bmatrix} \dot{\bar{X}}^1(t) \\ \vdots \\ \dot{\bar{X}}^{N_S}(t) \\ \dot{\bar{B}}(t) \\ \dot{\gamma}_I \end{bmatrix} \tag{2.3-2}*$$

where

$$\dot{\bar{X}}^n = \begin{bmatrix} \dot{\bar{R}} \\ \ddot{\bar{R}} \\ \Delta\dot{C}_D \\ \Delta\dot{C}_R \\ \dot{\bar{b}}_R \\ \dot{\bar{a}}_U \end{bmatrix}^n \tag{2.3-2a}$$

$$\dot{\overline{B}} = \begin{bmatrix} \dot{\overline{b}}_{\rho}^{G/W} \\ \dot{\overline{b}}_{d}^{G/W} \\ \dot{\overline{b}}_{\rho}^{CL} \\ \dot{\overline{b}}_{d}^{CL} \\ \dot{\overline{b}}^{CO} \\ \dot{\overline{b}}_{\rho}^{GS} \\ \dot{\overline{b}}_{d}^{GS} \\ \dot{\overline{b}}_{d}^{TDRS} \\ \dot{\overline{b}}_{\phi}^{G/W} \\ \dot{\overline{b}}_{\Delta\phi}^{G/W} \end{bmatrix} \tag{2.3-2b}$$

$$\dot{\gamma}_I = 0 \tag{2.3-2c}$$

The equations of motion for the spacecraft state vector components $(\overline{R}, \dot{\overline{R}})$ are defined in Section 4.1. These equations are numerically integrated using the Runge-Kutta algorithm defined in Section 4.2. This numerical integration starts from the most recent integration time, t_{i-1}, using $\overline{R}(t_{i-1})$ and $\dot{\overline{R}}(t_{i-1})$, the most recent propagated values based on an initial value equal to the state from the last measurement update, $\hat{\overline{X}}_{k-1}(+)$. Note that acceleration-related consider bias parameters (i.e. solar radiation pressure and drag coefficient corrections and acceleration biases) are included in the acceleration used in the state propagation. If relative state vectors are being estimated, the relative state vector components $(\overline{R}_{rel}^{n}, \dot{\overline{R}}_{rel}^{n})$ are propagated by forming the associated absolute position and velocity vectors, $\overline{R}^{n}(t_{i-1}) = \overline{R}^{1}(t_{i-1}) + \overline{R}_{rel}^{n}(t_{i-1}), \dot{\overline{R}}^{n}(t_{i-1}) = \dot{\overline{R}}^{1}(t_{i-1}) + \dot{\overline{R}}_{rel}^{n}(t_{i-1})$, propagating the absolute state, and then computing the propagated relative state. Propagation of the corrections to the nonspacecraft state vector components $(\Delta C_D, \Delta C_R, \overline{b}_R, \overline{a}_U, \overline{b}_{\rho}^{G/W}, \overline{b}_{d}^{G/W}, \overline{b}_{\rho}^{CL}, \overline{b}_{d}^{CL}, \overline{b}^{CO}, \overline{b}_{\rho}^{GS}, \overline{b}_{d}^{GS}, \overline{b}_{d}^{TDRS}, \overline{b}_{\phi}^{G/W}, \overline{b}_{\Delta\phi}^{G/W}$, and $\gamma_I)$ is performed analytically, as discussed in Section 4.3. The ground-based receiver state propagation equations are given in Section 4.6. This produces $\hat{\overline{X}}_i(-) \equiv \overline{X}(t_i)$. Note that, if t_i is the time at which receiver n acquires the signal from the j^{th} GPS/Galileo SV/WAAS GEO, the associated carrier phase bias state vector element, $b_{\phi_n}^{G/W_j}$, and singly differenced carrier phase bias state vector element, $b_{\Delta\phi_{1n}}^{G/W_j}$ are reinitialized.

2 Compute the state transition matrix from time t_{i-1} to time t_i using the algorithm given in Section 4.4.1. If the state vector consists entirely of absolute state vectors:

$$\Phi(t_i,t_{i-1})=\frac{\partial \overline{X}(t_i)}{\partial \overline{X}(t_{i-1})}=\begin{bmatrix} \frac{\partial \overline{X}^1(t_i)}{\partial \overline{X}^1(t_{i-1})} & \cdots & 0 & 0 & 0 \\ \vdots & \ddots & \vdots & \vdots & \vdots \\ 0 & \cdots & \frac{\partial \overline{X}^{N_S}(t_i)}{\partial \overline{X}^{N_S}(t_{i-1})} & 0 & 0 \\ 0 & \cdots & 0 & \frac{\partial \overline{B}(t_i)}{\partial \overline{B}(t_{i-1})} & 0 \\ 0 & \cdots & 0 & 0 & \frac{\partial \gamma_I(t_i)}{\partial \gamma_I(t_{i-1})} \end{bmatrix} \quad (2.3\text{-}3)^*$$

If the state vector includes relative states for the nonlocal satellites, the associated state transition matrix includes the correlation between the relative states and the local state

$$\Phi(t_i,t_{i-1})=\frac{\partial \overline{X}_{rel}(t_i)}{\partial \overline{X}_{rel}(t_{i-1})}=\begin{bmatrix} \frac{\partial \overline{X}^1(t_i)}{\partial \overline{X}^1(t_{i-1})} & 0 & \cdots & 0 & 0 & 0 \\ \frac{\partial \overline{X}^2(t_i)}{\partial \overline{X}^2(t_{i-1})}-\frac{\partial \overline{X}^1(t_i)}{\partial \overline{X}^1(t_{i-1})} & \frac{\partial \overline{X}^2(t_i)}{\partial \overline{X}^2(t_{i-1})} & \cdots & 0 & 0 & 0 \\ \vdots & \vdots & \ddots & \vdots & \vdots & \vdots \\ \frac{\partial \overline{X}^{N_S}(t_i)}{\partial \overline{X}^{N_S}(t_{i-1})}-\frac{\partial \overline{X}^1(t_i)}{\partial \overline{X}^1(t_{i-1})} & 0 & \cdots & \frac{\partial \overline{X}^{N_S}(t_i)}{\partial \overline{X}^{N_S}(t_{i-1})} & 0 & 0 \\ 0 & 0 & \cdots & 0 & \frac{\partial \overline{B}(t_i)}{\partial \overline{B}(t_{i-1})} & 0 \\ 0 & 0 & \cdots & 0 & 0 & \frac{\partial \gamma_I(t_i)}{\partial \gamma_I(t_{i-1})} \end{bmatrix} \quad (2.3\text{-}4)$$

where

$$\Phi(t_{i-1},\, t_{i-1})=I \quad \text{(Identity matrix)} \quad (2.3\text{-}5)^*$$

Equation Deleted (2.3-6)

3. Calculate the state process noise covariance matrix at time t_i, denoted by Q_{i-1}. The process noise algorithm for this step is described in Section 4.4.2. Factor into components G_d and Q_d using the algorithm provided in Section 2.2.

4. Propagate the state error covariance matrix factors to the time t_i to obtain U_k (–) and D_k (–). This propagation is performed by directly propagating the U and D matrices as shown in Section 4.4.3. If t_i is the time at which receiver n acquires the signal from the j^{th} GPS/Galileo SV/WAAS GEO, the associated carrier phase bias or singly differenced carrier phase bias state vector diagonal element are reinitialized to their initial values and the associated off-diagonal elements of the full covariance matrix are reinitialized to zero, and the covariance matrix is refactorized, using the algorithm defined in Section 2.2.1.

If t_i is not a valid measurement time, set $U_i(+) = U_i(-)$, $D_i(+) = D_i(-)$, and $X_i(+) = X_i(-)$ and terminate the time update process.

2.3.2 Measurement Update Process

The inputs to the measurement update process are the results of the time update, $\hat{\bar{X}}_k(-)$, $U_k(-)$, and $D_k(-)$, as well as the measurement noise covariance, R_k. The output from the measurement update process are the updated total state vector, $\hat{\bar{X}}_k(+)$, and the updated state error covariance matrix factors, $U_k(+)$ and $D_k(+)$. Section 2.3.2.1 discusses the process used to select valid measurements for processing. Section 2.3.2.2 defines the nominal scalar measurement update algorithm. Section 2.3.2.3 defines an alternate sequential measurement update algorithm that can be used when ground station range and Doppler measurements are processed at the same measurement time. Section 2.3.2.4 defines an alternate batch measurement update algorithm that can be used when multiple measurements are processed in the same filter update timespan.

2.3.2.1 Measurement Selection

The following criteria are used to select valid measurements for further processing:

- Time constraints, e.g. elapsed time from last successful measurement update is greater than or equal to the minimum specified measurement sampling interval
- Transmitter/sensor is enabled and has valid state vector or ephemeris
- Measurements do not occur during a maneuver time span (optional).
- Measurement-type specific selection criteria are satisfied (see Table 5.1 for details)
- Visibility criteria are satisfied

The visibility tests consist of the Height of Ray Path (HORP) test to eliminate measurements with long paths through the Earth's atmosphere for GPS/Galileo/WAAS, crosslink, or TDRSS measurements and a minimum elevation angle test for ground station measurements. These tests are defined below.

HORP Test: Edit a GPS/Galileo/WAAS, crosslink, or TDRSS measurement if the signal has a long path through the atmosphere (i.e., passes through the Earth's limb). The following updated HORP editing test is implemented in GEONS 3.0. Note that this test is more general than the original algorithm, which did not handle the case when the transmitter is at the minimum HORP altitude. In the ECEF frame, the HORP is computed as the altitude of the point on the line connecting the transmitter position and the receiver (predicted) position with minimum radius-squared (i.e., minimum altitude neglecting the oblateness of the Earth).

Compute the minimum radial distance (d):

Let $\bar{R}_R(t_k)$ be the receiver position and $\bar{R}_T(t_k)$ the transmitter position, then the set of points connecting them is given by

$$\left\{\left(1-\alpha\right)\bar{R}_R(t_k)+\alpha\bar{R}_T(t_k)\right\};\ \text{where}\ \alpha\in\left[0,1\right]$$

And their radial value is given by

$$f(\alpha)=\|(1-\alpha)\bar{R}_R(t_k)+\alpha\bar{R}_T(t_k)\|^2=\|\bar{R}_R(t_k)+\alpha(\bar{R}_T(t_k)-\bar{R}_R(t_k))\|^2 \qquad (2.3\text{-}7a)$$

By finding $\alpha=\alpha^*$ such that $\frac{df(\alpha)}{d\alpha}=0$, we find the minimum of (convex) f on the real line at

$$\alpha^*=-\frac{\bar{R}_R(t_k)\cdot(\bar{R}_T(t_k)-\bar{R}_R(t_k))}{\|\bar{R}_T(t_k)-\bar{R}_R(t_k)\|^2} \qquad (2.3\text{-}8)^*$$

If $\alpha^*<0$, the minimum radial distance (d) is the radial distance to the receiver. If $\alpha^*>1$, d is the radial distance to the transmitter; otherwise d is computed as $\sqrt{f\left(\alpha^*\right)}$.

a. The measurement is accepted if $d\geq R_e+h$ [case (a) in Figure 2-1], where R_e is the mean equatorial radius of the Earth and h is a specified minimum altitude. For GPS/ Galileo receivers located below the GPS/Galileo constellations, the minimum altitude is typically specified as the smaller of the height of the atmosphere or the height of the receiver. For Lunar spacecraft, the minimum altitude is typically specified as 0. For Ground Station tracking of Earth-orbiting spacecraft, the minimum altitude is typically specified as -50 km to account for Earth's ellipsoid.

b. If $d<R_e+h$, [case (b) in Figure 2-1], perform the following central angle test.

Equation Deleted (2.3-9)*

Equation Deleted (2.3-10)*

Compute the central angle and accept the measurement if $\alpha<\alpha_{max}$, where

$$\alpha=\cos^{-1}\left(\frac{\bar{R}_T\cdot\bar{R}_R}{R_T\,R_R}\right) \qquad (2.3\text{-}11)^*$$

and

R_T = magnitude of $\bar{R}_T(t_k)$

R_R = magnitude of $\bar{R}_R(t_k)$

α_{max} = maximum central angle (an input control parameter nominally equal to 70 degrees)

c. If the measurement is not accepted, terminate the update process.

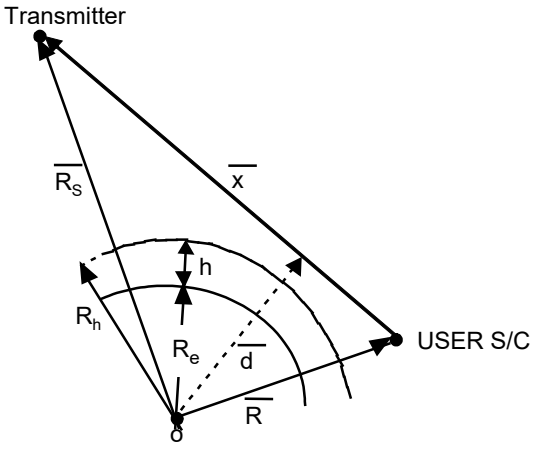

a. $d \geq R_e + h$

RAY PATH IS ABOVE
THE ATMOSPHERE

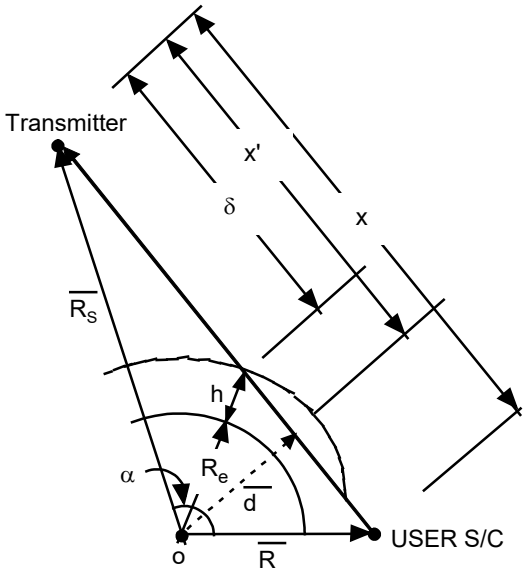

b. $d < R_e + h$

RAY PATH PASSES THROUGH
THE ATMOSPHERE

Figure 2-1. HORP Geometry

Elevation Angle Test: Edit a Ground Station (GS) one-way Doppler measurement if the elevation of the line-of-sight vector with respect to the local horizon is less than a minimum angle. This atmospheric editing test is performed as follows:

Compute the instantaneous line-of-sight vector from the receiving satellite to the transmitting GS as follows:

$$\bar{\rho}^{i} = \bar{R}(t_k) - \bar{R}^{i}_{GS}(t_k) \qquad \text{(2.3-11b)*}$$

where

$\bar{R}(t_k)$ =position vector of the receiving satellite at time t_k, referenced to the inertial Mean of J2000.0 reference frame

$\bar{R}^{i}_{GS}(t_k)$ =position of the transmitting GS at time t_k, referenced to the inertial Mean of J2000.0 reference frame

The GS position vectors are available in Earth-centered Earth-fixed (ECEF) coordinates. The GS position vector must be transformed from ECEF coordinates to J2000.0 inertial coordinates to using the transformations defined in Sections 3.2.1 through 3.2.3.

The atmospheric editing test is based on whether the elevation angle, *E*, of the line-of-sight vector with respect to the local horizon is greater than a minimum elevation angle, $E_{\min}$. Figure 2-2 illustrates the accepted (A) and edited (B) cases. The measurement is accepted if the following is true:

$$\sin E > \sin E_{\min} \qquad \text{(2.3-11c)*}$$

where $E_{\min}$ is a commandable minimum elevation angle within the ±90 degrees range, $E_{\min}$ and *E* are positive above the local horizon and negative below the horizon, and

$$\sin E = \frac{\bar{\rho}^{i} \cdot \bar{R}^{i}_{GS}(t_k)}{\left|\bar{\rho}^{i}\right| \left|\bar{R}^{i}_{GS}(t_k)\right|} \qquad \text{(2.3-11d)*}$$

If the measurement is edited, terminate the measurement update process.

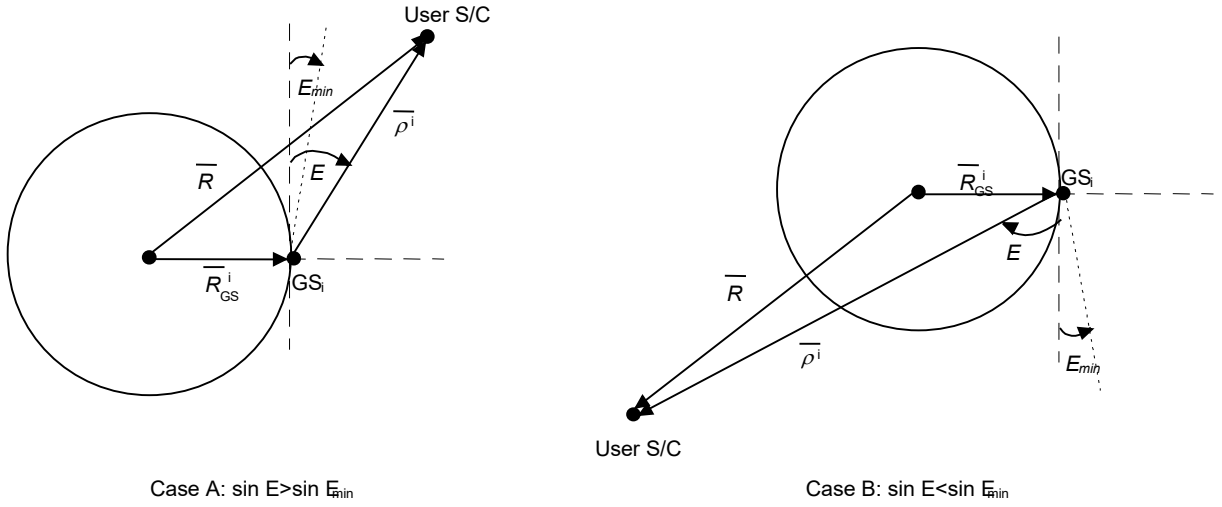

Figure 2-2. Atmospheric Editing Cases for GS Measurements

2.3.2.2 Scalar Measurement Update Procedures

Section 2.3.2.2.1 defines the default scalar measurement update process used in GEONS, which uses the Carlson Rank-One update algorithms based on Reference 5. Section 2.3.2.2.2 defines the scalar measurement update process when consider parameters are included. Either scalar update processes can be performed sequentially for each valid measurement at each measurement update epoch, t_k.

2.3.2.2.1 Default Scalar Measurement Update Procedure

1. Given the results of the time update, $\hat{\bar{X}}_k(-)$, $U_k(-)$, and $D_k(-)$, compute the predicted measurement, $\hat{Y}_k$, the measurement residual, y_k, and the measurement partial derivatives at the filter update epoch t_k, H_k,

$$\hat{Y}_k = G\left[\hat{\bar{X}}_k(-), t_k\right] \tag{2.3-12}*$$

$$y_k = Y_k - \hat{Y}_k \tag{2.3-13}*$$

$$H_k = \left[\frac{\partial G}{\partial \bar{X}}\right]_{\bar{X}=\hat{\bar{X}}_k(-)} \tag{2.3-14}*$$

where Y_k is the observed measurement. The measurement model equation, G, and associated partial derivatives, H, are given in Sections 5.3 through 5.9 of this document. If the

measurement time is not equal to the filter update epoch, the state can optionally be propagated from the filter update time to the measurement time.

2. Compute the predicted measurement residual variance, V_k, using Equations 2.3-15 through 2.3-18 in the Carlson Rank-One update algorithm defined in Section 2.3.2.4.1, where

$$V_k = a_N \tag{2.3-19}*$$

3. Perform the n-sigma measurement residual edit test:

   Calculate the sigma ratio

$$D_k = \frac{y_k}{\sqrt{V_k}} \tag{2.3-20}*$$

   If $|D_k| \leq N_\sigma$, accept the measurement and continue the measurement update. If $|D_k| > N_\sigma$, reject the measurement and the covariance updates and exit the calculation. In these tests, N_σ is a specifiable integer with a default value of 4.

4. Compute updated state error covariance factors and the Kalman gain vector, $\overline{K}_k$ using Equations 2.3-21 through 2.3-24 in the Carlson Rank-One update algorithm defined in Section 2.3.2.4.1, where

$$\overline{K}_k = \overline{b} / V_k \tag{2.3-25}*$$

   where $\overline{K}_k$ is the $[N \times 1]$ Kalman gain vector and the components of $\overline{b}$ are defined in Equation (2.3.2.4.1-14).

5. Update $\hat{\overline{X}}_k(-)$

$$\hat{\overline{X}}_k(+) = \hat{\overline{X}}_k(-) + \overline{K}_k y_k \tag{2.3-26}*$$

2.3.2.2.2 Scalar Measurement Update Procedure with Consider Parameters

When there are consider parameters, the state vector $\overline{X}_k$ is partitioned into estimated states (x) and consider states (p), where n_s=number of estimated parameters and n_p= number of consider parameters. Optionally, any parameter in the estimation state vector except for the satellite position and velocity can be processed as a consider parameter. However, GEONS 3.0 only supports the inclusion of the atmospheric drag coefficient correction and sensor and global biases as consider parameters. The value and covariance of a consider parameter is not updated by the filter measurement update process but the effects of consider parameter uncertainties are included in the calculation of corrections to and covariance of estimated parameters and in the error cross-covariance of estimated and consider parameters.

1. Given the results of the time update, $\hat{\bar{X}}_k(-)$, $U_k(-)$, and $D_k(-)$, compute the predicted measurement, $\hat{Y}_k$, the measurement residual, y_k, and the measurement partial derivatives at the measurement update epoch t_k, H_k,

$$\hat{Y}_k = G\left[\hat{\bar{X}}_k(-), t_k\right] \quad \text{(2.3.2.2.2-1)*}$$

$$y_k = Y_k - \hat{Y}_k \quad \text{(2.3.2.2.2-2)*}$$

$$H_k = \left[\frac{\partial G}{\partial \bar{X}}\right]_{\bar{X}=\hat{\bar{X}}_k(-)} \quad \text{(2.3.2.2.2-3)*}$$

where Y_k is the observed measurement. The measurement model equation, G, and associated partial derivatives, H, are given in Sections 5.3 through 5.9 of this document. Note that consider measurement bias parameters are included in the predicted measurement and measurement partial derivative calculations.

2. Perform a complete rank-one measurement update using the Carlson rank-one update given in Section 2.3.2.4.1 to compute the optimal Kalman gain, K_{opt}, covariance factors $U_{opt}(+)$ and $D_{opt}(+)$, and the predicted measurement residual variance, V_k .

3. If there are any consider parameters:

   For all parameters, set

$$K\ (i) = 0.0 \quad \text{(2.3.2.2.2-4)*}$$

   For each consider parameter, p, set the optimal Kalman gain to 0.0

$$K\ (p) = K_{opt}(p) \quad \text{(2.3.2.2.2-5)*}$$

$$K_{opt}(p) = 0.0 \quad \text{(2.3.2.2.2-6)*}$$

   Perform another rank-one measurement update using the Agee-Turner rank-one update procedure given in Section 2.3.2.4.2 with c=V_k and $x = K$ to solve

$$U_{con}(+)D_{con}(+)U_{con}(+)^T = U_{opt}(+)D_{opt}(+)U_{opt}(+)^T + V_k\,(K\ )(K\ )^T \quad \text{(2.3.2.2.2-7)*}$$

4. Perform the n-sigma measurement residual edit test. Calculate the sigma ratio

$$D_k = \frac{y_k}{\sqrt{V_k}} \qquad \text{(2.3.2.2.2-8)*}$$

If $|D_k| \le N_\sigma$, accept the measurement and continue the measurement update process.

If $|D_k| > N_\sigma$, reject the measurement, and the terminate processing of the ith measurement. In these tests, N_σ is a specifiable integer with a default value of 4.

5. If the measurement has not been edited, update $\hat{\overline{X}}_k(-)$ and the U and D covariance factors. Note that the following does not update the consider parameters or the covariance of the consider parameters:

$$\hat{\overline{X}}_k(+) = \hat{\overline{X}}_k(-) + \overline{K}_{opt}\, y_k \qquad \text{(2.3.2.2.2-9)*}$$

$$U_k(+) = U_{con}(+) \qquad \text{(2.3.2.2.2-10)*}$$

$$D_k(+) = D_{con}(+) \qquad \text{(2.3.2.2.2-11)*}$$

2.3.2.3 Simultaneous Measurement Update

(implemented only for ground station measurement processing in Release 2.10, replaced by Batch Measurement Update defined in Section 2.3.2.4 in GEONS Release 3.0)

2.3.2.4 Batch Measurement Update Procedure with Consider Option

The performance of an EKF is dependent on the order in which the measurements are processed. The following algorithm is discussed in detail in Section 3.2 of *Navigation Filter Best Practices* (Reference 59). As noted in that reference, "This is of particular import in the case when there is a powerful measurement coupled with a large *a priori* error. The state (and covariance) update will be large, very likely out of the linear range. Subsequent measurements which are processed may well be outside the residual edit thresholds, and hence will be rejected. In order to remedy this, we employ a hybrid Linear/Extended Kalman Filter measurement update. Recall that in an Extended Kalman Filter, the state is updated / relinearized / rectified after each measurement is processed. Hence, the solution is highly dependent on the order in which the measurements are processed. This is not a desirable situation in which to be."

This difficulty can be reduced by not applying the state updates until all the measurements associated with the same filter state epoch are processed. The state updates Δx are accumulated using a linear Kalman filter algorithm, which is mathematically equivalent to a sequential batch least-squares algorithm.

Optionally, any parameter in the estimation state vector except for the satellite position and velocity can be processed as a consider parameter. However, GEONS 3.0 only supports the inclusion of the atmospheric drag coefficient correction and sensor and global biases as consider parameters. The value and covariance of a consider parameter is not updated by the filter

measurement update process but the effects of consider parameter uncertainties are included in the calculation of corrections to and covariance of estimated parameters and in the error cross-covariance of estimated and consider parameters.

The inputs to the measurement update process are the results of the time update, $\hat{\bar{X}}_k(-)$, $U_k(-)$, and $D_k(-)$, as well as the measurement noise variance, R_k. The output from the measurement update process are the updated total state vector, $\hat{\bar{X}}_k(+)$, and the updated state error covariance matrix factors, $U_k(+)$ and $D_k(+)$ where t_k is the measurement update epoch time.

In general, the measurement time tags are not going to be equal to the current measurement update epoch time, t_k. In this case, the filter has propagated its state and covariance to the filter update time t = t_k from time $t = t_{k-1}$, and is subsequently given a measurement to be filtered (denoted by subscript m) that corresponds to the time $t = t_m$. If $\Delta t = t_m - t_k$ is significant (e.g. > 0.001 second), the time difference between the measurement and the filter state and covariance will need to be accounted for to accurately process the measurement. This time difference can be taken into account using either of the following options:

1. If the time difference is relatively small, e.g. < 1 second, the predicted measurements can be linearized about the current measurement update time. In GEONS 3.0, this correction is implemented for the GPS, Galileo, WAAS, TDRSS, and cross-link measurements.
2. The state can be computed at each measurement time by propagation and the measurement residual mapped to the filter epoch time using the state transition matrix. In GEONS 3.0, this approach is implemented for all celestial object and relative navigation camera measurements.

The following procedure assumes that the second option is used to compute the predicted measurement at the measurement time.

Given the results of the time update, $\hat{\bar{X}}_k(-)$, $U_k(-)$, and $D_k(-)$ at the current measurement update epoch, t_k, and a set of N_k measurements $\{Y_m^i\}$, with measurement times t_m that fall within the measurement update time interval $[t_k - \Delta t/2, t_k + \Delta t/2]$, the measurement update process consists of the following steps:

1. For each measurement Y_m^i, where i = 1, …, N_k,
   a. If $t_m = t_k$, set $\bar{X}_m^*(-) = \hat{\bar{X}}_k(-)$ for the associated satellite(s).
   b. If $t_m \neq t_k$, the state is propagated or interpolated to the time of the measurement to obtain $\bar{X}_m^*(-)$ for the associated satellite(s).
   c. Compute the predicted measurement, $\hat{Y}_m^i$, measurement residual, y_m^i, and measurement partial derivatives, H_m, at the measurement time t_m

$$\hat{Y}_m^i = G\left[\bar{X}_m^*(-),\ t_m\right] \qquad (2.3.2.4\text{-}1)^*$$

$$y_m^i = Y_m^i - \hat{Y}_m^i \qquad \text{(2.3.2.4-2)*}$$

$$H_m^i = \left[\frac{\partial G}{\partial \bar{X}}\right]_{\bar{X}=\bar{X}_m^*} \qquad \text{(2.3.2.4-3)*}$$

where Y_m^i is the observed measurement. The measurement model equation, *G*, and associated partial derivatives, *H*, are given in Sections 5.3 through 5.9.

d. If $t_m \neq t_k$, for celestial object measurements, compute the required submatrices of the state transition matrix from $t_k - t_m$, $\Phi(t_m, t_k)$, for the associated satellite(s) using equations given in Section 4.4.1. (Note that for celestial object measurements only the position submatrix is required.) Map the measurement partial derivatives to the current filter epoch time, t_k.

$$H_k^i = H_m^i \Phi(t_m, t_k) \qquad \text{(2.3.2.4-4)*}$$

e. Compute the predicted measurement residual variance, V_k^i, using the predicted covariance and perform the n-sigma measurement residual edit test. Calculate the sigma ratio

$$D_k = \frac{y_k^i}{\sqrt{V_k^i}} \qquad \text{(2.3.2.4-5)*}$$

where

$$V_k^i = H_k^i U_k(-) D_k(-) U_k(-)^T \left(H_k^i\right)^T + \left(\sigma^i\right)^2 \qquad \text{(2.3.2.4-6)*}$$

If $|D_k| \leq N_\sigma$, accept the measurement and continue the measurement update process. If $|D_k| > N_\sigma$, reject the measurement, and the terminate processing of the ith measurement. In these tests, N_σ is a specifiable integer with a default value of 4. Measurement residuals can exceed the acceptance threshold due clock anomalies and unplanned maneuvers in addition to measurement faults. The percentage of measurements that are rejected is tracked in measurement residual edit test defined in Section 2.3.3 and included in telemetry.

f. If the measurement is not edited, using the current values of $U_k^{i-1}(+)$ and $D_k^{i-1}(+)$ where $U_k^0(+) = U_k(-)$ and $D_k^0(+) = D_k(-)$ are from the time update, measurement update the covariance factors and compute the predicted measurement residual variance, V_k^i, and the optimal Kalman gain using the following procedure:

i. Perform a complete rank-one measurement update using the Carlson rank-one update given in Section 2.3.2.4.1 to compute the optimal Kalman gain, K^i_{opt}, covariance factors $U^i_{opt}(+)$ and $D^i_{opt}(+)$, and the predicted measurement residual variance, V^i_k.

ii. If there are any consider parameters, the state vector is partitioned into estimated states (x) and consider states (p), where n_s=number of estimated parameters and n_p= number of consider parameters

For all parameters, set

$$K^i(i) = 0.0 \qquad (2.3.2.4\text{-}7)^*$$

For each consider parameter, p, set the optimal Kalman gave to 0.0

$$K^i(p) = K^i_{opt}(p) \qquad (2.3.2.4\text{-}8)^*$$

$$K^i_{opt}(p) = 0.0 \qquad (2.3.2.4\text{-}9)^*$$

Perform another rank-one measurement update using the Agee-Turner rank-one update procedure given in Section 2.3.2.4.2 with c=V^i_k and $x = K^i$ to solve

$$U^i_{con}(+)D^i_{con}(+)U^i_{con}(+)^T = U^i_{opt}(+)D^i_{opt}(+)U^i_{opt}(+)^T + V^i_k\left(K^i\right)\left(K^i\right)^T \qquad (2.3.2.4\text{-}10)^*$$

g. Map the residual at the current filter epoch time, t_k

$$y^i_k = y^i_m - H^i_k \Delta\bar{x}^{i-1}_k \qquad (2.3.2.4\text{-}11)^*$$

Where $\Delta\bar{x}^{i-1}_k$ is the current accumulated state correction for the current batch measurement interval, where $\Delta\bar{x}^0_k = 0$ for the first measurement in each batch.

h. If measurement is not edited, update the accumulated the state update vector correction

$$\Delta\bar{x}^i_k = \Delta\bar{x}^{i-1}_k + K^i_{opt} y^i_k \qquad (2.3.2.4\text{-}12)^*$$

Where the Kalman gain is from step e.i if no consider parameters or step e.ii if there are consider parameters.

and the covariance factors

$$U_k^i(+) = \begin{cases} U_{opt}^i(+), \text{if no consider parameters} \\ U_{con}^i(+), \text{if there are consider parameters} \end{cases} \quad \text{(2.3.2.4-13)*}$$

$$D_k^i(+) = \begin{cases} D_{opt}^i(+), \text{if no consider parameters} \\ D_{con}^i(+), \text{if there are consider parameters} \end{cases} \quad \text{(2.3.2.4-13a)*}$$

2. After all N_k measurements have been processed, update $\hat{\bar{X}}_k(-)$ and the U and D covariance factors

$$\hat{\bar{X}}_k(+) = \hat{\bar{X}}_k(-) + \Delta\bar{x}_k^{N_k} \quad \text{(2.3.2.4-14)*}$$

$$U_k(+) = \begin{cases} U_{opt}^{N_k}(+), \text{if no consider parameters} \\ U_{con}^{N_k}(+), \text{if there are consider parameters} \end{cases} \quad \text{(2.3.2.4-15)*}$$

$$D_k(+) = \begin{cases} D_{opt}^{N_k}(+), \text{if no consider parameters} \\ D_{con}^{N_k}(+), \text{if there are consider parameters} \end{cases} \quad \text{(2.3.2.4-16)*}$$

2.3.2.4.1 Carlson Rank-One Update Algorithm with Underweighting

The Carlson Rank-One Update algorithm is discussed in detail in Appendix B.5 of *Navigation Filter Best Practices* (Reference 59). The Carlson Rank-One Update procedure with underweighting is as follows:

a. Compute

$$\bar{f} = \left[U_k^i(-)\right]^T \left[H_k^i\right]^T \quad \text{(2.3-15)*}$$

$$v_j = \left[D_k^i(-)\right]_{j,j} f_j \quad j = 1,2,\ldots,N \quad \text{(2.3-16)*}$$

where

N = dimension of the total state vector

$$U_k^i(-) = \begin{cases} U_k(-);\ i = 1, \text{ predicted value from time update} \\ U_k^{i-1}(+);\ i > 1, \text{ updated value after processing i - 1 measurements} \end{cases}$$

$$D_k^i(-) = \begin{cases} D_k(-);\ i = 1, \text{ predicted value from time update} \\ D_k^{i-1}(+);\ i > 1, \text{ updated value after processing i - 1 measurements} \end{cases}$$

H_k^i = [1 × N] measurement partial derivative matrix

b. Test for underweighting:

For j = 1, 2, ..., N, compute $HPH = H_k^i U_k^{i-1}(+) D_k^{i-1}(+) U_k^{i-1}(+)^T \left(H_k^i\right)^T$ as follows using values computed in Step a

$$\text{HPH}_j = HPH_{j-1} + f_j\, v_j \qquad \text{(2.3-16a)*}$$

If $HPH_N \le \alpha_{uw}^i$ set

$$a_0 = \left(\sigma^i\right)^2 \qquad \text{(2.3-17)*}$$

where

α_{uw}^i = Measurement underweighting threshold, a commanded parameter specified for each measurement type or each sensor type

σ^i = 1-sigma measurement error, a commanded parameter specified for each receiver and measurement type. Note that for GPS and Galileo receivers with large variations in the acquired signal strength (e.g. receivers in very high altitude and lunar orbits), the PR measurement standard deviation can optionally be computed based on based on standard GPS thermal noise theory as discussed in Section 12.4.2.

If $HPH_N > \alpha_{uw}^i$, set

$$a_0 = \left(\sigma^i\right)^2 + \beta_{uw}^i H_k^i P_k^i(-) H_k^{i\,T} \qquad \text{(2.3-17a)*}$$

where

β_{uw}^i = Measurement underweighting value, a commanded parameter specified for each measurement type or each sensor type

c. Compute updates to the state covariance based on the ith measurement:

$$a_1 = f_1\, v_1 + a_0 \qquad \text{(2.3-17b)*}$$

$$\left[D_k^i(+)\right]_{11} = \left[D_k^i(-)\right]_{11} a_0 / a_1 \qquad \text{(2.3-17c)*}$$

$$b_1 = v_1 \qquad \text{(2.3-17d)*}$$

$$\left[U_k^i(+)\right]_{11} = 1.0 \qquad \text{(2.3-17e)*}$$

For j = 2, ..., N,

$$a_j = a_{j-1} + f_j\, v_j \qquad \text{(2.3-18)*}$$

$$\left[D_k^i(+)\right]_{j,j} = \left[D_k^i(-)\right]_{j,j} a_{j-1} / a_j \qquad \text{(2.3-21)*}$$

$$b_j = v_j \qquad \text{(2.3-22)*}$$

$$\lambda_j = -f_j / a_{j-1} \qquad \text{(2.3-23)*}$$

$$\left.\begin{aligned} \left[U_k^i(+)\right]_{n,j} &= \left[U_k^i(-)\right]_{n,j} + \lambda_j\, b_n \\ b_n &= b_n + \left[U_k^i(-)\right]_{n,j} v_j \end{aligned}\right\} \quad \textit{for } n = 1,\ 2,\ \ldots,\ j-1 \qquad \text{(2.3-24)*}$$

d. Compute an update to the measurement residual variance, V_k^i, and the optimal Kalman gain

$$V_k^i = a_{\mathrm{N}} \qquad \text{(2.3-19)*}$$

and the optimal Kalman gain

$$K_{opt}^i = \frac{\overline{b}}{V_k^i} \qquad \text{(2.3-25)*}$$

2.3.2.4.2 Agee-Turner Rank-One Update Algorithm

The Agee-Turner Rank-One update is discussed in detail in Appendix B.3 of *Navigation Filter Best Practices* (Reference 59). This following recursive algorithm is taken from Section 7.3.2 of Reference 59. This algorithm is used to solve a matrix of the form

$$\tilde{U}\tilde{D}\tilde{U}^T = UDU^T + cxx^T \qquad (2.3.2.4.2\text{-}1)$$

where x is of rank 1. The following recursive algorithm is used to compute $\tilde{U}_{ij}$ and $\tilde{D}_{ii}$

Set $C^n = c$

For j = n, ..., 2, compute

$$\tilde{D}_{jj} = D_{jj} + C^j x_j^2 \qquad (2.3.2.4.2\text{-}2)^*$$

$$\tilde{U}_{jj} = 1 \qquad (2.3.2.4.2\text{-}3)^*$$

$$\beta_j = C^j / \tilde{D}_{jj} \qquad (2.3.2.4.2\text{-}4)^*$$

$$v_j = \beta_j x_j \qquad (2.3.2.4.2\text{-}5)^*$$

For i= 1, ..., j-1, compute

$$x_i = x_i - U_{ij} x_j \qquad (2.3.2.4.2\text{-}6)^*$$

$$\tilde{U}_{ij} = U_{ij} + x_i v_j \qquad (2.3.2.4.2\text{-}7)^*$$

End i loop

$$C^{j-1} = \beta_j D_{jj} \qquad (2.3.2.4.2\text{-}8)^*$$

End j loop

$$\tilde{D}_{11} = D_{11} + C^1 x_1^2 \qquad (2.3.2.4.2\text{-}9)^*$$

2.3.2.5 Measurement Underweighting

Measurement underweighting is an optional capability to underweight measurements when the absolute state covariance exceeds a commanded threshold for absolute measurements (i.e. GPS, Galileo, Ground Station, WAAS, Point Solutions, TDRSS, and all celestial object measurements except intersatellite) or when the relative state covariance exceeds a commanded threshold for relative measurements (i.e. crosslink and intersatellite line-of-sight/bearing). This capability is can be used to avoid initial filter divergence or post-maneuver divergence due to editing of valid measurements using an overly optimistic initial/post maneuver covariance relative to the actual errors when process noise is modeled to give good steady-state performance and adequate tracking is available. Underweighting is needed when accurate measurements are introduced at a time when the a priori covariance of the position and velocity is large and the measurement error due to the EKF linearization approximation is significant. Underweighting slows down the rate at which the covariance decreases to prevent the covariance matrix associated with these states from closing down too quickly. More detail is provided in the following reference: Renato Zanetti, Kyle J. DeMars, and Robert H. Bishop, "Underweighting Nonlinear Measurements," **Journal of Guidance, Control and Dynamics**, Vol. 33, No. 5, September-October 2010. Measurement underweighting is implemented as an option in the Carlson rank one algorithm defined in Section 2.3.2.4.1.

2.3.2.6 Efficiency Improvements in the UDU Algorithms

When the state vector is large containing many biases, which can either be estimated or consider states, the number of computations associated with the filter update process can be significantly reduced by separating the states into dynamic state and bias parameters. If the modified Gram-Schmidt algorithm is used to perform the filter update without taking advantage of the fact that the bias states are uncoupled with one another, there is a great deal of wasted computation, due to the large number of zeros in the state transition matrix associated with the bias states. However, if the dynamic states (position, velocity, attitude and clock states) are updated via the modified Gram-Schmidt process and if a more efficient algorithm is used for updating the bias states, the result is an efficient and a robust filter.

The GEONS filter algorithms incorporate several techniques to reduce computations. In GEONS, the dynamic states, which consist of the spacecraft position and velocity, are numerically integrated as discussed in Section 4.1 and 4.2. All other states are analytically integrated as discussed in Section 4.3. The state transition matrix, which is computed analytically as discussed in Section 4.4, has many zero elements. Sparse matrix multiplication techniques are used to reduce computations in the propagation of the covariance matrix.

The computational efficiency of the time update process in GEONS could be further improved by taking advantage of the block diagonal structure of the state transition matrix in the propagation of the covariance matrix. This improvement consists of a two-step process in which the modified Gram-Schmidt update is used for the first step and the Agee-Turner rank-one update is used for the second step. This improvement is discussed in detail in Section 7.3 of *Navigation Filter Best Practices* (Reference 59).

2.3.3 Fault Detection Tests

GEONS includes several tests that can be used to detect processing anomalies. However, anomaly investigation and resolution are performed external to the GEONS software library code. For example, the resolution of anomalies that result in filter divergence typically requires external intervention to halt processing and restart GEONS possibly with some adjustment of the filter tuning parameters.

If fault detection is enabled, GEONS performs the following navigation fault detection tests on the updated state and covariance for each receiver state being estimated:

a. Filter Convergence Test: Set the filter converged indicator to true if the RSS position sigma, RSS velocity sigma, and semimajor axis sigma are all below their respective ground commandable convergence tolerances.

b. RSS Position Difference Test:

   If an absolute comparison state is input, compute the RSS difference between the GEONS User position vector and the comparison ephemeris position vector (derived from either the GPS/Galileo Receiver's point solution or a backup ephemeris).

   If a relative comparison state is input, compute the RSS difference between the GEONS-estimated relative target position vector and the relative comparison position. In this case the GEONS-estimated relative target position vector state is computed by subtracting the absolute position vector of the local satellite from the absolute position vector of the target satellite

$$\bar{r}_{rel}^{GEONS} = \bar{r}_{abs}^{T\arg et} - \bar{r}_{abs}^{sat1} \qquad (2.3.3\text{-}1)^*$$

   Set the passed position difference test indicator to "false" (1) following initialization when there are not sufficient GEONS states to interpolate, (2) if a comparison state is not available for the current time, or (3) if the difference exceeds a ground commandable position difference tolerance. Set the indicator to "true" otherwise.

c. Covariance Factorization Test: Set the passed Covariance Matrix Divide by Zero Error Test Indicator to "false" if any of the following conditions have occurred, where the "zero" tolerance is a ground commandable value,

   - State error covariance matrix diagonalization divide by "zero"
   - State noise covariance matrix diagonalization divide by "zero"
   - State error covariance matrix propagation divide by "zero"
   - State error covariance matrix update divide by "zero"

   Otherwise, set the value to "true". When the covariance factorization test fails, autonomously transition from GEONS Filter Submode to GEONS Propagate Submode but without propagating covariance.

d. RSS Position Sigma Test: Set the passed position sigma test indicator to "false" if the state error covariance matrix RSS position sigma exceeds the ground commandable position sigma maximum tolerance. Different maximum tolerances are used for the preconvergence (i.e., when the filter convergence test has failed) and postconvergence (i.e., when the filter convergence test has passed) cases. Otherwise, set the indicator to "true".

e. RSS Velocity Sigma Test: Set the passed velocity sigma test indicator to "false" if the state error covariance matrix velocity variance exceeds a ground commandable velocity sigma maximum tolerance. Different maximum tolerances are used for the preconvergence and postconvergence cases. Otherwise, set the indicator to "true".

f. Measurement Residual Edit Test: Determine the percentage of measurements edited over a ground commandable sample size. Set the passed measurement edit test indicator to "false" if the percentage sigma-edited is larger than the ground commandable percentage tolerance. Otherwise, set the indicator to "true".

g. Covariance Overflow Test: Set the passed Covariance Overflow Error Test Indicator to "false" if any of the following conditions have occurred, where the overflow tolerance is a ground commanded value,

- State error covariance $[D]$ matrix element exceeds overflow tolerance
- State noise covariance $[Q_d]$ matrix element exceeds overflow tolerance

Otherwise, set the value to "true". When the covariance overflow test fails, autonomously transition from the GEONS primary mode from Normal to Halted.

h. Absolute Mahalanobis Measure Test (not implemented in GEONS 3.0): The absolute Mahalanobis measure threshold test is an optional test that can be performed if the absolute (e.g. Point Solution) comparison state and covariance are available for the satellite(s) being estimated. The test is performed as follows:

Compute the Mahalanobis measure from the absolute position differences and the respective absolute covariances:

$$d\left(\bar{r}_{abs}^{COMP}, \bar{r}_{abs}^{GEONS}\right) = \sqrt{\left(\bar{r}_{abs}^{COMP} - \bar{r}_{abs}^{GEONS}\right)^T S^{-1}\left(\bar{r}_{abs}^{COMP} - \bar{r}_{abs}^{GEONS}\right)} \qquad (2.3.3\text{-}2)^*$$

where

$\bar{r}_{abs}^{GEONS}$ =GEONS-computed absolute position vector of the satellite, referenced to the central-body inertial frame

$\bar{r}_{abs}^{COMP}$ = comparison absolute position vector of the satellite, referenced to the central-body inertial frame

$S = P_{abs}^{GEONS} + P_{abs}^{COMP}$ = Sum of the GEONS-computed covariance matrix and comparison covariance matrix (see note below) of the satellite position, referenced to the central-body inertial frame.

If the comparison covariance (or position variances) are not available within 1 second of the latest GEONS covariance, use the following approximations

- If PDOP is available for the Point Solution state data, use $P_{abs}^{COMP} = 10 * PDOP$
- If GDOP is available for the Point Solution state data but not PDOP, use $P_{abs}^{COMP} = 10 * GDOP$, and include the time bias in the state difference
- If no PDOP or GDOP, use $S = N * P_{abs}^{GEONS}$, where N is TBD multiplier

If $d\left(\bar{r}_{abs}^{COMP}, \bar{r}_{abs}^{GEONS}\right) \leq Commanded\ Threshold$, set the Mahalanobis measure test indicator to "true." If not set the indicator to "false."

i. Relative Mahalanobis Measure Test (not implemented in GEONS 3.0): The relative Mahalanobis measure threshold test is an optional test that can be performed if the relative comparison state and covariance are input for the satellite(s) being estimated. The test is performed as follows:

Compute the Mahalanobis measure from the relative position differences and the respective relative covariances:

$$d\left(\bar{r}_{rel}^{COMP}, \bar{r}_{rel}^{GEONS}\right) = \sqrt{\left(\bar{r}_{rel}^{COMP} - \bar{r}_{rel}^{GEONS}\right)^T S^{-1}\left(\bar{r}_{rel}^{COMP} - \bar{r}_{rel}^{GEONS}\right)} \qquad (2.3.3\text{-}3)^*$$

where

$\bar{r}_{rel}^{GEONS}$ = GEONS-computed relative position vector of the target satellite with respect to the local satellite, referenced to the central-body inertial frame

$\bar{r}_{rel}^{COMP}$ = comparison relative position vector of the target satellite with respect to the local satellite, referenced to the central-body inertial frame

$S = P_{rel}^{GEONS} + P_{rel}^{COMP}$ = Sum of the GEONS-computed relative position covariance matrix and externally-computed relative position covariance matrix of the target spacecraft with respect to the chaser satellite, referenced to the central-body inertial frame.

If $d\left(\bar{r}_{rel}^{COMP}, \bar{r}_{rel}^{GEONS}\right) \leq Commanded\ Threshold$, set the Mahalanobis measure test indicator to "true." If not set the indicator to "false."

2.3.4 GEONS Operational Modes

The GEONS modes and mode transitions are defined in this section.

The GEONS Navigation Modes are:

a. Initialize

b. Halted

c. Normal

The GEONS Navigation Mode transitions are shown in Figure 2-3. Each mode is discussed in the following subsections.

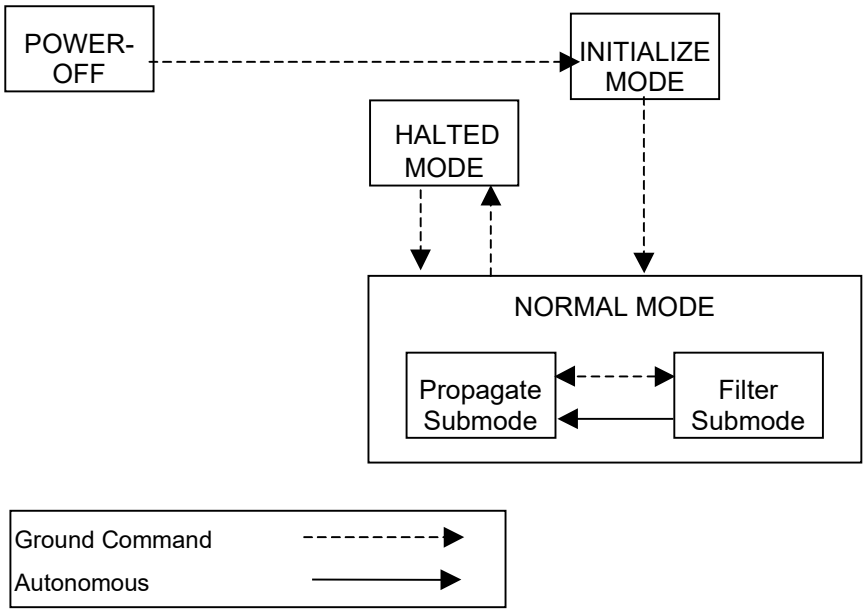

Figure 2-3. GEONS Mode State Transition Diagram

2.3.4.1 Initialize Mode

In Initialize Mode, the GEONS software processes are initialized from a power-off state and constants and initial values are loaded based on ground commands and/or the current receiver state solution.

2.3.4.2 Halted Mode

In Halted Mode, GEONS resets/reinitializes filter processing parameters (e.g., addition/deletion of solve-for parameters, change in atmospheric density) or state values (e.g., user state vector, covariance, process noise variances) based on ground commands and data values and/or the current receiver state solution.

2.3.4.3 Normal Mode

This section defines the execution sequence for major functions that can be executed in the Normal Mode.

Real-Time Prediction Processing

GEONS propagates the local and remote satellite position and velocity vectors obtained from the last available state estimate to the requested output time using a simplified real-time acceleration model.

Interface Processing

In Normal Mode, GEONS executes the following interface functions:

a. Process a GEONS command, when provided

b. Process receiver input data, when provided

c. Respond to telemetry data requests

State Estimation Processing

In Normal Mode, GEONS executes the following Propagate Submode or Filter Submode operations, depending upon the ground commanded GEONS Submode.

GEONS Propagate Submode

In the Propagate Submode, GEONS executes functions in the following sequence.

a. Determine if it is time to include measurements from selected measurement sources.

b. If it is time to include measurements from selected measurement sources, collect all valid measurements from all transmitters/sensors.

c. If the commanded maneuver time span falls within the propagation time span, update the spacecraft mass with the post-maneuver mass, and use the commanded maneuver noise variance to update the state covariance.

d. Propagate user state vector to measurement/intermediate request time, including externally-measured accelerations, if available.

e. Compute the state transition matrix.

f. Compute the process noise matrix.

g. Compute the diagonals of the process noise matrix corresponding to the measurement biases from the individual measurement sources, if measurement biases are to be included.

h. Propagate the covariance matrix.

i. For each measurement, compute the time and state of the transmitter/sensor, compute the predicted measurement, and perform the measurement editing tests.

j. Perform navigation fault detection checks

Filter Submode

In the Filter Submode, GEONS performs the same functions as for the Propagate function, except for step (i), which is replaced by:

i. For each measurement, compute the time and state of the transmitter, compute the predicted measurement, perform the measurement edit tests, and if the measurement edit tests are successful, update the user state vector with the measurement residual.

Backup Ephemeris Computation

The Backup Ephemeris Computation process is executed to compute averaged orbital elements and element rates using the real-time state vectors.

FCW Computation

The FCW Computation process is executed to compute the instantaneous Doppler shift and FCWs for a specific Ground Station using the real-time state vectors.

Maneuver Targeting

The Maneuver Targeting process is executed to compute initial and final maneuvers to transfer the satellite to a specified orbital position and velocity at a specified time and to perform these maneuvers at the specified time.

Initial State Vector Computation

The Initial State Vector Computation process is executed to compute an initial state vector based on nominal orbital elements using pseudorange and/or Doppler measurements.

2.4 Hierarchical Relative Navigation Capability (Future Release)

A number of distributed sparse aperture mission concepts (e.g. Stellar Imager, Solar Imaging Radio Array, various Terrestrial Planet Finder concepts) require dozens of spacecraft to precisely navigate in tightly controlled, close formations. Although GEONS can in principle simultaneously estimate several dozen-satellite states, the computational burden in terms of both memory and processing becomes excessive when the number of satellites becomes greater than about one dozen. This problem arises due to the high degree of correlation among formation flying satellite states when intersatellite crosslink measurements are processed. To properly model these correlations, an optimal navigation filter must maintain various data structures, such as a covariance matrix, that scale in size proportionally with the square of the number of satellites.

To reduce the computational burden for large formations, the following hierarchical nearest-neighbor algorithm provides the capability to estimate subclusters of satellites in a formation or constellation. In this case, the total set of N_s satellite state vectors to be estimated is divided into two or more independent segments with a maximum of $N_{\max}$ satellites each as follows.

The total estimation state vector with dimension $(n_s \times N_s + N_B + 1)$, where n_s is the size of each satellite/receiver's state vector, N_s is the number of satellite/receiver state vectors being estimated, and N_B is the number of measurement biases being estimated:

$$\overline{X} = \begin{bmatrix} \overline{X}^1 \\ \vdots \\ \overline{X}^{N_S} \\ \overline{B} \\ \gamma_I \end{bmatrix} \tag{2.4-1}$$

is divided into two or more independent segments of a maximum of $N_{\max}$ satellites each, with dimension $\leq (n_s \times N_{\max} + N_B + 1)$:

$$\overline{X}_n = \begin{bmatrix} \overline{X}_n^1 \\ \vdots \\ \overline{X}_n^{N_{\max}} \\ \overline{B} \\ \gamma_I \end{bmatrix}; n = 1,..,N \tag{2.4-2}$$

where $N = N_s / N_{\max}$ rounded up to an integer and the Nth segment can have smaller dimension than the others. The state vector segments are formed using the nominally closest $N_{\max}$ satellites. Each estimated satellite state vector $\overline{X}_n^i$ has the form defined in Equation (2.1-1b). The measurement bias vector $\overline{B}$ is defined in Equation (2.1-2b) and γ_I is the ionospheric delay scale factor. Note that $\overline{B}$ and γ_I are independently estimated in each partition.

Similarly the state transition, process noise, and covariance matrices are subdivided

$$\Phi_n(t_i,t_{i-1}) = \frac{\partial \overline{X}_n(t_i)}{\partial \overline{X}_n(t_{i-1})} = \begin{bmatrix} \frac{\partial \overline{X}_n^1(t_i)}{\partial \overline{X}_n^1(t_{i-1})} & \cdots & 0 & 0 & 0 \\ \vdots & \ddots & \vdots & \vdots & \vdots \\ 0 & \cdots & \frac{\partial \overline{X}_n^{N_{\max}}(t_i)}{\partial \overline{X}_n^{N_{\max}}(t_{i-1})} & 0 & 0 \\ 0 & \cdots & 0 & \frac{\partial \overline{B}(t_i)}{\partial \overline{B}(t_{i-1})} & 0 \\ 0 & \cdots & 0 & 0 & \frac{\partial \gamma_I(t_i)}{\partial \gamma_I(t_{i-1})} \end{bmatrix} \quad (2.4\text{-}3)^*$$

$$(Q_{i\text{-}1})_n = \begin{bmatrix} Q_{i\text{-}1}(\overline{X}_n^1) & \cdots & 0 & 0 & 0 \\ \vdots & \ddots & \vdots & \vdots & \vdots \\ 0 & \cdots & Q_{i\text{-}1}(\overline{X}_n^{N_{mas}}) & 0 & 0 \\ 0 & \cdots & 0 & Q_{i\text{-}1}(\overline{B}) & 0 \\ 0 & \cdots & 0 & 0 & Q_{i\text{-}1}(\gamma_I) \end{bmatrix} \quad (2.4\text{-}4)^*$$

$$[P_n] = [U_n][D_n][U_n]^T \quad (2.4\text{-}5)^*$$

Each covariance matrix partition is propagated and updated independent of the other partitions and each state vector segment is independently updated following the algorithm given in Section 2.3.2.2.

When crosslink measurements are processed as discussed in Section 5.5, the following procedure is used to calculate the position of the transmitting and receiving satellites:

1) If both the transmitting and receiving satellites are members of the same segment of the estimation state, e.g. $\overline{X}_n^i$ and $\overline{X}_n^j$, compute the crosslink range using the predicted states $\hat{\overline{X}}_n^i(-)$ and $\hat{\overline{X}}_n^j(-)$.

2) If the transmitting and receiving satellites are not members of the same segment of the estimation state, e.g. transmitting satellite state is $\overline{X}_m^i$ and receiving satellite state is $\overline{X}_n^j$, compute the crosslink range using the predicted state $\hat{\overline{X}}_n^j(-)$ for the receiving satellite state and compute the position of the transmitting satellite using a state vector that is either a) extracted from a ephemeris file (ground processing only) or b) propagated based on a periodically received state vector.

Section 3. Coordinate Systems, Transformations, and Time Systems

This section describes the coordinate systems, transformations, and time systems used in GEONS. It also contains the algorithm for the Greenwich hour angle calculation, which is used in the coordinate system transformations.

3.1 Coordinate Systems

Propagation of the satellite's state vector is performed using planet-centered rectangular coordinates and an acceleration vector referenced to a central-body-inertial (CBI) frame. The central body can be any planet, the Moon, or celestial object for which an ephemeris is available. The spacecraft acceleration due to a nonspherical gravitational field of a planet is computed using the satellite's planet-body fixed (PBF) coordinates and then transformed to the CBI frame. The propagated CBI state vector is transformed to the Earth-centered inertial (ECI) frame. Computation of the satellite's state transition matrix is performed using partial derivatives of the acceleration vector expressed in the ECI frame, which include the gravitational effects of other bodies. The tracking measurements are computed using state vectors referenced to the ECI frame. The GPS Space Vehicle (SV) positions and tracking station positions are expressed in Earth-centered Earth-fixed (ECEF) coordinates and must be transformed to the ECI frame. The radial (R), in-track (I), and cross-track (C) orbital frame coordinates are useful in expressing the position covariance and acceleration biases. These coordinate systems are defined in the following subsections. The required transformations are provided in Section 3.2.

3.1.1 Planet-Centered Inertial Systems

The CBI frames used in GEONS are obtained by translating the inertial frame used to develop the planetary ephemeris to the center of mass of the planet or Moon. Section 4.1.1 discusses the planetary ephemeris options that are available. For planetary ephemerides based on a series 400 Developmental Ephemeris, the CBI frames are obtained by translating from the International Celestial Reference Frame (ICRF). The ICRF is a realization of the International Celestial Reference System (ICRS), which was developed based on the recommendations of the International Astronomical Union (IAU). These recommendations stipulated that the origin of the ICRS is the solar system barycenter, the principal plane as close as possible to the Earth mean equator of J2000.0 and the origin of its principal plane as close as possible to the dynamical equinox of J2000.0. The ICRS is epoch-less with axis directions fixed with respect to the extragalactic radio sources. The ICRS, which officially replaced the IAU 1976 FK5 system definition on January 1, 1998, uses new precession-nutation models. Reference 49 provides a more complete discussion of the ICRF.

The equinox of the Earth's orbit is defined as the intersection of the plane of the Earth's equator and the plane of the ecliptic. The mean equator is the true equator with all nutation effects removed from the motion of the axis of rotation. The true Earth equator is defined as the plane normal to the Earth's instantaneous axis of rotation. The ecliptic plane is the Earth-Sun orbital plane.

The rectangular Cartesian coordinates (see Figure 3-1) associated with the ECI coordinate system are defined with respect to the following axes:

$\hat{X}_E$ axis = parallel to principal direction (dynamical equinox of J2000.0 in the IAU 1976 FK5 system; close to the dynamical equinox of J2000.0 in the ICRS)

$\hat{Y}_E$ axis = normal to the $\hat{X}_E$ and $\hat{Z}_E$ axes to form a right-hand system

$\hat{Z}_E$ axis = normal to the mean Earth's equator of J2000.0 in the direction of the Earth's mean spin axis in the IAU 1976 FK5 system; close to the mean equator of J2000.0 in the ICRS

The quantities $\overline{R}$, *X, Y,* and *Z* designate the position vector and Cartesian coordinates referenced to the inertial frame.

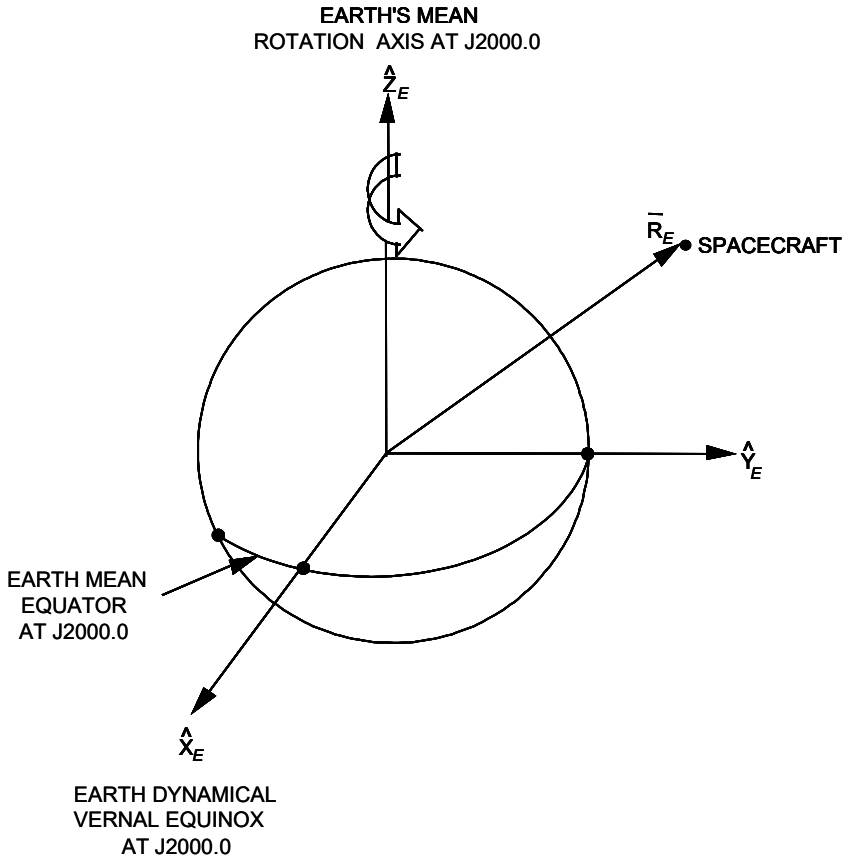

Figure 3-1. IAU 1976 FK5 ECI Coordinate System

3.1.2 Earth-Centered True Equator and Equinox of Date (TOD) Coordinate Systems

The Earth-centered true equator and equinox of date (TOD) system is defined as follows:

Origin:	Center of the Earth
Reference Time:	Reference Date
Reference Body:	Earth
Principal Plane:	True equator of the Earth, normal to the instantaneous Earth's rotation axis at the date
Principal Direction:	True vernal equinox of date

The TOD reference frame is defined with respect to the true equator and equinox at the time of computation, which differs from the mean of date reference system by the inclusion of the nutation of the true Earth spin axis about the mean pole. The true of date system is defined similarly to the mean of date system: a right-handed system with the $\hat{z}$ axis positive north and the $\hat{x}-\hat{y}$ plane defined as the true equatorial plane of date. The $\hat{x}$-axis direction is toward the true equinox of date. The quantities $\bar{r}$, x, y, and z designate the position vector and Cartesian coordinates referenced to the TOD frame.

The Earth's equator moves with time in response to perturbations exerted by the Sun, Moon, and planets. These motions explain the difference between the mean of date and true of date reference frames.

The motion of the equator consists of three elements: a smooth, long-term motion that carries the mean pole about the ecliptic pole at approximately 23.5 degrees; a short-period motion superimposed on the long-term motion; and the motion of the Earth's axis of figure with respect to the spin axis. The long-term motion is called the luni-solar precession and has a period of 26,000 years. The short-period motion is called nutation and is more irregular, with an amplitude of about 9 arc-seconds and a period of 18.6 years. The motion of the axis of figure is called polar motion and is considerably smaller and more irregular than the first two elements, but it should also be included for very-high-accuracy applications.

The motion of the ecliptic plane is a slow rotation, known as planetary precession. It carries the equinox, which is the intersection of the ecliptic plane and equator, eastward by approximately 12 arc-seconds per century. This also decreases the angle between the ecliptic and the equator, known as the obliquity of the ecliptic, by approximately 47 arc-seconds per century.

The long-period motions of the equator and equinox are considered together and are termed general precession. They are used to define the mean equator and equinox of a given date. The true equator and equinox of that date are determined by correcting the mean equator and equinox of date for the effects of nutation.

3.1.3 Earth-Centered Earth-Fixed (ECEF) Coordinate System

The ECEF/Geocentric Terrestrial Reference Frame (GTRF) is consistent with the International Terrestrial Reference Frame (ITRF) defined in Reference 49. The ECEF coordinate system is defined as follows:

Origin:	Center of mass of the Earth
Reference Time:	Reference Date
Reference Body:	Earth
Principal Plane:	Polar plane of the Earth, perpendicular to the adopted polar geographic axis (referred to as the International Reference Pole)
Principal Direction:	Intersection of the Greenwich meridian with the equator (referred to as the International Prime Meridian)

The Earth's axis of figure (i.e., principal moment of inertia) is not coincident with the Earth's instantaneous axis of rotation. It moves with respect to the latter, causing the polar motion effect. Therefore, the motion of the rotation axis pole is given with respect to the pole at some established epoch. The pole at the established epoch is referred to as the adopted geographic pole and corresponds to the Earth-fixed z axis, $\hat{z}_b$.

The Greenwich meridian is the plane containing the adopted polar axis that passes through the former Royal Observatory at Greenwich, England.

The rectangular Cartesian coordinates (see Figure 3-2) associated with the ECEF coordinate system are defined with respect to the following axes:

$\hat{x}_b$ axis = principal direction

$\hat{y}_b$ axis = normal to the $\hat{x}_b$ and $\hat{z}_b$ axes to form a right-hand system

$\hat{z}_b$ axis = axis along the vector passing through the adopted geographic pole

The quantities, $\bar{r}_b$, x_b, y_b and z_b designate the position vector and Cartesian coordinates referenced to the ECEF frame.

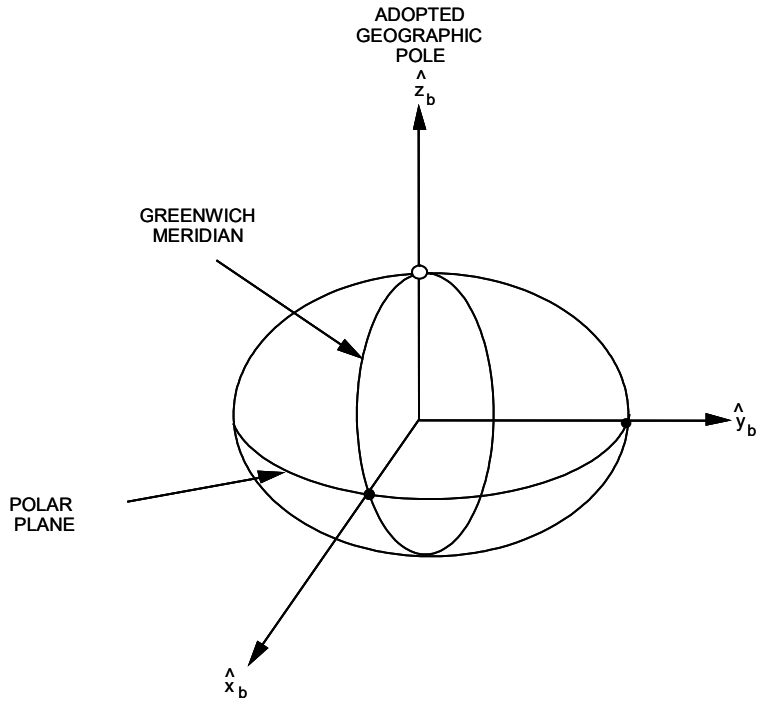

Figure 3-2. Earth-Centered Earth-Fixed Coordinate System

3.1.4 RIC Orbit Frame Coordinate System

The radial/in-track/cross-track (RIC) coordinate system is sometimes referred to as the orbit frame coordinate system. The RIC coordinate system is shown in Figure 3-3. Its origin and axes are defined as followed.

Origin:	Center of mass of the central body (Earth, Moon or planet)
Reference Time:	Reference Date
Reference Body:	Central body
Principal Plane:	Plane of the user spacecraft orbit
Principal Direction:	Radius vector from the origin to the user spacecraft

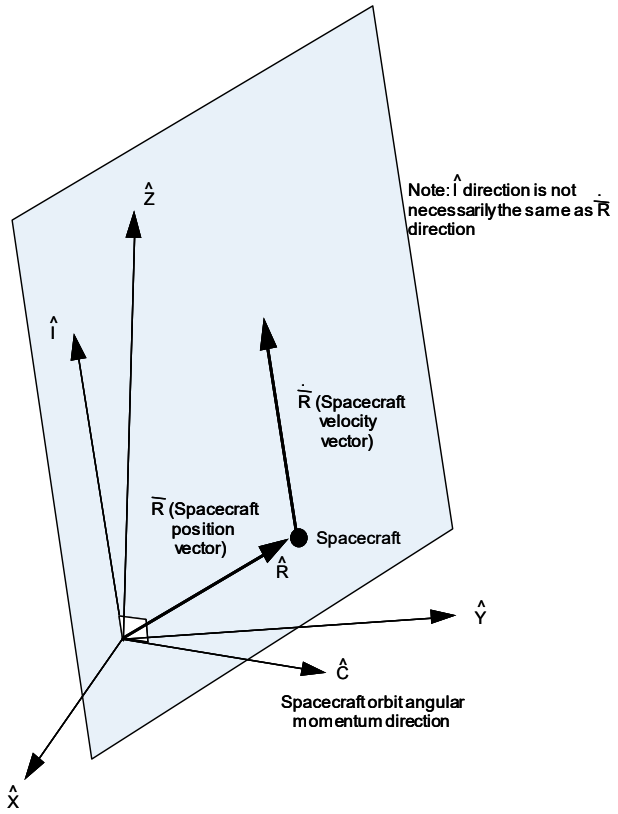

Figure 3-3. Radial/In-Track/Cross-Track (RIC) Orbit Frame Coordinate System

The rectangular coordinates for this system are the following;

$\hat{R}_C$ axis = (+) in direction from the center of the central body to the user spacecraft

$\hat{C}_C$ axis = (+) in direction of the orbital angular momentum vector

$\hat{I}_C$ axis = Completes the right-handed orthogonal coordinate system $\left(\hat{I} = \hat{C} \times \hat{R}\right)$, (+) direction has the same general sense as the velocity vector direction

Unit vectors defining the orientation of the RIC coordinate axes in the central-body J2000.0 coordinate system, a Cartesian XYZ coordinate system, are computed as follows:

$$\hat{R}_C = \frac{\overline{R}_C}{\left|\overline{R}_C\right|} \qquad (3.1\text{-}1)^*$$

$$\hat{C}_C = \frac{\overline{R}_C \times \dot{\overline{R}}_C}{\left|\overline{R}_C \times \dot{\overline{R}}_C\right|} \qquad (3.1\text{-}2)^*$$

$$\hat{I}_C = \hat{C}_C \times \hat{R}_C \qquad (3.1\text{-}3)^*$$

where

$\overline{R}_C = [XYZ]^T$ = spacecraft position vector in the central body frame (meters)

$\dot{\overline{R}}_C = [\dot{X}\dot{Y}\dot{Z}]^T$ = spacecraft velocity vector in the central body frame (meters/second)

$\hat{R}_C = [R_x R_y R_z]^T$ = radial unit vector in the central body coordinate frame (unitless)

$\hat{I}_C = [I_x I_y I_z]^T$ = in-track unit vector in the central body coordinate frame (unitless)

$\hat{C}_C = [C_x C_y C_z]^T$ = cross-track unit vector in the central body coordinate frame (unitless)

3.1.5 Rotating Libration Point Coordinate System (Future Release)

The rotating libration point (RLP) coordinate system is used for satellite orbits about to the Sun-Earth interior libration point, L_1. The L_1 point lies between the Sun and the Earth-Moon barycenter, approximately 1.5 x 10^6 kilometers (0.01 AU) from the Earth-Moon barycenter .

The RLP coordinate system is shown in Figure 3-4. Its origin and axes are defined as followed.

Origin:	L_1 libration point
Reference Time:	Reference Date
Reference Body:	L_1 libration point
Principal Plane:	Plane of the Earth-Moon barycenter's motion about the Sun
Principal Direction:	Vector from the Sun to the Earth-Moon barycenter

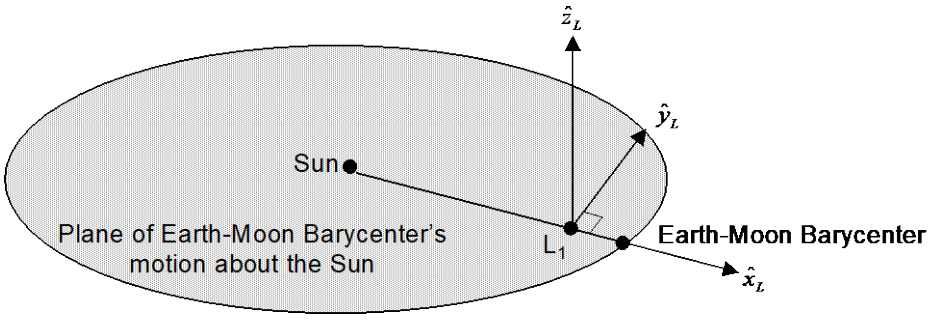

Figure 3-4. Rotating Libration Point Coordinate System

The rectangular coordinates for this system are defined with respect to the following axes:

$\hat{x}_L$ axis = principal direction

$\hat{y}_L$ axis = normal to the $\hat{x}_L$ and $\hat{z}_L$ axes to form a right-hand system

$\hat{z}_L$ axis = normal to plane containing the position and velocity vectors of the barycenter with respect to the Sun.

The quantities $\overline{R}_L$ and $\dot{\overline{R}}_L$ designate the satellite's position and velocity vectors in the RLP frame.

Unit vectors defining the orientation of the RLP coordinate axes in the Earth-centered inertial J2000.0 coordinate system are computed as follows:

$$\hat{x}_L = \frac{\overline{R}_B}{\left|\overline{R}_B\right|} \tag{3.1-4}*$$

$$\hat{z}_L = \frac{\overline{R}_B \times \dot{\overline{R}}_B}{\left|\overline{R}_B \times \dot{\overline{R}}_B\right|} \tag{3.1-5}*$$

$$\hat{y}_L = \hat{z}_L \times \hat{x}_L \tag{3.1-6}*$$

The inertial position and velocity of the Earth-Moon barycenter with respect to the Sun are given by

$$\overline{R}_B = \frac{\frac{m_E}{m_M}\overline{R}_E + \overline{R}_M}{\frac{m_E}{m_M} + 1} \tag{3.1-7}*$$

$$\dot{\overline{R}}_B = \frac{\frac{m_E}{m_M}\dot{\overline{R}}_E + \dot{\overline{R}}_M}{\frac{m_E}{m_M} + 1} \tag{3.1-8}*$$

where

$\overline{R}_E$ = inertial position vector of the Earth with respect to the Sun (meters)

$\dot{\overline{R}}_E$ = inertial velocity vector of the Earth with respect to the Sun (meters/second)

$\overline{R}_M$ = inertial position vector of the Moon with respect to the Sun (meters)

$\dot{\overline{R}}_M$ = inertial velocity vector of the Moon with respect to the Sun (meters/second)

m_E = mass of the Earth (5.9733328 x 10^{24} kilograms)

m_M = mass of the Moon (kilograms)

The rate of change of the libration coordinate axes is given by

$$\dot{\hat{x}}_L = \frac{\dot{\overline{R}}_B}{\left|\overline{R}_B\right|} - \frac{\overline{R}_B \bullet \dot{\overline{R}}_B}{\left|\overline{R}_B\right|^3}\overline{R}_B \tag{3.1-9}*$$

$$\dot{\hat{z}}_L = \frac{\overline{R}_B \times \overline{A}_B}{\left|\overline{R}_B \times \dot{\overline{R}}_B\right|} - \frac{\left[\left(\overline{R}_B \times \dot{\overline{R}}_B\right) \bullet \left(\overline{R}_B \times \overline{A}_B\right)\right]}{\left|\overline{R}_B \times \dot{\overline{R}}_B\right|^3} \overline{R}_B \times \dot{\overline{R}}_B \qquad (3.1\text{-}10)^*$$

$$\dot{\hat{y}}_L = \dot{\hat{z}}_L \times \hat{x}_L + \hat{z}_L \times \dot{\hat{x}}_L \qquad (3.1\text{-}11)^*$$

where

$$\overline{A}_B = -\mu_S \frac{\overline{R}_B}{\left|\overline{R}_B\right|^3} \qquad (3.1\text{-}12)^*$$

and μ_S is the gravitational constant of the Sun, 0.1327124×10^{21} meters^3/second^2.

3.1.6 Libration Point RIC Coordinate System (Future Release)

The libration-point-centered radial/in-track/cross-track (LRIC) coordinate system is shown in Figure 3-5. The origin and axes of the LRIC system are defined as followed.

Origin:	L_1 libration point
Reference Time:	Reference Date
Reference Body:	L_1 libration point
Principal Plane:	Plane of the user spacecraft orbit
Principal Direction:	Radius vector from the origin to the user spacecraft

The rectangular coordinates for this system are the following

$\hat{R}_L$ axis = (+) in direction from the libration point to the user spacecraft

$\hat{C}_L$ axis = (+) in direction of the orbital angular momentum vector

$\hat{I}_L$ axis = Completes the right-handed orthogonal coordinate system $\left(\hat{I}_L = \hat{C}_L \times \hat{R}_L\right)$, (+) direction has the same general sense as the velocity vector direction

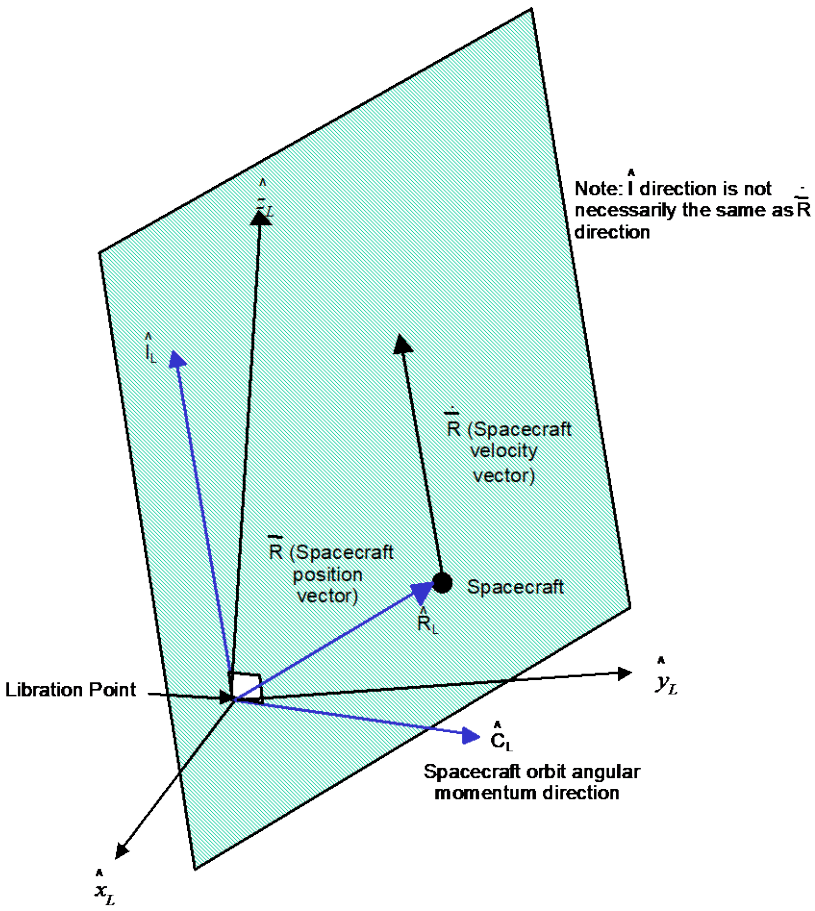

Figure 3-5. Libration-Point-Centered Radial/In-Track/Cross-Track (LRIC) Orbit Frame Coordinate System

Unit vectors defining the orientation of the LRIC coordinate axes in the RLP coordinate system defined in Section 3.1.5 are computed as follows:

$$\hat{R}_L = \frac{\overline{R}_L}{\left|\overline{R}_L\right|} \qquad (3.1\text{-}13)^*$$

$$\hat{C}_L = \frac{\overline{R}_L \times \dot{\overline{R}}_L}{\left|\overline{R}_L \times \dot{\overline{R}}_L\right|} \qquad (3.1\text{-}14)^*$$

$$\hat{I}_L = \hat{C}_L \times \hat{R}_L \qquad (3.1\text{-}15)^*$$

where

$\overline{R}_L$ = spacecraft position vector expressed in RLP coordinates (meters)

$\dot{\overline{R}}_L$ = spacecraft velocity vector expressed in RLP coordinates (meters/second)

$\hat{R}_L$ = radial unit vector in RLP coordinates (unitless)

$\hat{I}_L$ = in-track unit vector in RLP coordinates (unitless)

$\hat{C}_L$ = cross-track unit vector in RLP coordinates (unitless)

3.1.7 Lunar and Planet Body-Fixed Systems

The planet body-fixed frames are commonly defined using the IAU Cartographic Coordinates defined in Reference 48, which provide the orientation of the axis of rotation and location of the prime meridian with respect to the ICRF. The origin and axes of the IAU planet equator and prime meridian of date frame are defined as followed.

Origin: Center of mass of the planet

Reference Time: Reference Date

Reference Body: Planet

Principal Plane: Equator of the planet, perpendicular to the axis of rotation

Principal Direction: Intersection of the planetary prime meridian with the reference plane

The lunar principal axis coordinate frame is used to compute the spacecraft acceleration arising from the Moon's nonspherical gravitational potential. The associated coordinate axes are coincident with the principle axes of inertia of the Moon. The origin and axes of the lunar principle axis frame are defined as followed.

Origin: Center of mass of the Moon

Reference Time: Reference Date

Reference Body: Moon

Principal Plane: Equator of the Moon, perpendicular to the true axis of rotation

Principal Direction: Vector in the principal plane pointing to the 0 degree meridian

The rectangular coordinates for the lunar principal axis frame are the following

$\hat{x}_{LPA}$ axis = Unit vector along the principal direction

$\hat{y}_{LPA}$ axis = Unit vector in the equatorial plane of the Moon and normal to $\hat{x}_{LPA}$ and $\hat{z}_{LPA}$ such that $\hat{z}_{LPA} = \hat{x}_{LPA} \times \hat{y}_{LPA}$

$\hat{z}_{LPA}$ axis= Unit vector lying along the axis of rotation of the Moon

Note that the lunar principal axis frame is not the same as the IAU mean lunar pole frame that is commonly used in lunar geodesy. The IAU mean lunar pole frame uses the mean pole of rotation to define the principal plane and the mean axis of the Moon, which points to the center of the Earth, to define the principal direction.

3.1.8 VBN Coordinate System

The velocity/binormal/normal (VBN) coordinate system is defined as followed.

Origin:	Center of mass of the central body
Reference Time:	Reference Date
Reference Body:	Central Body
Principal Plane:	Plane of the user spacecraft orbit
Principal Direction:	Velocity vector of the user spacecraft

The rectangular coordinates for this system are the following;

$\hat{V}$ axis = (+) direction along the spacecraft velocity vector

$\hat{B}$ axis = Completes the right-handed orthogonal coordinate system $\left(\hat{B} = \hat{N} \times \hat{V}\right)$

$\hat{N}$ axis = (+) direction normal to the orbital plane (along the angular momentum vector)

Unit vectors defining the orientation of the VBN coordinate axes in the central body inertial J2000.0 coordinate system are computed as follows:

$$\hat{V}_C = \frac{\dot{\overline{R}}_C}{\left|\dot{\overline{R}}_C\right|} \tag{3.1-16}*$$

$$\hat{N}_C = \frac{\overline{R}_C \times \dot{\overline{R}}_C}{\left|\overline{R}_C \times \dot{\overline{R}}_C\right|} \tag{3.1-17}*$$

$$\hat{B}_C = \hat{N}_C \times \hat{V}_C \tag{3.1-18}*$$

where

$\overline{R}_C = \left[XYZ\right]^T$ = spacecraft position vector in the central body inertial frame (meters)

$\dot{\overline{R}}_C = \left[\dot{X}\dot{Y}\dot{Z}\right]^T$ = spacecraft velocity vector in the central body inertial frame (meters/second)

$\hat{V}_C = \left[V_x \; V_y \; V_z\right]^T$ = velocity unit vector in the central body inertial frame (unitless)

$\hat{B}_C = \left[B_x \; B_y \; B_z\right]^T$ = binormal unit vector in the central body inertial frame (unitless)

$\hat{N}_C = \left[N_x \; N_y \; N_z\right]^T$ = normal unit vector in the central body inertial frame (unitless)

3.2 Coordinate Transformations

GEONS supports two implementations of the ECI to ECEF coordinate transformation: the original IAU-76/FK5-based approach and the newer International Astronomical Union (IAU)-2000 Celestial Intermediate Origin (CIO) based approach. The IAU-76/FK5 transformation consists of three separate transformations, which are defined in Sections 3.2.1 through 3.2.3. The first relates the mean of J2000.0 frame to the mean of date (MOD) frame using the IAU 1976 Precession Model. The second relates the MOD frame to the true of date (TOD) frame using the IAU 1980 Theory of Nutation. The third relates the TOD frame to the ECEF frame. Sections 3.2.4 and 3.2.5 provide transformations associated with vectors and covariances expressed in radial, intrack, and crosstrack (RIC) coordinates. Sections 3.2.6 and 3.2.7 provide transformations associated with vectors expressed in a rotating libration point frame. Section 3.2.8 provides transformations associated with antenna offsets expressed in the spacecraft body frame. Section 3.2.9 discusses the coordinate transformation from the ECI to the lunar principal axis frame. Section 3.2.10 provides the transformation from the VBN to the central-body inertial frame. Sections 3.2.11 and 3.2.12 provide the transformations from the ECI to the CBI frame and the CBI to the PBF frames, respectively. Section 3.2.13 provides the transformation from the Ecliptic to the Mean of J2000 frame. Section 3.2.14 discusses calculation of the J2 mean semimajor axis error. Section 3.2.15 discusses the IAU-2000 CIO-based transformation from the ECI/ GCRF to the ECEF/ITRF using IAU-2000 precession/nutation models.

3.2.1 IAU-76/FK5 ECI Mean-of-J2000.0-to-Mean-of-Date Coordinate Transformation

The coordinate rotation between the IAU-76/FK5 mean equator and equinox of J2000.0 reference frame and other mean equator and equinox of date reference frames is a special case of the transformation between two mean equator and equinox of date coordinate systems. The Julian epoch J2000.0 is specifically defined to be the Julian epoch date of January 1.5, 2000, Julian date 2451545.0 barycentric dynamical time (TDB) [also known as ephemeris time (ET)].

The transformation of a fixed vector from one coordinate system to an alternate coordinate system can be accomplished by performing a series of frame rotations in succession. If a rotation matrix about a Cartesian $\hat{X}$ axis is denoted as *Q(a)*, a rotation matrix about a Cartesian $\hat{Y}$ axis is denoted as *P(a)*, and a rotation matrix about a Cartesian $\hat{Z}$ axis is denoted as *R(a)*, then as functions of the rotation angle, *a*, the elements of the rotation matrices are

$$Q(a) = \begin{bmatrix} 1 & 0 & 0 \\ 0 & \cos a & \sin a \\ 0 & -\sin a & \cos a \end{bmatrix} \tag{3.2-1}$$

$$P(a) = \begin{bmatrix} \cos a & 0 & -\sin a \\ 0 & 1 & 0 \\ \sin a & 0 & \cos a \end{bmatrix} \tag{3.2-2}$$

$$R(a) = \begin{bmatrix} \cos a & \sin a & 0 \\ -\sin a & \cos a & 0 \\ 0 & 0 & 1 \end{bmatrix} \tag{3.2-3}$$

The transformation matrix for processing from the mean equator and equinox of date for the reference epoch of J2000.0 to the mean equator and equinox of date for epoch E_2 is given by

$$A = R\left(-\frac{\pi}{2} - Z_A\right) Q(\theta_A)\, R\left(\frac{\pi}{2} - \varsigma_A\right) \tag{3.2-4}$$

where

$\frac{\pi}{2} - \varsigma_A$ = angle measured on the equator of the reference epoch of J2000.0 from the X axis to the intersection of the two equatorial planes

θ_A = angle of inclination of the equator at E_2 measured from the equator at J2000.0

$\frac{\pi}{2} + Z_A$ = angle measured on the equator of date, E_2, from the X_2 axis to the intersection of the two equatorial planes

The angles of the transformation are illustrated in Figure 3-6.

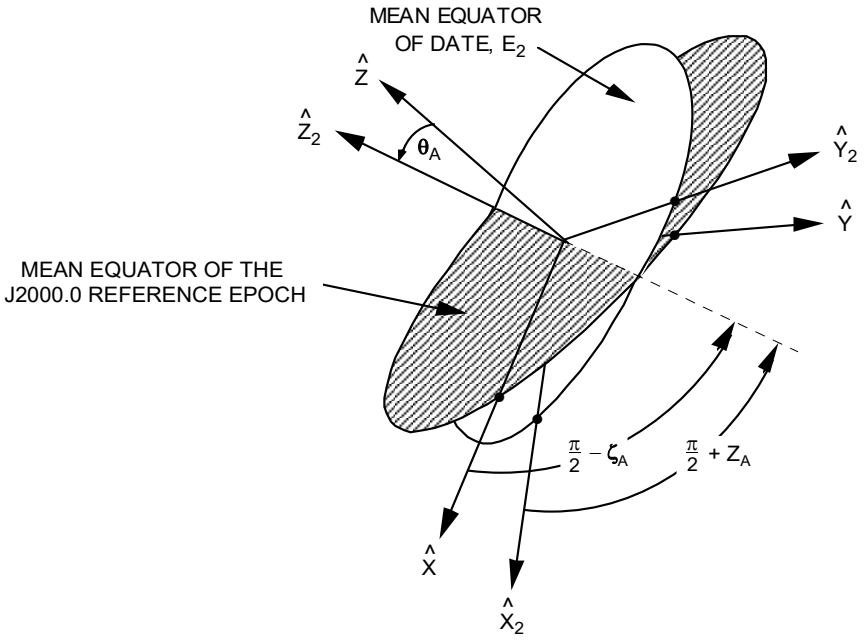

Figure 3-6. Precession Angles

This matrix is equivalent to

$$A = R(-Z_A)\, P(\theta_A)\, R(-\varsigma_A) \tag{3.2-5}*$$

Denoting the position vector expressed in mean equator and equinox of J2000.0 by $\overline{R}$ and the position vector expressed in mean equator and equinox of epoch E_2 by $\overline{R}_2$, the relationship can be expressed by

$$\overline{R}_2 = A\ \overline{R} \tag{3.2-6}*$$

The time derivative of A can be assumed to be small enough to ignore its effects on the transformation of the velocity, so that

$$\dot{\overline{R}}_2 = A\ \dot{\overline{R}} \tag{3.2-7}*$$

where $\dot{\overline{R}}_2$ is the time derivative of $\overline{R}_2$ and $\dot{\overline{R}}$ is the derivative of $\overline{R}$.

Due to the orthogonality of the transformation matrix, the precession transformation matrix from E_2 to J2000.0 is the transpose of A, so that

$$\overline{R} = A^T \overline{R}_2 \tag{3.2-8}*$$

and

$$\dot{\overline{R}} = A^T \dot{\overline{R}}_2 \tag{3.2-9}*$$

where A^T is the transpose of A.

The equations for ζ_A, θ_A, and Z_A in units of arcseconds are based on the IAU 1976 Precession Model

$$\varsigma_A = 2306.''2181\ T + 0.''30188\ T^2 + 0.''017998\ T^3 \tag{3.2-10}$$

$$\theta_A = 2004.''3109\ T - 0.''42665\ T^2 - 0.''041833\ T^3 \tag{3.2-11}$$

$$Z_A = 2306.''2181\ T + 1.''09468\ T^2 + 0.''018203\ T^3 \tag{3.2-12}$$

where

T = time interval in Julian centuries of 36525 days between the Julian date of epoch of J2000.0 and the Julian date for the epoch E_2, given by

$$T = \frac{E_2 - 2451545.0}{36525.0} \tag{3.2-13}*$$

The time interval T is defined in Julian centuries of TDB. The difference between TDB and Terrestrial Time (TT) is ignored in this calculation. Equation (3.2-13) is evaluated using TT computed using Equation (3.3-30).

3.2.2 Earth Mean-of-Date-to-True-of-Date Coordinate Transformation

The true Earth equator and equinox of date coordinate system is the Earth mean equator and equinox of date system corrected for nutation. Nutation is measured as cyclic changes in the obliquity of the ecliptic and the longitude of the equinox.

The rotation matrix from the mean equator and equinox of date system to the true equator and equinox of date system is given by

$$N = Q(-\varepsilon_t)\, R(-\delta\psi)\, Q(\varepsilon_m) \qquad (3.2\text{-}14)^*$$

where

ε_m = mean obliquity of the ecliptic, the angle from the mean equator to the true ecliptic plane

$\delta\psi$ = nutation in longitude

$\varepsilon_t = \varepsilon_m + \delta\varepsilon$ = true obliquity of the ecliptic, the angle from the true equator to the true ecliptic, where $\delta\varepsilon$ is the nutation in obliquity

These angles are illustrated in Figure 3-7. The Q and R matrices are defined in Section 3.2.1.

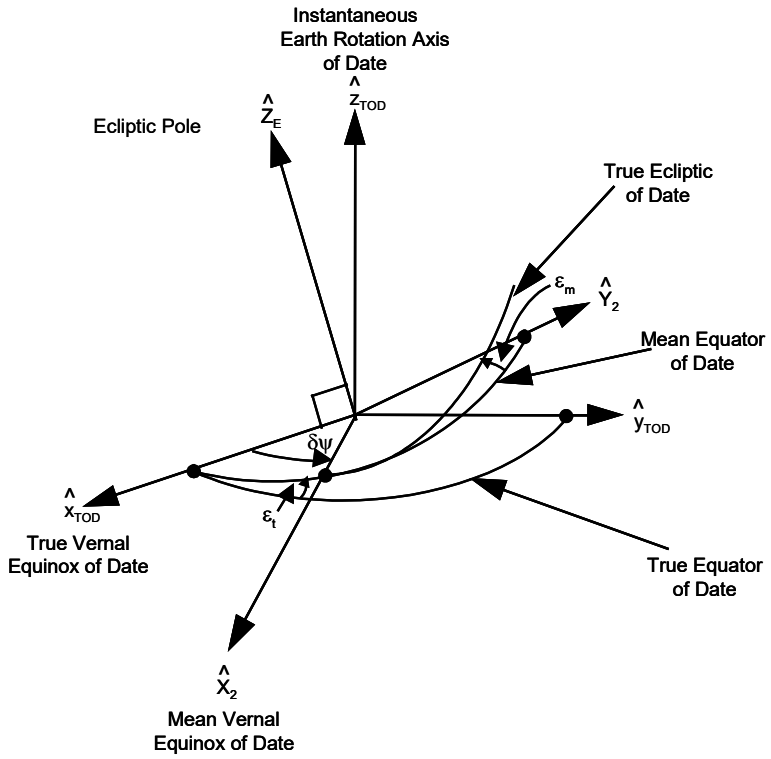

Figure 3-7. Nutation Angles

The transformation of position vectors from the mean of date system to the true of date system is then

$$\bar{r} = N\,\overline{R}_2 \qquad (3.2\text{-}15)^*$$

where

$\bar{r}$ = position vector in the true of date frame

$\overline{R}_2$ = position vector in the mean of date frame

The transformation for velocity vectors is also given by

$$\dot{\bar{r}} = N\,\dot{\overline{R}}_2 \qquad (3.2\text{-}16)^*$$

because the derivative of N is assumed to be negligible.

The mean obliquity and nutation angles are computed using the IAU 1980 Theory of Nutation (Reference 50). In the J2000.0 system, the mean obliquity in degrees is given by

$$\varepsilon_m = 23.43929111 - 0.01300417T - 0.1639(10^{-6})T^2 + 0.5036(10^{-6})T^3 \qquad (3.2\text{-}17)^*$$

The third-order term in the series for the mean obliquity is on the order of 10^{-9} for epochs near J2000.0 and therefore is currently not included in GEONS. In Equation 3.2-17), T = time interval in Julian centuries of 36525 days TBD between the Julian date E_2 and Julian date of epoch J2000.0, given by

$$T = \frac{E_2 - 2451545.0}{36525.0} \qquad (3.2\text{-}18)^*$$

Three options are available in GEONS for computing the values of the nutation in longitude, $\delta\psi$, and obliquity, $\delta\varepsilon$: (1) evaluating the full 106 term series based on the IAU 1980 Theory of Nutation, (2) evaluating the IAU 1980 Theory of Nutation series truncated to 35 terms (all terms for which both nutation in longitude and obliquity coefficients are less than 0.001 arcsec are excluded), and (3) evaluating the Chebyshev polynomial fits to the full 106 term series based on the IAU 1980 Theory of Nutation available from DE files.

The difference between TDB and Terrestrial Time (TT) is ignored in GEONS when the IAU 1980 Theory of Nutation is used and Equation (3.2-18) is evaluated using TT computed using Equation (3.3-30). When the nutation angles are computed by evaluating Chebyshev polynomial in the DE files, T can be evaluated using either TT or optionally TBD.

3.2.2.1 Nutation Computation Using IAU 1980 Theory of Nutation

The equations for the two series are

$$\delta\psi = \sum_{i=1}^{106}\left[\sin\left(a_{1i}\ell + a_{2i}\ell' + a_{3i}F + a_{4i}D + a_{5i}\Omega\right)\left(b_{1i} + b_{2i}T\right)\right] \qquad (3.2\text{-}19)^*$$

and

$$\delta\varepsilon = \sum_{i=1}^{106} \left[\cos\left(a_{1i}\ell + a_{2i}\ell' + a_{3i}F + a_{4i}D + a_{5i}\Omega\right)\left(c_{1i} + c_{2i}T\right)\right] \qquad (3.2\text{-}20)^*$$

where

a_{ji} = coefficients of the five fundamental arguments for the i^{th} term in the series

b_{1i} = coefficient for the nonsecular component of the i^{th} term in the longitude series

b_{2i} = coefficient for the secular component of the i^{th} term in the longitude series

c_{1i} = coefficient for the nonsecular component of the i^{th} term in the obliquity series

c_{2i} = coefficient for the secular component of the i^{th} term in the obliquity series

The quantities ℓ, ℓ', F, D, and Ω are the fundamental arguments and are defined as

ℓ = lunar mean anomaly (arcseconds)

ℓ' = mean anomaly of the Sun's (Earth's) orbit (arcseconds)

F = difference between the mean longitude of the Moon and Ω (mean longitude $-\Omega$) (arcseconds)

D = mean elongation of the Moon from the Sun (arcseconds)

Ω = longitude of the ascending node of the Moon's mean orbit on the ecliptic (arcseconds)

and are given by

$$\ell = 485866.733 + 1717915922.633\ T + 31.310\ T^2 + 0.064T^3 \qquad (3.2\text{-}21)^*$$

$$\ell' = 1287099.804 + 129596581.224\ T - 0.577\ T^2 - 0.012T^3 \qquad (3.2\text{-}22)^*$$

$$F = 335778.877 + 1739527263.137\ T - 13.257\ T^2 + 0.011T^3 \qquad (3.2\text{-}23)^*$$

$$D = 1072261.307 + 1602961601.328\ T - 6.891\ T^2 + 0.019T^3 \qquad (3.2\text{-}24)^*$$

$$\Omega = 450160.280 - 6962890.539\ T + 7.455\ T^2 + 0.008T^3 \qquad (3.2\text{-}25)^*$$

The third-order terms, involving T^3, in the above equations are very small and can be ignored for epochs near J2000.0. The full series for each computation has 106 trigonometric terms. The coefficients for the full series are given in Table 3-1a.

Table 3-1a. Coefficients for the Series for Nutation in Longitude $\delta\Psi$ ***and Obliquity*** $\delta\varepsilon$***, With T Measured in Julian Centuries From Epoch J2000.0***

ARGUMENT						LONGITUDE (0".0001)		OBLIQUITY (0".0001)	
i	ℓ a_{1i}	ℓ' a_{2i}	F a_{3i}	D a_{4i}	Ω a_{5i}	b_{1i}	b_{2i}	c_{1i}	c_{2i}
1	0	0	0	0	1	-171996.0	-174.2	92025.0	8.9
2	0	0	0	0	2	2062.0	0.2	-895.0	0.5
3	-2	0	2	0	1	46.0	0.0	-24.0	0.0
4	2	0	-2	0	0	11.0	0.0	0.0	0.0
5	-2	0	2	0	2	-3.0	0.0	1.0	0.0
6	1	-1	0	-1	0	-3.0	0.0	0.0	0.0
7	0	-2	2	-2	1	-2.0	0.0	1.0	0.0
8	2	0	-2	0	1	1.0	0.0	0.0	0.0
9	0	0	2	-2	2	-13187.0	-1.6	5736.0	-3.1
10	0	1	0	0	0	1426.0	-3.4	54.0	-0.1
11	0	1	2	-2	2	-517.0	1.2	224.0	-0.6

ARGUMENT						LONGITUDE (0''.0001)		OBLIQUITY (0''.0001)	
i	ℓ a_{1i}	ℓ' a_{2i}	F a_{3i}	D a_{4i}	Ω a_{5i}	b_{1i}	b_{2i}	c_{1i}	c_{2i}
12	0	-1	2	-2	2	217.0	-0.5	-95.0	0.3
13	0	0	2	-2	1	129.0	0.1	-70.0	0.0
14	2	0	0	-2	0	48.0	0.0	1.0	0.0
15	0	0	2	-2	0	-22.0	0.0	0.0	0.0
16	0	2	0	0	0	17.0	-0.1	0.0	0.0
17	0	1	0	0	1	-15.0	0.0	9.0	0.0
18	0	2	2	-2	2	-16.0	0.1	7.0	0.0
19	0	-1	0	0	1	-12.0	0.0	6.0	0.0
20	-2	0	0	2	1	-6.0	0.0	3.0	0.0
21	0	-1	2	-2	1	-5.0	0.0	3.0	0.0
22	2	0	0	-2	1	4.0	0.0	-2.0	0.0
23	0	1	2	-2	1	4.0	0.0	-2.0	0.0
24	1	0	0	-1	0	-4.0	0.0	0.0	0.0
25	2	1	0	-2	0	1.0	0.0	0.0	0.0
26	0	0	-2	2	1	1.0	0.0	0.0	0.0
27	0	1	-2	2	0	-1.0	0.0	0.0	0.0
28	0	1	0	0	2	1.0	0.0	0.0	0.0
29	-1	0	0	1	1	1.0	0.0	0.0	0.0
30	0	1	2	-2	0	-1.0	0.0	0.0	0.0
31	0	0	2	0	2	-2274.0	-0.2	977.0	-0.5
32	1	0	0	0	0	712.0	0.1	-7.0	0.0
33	0	0	2	0	1	-386.0	-0.4	200.0	0.0
34	1	0	2	0	2	-301.0	0.0	129.0	-0.1
35	1	0	0	-2	0	-158.0	0.0	-1.0	0.0
36	-1	0	2	0	2	123.0	0.0	-53.0	0.0
37	0	0	0	2	0	63.0	0.0	-2.0	0.0
38	1	0	0	0	1	63.0	0.1	-33.0	0.0
39	-1	0	0	0	1	-58.0	-0.1	32.0	0.0
40	-1	0	2	2	2	-59.0	0.0	26.0	0.0
41	1	0	2	0	1	-51.0	0.0	27.0	0.0
42	0	0	2	2	2	-38.0	0.0	16.0	0.0
43	2	0	0	0	0	29.0	0.0	-1.0	0.0
44	1	0	2	-2	2	29.0	0.0	-12.0	0.0
45	2	0	2	0	2	-31.0	0.0	13.0	0.0
46	0	0	2	0	0	26.0	0.0	-1.0	0.0
47	-1	0	2	0	1	21.0	0.0	-10.0	0.0
48	-1	0	0	2	1	16.0	0.0	-8.0	0.0
49	1	0	0	-2	1	-13.0	0.0	7.0	0.0
50	-1	0	2	2	1	-10.0	0.0	5.0	0.0
51	1	1	0	-2	0	-7.0	0.0	0.0	0.0
52	0	1	2	0	2	7.0	0.0	-3.0	0.0
53	0	-1	2	0	2	-7.0	0.0	3.0	0.0
54	1	0	2	2	2	-8.0	0.0	3.0	0.0
55	1	0	0	2	0	6.0	0.0	0.0	0.0
56	2	0	2	-2	2	6.0	0.0	-3.0	0.0
57	0	0	0	2	1	-6.0	0.0	3.0	0.0
58	0	0	2	2	1	-7.0	0.0	3.0	0.0
59	1	0	2	-2	1	6.0	0.0	-3.0	0.0
60	0	0	0	-2	1	-5.0	0.0	3.0	0.0
61	1	-1	0	0	0	5.0	0.0	0.0	0.0
62	2	0	2	0	1	-5.0	0.0	3.0	0.0
63	0	1	0	-2	0	-4.0	0.0	0.0	0.0
64	1	0	-2	0	0	4.0	0.0	0.0	0.0
65	0	0	0	1	0	-4.0	0.0	0.0	0.0
66	1	1	0	0	0	-3.0	0.0	0.0	0.0
67	1	0	2	0	0	3.0	0.0	0.0	0.0
68	1	-1	2	0	2	-3.0	0.0	1.0	0.0
69	-1	-1	2	2	2	-3.0	0.0	1.0	0.0
70	-2	0	0	0	1	-2.0	0.0	1.0	0.0
71	3	0	2	0	2	-3.0	0.0	1.0	0.0
72	0	-1	2	2	2	-3.0	0.0	1.0	0.0
73	1	1	2	0	2	2.0	0.0	-1.0	0.0
74	-1	0	2	-2	1	-2.0	0.0	1.0	0.0

ARGUMENT						LONGITUDE (0''.0001)		OBLIQUITY (0''.0001)	
i	ℓ a_{1i}	ℓ' a_{2i}	F a_{3i}	D a_{4i}	Ω a_{5i}	b_{1i}	b_{2i}	c_{1i}	c_{2i}
75	2	0	0	0	1	2.0	0.0	-1.0	0.0
76	1	0	0	0	2	-2.0	0.0	1.0	0.0
77	3	0	0	0	0	2.0	0.0	0.0	0.0
78	0	0	2	1	2	2.0	0.0	-1.0	0.0
79	-1	0	0	0	2	1.0	0.0	-1.0	0.0
80	1	0	0	-4	0	-1.0	0.0	0.0	0.0
81	-2	0	2	2	2	1.0	0.0	-1.0	0.0
82	-1	0	2	4	2	-2.0	0.0	1.0	0.0
83	2	0	0	-4	0	-1.0	0.0	0.0	0.0
84	1	1	2	-2	2	1.0	0.0	-1.0	0.0
85	1	0	2	2	1	-1.0	0.0	1.0	0.0
86	-2	0	2	4	2	-1.0	0.0	1.0	0.0
87	-1	0	4	0	2	1.0	0.0	0.0	0.0
88	1	-1	0	-2	0	1.0	0.0	0.0	0.0
89	2	0	2	-2	1	1.0	0.1	-1.0	0.0
90	2	0	2	2	2	-1.0	0.0	0.0	0.0
91	1	0	0	2	1	-1.0	0.0	0.0	0.0
92	0	0	4	-2	2	1.0	0.0	0.0	0.0
93	3	0	2	-2	2	1.0	0.0	0.0	0.0
94	1	0	2	-2	0	-1.0	0.0	0.0	0.0
95	0	1	2	0	0	1.0	0.0	0.0	0.0
96	-1	-1	0	2	1	1.0	0.0	0.0	0.0
97	0	0	-2	0	1	-1.0	0.0	0.0	0.0
98	0	0	2	-1	1	-1.0	0.0	0.0	0.0
99	0	1	0	2	2	-1.0	0.0	0.0	0.0
101	1	0	-2	-2	0	-1.0	0.0	0.0	0.0
102	0	-1	2	0	1	-1.0	0.0	0.0	0.0
103	1	1	0	-2	1	-1.0	0.0	0.0	0.0
104	1	0	-2	2	0	-1.0	0.1	0.0	0.0
105	2	0	0	2	0	1.0	0.0	0.0	0.0
106	0	0	2	4	2	-1.0	0.0	0.0	0.0

To reduce computation, the GEONS software can optionally compute the nutation series excluding those nonsecular or secular terms for which both nutation and obliquity coefficients are less than 0.001 arc-second. Table 3-1b lists only those coefficients included in the truncated series.

Table 3-1b. Coefficients for the Truncated Series for Nutation in Longitude $\delta\Psi$ and Obliquity $\delta\varepsilon$, With T Measured in Julian Centuries From Epoch J2000.0

ARGUMENT						PERIOD (DAYS)	LONGITUDE (0".0001)		OBLIQUITY (0".0001)	
i	ℓ a_{1i}	ℓ' a_{2i}	F a_{3i}	D a_{4i}	Ω a_{5i}		b_{1i}	b_{2i}	c_{1i}	c_{2i}
1	0	0	0	0	1	6798.4	-171996	-174.2	92025	8.9
2	0	0	0	0	2	3399.2	2062		-895	
3	-2	0	2	0	1	1305.5	46		-24	
4	2	0	-2	0	0	1095.2	11		0	
9	0	0	2	-2	2	182.6	-13187		5736	
10	0	1	0	0	0	365.3	1426		54	
11	0	1	2	-2	2	121.7	-517		224	
12	0	-1	2	-2	2	365.2	217		-95	
13	0	0	2	-2	1	177.8	129		-70	
14	2	0	0	-2	0	205.9	48		1	
15	0	0	2	-2	0	173.3	-22		0	
16	0	2	0	0	0	182.6	17		0	
17	0	1	0	0	1	386.0	-15		9	
18	0	2	2	-2	2	91.3	-16		7	
19	0	-1	0	0	1	346.6	-12		6	
31	0	0	2	0	2	13.7	-2274		977	
32	1	0	0	0	0	27.6	712		-7	
33	0	0	2	0	1	13.6	-386		200	
34	1	0	2	0	2	9.1	-301		129	
35	1	0	0	-2	0	31.8	-158		-1	
36	-1	0	2	0	2	27.1	123		-53	
37	0	0	0	2	0	14.8	63		-2	
38	1	0	0	0	1	27.7	63		-33	
39	-1	0	0	0	1	27.4	-58		32	
40	-1	0	2	2	2	9.6	-59		26	
41	1	0	2	0	1	9.1	-51		27	
42	0	0	2	2	2	7.1	-38		16	
43	2	0	0	0	0	13.8	29		-1	
44	1	0	2	-2	2	23.9	29		-12	
45	2	0	2	0	2	6.9	-31		13	
46	0	0	2	0	0	13.6	26		-1	
47	-1	0	2	0	1	27.0	21		-10	
48	-1	0	0	2	1	32.0	16		-8	
49	1	0	0	-2	1	31.7	-13		7	
50	-1	0	2	2	1	9.5	-10		5	

Comparisons were made between the nutation matrices computed from the full series and the truncated series and were tabulated from the Astronomical Almanac (Reference 8) at several dates. Elements of the nutation matrix computed using the full series agreed with the Astronomical Almanac values to the eight published digits for all cases. The largest difference between an element of the full series matrix and the corresponding element of the truncated series matrix was less than 2×10^{-8}. It may be possible to make further reductions for cases in which only times within 10 years of J2000.0 are considered; however, this reduction would require further analysis.

3.2.2.2 Nutation Calculation Using Chebyshev Series Representation

The DE files provide Chebyshev coefficients for the nutation in longitude and obliquity referenced to TT, which have been computed based on the full 1980 Theory of Nutation. These coefficients can optionally be used in GEONS to compute the nutation terms using the following formulas:

Each nutation angle $(\delta\psi, \delta\varepsilon)$ is computed as follows:

$$x(t_{TT}) = \sum_{n=0}^{N} c_n T_n(\tau) \qquad \text{(3.2-25a)*}$$

where t_{TT} is the request time in TT (computed using Equations 4.1-28b and 4.1-28c), c_n are the associated Chebyshev coefficients, $T_n(\tau)$ are the Chebyshev polynomials, and N is the degree of the expansion. The Chebyshev polynomials are computed using the following recursion formula:

$$T_n(\tau) = 2\tau T_{n-1}(\tau) - T_{n-2}(\tau), \quad n = 2,3,... \qquad \text{(3.2-25b)*}$$

where $T_0(\tau) = 1$ and $T_1(\tau) = \tau$.

The applicable range of interpolation for the Chebyshev time parameter τ is $-1 \le \tau \le 1$, which is computed as follows:

$$\tau = \frac{2\Delta t_{TT}}{\Delta T_C} - 1 \qquad \text{(3.2-25c)*}$$

where $\Delta t_{TT} = t_{TT} - T_C^{Start}$ is the elapsed time from the start time of the polynomial fit interval, T_C^{Start}, and ΔT_C is the length associated Chebyshev polynomial fit interval. The fit interval is 32 days for the nutation angles.

3.2.2.3 Earth-Mean-of-J2000.0 to True-of-Date Transformation Matrix

The transformation matrix from the mean equator of J2000.0 to the true equator of date is computed by multiplying the two transformation matrices, *A* and *N*, so that

$$C = N\,A \qquad \text{(3.2-26)*}$$

where *A* is the precession matrix from the reference epoch, J2000.0, as defined in Section 3.2.1.

The transformation of position vectors from the mean equator of J2000.0 to the true equator of date is then

$$\bar{r} = C\,\overline{R} \qquad \text{(3.2-27)}$$

where $\bar{r}$ is a position vector in the true of date frame and $\overline{R}$ is a position vector in the mean of J2000.0 frame. The transformation of velocity vectors is also given by

$$\dot{\bar{r}} = C\,\dot{\overline{R}} \qquad \text{(3.2-28)}$$

because the derivative of *C* is assumed to be negligible.

Because both the *A* and *N* matrices are orthogonal, their product is orthogonal. The transformation matrix from true of date to mean of J2000.0 is then given by C^T

$$\overline{R} = C^T \bar{r} \qquad \text{(3.2-29)}$$

$$\dot{\bar{R}} = C^T \dot{\bar{r}} \tag{3.2-30}$$

3.2.3 Earth True-of-Date-to-ECEF Coordinate Transformation

The transformation that relates the TOD coordinates to the ECEF coordinates accounts for two separate effects. The first relates the true vernal equinox to the prime meridian of the rotating Earth by means of the angle a_g, the true of date right ascension of Greenwich. The second effect, called polar motion, accounts for the fact that the pole of the ECEF body-fixed axis does not coincide with the Earth's spin axis. The first of these effects, which transforms the TOD coordinates to pseudo-body-fixed coordinates, is defined in Section 3.2.3.1. Polar motion is not required for Doppler measurement processing but should be included to process the pseudorange measurements. The transformation from pseudo-body-fixed coordinates to ECEF coordinates is defined in Section 3.2.3.2.

3.2.3.1 True-of-Date-to-Pseudo-Body-Fixed Coordinate Transformation

The transformation from true of date coordinates to ECEF coordinates uncorrected for polar motion (also referred to as pseudo-body-fixed coordinates) is

$$\bar{r}_P = R\left(a_g\right)\bar{r} = R_g\,\bar{r} \tag{3.2-31}*$$

where

R = $\hat{Z}$ axis rotation matrix defined in Section 3.2.1

$\bar{r}$ = true equator and equinox of date position vector

$\bar{r}_P$ = pseudo-body-fixed position vector

a_g = TOD right ascension of the Greenwich prime meridian, which is equal in value to the Greenwich hour angle

The transformation of a velocity vector is

$$\dot{\bar{r}}_P = \frac{d}{dt}\left[R\left(a_g\right)\right]\bar{r} + R\left(a_g\right)\dot{\bar{r}} \tag{3.2-32}*$$

where

$$\frac{d}{dt}\left[R\left(a_g\right)\right] = \begin{bmatrix} -\omega_e \sin\left(a_g\right) & \omega_e \cos\left(a_g\right) & 0 \\ -\omega_e \cos\left(a_g\right) & -\omega_e \sin\left(a_g\right) & 0 \\ 0 & 0 & 0 \end{bmatrix} \tag{3.2-33}*$$

and

$\bar{r}$ = true equator and equinox of date position vector

$\dot{\bar{r}}$ = true equator and equinox of date velocity vector

$\dot{\bar{r}}_P$ = pseudo-body-fixed velocity vector

ω_e = Earth rotation rate equal to 7.2921158553 x 10^{-5} radians per second

Correction for polar motion converts the pseudo-body-fixed coordinates to body-fixed coordinates, $\bar{r}_b$. If the polar motion effects are ignored, then $\bar{r}_b = \bar{r}_P$ and $\dot{\bar{r}}_b = \dot{\bar{r}}_P$.

Because the *R* matrix is orthogonal, the transformation from the pseudo-body-fixed coordinate system to true equator and equinox of date coordinates is

$$\bar{r} = R^T\left(a_g\right)\bar{r}_p \tag{3.2-34}$$

$$\dot{\bar{r}} = R^T\left(a_g\right)\left(\dot{\bar{r}}_P - \frac{\mathrm{d}}{\mathrm{d}t}\left[R\left(a_g\right)\right]\bar{r}\right) \tag{3.2-35}$$

where $R^T(a_g)$ is the transpose of the $R(a_g)$ matrix.

The true of date right ascension of the Greenwich prime meridian, a_g, is measured easterly from the true vernal equinox to the Greenwich meridian along the equator. A related quantity is the Greenwich hour angle (GHA), also called the true Greenwich sidereal time, which measures the angular distance of the true vernal equinox west along the equator from the Greenwich meridian. The GHA and a_g are equal in value, and both increase as the Earth rotates.

The GHA is computed from the Greenwich mean sidereal time (a_{GM}) and a correction due to nutation in longitude and obliquity, known as the equation of equinoxes.

The Greenwich mean sidereal time, a_{GM}, is defined as the right ascension of the fictitious mean Sun minus 12 hours plus the time of day in UT1 (universal time, corrected to remove polar motion effects). The Greenwich mean sidereal time at 0h 0min 0s UT1 is expressed in units of radians, following the expression presented in Reference 50

$$a_{GM} = \begin{matrix}[24110.54841^s + 8640184.812866\, T_{UT1} \\ +0.093104\, T_{UT1}^2 - 6.2\times 10^{-6} T_{UT1}^3]\frac{2\pi}{86400}\end{matrix} \tag{3.2-36}*$$

where

T_{UT1}= number of Julian centuries elapsed from epoch J2000.0 UT1 to the JD at 0h 0min 0s UT1 = (JD_{UT1} – 2451545.0)/36525, where JD is the integer part of the Julian date for 0h 0min 0s UT1 on the date of interest

The superscript *s* indicates seconds. The algorithm for converting from UTC to UT1 time is provided in Section 3.3.

The elapsed UT1 time on the day of interest is added in as follows:

$$a_{GM}(t) = a_{GM} + \omega_e(t - t_{ref})$$

where

a_{GM} = mean Greenwich sidereal time computed using Equation (3.2-36) at 0h 0min 0s UT1 of the day of interest

ω_e = rotation rate of the Earth

t_{ref} = 0h 0min 0s UT1 of the day of interest

The true Greenwich sidereal time is computed by applying the correction, δH , from the nutation in longitude and obliquity to the $a_{GM}(t)$, as

$$GHA = a_g = a_{GM}(t) + \delta H \quad (3.2\text{-}37)^*$$

where

$$\delta H = \delta\psi \cos(\varepsilon_m) + f(0.00264 \sin\Omega + 0.000063 \sin 2\Omega) \quad (3.2\text{-}38)^*$$

The computation of the mean obliquity, ε_m , is defined in Equation 3.2-17. The computation of the nutation in longitude, $\delta\psi$, is discussed in Section 3.2.2.1, as part of the transformation to the true of date coordinate frame. The function f(x) converts arcseconds to radians and Ω is the longitude of the ascending node of the Moon's mean orbit on the ecliptic as defined for nutation in Section 3.2.2.1.

(*Equation deleted)* (3.2-39)

3.2.3.2 Earth Pseudo-Body-Fixed-to-ECEF Coordinate Transformation

The polar motion correction takes into account the fact that the Earth's principal moment of inertia is not coincident with the Earth's rotation axis. The coordinates of the Celestial Ephemeris Pole (which differs from the Earth's instantaneous rotation axis by quasi-diurnal terms with amplitudes under 0.01 arcseconds) are measured relative to the International Reference Pole in terms of its x_p and y_p components in the polar plane, which is perpendicular to the z body-fixed axis. The z body-fixed axis is coincident with the rotation axis at an established epoch referred to as the adopted reference pole, called the International Reference Pole. The coordinates x_p and y_p are periodically measured by the International Earth Rotation Service (IERS) and supplied to users daily via the IERS website (http://www.iers.org). The IERS polar motion coordinates describe the instantaneous rotation axis of the ITRF with respect to the ICRF, when used with the conventional 1976 Precession Model and 1980 Nutation Theory.

The instantaneous coordinates of the pole in arc-seconds, x_p and y_p, are obtained by evaluating the following trigonometric function for the date of interest:

$$x_p = a_1 + a_2 \cos A + a_3 \sin A + a_4 \cos C + a_5 \sin C \text{ (arc-seconds)} \quad (3.2\text{-}40)^*$$

$$y_p = a_6 + a_7 \cos A + a_8 \sin A + a_9 \cos C + a_{10} \sin C \text{ (arc-seconds)} \quad (3.2\text{-}41)^*$$

where the coefficients a_i are determined in the USNO polar motion prediction published in the IERS Bulletin-A. The angles A and C are computed as follows:

$$A = \frac{2\pi}{365.25}\left(MJD - T_p\right) \text{ (radians)} \quad (3.2\text{-}42)^*$$

$$C = \frac{2\pi}{435}\left(MJD - T_p\right) \quad \text{(radians)} \quad (3.2\text{-}43)^*$$

where *MJD* is the modified Julian date of the request time and T_p is the epoch time of the prediction, also published in IERS Bulletin-A. The *MJD* is computed as follows:

$$MJD = JD - 2400000.5 \text{ days} \qquad (3.2\text{-}44)^*$$

where *JD* is the Julian date of the request time computed using Equation (4.1-11). The estimated accuracies of these predictions are 0.002 arc-second and 0.005 arc-second for the 10- and 40-day predictions, respectively. The 10 a_i coefficients and the epoch time of the prediction will be uplinked to the spacecraft monthly.

When the GPS-ICE Earth Orientation Parameters (EOP) messages are available from the GPS Broadcast Message, x_p and y_p are computed as follows:

$$\begin{aligned} x_p &= PM\_X + PM\_\dot{X}(t - t_{EOP}) \\ y_p &= PM\_Y + PM\_\dot{Y}(t - t_{EOP)}) \end{aligned} \qquad (3.2\_44b)$$

The coefficients *PM_X, PM_Y*, $PM\_\dot{X}$ and $PM\_\dot{Y}$ are provided as part of the GPS Broadcast message type 32 (see Table 3-2). Section 30.3.3.5 in Reference 10 provides a detailed discussion of the EOP.

Table 3-2. GPS Earth Orientation Parameters

Parameter	Units	Description
t_{EOP}	Second	EOP Data Reference Time in seconds from the start of the GPS week
PM_X	Arcseconds	X-Axis Polar Motion Value at Reference Time
$PM\_\dot{X}$	Arcseconds/ day	X-Axis Polar Motion Drift at Reference Time
PM_Y	Arcseconds	Y-Axis Polar Motion Value at Reference Time
$PM\_\dot{Y}$	Arcseconds/ day	Y-Axis Polar Motion Drift at Reference Time
$\Delta UT1$	Seconds	UT1-GPS Difference at Reference Time
$\Delta\dot{UT}1$	Seconds/day	Rate of UT1-GPS Difference at Reference Time

Alternatively, when TDRSS Augmentation Service for Satellites (TASS) messages are available, the current Earth Orientation Parameters, x_p and y_p, can be obtained directly from the values in these messages.

The additional transformation from the pseudo-body-fixed coordinates defined in Equations (3.2-31) and (3.2-32) to the body-fixed ECEF frame is as follows:

$$\bar{r}_{EF} = B\left(x'_p, y'_p\right)\bar{r}_p \tag{3.2-45}*$$

$$\dot{\bar{r}}_{EF} = B\left(x'_p, y'_p\right)\dot{\bar{r}}_p \tag{3.2-46}*$$

where

$$B\left(x'_p, y'_p\right) = \begin{bmatrix} 1 & 0 & x'_p \\ 0 & 1 & -y'_p \\ -x'_p & y'_p & 1 \end{bmatrix} \tag{3.2-47}*$$

and x'_p and y'_p are the pole coordinates expressed in radians, where 1 arc-second = $0.4848136811095 \times 10^{-5}$ radians.

In summary, the coordinate transformation from the mean equator and equinox of J2000.0 to ECEF is given by

$$\bar{r}_{ECEF} = B\,R_g\,C\,\bar{R}_{J2000} \tag{3.2-48a}*$$

$$\dot{\bar{r}}_{ECEF} = B\left(\frac{d}{dt}\left[R(a_g)\right]\right)C\bar{R}_{J2000} + BR_gC\dot{\bar{R}}_{J2000} \tag{3.2-48b}*$$

The coordinate transformation from ECEF to the mean equator and equinox of J2000.0 is given by

$$\bar{R}_{J2000} = C^T\ R_g^T\ B^T\bar{r}_{ECEF} \tag{3.2-49a}*$$

$$\dot{\bar{R}}_{J2000} = C^T\left(\frac{d}{dt}\left[R(a_g)\right]\right)^T B^T\bar{r}_{ECEF} + C^T R_g^T B^T\dot{\bar{r}}_{ECEF} \tag{3.2-49b}*$$

3.2.4 Central-Body Inertial-to-RIC Coordinate Transformation

The matrix that transforms a vector in the central-body inertial frame to the RIC frame is formed using RIC unit vectors expressed in the central body inertial frame defined in Equations 3.1-1 through 3.1-3:

$$\left[T_{RIC\leftarrow XYZ}\right]_C = \begin{bmatrix} \hat{R}_C\cdot\hat{X}_C & \hat{R}_C\cdot\hat{Y}_C & \hat{R}_C\cdot\hat{Z}_C \\ \hat{I}_C\cdot\hat{X}_C & \hat{I}_C\cdot\hat{Y}_C & \hat{I}_C\cdot\hat{Z}_C \\ \hat{C}_C\cdot\hat{X}_C & \hat{C}_C\cdot\hat{Y}_C & \hat{C}_C\cdot\hat{Z}_C \end{bmatrix} \tag{3.2-50}*$$

A vector expressed in the central-body mean of J2000.0 frame is transformed to RIC coordinates with respect to the central-body frame as follows

$$\begin{bmatrix} R_C \\ I_C \\ C_C \end{bmatrix} = \left[T_{RIC \leftarrow XYZ}\right]_C \begin{bmatrix} X_C \\ Y_C \\ Z_C \end{bmatrix} \tag{3.2-51}*$$

A vector in RIC coordinates is transformed to mean of J2000.0 coordinates with respect to the central-body frame as follows

$$\begin{bmatrix} X_C \\ Y_C \\ Z_C \end{bmatrix} = \left[T_{RIC \leftarrow XYZ}\right]_C^T \begin{bmatrix} R_C \\ I_C \\ C_C \end{bmatrix} \tag{3.2-52}*$$

3.2.5 Central-Body Inertial to RIC Covariance Transformation

A [6 × 6] position and velocity covariance matrix [*P*] in RIC coordinates with respect to the central-body frame is transformed into central-body mean of J2000.0 coordinates as shown below:

$$\left[P\right]_{XYZ_C} = \begin{bmatrix} \left[T_{RIC \leftarrow XYZ}\right]_C & 0_{3\times3} \\ 0_{3\times3} & \left[T_{RIC \leftarrow XYZ}\right]_C \end{bmatrix}^T \left[P\right]_{RIC_C} \begin{bmatrix} \left[T_{RIC \leftarrow XYZ}\right]_C & 0_{3\times3} \\ 0_{3\times3} & \left[T_{RIC \leftarrow XYZ}\right]_C \end{bmatrix} \tag{3.2-53}*$$

This transformation is used when transforming the initial RIC state error covariance matrix into Mean of J2000.0 XYZ coordinates and when transforming the RIC state noise covariance matrix into Mean of J2000.0 XYZ coordinates.

A [6 × 6] position and velocity covariance matrix [*P*] in XYZ coordinates is transformed into RIC coordinates as shown below:

$$\left[P\right]_{RIC_C} = \begin{bmatrix} \left[T_{RIC \leftarrow XYZ}\right]_C & 0_{3\times3} \\ 0_{3\times3} & \left[T_{RIC \leftarrow XYZ}\right]_C \end{bmatrix} \left[P\right]_{XYZ_C} \begin{bmatrix} \left[T_{RIC \leftarrow XYZ}\right]_C & 0_{3\times3} \\ 0_{3\times3} & \left[T_{RIC \leftarrow XYZ}\right]_C \end{bmatrix}^T \tag{3.2-54}*$$

This transformation is used when transforming the state error covariance matrix into RIC coordinates.

3.2.6 Inertial Cartesian to Rotating Libration Point Coordinate Transformation

(Future Release)

The transformation of the satellite position and velocity vectors expressed in the inertial mean of J2000.0 frame, $\overline{R}$ and $\dot{\overline{R}}$, to the rotating libration point (RLP) frame defined in Section 3.1.5, $\overline{R}_L$ and $\dot{\overline{R}}_L$, is computed as follows:

$$\begin{bmatrix} \overline{R}_L \\ \dot{\overline{R}}_L \end{bmatrix} = \begin{bmatrix} T_{RLP \leftarrow XYZ} & 0_{3\times3} \\ \dot{T}_{RLP \leftarrow XYZ} & T_{RLP \leftarrow XYZ} \end{bmatrix} \begin{bmatrix} \overline{R} \\ \dot{\overline{R}} \end{bmatrix} \tag{3.2-55}*$$

where

$$\left[T_{RLP\leftarrow XYZ}\right]=\begin{bmatrix}\hat{x}_{Lx} & \hat{x}_{Ly} & \hat{x}_{Lz}\\ \hat{y}_{Lx} & \hat{y}_{Ly} & \hat{y}_{Lz}\\ \hat{z}_{Lx} & \hat{z}_{Ly} & \hat{z}_{Lz}\end{bmatrix} \tag{3.2-56}*$$

$$\left[\dot{T}_{RLP\leftarrow XYZ}\right]=\begin{bmatrix}\dot{\hat{x}}_{Lx} & \dot{\hat{x}}_{Ly} & \dot{\hat{x}}_{Lz}\\ \dot{\hat{y}}_{Lx} & \dot{\hat{y}}_{Ly} & \dot{\hat{y}}_{Lz}\\ \dot{\hat{z}}_{Lx} & \dot{\hat{z}}_{Ly} & \dot{\hat{z}}_{Lz}\end{bmatrix} \tag{3.2-57}*$$

The inertial coordinates of the RLP unit vectors $\hat{x}_L$, $\hat{y}_L$, and $\hat{z}_L$ are defined in Equations 3.1-4 through 3.1-6. The rates of change of the inertial coordinates of the RLP unit vectors $\dot{\hat{x}}_L$, $\dot{\hat{y}}_L$, and $\dot{\hat{z}}_L$ are defined in Equations 3.1-9 through 3.1-11.

3.2.7 Rotating Libration Point to Libration-Point-RIC Coordinate Transformation

(Future Release)

The LRIC unit vectors defined in Section 3.1.6 can be formed into a matrix that transforms RLP coordinates into LRIC coordinates:

$$\left[T_{LRIC\leftarrow RLP}\right]=\begin{bmatrix}\hat{R}_{Lx} & \hat{R}_{Ly} & \hat{R}_{Lz}\\ \hat{I}_{Lx} & \hat{I}_{Ly} & \hat{I}_{Lz}\\ \hat{C}_{Lx} & \hat{C}_{Ly} & \hat{C}_{Lz}\end{bmatrix} \tag{3.2-58}*$$

A vector in RLP coordinates, such as a line-of-sight position vector from the libration point to the user satellite, is transformed into LRIC coordinates as follows

$$\begin{bmatrix}R_L\\ I_L\\ C_L\end{bmatrix}=\left[T_{LRIC\leftarrow RLP}\right]\begin{bmatrix}x_L\\ y_L\\ z_L\end{bmatrix} \tag{3.2-59}*$$

A vector in LRIC coordinates, such as a thrust acceleration vector, is transformed into RLP coordinates as

$$\begin{bmatrix}x_L\\ y_L\\ z_L\end{bmatrix}=\left[T_{LRIC\leftarrow RLP}\right]^T\begin{bmatrix}R_L\\ I_L\\ C_L\end{bmatrix} \tag{3.2-60}*$$

3.2.8 Spacecraft Antenna Offset Transformations

This section provides transformations that are used to transform antenna offset vectors expressed in a spacecraft body-fixed frame to an offset vector in the inertial frame.

The position and velocity of antenna *m* on spacecraft *n* are computed as follows in terms of constant antenna offsets expressed in the spacecraft body frame $\left[\left(\Delta x^n_{A_m}\right)_B, \left(\Delta y^n_{A_m}\right)_B, \left(\Delta z^n_{A_m}\right)_B\right]$:

$$\begin{aligned}
\overline{R}_{A_m}{}^n(t^n_R) &= \overline{R}^n(t^n_R) + T^n_{XYZ\leftarrow B}\begin{bmatrix}\left(\Delta x^n_{A_m}\right)_B\\ \left(\Delta y^n_{A_m}\right)_B\\ \left(\Delta z^n_{A_m}\right)_B\end{bmatrix}\\
\dot{\overline{R}}_{A_m}{}^n(t^n_R) &= \dot{\overline{R}}^n(t^n_R) + \dot{T}^n_{XYZ\leftarrow B}\begin{bmatrix}\left(\Delta x^n_{A_m}\right)_B\\ \left(\Delta y^n_{A_m}\right)_B\\ \left(\Delta z^n_{A_m}\right)_B\end{bmatrix}
\end{aligned} \qquad \text{(3.2-61)*}$$

where $\overline{R}(t_R)$ and $\dot{\overline{R}}(t_R)$ are the position and velocity of the spacecraft center of mass and $T^n_{XYZ\leftarrow B}$ and $\dot{T}^n_{XYZ\leftarrow B}$ are the transformation matrix from the local body frame to the J2000.0 inertial frame and its time derivative, respectively.

Sections 3.2.8.1 and 3.2.8.2 define the transformation matrices $T^n_{XYZ\leftarrow B}$ used for 3-axis stabilized spacecraft and spin-stabilized spacecraft, respectively.

3.2.8.1 Three-Axis Stabilized Spacecraft

For a three-axis stabilized spacecraft, the transformation matrix $T^n_{XYZ\leftarrow B}$ is equal to the transpose of the attitude matrix $A(t)$, which maps vectors from the J2000.0 inertial frame to the satellite body frame.

$$\begin{aligned}
T^n_{XYZ\leftarrow B} &= A^T(t)\\
\dot{T}^n_{XYZ\leftarrow B} &\cong 0
\end{aligned} \qquad \text{(3.2-62)*}$$

At time t, the attitude matrix is given by

$$A(t) = \begin{bmatrix}
\cos\psi\cos\phi - \sin\psi\cos\theta\sin\phi & \cos\psi\sin\phi + \sin\psi\cos\theta\cos\phi & \sin\psi\sin\theta\\
-\sin\psi\cos\phi - \cos\psi\cos\theta\sin\phi & -\sin\psi\sin\phi + \cos\psi\cos\theta\sin\phi & \cos\psi\sin\theta\\
\sin\theta\sin\phi & -\sin\theta\cos\phi & \cos\theta
\end{bmatrix} \qquad \text{(3.2-63)}$$

where

ϕ, θ, ψ = satellite body yaw, pitch, and roll angles at time t with respect to the inertial frame, corresponding to a 3-1-3 sequence of Euler angle rotations

or equivalently

$$A(t) = \begin{bmatrix}
q_1^2 - q_2^2 - q_3^2 + q_4^2 & 2(q_1q_2 + q_3q_4) & 2(q_1q_3 - q_2q_4)\\
2(q_1q_2 - q_3q_4) & -q_1^2 + q_2^2 - q_3^2 + q_4^2 & 2(q_2q_3 + q_1q_4)\\
2(q_1q_3 + q_2q_4) & 2(q_2q_3 - q_1q_4) & -q_1^2 - q_2^2 + q_3^2 + q_4^2
\end{bmatrix} \qquad \text{(3.2-64)*}$$

where

q_1, q_2, q_3, q_4 = quaternion elements or Euler symmetric parameters defining the orientation of the satellite body at time t with respect to the inertial frame

The capability is available in GEONS to input an attitude history file that contains the values of the quaternion elements at specific times. Operationally, this attitude information could be provided by an onboard attitude estimator operating in parallel with the GEONS orbit estimator or by an advanced star tracking system that provides the attitude quaternion directly.

Definitions of the spacecraft body frames are spacecraft specific; however, the target attitude frame is often defined with the z_B – axis along the radial or anti-radial direction, the x_B – axis along the in-track or anti-in-track direction, and y_B – axis along the cross-track or anti-cross-track direction. For the case of a nadir-pointing spacecraft rotating at 1 revolution per orbit with negligible attitude control errors, the transformation matrix $T^n_{XYZ\leftarrow B}$ in Equation (3.2-61) is equivalent to the matrix $[T_{RIC\leftarrow XYZ}]^T$, defined in Section 3.2-50, which maps a vector in the RIC frame to the inertial frame. If the antenna offsets are expressed in terms of RIC components in the central body frame, Equation (3.2-61) reduces to

$$\overline{R}_{A_m}{}^n(t^n_R) = \overline{R}^n(t^n_R) + [T^n_{RIC\leftarrow XYZ}]_C{}^T \begin{bmatrix} \Delta R^n_{A_m} \\ \Delta I^n_{A_m} \\ \Delta C^n_{A_m} \end{bmatrix} \tag{3.2-65}*$$

3.2.8.2 Spin-Stabilized Spacecraft

For spin-stabilized spacecraft, $T^n_{XYZ\leftarrow B}$ is the transformation matrix from the rotating local body frame to the J2000.0 inertial frame. Figure 3-8 illustrates this rotating body frame. The satellite spins at a rate ω_B about the spacecraft spin axis, nominally parallel to the geometric axis of the satellite. The rotating body frame is centered at the spacecraft center of mass with the z_B axis along the spin axis direction and the x_B and y_B axes in the plane perpendicular to the spin axis. The location of the x_B and y_B axes is satellite specific; one axis is usually chosen to be aligned with a specific hardware element such as a solar panel or a sensor. The phase angle ϕ_B defines the instantaneous location of the x_B axis relative to a body-centered non-rotating frame.

The orientation of the spin-axis with respect to the geocentric inertial J2000 frame is expressed as follows:

$$\hat{A} = \begin{bmatrix} \cos\alpha_B \ \cos\delta_B \\ \sin\alpha_B \ \cos\delta_B \\ \sin\delta_B \end{bmatrix} \tag{3.2-66}$$

where

$\hat{A}$ = unit vector along the spacecraft spin axis

α_B = the right ascension of the spin axis

δ_B = declination of the spin axis

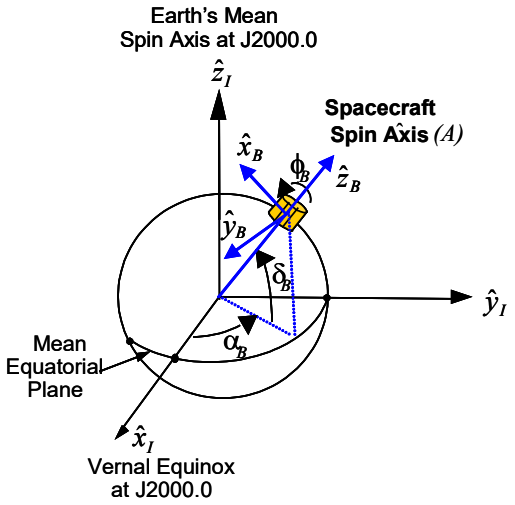

Figure 3-8. Definition of Rotating Body Frame

The transformation matrix $T^n_{XYZ\leftarrow B}$ from a vector expressed in this rotating body-fixed frame to a vector expressed in the inertial frame can be written in terms of three rotations:

$$T^n_{XYZ\leftarrow B} = \left[R_3(\phi_B) R_2(\frac{\pi}{2} - \delta_B) R_3(\alpha_B) \right]^T$$

$$= \begin{bmatrix} \cos\phi_B \sin\delta_B \cos\alpha_B - \sin\phi_B \sin\alpha_B & -\sin\phi_B \sin\delta_B \cos\alpha_B - \cos\phi_B \sin\alpha_B & \cos\delta_B \cos\alpha_B \\ \cos\phi_B \sin\delta_B \sin\alpha_B + \sin\phi_B \cos\alpha_B & -\sin\phi_B \sin\delta_B \sin\alpha_B + \sin\phi_B \cos\alpha_B & \cos\delta_B \sin\alpha_B \\ -\cos\phi_B \cos\delta_B & \sin\phi_B \cos\delta_B & \sin\delta_B \end{bmatrix} \quad (3.2\text{-}67)^*$$

$$= \begin{bmatrix} \hat{x}_B \cdot \hat{x}_I & \hat{y}_B \cdot \hat{x}_I & \hat{z}_B \cdot \hat{x}_I \\ \hat{x}_B \cdot \hat{y}_I & \hat{y}_B \cdot \hat{y}_I & \hat{z}_B \cdot \hat{y}_I \\ \hat{x}_B \cdot \hat{z}_I & \hat{y}_B \cdot \hat{z}_I & \hat{z}_B \cdot \hat{z}_I \end{bmatrix}$$

$$\dot{T}^n_{XYZ\leftarrow B} = \omega_B \begin{bmatrix} -\sin\phi_B \sin\delta_B \cos\alpha_B - \cos\phi_B \sin\alpha_B & -\cos\phi_B \sin\delta_B \cos\alpha_B + \sin\phi_B \sin\alpha_B & 0 \\ -\sin\phi_B \sin\delta_B \sin\alpha_B + \cos\phi_B \cos\alpha_B & -\cos\phi_B \sin\delta_B \sin\alpha_B + \cos\phi_B \cos\alpha_B & 0 \\ \sin\phi_B \cos\delta_B & \cos\phi_B \cos\delta_B & 0 \end{bmatrix} \quad (3.2\text{-}68)^*$$

The capability is available in GEONS to input an attitude history file that contains the values of the right ascension and declination of the spin axis with respect to the inertial reference frame, the rotation rate, and the phase at specific times. The value of the phase at any time is computed as follows based on the most recent input values for ϕ_B and ω_B:

$$\phi_B(t^n_k) = \mathrm{mod}\left[\phi_B(t^n_{last}) + \omega_B(t^n_k - t^n_{last}), 2\pi\right] \quad (3.2\text{-}69)^*$$

3.2.9 ECI to Lunar Principal Axis Frame Coordinate Transformation

The Lunar Principal Axis (LPA) (also referred to as selenographic) coordinate frame is used to define positions on the Lunar surface and to compute the spacecraft acceleration arising from the Moon's nonspherical gravitational potential. The coordinate axes are the principal axes of inertia of the Moon, defined in Section 3.1.7. The orientation of the lunar principal axes with respect to the mean of J2000 frame is given by three Euler angles: (1) the rotation by angle φ about the Z-axis from the vernal equinox (X-axis of J2000.0 frame) to the intersection of the ascending node of the lunar equator, (2) the tilt up about the X-axis by θ to match the lunar equator, and (3) the rotation by ψ along the lunar equator to the lunar prime meridian.

The transformation of position and velocity vectors from the Earth-centered Mean of J2000.0 frame (ECI) to the Lunar-centered Mean of J2000 reference frame (LCI) is given by

$$\begin{aligned} \overline{R}_{J2000\ LCI} &= \overline{R}_{J2000\ ECI} - \overline{R}_{Moon\ ECI} \\ \dot{\overline{R}}_{J2000\ LCI} &= \dot{\overline{R}}_{J2000\ ECI} - \dot{\overline{R}}_{Moon\ ECI} \end{aligned} \tag{3.2-70}*$$

where $\overline{R}_{Moon\ ECI}$ and $\dot{\overline{R}}_{Moon\ ECI}$ are the position and velocity of the Moon in the Mean of J2000.0 geocentric frame.

The transformation of a position and velocity vector from the LCI frame, $\overline{R}_{J2000\ LCI}$, to the LPA frame, $\bar{r}_{LPA}$, is given by

$$\begin{aligned} \bar{r}_{LPA} &= T_{LPA \leftarrow J2000\ LCI}\, \overline{R}_{J2000\ LCI} \\ \dot{\bar{r}}_{LPA} &= T_{LPA \leftarrow J2000\ LCI}\, \dot{\overline{R}}_{J2000\ LCI} + \dot{T}_{LPA \leftarrow J2000\ LCI}\, \overline{R}_{J2000\ LCI} \end{aligned} \tag{3.2-71}*$$

where the rotation matrix, $T_{LPA \leftarrow J2000\ LCI}$, transforms the vector from the Mean of J2000.0 lunar-centered frame to the lunar principal axis frame.

In terms of the Euler angles of the lunar principal axes relative to the J2000 reference frame, the rotation matrix $T_{LPA \leftarrow J2000\ LCI}$ is given by

$$T_{LPA \leftarrow J2000\ LCI} = R(\psi)Q(\theta)R(\phi) \tag{3.2-72}$$

where the elementary rotation matrices are defined in Section 3.2.

3.2.9.1 Transformation Using Chebyshev Series Representation

The most accurate source for the lunar Euler angles is a modern high precision planetary ephemeris (accurate to less than 1 meter). Note that the Euler angles provided in DE403 were used to develop the LP100K nonspherical lunar gravity model and are therefore the best choice for use with that gravity model. The DE series 400 files provide Chebyshev coefficients for the Euler angles referenced to TT. These coefficients can optionally be used in GEONS to compute the transformation given in Equation (3.2-72). In this case the Euler angles are evaluated using the following formulas:

Each Euler angle (ϕ, θ, ψ) and the associated rates are computed as follows:

$$x(t_{TT}) = \sum_{n=0}^{N} c_n T_n(\tau)$$
$$\dot{x}(t_{TT}) = \sum_{n=0}^{N} c_n \dot{T}_n(\tau) \qquad \text{(3.2-72a)*}$$

where t_{TT} is the request time in TT (computed using Equations 4.1-28b and 4.1-28c), c_n are the associated Chebyshev coefficients, $T_n(\tau)$ and $\dot{T}_n(\tau)$ are the Chebyshev polynomials for the angles and angular rates respectively, and N is the degree of the expansion. The Chebyshev polynomials are computed using the following recursion formula:

$$T_n(\tau) = 2\tau T_{n-1}(\tau) - T_{n-2}(\tau), \quad n = 2,3,... \qquad \text{(3.2-72b)*}$$

where $T_0(\tau) = 1$ and $T_1(\tau) = \tau$.

The applicable range of interpolation for the Chebyshev time parameter τ is $-1 \le \tau \le 1$, which is computed as follows:

$$\tau = \frac{2\Delta t_{TT}}{\Delta T_C} - 1 \qquad \text{(3.2-72c)*}$$

where $\Delta t_{TT} = t_{TT} - T_C^{Start}$ is the elapsed time from the start time of the polynomial fit interval, T_C^{Start}, and ΔT_C is the length associated Chebyshev polynomial fit interval. The fit interval is 32 days for the Euler angles.

The transformation is computed as follows:

$$T_{LPA \leftarrow J2000_{LCI}} = \begin{pmatrix} \cos\psi\cos\phi - \sin\psi\sin\phi\cos\theta & \cos\psi\sin\phi + \sin\psi\cos\phi\cos\theta & \sin\psi\sin\theta \\ -\sin\psi\cos\phi - \cos\psi\sin\phi\cos\theta & -\sin\psi\sin\phi + \cos\psi\cos\phi\cos\theta & \cos\psi\sin\theta \\ \sin\phi\sin\theta & -\cos\phi\sin\theta & \cos\theta \end{pmatrix} \qquad \text{(3.2-72d)*}$$

The time derivative of the rotation matrix, $\dot{T}_{LPA \leftarrow J2000_{LCI}}$, is obtained by differentiating its elements:

$$\dot{T}_{LPA\leftarrow J2000_{LCI}} = \begin{pmatrix} \begin{pmatrix} -\dot{\psi}\sin\psi\cos\phi \\ -\dot{\phi}\cos\psi\sin\phi \\ -\dot{\psi}\cos\psi\sin\phi\cos\theta \\ -\dot{\phi}\sin\psi\cos\phi\cos\theta \\ +\dot{\theta}\sin\psi\sin\phi\sin\theta \end{pmatrix} & \begin{pmatrix} -\dot{\psi}\sin\psi\sin\phi \\ +\dot{\phi}\cos\psi\cos\phi \\ +\dot{\psi}\cos\psi\cos\phi\cos\theta \\ -\dot{\phi}\sin\psi\sin\phi\cos\theta \\ -\dot{\theta}\sin\psi\cos\phi\sin\theta \end{pmatrix} & \begin{matrix} \dot{\psi}\cos\psi\sin\theta \\ +\dot{\theta}\sin\psi\cos\theta \end{matrix} \\ \begin{pmatrix} -\dot{\psi}\cos\psi\cos\phi \\ +\dot{\phi}\sin\psi\sin\phi \\ +\dot{\psi}\sin\psi\sin\phi\cos\theta \\ -\dot{\phi}\cos\psi\cos\phi\cos\theta \\ +\dot{\theta}\cos\psi\sin\phi\sin\theta \end{pmatrix} & \begin{pmatrix} -\dot{\psi}\cos\psi\sin\phi \\ -\dot{\phi}\sin\psi\cos\phi \\ -\dot{\psi}\sin\psi\cos\phi\cos\theta \\ -\dot{\phi}\cos\psi\sin\phi\cos\theta \\ -\dot{\theta}\cos\psi\cos\phi\sin\theta \end{pmatrix} & \begin{matrix} -\dot{\psi}\sin\psi\sin\theta \\ +\dot{\theta}\cos\psi\cos\theta \end{matrix} \\ \begin{pmatrix} \dot{\phi}\cos\phi\sin\theta \\ +\dot{\theta}\sin\phi\cos\theta \end{pmatrix} & \begin{pmatrix} \dot{\phi}\sin\phi\sin\theta \\ -\dot{\theta}\cos\phi\cos\theta \end{pmatrix} & -\dot{\theta}\sin\theta \end{pmatrix} \quad \text{(3.2-72e)*}$$

and $\dot{T}_{J2000_{LCI}\leftarrow LPA} = \left[\dot{T}_{LPA\leftarrow J2000_{LCI}}\right]^T$.

3.2.9.2 Transformation Using Analytical Series

GEONS also provides the following analytical approach to compute this transformation, which is based on a conversion of the IAU 1994 series for lunar physical librations of the mean lunar pole frame to the DE403 lunar principle axis frame. This approach is less accurate (accurate to about 100 meters on the lunar surface) than using the Euler angles provided in the high precision planetary ephemeris but is more appropriate for implementation in flight software. In terms of the IAU 1994 series, the transformation matrix $T_{LPA\leftarrow J2000_{LCI}}$ is computed as follows:

$$T_{LPA\leftarrow J2000_{LCI}} = T_{LPA\leftarrow MP}\ T_{MP\leftarrow J2000_{LCI}} \quad \text{(3.2-73)}$$

where $T_{LPA\leftarrow MP}$ is the transformation from the IAU mean lunar pole frame to the DE403 lunar principle axis frame and $T_{MP\leftarrow J2000_{LCI}}$ is the transformation from the IAU mean lunar pole frame to the mean of J2000.0 frame.

References 44 and 45 provide modifications to the IAU lunar physical libration series given in Reference 43 to account for the differences between the IAU mean lunar pole and principle axis frames based on a body-fixed lunar orientation of DE403. The resultant transformation is given by

$$\begin{aligned} T_{LPA\leftarrow J2000_{LCI}} &= R(\Lambda)Q(90^\circ-\delta_0)R(\alpha_0+90^\circ) \\ &= \begin{bmatrix} -\cos\Lambda\sin\alpha_0 - \sin\Lambda\sin\delta_0\cos\alpha_0 & \cos\Lambda\cos\alpha_0 - \sin\Lambda\sin\delta_0\sin\alpha_0 & \sin\Lambda\cos\delta_0 \\ \sin\Lambda\sin\alpha_0 - \cos\Lambda\sin\delta_0\cos\alpha_0 & -\sin\Lambda\cos\alpha_0 - \cos\Lambda\sin\delta_0\sin\alpha_0 & \cos\Lambda\cos\delta_0 \\ \cos\delta_0\cos\alpha_0 & \cos\delta_0\sin\alpha_0 & \sin\delta_0 \end{bmatrix} \end{aligned} \quad \text{(3.2-74)*}$$

where $\alpha_0 = \varphi - 90^\circ$ is the right ascension of the lunar north pole with respect to the mean of J2000 frame

$$\begin{aligned}\alpha_0 = {} & 269.9949 + 0.0031\,T_e - 3.8787\sin E_1 - 0.1204\sin E_2 + 0.070\sin E_3 \\ & - 0.0172\sin E_4 + 0.0072\sin E_6 - 0.0052\ \sin\ E_{10} + 0.0043\ \sin E_{13} \\ & + 0.0553\cos \Lambda_p + 0.0034\cos(\Lambda_p + E_1) \quad \text{(degrees)}\end{aligned} \tag{3.2-75}*$$

$\delta_0 = 90^\circ - \theta$ is the declination of the lunar north pole with respect to the mean of J2000 frame

$$\begin{aligned}\delta_0 = {} & 66.5392 + 0.0130\,T_e + 1.5419\cos E_1 + 0.0239\cos E_2 - 0.0278\cos E_3 \\ & + 0.0068\cos E_4 - 0.0029\cos E_6 + 0.0009\cos E_7 + 0.0008\cos E_{10} \\ & - 0.0009\cos E_{13} + 0.0220\sin \Lambda_p + 0.0007\sin(\Lambda_p + E_1) \quad \text{(degrees)}\end{aligned} \tag{3.2-76}*$$

and $\Lambda = \psi$ is the lunar prime meridian with respect to the mean of J2000 frame

$$\begin{aligned}\Lambda = {} & \Lambda_p + 3.5610\sin E_1 + 0.1208\sin E_2 \\ & - 0.0642\sin E_3 + 0.0158\sin E_4 + 0.0252\sin E_5 - 0.0066\sin E_6 - 0.0047\sin E_7 \\ & - 0.0046\sin E_8 + 0.0028\sin E_9 + 0.0052\sin E_{10} + 0.0040\sin E_{11} \\ & + 0.0019\sin E_{12} - 0.0044\sin E_{13} + 0.01775 - 0.0507\cos \Lambda_p - 0.0034\cos(\Lambda_p + E_1) \quad \text{(degrees)}\end{aligned} \tag{3.2-77}*$$

where

$$E_1 = 125.045 - 0.0529921\,d_e \quad \text{(degrees)} \tag{3.2-78}*$$

$$E_2 = 250.089 - 0.1059842\,d_e \quad \text{(degrees)} \tag{3.2-79}*$$

$$E_3 = 260.008 + 13.0120009\,d_e \quad \text{(degrees)} \tag{3.2-80}*$$

$$E_4 = 176.625 + 13.3407154\,d_e \quad \text{(degrees)} \tag{3.2-81}*$$

$$E_5 = 357.529 + 0.9856003\,d_e \quad \text{(degrees)} \tag{3.2-82}*$$

$$E_6 = 311.589 + 26.4057084\,d_e \quad \text{(degrees)} \tag{3.2-83}*$$

$$E_7 = 134.963 + 13.0649930\,d_e \quad \text{(degrees)} \tag{3.2-84}*$$

$$E_8 = 276.617 + 0.3287146\,d_e \quad \text{(degrees)} \tag{3.2-85}*$$

$$E_9 = 34.226 + 1.7484877\,d_e \quad \text{(degrees)} \tag{3.2-86}*$$

$$E_{10} = 15.134 - 0.1589763\,d_e \quad \text{(degrees)} \tag{3.2-87}*$$

$$E_{11} = 119.743 + 0.0036096\,d_e \quad \text{(degrees)} \tag{3.2-88}*$$

$$E_{12} = 239.961 + 0.1643573\,d_e \quad \text{(degrees)} \tag{3.2-89}*$$

$$E_{13} = 25.053 + 12.9590088\, d_e \quad \text{(degrees)} \tag{3.2-90}*$$

$$\Lambda_p = 38.3213 + 13.17635815\, d_e - 1.4 \times 10^{-12} d_e^{\,2} \quad \text{(degrees)} \tag{3.2-91}*$$

where d_e is the time interval in days from January 1.5, 2000 TCB (Julian date: 2451545.0) and T_e is the time interval in Julian centuries of 36525 ephemeris days, i.e. $T_e = \dfrac{d_e}{36525}$.

The time derivative of the rotation matrix, $\dot{T}_{LPA \leftarrow J2000\ LCI}$, is obtained by differentiating its elements, assuming that $\dot{\alpha}_0$ and $\dot{\delta}_0$ are zero:

$$\dot{T}_{LPA \leftarrow J2000\ LCI} = \dot{\Lambda} \begin{bmatrix} \sin\Lambda \sin\alpha_0 - \cos\Lambda \sin\delta_0 \cos\alpha_0 & -\sin\Lambda \cos\alpha_0 - \cos\Lambda \sin\delta_0 \sin\alpha_0 & \cos\Lambda \cos\delta_0 \\ \cos\Lambda \sin\alpha_0 + \sin\Lambda \sin\delta_0 \cos\alpha_0 & -\cos\Lambda \cos\alpha_0 + \sin\Lambda \sin\delta_0 \sin\alpha_0 & -\sin\Lambda \cos\delta_0 \\ 0 & 0 & 0 \end{bmatrix} \tag{3.2-91a}*$$

and $\dot{T}_{J2000_{LCI} \leftarrow LPA} = \left[\dot{T}_{LPA \leftarrow J2000\ LCI}\right]^T$.

where $\dot{\Lambda} \cong 13.17635815$ degrees per day $= \dot{\Lambda} \cong \dfrac{13.17635815}{86400} \times \dfrac{\pi}{180}$ radians per second, the first order rotation rate of the Moon.

3.2.10 VBN to CBI Coordinate Transformation

The transformation of a vector expressed in the VBN frame defined in Section 3.1.8 to the central-body inertial mean of J2000.0 frame is computed as follows:

$$\begin{bmatrix} X_C \\ Y_C \\ Z_C \end{bmatrix} = \left[T_{XYZ \leftarrow VBN}\right]_C \begin{bmatrix} V_C \\ B_C \\ N_C \end{bmatrix} \tag{3.2-92}*$$

where

$$\left[T_{XYZ \leftarrow VBN}\right]_C = \begin{bmatrix} \hat{V}_C \cdot \hat{X}_C & \hat{B}_C \cdot \hat{X}_C & \hat{N}_C \cdot \hat{X}_C \\ \hat{V}_C \cdot \hat{Y}_C & \hat{B}_C \cdot \hat{Y}_C & \hat{N}_C \cdot \hat{Y}_C \\ \hat{V}_C \cdot \hat{Z}_C & \hat{B}_C \cdot \hat{Z}_C & \hat{N}_C \cdot \hat{Z}_C \end{bmatrix} \tag{3.2-93}*$$

3.2.11 ECI to Non-Earth CBI Coordinate Transformation

The transformation of position and velocity vectors from the Mean of J2000.0 Earth-centered frame (ECI) to the Mean of J2000 reference frame of a non-Earth central body (CBI) is given by

$$\begin{aligned} \overline{R}_{J2000\ PCI} &= \overline{R}_{J2000\ ECI} - \overline{R}_{Planet\ ECI} \\ \dot{\overline{R}}_{J2000\ PCI} &= \dot{\overline{R}}_{J2000\ ECI} - \dot{\overline{R}}_{Planet\ ECI} \end{aligned} \tag{3.2-94}*$$

where $\overline{R}_{Planet\ ECI}$ and $\dot{\overline{R}}_{Planet\ ECI}$ are the position and velocity of the non-Earth central body in the Mean of J2000.0 Earth-centered frame.

3.2.12 Non-Earth CBI to PBF Coordinate Transformation

The transformation from the non-Earth CBI to PBF frame is performed using the cartographic coordinates of the body provided in Reference 48. The cartographic coordinates of the body consist of the orientation of the axis of rotation (north pole) and the prime meridian of the object with respect to the inertial ICRF. In the absence of other information, the axis of rotation is assumed to be normal to the mean orbital plane.

The transformation is given by

$$T_{PBF\leftarrow J2000\ CBI} = R(\Lambda)Q(90^\circ - \delta_0)R(\alpha_0 + 90^\circ)$$

$$= \begin{bmatrix} -\cos\Lambda\sin\alpha_0 - \sin\Lambda\sin\delta_0\cos\alpha_0 & \cos\Lambda\cos\alpha_0 - \sin\Lambda\sin\delta_0\sin\alpha_0 & \sin\Lambda\cos\delta_0 \\ \sin\Lambda\sin\alpha_0 - \cos\Lambda\sin\delta_0\cos\alpha_0 & -\sin\Lambda\cos\alpha_0 - \cos\Lambda\sin\delta_0\sin\alpha_0 & \cos\Lambda\cos\delta_0 \\ \cos\delta_0\cos\alpha_0 & \cos\delta_0\sin\alpha_0 & \sin\delta_0 \end{bmatrix} \quad (3.2\text{-}95)^*$$

where $\alpha_0 = \varphi - 90^\circ$ is the right ascension of date of the axis of rotation (north pole) with respect to the ICRF frame, $\delta_0 = 90^\circ - \theta$ is the declination of date of the axis of rotation with respect to the ICRF, and $\Lambda = \psi$ is the prime meridian with respect to the ICRF.

The time derivative of the rotation matrix, $\dot{T}_{PBF\leftarrow J2000\ CBI}$, is obtained by differentiating its elements, assuming that $\dot{\alpha}_0$ and $\dot{\delta}_0$ are zero:

$$\dot{T}_{PBF\leftarrow J2000\ CBI} = \dot{\Lambda}\begin{bmatrix} \sin\Lambda\sin\alpha_0 - \cos\Lambda\sin\delta_0\cos\alpha_0 & -\sin\Lambda\cos\alpha_0 - \cos\Lambda\sin\delta_0\sin\alpha_0 & \cos\Lambda\cos\delta_0 \\ \cos\Lambda\sin\alpha_0 + \sin\Lambda\sin\delta_0\cos\alpha_0 & -\cos\Lambda\cos\alpha_0 + \sin\Lambda\sin\delta_0\sin\alpha_0 & -\sin\Lambda\cos\delta_0 \\ 0 & 0 & 0 \end{bmatrix} \quad (3.2\text{-}96)^*$$

and $\dot{T}_{J2000_{CBI}\leftarrow PBF} = \left[\dot{T}_{PBF\leftarrow J2000\ PCI}\right]^T$.

Table 1 in Reference 48 provides the following approximate expressions (accurate to 0.1 degree) for computing these angles, which are summarized in Table 3-3.

Table 3-3. Values for the Direction of the North Pole of Rotation and Prime Meridian of the Sun and Planets

Body	Right Ascension (α_0) (degrees)	Declination (δ_0) (degrees)	Prime Meridian (Λ) (degrees)	Rotation Rate ($\dot{\Lambda}$) (degrees/day)
Sun	286.13	63.87	84.10 +14.1844000d	14.1844000
Mercury	281.01 - 0.033T	61.45 – 0.005T	329.548 + 6.1385025d	6.1385025
Venus	272.76	67.16	160.20 – 1.4813688d	– 1.4813688
Mars	317.68143 – 0.1061T	52.88650 - 0.0609T	176.630 + 350.89198226d	350.89198226

Body	Right Ascension (α_0) (degrees)	Declination (δ_0) (degrees)	Prime Meridian (Λ) (degrees)	Rotation Rate ($\dot{\Lambda}$) (degrees/day)
Jupiter	268.05 – 0.009T	64.49 + 0.003T	284.95 + 870.5366420d	870.5366420
Saturn	40.589 – 0.036T	83.537 – 0.004T	38.90 + 810.7939024d	810.7939024

where d is the time interval in days from January 1.5, 2000 TCB (Julian date: 2451545.0) and T is the time interval in Julian centuries of 36525 ephemeris days from January 1.5, 2000 TCB (Julian date: 2451545.0 TCB), i.e. $T = \frac{d}{36525}$.

3.2.13 Ecliptic to CBI Coordinate Transformation

The ecliptic coordinate frame is defined as follows:

- x-axis is pointing from the center of the Earth towards the vernal equinox of epoch J2000.0
- z-axis is perpendicular to the ecliptic (Earth-Sun) plane
- y-axis completes the right-handed system

The transformation matrix from the ecliptic frame to the inertial frame is given by:

$$T_{J2000 \leftarrow ecl} = R_x(-\varepsilon_m) = \begin{pmatrix} 1 & 0 & 0 \\ 0 & \cos(\varepsilon_m) & -\sin(\varepsilon_m) \\ 0 & \sin(\varepsilon_m) & \cos(\varepsilon_m) \end{pmatrix} \tag{3.2.13-1}$$

where the mean obliquity of the Ecliptic, ε_m, is computed using Equations (3.2-17) and (3.2-18).

3.2.14 J2 Mean Semimajor Axis Error

The J2 mean semimajor axis error is computed as the difference of the truth J2 mean semimajor axis and the estimated J2 mean semimajor axis.

$$\Delta a = a_{J2}^{True} - a_{J2}^{Estimated} \tag{3.2.14-1}*$$

The J2 mean semimajor axis is defined to be

$$a_{J2} = \frac{\mu_E}{2}\left[\Psi_{PM+J2_E} - \frac{\left|\dot{\bar{R}}\right|^2}{2}\right]^{-1} \tag{3.2.14-2}*$$

where μ_E is the gravitational constant of the Earth and ψ_{PM+J2_E} is the sum of the gravitational potential due to the Earth's point mass and J2

$$\psi_{PM+J2_E} = \frac{\mu_E}{R}[1 + C_2^0\left(\frac{R_e}{R}\right)^2 P_2^0(\sin\phi)] \tag{3.2.14-3}$$

where

R = magnitude of the vector from the Earth's center of mass to the satellite

μ_E = gravitational constant of the Earth (398600.4415 x 10^9 meters^3/second^2 for consistency with the JGM-2 gravitational model)

R_e = equatorial radius of the Earth

$C_n^0 = -J_2 =$ second order zonal harmonic coefficient for the Earth

ϕ = geocentric latitude

$P_2^0(\sin\phi) = \frac{1}{2}\left[3\sin^2\phi - 1\right]$

Ignoring polar motion effects, the geocentric latitude is computed as follows:

$$\phi = \sin^{-1}\left(\frac{z}{r}\right) \tag{3.2.14-4}*$$

where $(\bar{r},\ x,\ y,\ z)$ are the TOD components of the spacecraft position vector. The spacecraft state in the TOD frame is computed from the vector in the Mean of J2000.0 frame as follows

$$\bar{r} = C\bar{R} \tag{3.2.14-5}*$$

where the C matrix is defined in Equation 3.2-26).

Using Equation 3.2.14-4, Equation 3.2.14-3 reduces to the following:

$$\psi_{PM+J2_E} = \frac{\mu_E}{R}\left[1 + \frac{C_2^0}{2}\left(\frac{R_e}{R}\right)^2\left(3\frac{z^2}{r^2} - 1\right)\right] \tag{3.2.14-6}*$$

Note that Equation (3.2.14-3) is an extension of the definition of the semimajor axis to include the J2 potential. The standard definition of the semimajor axis given by

$$a = \left[\frac{2}{R} - \frac{\left|\dot{\bar{R}}\right|^2}{\mu_E}\right]^{-1} \tag{3.2.14-7}$$

which can be rewritten as follows

$$a = \frac{\mu_E}{2}\left[\psi_{PM} - \frac{\left|\dot{\bar{R}}\right|^2}{2}\right]^{-1} \qquad (3.2.14\text{-}8)$$

where $\psi_{PM} = \dfrac{\mu_E}{R}$ is the gravitational potential due to the Earth's point mass gravitational term.

3.2.15 IAU-2000 ECI/GCRF to ECEF/ITRF Coordinate Transformation (Planned for GEONS 3.1)

The IAU-2000 GCRF to ITRF transformation is discussed in detail in Reference 49. GEONS implements the following CIO-based computation approach, which is consistent with the recommendations provided in Reference 62, to relate the International Terrestrial Reference Frame (ITRF) to the Geocentric Celestial Reference Frame (GCRF) at the date t:

$$\bar{R}_{GCRF}(t) = Q(t)\, R(t)\, W(t)\bar{r}_{ITRF}(t) \qquad (3.2.15\text{-}1)^*$$

where *Q(t)* is the transformation matrix arising from the combined effects of nutation, precession and frame bias (Celestial Intermediate Reference Frame (CIRF) to GCRF rotation), *R(t)* is the transformation matrix arising from the rotation of the Earth around the axis associated with the pole (Terrestrial Intermediate Reference Frame (TIRF) to CIRF rotation), and *W(t)* is the transformation matrix for polar motion and from the ITRF origin (ITRF to the TIRF rotation). The parameter t, used in Eq. (3.2.15-1) is defined by

$$t = (TT - 2000\text{ January 1d 12h TT) in days / 36525} \qquad (3.2.15\text{-}2)^*$$

where TT=TAI + 32.184s is Terrestrial Time.

The corresponding transformation for the velocity vector is obtained by taking the time derivative of Eq. (3.2.15-1). The time derivatives of the *Q(t)* and *W(t)* rotation matrices are negligible; however, for the *R(t)* rotation, the derivative of the rotation matrix around the equator must be included:

$$\dot{\bar{R}}_{GCRF} = Q(t)\left(\frac{d}{dt}\left[R(t)\right]\right)W(t)\bar{r}_{ITRF} + Q(t)\, R(t)\, W(t)\dot{\bar{r}}_{ITRF} \qquad (3.2.15\text{-}3)^*$$

where

$$\left(\frac{d}{dt}\left[R(t)\right]\right) = \omega_e \begin{bmatrix} -\sin(ERA) & \cos(ERA) & 0 \\ -\cos(ERA) & -\sin(ERA) & 0 \\ 0 & 0 & 0 \end{bmatrix} \qquad (3.2.15\text{-}4)^*$$

and

ω_e = Earth rotation rate equal to 7.2921158553 x 10^{-5} radians per second

ERA = Earth Rotation Angle between the Celestial Intermediate Origin (CIO) and the Terrestrial Intermediate Origin (TIO) at date t on the equator of the Celestial Intermediate Pole (CIP)

The definition of the GCRS and ITRS and the procedures for the ITRS to GCRS transformation that are provided in Reference 49 comply with the IAU 2000/2006 resolutions. More detailed explanations about the relevant concepts, software and IERS products corresponding to the IAU 2000 resolutions can be found in IERS Technical Note 29 (Capitaine et al., 2002).

Software routines to implement the IAU 2006/2000A transformations are provided by the IAU Standards Of Fundamental Astronomy (SOFA) service. Implementations in Fortran77 and C are available. The SOFA software supports both the CIO-based and classical Equinox-based approaches for implementing the IAU resolutions in the transformation from ITRS to GCRS provided by Eq. (3.2.15-1). For both transformations, the procedure is to form the various components of Eq. (3.2.15-1), choosing for the *Q(t)* and *R(t)* pair either the CIO based or classical forms, and then to combine these components into the complete terrestrial-to-celestial matrix. Formulations for *Q(t)* using either the full IAU-2000A or truncated IAU-2000B nutation models are provided. The GEONS implementation makes use of the CIO-based routines available in the open-source Essential Routines for Fundamental Astronomy (ERFA) library, which are based on the SOFA library routines.

3.3 Time Systems

GPS time is the basic time system for the GPS SV ephemerides and the GPS Tensor™ receiver computations. Coordinated universal time (UTC) is the basic time system for GEONS' internal computations. Universal time corrected for polar motion (UT1) is used in computing the GHA, which is used in transformations between the inertial and ECEF coordinate frames. The transformations between these time systems are provided in this section.

3.3.1 Conversion From GPS System Time to UTC

GPS time is measured in terms of the number of weeks elapsed from the GPS standard epoch and the number of seconds from the beginning of the GPS week (00:00 Sunday). The GPS time system (GPST) has a constant offset of 19 seconds with respect to the International Atomic Time (TAI) and was coincident with UTC at the GPS standard epoch. Table 3-4 lists the standard GPS and J2000.0 epoch dates. Reference 9 provides a detailed discussion of the GPS time system.

Table 3-4. Standard Epochs

Epoch	Calendar Date	Time System	Julian Date
GPS	1980 January $6^d.0$	UTC	2444244.5
J2000.0	2000 January $1^d.5$	TT	2451545.0

The GPS Week count (WN) starts at the GPS standard epoch and is modulo 1024. Therefore, the week count will roll over at Julian Date 2442444.5+7*1024 = 2451412.5, which is midnight 21-22 August 1999 UTC.

The following basic relations hold between these time systems for calendar years 1972 and later:

$$TAI = GPST + 19.^s000 \quad \text{(constant offset)} \tag{3.3-1}$$

$$TAI = UTC + 1.^s000\ n \tag{3.3-2}$$

where n is the accumulated integer leap second offset

Using these relations, *UTC* can be obtained from *GPST* as follows:

$$UTC = GPST + (19.^s000 - 1.^s000\ n) \tag{3.3-3}*$$

At the GPS standard epoch, $UTC = GPST$. In late 1991, the value of n was 26, leading to a 7-second difference between *GPST* and *UTC*. Note that *GPST* always goes ahead of *UTC*. For example, the beginning of the GPS week will precede the beginning of the corresponding UTC calendar week by an integer (= n – 19) seconds.

For conversion of GPS time to UTC using Equation (3.3-3), the GPS week count roll over must be taken into account. The current GPS week number can be derived from the Week Number contained in word 3 of subframe 1 of the navigation message (*WN*) , taking into account the roll over every 1024 weeks, as follows:

$$WN' = WN + 1024N \qquad \text{(3.3-3a)*}$$

where N is initialized to zero for initialization times prior to midnight 21-22 August 1999 and to 1 for initialization times after to midnight 21-22 August 1999. The value of N is incremented by 1 when the roll over occurs (first message for which previous WN =1023, current WN = 0). The relation given by Equation (3.3-3) is correct to within 1 microsecond.

The broadcast SV ephemeris message contains GPS-UTC clock correction terms that can be used to compute the offset of the broadcast GPS time from UTC to within 90 nanoseconds. However, these corrections are not currently implemented in GEONS. Page 18 of subframe 4 of the navigation message includes the UTC conversion parameters that are shown in Table 3-5.

Table 3-5. GPS-to-UTC Time Conversion Parameters Included in Page 18 of Subframe 4

Parameter	Units	Description
A_0	Second	Constant term of the polynomial
A_1	Seconds/ second	Coefficient of the first-order term of the polynomial
Δt_{LS}	Second	Delta time due to leap seconds (definitive)
t_{ot}	Second	Reference time for UTC data
WN_t	Week	Reference week number for UTC data
WN_{LSF}	Week	Week number for the scheduled leap second
DN	Day	Day number for the scheduled leap second
Δt_{LSF}	Second	Scheduled delta time due to leap seconds

There is one additional time parameter needed for the UTC conversion, the user estimated time (t_e). The user estimated time (t_e) (user's current time) should be in seconds from start of the current week. The last three parameters in Table 3-3 describe the scheduled future (with respect to the reference time for the UTC data) leap second update. The day associated with the week number (WN_{LSF}) and the day number (DN) Δt_{LSF} becomes effective is referred to as the effectivity date. Note that 'day one' is the first day relative to the start of week.

Reference 10 gives three different UTC computation algorithms. The relationship of the effectivity date to the user's current GPS time will determine that algorithm should be used, as shown below:

(a) Whenever the effectivity date is not in the past relative to the user's current time and the user's current time does not fall in the timespan that starts at DN+3/4 and ends at DN+5/4, the UTC time (in seconds from start of the current week) is obtained from the GPS time using the following equations:

$$t_{UTC} = (t_e - \Delta t_{UTC}) \text{ [mod 86400]} \qquad \text{(3.3-4)}$$

where the UTC conversion term, Δt_{UTC}, is computed using the following expression:

$$\Delta t_{UTC} = \Delta t_{LS} + A_0 + A_1[t_e - t_{0t} + 604800(WN - WN_t)] \quad (3.3\text{-}5)$$

(b) Whenever the user's current time falls within the timespan of *DN*+3/4 to *DN*+5/4, the following UTC time conversion equations will accommodate the leap second event with a possible week number transition:

$$t_{UTC} = W \ [\text{mod } (86400 + \Delta t_{LSF} - \Delta t_{LS})] \quad (3.3\text{-}6)$$

where

$$W = (t_e - \Delta t_{UTC} - 43200) \ [\text{mod } 86400] + 43200 \quad (3.3\text{-}7)$$

The term Δt_{UTC} in the above equation is computed using Equation (3.3-5) as in the case of (a).

(c) Whenever the effectivity date is in the 'past' relative to the user's current time, the relationship given for UTC in the case of (a) above is valid except that the value of Δt_{LSF} is substituted for Δt_{LS} in computing Δt_{UTC}, i.e.,

$$\Delta t_{UTC} = \Delta t_{LSF} + A_0 + A_1[t_e - t_{0t} + 604800(WN - WN_t)] \quad (3.3\text{-}8)$$

The UTC conversion parameters used in Equation (3.3-5) [all the parameters on the right-hand side of this equation] are contained in the GPS navigation message (page 18 of subframe 4 in Reference 10). The corrections associated with the A_0 and A_1 terms are on the order of nanoseconds.

3.3.2 Conversion From GPS SV Clock Time (t_{sv}) to GPS System Time

GPS SV clock time is converted to the GPS system time using the following equation:

$$t = t^{(SC)} - \delta t_{Sj} \quad (3.3\text{-}9)^*$$

The SV time offset, δt_{Sj}, from the GPS system time is computed using the time offset correction parameter t_{OC} and the SV clock polynomial parameters (a_0, a_1, and a_2), all of which are available from the broadcast navigation message for GPS SV j. This offset is given by the following expression taken from Section 20.3.3.3.3.1 of Reference 10 with the addition of the clock correction parameters $\Delta\delta t_{Sj}^{DC}(t)$ when available from the TDRSS Augmentation Service for Satellites (TASS) broadcast messages:

$$\delta t_{Sj} = a_0 + a_1(t - t_{OC}) + a_2(t - t_{OC})^2 + FeA^{1/2} \sin E_k + \Delta\delta t_{Sj}^{DC}(t) \quad (3.3\text{-}10)^*$$

and the rate of change of the SV time offset is given by

$$\dot{\delta t}_{Sj} = a_1 + 2a_2(t - t_{OC}) + \dot{E}FeA^{1/2} \cos E_k \quad (3.3\text{-}10b)^*$$

where

F = $-4.442807633 \times 10^{-10}$ seconds/(meter)$^{1/2}$

e = eccentricity

$A^{1/2}$ = square-root of semimajor axis

E_k = eccentric anomaly

$\dot{E}$ = rate of change of the eccentric anomaly, $\frac{n}{1-e\,cosE_k}$ where $n = \sqrt{\mu}\left(A^{1/2}\right)^{-3} + \Delta n$

The Keplerian orbit parameters e and $A^{1/2}$ and the mean motion correction Δn are available from the ephemeris parameters included in the broadcast navigation message, and the eccentric anomaly E_k can be computed using Kepler's equation (see Section 5.2.2).

The term $FeA^{1/2} \sin E_k$ represents the relativistic correction that depends on the eccentricity of the GPS orbit, which can also be computed using an equivalent expression, $-2\overline{R} \cdot \overline{V} / c^2$. The clock polynomial coefficients (a_0, a_1, a_2) and the clock data reference time (t_{OC}) are given in subframe 1 of the navigation message. The SV clock offset is used in the pseudorange measurement model given by Equation 5.3-20 in Section 5.3.2.

The TASS messages will provide precise GPS differential corrections and other ancillary data to enable decimeter level orbit determination accuracy and nanosecond time-transfer accuracy, onboard in real-time. TASS will broadcast its message on the S-band multiple access channel of NASA's TDRSS. Broadcasts will be available from three or more TDRSS satellites, providing global coverage.

When the GPS ICE differential correction (DC) messages are available, Equation (3.3-10) is computed as follows:

$$\delta t_{Sj} = (a_0 + \delta a_{f0}) + (a_1 + \delta a_{f1})(t - t_{OC}) + a_2 (t - t_{OC})^2 + FeA^{1/2} \sin E_k \qquad \text{(3.3-10c)*}$$

Equation (3.3-10b) is also corrected as follows:

$$\delta \dot{t}_{Sj} = a_1 + \delta a_{f1} + 2a_2 (t - t_{OC}) + \dot{E} FeA^{1/2} \cos E_k \qquad \text{(3.3-10d)*}$$

The clock DC coefficients will be transmitted as part of the GPS Broadcast messages. Table 5-2 provides a description of these parameters. Section 30.3.3.7 of Reference 10 provides a detailed discussion of these corrections.

When the GPS SV ephemeris is obtained from a precise ephemeris, which contains position, velocity, and clock polynomial coefficients (a_0, a_1) at equally spaced points in time, rather than a broadcast navigation message, the following equation is used to compute the SV time offset and offset rate of change at time t:

$$\delta t_{Sj} = a_0 + a_1 (t - t_A) - 2\frac{\overline{R}(t) \cdot \overline{V}(t)}{c^2} \qquad \text{(3.3-11)*}$$

$$\delta \dot{t}_{Sj} \cong a_1 - \frac{2}{c^2}\left(v^2 - \frac{\mu_E}{R}\right) \qquad \text{(3.3-11b)*}$$

where t_A is the time point immediately preceding the time t and $\overline{R}(t)$ and $\overline{V}(t)$ are obtained by interpolation of the precise ephemeris data.

In addition, there are group delay correction terms for L1, L2, and L5 users and ionospheric correction parameters for single frequency L1 P, L1 C/A, L2 P, and L2 C users and dual frequency L1/L2 users. These include the L1-L2 group delay differential correction parameter, $T_{GD,}$ and inter-signal group delay corrections (ISC) associated with the mean SV group delay differential between the L1 P and the L1 C/A codes ($ISC_{L1C/A}$), the L1 P and the L2 C codes (ISC_{L2C}), the L1 P and the L5 I5 codes (ISC_{L5I5}), and the L1 P and the L5-Q5 codes (ISC_{L5Q5}), (Reference 10 (Section 30.3.3.3.1.1) and Reference 46 (Section 20.3.3.3.1). The group delay correction parameters, $T_{GD,}$ and the ISC values are provided to the user as message type 30 data (Table 30-IV in Reference 10 and Table 20-IV in Reference 46).

Including these corrections, the additional single frequency SV clock correction is given by

$$\left(\delta t_{S_j}^{SF}\right)_{L1C/A} = -T_{GD_j} + ISC_j^{L1C/A} \qquad \text{(3.3-12)*}$$

$$\left(\delta t_{S_j}^{SF}\right)_{L2C} = -T_{GD_j} + ISC_j^{L2C} \qquad \text{(3.3-12a)*}$$

$$\left(\delta t_{S_j}^{SF}\right)_{L5I5} = -T_{GD_j} + ISC_j^{L5I5} \qquad \text{(3.3-12b)*}$$

$$\left(\delta t_{S_j}^{SF}\right)_{L5Q5} = -T_{GD_j} + ISC_j^{L5Q5} \qquad \text{(3.3-12c)*}$$

The user who uses both frequencies does not require this correction since the clock parameters account for the induced effects. See Section 5.3.1.2 for description of group delay and ionospheric corrections for dual-frequency pseudorange measurements.

3.3.3 Conversion From Julian Date to Calendar Date

The conversion from Julian date (*JD*) to calendar date is performed using the following algorithm:

$$L_1 = JD + 68569 \qquad \text{(3.3-13)*}$$

$$N = 4L_1 / 146097 \qquad \text{(3.3-14)*}$$

$$L_2 = L_1 - (146097N + 3)/4 \qquad \text{(3.3-15)*}$$

$$I_1 = 4000(L_2 + 1)/1461001 \qquad \text{(3.3-16)*}$$

$$L_3 = L_2 - 1461I_1/4 + 31 \qquad \text{(3.3-17)*}$$

$$J_1 = 80L_3 / 2447 \quad (3.3\text{-}18)^*$$

$$K = L_3 - 2447J_1 / 80 \quad (3.3.19)^*$$

$$L_4 = J_1 / 11 \quad (3.3\text{-}20)^*$$

$$J = J_1 + 2 - 12L_4 \quad (3.3\text{-}21)^*$$

$$I = 100(N - 49) + I_1 + L_4 \quad (3.3\text{-}22)^*$$

where *JD* is the Julian Date + 0.5 truncated to an integer, *I* is the year, *J* is the month, and *K* is the day of the month. In this computation, all variables are integers and a division by integers implies truncation of the quotients to integers.

3.3.4 Conversion From Calendar Date to Julian Date

The conversion from calendar date to Julian date (*JD*) can be performed using the following algorithm:

$$JD = \begin{pmatrix} D - 32075 + 1461(Y + 4799) / 4 + 336 \\ -3[(Y + 4899) / 100] / 4 \end{pmatrix} - 0.5 + S / 86400.0 \quad (3.3\text{-}23)^*$$

where *Y* is the year, *D* is the day of the year, and *S* is seconds of the day.

(equation deleted) (3.3-24)*

In these computations, division by integers implies truncation of the quotients to integers.

The calculation of the Greenwich sidereal time [Equation (3.2-36)] requires time values in the UT1 system. Therefore, a conversion algorithm between the UTC and UT1 time systems is required. The conversion from UTC to UT1 is, in theory, a continuous function. The USNO distributes predictions for the UT1-UTC corrections in IERS Bulletin-A. The UT1-UTC corrections are computed for the date of interest using the following polynomial fit to these predictions:

$$\Delta UT1 = UT1 - UTC = u_1 + u_2(MJD - T_{UT1}) + u_3(MJD - T_{UT1})^2 \text{ (seconds)} \quad (3.3\text{-}25)^*$$

where *MJD* is the modified Julian date of the request date, defined by Equation (3.2-44), and T_{UT1} is the modified Julian date of the epoch of the prediction and u_1, u_2, u_3 are commanded values.

If the GPS Earth Orientation Parameters are made available, ΔUT1 is computed as follows:

$$\Delta UT1 = \Delta UT1_{GPS} + \Delta \dot{UT}1_{GPS}[t - t_{EOP}] \quad (3.3\text{-}25b)^*$$

The coefficients $\Delta UT1_{GPS}$ and $\Delta \dot{UT}1_{GPS}$ are provided as part of the GPS CNAV message type 32 on the L2C signal. Note that this option is not implemented in GEONS 3.0 but is planned for

GEONS 3.1. Section 30.3.3.5 in Reference 10 provides a detailed discussion of the user algorithm for application of the GPS EOP parameters. Table 3-2 provides a description of these parameters.

(Equation deleted) (3.3-26)

The coefficients u_i are precomputed by performing a quadratic fit to the USNO UT1-UTC predictions published in the IERS Bulletin-A.

(Equation deleted) (3.3-27)

The estimated accuracies of these predictions are 0.0017 second and 0.0048 second for 10- and 40-day predictions, respectively. The 3 u_i coefficients and the epoch time of the prediction will be uplinked to the spacecraft monthly.

The current UT1 time is then computed from the current UTC time as follows:

$$UT1 = UTC + \Delta UT1 \quad \text{(3.3-28)*}$$

3.3.5 Conversion From UTC to TAI and Terrestrial Time

International Atomic Time (TAI) is related to UTC as follows:

$$TAI = UTC + 1.^{s}000n \text{ seconds} \quad \text{(3.3-29a)*}$$

where n equals the total number of elapsed leap seconds (i.e.,10 plus the number since 1972).

Terrestrial Time (TT) is the time scale of the apparent geocentric ephemerides of the bodies in the solar system. It is used in the evaluation of the precise analytic solar/lunar ephemeris series described in Section 4.1.1.2. TT replaces the now obsolete Terrestrial Dynamical Time (TDT) and ephemeris time (ET). TT is related to TAI as follows:

$$TT = TAI + 32.184 \text{ seconds} \quad \text{(3.3-29)}$$

Using Equation (3.3-2), TT is computed from UTC as follows:

$$TT = UTC + 1.^{s}000\ n\ + 32.184 \text{ seconds} \quad \text{(3.3-30)*}$$

The conversion from TT to TDB is performed for evaluation of the DE planetary ephemeris using ERFA library Time and Calendar routines.

3.3.6 Relativistic Clock Corrections

This section discusses the effect of special and general relativity on spacecraft clocks. The primary relativistic effects on a satellite clock are the second order Doppler shift and the gravitational frequency shift. Clocks moving in space run faster than clocks at rest on the surface of the Earth due to the lower gravitational potential in satellite orbit but run slower due to their higher velocity. For more detail see Reference 57 for the effect on GPS orbits and Reference 70 for the effect on lunar orbits.

Reference 70 provides the following formula for computing the total time difference of clock A with respect to clock B accumulated from coordinate time t_1 to coordinate time t_2:

$$\Delta t = \int_{t_1}^{t_2} \left[\frac{\Phi_A(t)}{c^2} - \frac{v_A(t)^2}{2c^2} - \frac{\Phi_B(t)}{c^2} + \frac{v_B(t)^2}{2c^2} \right] dt \tag{3.3-31}$$

where Φ_A and Φ_B are the associated gravitational potentials and v_A and v_B are the associated clock speeds with respect to the inertial frame.

UTC and TAI are based on time measured by clocks at rest on the surface of the Earth. A time interval recorded by a clock at rest on the surface of the Earth is given by:

$$d\tau_E = \left(1 + \frac{\Phi_0}{c^2} \right) dt \tag{3.3-32}$$

or equivalently

$$\Delta\tau_E = \left(1 + \frac{\Phi_0}{c^2} \right) \Delta t \tag{3.3-32b))}$$

where $\Phi_0 / c^2 = -6.96929 \times 10^{-10}$ is the effective geopotential at the equator in the rotating ECEF frame. In Equation (3.3-32b), Δt denotes a finite time interval, not necessarily an infinitesimally small interval, and t denotes the coordinate time measured at infinity (the independent variable in the spacecraft equations of motion). In the following sections, the gravitational potentials for a clock on a satellite orbiting the Earth or Moon are approximated using only the point mass gravitational contributions.

3.3.6.1 Relativistic Clock Corrections for Earth Orbiting Satellites

The effect of the Earth's point mass gravitational potential on a time interval recorded by a clock on a satellite orbiting the Earth relative to a clock at rest on the surface of the Earth is approximated by

$$d\tau_S = \left(1 - \frac{\mu_E}{R_S^E c^2} - \frac{\left(\dot{R}_S^E\right)^2}{2c^2} - \frac{\Phi_0}{c^2} \right) d\tau_E \tag{3.3-33}$$

where the subscript S stands for satellite and R_S^E and $\dot{R}_S^E$ are the magnitudes of the position and velocity vectors in the Earth-centered inertial frame, respectively. Using the following relationship for the total energy

$$\frac{\dot{R}_S^2}{2} - \frac{\mu_E}{R_S} = -\frac{\mu_E}{2a_S} \tag{3.3-34}$$

for $\dot{R}_S^2$ in Equation 3.3-33 yields

$$d\tau_S = \left[\left(1 - \frac{3\mu_E}{2a_S c^2} - \frac{\Phi_0}{c^2}\right) + \frac{2\mu_E}{c^2}\left(\frac{1}{a_S} - \frac{1}{R_S}\right)\right] d\tau_E \tag{3.3-35}$$

The integrated form of this equation (assuming that the satellite is in an elliptical orbit) is given by:

$$\Delta\tau_S \cong \left(1 - \frac{3\mu_E}{2a_S c^2} - \frac{\Phi_0}{c^2}\right)\Delta\tau_E - \frac{2e_S\sqrt{\mu_E a_S}\sin E}{c^2} + C \tag{3.3-36}$$

The integration constant C can be assumed to be zero using appropriate initial conditions or can be omitted assuming that it will be absorbed in the estimated clock bias term.

The relative time bias due to the relativistic effects of the clock onboard the spacecraft with respect to the Earth bound clock is given by:

$$\Delta^2\tau_S = \Delta\tau_S - \Delta\tau_E = \left(-\frac{3\mu_E}{2a_S c^2} - \frac{\Phi_0}{c^2}\right)\Delta\tau_E - \frac{2e_S\sqrt{\mu_E a_S}\sin E}{c^2} \tag{3.3-37}$$

The eccentricity dependent term is always included in GEONS when computing GPS transmit times (see Section 3.3.2). The terms inside the parenthesis are the ones used by GPS project to calibrate the oscillators onboard GPS SVs. In the case of GPS satellites, un-calibrated clock onboard GPS satellite will run faster than an Earth fixed clock, by approximately 38.6 micro-seconds per day. A typical GPS clock behavior is shown in Figure 3-9. With some GPS SVs, the eccentricity could be as large as 0.02.

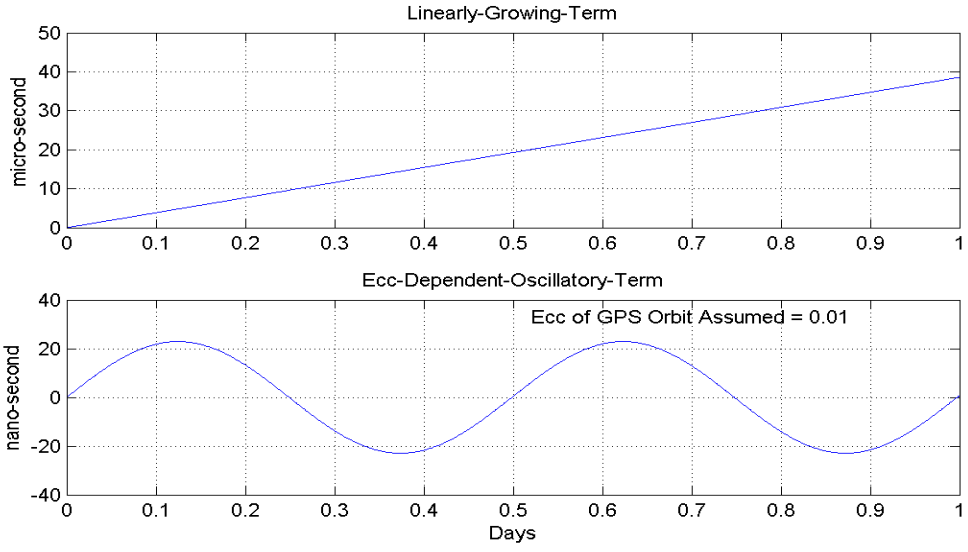

Figure 3-9. Relativistic Effects on a GPS SV Clock

Figure 3-10 shows the relativistic effect on a satellite clock in a high-altitude Earth orbit (HEO) with a semimajor axis of 42095.7 km and eccentricity of 0.82.

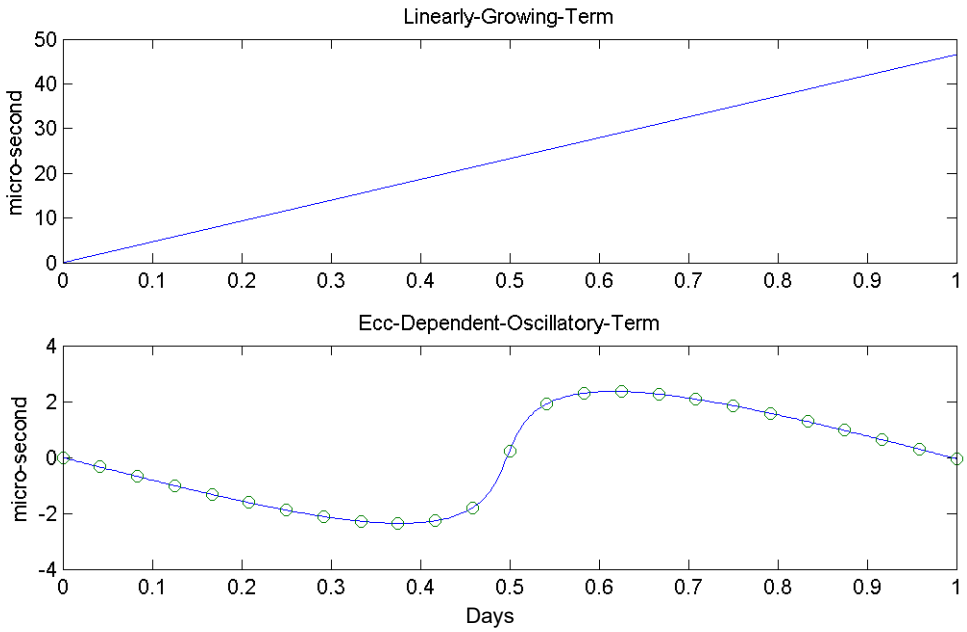

Figure 3-10. Relativistic Effects on a HEO Satellite Clock

If the relativistic effects in Equation (3.3-37) are not modeled explicitly, the linear effect will be absorbed in the time bias drift estimate and the periodic effect will be absorbed in both the time bias and time bias drift estimates, requiring a somewhat larger process noise value for the time bias and/or drift than would be needed if the effect were modeled. To improve estimation of the time bias and drift, the relativistic effects can be optionally included in the propagation of the receiver time.

3.3.6.2 Relativistic Clock Corrections for Lunar Orbiting Satellites (Not implemented in GEONS 3.0)

3.3.7 Conversion From Galileo System Time (GST) to UTC

Galileo System Time (GST) is measured in terms of the Week Number (number of weeks elapsed from the GST start epoch) and the Time of Week (number of seconds from the beginning of the previous week (00:00 Sunday). Table 3-6 lists the GPS, J2000.0 and Galileo epoch dates. Reference 63 provides a more detailed discussion of the GST.

Table 3-6. Standard Epochs

Epoch	Calendar Date	Time System	Julian Date
GPS	1980 January $6^d.0$	UTC	2444244.5
J2000.0	2000 January $1^d.5$	TT	2451545.0
Galileo	1999 August 21 23:59:47	UTC	2451412.5

The GST Week Number (WN) starts at the GST start epoch and is modulo 4096 (about 78 years). Note that the GST start epoch is 1999 August $22^d.0$ GPST, which coincides with the roll-over of the GPS Week Number that occurred in August 1999 when the number of leap seconds was 13. The Time of Week (TOW) is defined as the number of seconds that have occurred since the transition from the previous week. The TOW covers an entire week from 0 to 604799 seconds and is reset to zero at the end of each week.

Note that the following procedure for conversion from GST to UTC is identical to that defined in Section 3.3.1 for conversion of GPST to UTC; however, the values of the GST conversion parameters will be different than those for GPST conversion. The format of the Galileo C/NAV navigation message is the same as the format of the GPS navigation message. The format of the Galileo F/NAV and I/NAV messages is defined in Section 4 of Reference 63.

Following the procedure defined in Section 5.1.7 of Reference 63, UTC can be obtained from GST using the GST-UTC conversion parameters listed in Table 3.7 for 3 different cases depending on the epoch of the possible leap second adjustment (scheduled future or recent past) given by DN, the day at the end of which the leap second becomes effective, and week number WN_{LSF} to which DN is referenced. "Day one" of *DN* is the first day relative to the end/start of week and the WN_{LSF} value consists of eight bits which are a modulo 256 binary representation of the Galileo week number to which the *DN* is referenced.

Table 3-7. GST-to-UTC Time Conversion Parameters (from Table 65 in Reference 63)

Parameter	Unit	Description
A_0	Second	Constant term of the polynomial
A_1	Seconds/ second	Coefficient of the first-order term of the polynomial
Δt_{LS}	Second	Leap second count before leap second adjustment
t_{ot}	Second	Reference Time of Week for UTC data
WN_{0t}	Week	Reference Week Number for UTC data
WN_{LSF}	Week	Week number for the scheduled leap second adjustment
DN	Day	Day number at the end of which a leap second adjustment becomes effective
Δt_{LSF}	Second	Leap second count after leap second adjustment

In all computations the user must account for the truncated nature (roll-over) of the parameters (DN, WN, WN_{0t}, and WN_{LSF}), considering the following properties:

At the time of broadcast of the GST -UTC parameters,

- The absolute value of the difference between untruncated WN and WN_{0t} values does not exceed 127
- When Δt_{LS} and Δt_{LSF} differ, the absolute value of the difference between the untruncated WN and WN_{LSF} values received within the same subframe does not exceed 127.

In addition to the parameters listed in Table 3-6, the following parameters are used in the GST – UTC conversion algorithm:

- t_E is the GST as estimated by the user through its GST determination algorithm in seconds from start of the current week
- WN is the week number to which t_E is referenced.

Case a

Whenever the leap second adjustment time indicated by WN_{LSF} and DN is not in the past (relative to the user's present time) and the user's present time does not fall in the time span which starts six hours prior to the effective time and ends six hours after the effective time, t_{UTC} is computed according to the following equations:

$$t_{UTC} = \left(t_E - \Delta t_{UTC}\right) [\text{Modulo } 86400] \qquad (3.3.7\text{-}1)^*$$

where

$$\Delta t_{UTC} = \Delta t_{LS} + A_0 + A_1\left(t_E - t_{0t} + 604800\left(WN - WN_{0t}\right)\right) \qquad (3.3.7\text{-}2)^*$$

Case b

Whenever the user's current time falls within the time span of six hours prior to the leap second adjustment time to six hours after the adjustment time, t_{UTC} is computed according to the following equations (Δt_{UTC} as defined in case a):

$$t_{UTC} = W[\text{Modulo } \left(86400 + \Delta t_{LSF} - \Delta t_{LS}\right)] \qquad (3.3.7\text{-}3)^*$$

where

$$W = \left(t_E - \Delta t_{UTC} - 43200\right)\left[\text{Modulo } 86400\right] + 43200 \qquad (3.3.7\text{-}4)^*$$

Case c

Whenever the leap second adjustment time, as indicated by the WN_{LSF} and DN values, is in the "past" (relative to the user's current time) and the user's present time does not fall in the time span which starts six hours prior to the leap second adjustment time and ends six hours after the adjustment time, t_{UTC} is computed according to the following equation:

$$t_{UTC} = \left(t_E - \Delta t_{UTC}\right) [\text{Modulo } 86400] \qquad (3.3.7\text{-}5)^*$$

where

$$\Delta t_{UTC} = \Delta t_{LSF} + A_0 + A_1\left(t_E - t_{0t} + 604800\left(WN - WN_{0t}\right)\right) \qquad (3.3.7\text{-}6)^*$$

3.3.8 Conversion From Galileo System Time (GST) to GPS Time (GPST)

The procedure for converting between Galileo System Time (GST) and GPS Time (GPST) is defined in Section 5.1.8 of Reference 63. The difference between the Galileo and the GPS time scales, expressed in seconds, is given by the equation below:

$$\Delta t_{Systems} = t_{Galileo} - t_{GPS} = A_{0G} + A_{1G}\left(TOW - t_{0G} + 604800\left(WN - WN_{0G}\right)\right) \qquad (3.3.8\text{-}1)^*$$

where

$t_{Galileo}$ = GST time in seconds

t_{GPS} = GPS time in seconds

A_{0G} = constant term of the offset $\Delta t_{Systems}$

A_{1G} = rate of change of the offset $\Delta t_{Systems}$

t_{0G} = reference GST TOW for the GGTO data

TOW = GST Time of Week in seconds

WN = GST Week Number

WN_{0G} = Week Number of the GPS/Galileo Time Offset reference

The user must account in the above formula for the truncated nature (roll-over) of the weekly parameters (WN, $WN0G$), considering that at the time of broadcast of the GGTO parameters, the absolute value of the difference between untruncated WN and $WN0G$ values does not exceed 31. The GGTO parameters are formatted according to the values in Table 3.8. When the GGTO is not available, the GGTO parameters disseminated are: $A0G$ (all ones -16 bits), $A1G$ (all ones - 12 bits), $t0G$ (all ones - 8 bits), $WN0G$ (all ones - 6 bits). When a user receives all four parameters set to all ones the GGTO is considered as not valid.

Table 3-8. GGTO Parameters for the GPS Time to GST Offset Computation (from Table 66 in Reference 63)

Parameter	Definition	Bits	Scale factor	Unit
A_{0G}	Constant term of the polynomial describing the offset $\Delta t_{systems}$	16*	2^{-35}	s
A_{1G}	Rate of change of the offset $\Delta t_{systems}$	12*	2^{-51}	s/s
t_{0G}	Reference time for GGTO data	8	3600	s
WN_{0G}	Week number of GGTO reference	6	1	week
Total GST-GPS Conversion Size		**42**		

3.3.9 Conversion From Galileo Satellite Clock Time to Galileo System Time (GST)

The procedure for computing the offset of the physical Galileo Satellite signal time of transmission relative to the satellite signal time of transmission in Galileo System Time (GST) is defined in Sections 5.1.3 through 5.1.5 of Reference 63. Each Galileo satellite transmits the satellite clock correction data defined in Table 3-9.

Table 3-9. Galileo Clock Correction Parameters (from Table 60 in Reference 63)

Parameter	Definition	Bits	Scale factor	Unit
t_{0c}	clock correction data reference Time of Week	14	60	s
a_{f0}	SV clock bias correction coefficient	31*	2^{-34}	s
a_{f1}	SV clock drift correction coefficient	21*	2^{-46}	s/s
a_{f2}	SV clock drift rate correction coefficient	6*	2^{-59}	s/s^2
Total Clock Correction Size		**72**		

The total Galileo satellite time correction consists of a satellite time correction $\delta t_{GAL_j}(X)$ for both single and dual frequency GPS users and an additional Broadcast Group Delay correction $\delta t^{SF}_{GAL_j}(X)$ for only single frequency GPS users.

$$\Delta t_{GST_j}(X) = \delta t_{GAL_j}(X) + \delta t^{SF}_{GAL_j}(X) \qquad (3.3.9\text{-}1)$$

The satellite time correction (in seconds), $\delta t_{GAL_j}(X)$, is computed using the GST signal time of transmission in seconds (t_{GST}), time correction GST reference Time of Week, $(t_{OC}(X))$, and the SV clock polynomial parameters (a_{f0}, a_{f1}, and a_{f2}). These data are available from the broadcast navigation message for Galileo SVj for the associated dual frequency combination $(X) = (E1, E5a)$ and $(X) = (E1, E5b)$ as defined in Table 61 in Reference 63.

$$\delta t_{GAL_j}(X) = a_{f0}(X) + a_{f1}(X)\left[t_{GST} - t_{OC}(X)\right] + a_{f2}(X)\left[t_{GST} - t_{OC}(X)\right]^2 + F_{GAL} e A^{1/2} \sin E \quad (3.3.9\text{-}2)^*$$

The rate of change of the satellite time correction is given by

$$\delta \dot{t}_{GAL_j}(X) = a_{f1}(X) + 2a_{f2}(X)\left[t_{GST} - t_{OC}(X)\right] + \dot{E} F_{GAL} e A^{1/2} \cos E \qquad (3.3.9\text{-}3)^*$$

where

F_{GAL} = $-4.442807309 \times 10^{-10}$ seconds/(meter)^{½}

e = eccentricity

$A^{1/2}$ = square-root of semimajor axis

E = eccentric anomaly

$\dot{E}$ = rate of change of the eccentric anomaly, approximated by $\dot{E} \cong n = \sqrt{\mu}\left(A^{1/2}\right)^{-3} + \Delta n$

The term $FeA^{1/2} \sin E_k$ represents the relativistic correction that depends on the eccentricity of the Galileo orbit. The Keplerian orbit parameters e and $A^{1/2}$ and the mean motion correction Δn

are available from the Galileo satellite ephemeris parameters included in the broadcast navigation message, and the eccentric anomaly E can be computed using Kepler's equation (see Section 5.2.2).

In addition, each Galileo satellite broadcast has its own Broadcast Group Delay (BGD) correction terms for single frequency users. The additional single frequency satellite clock correction is given by

$$\delta t_{GAL_j}^{SF}\left(f_1\right) = -BGD_j\left(f_1, f_2\right) \tag{3.3.9-4}*$$

$$\delta t_{GAL_j}^{SF}\left(f_2\right) = -\left(\frac{f_1}{f_2}\right)^2 BGD_j\left(f_1, f_2\right) \tag{3.3.9-5}*$$

Section 4. State Propagation

The GEONS propagator will propagate the user state vectors between measurement updates. In addition, the TDRSS transmitter states and optionally the crosslink transmitter states are propagated if they are not being estimated. The forces modeled in the equations of motion include atmospheric drag, solar radiation pressure, non-spherical gravitational field for central body, and point-mass gravitational effects of the Earth, Sun, Moon, Venus, Mars, Jupiter, and Saturn. The gravitational effect of the Earth and the J_2 zonal coefficient are included in the computation of the position and velocity state transition matrix components.

The spacecraft equations of motion are given in Section 4.1. The numerical integration algorithm is defined in Section 4.2. The equations of motion for the nonspacecraft state vector components are given in Section 4.3. The state covariance propagation algorithms are defined in Section 4.4. Procedures for handling maneuvers are addressed in Section 4.5. The ground-based receiver state propagation algorithms are described in Section 4.6.

4.1 Spacecraft Equations of Motion

The spacecraft equations of motion, expressed in Cartesian coordinates, are

$$\frac{d^2\overline{R}}{dt^2} = \overline{a} \tag{4.1-1}$$

where

$\overline{R}$ = satellite position vector in the mean of J2000.0 coordinate frame

$\overline{a}$ = total acceleration vector in the mean of J2000.0 coordinate frame

This set of three second-order differential equations is transformed to an equivalent set of six first-order differential equations

$$\frac{\mathrm{d}\overline{R}}{\mathrm{d}t} = \dot{\overline{R}} \tag{4.1-2}*$$

$$\frac{\mathrm{d}\dot{\overline{R}}}{\mathrm{d}t} = \overline{a} \tag{4.1-3}*$$

where $\dot{\overline{R}}$ is the satellite velocity expressed in the mean of J2000.0 coordinate frame.

The total acceleration of the satellite, $\overline{a}$, includes the following components:

- Gravitational acceleration (point-mass contributions) of the satellite due to the Earth's mass ($\overline{a}_E$) and the solar, lunar and other planet masses ($\overline{a}_S$, $\overline{a}_M$ and $\overline{a}_P$, respectively)
- Gravitational acceleration of the satellite due to the nonsphericity of the Earth's gravitational potential ($\overline{a}_{NS_E}$) and the Moon's gravitational potential ($\overline{a}_{NS_M}$)

- Satellite acceleration due to atmospheric drag forces ($\bar{a}_D$)
- Satellite acceleration due to solar radiation pressure ($\bar{a}_{SRP}$)
- Satellite acceleration measured externally ($\bar{a}_{ext}$)
- Satellite acceleration due to unmodeled accelerations ($\bar{a}_U$) expressed in the Mean of J2000.0 frame

The total acceleration, $\bar{a}$, is expressed in terms of these components as

$$\bar{a} = \bar{a}_E + \bar{a}_S + \bar{a}_M + \bar{a}_P + \bar{a}_{NS_E} + \bar{a}_{NS_M} + \bar{a}_D + \bar{a}_{SRP} + \bar{a}_{ext} + \bar{a}_U \qquad (4.1\text{-}4)^*$$

All or any subset of these effects can be included in the acceleration vector, which is used in constructing the equations of motion. These accelerations are discussed in the following subsections. In addition, when a maneuver is modeled as an impulsive velocity change (delta-V), the satellite equations of motion are integrated to the maneuver time, the velocity change is added to the velocity vector at the maneuver time, and integration of the equations of motion continues using the post-maneuver state vector.

4.1.1 Earth, Solar, Lunar, and Planetary Point-Mass Accelerations

To first order, the gravitational attraction of a body of mass *m* can be approximated as that arising from a dimensionless particle of mass *m* located at the center of mass of the body. Point-mass accelerations arising from the following bodies can be included in the acceleration model: Earth, Moon, Sun, Mars, Venus, Jupiter, and Saturn.

The motion of the satellite is referenced to the central body's position, i.e., the central-body mean of J2000.0 coordinate system is used in the integration of the spacecraft equations of motion. Any of these bodies can be the central body. The total point mass acceleration is given by

$$\frac{\mathrm{d}^2 \bar{R}_C^n}{\mathrm{d}t^2} = -\frac{\mu_C \bar{R}_C^n}{\left(R_C^n\right)^3} + \sum_{p=1}^{P} \mu_p \left(\frac{\bar{R}_C^p - \bar{R}_C^n}{|\bar{R}_C^p - \bar{R}_C^n|^3} - \frac{\bar{R}_C^p}{|\bar{R}_C^p|^3} \right) \qquad (4.1\text{-}5)^*$$

(Equation removed) (4.1-6)

(Equation removed) (4.1-7)

(Equation removed) (4.1-8)

where

$\bar{R}_C^n$ = position vector of the satellite n referenced to the central-body mean of J2000.0 frame

$\bar{R}_C^p$ = position vector of perturbing planetary body p referenced to the central-body mean of J2000.0 frame

μ_C = gravitational constant of the central body

μ_p = gravitational constant of the perturbing body

The following are the recommended values for these constants

μ_E = gravitational constant of the Earth (398600.4415 x 10^9 meters^3/sec^2 consistent with JGM-2)

μ_S = gravitational constant of the Sun (1.327124 x 10^{20} meters^3/sec^2)

μ_M = gravitational constant of the Moon (4.902799 x 10^{12} meters^3/sec^2)

μ_{Mars} = gravitational constant of Mars (4.2828286588769 x 10^{13} meters^3/sec^2)

μ_{Venus} = gravitational constant of Venus (3.2485876561687 x 10^{14} meters^3/sec^2)

$\mu_{Jupiter}$ = gravitational constant of Jupiter (1.2671259708179 x 10^{17} meters^3/sec^2)

μ_{Saturn} = gravitational constant of Saturn (3.793951970883 x 10^{16} meters^3/sec^2)

Three models are available for computing the positions of the Sun and Moon: a low precision method based on an article by by Van Flandern and Pulkkinen (Reference 11), a more precise method developed by Steven Moshier (Reference 26), and a high-precision method using Chebyshev coefficients extracted from a JPL Definitive Ephemeris (DE) file and saved in memory. These methods are described in Section 4.1.1.1, 4.1.1.2, and 4.1.1.3. The precise method developed by Moshier and DE method are also used to compute the positions of the other planets. Note that both models provide the Sun, Moon, or planetary positions referenced to the Earth-centered mean of J2000.0 frame and therefore must be transformed to the central-body frame if the central body is not the Earth, using the transformation defined in Section 3.2.11. In addition, the Moon, Sun, planetary and asteroid positions can be read in on a file.

4.1.1.1 Low Precision Planetary Ephemeris

The mean of date positions of the Sun and the Moon are determined by evaluating the low-precision (i.e., approximately 1 minute of arc) series expansions for the mean of date coordinates provided in an article by Van Flandern and Pulkkinen (Reference 11). The associated velocities are computed using finite differencing of the position vectors. Formulas for the positions of the planets are also provided in Reference 11; however, only the components relevant to the positions of the Sun and Moon are implemented in GEONS. This low-precision method is computationally more efficient than the more precise method and sufficiently accurate for use in GEONS navigation processing of near-Earth satellites. Reference 12 presents an approach for augmenting the algorithm presented above to provide a solar position accuracy of better than 10 arc-seconds.

In the following equations, the time t_{TT} is expressed as the number of days measured from the standard epoch, 2000 January 1.5 Terrestrial Time (TT) (Julian date of 2,451,545.0). Therefore,

$$t_{TT} = JD_{TT} - 2451545.0 \qquad (4.1\text{-}9)^*$$

where JD_{TT} is the given Julian date TT including fractional days.

The time parameter T, used as a polynomial variable, is the time in Julian centuries from the epoch B1900.0, given by

$$T = \frac{t_{TT}}{36525} + 1 \qquad (4.1\text{-}10)^*$$

The equation to convert a Gregorian calendar date to a Julian day number at Greenwich noon (JD) is as follows:

$$\begin{aligned} JD_{TT} = \; & \big(D - 32075 + 1461(Y + 4799)/4 + 336 \\ & - 3\big[(Y + 4899)/100\big]/4\big) - 0.5 + S/86400.0 \end{aligned} \qquad (4.1\text{-}11)^*$$

where Y is the year, D is the day of the year, and S is seconds of the day, TT. In this statement, Y, M, D, and S are input as integers, and a division by integers implies truncation of the quotients to integers (decimals are not carried).

For evaluation of the low precision ephemeris series, the difference between TT and UTC has neglible impact and is ignored.

In terms of the time t_{TT}, the following fundamental arguments are needed in the calculation of the solar and lunar positions:

- L represents the mean longitude
- F denotes the argument of latitude
- G denotes the mean anomaly

The expressions for each fundamental argument, A_j, given below, are in units of revolutions (one revolution equals 360 degrees). For practical calculations, the integral number of revolutions should be discarded.

Moon

$$A_1 = L_M = 0.606434 + 0.03660110129\ t_{TT} \qquad (4.1\text{-}12)^*$$

$$A_2 = G_M = 0.374897 + 0.03629164709\ t_{TT} \qquad (4.1\text{-}13)^*$$

$$A_3 = F_M = 0.259091 + 0.03674819520\ t_{TT} \qquad (4.1\text{-}14)^*$$

$$A_4 = D = L_M - L_S = -0.172638 + 0.03386319198\ t_{TT} \qquad (4.1\text{-}15)^*$$

$$A_5 = \Omega_M = L_M - F_M = 0.347343 - 0.00014709391\ t_{TT} \qquad (4.1\text{-}16)^*$$

Sun

$$A_7 = L_S = 0.779072 + 0.00273790931\ t_{TT} \qquad (4.1\text{-}17)^*$$

$$A_8 = G_S = 0.993126 + 0.00273777850\ t_{TT} \qquad (4.1\text{-}18)^*$$

Venus

$$A_{12} = L_2 = 0.505498 + 0.00445046867\ t_{TT} \quad (4.1\text{-}19)^*$$

$$A_{13} = G_2 = 0.140023 + 0.00445036173\ t_{TT} \quad (4.1\text{-}20)^*$$

Mars

$$A_{16} = G_4 = 0.053856 + 0.00145561327\ t_{TT} \quad (4.1\text{-}21)^*$$

Jupiter

$$A_{19} = G_5 = 0.056531 + 0.00023080893\ t_{TT} \quad (4.1\text{-}22)^*$$

Only the fundamental arguments needed to calculate the positions of the Sun and Moon (Reference 11) are given above (thus the absence of some argument numbers). The quantity D is the mean elongation of the Moon from the Sun, and Ω_M is the longitude of the lunar ascending nodes. Only those planets that have significant perturbation effects on the orbits of the Sun and Moon are included in the series expansions.

The geocentric equatorial coordinates are the right ascension, a, declination, δ, and geocentric distance, ρ. These coordinates are expressed in terms of a compact series denoted by U, V, and W, as follows:

$$a = L + \sin^{-1}\left[\frac{W}{\sqrt{U - V^2}}\right] \quad (4.1\text{-}23)^*$$

$$\delta = \sin^{-1}\left(\frac{V}{\sqrt{U}}\right) \quad (4.1\text{-}24)^*$$

$$\rho = \overline{\Delta}\sqrt{U} \quad (4.1\text{-}25)^*$$

In Equation (4.1-23), L is understood to be L_M for the Moon and L_S for the Sun. The scaling factor in Equation (4.1-25), $\overline{\Delta}$, is equal to 1.00021 astronomical units for the Sun and equal to 60.40974 in units of equatorial Earth radii for the Moon. The corresponding position vector in the mean of date coordinate frame is given by

$$\begin{bmatrix} X \\ Y \\ Z \end{bmatrix} = \rho \begin{bmatrix} \cos\delta \quad \cos a \\ \cos\delta \quad \sin a \\ \sin\delta \end{bmatrix} \quad (4.1\text{-}26)^*$$

The mean of J2000.0 vectors are computed using transformation matrix A given in Section 3.2.1.

The series for U, V, and W in Equations (4.1-23) through (4.1-25) is presented in the form

$$\sum_i c_i T^{n_i} \begin{matrix} \sin \\ or \\ \cos \end{matrix} \left(\sum_j b_j A_j \right) \qquad (4.1\text{-}27)^*$$

The coefficients c_i, n_i, and b_j are presented in Tables 4-1 and 4-2, which have been extracted from Reference 11. The parameters A_j are fundamental arguments [Equations (4.1-12) through (4.1-22)] calculated for the required time. As an example, the U series for the Sun from Table 4-1 would be the following:

$$\begin{aligned} U = {} & 1 - 0.03349 \cos G_S - 0.00014 \cos 2G_S \\ & - 0.00008T \cos G_S - 0.00003 \sin (G_S - G_5) \end{aligned} \qquad (4.1\text{-}28)^*$$

The value of T can be evaluated using Equation (4.1-10), and the fundamental arguments G_S and G_5 corresponding to T can be calculated using the expressions given in Equations (4.1-17) and (4.1-22), respectively.

Table 4-1. Trigonometric Series for the Sun

SERIES	COEFFICIENT	POWER OF T	TRIGONOMETRIC FUNCTIONS AND COEFFICIENTS (b_j) FOR FUNDAMENTAL ARGUMENTS (A_j)							
	(c_i)	(n_i)	SIN/COS	j = 1	j = 5	j = 7	j = 8	j = 13	j = 16	j = 19
V	0.39785	0	SIN	0	0	1	0	0	0	0
	–0.01000	0	SIN	0	0	1	–1	0	0	0
	0.00333	0	SIN	0	0	1	1	0	0	0
	–0.00021	1	SIN	0	0	1	0	0	0	0
	0.00004	0	SIN	0	0	1	2	0	0	0
	–0.00004	0	COS	0	0	1	0	0	0	0
	–0.00004	0	SIN	0	1	–1	0	0	0	0
	0.00003	1	SIN	0	0	1	–1	0	0	0
U	1.00000	0	COS	0	0	0	0	0	0	0
	–0.03349	0	COS	0	0	0	1	0	0	0
	–0.00014	0	COS	0	0	0	2	0	0	0
	0.00008	1	COS	0	0	0	1	0	0	0
	–0.00003	0	SIN	0	0	0	1	0	0	–1
W	–0.04129	0	SIN	0	0	2	0	0	0	0
	0.03211	0	SIN	0	0	0	1	0	0	0
	0.00104	0	SIN	0	0	2	–1	0	0	0
	–0.00035	0	SIN	0	0	2	1	0	0	0
	–0.00010	0	COS	0	0	0	0	0	0	0
	–0.00008	1	SIN	0	0	0	1	0	0	0
	–0.00008	0	SIN	0	1	0	0	0	0	0
	0.00007	0	SIN	0	0	0	2	0	0	0
	0.00005	1	SIN	0	0	2	0	0	0	0
	0.00003	0	SIN	1	0	–1	0	0	0	0
	–0.00002	0	COS	0	0	0	1	0	0	–1
	0.00002	0	SIN	0	0	0	4	0	–8	3
	–0.00002	0	SIN	0	0	0	1	–1	0	0
	–0.00002	0	COS	0	0	0	2	–2	0	0

Table 4-2. Trigonometric Series for the Moon (1 of 4)

SERIES	COEFFICIENT	POWER OF T	TRIGONOMETRIC FUNCTIONS AND COEFFICIENTS (b_j) FOR FUNDAMENTAL ARGUMENTS (A_j)							
	(c_i)	(n_i)	SIN/COS	j = 2	j = 3	j = 4	j = 5	j = 7	j = 8	j = 12
V	0.39558	0	SIN	0	1	0	1	0	0	0
	0.08200	0	SIN	0	1	0	0	0	0	0
	0.03257	0	SIN	1	–1	0	–1	0	0	0
	0.01092	0	SIN	1	1	0	1	0	0	0
	0.00666	0	SIN	1	–1	0	0	0	0	0
	–0.00644	0	SIN	1	1	–2	1	0	0	0
	–0.00331	0	SIN	0	1	–2	1	0	0	0
	–0.00304	0	SIN	0	1	–2	0	0	0	0
	–0.00240	0	SIN	1	–1	–2	–1	0	0	0
	0.00226	0	SIN	1	1	0	0	0	0	0
	–0.00108	0	SIN	1	1	–2	0	0	0	0
	–0.00079	0	SIN	0	1	0	–1	0	0	0
	0.00078	0	SIN	0	1	2	1	0	0	0
	0.00066	0	SIN	0	1	0	1	0	–1	0
	–0.00062	0	SIN	0	1	0	1	0	1	0
	–0.00050	0	SIN	1	–1	–2	0	0	0	0
	0.00045	0	SIN	2	1	0	1	0	0	0
	–0.00031	0	SIN	2	1	–2	1	0	0	0
	–0.00027	0	SIN	1	1	–2	1	0	1	0
	–0.00024	0	SIN	0	1	–2	1	0	1	0
	–0.00021	1	SIN	0	1	0	1	0	0	0
	0.00018	0	SIN	0	1	–1	1	0	0	0
	0.00016	0	SIN	0	1	2	0	0	0	0
	0.00016	0	SIN	1	–1	0	–1	0	–1	0
	–0.00016	0	SIN	2	–1	0	–1	0	0	0
	–0.00015	0	SIN	0	1	–2	0	0	1	0
	–0.00012	0	SIN	1	–1	–2	–1	0	1	0
	–0.00011	0	SIN	1	–1	0	–1	0	1	0
	0.00009	0	SIN	1	1	0	1	0	–1	0
	0.00009	0	SIN	2	1	0	0	0	0	0
	0.00008	0	SIN	2	–1	0	0	0	0	0
	0.00008	0	SIN	1	1	2	1	0	0	0
	–0.00008	0	SIN	0	3	–2	1	0	0	0
	0.00007	0	SIN	1	–1	2	0	0	0	0
	–0.00007	0	SIN	2	–1	–2	–1	0	0	0
	–0.00007	0	SIN	1	1	0	1	0	1	0
	–0.00006	0	SIN	0	1	1	1	0	0	0
	0.00006	0	SIN	0	1	–2	0	0	–1	0
	0.00006	0	SIN	1	–1	0	1	0	0	0
	0.00006	0	SIN	0	1	2	1	0	–1	0
	–0.00005	0	SIN	1	1	–2	0	0	1	0
	–0.00004	0	SIN	2	1	–2	0	0	0	0
	0.00004	0	SIN	1	–3	0	–1	0	0	0
	0.00004	0	SIN	1	–1	0	0	0	–1	0
	–0.00003	0	SIN	1	–1	0	0	0	1	0
	0.00003	0	SIN	0	1	–1	0	0	0	0

Table 4-2. Trigonometric Series for the Moon (2 of 4)

SERIES	COEFFICIENT	POWER OF T	TRIGONOMETRIC FUNCTIONS AND COEFFICIENTS (b_j) FOR FUNDAMENTAL ARGUMENTS (A_j)							
	(c_i)	(n_i)	SIN/COS	j = 2	j = 3	j = 4	j = 5	j = 7	j = 8	j = 12
V	0.00003	0	SIN	0	1	–2	1	0	–1	0
(Cont'd)	–0.00003	0	SIN	0	1	–2	–1	0	0	0
	0.00003	0	SIN	1	1	–2	1	0	–1	0
	0.00003	0	SIN	0	1	0	0	0	–1	0
	–0.00003	0	SIN	0	1	–1	1	0	–1	0
	–0.00002	0	SIN	1	–1	–2	0	0	1	0
	–0.00002	0	SIN	0	1	0	0	0	1	0
	0.00002	0	SIN	1	1	–1	1	0	0	0
	–0.00002	0	SIN	1	1	0	–1	0	0	0
	0.00002	0	SIN	3	1	0	1	0	0	0
	–0.00002	0	SIN	2	–1	–4	–1	0	0	0
	0.00002	0	SIN	1	–1	–2	–1	0	–1	0
	–0.00002	1	SIN	1	–1	0	–1	0	0	0
	–0.00002	0	SIN	1	–1	–4	–1	0	0	0
	–0.00002	0	SIN	1	1	–4	0	0	0	0
	–0.00002	0	SIN	2	–1	–2	0	0	0	0
	0.00002	0	SIN	1	1	2	0	0	0	0
	0.00002	0	SIN	1	1	0	0	0	–1	0
U	1.00000	0	COS	0	0	0	0	0	0	0
	–0.10828	0	COS	1	0	0	0	0	0	0
	–0.01880	0	COS	1	0	–2	0	0	0	0
	–0.01479	0	COS	0	0	2	0	0	0	0
	0.00181	0	COS	2	0	–2	0	0	0	0
	–0.00147	0	COS	2	0	0	0	0	0	0
	–0.00105	0	COS	0	0	2	0	0	–1	0
	–0.00075	0	COS	1	0	–2	0	0	1	0
	–0.00067	0	COS	1	0	0	0	0	–1	0
	0.00057	0	COS	0	0	1	0	0	0	0
	0.00055	0	COS	1	0	0	0	0	1	0
	–0.00046	0	COS	1	0	2	0	0	0	0
	0.00041	0	COS	1	–2	0	0	0	0	0
	0.00024	0	COS	0	0	0	0	0	1	0
	0.00017	0	COS	0	0	2	0	0	1	0
	0.00013	0	COS	1	0	–2	0	0	–1	0
	–0.00010	0	COS	1	0	–4	0	0	0	0
	–0.00009	0	COS	0	0	1	0	0	1	0
	0.00007	0	COS	2	0	–2	0	0	1	0
	0.00006	0	COS	3	0	–2	0	0	0	0
	0.00006	0	COS	0	2	–2	0	0	0	0
	–0.00005	0	COS	0	0	2	0	0	–2	0
	–0.00005	0	COS	2	0	–4	0	0	0	0
	0.00005	0	COS	1	2	–2	0	0	0	0
	–0.00005	0	COS	1	0	–1	0	0	0	0
	–0.00004	0	COS	1	0	2	0	0	–1	0
	–0.00004	0	COS	3	0	0	0	0	0	0
	–0.00003	0	COS	1	0	–4	0	0	1	0
	–0.00003	0	COS	2	–2	0	0	0	0	0
	–0.00003	0	COS	0	2	0	0	0	0	0

Table 4-2. Trigonometric Series for the Moon (3 of 4)

SERIES	COEFFICIENT	POWER OF T	TRIGONOMETRIC FUNCTIONS AND COEFFICIENTS (b_j) FOR FUNDAMENTAL ARGUMENTS (A_j)							
	(c_i)	(n_i)	SIN/COS	j = 2	j = 3	j = 4	j = 5	j = 7	j = 8	j = 12
W	0.10478	0	SIN	1	0	0	0	0	0	0
	–0.04105	0	SIN	0	2	0	2	0	0	0
	–0.02130	0	SIN	1	0	–2	0	0	0	0
	–0.01779	0	SIN	0	2	0	1	0	0	0
	0.01774	0	SIN	0	0	0	1	0	0	0
	0.00987	0	SIN	0	0	2	0	0	0	0
	–0.00338	0	SIN	1	–2	0	–2	0	0	0
	–0.00309	0	SIN	0	0	0	0	0	1	0
	–0.00190	0	SIN	0	2	0	0	0	0	0
	–0.00144	0	SIN	1	0	0	1	0	0	0
	–0.00144	0	SIN	1	–2	0	–1	0	0	0
	–0.00113	0	SIN	1	2	0	2	0	0	0
	–0.00094	0	SIN	1	0	–2	0	0	1	0
	–0.00092	0	SIN	2	0	–2	0	0	0	0
	0.00071	0	SIN	0	0	2	0	0	–1	0
	0.00070	0	SIN	2	0	0	0	0	0	0
	0.00067	0	SIN	1	2	–2	2	0	0	0
	0.00066	0	SIN	0	2	–2	1	0	0	0
	–0.00066	0	SIN	0	0	2	1	0	0	0
	0.00061	0	SIN	1	0	0	0	0	–1	0
	–0.00058	0	SIN	0	0	1	0	0	0	0
	–0.00049	0	SIN	1	2	0	1	0	0	0
	–0.00049	0	SIN	1	0	0	–1	0	0	0
	–0.00042	0	SIN	1	0	0	0	0	1	0
	0.00034	0	SIN	0	2	–2	2	0	0	0
	–0.00026	0	SIN	0	2	–2	0	0	0	0
	0.00025	0	SIN	1	–2	–2	–2	0	0	0
	0.00024	0	SIN	1	–2	0	0	0	0	0
	0.00023	0	SIN	1	2	–2	1	0	0	0
	0.00023	0	SIN	1	0	–2	–1	0	0	0
	0.00019	0	SIN	1	0	2	0	0	0	0
	0.00012	0	SIN	1	0	–2	0	0	–1	0
	0.00011	0	SIN	1	0	–2	1	0	0	0
	0.00011	0	SIN	1	–2	–2	–1	0	0	0
	–0.00010	0	SIN	0	0	2	0	0	1	0
	0.00009	0	SIN	1	0	–1	0	0	0	0
	0.00008	0	SIN	0	0	1	0	0	1	0
	–0.00008	0	SIN	0	2	2	2	0	0	0
	–0.00008	0	SIN	0	0	0	2	0	0	0
	–0.00007	0	SIN	0	2	0	2	0	–1	0
	0.00006	0	SIN	0	2	0	2	0	1	0
	–0.00005	0	SIN	1	2	0	0	0	0	0
	0.00005	0	SIN	3	0	0	0	0	0	0
	–0.00005	0	SIN	1	0	0	0	16	0	–18
	–0.00005	0	SIN	2	2	0	2	0	0	0
	0.00004	1	SIN	0	2	0	2	0	0	0

Table 4-2. Trigonometric Series for the Moon (4 of 4)

SERIES	COEFFICIENT	POWER OF T	TRIGONOMETRIC FUNCTIONS AND COEFFICIENTS (b_j) FOR FUNDAMENTAL ARGUMENTS (A_j)							
	(c_i)	(n_i)	SIN/COS	j = 2	j = 3	j = 4	j = 5	j = 7	j = 8	j = 12
W	0.00004	0	COS	1	0	0	0	16	0	–18
(Cont'd)	–0.00004	0	SIN	1	–2	2	0	0	0	0
	–0.00004	0	SIN	1	0	–4	0	0	0	0
	–0.00004	0	SIN	3	0	–2	0	0	0	0
	–0.00004	0	SIN	0	2	2	1	0	0	0
	–0.00004	0	SIN	0	0	2	–1	0	0	0
	–0.00003	0	SIN	0	0	0	0	0	2	0
	–0.00003	0	SIN	1	0	–2	0	0	2	0
	0.00003	0	SIN	0	2	–2	1	0	1	0
	–0.00003	0	SIN	0	0	2	1	0	–1	0
	0.00003	0	SIN	2	2	–2	2	0	0	0
	0.00003	0	SIN	0	0	2	0	0	–2	0
	–0.00003	0	SIN	2	0	–2	0	0	1	0
	0.00003	0	SIN	1	2	–2	2	0	1	0
	–0.00003	0	SIN	2	0	–4	0	0	0	0
	0.00002	0	SIN	0	2	–2	2	0	1	0
	–0.00002	0	SIN	2	2	0	1	0	0	0
	–0.00002	0	SIN	2	0	0	–1	0	0	0
	0.00002	1	COS	1	0	0	0	16	0	–18
	0.00002	0	SIN	0	0	4	0	0	0	0
	–0.00002	0	SIN	0	2	–1	2	0	0	0
	–0.00002	0	SIN	1	2	–2	0	0	0	0
	–0.00002	0	SIN	2	0	0	1	0	0	0
	–0.00002	0	SIN	2	–2	0	–1	0	0	0
	0.00002	0	SIN	1	0	2	0	0	–1	0
	0.00002	0	SIN	2	0	0	0	0	–1	0
	–0.00002	0	SIN	1	0	–4	0	0	1	0
	0.00002	1	SIN	1	0	0	0	16	0	–18
	–0.00002	0	SIN	1	–2	0	–2	0	–1	0
	0.00002	0	SIN	2	–2	0	–2	0	0	0
	–0.00002	0	SIN	1	0	2	1	0	0	0
	–0.00002	0	SIN	1	–2	2	–1	0	0	0

4.1.1.2 Intermediate Precision Planetary Ephemeris

A more precise analytical planetary ephemeris is available for propagation of high-Earth orbits, e.g. geosynchronous and higher. This method consists of the evaluation of series developed by Steven Moshier (Reference 26). It uses tables of coefficients derived by a least-squares fit to the Jet Propulsion Laboratory's DE404 ephemeris and is therefore referenced to the ICRF. The periodic frequencies used were determined by spectral analysis of the ephemeris and comparison with other analytical planetary theories. The least-squares fit covers the interval from –1350 to +3000 for the inner planets.

The method uses numerical tables to compute the geocentric polar coordinates (i.e. longitude, latitude, and distance) of the Moon referenced to the mean equinox and ecliptic of date and the heliocentric polar coordinates of the Earth-Moon barycenter and the planets referenced to the mean ecliptic of J2000. The series are evaluated in the following order:

1. The geocentric Cartesian coordinates of the Moon, $\overline{R}^{E}_{Moon}$, are computed from the geocentric polar coordinates and rotated from the Mean of Date to the Mean of J2000 frame.

2. The heliocentric ecliptic Cartesian coordinates of the Earth-Moon barycenter, $\overline{R}^{S}_{EMB}$, are computed from the heliocentric polar coordinates and then rotated to the mean equator of J2000 frame. The geocentric Sun vector is then computed as follows:

$$\overline{R}^{E}_{Sun} = -\overline{R}^{S}_{EMB} + \left[\frac{m_{Moon}}{m_{Moon} + m_{Earth}}\right]\overline{R}^{E}_{Moon} \qquad \text{(4.1-28a)*}$$

3. The heliocentric ecliptic Cartesian coordinates of the planets are computed from the heliocentric polar coordinates and then rotated to the mean equator of J2000 frame and translated to the geocentric frame using the geocentric position vector of the Sun, $\overline{R}^{E}_{Sun}$.

4. The associated velocities are computed using finite differencing of the position vectors.

The method used requires the Julian date in TT. The TT calendar date corresponding to the current UTC time is computed using Equation (3.3-30) given in Section 3.3.5.

$$TT = UTC + 1.^{s}0\ n + 32.184 \text{ seconds} \qquad \text{(4.1-28b)*}$$

where n equals 10 plus the total number of elapsed leap seconds since 1972. The equation to convert a Gregorian calendar date to a Julian day number at Greenwich noon (JD) is as follows:

$$\begin{aligned} JD_{TT} = \ & \big(D - 32075 + 1461(Y + 4799)/4 + 336 \\ & - 3\big[(Y + 4899)/100\big]/4\big) - 0.5 + S/86400.0 \end{aligned} \qquad \text{(4.1-28c)*}$$

where Y is the year, D is the day of the year, and S is seconds of the day, TT. In this statement, *Y, M, D,* and *S* are input as integers, and a division by integers implies truncation of the quotients to integers (decimals are not carried).

Over the 2000 to 2500 time period, the root-mean-square error for the Moon' position is approximately 0.06 arc seconds in longitude, 0.04 arc seconds in latitude, and 60 meters in distance. For time periods near J2000, comparisons with the high precision lunar ephemeris available from the JPL DE405 Ephemeris indicate a total position difference on the order of 100 to 200 meters.

4.1.1.3 High Precision Planetary Ephemeris

The capability is also available to use a high precision planetary ephemeris consisting of Chebyshev polynomial coefficients for each position component extracted from a JPL series 4xx DE for a specific time span for any of the following bodies: Mercury, Venus, Earth-Moon barycenter, Mars, Jupiter, Saturn, Uranus, Neptune, Pluto, Sun, and Moon (geocentric). The coefficients for the planets represent the solar system barycentric (SSB) positions of the centers of the planetary systems with respect to the International Celestial Reference Frame (ICRF) referenced to Barycentric Dynamical Time (TDB). Reference 51 provides a detailed description

of the contents of these files and sample subroutines for retrieving their contents. Chebyshev polynomial coefficients from DE421 are available in the GEONS flight software and the capability is available to update to a later DE version, when available.

Each position and corresponding velocity component is computed as follows:

$$\begin{aligned} x(t_{TT}) &= \sum_{n=0}^{N} c_n T_n(\tau) \\ \dot{x}(t_{TT}) &= \sum_{n=1}^{N} c_n \dot{T}_n(\tau) \end{aligned} \qquad \text{(4.1-28d)*}$$

where t_{TT} is the request time in TT (computed using Equations 4.1-28b and 4.1-28c), c_n are the associated Chebyshev coefficients, $T_n(\tau)$ are the Chebyshev polynomials of the first kind, and N is the degree of the expansion. The Chebyshev polynomials are computed using the following recursion formula:

$$T_n(\tau) = 2\tau T_{n-1}(\tau) - T_{n-2}(\tau), \quad n = 2,3,... \qquad \text{(4.1-28e)*}$$

where $T_0(\tau) = 1$ and $T_1(\tau) = \tau$.

The applicable range of interpolation for the Chebyshev time parameter τ is $-1 \le \tau \le 1$, which is computed as follows:

$$\tau = \frac{2\Delta t_{TT}}{\Delta T_C} - 1 \qquad \text{(4.1-28f)*}$$

where $\Delta t_{TT} = t_{TT} - T_C^{Start}$ is the elapsed time from the start time of the polynomial fit interval, T_C^{Start}, and ΔT_C is the length associated Chebyshev polynomial fit interval. The fit intervals are as follows: 4 days for the Moon, 8 days for Mercury, 16 days for the Sun, Venus, and the Earth-Moon barycenter, and 32 days for the remaining planets.

The derivatives of the Chebyshev polynomials are computed by differentiating Equation (4.1-28e) by time:

$$\dot{T}_n(\tau) = \left[2\dot{\tau}T_{n-1}(\tau) + 2\tau\dot{T}_{n-1}(\tau) - \dot{T}_{n-2}(\tau)\right] \quad n = 2,3,\ldots \qquad \text{(4.1-28g)*}$$

where $\dot{T}_1(\tau) = \dot{\tau}$, $\dot{T}_2(\tau) = 4\dot{\tau}\tau$, and

$$\dot{\tau} = \frac{2}{\Delta T_C} \qquad \text{(4.1-28h)*}$$

For use in GEONS, the planetary positions and velocities and velocities are transformed to the mean of J2000.0 ECI frame as follows:

$$\begin{aligned} \overline{R}_{Planet\ ECI} &= \overline{R}_{Planet\ SSB} - \overline{R}_{Earth\ SSB} \\ \dot{\overline{R}}_{Planet\ ECI} &= \dot{\overline{R}}_{Planet\ SSB} - \dot{\overline{R}}_{Earth\ SSB} \end{aligned} \qquad \text{(4.1-28i)*}$$

where

$$\bar{R}_{Earth_{SSB}} = \bar{R}_{EMB_{SSB}} - \left[\frac{m_{Moon}}{m_{Moon}+m_{Earth}}\right]\bar{R}_{Moon_{ECI}}$$

$$\dot{\bar{R}}_{Earth_{SSB}} = \dot{\bar{R}}_{EMB_{SSB}} - \left[\frac{m_{Moon}}{m_{Moon}+m_{Earth}}\right]\dot{\bar{R}}_{Moon_{ECI}}$$

Or equivalently

$$\bar{R}_{Earth_{SSB}} = \bar{R}_{EMB_{SSB}} - \left[\frac{\bar{R}_{Moon_{ECI}}}{1+R_{E/M}}\right]$$

$$\dot{\bar{R}}_{Earth_{SSB}} = \dot{\bar{R}}_{EMB_{SSB}} - \left[\frac{\dot{\bar{R}}_{Moon_{ECI}}}{1+R_{E/M}}\right] \qquad (4.1\text{-}28j)^*$$

where $\overline{R}_{Planet\ _{SSB}}$ and $\dot{\overline{R}}_{Planet\ _{SSB}}$ are the position and velocity of the Planet in the Mean of J2000.0 SSB frame, $\overline{R}_{EMB\ _{SSB}}$ and $\dot{\overline{R}}_{EMB\ _{SSB}}$ are the position and velocity of the Earth-Moon barycenter in the Mean of J2000.0 SSB frame, and $\overline{R}_{Moon\ _{ECI}}$ and $\dot{\overline{R}}_{Moon\ _{ECI}}$ are the position and velocity of the Moon in the Mean of J2000.0 geocentric frame, which are computed by evaluating Equation (4.1-28d). $\overline{R}_{Earth\ _{SSB}}$ and $\dot{\overline{R}}_{Earth\ _{SSB}}$ are the position and velocity of the Earth in the Mean of J2000.0 SSB frame computed using Equation (4.1-28j). $R_{E/M}$ is the Earth/Moon mass ratio equal to 0.813005600000000044e+02.

4.1.2 Nonspherical Gravitational Acceleration

GEONS includes the capability to model nonspherical gravitational effects from the Earth or non-Earth central body (e.g. Moon, other planets or asteroid). The inertial acceleration vector resulting from nonspherical gravitational effects is given by the gradient of the nonspherical terms in the gravitational potential function, ψ_{NS}, as follows:

$$\overline{a}_{NS} = \nabla \psi_{NS} \qquad (4.1\text{-}29)^*$$

The default geopotential model is the 30x30 Joint Gravity Model-2 (JGM-2). The 360x360 Earth Gravitational Model 96 (EGM96) geopotential model is also available in GEONS 3.0. The default lunar potential model is the 100x100 Lunar Prospector (LP) 100K model. To avoid numerical precision problems, the JGM-2 gravitational potential is computed using scaled coefficients with unnormalized associated Legendre functions (Section 4.1.2.1); all other Earth, lunar, and planetary gravitational potentials are computed using normalized coefficients with normalized associated Legendre functions (Section 4.1.2.2).

4.1.2.1 Nonspherical Gravitational Acceleration of the Earth Using Unnormalized Coefficients (replaced with normalized algorithm in GEONS 3.0)

This algorithm is used with the default Joint Gravity Model-2 (JGM-2) 30x30 geopotential model. The nonspherical geopotential, ψ_{NS_E}, is given by

$$\psi_{NS_E}(r,\phi,\lambda) = \frac{\mu}{r}\sum_{n=2}^{N} C_n^0\left(\frac{R_e}{r}\right)^n P_n^0(\sin\phi) + \frac{\mu}{r}\sum_{n=2}^{N}\sum_{m=1}^{n}\left[\frac{R_e}{r}\right]^n P_n^m(\sin\phi)\left[S_n^m \sin(m\lambda) + C_n^m \cos(m\lambda)\right] \tag{4.1-30}$$

where

r = magnitude of the vector from the Earth's center of mass to the satellite

ϕ = geocentric latitude

λ = geocentric longitude (measured east from the prime meridian)

μ = gravitational constant of the Earth (398600.4415 x 10^9 meters^3/second^2 for consistency with the JGM-2 gravitational model)

R_e = equatorial radius of the Earth

N = maximum degree included in the expansion

$P_n^m(sin\phi)$ = associated Legendre function

$(S_n^m)_E$, $(C_n^m)_E$ = harmonic coefficients for the Earth (zonal harmonics for $m = 0$, sectoral harmonics for $m = n$, and tesseral harmonics for $n > m \neq 0$)
(Note: $J_n = -C_n^0$, where J are the zonal coefficients)

The first and second terms are the nonspherical potential due to the sum of zonal and tesseral harmonics, respectively. The term $n = 1$ is not present, since the origin of the coordinate system is placed at the center of mass of the Earth. For GEONS, the value of N, the maximum degree included in the expansion, will be an input parameter and will not exceed 30 for the Earth. The default geopotential model is the Joint Gravity Model-2 (JGM-2).

The Earth's gravitational coefficients and associated Legendre polynomials are scaled as follows:

$$\widetilde{C}_n^m = F(C_n^m)_E \tag{4.1-31}$$

$$\widetilde{S}_n^m = F(S_n^m)_E \tag{4.1-32}$$

$$\widetilde{P}_n^m = \frac{1}{F}P_n^m \tag{4.1-33}$$

The scaled coefficients and unnormalized associated Legendre functions are used in the calculations. The following nominal scale factor is used for JGM-2:

$$F = 10^{25} \tag{4.1-34}$$

Expressing the gradient in ECEF coordinates, $\bar{r}_b^T = (x_b, y_b, z_b)$ (see Section 3.1.3), the form for the inertial acceleration vector is obtained as follows:

$$\bar{a}_{NS_b E} = \begin{bmatrix} \ddot{x}_{NS_b} \\ \ddot{y}_{NS_b} \\ \ddot{z}_{NS_b} \end{bmatrix} = \frac{\partial \psi_{NS_E}}{\partial r}\left(\frac{\partial r}{\partial \bar{r}_b}\right)^T + \frac{\partial \psi_{NS_E}}{\partial \phi}\left(\frac{\partial \phi}{\partial \bar{r}_b}\right)^T + \frac{\partial \psi_{NS_E}}{\partial \lambda}\left(\frac{\partial \lambda}{\partial \bar{r}_b}\right)^T \tag{4.1-35}$$

where $\ddot{x}_{NS_b}$, $\ddot{y}_{NS_b}$, and $\ddot{z}_{NS_b}$ are the components of the inertial acceleration expressed in ECEF coordinates and not the acceleration with respect to the ECEF coordinate system. Thus, it is necessary to transform these components into the mean of J2000.0 coordinate system in which the spacecraft equations of motion are expressed.

This transformation is given by

$$\bar{a}_{NS_E} = C^T R_g^T B^T \bar{a}_{NS_b E} \tag{4.1-36}$$

where $R_g^T B^T$ transforms from ECEF to TOD coordinates and C^T transforms from TOD to mean of J2000.0 coordinates. Assuming that the geographic pole axis, $\hat{z}_b$, is aligned with the instantaneous spin axis, $\hat{z}$, of the TOD coordinate system, the $R_g^T B^T$ rotation reduces to $R^T(a_g)$, which is equivalent to replacing $(\bar{r}_b, x_b, y_b, z_b)$ in Equation (4.1-35) by $(\bar{r}, x, y, z)$, the TOD components, and calculating the longitude and latitude as follows:

$$\lambda = a - a_g \tag{4.1-37}*$$

$$\phi = \sin^{-1}\left(\frac{z}{r}\right) \tag{4.1-38}*$$

where

a = right ascension of the spacecraft $\left[a = \tan^{-1}(y/x)\right]$

a_g = TOD right ascension of Greenwich

The C^T rotation matrix is defined in Sections 3.2.1 and 3.2.1.

The inertial acceleration vector can then be written as

$$\bar{a}_{NS_E} = C^T \begin{bmatrix} \ddot{x}_{NS_{E_{TOD}}} \\ \ddot{y}_{NS_{E_{TOD}}} \\ \ddot{z}_{NS_{E_{TOD}}} \end{bmatrix} = C^T \left[\frac{\partial \psi_{NS_E}}{\partial r}\left(\frac{\partial r}{\partial \bar{r}}\right)^T + \frac{\partial \psi_{NS_E}}{\partial \phi}\left(\frac{\partial \phi}{\partial \bar{r}}\right)^T + \frac{\partial \psi_{NS_E}}{\partial \lambda}\left(\frac{\partial \lambda}{\partial \bar{r}}\right)^T \right] \tag{4.1-39}*$$

where the partial derivatives are evaluated using the TOD coordinates $(\bar{r}, x, y, z)$.

The partial derivatives of the nonspherical portion of the Earth's potential with respect to r, ϕ, and λ are given by

$$\frac{\partial \psi_{NS_E}}{\partial r} = -\frac{1}{r}\frac{\mu_E}{r}\sum_{n=2}^{N}\left(\frac{R_e}{r}\right)^n (n+1)\sum_{m=0}^{n}\left[\widetilde{C}_n^m \cos(m\lambda) + \widetilde{S}_n^m \sin(m\lambda)\right]\widetilde{P}_n^m(\sin\phi) \qquad (4.1\text{-}40)^*$$

$$\frac{\partial \psi_{NS_E}}{\partial \phi} = \frac{\mu_E}{r}\sum_{n=2}^{N}\left(\frac{R_e}{r}\right)^n \sum_{m=0}^{n}\left[\widetilde{C}_n^m \cos(m\lambda) + \widetilde{S}_n^m \sin(m\lambda)\right] \times\left[\widetilde{P}_n^{m+1}(\sin\phi) - m\tan\phi\,\widetilde{P}_n^m(\sin\phi)\right] \qquad (4.1\text{-}41)^*$$

$$\frac{\partial \psi_{NS_E}}{\partial \lambda} = \frac{\mu_E}{r}\sum_{n=2}^{N}\left(\frac{R_e}{r}\right)^n \sum_{m=0}^{n} m\left[\widetilde{S}_n^m \cos(m\lambda) - \widetilde{C}_n^m \sin(m\lambda)\right]\widetilde{P}_n^m(\sin\phi) \qquad (4.1\text{-}42)^*$$

The Legendre functions and the terms $\cos(m\lambda)$, $\sin(m\lambda)$, and $m\tan\phi$ are computed via recursion formulas, as follows:

$$\widetilde{P}_n^0(\sin\phi) = \frac{1}{n}\left[(2n-1)\sin\phi\,\widetilde{P}_{n-1}^0(\sin\phi) - (n-1)\widetilde{P}_{n-2}^0(\sin\phi)\right] \qquad (4.1\text{-}43)^*$$

$$\widetilde{P}_n^m(\sin\phi) = \widetilde{P}_{n-2}^m(\sin\phi) + (2n-1)\cos\phi\;\widetilde{P}_{n-1}^{m-1}(\sin\phi) \quad (m \neq 0;\ m < n) \qquad (4.1\text{-}44)^*$$

$$\widetilde{P}_n^m(\sin\phi) = 0 \quad (m > n) \qquad (4.1\text{-}45)^*$$

$$\widetilde{P}_n^n(\sin\phi) = (2n-1)\cos\phi\;\widetilde{P}_{n-1}^{n-1}(\sin\phi) \quad (m \neq 0;\ m = n) \qquad (4.1\text{-}46)^*$$

with initial values

$$\widetilde{P}_0^0(\sin\phi) = \frac{1}{F}P_0^0(\sin\phi) = \frac{1}{F} \qquad (4.1\text{-}47)^*$$

$$\widetilde{P}_1^0(\sin\phi) = \frac{1}{F}P_1^0(\sin\phi) = \frac{\sin\phi}{F} \qquad (4.1\text{-}48)^*$$

$$\widetilde{P}_1^1(\sin\phi) = \frac{1}{F}P_1^1(\sin\phi) = \frac{\cos\phi}{F} \qquad (4.1\text{-}49)^*$$

and

$$\sin(m\lambda) = 2\cos\lambda\sin\left[(m-1)\lambda\right] - \sin\left[(m-2)\lambda\right];\ m \geq 2 \qquad (4.1\text{-}50)^*$$

$$\cos(m\lambda) = 2\cos\lambda\cos\left[(m-1)\lambda\right] - \cos\left[(m-2)\lambda\right];\ m \geq 2 \qquad (4.1\text{-}51)^*$$

$$m\tan\phi = (m-1)\tan\phi + \tan\phi \qquad (4.1\text{-}52)^*$$

The partial derivatives of r, ϕ, and λ, with respect to x, y, and z, are computed from the expressions

$$\frac{\partial r}{\partial \bar{r}} = \frac{\bar{r}^T}{r} \tag{4.1-53}$$

$$\frac{\partial \phi}{\partial \bar{r}} = \frac{1}{\sqrt{x^2 + y^2}} \left[-\frac{z\,\bar{r}^T}{r^2} + \frac{\partial z}{\partial \bar{r}} \right] \tag{4.1-54}$$

$$\frac{\partial \lambda}{\partial \bar{r}} = \frac{1}{x^2 + y^2} \left[x\frac{\partial y}{\partial \bar{r}} - y\frac{\partial x}{\partial \bar{r}} \right] \tag{4.1-55}$$

where the position partial derivatives are equal to the following:

$$\frac{\partial x}{\partial \bar{r}} = (1, 0, 0) \qquad \frac{\partial y}{\partial \bar{r}} = (0, 1, 0) \qquad \frac{\partial z}{\partial \bar{r}} = (0, 0, 1)$$

Substituting Equations (4.1-53) through (4.1-55) into Equation (4.1-39) yields the TOD components of the acceleration vector

$$\ddot{x}_{NS_{TOD}} = \left(\frac{1}{r}\frac{\partial \psi_{NS_E}}{\partial r} - \frac{z}{r^2\sqrt{x^2 + y^2}}\frac{\partial \psi_{NS_E}}{\partial \phi} \right) x - \left(\frac{1}{x^2 + y^2}\frac{\partial \psi_{NS_E}}{\partial \lambda} \right) y \tag{4.1-56}*$$

$$\ddot{y}_{NS_{TOD}} = \left(\frac{1}{r}\frac{\partial \psi_{NS_E}}{\partial r} - \frac{z}{r^2\sqrt{x^2 + y^2}}\frac{\partial \psi_{NS_E}}{\partial \phi} \right) y + \left(\frac{1}{x^2 + y^2}\frac{\partial \psi_{NS_E}}{\partial \lambda} \right) x \tag{4.1-57}*$$

$$\ddot{z}_{NS_{TOD}} = \left(\frac{1}{r}\frac{\partial \psi_{NS_E}}{\partial r} \right) z + \frac{\sqrt{x^2 + y^2}}{r^2}\frac{\partial \psi_{NS_E}}{\partial \phi} \tag{4.1-58}*$$

which are then transformed to the mean of J2000.0 reference frame using Equation (4.1-39).

4.1.2.2 Nonspherical Gravitational Acceleration Using Normalized Coefficients

Note that in GEONS 3.0, all nonspherical gravitational acceleration are computed using this algorithm. The original baseline JGM-2 unnormalized coefficients are re-scaled by the 1e25 factor and normalized according to the normalized Legendre polynomial scaling. Note that the recursion formula for computing the acceleration due to non-spherical gravity given below is singular at the poles (x = y = 0 in planet fixed coordinates). A different recursion should be used for any mission with an inclination close to 90 deg.

The normalized associated Legendre functions are defined in terms of the unnormalized functions as follows

$$\overline{P}_n^m(\sin\phi) = N(n,m)P_n^m(\sin\phi) \tag{4.1.2-1}$$

where the normalization factor $N(n,m)$ is given by

$$N(n,m) \equiv \left[\frac{(n-m)!(2n+1)(2-\delta_{m,0})}{(n+m)!}\right]^{\frac{1}{2}} \tag{4.1.2-2}$$

Expressing the nonspherical lunar potential, ψ_{NS_M}, in terms of $\overline{P}_n^m(\sin\phi)$ gives

$$\begin{aligned}\psi_{NS_M}(r,\phi,\lambda) = {} & \frac{\mu}{r}\sum_{n=2}^{N}\overline{C}_n^0\left(\frac{R_e}{r}\right)^n\overline{P}_n^0(\sin\phi) \\ & + \frac{\mu}{r}\sum_{n=2}^{N}\sum_{m=1}^{n}\left[\frac{R_e}{r}\right]^n\overline{P}_n^m(\sin\phi)\left[\overline{S}_n^m\sin(m\lambda) + \overline{C}_n^m\cos(m\lambda)\right]\end{aligned} \tag{4.1.2-3}$$

where

r = magnitude of the vector from the central body's center of mass to the satellite

ϕ = latitude of the satellite in the planet body fixed (PBF) frame (e.g. geographic or selenographic latitude)

λ = longitude of the satellite in the PBF frame (e.g. geographic or selenographic longitude)

μ = gravitational constant of the central body (e.g. 4902.800238 x 10^9 meters^3/second^2 for the LP100K gravitational model)

R_e = equatorial radius of the central body (e.g. 1738 kilometers for the LP100K gravitational model)

N = maximum degree included in the expansion (e.g. 100 for the LP100K model)

$\overline{P}_n^m(\sin\varphi)$ = normalized associated Legendre function

$\overline{S}_n^m$, $\overline{C}_n^m$ = normalized harmonic coefficients for the central body:

$$\begin{aligned}\overline{C}_n^m &= \frac{(C_n^m)_M}{N(n,m)} \\ \overline{S}_n^m &= \frac{(S_n^m)_M}{N(n,m)}\end{aligned} \tag{4.1.2-4}$$

Expressing the gradient of the nonspherical potential in PBF coordinates (e.g. the International Terrestrial Reference Frame (ITRF) in the case of the Earth or the lunar principal axis frame in the case of the Moon), the associated acceleration vector in the planet-centered inertial (PCI) mean of J2000 frame is obtained as follows:

$$\bar{a}_{NS} = \left[T_{PBF \leftarrow J2000_{PCI}}\right]^T \begin{bmatrix} \ddot{x}_{NS_{PBF}} \\ \ddot{y}_{NS_{PBF}} \\ \ddot{z}_{NS_{PBF}} \end{bmatrix} \tag{4.1.2-5}*$$

where the rotation, $\left[T_{PBF \leftarrow J2000_{PCI}}\right]^T$, which transforms the acceleration vector from the PBF to the PCI coordinate frame, is discussed in Sections 3.2.1 through 3.2.3 for the Earth and Sections 3.2.9 and 3.2.12 for the Moon and other planets, respectively. The acceleration components $\ddot{x}_{NS_{PBF}}, \ddot{y}_{NS_{PBF}}$, and $\ddot{z}_{NS_{PBF}}$, which are the components of the inertial acceleration expressed in PBF coordinates (not the acceleration with respect to the PBF system) are given by

$$\begin{bmatrix} \ddot{x}_{NS_{PBF}} \\ \ddot{y}_{NS_{PBF}} \\ \ddot{z}_{NS_{PBF}} \end{bmatrix} = \left[\frac{\partial \psi_{NS}}{\partial r} \left(\frac{\partial r}{\partial \bar{r}_{PBF}} \right)^T + \frac{\partial \psi_{NS}}{\partial \phi} \left(\frac{\partial \phi}{\partial \bar{r}_{PBF}} \right)^T + \frac{\partial \psi_{NS}}{\partial \lambda} \left(\frac{\partial \lambda}{\partial \bar{r}_{PBF}} \right)^T \right] \tag{4.1.2-6}*$$

The spacecraft position vector in the PBF frame $\bar{r}_{PBF}$ is computed as follows

$$\bar{r}_{PBF} = T_{PBF \leftarrow J2000_{PCI}} \left(\bar{R}_{J2000_{ECI}} - \bar{R}_{Planet_{PCI}} \right) \tag{4.1.2-7}*$$

where $\bar{R}_{J2000_{ECI}}$ is the spacecraft position vector in the Mean of J2000 geocentric frame and $\bar{R}_{Planet_{ECI}}$ is the position of the central body in the Mean of J2000 geocentric frame.

The partial derivatives of the nonspherical portion of the central body potential with respect to *r*, ϕ, and λ are given by

$$\frac{\partial \psi_{NS}}{\partial r} = -\frac{\mu}{r^2} \sum_{n=2}^{N} \left(\frac{R_e}{r} \right)^n (n+1) \sum_{m=0}^{n} \left[\bar{C}_n^m \cos(m\lambda) + \bar{S}_n^m \sin(m\lambda) \right] \bar{P}_n^m (\sin\phi) \tag{4.1.2-8}*$$

$$\begin{aligned} \frac{\partial \psi_{NS}}{\partial \phi} = \frac{\mu}{r} \sum_{n=2}^{N} \left(\frac{R_e}{r} \right)^n \sum_{m=0}^{n} \left[\bar{C}_n^m \cos(m\lambda) + \bar{S}_n^m \sin(m\lambda) \right] \\ \times \left[\zeta(n,m) \bar{P}_n^{m+1} (\sin\phi) - m \tan\phi \bar{P}_n^m (\sin\phi) \right] \end{aligned} \tag{4.1.2-9}*$$

where

$$\lambda = \tan^{-1} \left(\frac{y_{PBF}}{x_{PBF}} \right) \tag{4.1.2-10}*$$

$$\phi = \sin^{-1} \left(\frac{z_{PBF}}{r_{PBF}} \right) \tag{4.1.2-11}*$$

$$\zeta(n,m) = \sqrt{(n-m)(n+m+1) \frac{2 - \delta_{m,0}}{2}} \tag{4.1.2-12}*$$

$$\frac{\partial \psi_{NS}}{\partial \lambda} = \frac{\mu}{r}\sum_{n=2}^{N}\left(\frac{R_e}{r}\right)^n \sum_{m=0}^{n} m\left[\overline{S}_n^m \cos(m\lambda) - \overline{C}_n^m \sin(m\lambda)\right]\overline{P}_n^m(\sin\phi) \qquad (4.1.2\text{-}13)^*$$

The normalized Legendre functions and the terms $\cos(m\lambda)$, $\sin(m\lambda)$, and $m \tan\phi$ are computed via recursion formulas, as follows:

For n=m:

$$\overline{P}_m^m(\sin\phi) = \begin{cases} 1.0; & m = 0 \\ \sqrt{2(2m+1)\kappa(m)}\cos^m\phi; & m > 0 \end{cases} \qquad (4.1.2\text{-}14)^*$$

where

$$\kappa(m) = \frac{(2m-1)!!}{(2m)!!} = \left(\frac{1}{2}\right)\left(\frac{3}{4}\right)....\left(\frac{2m-1}{2m}\right) \qquad (4.1.2\text{-}15)^*$$

For n = m+1 and m ≥ 0:

$$\overline{P}_{m+1}^m(\sin\phi) = \sqrt{2m+3}\sin\phi\,\overline{P}_m^m(\sin\phi) \qquad (4.1.2\text{-}16)^*$$

For n $\geq$ m+2 and m ≥ 0:

$$\overline{P}_n^m(\sin\phi) = \alpha(n,m)\sin\phi\,\overline{P}_{n-1}^m(\sin\phi) - \beta(n,m)\overline{P}_{n-2}^m(\sin\phi) \qquad (4.1.2\text{-}17)^*$$

where

$$\alpha(n,m) = \sqrt{\frac{(2n+1)(2n-1)}{(n-m)(n+m)}} \qquad (4.1.2\text{-}18)^*$$

$$\beta(n,m) = \sqrt{\frac{(2n+1)(n+m-1)(n-m-1)}{(2n-3)(n+m)(n-m)}} \qquad (4.1.2\text{-}19)^*$$

and for m ≥ 2:

$$\sin(m\lambda) = 2\cos\lambda\sin\left[(m-1)\lambda\right] - \sin\left[(m-2)\lambda\right] \qquad (4.1.2\text{-}20)^*$$

$$\cos(m\lambda) = 2\cos\lambda\cos\left[(m-1)\lambda\right] - \cos\left[(m-2)\lambda\right] \qquad (4.1.1\text{-}21)^*$$

$$m\tan\phi = (m-1)\tan\phi + \tan\phi \qquad (4.1.2\text{-}22)^*$$

(Equations 4.1.2-23 through 4.1.2-28 removed)

The partial derivatives of r, ϕ, and λ, with respect to x_{PBF}, y_{PBF}, and z_{PBF}, are computed from the expressions

$$\frac{\partial r}{\partial \bar{r}_{PBF}} = \frac{\bar{r}_{PBF}^{\ T}}{r_{PBF}} \tag{4.1.2-29}*$$

$$\frac{\partial \phi}{\partial \bar{r}_{PBF}} = \frac{1}{\sqrt{x_{PBF}^{\ 2} + y_{PBF}^{\ 2}}} \left[-\frac{z_{PBF}\, \bar{r}_{PBF}^{\ T}}{r_{PBF}^{\ 2}} + \frac{\partial z_{PBF}}{\partial \bar{r}_{PBF}} \right] \tag{4.1.2-30}*$$

$$\frac{\partial \lambda}{\partial \bar{r}_{PBF}} = \frac{1}{x_{PBF}^{\ 2} + y_{PBF}^{\ 2}} \left[x_{PBF} \frac{\partial y_{PBF}}{\partial \bar{r}_{PBF}} - y_{PBF} \frac{\partial x_{PBF}}{\partial \bar{r}_{PBF}} \right] \tag{4.1.2-31}*$$

where the position partial derivatives are equal to the following:

$$\frac{\partial x_{PBF}}{\partial \bar{r}_{PBF}} = (1,0,0) \qquad \frac{\partial y_{PBF}}{\partial \bar{r}_{PBF}} = (0,1,0) \qquad \frac{\partial z_{PBF}}{\partial \bar{r}_{PBF}} = (0,0,1) \tag{4.1.2-32}$$

Substituting Equations (4.1.2-29) through (4.1.2-31) into Equation (4.1.2-6) yields the selenographic components of the acceleration vector

$$\ddot{x}_{NS_{PBF}} = \left(\frac{1}{r_{SG}} \frac{\partial \psi_{NS}}{\partial r_{PBF}} - \frac{z_{PBF}}{r_{PBF}^{\ 2} \sqrt{x_{PBF}^{\ 2} + y_{PBF}^{\ 2}}} \frac{\partial \psi_{NS}}{\partial \phi} \right) x_{PBF} - \left(\frac{1}{x_{PBF}^{\ 2} + y_{PBF}^{\ 2}} \frac{\partial \psi_{NS}}{\partial \lambda} \right) y_{PBF} \tag{4.1.2-33}$$

$$\ddot{y}_{NS_{PBF}} = \left(\frac{1}{r_{PBF}} \frac{\partial \psi_{NS}}{\partial r} - \frac{z_{PBF}}{r_{PBF}^{\ 2} \sqrt{x_{PBF}^{\ 2} + y_{PBF}^{\ 2}}} \frac{\partial \psi_{NS}}{\partial \phi} \right) y_{PBF} + \left(\frac{1}{x_{PBF}^{\ 2} + y_{PBF}^{\ 2}} \frac{\partial \psi_{NS}}{\partial \lambda} \right) x_{PBF} \tag{4.1.2-34}$$

$$\ddot{z}_{NS_{PBF}} = \left(\frac{1}{r_{PBF}} \frac{\partial \psi_{NS}}{\partial r} \right) z_{PBF} + \frac{\sqrt{x_{PBF}^{\ 2} + y_{PBF}^{\ 2}}}{r_{PBF}^{\ 2}} \frac{\partial \psi_{NS}}{\partial \phi} \tag{4.1.2-35}$$

which are transformed to the mean of J2000.0 geocentric reference frame using Equation (4.1.2-5).

4.1.2.3 Reduction in Nonspherical Gravitational Acceleration Calculations

State propagation using a Runge-Kutta integrator requires multiple evaluations of the acceleration model for each integration step. The GEONS flight code includes a fourth-order integrator, which requires four acceleration evaluations, and an eighth-order integrator, which requires ten acceleration evaluations. These integration methods are discussed in detail in Section 4.2. The fourth-order integrator was selected for use in flight applications where computational efficiency is critical. To further reduce computation, an option is available to compute the Sun and Moon positions and rotation matrices used in the evaluation of the acceleration models only at the initial time.

If the size of the nonspherical gravitational model that is being evaluated is moderately large, calculation of the nonspherical gravitational acceleration will be the major contributor to the computational time for each acceleration evaluation. This cost can be reduced by using a first-

order Taylor series approximation to the nonspherical gravitational acceleration centered at the location of the spacecraft at the beginning of the integration step.

The following description of this capability, which has been implemented for propagation of the Orion spacecraft, is based on the state propagation discussion in Section 6.6.5 of Reference 59. The nonspherical gravity acceleration is computed using the following Taylor series about the spacecraft position at the beginning of each integration step, $\overline{R}^n(t_0)$. Truncating after the first order in $\left[R^n(t_i) - R^n(t_0)\right]$ gives

$$\overline{a}_{NS}\left(R^n(t_i)\right) = \overline{a}_{NS}\left(R^n(t_0)\right) + \left.\frac{\partial \overline{a}_{NS}}{\partial R^n(t)}\right|_{t=t_0} \left[R^n(t_i) - R^n(t_0)\right] \qquad (4.1.2\text{-}36)^*$$

where $\frac{\partial \overline{a}_{NS}}{\partial R^n(t)}$ is the gravity gradient matrix. This approximation requires calculation of the nonspherical gravitational acceleration and the associated gravity gradient matrix at only the initial integration step time. A less accurate but more computationally efficient approach would be to only reevaluate the point-mass and possibly J_2 gravity contributions at each intermediate time following the initial integration step time.

4.1.3 Atmospheric Drag Acceleration

Atmospheric drag acceleration is modeled for the user spacecraft as a drag force in the direction of the relative wind vector acting on a satellite of constant surface area. This model applies only to the Earth. The velocity of the satellite relative to the atmosphere is computed in the inertial coordinate system by subtracting the motion of the atmosphere, assumed to rotate with the Earth, from that of the satellite, as follows:

$$\overline{V}_{rel} = \dot{\overline{R}} - \overline{\omega} \times \overline{R} \qquad (4.1\text{-}59)^*$$

The Earth's rotation vector, $\overline{\omega}$, is directed along the Earth's instantaneous spin axis with a magnitude equal to the rotation rate of the Earth and components $(\omega_1, \omega_2, \omega_3)$. The Earth's rotation vector is computed in the inertial mean of J2000.0 frame as follows:

$$\overline{\omega}^T = \omega_e \left[C(3,1); C(3,2); C(3,3)\right] \qquad (4.1\text{-}60)^*$$

where ω_e is the rotation rate of the Earth in radians per second (7.2921158553 x 10^{-5} radians/second and the C matrix, which provides the transformation from the ECI to the TOD frame is used to rotate the spin axis to the inertial frame, is defined in Equation (3.2-26).

For the case of a spherical satellite, the atmospheric drag acceleration is computed as

$$\overline{a}_D = -\frac{1}{2}\left(\frac{C_D(t_k)\,A}{m}\right)\rho_a\ \overline{V}_{rel}\,|\overline{V}_{rel}| \qquad (4.1\text{-}61)^*$$

where

$C_D(t_k)$ = aerodynamic force coefficient, computed using Equation (4.3-13)

A = surface area of the satellite (meters^2)

m = mass of the satellite (kilograms)

ρ_a = density function computed from the atmospheric drag model (kilograms/ meters^3)

Nominally, for a spherical satellite, the aerodynamic force coefficient, C_D, is equal to 2.0. In order to absorb an error in any of the above terms, an adjustment to C_D, $\Delta C_D(t_k)$, can be estimated. The computation of $\Delta C_D(t_k)$ is discussed further in Section 4.3.

The atmospheric density function, ρ_a, is modeled using an analytic approximation to the Harris-Priester atmospheric model. Harris and Priester determined the physical properties of the upper atmosphere theoretically by solving the heat conduction equation under quasi-hydrostatic conditions (see References 13 through 15). Approximations for fluxes from the extreme ultraviolet and corpuscular heat sources were included, but the model averages the semiannual and seasonal-latitudinal variations and does not attempt to account for the extreme ultraviolet 27-day effect.

The atmospheric model presented here is a modification of the Harris-Priester concept. The modification attempts to account for the diurnal bulge by including a cosine variation between a maximum density profile at the apex of the diurnal bulge (which is located approximately 30 degrees east of the subsolar point) and a minimum density profile at the antapex of the diurnal bulge.

The variation of the atmospheric density depends on the solar flux value and the altitude. In the Harris-Priester model, tables corresponding to the anticipated solar flux value are used. The approximation in GEONS is based on an analytic formula [see Equation (4.1-61) below] that applies to all solar flux values of interest and requires limited tables (which can be uplinked once during the initialization stage). The result is a gain in operational simplicity without significant loss of accuracy (between 5 and 10 percent).

The density values at a fixed height h above the reference ellipsoid for either the minimum atmospheric density ($\rho_{\min}$) or the maximum atmospheric density ($\rho_{\max}$) can be represented by the following simple analytic formula (Reference 16):

$$\rho_m(f, h) = A_m(f - 65)^{\alpha_m} + B_m\left[2 - e^{-\beta_m(f-65)}\right] \qquad (4.1\text{-}62)^*$$

where

ρ_m = maximum ($\rho_{\max}$) or minimum ($\rho_{\min}$)density

$A_m, B_m, \alpha_m, \beta_m$ = height-dependent, best-fit parameters to fit the tabulated Harris-Priester density values

f = 10.7-centimeter solar flux level in units of 10^{-22} watts/meter^2/hertz, an uplinkable parameter, commonly referred to as $F_{10.7}$

The solar flux value is also available in the TDRSS Augmentation Service for Satellites (TASS) broadcast messages.

The best-fit parameters for $\rho_{\min}$ and $\rho_{\max}$ are provided in Tables 4-3 and 4-4, respectively. The tables are associated with altitudes between 110 and 2000 kilometers. Values for the altitude region associated with the nominal spacecraft mission orbit should be available in the flight software.

For any given height h, $\rho_{\min}$ and $\rho_{\max}$ can be obtained by interpolating between the two adjacent heights, h_1 and h_2, for which parametric equations are available, as follows:

$$\rho_m(f,\ h) = \rho_m(f,\ h_1)\left[\frac{\rho_m(f,\ h_2)}{\rho_m(f,\ h_1)}\right]^k \tag{4.1-63}*$$

where

$$h_1 < h < h_2 \tag{4.1-64}$$

and

$$k = \frac{h - h_1}{h_2 - h_1} \tag{4.1-65}*$$

If h< the minimum altitude in the tables (i.e. 110 kilometers), the value h = the minimum altitude in the tables is used in the evaluation of Equation (4.1-62).

If h> the maximum altitude in the tables (i.e. 2000 kilometers), the density is zero.

A good approximation (neglecting polar motion) for the satellite height, h, is given by

$$h = r - R_E \tag{4.1-66}*$$

where R_E is the mean radius of the Earth, given as

$$R_E = \frac{R_e(1 - f_E)}{\sqrt{1 - (2f_E - f_E^2)\cos^2\delta}} \tag{4.1-67}*$$

$$cos\delta = \frac{\sqrt{x_{ECEF}^2 + y_{ECEF}^2}}{r} \tag{4.1-68}*$$

and

r = magnitude of the satellite position vector

R_e = equatorial radius of the Earth

f_E = Earth's flattening coefficient

δ = declination of the satellite (it is assumed that δ equals the geocentric latitude of the subsatellite point)

x_{ECEF}, y_{ECEF} = components of the satellite position vector, $\bar{r}_{ECEF}$

The density, ρ_a, is then computed by including the diurnal variation effect

$$\rho_a = \rho_{min}(f,\ h) + \left[\rho_{max}(f,\ h) - \rho_{min}(f,\ h)\right] \cos^n\left(\frac{\gamma}{2}\right) \tag{4.1-69}*$$

where γ is the angle between the satellite position vector and the apex of the diurnal bulge.

The cosine function in Equation (4.1-68) can be determined directly as

$$\cos^n\left(\frac{\gamma}{2}\right) = \left(\frac{1+\cos\gamma}{2}\right)^{n/2} = \left[\frac{1}{2} + \frac{\bar{R}\cdot\hat{U}_B}{2R}\right]^{n/2} \tag{4.1-70}*$$

where

$\bar{R}$ = satellite position vector (in mean of J2000.0 coordinates)

$\hat{U}_B$ = unit vector directed toward the apex of the diurnal bulge (in mean of J2000.0 coordinates)

For GEONS, *n* is an input parameter, which is typically equal to 2 for low-inclination orbits and 6 for polar orbits.

The vector $\hat{U}_B$ has the following components:

$$U_{B_x} = \cos\delta_S \cos\left(a_S + \bar{\lambda}\right) \tag{4.1-71}*$$

$$U_{B_y} = \cos\delta_S \sin\left(a_S + \bar{\lambda}\right) \tag{4.1-72}*$$

$$U_{B_z} = \sin\delta_S \tag{4.1-73}*$$

where

δ_S = declination of the Sun, defined in Equation (4.1-24)

a_S = right ascension of the Sun, defined in Equation (4.1-23)

$\bar{\lambda}$ = lag angle between the Sun line and the apex of the diurnal bulge (approximately 30 degrees)

Table 4-3. Best-Fit Parameters for the Harris-Priester Minimum Atmospheric Density, $\rho_{\min}$

Altitude, *h* (kilometers)	Best-Fit Parameters			
	A **(kilograms/ kilometers^3)**	**α (unitless)**	***B*** **(kilograms/ kilometers^3)**	**β (unitless)**
110	7.8000D+01	0.0	0.0	0.0
120	2.4900D+01	0.0	0.0	0.0
130	-1.1939D-02	0.8751	8.9780D+00	0.0
140	-3.3128D-03	0.8803	4.0690D+00	0.0
150	3.0904D-03	0.5179	2.0860D+00	0.0
160	3.8306D-03	0.7550	1.1460D+00	0.0
170	3.8433D-03	0.7929	6.6160D-01	0.0
180	2.6344D-03	0.8610	4.0160D-01	0.0
190	1.9229D-03	0.8996	2.5300D-01	0.0
200	1.4409D-03	0.9285	1.6280D-01	0.0
210	9.3739D-04	0.9807	1.0760D-01	0.0
220	5.8783D-04	1.0373	7.2870D-02	0.0
230	3.8447D-04	1.0837	5.0380D-02	0.0
240	2.5352D-04	1.1285	3.5490D-02	0.0
250	1.6852D-04	1.1720	2.5410D-02	0.0
260	1.1296D-04	1.2142	1.8460D-02	0.0
270	7.7290D-05	1.2528	1.3580D-02	0.0
280	5.3951D-05	1.2880	1.0100D-02	0.0
290	3.8363D-05	1.3198	7.5880D-03	0.0
300	2.7122D-05	1.3533	5.7190D-03	0.0
320	5.7779D-06	1.5646	3.3050D-03	6.6739D.03
340	2.4895D-06	1.6656	1.9530D-03	8.8782D-03
360	1.1952D-06	1.7486	1.1750D-03	1.0875D-02
380	6.0302D-07	1.8240	7.1670D-04	1.3006D-02
400	3.1547D-07	1.8940	4.4280D-04	1.5129D-02
420	1.7111D-07	1.9579	2.7790D-04	1.7603D-02
440	9.1715D-08	2.0256	1.7600D-04	1.9867D-02

Altitude, *h* (kilometers)	Best-Fit Parameters			
	A **(kilograms/ kilometers^3)**	**α (unitless)**	***B*** **(kilograms/ kilometers^3)**	**β (unitless)**
460	4.9008D-08	2.0947	1.1280D-04	2.2358D-02
480	2.5849D-08	2.1671	7.3460D-05	2.4837D-02
500	1.3512D-08	2.2420	4.8660D-05	2.7228D-02
520	6.9794D-09	2.3197	3.2910D-05	2.9303D-02
540	3.5672D-09	2.4001	2.2790D-05	3.0905D-02
560	1.7865D-09	2.4851	1.6220D-05	3.1924D-02
580	8.9173D-10	2.5712	1.1880D-05	3.2157D-02
600	4.3949D-10	2.6602	8.9780D-06	3.1651D-02
620	2.1604D-10	2.7503	6.9870D-06	3.0602D-02
640	1.0590D-10	2.8414	5.5930D-06	2.9273D-02
660	5.2157D-11	2.9322	4.5890D-06	2.7841D-02
680	2.6007D-11	3.0211	3.8460D-06	2.6423D-02
700	1.3122D-11	3.1084	3.2810D-06	2.5185D-02
720	6.7645D-12	3.1921	2.8380D-06	2.4270D-02
740	3.6011D-12	3.2702	2.4820D-06	2.3581D-02
760	1.9792D-12	3.3428	2.1900D-06	2.3164D-02
780	1.1312D-12	3.4087	1.9440D-06	2.3068D-02
800	6.8348D-13	3.4647	1.7360D-06	2.3083D-02
850	2.6558D-12	3.0991	1.1800D-06	2.6181D-02
900	1.4314D-12	3.1164	8.7000D-07	3.0263D-02
950	9.7814D-13	3.0982	6.6000D-07	3.8122D-02
1000	1.5905D-12	2.9272	4.8000D-07	4.7237D-02
1100	1.3351D-11	2.3794	3.0000D-07	3.5909D-02
1200	6.4934D-11	1.9547	1.8500D-07	2.9814D-02
1300	3.6950D-10	1.5317	1.1300D-07	1.7111D-02
1400	1.1825D-09	1.2630	7.3000D-08	1.0000D-03
1500	7.2326D-10	1.3027	5.2000D-08	2.5822D-04
1600	3.9700D-10	1.3579	3.7000D-08	1.0000D-03
1700	3.1532D-10	1.3817	2.5500D-08	1.0000D-03
1800	1.8189D-10	1.4228	1.8200D-08	1.0000D-03
1900	1.3933D-10	1.4313	1.3000D-08	1.0000D-03
2000	9.5796D-11	1.4598	1.0000D-08	1.0000D-03

NOTE: This table was derived from Reference 16.

Table 4-4. Best-Fit Parameters for the Harris-Priester Maximum Atmospheric Density, $\rho_{\max}$

Altitude, *h* (kilometers)	Best-Fit Parameters			
	A **(kilograms/ kilometers^3)**	**α (unitless)**	***B*** **(kilograms/ kilometers^3)**	**β (unitless)**
110	7.8000D+01	0.0	0.0	0.0
120	2.4900D+01	0.0	0.0	0.0
130	-1.0288D-02	0.9124	9.3310D+00	0.0
140	-1.5957D-03	1.0205	4.2120D+00	0.0
150	6.0816D-03	0.4198	2.1680D+00	0.0
160	4.3565D-03	0.7089	1.2360D+00	0.0
170	3.7004D-03	0.7724	7.5580D-01	0.0
180	2.9642D-03	0.8090	4.8850D-01	0.0
190	2.4927D-03	0.8261	3.2740D-01	0.0
200	1.8838D-03	0.8559	2.2840D-01	0.0
210	1.5208D-03	0.8719	1.6340D-01	0.0
220	1.2219D-03	0.8895	1.1920D-01	0.0
230	9.5705D-04	0.9114	8.8510D-02	0.0
240	7.4926D-04	0.9332	6.6660D-02	0.0
250	5.8527D-04	0.9554	5.0830D-02	0.0
260	4.5493D-04	0.9787	3.9190D-02	0.0
270	3.5273D-04	1.0027	3.0500D-02	0.0
280	2.7128D-04	1.0288	2.3940D-02	0.0
290	2.0847D-04	1.0555	1.8940D-02	0.0
300	1.6154D-04	1.0809	1.5100D-02	0.0
320	1.0021D-04	1.1258	9.8860D-03	0.0
340	6.3023D-05	1.1692	6.6080D-03	0.0
360	4.0140D-05	1.2115	4.4940D-03	0.0
380	2.5853D-05	1.2529	3.1000D-03	0.0
400	1.6829D-05	1.2934	2.1630D-03	0.0
420	2.1107D-05	1.3320	1.5260D-03	0.0
440	7.3292D-06	1.3719	1.0850D-03	0.0
460	4.8575D-06	1.4120	7.7670D-04	0.0
480	3.2318D-06	1.4521	5.5990D-04	0.0
500	2.1442D-06	1.4936	4.0610D-04	0.0
520	1.1880D-06	1.5650	2.9630D-04	2.8426D-03
540	7.4848D-07	1.6173	2.1740D-04	3.8473D-03

Altitude, *h* (kilometers)	Best-Fit Parameters			
	A **(kilograms/ kilometers^3)**	***α*** **(unitless)**	***B*** **(kilograms/ kilometers^3)**	**β (unitless)**
560	4.7709D-07	1.6685	1.6050D-04	4.7660D-03
580	3.0399D-07	1.7205	1.1920D-04	5.7479D-03
600	1.9500D-07	1.7720	8.9100D-05	6.6919D-03
620	1.2570D-07	1.8231	8.7080D-05	7.5966D-03
640	8.1577D-08	1.8734	5.0900D-05	8.4180D-03
660	5.2632D-08	1.9253	3.8960D-05	9.3167D-03
680	3.4199D-08	1.9763	3.0110D-05	1.0066D-02
700	2.2130D-08	2.0285	2.3510D-05	1.0866D-02
720	1.4432D-08	2.0795	1.8570D-05	1.1472D-02
740	9.3506D-09	2.1321	1.4840D-05	1.2121D-02
760	6.0874D-09	2.1841	1.2020D-05	1.2575D-02
780	3.9601D-09	2.2365	9.8670D-06	1.3009D-02
800	2.5823D-09	2.2888	8.1930D-06	1.3276D-02
850	2.1946D-09	2.2422	6.2000D-06	2.5529D-03
900	2.0811D-09	2.1776	4.4000D-06	-1.9168D-03
950	4.5331D-10	2.3997	3.3000D-06	5.0229D-03
1000	1.2710D-10	2.5811	2.7000D-06	1.2919D-02
1100	1.2207D-11	2.9070	1.7500D-06	2.7866D-02
1200	2.6581D-12	3.0632	1.2000D-06	3.2416D-02
1300	7.4153D-13	3.1939	8.5000D-07	3.9225D-02
1400	5.4632D-14	3.5853	6.2000D-07	4.1313D-02
1500	7.7086D-15	3.8596	4.7500D-07	3.4612D-02
1600	1.7322D-15	4.0683	3.6500D-07	3.5450D-02
1700	6.3293D-15	3.7397	3.0000D-07	3.4738D-02
1800	2.1463D-13	2.9859	2.2000D-07	4.1007D-02
1900	9.0409D-13	2.6444	1.8000D-07	3.5595D-02
2000	5.9649D-12	2.2291	1.4600D-07	3.1280D-02

NOTE: This table was derived from Reference 16.

4.1.4 Solar Radiation Pressure Acceleration Model

This section provides solar radiation pressure acceleration models based on a simple spherical satellite model with constant spacecraft area and a higher fidelity model that takes into account the changing spacecraft surface area due to changing attitude with respect to the Sun.

4.1.4.1 Solar Radiation Pressure Acceleration with Spherical Area Model

The model for the acceleration, $\bar{a}_{SRP}$, due to direct solar radiation pressure acting on a spherical satellite is given by

$$\bar{a}_{SRP} = \upsilon P_S R_{Sun}^2 \frac{C_R(t_k) A}{m} \frac{\bar{r}_{vs}}{r_{vs}^3} \qquad \text{(4.1-73a)*}$$

where the eclipse factor υ is defined as follows

υ = 0 if the spacecraft is shadowed by the central body

υ = 1 if the spacecraft is sunlit

where the vector from the sun to the spacecraft, $\bar{r}_{vs}$, is computed as follows:

$$\bar{r}_{vs} = \bar{R}_C^n - \bar{R}_C^S \qquad \text{(4.1-74)*}$$

and P_S = mean solar flux at one astronomical unit, divided by the speed of light (4.57×10^{-6} Newtons/meter^2)

$\bar{R}_C^n$ = position vector of satellite n referenced to the central-body mean of J2000 frame

$\bar{R}_C^S$ = position vector of the Sun referenced to the central-body mean of J2000 frame, computed as described in Section 4.1.1

R_{Sun} = one astronomical unit ($1.49597893 \times 10^{+11}$ meters)

$C_R(t_k)$ = solar radiation pressure coefficient, computed using Equation (4.3-13a)

A = surface area of the spacecraft (meter^2)

m = mass of the spacecraft (kilograms)

r_{vs} = magnitude of the vector $\bar{r}_{vs}$ (meters)

Note that partial shadowing, i.e., penumbra and umbra, is not modeled. The following cylindrical shadow model is used to detect eclipse events at each time that the acceleration is computed. The spacecraft is assumed to be in sunlight (υ = 1) if

$$\bar{R}_C^n \bullet \frac{\bar{R}_C^S}{\left|\bar{R}_C^S\right|} \geq 0 \qquad \text{(4.1-75)*}$$

The spacecraft is fully in shadow ($\upsilon = 0$) if

$$\overline{R}_C^n \bullet \frac{\overline{R}_C^S}{\left|\overline{R}_C^S\right|} < 0 \qquad (4.1\text{-}76)^*$$

and if the vector to the spacecraft along the normal to the sun vector has a magnitude less than the central body radius, R_C,

$$\left|\overline{R}_C^n - \left(\overline{R}_C^n \bullet \frac{\overline{R}_C^S}{\left|\overline{R}_C^S\right|}\right)\frac{\overline{R}_C^S}{\left|\overline{R}_C^S\right|}\right| < R_C \qquad (4.1\text{-}77)^*$$

4.1.4.2 Solar Radiation Pressure Acceleration with Multiplate Area Model (not currently implemented)

The solar radiation pressure acceleration at a specific time is computed for each illuminated flat plate in the multiplate spacecraft model based on the following high-fidelity model defined Reference 54.

$$\overline{a}_{SRP} = -C_R(t_k)\frac{P_S R_{Sun}^2 \upsilon}{mS^2}\sum_{i=1}^{nplate} A_i\left|\hat{n}_i \cdot \hat{S}\right|\left[2\left(\frac{\delta_i}{3} + \rho_i(\hat{n}_i \cdot \hat{S})\right)\hat{n}_i + (1-\rho_i)\hat{S}\right] \qquad (4.1\text{-}77a)$$

where

$C_R(t_k) =$ solar radiation pressure coefficient computed using Equation (4.3-13a)

$P_S =$ mean solar flux at one astronomical unit, divided by the speed of light (4.57×10^{-6} Newtons/meter^2)

$R_{Sun} =$ one astronomical unit ($1.49597893 \times 10^{+11}$ meters)

$\upsilon =$ eclipse factor, equal to the fraction of the solar radiation pressure flux at the spacecraft taking into account shadowing by the Moon and the Earth as defined in Section 4.1.4.1

$m =$ spacecraft mass (kilograms) (satellite-specific commanded parameter)

$A_i =$ surface area of the ith plate (meter^2) (satellite-specific commanded parameter)

$\hat{n}_i =$ surface normal unit vector for the ith plate in the central-body inertial frame

$S = \left|\overline{R}_C^S - \overline{R}_C^n\right|$ magnitude of the satellite-to-sun vector (meters)

$\hat{S} = \dfrac{\overline{R}_C^S - \overline{R}_C^n}{\left|\overline{R}_C^S - \overline{R}_C^n\right|}$, satellite-to-sun unit vector in the central-body inertial frame

$\delta_i =$ diffusive reflectivity for the ith plate (satellite-specific commanded parameter)

ρ_i = specular reflectivity for the ith plate (satellite-specific commanded parameter)

The summation is performed for each illuminated plate *i*, i.e. when

$$\hat{S} \cdot \hat{n}_i > 0 \tag{4.1-77b}$$

Spin-Stabilized Macromodel and Associated Partial Derivatives (Future Release)

For the MMS spacecraft, an approximate area model consists of a regular octagonal cylinder composed of 8 solar array side panels and top and bottom plates and an inner column. The total acceleration is equal to the contributions from each of these components:

$$\bar{a}_{SRP} = \bar{a}_{SRP}^{oct} + \bar{a}_{SRP}^{top/bot} + \bar{a}_{SRP}^{col} \tag{4.1-77c}*$$

The spacecraft rotation period (20-24 seconds) is comparable to the integration stepsize (nominally 30 seconds). Therefore, the acceleration computed using Equation 4.1-77a should be averaged over the rotation period.

Reference 55 provides a similar solar radiation pressure model for the spin-stabilized SELENE relay spacecraft. In Reference 55, the solar radiation pressure acceleration is derived in the spacecraft-centered body frame defined as follows:

$\hat{z}_B$ is parallel to the spin axis $\hat{A}$

$\hat{x}_B = \hat{S} \times \hat{z}_B$, normal to $\hat{z}_B$ and the Sun direction $\hat{S}$ (4.1-77d)*

$\hat{y}_B = \hat{z}_B \times \hat{x}_B$, in the plane defined by $\hat{A}$ and $\hat{S}$

The angle θ between the spin axis and the Sun direction is given by

$$\cos\theta = \hat{A} \cdot \hat{S} \tag{4.1-77e}*$$

where $\hat{A}$ is the spin axis direction expressed in the inertial frame

$$\hat{A} = \begin{bmatrix} \cos\alpha_B & \cos\delta_B \\ \sin\alpha_B & \cos\delta_B \\ & \sin\delta_B \end{bmatrix} \tag{4.1-77f}*$$

α_B is the right ascension of the spin axis with respect to the inertial frame, and δ_B is the declination of the spin axis with respect to the inertial frame (defined in Section 3.2.8.2).

The model in Reference 55 is based on the following assumptions: (1) the spacecraft rotation period is much smaller than the orbital period so that the solar radiation force acting on the spacecraft can be modeled as constant over one rotation period, (2) the orientation of the spin axis does not change over the rotation period, and (3) the effects of shadowing and reflection by the different parts of the spacecraft can be neglected. The accelerations in the spacecraft-centered body

frame defined in Equation (4.1.4-77d) are then rotated to the inertial frame for inclusion in the equations of motion

$$\bar{a}_{SRP} = T^{n}_{XYZ \leftarrow B}\left[\left(\bar{a}^{oct}_{SRP}\right)_B + \left(\bar{a}^{top/bot}_{SRP}\right)_B + \left(\bar{a}^{col}_{SRP}\right)_B\right] \tag{4.1-77g)*}$$

where

$$T^{n}_{XYZ \leftarrow B} = \begin{bmatrix} \hat{x}_B \cdot \hat{x}_I & \hat{y}_B \cdot \hat{x}_I & \hat{z}_B \cdot \hat{x}_I \\ \hat{x}_B \cdot \hat{y}_I & \hat{y}_B \cdot \hat{y}_I & \hat{z}_B \cdot \hat{y}_I \\ \hat{x}_B \cdot \hat{z}_I & \hat{y}_B \cdot \hat{z}_I & \hat{z}_B \cdot \hat{z}_I \end{bmatrix} \tag{4.1-77h)*}$$

This model assumes that the top and bottom of the cylinder are identical and that only one will be illuminated at any time. The acceleration due to solar radiation pressure acting on the top/bottom plate is obtained using Equation (4.1.4-77a) directly:

$$\left(\bar{a}^{top/bot}_{SRP}\right)_B = -C_R \frac{P_S R^2_{Sun} \upsilon}{mS^2} \begin{pmatrix} 0 \\ A_{top}(1-\rho_t)\sin\theta\cos\theta \\ A_{top}\cos\theta\left[(1+\rho_t)\cos\theta + \frac{2\delta_t}{3}\right] \end{pmatrix}, \theta \le \pi/2$$

$$\left(\bar{a}^{top/bot}_{SRP}\right)_B = -C_R \frac{P_S R^2_{Sun} \upsilon}{mS^2} \begin{pmatrix} 0 \\ -A_{top}(1-\rho_t)\sin\theta\cos\theta \\ -A_{top}\cos\theta\left[(1+\rho_t)\cos\theta + \frac{2\delta_t}{3}\right] \end{pmatrix}, \theta > \pi/2 \tag{4.1-77i)*}$$

where

A_{top} = area of the top/bottom of the cylinder, assumed to be identical (an input parameter)

δ_t = diffusive reflectivity for the top/bottom (an input parameter)

ρ_t = specular reflectivity for the top/bottom (an input parameter)

The mean acceleration over one spacecraft rotation due to solar radiation pressure acting on the 8 sides of the octagonal cylinder is computed by summing up the forces acting on each sunlit solar array plate and averaging over the rotational period. In the satellite-centered frame, this yields:

$$\left(\bar{a}^{oct}_{SRP}\right)_B = -C_R \frac{P_S R^2_{Sun} \upsilon}{mS^2} \begin{pmatrix} 0 \\ \frac{8A_{oct}}{3}\sin\theta\left[\frac{3+\rho_s}{\pi}\sin\theta + \frac{\delta_s}{2}\right] \\ \frac{8A_{oct}}{\pi}(1-\rho_s)\sin\theta\cos\theta \end{pmatrix} \tag{4.1-77j)*}$$

where

A_{oct} = Area of each solar array panel (an input parameter)

δ_s = diffusive reflectivity for the solar array (an input parameter)

ρ_s = specular reflectivity for the solar array (an input parameter)

Using a similar approach, the mean acceleration over one spacecraft rotation due to solar radiation pressure acting on the column is given by

$$\left(\bar{a}_{SRP}^{col}\right)_B = -C_R \frac{P_S R_{Sun}^2 \upsilon}{mS^2} \begin{pmatrix} 0 \\ \frac{2\pi rh}{3}\sin\theta\left[\frac{3+\rho_c}{\pi}\sin\theta + \frac{\delta_c}{2}\right] \\ 2rh(1-\rho_c)\sin\theta\cos\theta \end{pmatrix} \qquad \text{(4.1-77k)*}$$

where

r = radius of the column (an input parameter)

h = height of exposed portion of the column (an input parameter)

δ_c = diffusive reflectivity for the column (an input parameter, equal to 0.20 for Germanium Black Kapton)

ρ_c = specular reflectivity for the column (an input parameter, equal to 0.30 for Germanium Black Kapton)

The associated partial derivative matrix [D] referenced in Section 4.4.1.3 is given by

$$\frac{\partial \bar{a}_{SRP}}{\partial C_R} = T_{XYZ\leftarrow B}^n \left[\frac{\left(\bar{a}_{SRP}^{oct}\right)_B}{\partial C_R} + \frac{\left(\bar{a}_{SRP}^{top/bot}\right)_B}{\partial C_R} + \frac{\left(\bar{a}_{SRP}^{col}\right)_B}{\partial C_R} \right] \qquad \text{(4.1-77l)*}$$

where

$$\frac{\partial\left(\bar{a}_{SRP}^{oct}\right)_B}{\partial C_R} = -\frac{P_S R_{Sun}^2 \upsilon}{mS^2} \begin{pmatrix} 0 \\ \frac{8A_{oct}}{3}\sin\theta\left[\frac{3+\rho_s}{\pi}\sin\theta + \frac{\delta_s}{2}\right] \\ \frac{8A_{oct}}{\pi}(1-\rho_s)\sin\theta\cos\theta \end{pmatrix} \qquad \text{(4.1-77m)*}$$

$$\frac{\partial\left(\bar{a}_{SRP}^{top/bot}\right)_B}{\partial C_R} = -\frac{P_S R_{Sun}^2 \upsilon}{mS^2}\begin{pmatrix} 0 \\ A_{top}(1-\rho_t)\sin\theta\cos\theta \\ A_{top}\cos\theta\left[(1+\rho_t)\cos\theta + \frac{2\delta_t}{3}\right] \end{pmatrix}, \theta \le \pi/2 \quad \text{(4.1-77n)*}$$

$$\frac{\partial\left(\bar{a}_{SRP}^{top/bot}\right)_B}{\partial C_R} = -\frac{P_S R_{Sun}^2 \upsilon}{mS^2}\begin{pmatrix} 0 \\ -A_{top}(1-\rho_t)\sin\theta\cos\theta \\ -A_{top}\cos\theta\left[(1+\rho_t)\cos\theta + \frac{2\delta_t}{3}\right] \end{pmatrix}, \theta > \pi/2$$

$$\frac{\partial\left(\bar{a}_{SRP}^{col}\right)_B}{\partial C_R} = -\frac{P_S R_{Sun}^2 \upsilon}{mS^2}\begin{pmatrix} 0 \\ \frac{2\pi rh}{3}\sin\theta\left[\frac{3+\rho_c}{\pi}\sin\theta + \frac{\delta_c}{2}\right] \\ 2rh(1-\rho_c)\sin\theta\cos\theta \end{pmatrix} \quad \text{(4.1-77o)*}$$

4.1.5 Externally Measured Accelerations

This acceleration model is suitable for modeling thrust accelerations associated with a spacecraft maneuver. This model assumes that the externally measured accelerations have been averaged over the propagation interval. These accelerations can be input in any of the following frames: Mean of J2000.0 with respect to the central body, RIC or VBN defined with respect to the central-body frame or three-axis stabilized or spin-stabilized spacecraft body frames. The externally measured acceleration associated with the current propagation interval is converted to the inertial Mean of J2000 coordinate frame using the appropriate transformation (i.e. Equation 3.2-52, 3.2-92, 3.2-62, or 3.2-67). Note that averaging of the externally measured accelerations is not currently implemented in GEONS. In addition, a maneuver can be modeled as an impulsive velocity change (delta-V) that is added to the velocity vector at the maneuver time. When accelerometer sensor measurements are used to model the non-conservative forces, the averaged acceleration is included in the total acceleration in the central-body inertial frame:

$$\bar{a} = \bar{a}_E + \bar{a}_S + \bar{a}_P + \bar{a}_{NS_E} + \bar{a}_{NS_M} + \bar{a}_{ext}^{Average} \quad \text{(4.1-77p)*}$$

External accelerations are typically obtained from an accelerometer onboard the spacecraft. An accelerometer measures the non-conservative forces acting on a spacecraft at any time, if they exceed the accelerometer thresholds. The non-conservative forces, which are typically dominated by any propulsive forces, also include atmospheric drag and solar radiation pressure forces. Accelerometer sensor measurements are typically used to model the propulsive force only when the spacecraft is thrusting. Estimated accelerometer sensor biases are used to correct the accelerometer measurements prior to including them in the total acceleration vector.

Correction of the accelerometer sensor measurements is not currently implemented in GEONS. The corrected accelerometer acceleration is given by

$$\tilde{a}_{ext}^{Corrected} = [T_{XYZ\leftarrow B}]_C \; [T_{B\leftarrow IMU}] \begin{bmatrix} \left(a_{IMU_x}^{Measured} - b_{IMU_x}^A\right)/\left(1 + s_{IMU_x}^A\right) \\ \left(a_{IMU_y}^{Measured} - b_{IMU_y}^A\right)/\left(1 + s_{IMU_y}^A\right) \\ \left(a_{IMU_z}^{Measured} - b_{IMU_z}^A\right)/\left(1 + s_{IMU_z}^A\right) \end{bmatrix} \tag{4.1-77q}$$

where

$\left[T_{XYZ\leftarrow B}\right]_C$ = rotation matrix from the spacecraft body frame to the central body inertial frame defined in Section 3.2.8

$\left[T_{B\leftarrow IMU}\right]$ = rotation matrix from the IMU sensor frame to the body frame

$\left[s_{IMU_x}^A, s_{IMU_y}^A, s_{IMU_z}^A\right]$ = scale factors, representing the error in the conversion from raw sensor outputs to engineering units

$\bar{a}_{IMU}^{Measured}$ = Measured accelerometer accelerations in the IMU sensor frame

$\left[b_{IMU_x}^A, b_{IMU_y}^A, b_{IMU_z}^A\right]$ = component of the accelerometer measurement bias in the IMU sensor frame

$\bar{b}_{IMU}^A$ = vector of all accelerometer measurement biases

$$\bar{b}_{IMU}^A = \begin{bmatrix} b_{IMU_x}^A \\ b_{IMU_y}^A \\ b_{IMU_y}^A \\ s_{IMU_x}^A \\ s_{IMU_y}^A \\ s_{IMU_y}^A \end{bmatrix} \tag{4.1-77r}$$

4.1.6 Unmodeled Accelerations

Unmodeled accelerations can be represented by acceleration biases defined with respect to any of the following coordinate frames:

- $\left(\bar{a}_U\right)_{RIC}$, acceleration biases expressed in the Radial/In-track/Crosstrack (RIC) coordinates with respect to the central body frame defined in Section 3.1.4
- $\left(\bar{a}_U\right)_{VBN}$, acceleration biases expressed in the Velocity/Binormal/Normal (VBN) coordinates with respect to the central body frame defined in Section 3.1.8
- $\left(\bar{a}_U\right)_B$, acceleration biases expressed in the spacecraft body frame

These acceleration biases are modeled as either random constants or Gauss-Markov processes using the models defined in Section 4.3. The estimated "unmodeled" acceleration bias values are included in the total acceleration that is used to propagate the position and velocity components of the estimated state vector. The acceleration biases must be transformed to the inertial Mean of J2000.0 frame for inclusion in the total acceleration vector defined in Equation 4.1-4. The transformations are as follows, depending on the frame used to define the bias:

$$\left(\bar{a}_U\right)_{J2000} = \begin{cases} \left[T_{RIC\leftarrow XYZ}\right]_C^{\ T}\left(\bar{a}_U\right)_{RIC}, \text{ for acceleration biases expressed in the RIC frame} \\ \left[T_{XYZ\leftarrow VBN}\right]_C\left(\bar{a}_U\right)_{VBN}, \text{ for acceleration biases expressed in the VBN frame} \\ \left[T_{XYZ\leftarrow B}\right]\left(\bar{a}_U\right)_B, \text{ for acceleration biases expressed in the body frame} \end{cases} \quad (4.1\text{-}78)^*$$

The associated transformation matrices are defined in Sections 3.2.4, 3.2.8, and 3.2.10.

4.2 Runge-Kutta Integration Algorithm

The Runge-Kutta method is a self-starting, single-step numerical integration technique by which the value of the dependent variable, x, at some future time, $t_1 + \tau$ (where τ is the integration step size), can be calculated from a weighted summation formula and the value of the dependent variable at t_1. GEONS includes both fourth-order and eighth-order integration algorithms.

The fourth-order integration algorithm, which is described below, was selected for computational efficiency. The following formulas apply to a single component of the vector of quantities being integrated, $\bar{x}(t)$.

Given a first-order differential equation of the form

$$\frac{dx}{dt} = F(\bar{x}, t) \tag{4.2-1}$$

and an initial value

$$x_0 = x(t_0) \tag{4.2-2}$$

the dependent variable, x, at time $t_1 + \tau$ is computed as follows:

$$x(t_0 + \tau) = x_0 + \tfrac{\tau}{6}(F_0 + 2F_1 + 2F_2 + F_3) \tag{4.2-3}*$$

where

$$F_0 = F(\bar{x}_0, t_0) \tag{4.2-4}*$$

$$F_1 = F\left(\bar{x}_0 + \frac{\tau}{2}F_0,\ t_0 + \frac{\tau}{2}\right) \tag{4.2-5}*$$

$$F_2 = F\left(\bar{x}_0 + \frac{\tau}{2}F_1,\ t_0 + \frac{\tau}{2}\right) \tag{4.2-6}*$$

$$F_3 = F(\bar{x}_0 + \tau F_2,\ t_0 + \tau) \tag{4.2-7}*$$

The function F is given by the user spacecraft equations of motion defined in Section 4.1. To reduce computation, an option is available to compute the Sun and Moon positions and rotation matrices used in the evaluation of the acceleration models only at the initial time t_0. A fixed maximum value will be assigned to the stepsize τ for the user spacecraft. The actual stepsize will be an adjustable variable smaller than or equal to the fixed maximum value.

The Shanks eighth order Runge-Kutta algorithm was selected to provide higher accuracy using larger stepsizes (Reference 56). The following Shanks Runge-Kutta algorithm requires 10 function evaluations.

The dependent variable, x, at time $t_0 + \tau$ is computed as follows:

$$x\left(t_0+\tau\right)=x_0+\tau\sum_{i=0}^{9}c_i F_i \qquad (4.2\text{-}8)^*$$

where

$$F_0 = F\left(\bar{x}_0, t_0\right) \qquad (4.2\text{-}9)^*$$

$$F_i = F\left(\bar{x}_0 + k_i,\ t_0 + a_i\tau\right) \qquad \text{i} = 1,\ldots, 9 \qquad (4.2\text{-}10)^*$$

$$k_i = a_i\tau\sum_{j=0}^{i-1} b_{i,j}F_j \qquad \text{i} = 1,\ldots, 9 \qquad (4.2\text{-}11)^*$$

Table 4-5 contains the values for the coefficients used in these formulas.

Table 4-5. Coefficients for the Eighth Order Runge-Kutta Method

i	c_i	a_i	$a_i b_{i,j}$								
			J=0	J=1	J=2	J=3	J=4	J=5	J=6	J=7	J=8
0	41/840										
1	0	4/27	4/27								
2	0	2/9	1/18	3/18							
3	27/840	1/3	1/12	0	3/12						
4	272/840	1/2	1/8	0	0	3/8					
5	27/840	2/3	13/54	0	-27/54	42/54	8/54				
6	216/840	1/6	389/4320	0	-54/4320	966/4320	-824/4320	243/4320			
7	0/840	1	-231/20	0	81/20	-1164/20	656/20	-122/20	800/20		
8	216/840	5/6	-127/288	0	18/288	-678/288	456/288	-9/288	576/288	4/288	
9	41/840	1	1481/820	0	-81/820	7104/820	-3376/820	72/820	-5040/820	-60/820	720/820

4.3 Nonspacecraft State Vector Propagation

This section provides the state propagation and state transition matrix equations for the atmospheric drag coefficient correction (ΔC_D), solar radiation pressure coefficient correction (ΔC_R), receiver time bias (b_R), receiver time bias rate and acceleration (d_R and $\dot{d}_R$), acceleration biases ($\bar{a}_U$),GPS/WAAS pseudorange biases ($\bar{b}_\rho^{G/W}$), GPS/WAAS Doppler biases ($\bar{b}_d^{G/W}$), GPS/WAAS carrier phase biases ($\bar{b}_\phi^{G/W}$), GPS/WAAS singly differenced carrier phase biases ($\Delta\bar{b}_\phi^{G/W}$), cross-link pseudorange biases ($\bar{b}_\rho^{CL}$), cross-link Doppler biases ($\bar{b}_d^{CL}$), celestial object sensor biases ($\bar{b}^{CO}$), GS range biases ($\bar{b}_\rho^{GS}$), GS Doppler biases ($\bar{b}_d^{GS}$), TDRSS Doppler biases ($\bar{b}_d^{TDRS}$), accelerometer sensor measurement biases in the IMU frame ($\bar{b}_{IMU}^{A}$), and ionospheric scale factor (γ_I). Each of these biases can be modeled as either a random walk or first-order Gauss-Markov (FOGM) process using the equations provided in Sections 4.3.1 and 4.3.2, respectively. In addition, the time bias drift can be modeled as a second-order Gauss-Markov (SOGM) process using the equations provided in Section 4.3.3.

The atmospheric drag coefficient for satellite n at time *t* is computed as follows

$$C_D^n(t) = \left(C_D^n\right)_{ref} + \Delta C_D^n(t) \qquad \text{(4.3-1)*}$$

where

$\left(C_D^n\right)_{ref}$ = constant reference value for C_D^n (commandable parameter)

$\Delta C_D^n(t)$ = correction to C_D^n at time *t*

The solar radiation pressure coefficient for satellite n at time *t* is computed as follows

$$C_R^n(t) = \left(C_R^n\right)_{ref} + \Delta C_R^n(t) \qquad \text{(4.3-1a)*}$$

where

$\left(C_R^n\right)_{ref}$ = constant reference value for C_R^n (commandable parameter)

$\Delta C_R^n(t)$ = correction to C_R^n at time *t*

Some GPS receivers estimate the receiver clock's offset from GPS time and increase/decrease the receiver's clock time by 1 millisecond whenever the magnitude of the estimated offset exceeds 0.5 milliseconds. (If the estimated offset is less than -0.5 milliseconds, the clock time is increased by 1 millisecond. If the offset is greater than +0.5 milliseconds, the clock time is decreased by 1 millisecond.) To accommodate such receivers, the residual receiver time bias for satellite n, $\tilde{b}_R^n(t)$, can optionally be modeled as

$$\tilde{b}_R^n(t) = b_R^n(t) - q\left[\frac{b_R^n(t) + sign[b_R^n(t)]\times 0.5q}{q}\right]_{INT} \qquad \text{(4.3-2a)*}$$

where

$b_R^n(t)$ = accumulated time bias (meters) at time t for receiver n

$[x]_{\text{INT}}$ = designates the greatest integer contained in the value of x

$sign[x]$ = designates the sign of the value of x

q = distance that a signal travels in 1 millisecond (299792.458 meters)

The accumulated receiver time bias $b_R^n(t)$ is related to the time bias rate, optional time bias acceleration, and optional correction to model relativistic drift effects on the spacecraft clock relative to a UTC reference clock at rest in the ECI frame on the Earth's geoid, $\Delta\dot{d}_{R_{\text{Rel}}}^n$, as follows

$$b_R^n(t) = b_R^n(t-\Delta t) + [d_R^n(t-\Delta t) + \Delta d_{R_{\text{Rel}}}^n(t-\Delta t)] \cdot \Delta t + \dot{d}_R^n(t-\Delta t) \cdot \frac{\Delta t^2}{2} \quad (4.3\text{-}2)$$

The accumulated receiver time bias rate $d_R^n(t)$ is related to the optional time bias acceleration as follows

$$d_R^n(t) = d_R^n(t-\Delta t) + \dot{d}_R^n(t-\Delta t) \cdot \Delta t + \Delta d_{R_{rel}}^n(t-\Delta t) \quad (4.3\text{-}3)$$

where

$b_R^n(t)$ = accumulated GPS receiver time bias (meters) at time t

$b_R^n(0)$ = initial receiver time bias (meters) (commandable parameter)

$d_R^n(t)$ = value of the receiver time bias rate at time t (meters/second)

$d_R^n(0)$ = initial receiver time bias rate (meters/second) (commandable parameter)

$\dot{d}_R^n(t)$ = value of the optional receiver time bias acceleration at time t (meters/second^2)

$\dot{d}_R^n(0)$ = initial receiver time bias acceleration value (meters/second^2) (commandable parameter)

$\Delta d_{R_{\text{Rel}}}^n(t)$ = drift of the satellite clock versus a clock at rest on the surface of the Earth due to relativity (meters/second)

The value of $\widetilde{b}_R^n(t)$ is related to the receiver's residual time offset term δt_R^n as follows:

$$\widetilde{b}_R^n(t) = c\delta t_R^n \quad (4.3\text{-}4)$$

The value of $d_R^n(t)$ is related to the receiver frequency offset (in hertz), δF_{REF}, as follows:

$$d_R^n(t) = c\frac{\delta F_{REF}^n}{F_T} \quad (4.3\text{-}5)$$

Where F_T is the nominal carrier frequency (e.g. 1575.42 megahertz for L1).

Note that the model for the residual receiver clock bias given in Equation (4.3-2a) is receiver specific. If the receiver does not increase (decrease) the clock time to accommodate offsets of 1 millisecond, the accumulated bias model given in Equation (4.3-2) should be used.

The primary relativistic effects on a satellite clock are the second order Doppler shift and the gravitational frequency shift. Clocks moving in space run faster than clocks at rest on the surface of the Earth due to the lower gravitational potential in satellite orbit but run slower due to their higher velocity. The fractional frequency shift of the receiver's clock relative to a reference clock fixed on the Earth's geoid can be approximated as follows (see Equations 27 and 53 in Reference 57 for more detail) for an Earth-orbiting satellite

$$\frac{\Delta F_{\text{Rel}}}{F_T} = -\frac{\left(\dot{R}_S^n\right)^2}{2c^2} - \frac{\mu_E}{R_S^n c^2} - \frac{\Phi_0}{c^2} \tag{4.3-6}$$

where

$-\frac{\mu_E}{R_S^n}$ = Earth's Gravitational point mass potential at the satellite's position

R_S^n = Magnitude of the satellite's ECI position vector

$\dot{R}_S^n$ = Magnitude of the satellite's ECI velocity vector

$\frac{\Phi_0}{c^2} = -6.96929\text{x}10^{-10}$ =Effective geopotential at the equator in the ECEF frame (included because reference clocks are fixed on the Earth's surface)

Based on Equations 4.3-5 and 4.3-6, the relativistic contribution to the drift of the receiver's clock relative to a reference clock fixed on the Earth's geoid can be approximated as follows for an Earth-orbiting satellite

$$\Delta d_{R_{\text{Rel}}}^n(t) = c\left(-\frac{1}{c^2}\left(\frac{\mu_E}{R_S^n} + \frac{\left(\dot{R}_S^n\right)^2}{2}\right) + 6.96929\text{x}10^{-10}\right) \text{ (m/s)} \tag{4.3-7}*$$

Components of an acceleration bias vector $\bar{a}_U$ can be estimated to account for unmodeled accelerations. The acceleration bias vector can be modeled in trajectory-fixed coordinates (RIC or VBN) or a spacecraft body-fixed frame dependent on the spacecraft attitude using the equations given in Section 4.1.6. Each component of the acceleration bias vector can be modeled as either a random walk or Gauss-Markov process.

(Equation Deleted) (4.3-8)

(Equation Deleted) (4.3-9)

(Equation Deleted) (4.3-10)

(Equation Deleted) (4.3-11)

(Equation Deleted) (4.3-12)

(same as Equation 4.3-1) (4.3-13)

(same as Equation 4.3-1a) (4.3-13a)

(same as Equation 4.3-2a) (4.3-14a)

4.3.1 Random Walk Processes

The predicted values for the random walk biases that can be estimated in GEONS are as follows:

$$b_R^n(t_k) = b_R^n(t_{k-1}) + [d_R^n(t_{k-1}) + \Delta d_{R_{\text{Rel}}}^n(t_{k-1})][t_k - t_{k-1}] + \dot{d}_R^n(t_{k-1})[t_k - t_{k-1}]^2/2 \quad (4.3\text{-}14)^*$$

$$\Delta C_D^n(t_k) = \Delta C_D^n(t_{k-1}) \quad (4.3\text{-}15)^*$$

$$\Delta C_R^n(t_k) = \Delta C_R^n(t_{k-1}) \quad (4.3\text{-}15a)^*$$

$$\left(\overline{a}_U^n(t_k)\right)_{RIC} = \left(\overline{a}_U^n(t_{k-1})\right)_{RIC} \quad (4.3\text{-}16)^*$$

$$\left(\overline{a}_U^n(t_k)\right)_{VBN} = \left(\overline{a}_U^n(t_{k-1})\right)_{VBN} \quad (4.3\text{-}17)^*$$

$$\left(\overline{a}_U^n(t_k)\right)_B = \left(\overline{a}_U^n(t_{k-1})\right)_B \quad (4.3\text{-}18)^*$$

$$d_R^n(t_k) = d_R^n(t_{k-1}) + \dot{d}_R^n(t_{k-1})[t_k - t_{k-1}] \quad (4.3\text{-}19)^*$$

$$\dot{d}_R^n(t_k) = \dot{d}_R^n(t_{k-1}) \quad (4.3\text{-}19a)^*$$

$$\overline{b}_\rho^{G/W}(t_k) = \overline{b}_\rho^{G/W}(t_{k-1}) \quad (4.3\text{-}19a)^*$$

$$\overline{b}_d^{G/W}(t_k) = \overline{b}_d^{G/W}(t_{k-1}) \quad (4.3\text{-}19b)^*$$

$$\overline{b}_\rho^{CL}(t_k) = \overline{b}_\rho^{CL}(t_{k-1}) \quad (4.3\text{-}19c)^*$$

$$\overline{b}_d^{CL}(t_k) = \overline{b}_d^{CL}(t_{k-1}) \quad (4.3\text{-}19d)^*$$

$$\overline{b}^{CO}(t_k) = \overline{b}^{CO}(t_{k-1}) \quad (4.3\text{-}19e)^*$$

$$b_{\phi_n}^{G/W_i}(t_k) = \begin{cases} b_{\phi_n}^{G/W_i}(t_{k-1}), & t_k \neq \text{time of signal acquisition} \\ b_{\phi_n}^{G/W_i}(t_{acq}), & t_k = \text{time of signal acquisition for G/W}_\text{i} \text{ by receiver n} \end{cases} \quad (4.3\text{-}19f)^*$$

where $i = 1,\ldots 40$, $n = 1,\ldots, N_S$ and $b_{\phi_n}^{G/W_i}(t_{acq})$ is defined in Equation (5.3 - 51)

$$b_{\Delta\phi_{1n}}^{G/W_i}(t_k) = \begin{cases} b_{\Delta\phi_{1n}}^{G/W_i}(t_{k-1}), & t_k \neq \text{time of signal acquisition} \\ b_{\Delta\phi_{1n}}^{G/W_i}(t_{acq}), & t_k = \text{time of signal acquisition for G/W}_i \text{ by receiver 1 or receiver n} \end{cases} \quad \text{(4.3-19g)*}$$

where $i = 1,...40$, $n = 2,...,N_S$ and $b_{\Delta\phi_{1n}}^{G/W_i}(t_{acq})$ is defined in Equation (5.4-19)

$$\gamma_I(t_k) = \gamma_I(t_{k-1}) \quad \text{(4.3-19h)*}$$

$$\overline{b}_{\rho}^{GS}(t_k) = \overline{b}_{\rho}^{GS}(t_{k-1}) \quad \text{(4.3-19i)*}$$

$$\overline{b}_{d}^{GS}(t_k) = \overline{b}_{d}^{GS}(t_{k-1}) \quad \text{(4.3-19j)*}$$

$$\overline{b}_{d}^{TDRS}(t_k) = \overline{b}_{d}^{TDRS}(t_{k-1}) \quad \text{(4.3-19k)*}$$

$$\overline{b}_{IMU}^{A}(t_k) = \overline{b}_{IMU}^{A}(t_{k-1}) \quad \text{(4.3-19k)*}$$

The following are the nonzero partial derivatives for the random-walk variables that are used in computing the state transition matrix:

$$\frac{\partial \Delta C_D^n(t_k)}{\partial \Delta C_D^n(t_{k-1})} = 1 \quad \text{(4.3-20)*}$$

$$\frac{\partial \Delta C_R^n(t_k)}{\partial \Delta C_R^n(t_{k-1})} = 1 \quad \text{(4.3-20a)*}$$

$$\frac{\partial b_R^n(t_k)}{\partial b_R^n(t_{k-1})} = 1 \quad \text{(4.3-21)*}$$

$$\frac{\partial b_R^n(t_k)}{\partial d_R^n(t_{k-1})} = t_k - t_{k-1} \quad \text{(4.3-21a)*}$$

$$\frac{\partial b_R^n(t_k)}{\partial \dot{d}_R^n(t_{k-1})} = \frac{[t_k - t_{k-1}]^2}{2} \quad \text{(4.3-21b)*}$$

$$\frac{\partial d_R^n(t_k)}{\partial d_R^n(t_{k-1})} = 1 \quad \text{(4.3-22)*}$$

$$\frac{\partial d_R^n(t_k)}{\partial \dot{d}_R^n(t_{k-1})} = t_k - t_{k-1} \quad \text{(4.3-22a)*}$$

$$\frac{\partial \dot{d}_R^n(t_k)}{\partial \dot{d}_R^n(t_{k-1})} = 1 \qquad \text{(4.3-22aa)*}$$

$$\frac{\partial\left(a_{U_i}^n(t_k)\right)_{RIC}}{\partial\left(a_{U_i}^n(t_{k-1})\right)_{RIC}} = 1; \quad i = 1,...3 \qquad \text{(4.3-22b)*}$$

$$\frac{\partial\left(a_{U_i}^n(t_k)\right)_{VBN}}{\partial\left(a_{U_i}^n(t_{k-1})\right)_{VBN}} = 1; \quad i = 1,...3 \qquad \text{(4.3-22c)*}$$

$$\frac{\partial\left(a_{U_i}^n(t_k)\right)_{B}}{\partial\left(a_{U_i}^n(t_{k-1})\right)_{B}} = 1; \quad i = 1,...3 \qquad \text{(4.3-22d)*}$$

$$\frac{\partial b_{\rho}^{G/W_i}(t_k)}{\partial b_{\rho}^{G/W_i}(t_{k-1})} = 1; \quad i = 1,...40 \qquad \text{(4.3-23)*}$$

$$\frac{\partial b_{d}^{G/W_i}(t_k)}{\partial b_{d}^{G/W_i}(t_{k-1})} = 1; \quad i = 1,...40 \qquad \text{(4.3-24)*}$$

$$\frac{\partial b_{\rho_j}^{CL}(t_k)}{\partial b_{\rho_j}^{CL}(t_{k-1})} = 1; \quad j = 1,...N_S \qquad \text{(4.3-25)*}$$

$$\frac{\partial b_{d_j}^{CL}(t_k)}{\partial b_{d_j}^{CL}(t_{k-1})} = 1; \quad j = 1,...N_S \qquad \text{(4.3-26)*}$$

$$\frac{\partial b_{n}^{CO_j}(t_k)}{\partial b_{n}^{CO_j}(t_{k-1})} = 1; \quad n = 1,..., N_S;\ j = 1, ..., n_{sensor} \qquad \text{(4.3-27)*}$$

$$\frac{\partial b_{\phi_n}^{G/W_i}(t_k)}{\partial b_{\phi_n}^{G/W_i}(t_{k-1})} = 1; \quad n = 1,..., N_S;\ i = 1,...40 \qquad \text{(4.3-27a)*}$$

$$\frac{\partial b_{\Delta\phi_{1n}}^{G/W_i}(t_k)}{\partial b_{\Delta\phi_{1n}}^{G/W_i}(t_{k-1})} = 1; \quad n = 2,..., N_S;\ i = 1,...40 \qquad \text{(4.3-27b)*}$$

$$\frac{\partial \gamma_I(t_k)}{\partial \gamma_I(t_{k-1})} = 1 \qquad \text{(4.3-27c)*}$$

$$\frac{\partial b_{\rho}^{GS_j}(t_k)}{\partial b_{\rho}^{GS_j}(t_{k-1})} = 1; \quad j = 1,...n_{GS} \tag{4.3-27d}*$$

$$\frac{\partial b_{d}^{GS_j}(t_k)}{\partial b_{d}^{GS_j}(t_{k-1})} = 1; \quad j = 1,...n_{GS} \tag{4.3-27e}*$$

$$\frac{\partial b_{d}^{TDRS_j}(t_k)}{\partial b_{d}^{TDRS_j}(t_{k-1})} = 1; \quad j = 1,...,n_{TDRS} \tag{4.3-27f}*$$

$$\frac{\partial b_{IMU}^{A_i}(t_k)}{\partial b_{IMU}^{A_i}(t_{k-1})} = 1; \quad i = 1,...3 \tag{4.3-27g}*$$

where n_{GS} is the number of transmitting ground stations, n_{sensor} is the number of celestial object sensors, and n_{TDRS} is the number of TDRSS satellite transmitters.

4.3.2 First-Order Gauss-Markov Processes

The predicted values for the Gauss-Markov biases that can be estimated in GEONS are as follows:

$$\Delta C_D^n(t_k) = e^{-\frac{\Delta T}{\tau_{C_D}}} \Delta C_D^n(t_{k-1}) \tag{4.3-28}*$$

$$\Delta C_R^n(t_k) = e^{-\frac{\Delta T}{\tau_{C_R}}} \Delta C_R^n(t_{k-1}) \tag{4.3-29}*$$

$$b_R^n(t_k) = b_R^n(t_{k-1}) + \tau_R \left(1 - e^{-\frac{\Delta T}{\tau_R}}\right) d_R^n(t_{k-1}) \tag{4.3-29a}*$$

$$\left(\bar{a}_U^n(t_k)\right)_{RIC} = e^{-\frac{\Delta T}{\tau_{a_U}}} \left(\bar{a}_U^n(t_{k-1})\right)_{RIC} \tag{4.3-29b}*$$

$$\left(\bar{a}_U^n(t_k)\right)_{VBN} = e^{-\frac{\Delta T}{\tau_{a_U}}} \left(\bar{a}_U^n(t_{k-1})\right)_{VBN} \tag{4.3-29c}*$$

$$\left(\bar{a}_U^n(t_k)\right)_{B} = e^{-\frac{\Delta T}{\tau_{a_U}}} \left(\bar{a}_U^n(t_{k-1})\right)_{B} \tag{4.3-29d}*$$

$$d_R^n(t_k) = e^{-\frac{\Delta T}{\tau_R}} d_R^n(t_{k-1}) \tag{4.3-29e}*$$

$$\bar{b}_{\rho}^{G/W}(t_k) = e^{-\frac{\Delta T}{\tau_{\rho}^{G/W}}} \bar{b}_{\rho}^{G/W}(t_{k-1}) \tag{4.3-29f}*$$

$$\overline{b}_d^{G/W}(t_k) = e^{-\frac{\Delta T}{\tau_d^{G/W}}} \overline{b}_d^{G/W}(t_{k-1}) \qquad \text{(4.3-29g)*}$$

$$\overline{b}_\rho^{CL}(t_k) = e^{-\frac{\Delta T}{\tau_\rho^{CL}}} \overline{b}_\rho^{CL}(t_{k-1}) \qquad \text{(4.3-29h)*}$$

$$\overline{b}_d^{CL}(t_k) = e^{-\frac{\Delta T}{\tau_d^{CL}}} \overline{b}_d^{CL}(t_{k-1}) \qquad \text{(4.3-29i)*}$$

$$\overline{b}^{CO}(t_k) = e^{-\frac{\Delta T}{\tau^{CO}}} \overline{b}^{CO}(t_{k-1}) \qquad \text{(4.3-29j)*}$$

$$b_{\phi_n}^{G/W_i}(t_k) = \begin{cases} e^{-\frac{\Delta T}{\tau_\phi^{G/W}}} b_{\phi_n}^{G/W_i}(t_{k-1}), \; t_k \neq \text{time of signal acquisition} \\ b_{\phi_n}^{G/W_i}(t_{acq}), \; t_k = \text{time of signal acquisition for G/W}_\text{i} \text{ by receiver n} \end{cases} \qquad \text{(4.3-29k)*}$$

where $i = 1,...40$, $n = 1,..., N_S$ and $b_{\phi_n}^{G/W_i}(t_{acq})$ is defined in Equation (5.3-51)

$$b_{\Delta\phi_{1n}}^{G/W_i}(t_k) = \begin{cases} e^{-\frac{\Delta T}{\tau_{\Delta\phi}^{G/W}}} b_{\Delta\phi_{1n}}^{G/W_i}(t_{k-1}), \; t_k \neq \text{time of signal acquisition} \\ b_{\Delta\phi_{1n}}^{G/W_i}(t_{acq}), \; t_k = \text{time of signal acquisition for G/W}_\text{i} \text{ by receiver 1 or receiver n} \end{cases} \qquad \text{(4.3-29l)*}$$

where $i = 1,...40$, $n = 2,..., N_S$ and $b_{\phi_{1n}}^{G/W_i}(t_{acq})$ is defined in Equation (5.4-19)

$$\gamma_1(t_k) = e^{-\frac{\Delta T}{\tau_{\gamma_1}}} \gamma_1(t_{k-1}) \qquad \text{(4.3-29m)*}$$

$$\overline{b}_\rho^{GS}(t_k) = e^{-\frac{\Delta T}{\tau_\rho^{GS}}} \overline{b}_\rho^{GS}(t_{k-1}) \qquad \text{(4.3-30a)*}$$

$$\overline{b}_d^{GS}(t_k) = e^{-\frac{\Delta T}{\tau_d^{GS}}} \overline{b}_d^{GS}(t_{k-1}) \qquad \text{(4.3-30)*}$$

$$\overline{b}_d^{TDRS}(t_k) = e^{-\frac{\Delta T}{\tau_d^{TDRS}}} \overline{b}_d^{TDRS}(t_{k-1}) \qquad \text{(4.3-31)*}$$

$$\overline{b}_{IMU}^{A}(t_k) = e^{-\frac{\Delta T}{\tau^{A}}} \overline{b}_{IMU}^{A}(t_{k-1}) \qquad \text{(4.3-31a)*}$$

where

ΔT = $t_k - t_{k-1}$

τ = correlation time associated with the bias, a commanded parameter (seconds)

The following are the nonzero partial derivatives for Gauss Markov biases, which are used in computing the state transition matrix:

$$\frac{\partial \Delta C_D^n(t_k)}{\partial \Delta C_D^n(t_{k-1})} = e^{-\frac{\Delta T}{\tau_{C_D}}} \tag{4.3-31b)*}$$

$$\frac{\partial \Delta C_R^n(t_k)}{\partial \Delta C_R^n(t_{k-1})} = e^{-\frac{\Delta T}{\tau_{C_R}}} \tag{4.3-31c)*}$$

$$\frac{\partial b_R^n(t_k)}{\partial b_R^n(t_{k-1})} = 1 \tag{4.3-31d)*}$$

$$\frac{\partial b_R^n(t_k)}{\partial d_R^n(t_{k-1})} = \tau\left(1 - e^{-\frac{\Delta T}{\tau_R}}\right) \tag{4.3-31e)*}$$

$$\frac{\partial d_R^n(t_k)}{\partial d_R^n(t_{k-1})} = e^{-\frac{\Delta T}{\tau_R}} \tag{4.3-31f)*}$$

$$\frac{\partial\left(a_{U_i}^n(t_k)\right)_{RIC}}{\partial\left(a_{U_i}^n(t_{k-1})\right)_{RIC}} = e^{-\frac{\Delta T}{\tau_{a_U}}}; \quad i = 1,...3 \tag{4.3-31g)*}$$

$$\frac{\partial\left(a_{U_i}^n(t_k)\right)_{VBN}}{\partial\left(a_{U_i}^n(t_{k-1})\right)_{VBN}} = e^{-\frac{\Delta T}{\tau_{a_U}}}; \quad i = 1,...3 \tag{4.3-31h)*}$$

$$\frac{\partial\left(a_{U_i}^n(t_k)\right)_{B}}{\partial\left(a_{U_i}^n(t_{k-1})\right)_{B}} = e^{-\frac{\Delta T}{\tau_{a_U}}}; \quad i = 1,...3 \tag{4.3-31i)*}$$

$$\frac{\partial b_\rho^{G/W_i}(t_k)}{\partial b_\rho^{G/W_i}(t_{k-1})} = e^{-\frac{\Delta T}{\tau_\rho^{G/W}}}; \quad i = 1,...40 \tag{4.3-31j)*}$$

$$\frac{\partial b_d^{G/W_i}(t_k)}{\partial b_d^{G/W_i}(t_{k-1})} = e^{-\frac{\Delta T}{\tau_d^{G/W}}}; \quad i = 1,...40 \tag{4.3-31k)*}$$

$$\frac{\partial b_{\rho_j}^{CL}(t_k)}{\partial b_{\rho_j}^{CL}(t_{k-1})} = e^{-\frac{\Delta T}{\tau_\rho^{CL}}}; \quad j = 1,...N_S \tag{4.3-31l)*}$$

$$\frac{\partial b_{d_j}^{CL}(t_k)}{\partial b_{d_j}^{CL}(t_{k-1})} = e^{-\frac{\Delta T}{\tau_d^{CL}}}; \quad j = 1,...N_S \tag{4.3-31m)*}$$

$$\frac{\partial b_n^{CO_j}(t_k)}{\partial b_n^{CO_j}(t_{k-1})} = e^{-\frac{\Delta T}{\tau^{CO}}}; \quad n = 1,..., N_S;\ j = 1, ..., n_{sensor} \tag{4.3-31n)*}$$

$$\frac{\partial b_{\phi_n}^{G/W_i}(t_k)}{\partial b_{\phi_n}^{G/W_i}(t_{k-1})} = e^{-\frac{\Delta T}{\tau_\phi^{G/W}}}; \quad n = 1,..., N_S;\ i = 1,...40 \tag{4.3-31o)*}$$

$$\frac{\partial b_{\Delta\phi_{1n}}^{G/W_i}(t_k)}{\partial b_{\Delta\phi_{1n}}^{G/W_i}(t_{k-1})} = e^{-\frac{\Delta T}{\tau_{\Delta\phi}^{G/W}}}; \quad n = 2,..., N_S;\ i = 1,...40 \tag{4.3-31p)*}$$

$$\frac{\partial \gamma_I(t_k)}{\partial \gamma_I(t_{k-1})} = e^{-\frac{\Delta T}{\tau_{\gamma I}}} \tag{4.3-31q)*}$$

$$\frac{\partial b_\rho^{GS_j}(t_k)}{\partial b_\rho^{GS_j}(t_{k-1})} = e^{-\frac{\Delta T}{\tau_\rho^{GS}}}; \quad j = 1,...n_{GS} \tag{4.3-32a)*}$$

$$\frac{\partial b_d^{GS_j}(t_k)}{\partial b_d^{GS_j}(t_{k-1})} = e^{-\frac{\Delta T}{\tau_d^{GS}}}; \quad j = 1,...n_{GS} \tag{4.3-32)*}$$

$$\frac{\partial b_d^{TDRS_j}(t_k)}{\partial b_d^{TDRS_j}(t_{k-1})} = e^{-\frac{\Delta T}{\tau_d^{TDRS}}}; \quad j = 1,..., n_{TDRS} \tag{4.3-33)*}$$

$$\frac{\partial b_{IMU}^{A_i}(t_k)}{\partial b_{IMU}^{A_i}(t_{k-1})} = e^{-\frac{\Delta T}{\tau^A}}; \quad i = 1,...,3 \tag{4.3-33a)*}$$

where n_{GS} is the number of transmitting ground stations, n_{sensor} is the number of celestial object sensors, and n_{TDRS} is the number of TDRSS satellite transmitters.

4.3.3 Second-Order Gauss-Markov Processes

When the time bias is modeled as a FOGM process and the time bias drift is modeled as a SOGM process, the maximum value of the time bias covariance can be limited. In this case, the predicted values are as follows:

$$b_R^n(t_k) = \frac{\partial b_R^n(t_k)}{\partial b_R^n(t_{k-1})} b_R^n(t_{k-1}) + \frac{\partial b_R^n(t_k)}{\partial d_R^n(t_{k-1})} d_R^n(t_{k-1}) \tag{4.3-34}*$$

$$d_R^n(t_k) = \frac{\partial d_R^n(t_k)}{\partial b_R^n(t_{k-1})} b_R^n(t_{k-1}) + \frac{\partial d_R^n(t_k)}{\partial d_R^n(t_{k-1})} d_R^n(t_{k-1}) \tag{4.3-35}*$$

where the following partial derivatives are used in computing the state transition matrix:

$$\frac{\partial b_R^n(t_k)}{\partial b_R^n(t_{k-1})} = \frac{e^{a\Delta T}}{b}\left(b\cos(b\Delta T) + (a + 2\varsigma_d\omega_n)\sin(b\Delta T)\right) \tag{4.3-36}*$$

$$\frac{\partial b_R^n(t_k)}{\partial d_R^n(t_{k-1})} = \frac{e^{a\Delta T}}{b}\sin(b\Delta T) \tag{4.3-37}*$$

$$\frac{\partial d_R^n(t_k)}{\partial b_R^n(t_{k-1})} = -\frac{e^{a\Delta T}}{b}\omega_n^2\sin(b\Delta T) \tag{4.3-38}*$$

$$\frac{\partial d_R^n(t_k)}{\partial d_R^n(t_{k-1})} = \frac{e^{a\Delta T}}{b}\left(b\cos(b\Delta T) + (a + \beta)\sin(b\Delta T)\right) \tag{4.3-39}*$$

where

$$a = -\frac{1}{2}\left(\beta + 2\varsigma_d\omega_n\right) \tag{4.3-40}*$$

$$b = \sqrt{\omega_n^2(1-\varsigma_d{}^2) + \beta\varsigma_d\omega_n - \frac{1}{4}\beta^2} = \sqrt{\omega_d^2 + \beta\varsigma_d\omega_n - \frac{1}{4}\beta^2} \tag{4.3-41}*$$

$$\omega_d = \sqrt{\omega_n^2\left(1-\zeta_d{}^2\right)} \tag{4.3-42}*$$

where

$$\Delta T = t_k - t_{k-1}$$

$\beta = 1/\tau_R$ = where τ_R is the FOGM correlation time associated with the receiver time bias, a commanded parameter (seconds) with recommended values 43200 s$\leq \tau_R \leq$43200000 s

ω_n = SOGM natural frequency, a commanded parameter (radians per second) with recommended values $6x10^{-5} \leq \omega_n \leq 3x10^{-4}$

ζ_d = SOGM damping ratio, a commanded parameter (unitless) with recommended values $0 \leq \zeta_d < 1$

If the values for τ_R, ω_n, and ζ_d are selected such that $1/a$ is much larger than ΔT, the FOGM/SOGM process resembles a random walk process over intervals shorter than $1/a$. Reference 53 provides a more detailed discussion of the performance of this model.

4.4 State Error Covariance Propagation

Sections 4.4.1 through 4.4.3 present the algorithms for computing the state transition matrix, computing the state process noise covariance matrix, and propagating the covariance matrix factors, respectively. Note that the timestep used for state error covariance propagation is the same as the time interval used in the filter time update processing discussed in Section 2.3.1.

4.4.1 State Transition Matrix Computation

The state transition matrix is used to propagate the state error covariance matrix. Note that the state transition matrix is computed in ECI frame, regardless of the central body that is being used to integrate the satellite state vector.

The state transition matrix at time t_i is defined as

$$\Phi(t_i,t_{i-1})=\frac{\partial \bar{X}(t_i)}{\partial \bar{X}(t_{i-1})}=\begin{bmatrix} \frac{\partial \bar{X}^1(t_i)}{\partial \bar{X}^1(t_{i-1})} & \cdots & 0 & 0 & 0 \\ \vdots & \ddots & \vdots & \vdots & \vdots \\ 0 & \cdots & \frac{\partial \bar{X}^{N_S}(t_i)}{\partial \bar{X}^{N_S}(t_{i-1})} & 0 & 0 \\ 0 & \cdots & 0 & \frac{\partial \bar{B}(t_i)}{\partial \bar{B}(t_{i-1})} & 0 \\ 0 & \cdots & 0 & 0 & \frac{\partial \gamma_I(t_i)}{\partial \gamma_I(t_{i-1})} \end{bmatrix} \qquad (4.4\text{-}1)^*$$

where

$$\frac{\partial \bar{X}^n(t_i)}{\partial \bar{X}^n(t_{i-1})}=\begin{bmatrix} \frac{\partial \bar{R}(t_i)}{\partial \bar{R}(t_{i-1})} & \frac{\partial \bar{R}(t_i)}{\partial \dot{\bar{R}}(t_{i-1})} & \frac{\partial \bar{R}(t_i)}{\partial \Delta C_D(t_{i-1})} & \frac{\partial \bar{R}(t_i)}{\partial \Delta C_R(t_{i-1})} & 0_{3\times2} & \frac{\partial \bar{R}(t_i)}{\partial \bar{a}_U(t_{i-1})} & \frac{\partial \bar{R}(t_i)}{\partial \bar{b}^A_{IMU}(t_{i-1})} \\ \frac{\partial \dot{\bar{R}}(t_i)}{\partial \bar{R}(t_{i-1})} & \frac{\partial \dot{\bar{R}}(t_i)}{\partial \dot{\bar{R}}(t_{i-1})} & \frac{\partial \dot{\bar{R}}(t_i)}{\partial \Delta C_D(t_{i-1})} & \frac{\partial \dot{\bar{R}}(t_i)}{\partial \Delta C_R(t_{i-1})} & 0_{3\times2} & \frac{\partial \dot{\bar{R}}(t_i)}{\partial \bar{a}_U(t_{i-1})} & \frac{\partial \dot{\bar{R}}(t_i)}{\partial \bar{b}^A_{IMU}(t_{i-1})} \\ 0_{1\times3} & 0_{1\times3} & \frac{\partial \Delta C_D(t_i)}{\partial \Delta C_D(t_{i-1})} & 0 & 0_{1\times2} & 0_{1\times3} & 0_{1\times3} \\ 0_{1\times3} & 0_{1\times3} & 0 & \frac{\partial \Delta C_R(t_i)}{\partial \Delta C_R(t_{i-1})} & 0_{1\times2} & 0_{1\times3} & 0_{1\times3} \\ 0_{2\times3} & 0_{2\times3} & 0_{2\times1} & 0_{2\times1} & \frac{\partial \bar{b}_R(t_i)}{\partial \bar{b}_R(t_{i-1})} & 0_{2\times3} & 0_{2\times3} \\ 0_{3\times3} & 0_{3\times3} & 0_{3\times1} & 0_{3\times1} & 0_{3\times2} & \frac{\partial \bar{a}_U(t_i)}{\partial \bar{a}_U(t_{i-1})} & 0_{3\times3} \\ 0_{3\times3} & 0_{3\times3} & 0_{3\times1} & 0_{3\times1} & 0_{3\times2} & 0_{3\times3} & \frac{\partial \bar{b}^A_{IMU}(t_i)}{\partial \bar{b}^A_{IMU}(t_{i-1})} \end{bmatrix} \qquad (4.4\text{-}1a)^*$$

If the state vector includes relative states for the nonlocal satellites, the associated state transition matrix includes the correlation between the relative states and the local state

$$\Phi(t_i,t_{i-1})=\frac{\partial \overline{X}_{rel}(t_i)}{\partial \overline{X}_{rel}(t_{i-1})}=\begin{bmatrix} \frac{\partial \overline{X}^1(t_i)}{\partial \overline{X}^1(t_{i-1})} & 0 & \cdots & 0 & 0 & 0 \\ \frac{\partial \overline{X}^2(t_i)}{\partial \overline{X}^2(t_{i-1})}-\frac{\partial \overline{X}^1(t_i)}{\partial \overline{X}^1(t_{i-1})} & \frac{\partial \overline{X}^2(t_i)}{\partial \overline{X}^2(t_{i-1})} & \cdots & 0 & 0 & 0 \\ \vdots & \vdots & \ddots & \vdots & \vdots & \vdots \\ \frac{\partial \overline{X}^{N_S}(t_i)}{\partial \overline{X}^{N_S}(t_{i-1})}-\frac{\partial \overline{X}^1(t_i)}{\partial \overline{X}^1(t_{i-1})} & 0 & \cdots & \frac{\partial \overline{X}^{N_S}(t_i)}{\partial \overline{X}^{N_S}(t_{i-1})} & 0 & 0 \\ 0 & 0 & \cdots & 0 & \frac{\partial \overline{B}(t_i)}{\partial \overline{B}(t_{i-1})} & 0 \\ 0 & 0 & \cdots & 0 & 0 & \frac{\partial \gamma_I(t_i)}{\partial \gamma_I(t_{i-1})} \end{bmatrix} \quad \text{(4.4-1b)}$$

Note that, if the atmospheric drag coefficient correction, the solar radiation pressure coefficient correction and/or the acceleration biases are not being estimated, the associated columns are not present in the state transition matrix given in Equation (4.4.1a).

The position and velocity components are computed by the following semianalytic approximation

$$\begin{bmatrix} \frac{\partial \overline{R}(t_i)}{\partial \overline{R}(t_{i-1})} & \frac{\partial \overline{R}(t_i)}{\partial \dot{\overline{R}}(t_{i-1})} \\ \frac{\partial \dot{\overline{R}}(t_i)}{\partial \overline{R}(t_{i-1})} & \frac{\partial \dot{\overline{R}}(t_i)}{\partial \dot{\overline{R}}(t_{i-1})} \end{bmatrix}=\begin{bmatrix} I+A_{i-1}\frac{\Delta T^2}{2} & I\left(\Delta T-\beta\frac{\Delta T^2}{2}\right) \\ (A_{i-1}+A_i)\frac{\Delta T}{2}-\beta A_{i-1}\frac{\Delta T^2}{2} & I+A_i\frac{\Delta T^2}{2}+I\left(-\beta\Delta T+\beta^2\frac{\Delta T^2}{2}\right) \end{bmatrix} \quad \text{(4.4-2)*}$$

where $\Delta T = t_i - t_{i-1}$ (seconds) and $\beta = 2\varsigma \cdot \omega_n$, where ς is the SOGM orbital covariance artificial damping ratio (a commandable parameter) and ω_n is the orbital rate given by (Reference 52)

$$\omega_n = \frac{2\pi}{P} = \sqrt{\frac{\mu_C}{a^3}} \quad \text{(4.4-3)*}$$

where the semimajor axis is given by

$$a = \left[\frac{2}{|\overline{R}|}-\frac{|\dot{\overline{R}}|^2}{\mu_C}\right]^{-1} \quad \text{(4.4-3a)*}$$

The [3 × 3] [A_i] matrix consists of the partial derivatives of the acceleration vector, $\ddot{\overline{R}}(t_i)$, with respect to the position vector at time t_i. Computation of the [A_i] matrix is discussed in Section 4.4.1.1. The [3 × 3] [I] matrix is the identity matrix. This semianalytic second-order formulation of the position and velocity state transition submatrix, which is based on Method H in Reference 17 and Reference 59, is obtained using the following second-order Runge-Kutta integration formula:

$$\Phi(t_i, t_{i-1}) = I + \frac{A(t_{i-1})+A(t_i)}{2}\Delta T + A(t_{i-1})A(t_i)\frac{\Delta T^2}{2} \tag{4.4-4}$$

Based on analysis presented in Reference 17, this approximation will propagate the state error covariance matrix around one orbit (for a low Earth orbit) with an accuracy of approximately 1 percent if a maximum time step of 16 seconds is used.

If the atmospheric drag coefficient correction is estimated, the atmospheric drag correction components are computed by the approximation

$$\begin{bmatrix} \dfrac{\partial \overline{R}(t_i)}{\partial \Delta C_D(t_{i-1})} \\ \dfrac{\partial \dot{\overline{R}}(t_i)}{\partial \Delta C_D(t_{i-1})} \end{bmatrix} = \begin{bmatrix} B_{i-1}\dfrac{\Delta T^2}{2} \\ B_{i-1}\Delta T \end{bmatrix} \tag{4.4-5}*$$

The $[B_{i\text{-}1}]$ matrix represents the partial derivatives of the acceleration vector with respect to the drag scale factor at time $t_{i\text{-}1}$. The $[B]$ matrix is computed in Section 4.4.1.2.

If the solar radiation pressure coefficient correction is estimated, the solar radiation pressure coefficient correction components are computed by the approximation

$$\begin{bmatrix} \dfrac{\partial \overline{R}(t_i)}{\partial \Delta C_R(t_{i-1})} \\ \dfrac{\partial \dot{\overline{R}}(t_i)}{\partial \Delta C_R(t_{i-1})} \end{bmatrix} = \begin{bmatrix} D_{i-1}\dfrac{\Delta T^2}{2} \\ D_{i-1}\Delta T \end{bmatrix} \tag{4.4-5a}*$$

The $[D_{i\text{-}1}]$ matrix represents the partial derivatives of the acceleration vector with respect to the solar radiation pressure coefficient at time $t_{i\text{-}1}$. The $[D]$ matrix is computed in Section 4.4.1.3.

If the acceleration biases are estimated, the acceleration bias components are computed by the approximation

$$\begin{bmatrix} \dfrac{\partial \overline{R}(t_i)}{\partial \overline{a}_u(t_{i-1})} \\ \dfrac{\partial \dot{\overline{R}}(t_i)}{\partial \overline{a}_u(t_{i-1})} \end{bmatrix} = \begin{bmatrix} E_{i-1}\dfrac{\Delta T^2}{2} \\ E_{i-1}\Delta T \end{bmatrix} \tag{4.4-5b}*$$

The $[E_{i\text{-}1}]$ matrix represents the partial derivatives of the mean of J2000.0 acceleration vector with respect to the acceleration biases at time $t_{i\text{-}1}$. The $[E]$ matrix is computed in Section 4.4.1.4.

If the accelerometer sensor biases are estimated, the accelerometer bias components are computed by the approximation

$$\begin{bmatrix} \dfrac{\partial \bar{R}(t_i)}{\partial \bar{b}^{A}_{IMU}(t_{i-1})} \\ \dfrac{\partial \dot{\bar{R}}(t_i)}{\partial \bar{b}^{A}_{IMU}(t_{i-1})} \end{bmatrix} = \begin{bmatrix} F_{i-1}\dfrac{\Delta T^2}{2} \\ F_{i-1}\Delta T \end{bmatrix} \qquad \text{(4.4-5c)*}$$

The $[F_{i\text{-}1}]$ matrix represents the partial derivatives of the mean of J2000.0 acceleration vector with respect to the accelerometer sensor biases at time $t_{i\text{-}1}$. The $[F]$ matrix is computed as defined in Section 4.4.1.5.

The remaining partial derivatives in Equation 4.4-1a are defined in Section 4.3.1 (Equations 4.3-20 through 4.3-22d) and Section 4.3.2 (Equations 4.3-31b through 4.3-31i) for random walk or first-order Gauss Markov bias processes, respectively and in Section 4.3.3 when the time bias drift is modeled as a second-order Gauss-Markov process (Equations 4.3-37 through 4.3-40).

$$\frac{\partial \bar{B}(t_i)}{\partial \bar{B}(t_{i-1})} = \begin{bmatrix}
\dfrac{\partial \bar{b}_p^{G/W}(t_i)}{\partial \bar{b}_p^{G/W}(t_{i-1})} & 0 & 0 & 0 & 0 & 0 & 0 & 0 & 0 & 0 \\
0 & \dfrac{\partial \bar{b}_d^{G/W}(t_i)}{\partial \bar{b}_d^{G/W}(t_{i-1})} & 0 & 0 & 0 & 0 & 0 & 0 & 0 & 0 \\
0 & 0 & \dfrac{\partial \bar{b}_p^{CL}(t_i)}{\partial \bar{b}_p^{CL}(t_{i-1})} & 0 & 0 & 0 & 0 & 0 & 0 & 0 \\
0 & 0 & 0 & \dfrac{\partial \bar{b}_d^{CL}(t_i)}{\partial \bar{b}_d^{CL}(t_{i-1})} & 0 & 0 & 0 & 0 & 0 & 0 \\
0 & 0 & 0 & 0 & \dfrac{\partial \bar{b}^{CO}(t_i)}{\partial \bar{b}^{CO}(t_{i-1})} & 0 & 0 & 0 & 0 & 0 \\
0 & 0 & 0 & 0 & 0 & \dfrac{\partial \bar{b}_p^{GS}(t_i)}{\partial \bar{b}_p^{GS}(t_{i-1})} & 0 & 0 & 0 & 0 \\
0 & 0 & 0 & 0 & 0 & 0 & \dfrac{\partial \bar{b}_d^{GS}(t_i)}{\partial \bar{b}_d^{GS}(t_{i-1})} & 0 & 0 & 0 \\
0 & 0 & 0 & 0 & 0 & 0 & 0 & \dfrac{\partial \bar{b}_d^{TDRS}(t_i)}{\partial \bar{b}_d^{TDRS}(t_{i-1})} & 0 & 0 \\
0 & 0 & 0 & 0 & 0 & 0 & 0 & 0 & \dfrac{\partial \bar{b}_\phi^{G/W}(t_i)}{\partial \bar{b}_\phi^{G/W}(t_{i-1})} & 0 \\
0 & 0 & 0 & 0 & 0 & 0 & 0 & 0 & 0 & \dfrac{\partial \bar{b}_{\Delta\phi}^{G/W}(t_i)}{\partial \bar{b}_{\Delta\phi}^{G/W}(t_{i-1})}
\end{bmatrix} \qquad \text{(4.4-5e)*}$$

The partial derivatives of the measurement biases in Equation (4.4-5e) and the partial derivative of the ionospheric scale factor are defined in Section 4.3.1 (Equations 4.3-23 through 4.3-27f) and Section 4.3.2 (Equations 4.3-31j through 4.3-33) for random walk or Gauss Markov bias processes, respectively.

4.4.1.1 Acceleration Partial Derivatives

If the covariance damping ratio ς equals zero, the [3 × 3] acceleration partial derivatives matrix $[A_i]$ includes all point mass accelerations for all perturbing bodies included in the acceleration model and the Earth J_2 zonal harmonic acceleration, $\bar{a}_{J_2}$, if the degree of the nonspherical Earth

gravitational model is greater than or equal to 2. If the covariance damping ratio ς is greater than zero, the [3 × 3] acceleration partial derivatives matrix [A_i] includes only the central body point mass acceleration. Note that this matrix is computed in the ECI frame regardless of which body is used as the central body for state integration. This matrix can be approximated as follows in the ECI frame, if the effects of precession and nutation are ignored:

$$[A] = \begin{bmatrix} \frac{\partial a_{gx}}{\partial X} & \frac{\partial a_{gx}}{\partial Y} & \frac{\partial a_{gx}}{\partial Z} \\ \frac{\partial a_{gy}}{\partial X} & \frac{\partial a_{gy}}{\partial Y} & \frac{\partial a_{gy}}{\partial Z} \\ \frac{\partial a_{gz}}{\partial X} & \frac{\partial a_{gz}}{\partial Y} & \frac{\partial a_{gz}}{\partial Z} \end{bmatrix} \tag{4.4-6}*$$

where

$$\bar{a}_g = \begin{cases} \bar{a}_E + \sum_p \mu_p \left(\frac{\bar{R}^p - \bar{R}}{\left|\bar{R}^p - \bar{R}\right|^3} - \frac{\bar{R}^p}{\left|\bar{R}^p\right|^3} \right); & \varsigma = 0,\ N_{NS}^{Earth} < 2 \\ \bar{a}_E + \bar{a}_{J_2} + \sum_p \mu_p \left(\frac{\bar{R}^p - \bar{R}}{\left|\bar{R}^p - \bar{R}\right|^3} - \frac{\bar{R}^p}{\left|\bar{R}^p\right|^3} \right); & \varsigma = 0,\ N_{NS}^{Earth} \geq 2 \\ \bar{a}_C; & \varsigma > 0 \end{cases} \tag{4.4-7}$$

$$\bar{a}_E = -\frac{\mu_E \bar{R}}{R^3} \tag{4.4-8}$$

$$\bar{a}_{J_2} = -\frac{3\mu_E R_e^2 C_2^0}{2R^5} \begin{bmatrix} (5\frac{Z^2}{R^2} - 1)X \\ (5\frac{Z^2}{R^2} - 1)Y \\ (5\frac{Z^2}{R^2} - 3)Z \end{bmatrix} \tag{4.4-9}$$

$$R = \sqrt{X^2 + Y^2 + Z^2} \tag{4.4-10}*$$

and $\bar{a}_C$ is the non-Earth central body acceleration expressed in the ECI frame

$$\bar{a}_C = \mu_P \left(\frac{\bar{R}^p - \bar{R}}{\left|\bar{R}^p - \bar{R}\right|^3} - \frac{\bar{R}^p}{\left|\bar{R}^p\right|^3} \right) \tag{4.4-10a}$$

where μ_P is the gravitational constant of the non-Earth central body and $\overline{R}^p$ is the position vector of the non-Earth central body expressed in the ECI frame

In Equation 4.4-7, the summation over p includes all bodies other than the Earth that are included in the gravitational point mass acceleration and $\overline{R} = \overline{R}^n_{ECI}$ and $\overline{R}^p = \overline{R}^p_{ECI}$.

When the covariance damping ratio ς equals zero, the gravitational acceleration can be written in the form:

$$\bar{a}_g = \begin{bmatrix} -\frac{\mu_x}{R^3}X + \sum_p \mu_p \left(\frac{X^p - X}{|\bar{R}^p - \bar{R}|^3} - \frac{X^p}{|R^p|^3}\right) \\ -\frac{\mu_x}{R^3}Y + \sum_p \mu_p \left(\frac{Y^p - Y}{|R^p - \bar{R}|^3} - \frac{Y^p}{|\bar{R}^p|^3}\right) \\ (-\frac{\mu_x}{R^3} + 3\frac{\mu_E C_2^0 R_e^2}{R^5})Z + \sum_p \mu_p \left(\frac{Z^p - Z}{|\bar{R}^p - \bar{R}|^3} - \frac{Z^p}{|\bar{R}^p|^3}\right) \end{bmatrix} \quad (4.4\text{-}11)^*$$

where

$$\mu_x = \mu_E \left[1 + \frac{3}{2} C_2^0 \frac{R_e^2}{R^2}\left(5\frac{Z^2}{R^2} - 1\right)\right] \quad (4.4\text{-}12)^*$$

When the covariance damping ratio ς equals zero, the following acceleration partial derivatives (taken from Reference 17) are valid for the J2000.0 coordinate system:

$$\frac{\partial a_{gx}}{\partial X} = -\frac{\mu_x}{R^3} + \frac{X^2}{R^5}\left[7\mu_x - 4\mu_E + 3\mu_E\ C_2^0 \frac{R_e^2}{R^2}\right] + \sum_p \mu_p \left(\frac{-1}{|\bar{R}^p - \bar{R}|^3} + 3\frac{X^p - X}{|\bar{R}^p - \bar{R}|^5}\right) \quad (4.4\text{-}13)^*$$

$$\frac{\partial a_{gx}}{\partial Y} = \frac{X\ Y}{R^5}\left[7\mu_x - 4\mu_E + 3\mu_E\ C_2^0 \frac{R_e^2}{R^2}\right] + \sum_p \mu_p \left(3\frac{(X^p - X)(Y^p - Y)}{|\bar{R}^p - \bar{R}|^5}\right) \quad (4.4\text{-}14)^*$$

$$\frac{\partial a_{gx}}{\partial Z} = \frac{X\ Z}{R^5}\left[7\mu_x - 4\mu_E - 12\mu_E\ C_2^0 \frac{R_e^2}{R^2}\right] + \sum_p \mu_p \left(3\frac{(X^p - X)(Z^p - Z)}{|\bar{R}^p - \bar{R}|^5}\right) \quad (4.4\text{-}15)^*$$

$$\frac{\partial a_{gy}}{\partial X} = \frac{\partial a_{gx}}{\partial Y} \quad (4.4\text{-}16)^*$$

$$\frac{\partial a_{gy}}{\partial Y} = -\frac{\mu_x}{R^3} + \frac{Y^2}{R^5}\left[7\mu_x - 4\mu_E + 3\mu_E\ C_2^0 \frac{R_e^2}{R^2}\right] + \sum_p \mu_p \left(\frac{-1}{|\bar{R}^p - \bar{R}|^3} + 3\frac{(Y^p - Y)^2}{|\bar{R}^p - \bar{R}|^5}\right) \quad (4.4\text{-}17)^*$$

$$\frac{\partial a_{gy}}{\partial Z} = \frac{Y\ Z}{R^5}\left[7\mu_x - 4\mu_E - 12\mu_E C_2^0 \frac{R_e^2}{R^2}\right] + \sum_p \mu_p \left(3\frac{(Y^p - Y)(Z^p - Z)}{|\bar{R}^p - \bar{R}|^5}\right) \quad (4.4\text{-}18)^*$$

$$\frac{\partial a_{gz}}{\partial X} = \frac{\partial a_{gx}}{\partial Z} \quad (4.4\text{-}19)^*$$

$$\frac{\partial a_{gz}}{\partial Y} = \frac{\partial a_{gy}}{\partial Z} \quad (4.4\text{-}20)^*$$

$$\frac{\partial a_{gz}}{\partial Z} = -\frac{\partial a_{gx}}{\partial X} - \frac{\partial a_{gy}}{\partial Y} \qquad (4.4\text{-}21)^*$$

When the covariance damping ratio ς is greater than zero,

$$\frac{\partial a_{gx}}{\partial X} = \mu_p \left(\frac{-1}{|\bar{R}^p - \bar{R}|^3} + 3\frac{(X^p - X)^2}{|\bar{R}^p - \bar{R}|^5} \right) \qquad (4.4\text{-}21a)^*$$

$$\frac{\partial a_{gx}}{\partial Y} = \mu_p \left(3\frac{(X^p - X)(Y^p - Y)}{|\bar{R}^p - \bar{R}|^5} \right) \qquad (4.4\text{-}21b)^*$$

$$\frac{\partial a_{gx}}{\partial Z} = \mu_p \left(3\frac{(X^p - X)(Z^p - Z)}{|\bar{R}^p - \bar{R}|^5} \right) \qquad (4.4\text{-}21c)^*$$

$$\frac{\partial a_{gy}}{\partial X} = \frac{\partial a_{gx}}{\partial Y} \qquad (4.4\text{-}21d)^*$$

$$\frac{\partial a_{gy}}{\partial Y} = \mu_p \left(\frac{-1}{|\bar{R}^p - \bar{R}|^3} + 3\frac{(Y^p - Y)^2}{|\bar{R}^p - \bar{R}|^5} \right) \qquad (4.4\text{-}21e)^*$$

$$\frac{\partial a_{gy}}{\partial Z} = \mu_p \left(3\frac{(Y^p - Y)(Z^p - Z)}{|\bar{R}^p - \bar{R}|^5} \right) \qquad (4.4\text{-}21f)^*$$

$$\frac{\partial a_{gz}}{\partial X} = \frac{\partial a_{gx}}{\partial Z} \qquad (4.4\text{-}21g)^*$$

$$\frac{\partial a_{gz}}{\partial Y} = \frac{\partial a_{gy}}{\partial Z} \qquad (4.4\text{-}21h)^*$$

$$\frac{\partial a_{gz}}{\partial Z} = -\frac{\partial a_{gx}}{\partial X} - \frac{\partial a_{gy}}{\partial Y} \qquad (4.4\text{-}21i)^*$$

4.4.1.2 Drag Scale Factor Partial Derivatives

The [3 × 1] drag scale factor partial derivative matrix [*B*] is given below:

$$[B] = -\frac{\rho_a A}{2m} \left| \overline{V}_{rel} \right| \overline{V}_{rel} \qquad (4.4\text{-}22)^*$$

where all the parameters on the right hand side of Equation (4.4-22) are defined in Section 4.1.3.

Equation deleted (4.4-23)

Equation deleted (4.4-24)

Equation deleted (4.4-25)

Equation deleted (4.4-26)

4.4.1.3 Solar Radiation Pressure Coefficient Partial Derivatives

The [3 × 1] solar radiation pressure coefficient partial derivative matrix [*D*] is given below for the spherical area model:

$$[D] = \nu P_S R_{Sun}^2 \frac{A}{m} \frac{\bar{r}_{vs}}{r_{vs}^3} \qquad \text{(4.4-26a)*}$$

The parameters on the right hand side of Equation (4.4-26a) are defined in Section 4.1.4.1 and are computed in the ECI frame. The corresponding partial derivative matrix for the MMS spin-stabilized macromodel is defined in Section 4.1.4.2.

4.4.1.4 Acceleration Bias Partial Derivatives

The [3 × 3] acceleration bias partial derivative matrix [*E*] is given below:

$$[E] = \begin{cases} [T_{XYZ \leftarrow RIC}]_C, \text{ for acceleration biases expressed in the RIC frame, } (\bar{a}_U)_{RIC} \\ [T_{XYZ \leftarrow VBN}]_C, \text{ for acceleration biases expressed in the VBN frame, } (\bar{a}_U)_{VBN} \\ T_{XYZ \leftarrow B}, \text{ for acceleration biases expressed in the body frame, } (\bar{a}_U)_B \end{cases} \qquad \text{(4.4-26b)*}$$

The transformation matrices in Equation (4.4-26b) are defined in Sections 3.2.4, 3.2.8 and 3.2.10.

4.4.1.5 Accelerometer Sensor Bias Partial Derivatives

The components of the [3 × 6] partial derivative matrix [*F*] of the accelerometer acceleration with respect to the accelerometer measurement bias components in the IMU sensor frame and the accelerometer scale factor bias components defined in Section 4.1.5 have the following values during thrusting and are 0 otherwise:

$$[F] = -[T_{XYZ \leftarrow B}]_C \; [T_{B \leftarrow IMU}] \begin{bmatrix} 1 & 0 & 0 & a_{IMU_x}^{Measured} & 0 & 0 \\ 0 & 1 & 0 & 0 & a_{IMU_y}^{Measured} & 0 \\ 0 & 0 & 1 & 0 & 0 & a_{IMU_z}^{Measured} \end{bmatrix} \qquad \text{(4.4-26c)*}$$

The transformation matrices are defined in Sections 3.2.8 and 3.2.10.

4.4.2 Process Noise Covariance Matrix

The process noise covariance matrix, Q_k, is used in the Kalman filter algorithms to correct the state error covariance for errors in the force model. The GEONS extended Kalman filter uses a physically connected algorithm (see References 18 and 19) for calculating the gravitational contribution to the spacecraft state error covariance and uses random-walk algorithms for calculating the contribution from other sources. This section presents these algorithms. Section 4.4.2.1 describes the block structure of the process noise covariance matrix and the nonspacecraft state process noise block. Section 4.4.2.2 discusses the computation of the gravitational process noise contribution.

4.4.2.1 Block Structure of the Process Noise Covariance Matrix

The total process noise covariance matrix has the form:

$$Q_{i\text{-}1} = \begin{bmatrix} Q_{i\text{-}1}(\overline{X}_1) & \cdots & 0 & 0 & 0 \\ \vdots & \ddots & \vdots & \vdots & \vdots \\ 0 & \cdots & Q_{i\text{-}1}(\overline{X}_{N_S}) & 0 & 0 \\ 0 & \cdots & 0 & Q_{i\text{-}1}(\overline{B}) & 0 \\ 0 & \cdots & 0 & 0 & Q_{i\text{-}1}(\gamma_I) \end{bmatrix} \qquad (4.4\text{-}27)^*$$

The GEONS state vector components for each user satellite can be partitioned into two parts: (1) spacecraft position and velocity elements and (2) other satellite state parameters, which include receiver time bias and time bias drift corrections and optionally the atmospheric drag coefficient correction and solar radiation pressure coefficient correction. This can be represented as follows:

$$\overline{X}^n = \begin{bmatrix} \overline{S} \\ \overline{g} \end{bmatrix}^n \qquad (4.4\text{-}27a)^*$$

where $\overline{S}$ is composed of the position and velocity vectors, $\overline{R}$ and $\dot{\overline{R}}$, of the nth user spacecraft ($\overline{S}$ is a six-component vector).

The quantity $\overline{g}$ is given by

$$\overline{g} = \begin{bmatrix} \Delta C_D \\ \Delta C_R \\ \overline{b}_R \\ \overline{a}_U \end{bmatrix} \qquad (4.4\text{-}28)^*$$

where

ΔC_D = the atmospheric drag coefficient correction

ΔC_R = the solar radiation pressure coefficient correction

$\overline{b}_R$ = GPS receiver time-bias vector, which includes b_R, d_R, and optionally $\dot{d}_R$

$\overline{u}_U$ = Unmodeled acceleration biases expressed in either the RIC, VBN or body frame

The gravitational process noise contribution to the covariance matrix for the orbital elements vector, $\overline{S}$, is computed using the physically connected algorithm described in Section 4.4.2.2. The quantities contained in the vector $\overline{g}$ are random variables, and the contribution of the process noise to the covariance matrix for these parameters is described at the end of this section.

The process noise covariance matrix components for each user satellite [needed to evaluate Equations (4.4-62) and (4.4-63) in Section 4.4.3] have a block structure that can be represented as follows:

$$Q_{i-1}(\bar{X}^n) = \begin{bmatrix} Q_{i-1}(\bar{S}^n) & 0 \\ 0 & Q_{i-1}(\bar{g}^n) \end{bmatrix} \quad (4.4\text{-}29)^*$$

where

$Q(\bar{S}^n)$ = process noise covariance matrix for the position and velocity vectors of satellite n [defined in Equation (4.4-30)]

$Q(\bar{g}^n)$ = process noise covariance matrix for the other state variables of satellite n [defined in Equation (4.4-35)]

The position and velocity submatrix is computed in RIC components in the central body frame and then transformed into XYZ mean of J2000 coordinates as shown below; where the transformation matrix, $[T_{RIC \leftarrow XYZ}]_C$, is computed using the position and velocity in the central body frame at time (t_{i-1}):

$$Q_{i-1}(\bar{S}^n) = \begin{bmatrix} [T_{RIC \leftarrow XYZ}]_C & 0_{3\times3} \\ 0_{3\times3} & [T_{RIC \leftarrow XYZ}]_C \end{bmatrix}^T [Q_{RIC_C}]_n \begin{bmatrix} [T_{RIC \leftarrow XYZ}]_C & 0_{3\times3} \\ 0_{3\times3} & [T_{RIC \leftarrow XYZ}]_C \end{bmatrix} \quad (4.4\text{-}30)$$

where

$$\left[Q_{RIC}\right]^n = \begin{bmatrix} Q_r\frac{\Delta T^3}{3}+Q_\mu\frac{\Delta T^4}{4} & 0 & 0 & Q_r\frac{\Delta T^2}{2}+Q_\mu\frac{\Delta T^3}{2} & 0 & 0 \\ 0 & Q_i\frac{\Delta T^3}{3} & 0 & 0 & Q_i\frac{\Delta T^2}{2} & 0 \\ 0 & 0 & Q_c\frac{\Delta T^3}{3} & 0 & 0 & Q_c\frac{\Delta T^2}{2} \\ Q_r\frac{\Delta T^2}{2}+Q_\mu\frac{\Delta T^3}{2} & 0 & 0 & Q_r\,\Delta T+Q_\mu\Delta T^2 & 0 & 0 \\ 0 & Q_i\frac{\Delta T^2}{2} & 0 & 0 & Q_i\,\Delta T & 0 \\ 0 & 0 & Q_c\frac{\Delta T^2}{2} & 0 & 0 & Q_c\,\Delta T \end{bmatrix}^n \quad (4.4\text{-}31)^*$$

where

Q_r = radial velocity noise variance rate (meters^2/second^3) in the central body frame

Q_i = in-track velocity noise variance rate (meters^2/second^3) in the central body frame

Q_c = cross-track velocity noise variance rate (meters^2/second^3) in the central body frame

ΔT = $t_i - t_{i-1}$ = time step (seconds)

Q_μ = radial Earth gravity state noise variance rate for geosynchronous orbits computed using Equation (4.4-61b) (meters^2/second^4)

Note that this formulation for the state process noise assumes that the velocity errors are uncorrelated in time. The radial, in-track, and cross-track variance rates (*Q's*) each have two components as shown below:

$$Q_r = Q_{r,eg} + Q_{r,o} \quad (4.4\text{-}32)^*$$

$$Q_i = Q_{i,eg} + Q_{i,o} \quad (4.4\text{-}33)^*$$

$$Q_c = Q_{c,eg} + Q_{c,o} \quad (4.4\text{-}34)^*$$

where

$Q_{r,eg}$ = Earth gravity radial state noise variance rate for low-Earth-orbiting (LEO) satellites (meters^2/second^3), computed using Equation (4.4-59), which is only value if the Earth is the central body.

$Q_{r,o}$ = other radial velocity noise variance rate (meters^2/second^3), commandable parameter

$Q_{i,eg}$ = Earth gravity in-track velocity noise variance rate for LEO satellites (meters^2/second^3), computed using Equation (4.4-60), which is only value if the Earth is the central body.

$Q_{i,o}$ = other in-track velocity noise variance rate (meters^2/second^3), commandable parameter

$Q_{c,eg}$ = Earth gravity cross-track state noise variance rate for LEO satellites (meters^2/second^3), computed using Equation (4.4-61), which is only value if the Earth is the central body.

$Q_{c,o}$ = other cross-track state noise variance rate (meters^2/second^3), commandable parameter

Variances are added because the component error sources are independent. This model assumes timewise uncorrelated random acceleration errors, sometimes referred to as a random-walk model.

For orbits where the dynamic modeling errors are fairly constant in the radial, in-track, and cross-track directions (e.g. near-circular and libration point orbits), constant values for the other velocity noise variance rates are usually adequate. However, for highly elliptic orbits where the dynamic modeling errors vary by more than an order of magnitude with distance from the central body (e.g. highly elliptic lunar orbits), a model that increases the velocity noise variance rates based on the square of the inverse of the distance from the central body can provide a more realistic covariance. Note that this type of scaled model is not currently implemented in the GEONS 3.0 source code.

Other state noise refers to small unmodeled accelerations from polar motion, tidal effects, random venting, etc. Other state noise includes small errors in the acceleration models for solar gravity, lunar gravity, and solar pressure. If the unmodeled acceleration effects are estimated, the state noise is covered by its own state vector element process noise. Note that atmospheric drag or solar radiation pressure coefficient correction state noise is covered by its own state vector element. The derivation of the Earth gravity state noise model is given Section 4.4.2.2.

The process noise contributions for the remaining state vector elements for satellite n and the measurement biases are modeled as either random-walk or Gauss-Markov processes. When the time bias, drift and optional acceleration are modeled as random walk processes, the associated process noise matrix elements are given by

$$Q_{b_R}^{RW} = \begin{bmatrix} \dot{Q}_{b_R}\Delta T + \dot{Q}_{d_R}\dfrac{\Delta T^3}{3} + \dot{Q}_{\dot{d}_R}\dfrac{\Delta T^5}{20} & \dot{Q}_{d_R}\dfrac{\Delta T^2}{2} + \dot{Q}_{\dot{d}_R}\dfrac{\Delta T^4}{8} & \dot{Q}_{\dot{d}_R}\dfrac{\Delta T^3}{6} \\ \dot{Q}_{d_R}\dfrac{\Delta T^2}{2} + \dot{Q}_{\dot{d}_R}\dfrac{\Delta T^4}{8} & \dot{Q}_{d_R}\Delta T + \dot{Q}_{\dot{d}_R}\dfrac{\Delta T^3}{3} & \dot{Q}_{\dot{d}_R}\dfrac{\Delta T^2}{2} \\ \dot{Q}_{\dot{d}_R}\dfrac{\Delta T^3}{6} & \dot{Q}_{\dot{d}_R}\dfrac{\Delta T^2}{2} & \dot{Q}_{\dot{d}_R}\Delta T \end{bmatrix} \quad \text{(4.4-34a)*}$$

where

$\dot{Q}_{b_R}$ = GPS receiver time bias process noise variance rate (meters^2/second)

$\dot{Q}_{d_R}$ = GPS receiver time bias rate process noise variance rate (meters^2/second^3)

$\dot{Q}_{\dot{d}_R}$ = GPS receiver time bias acceleration process noise variance rate (meters^2/second^5)

For all other elements modeled as random walk processes, the process noise variance is given by

$$Q_{RW} = \dot{Q}_{RW}\Delta T \tag{4.4-34b)*}$$

where

$\dot{Q}_{RW}$ = the associated process noise variance rate (one per second)

When the time bias drift is modeled as a first-order Gauss-Markov process, the maximum value of the time drift process noise variance is bounded and the time bias process noise variance grows linearly with ΔT. The associated process noise matrix elements are given by

$$Q_{\bar{b}_R}^{FOGM} = \begin{bmatrix} \frac{S_{d_R}\tau_R^3}{2}\left[\left(1-e^{-\frac{2\Delta T}{\tau_R}}\right)+2\frac{\Delta T}{\tau_R}-4\left(1-e^{-\frac{\Delta T}{\tau_R}}\right)\right] & \frac{S_{d_R}\tau_R^2}{2}\left(1-e^{-\frac{\Delta T}{\tau_R}}\right)^2 \\ \frac{S_{d_R}\tau_R^2}{2}\left(1-e^{-\frac{\Delta T}{\tau_R}}\right)^2 & \frac{S_{d_R}\tau_R}{2}\left(1-e^{-\frac{2\Delta T}{\tau_R}}\right) \end{bmatrix} \tag{4.4-34c)*}$$

where

τ_R = GPS receiver time bias drift correlation time, a commanded parameter (seconds)

S_{d_R} = Power spectral density of the receiver time bias drift noise, a commanded parameter (meters^2/second^3)

For all elements modeled as first-order Gauss-Markov processes except for the time bias and drift, the process noise variance is bounded and given by

$$Q_{FOGM} = \left(\sigma_{FOGM}\right)^2\left[1-e^{-\frac{2\Delta T}{\tau}}\right] \tag{4.4-34d)*}$$

where

σ_{FOGM} = the associated maximum root variance, a commanded parameter

τ = the associated correlation time, a commanded parameter (seconds)

When the receiver time bias is modeled as a first-order Gauss-Markov process and the time bias drift is modeled as a second-order Gauss-Markov process, the maximum propagated process noise

variances for the time bias and time bias drift are bounded. The associated process noise matrix elements are given by

$$Q_{\bar{b}_R}^{SOGM} = \begin{bmatrix} Q_{11} & Q_{12} \\ Q_{21} & Q_{22} \end{bmatrix} \tag{4.4-34e}*$$

where

$$Q_{11} = S_{b_R} \Delta T \tag{4.4-34f}*$$

$$Q_{12} = Q_{21} = 0 \tag{4.4-34g}*$$

$$Q_{22} = S_{d_R} \Delta T \tag{4.4-34h}*$$

where

S_{b_R} = Power spectral density of the receiver time bias noise, a commanded parameter (meters^2/second)

S_{d_R} = Power spectral density of the receiver time bias drift noise, a commanded parameter (meters^2/second^3)

ΔT = $t_i - t_{i-1}$ = time step (seconds)

When the FOGM/SOGM time bias/drift model is used, the behavior of the associated covariance is controlled by the selection of the power spectral densities and the values for τ_R, ω_n, and ζ_d defined in Section 4.3.3. Reference 53 provides a more detailed discussion of the performance of this model.

The process noise covariance submatrix for the remaining state vector elements for satellite n are given by

$$Q_{i-1}(\bar{g}^n) = \begin{bmatrix} Q_{C_D} & 0 & 0 & 0 \\ 0 & Q_{C_R} & 0 & 0 \\ 0 & 0 & Q_{\bar{b}_R} & 0 \\ 0 & 0 & 0 & Q_{\bar{a}_U} \end{bmatrix}^n \tag{4.4-35}*$$

where

Q_{C_D} = the atmospheric drag coefficient correction process noise variance; note that the associated row and column is not included if the atmospheric drag coefficient correction is not estimated

Q_{C_R} = the solar radiation pressure coefficient correction process noise variance; note that the associated row and column is not included if the solar radiation pressure coefficient correction is not estimated

$Q_{\bar{b}_R}$ = GPS receiver time bias process noise matrix given by either Equation 4.4-34a or 4.4-34c

$Q_{\bar{a}_U}$ = Acceleration bias process noise variance (meters^2/second^3)

The components of the diagonal measurement bias process noise submatrix are computed as follows:

$$Q_{i-1}(\bar{B}) = \begin{bmatrix} \bar{Q}_\rho^{G/W} & 0 & 0 & 0 & 0 & 0 & 0 & 0 & 0 & 0 \\ 0 & \bar{Q}_d^{G/W} & 0 & 0 & 0 & 0 & 0 & 0 & 0 & 0 \\ 0 & 0 & \bar{Q}_\rho^{CL} & 0 & 0 & 0 & 0 & 0 & 0 & 0 \\ 0 & 0 & 0 & \bar{Q}_d^{CL} & 0 & 0 & 0 & 0 & 0 & 0 \\ 0 & 0 & 0 & 0 & \bar{Q}^{CO} & 0 & 0 & 0 & 0 & 0 \\ 0 & 0 & 0 & 0 & 0 & \bar{Q}_\rho^{GS} & 0 & 0 & 0 & 0 \\ 0 & 0 & 0 & 0 & 0 & 0 & \bar{Q}_d^{GS} & 0 & 0 & 0 \\ 0 & 0 & 0 & 0 & 0 & 0 & 0 & \bar{Q}_d^{TDRS} & 0 & 0 \\ 0 & 0 & 0 & 0 & 0 & 0 & 0 & 0 & \bar{Q}_\phi^{G/W} & 0 \\ 0 & 0 & 0 & 0 & 0 & 0 & 0 & 0 & 0 & \bar{Q}_{\Delta\phi}^{G/W} \end{bmatrix} \quad \text{(4.4-35a)*}$$

where

$\bar{Q}_\rho^{G/W}$ = diagonal matrix containing pseudorange bias process noise variances for 32 GPS SVs and 8 WAAS GEOs, where the rate is a commanded parameter (meters^2/second)

$\bar{Q}_d^{G/W}$ = diagonal matrix containing Doppler bias process noise variances for 32 GPS SVs and 8 WAAS GEOs, where the rate is a commanded parameter (hertz^2/second)

$\bar{Q}_\rho^{CL}$ = diagonal matrix containing cross-link pseudorange bias process noise variances for all transmitters, where the rate is a commanded parameter (meters^2/second)

$\bar{Q}_d^{CL}$ = diagonal matrix containing cross-link Doppler bias process noise variances for all transmitters, where the rate is a commanded parameter (hertz^2/second)

$\bar{Q}^{CO}$ = diagonal matrix containing celestial object sensor bias process noise variances for N_S satellites, where the rate is a commanded parameter

$\overline{Q}_{\rho}^{GS}$ = diagonal matrix containing range bias process noise variances $Q_{\rho}^{GS_j}$ for all transmitting ground stations (meter^2)

$\overline{Q}_{d}^{GS}$ = diagonal matrix containing Doppler bias process noise variances $Q_{d}^{GS_j}$ for all transmitting ground stations (hertz^2)

$\overline{Q}_{d}^{TDRS}$ = diagonal matrix containing Doppler bias process noise variances $Q_{d}^{TDRS_j}$ for all TDRSS transmitters (hertz^2)

$\overline{Q}_{\phi}^{G/W}$ = diagonal matrix containing process noise variances for carrier phase biases between N_S receivers and 32 GPS SVs and 8 WAAS GEOs, where the rate is a commanded parameter (meters^2/second)

$\overline{Q}_{\Delta\phi}^{G/W}$ = diagonal matrix containing process noise variances for the singly differenced carrier phase biases between the local receiver (1) and $N_S - 1$ remote receivers and 32 GPS SVs and 8 WAAS GEOs, where the rate is a commanded parameter (meters^2/second)

(Equation replaced by Equations 4.4-34a and b) (4.4-35b)*

(Equation replaced by Equations 4.4-34a and b) (4.4-35c)*

Finally, the process noise matrix element for the ionospheric scale factor, $Q_{i-1}(\gamma_I)$, is computed using Equation 4.4-34b or d.

4.4.2.2 Earth Gravity State Noise Model for LEO Satellites

GEONS uses a semianalytic Earth gravity state noise model derived from algorithms presented in References 18 through 20. The algorithm in Reference 19 computes a state noise covariance matrix for a state vector defined in terms of equinoctial orbital elements. The algorithm in Reference 3 uses the state noise covariance matrix formulation in equinoctial orbital elements but transforms it to XYZ (Cartesian) coordinates. The algorithm in this document avoids the use of equinoctial orbital elements by computing the state noise covariance matrix in RIC coordinates and then transforming it to XYZ (Cartesian) coordinates.

The following algorithm models the state noise contribution for LEO satellites due to errors of omission and errors of commission in the gravity model coefficients.

The following derivation is adapted from Reference 3. The Earth gravity state noise in RIC coordinates is derived from the following integral:

$$[Q(t_k)]_{RIC,EG} = \int_{t_k}^{t_{k+1}} \phi(t_{k+1}, t)\ B(t)\ C(t, 0)\ T\ B^T(t)\ \phi^T(t_{k+1}, t)\, \mathrm{d}t \qquad (4.4\text{-}36)$$

where

$[Q]_{RIC,EG}$ = [6 × 6] RIC Earth gravity state noise matrix

$[\phi]$ = [6 × 6] RIC state transition matrix

$[B]$ = [6 × 3] RIC matrix of partial derivatives of the RIC coordinates with respect to the velocity vector

$[C]$ = [3 × 3] RIC gravity error covariance matrix

$[T]$ = [3 × 3] RIC correlation time matrix

The quantities in the integral are computed as follows:

$$T = \int_{-\bar{\gamma}}^{\bar{\gamma}} \rho(\gamma)\, d\gamma \tag{4.4-37}$$

where $\bar{\gamma}$ is a gravity autocorrelation cutoff time that satisfies the condition

$$\frac{2}{9} \le \frac{\bar{\gamma}}{P} \le \frac{4}{9} \tag{4.4-38}$$

where P is the orbital period.

The matrix $\rho(\gamma)$ has the following form:

$$\rho(\gamma) = \begin{bmatrix} \dfrac{C_R(t,\gamma)}{C_R(t,0)} & 0 & 0 \\ 0 & \dfrac{C_I(t,\gamma)}{C_I(t,0)} & 0 \\ 0 & 0 & \dfrac{C_C(t,\gamma)}{C_C(t,0)} \end{bmatrix} \tag{4.4-39}$$

where

$$C_R(t,\ \gamma) = \sum_{n=2}^{N_{Max}} \left[\frac{R_e}{R(t)}\right]^{2n+4} \sigma^2(n)\ P_n^0(cos\ \ [\psi(\gamma)]) \tag{4.4-40}$$

$$C_I(t,\ \gamma) = \sum_{n=2}^{N_{Max}} \frac{n(n+1)}{2(n-1)^2} \left[\frac{R_e}{R(t)}\right]^{2n+4} \sigma^2(n)\ \left[P_n^0(cos\ \ [\psi(\gamma)]) - \frac{P_n^2(cos\ [\psi(\gamma)])}{n(n+1)}\right] \tag{4.4-41}$$

$$C_C(t,\ \gamma) = \sum_{n=2}^{N_{Max}} \frac{n(n+1)}{2(n-1)^2} \left[\frac{R_e}{R(t)}\right]^{2n+4} \sigma^2(n)\ \left[P_n^0(cos\ \ [\psi(\gamma)]) + \frac{P_{n-1}^2(cos\ [\psi(\gamma)])}{n(n+1)}\right] \tag{4.4-42}$$

Where P_n^0 is the Legendre polynomial of degree n and P_n^2 is the associated Legendre function of degree n and order 2. These sums are computed so that convergence is achieved, where $N_{Max} \le 100$.

The symbols $\sigma^2(n)$ occurring in the equations for $C_R(t,\gamma)$, $C_I(t,\gamma)$, and $C_C(t,\gamma)$ are called the generalized degree variances. The degree variances for errors of commission, terms 2 through

degree $N_{Commission}$, are obtained from the formal errors associated with the gravity model coefficients. The degree variances for the errors of omission, terms $N_{Omission}$ through N_{Max}, are obtained from the magnitudes of the omitted coefficients and extrapolation of the magnitudes of the coefficients for the JGM2 gravity model.

The matrix $C(t, 0)$ is defined as follows:

$$C(t, 0) = \begin{bmatrix} C_R(t,0) & 0 & 0 \\ 0 & C_I(t,0) & 0 \\ 0 & 0 & C_C(t,0) \end{bmatrix} \tag{4.4-43}$$

The components of the matrix $C(t, 0)$ are obtained from the equations for $C_R(t,\gamma)$, $C_I(t,\gamma)$, and $C_C(t,\gamma)$ by setting $\gamma = 0$. In this case, $\Psi(0) = 0$ and $\cos \Psi(0) = 1$; therefore, $P_n^0(1) = 1$ and $P_n^m(1) = 0$ for $m \neq 0$. The equations for $C_R(t,\gamma)$, $C_I(t,\gamma)$, and $C_C(t,\gamma)$ then take the following form:

$$C_R(t,\ 0) = \sum_{n=2}^{N_{Commission}} \left(\frac{n+1}{n-1}\right)^2 \left[\frac{R_e}{R(t)}\right]^{2n+4} \sigma^2(n) + \sum_{n=N_{Omission}}^{N_{Max}} \left(\frac{n+1}{n-1}\right)^2 \left[\frac{R_e}{R(t)}\right]^{2n+4} \sigma^2(n) \tag{4.4-44}*$$

$$C_I(t,\ 0) = \sum_{n=2}^{N_{Commission}} \frac{n(n+1)}{2(n-1)^2} \left[\frac{R_e}{R(t)}\right]^{2n+4} \sigma^2(n) + \sum_{n=N_{Omission}}^{N_{Max}} \frac{n(n+1)}{2(n-1)^2} \left[\frac{R_e}{R(t)}\right]^{2n+4} \sigma^2(n) \tag{4.4-45}*$$

$$C_C(t, 0) = C_I(t, 0) \tag{4.4-46}*$$

These sums are computed so that convergence is achieved using a value of $N \leq 100$. The following abbreviations will be used for the $[C]$ matrix elements:

$$C_R = C_R(t, 0) \tag{4.4-47}$$

$$C_I = C_I(t, 0) \tag{4.4-48}$$

$$C_C = C_C(t, 0) \tag{4.4-49}$$

In the above equations, R_e is the Earth's equatorial radius, $R(t)$ is the magnitude of the spacecraft position vector, and $\psi(t)$ is the displacement in the central angle measured in the orbit plane, such that

$$U(\tau) = U(t) + \psi(t - \tau) \tag{4.4-50}$$

where $U(\tau)$ is the argument of latitude, i.e., the angle in the orbit plane between the ascending node and the radius vector to the instantaneous position of the spacecraft at time τ.

According to References 18 through 20, $\rho(\gamma)$ is insensitive to small variations in $R(t)$. Therefore, the expressions for $C_R(t, \gamma)$, $C_I(t, \gamma)$, and $C_C(t, \gamma)$ can be evaluated for a constant value of $R(t)$, typically chosen to be perigee

$$R(t) \approx R \quad \text{(at perigee)} \tag{4.4-51}$$

Thus, the constant components of the $[T]$ matrix are precomputed using an offline utility for a given orbit, gravity model, and degree of truncation. The $[T]$ matrix is therefore composed of uplinkable parameters as defined below:

$$[T] = \begin{bmatrix} T_R & 0 & 0 \\ 0 & T_1 & 0 \\ 0 & 0 & T_C \end{bmatrix} \tag{4.4-52}$$

where

T_R = radial correlation time (seconds)

T_I = in-track correlation time (seconds)

T_C = cross-track correlation time (seconds)

(Equation deleted) (4.4-53)

In the derivation of the Earth gravity state noise matrix, the following RIC transition matrix, ϕ, is used for the RIC position and velocity vector components:

$$\phi(t_{k+1}, t_k) = \frac{\partial \overline{RIC}(t_{k+1})}{\partial \overline{RIC}(t_k)} = \begin{bmatrix} 1 & 0 & 0 & \Delta T & 0 & 0 \\ 0 & 1 & 0 & 0 & \Delta T & 0 \\ 0 & 0 & 1 & 0 & 0 & \Delta T \\ 0 & 0 & 0 & 1 & 0 & 0 \\ 0 & 0 & 0 & 0 & 1 & 0 \\ 0 & 0 & 0 & 0 & 0 & 1 \end{bmatrix} \tag{4.4-54}$$

Matrix B is a $[6 \times 3]$ matrix that consists of the partial derivatives of the RIC coordinates with respect to the velocity vector expressed in orbit plane coordinates (i.e., radial, in-track, and cross-track), with the following components:

$$\dot{\overline{R}}_{op} = (\dot{r}_R, \dot{r}_I, \dot{r}_C) \tag{4.4-55}$$

$$B = \frac{\partial \overline{RIC}}{\partial \dot{\bar{R}}_{op}} = \begin{bmatrix} 0 & 0 & 0 \\ 0 & 0 & 0 \\ 0 & 0 & 0 \\ 1 & 0 & 0 \\ 0 & 1 & 0 \\ 0 & 0 & 1 \end{bmatrix} \tag{4.4-56}$$

The [ϕ] [B], [C], and [T] matrices are multiplied out as shown below:

$$\left[Q_{RIC,EG}\right] = \int \begin{bmatrix} C_R T_R \Delta T^2 & 0 & 0 & C_R T_R \Delta T & 0 & 0 \\ 0 & C_I T_I \Delta T^2 & 0 & 0 & C_I T_I \Delta T & 0 \\ 0 & 0 & C_C T_C \Delta T^2 & 0 & 0 & C_C T_C \Delta T \\ C_R T_R \Delta T & 0 & 0 & C_R T_R & 0 & 0 \\ 0 & C_I T_I \Delta T & 0 & 0 & C_I T_I & 0 \\ 0 & 0 & C_C T_C \Delta T & 0 & 0 & C_C T_C \end{bmatrix} d\tau \tag{4.4-57}$$

The derivation is completed by evaluating the integral as shown below:

$$\left[Q_{RIC,EG}\right] = \begin{bmatrix} C_R T_R \frac{\Delta T^3}{3} & 0 & 0 & C_R T_R \frac{\Delta T^2}{2} & 0 & 0 \\ 0 & C_I T_I \frac{\Delta T^3}{3} & 0 & 0 & C_I T_I \frac{\Delta T^2}{2} & 0 \\ 0 & 0 & C_C T_C \frac{\Delta T^3}{3} & 0 & 0 & C_C T_C \frac{\Delta T^2}{2} \\ C_R T_R \frac{\Delta T^2}{2} & 0 & 0 & C_R T_R \Delta T & 0 & 0 \\ 0 & C_I T_I \frac{\Delta T^2}{2} & 0 & 0 & C_I T_I \Delta T & 0 \\ 0 & 0 & C_C T_C \frac{\Delta T^2}{2} & 0 & 0 & C_C T_C \Delta T \end{bmatrix} \tag{4.4-58}*$$

The equivalent Earth gravity state noise variance rates are then computed as shown below:

$$Q_{r,eg} = C_R \; T_R \tag{4.4-59}*$$

$$Q_{i,eg} = C_I \; T_I \tag{4.4-60}*$$

$$Q_{c,eg} = C_C \; T_C \tag{4.4-61}*$$

The Earth gravity state noise variance rates given in Equations 4.4-59 through 4.4-61 were derived assuming that the satellite orbit is nearly circular. To accommodate eccentric LEO orbits, the option is provided to scale the Earth gravity state noise spectral densities as shown below:

$$Q_{r,eg} = C_R \; T_R \left(\frac{R(t)}{R_{ref}} \right)^{N_r} \tag{4.4-59a)*}$$

$$Q_{i,eg} = C_I \; T_I \left(\frac{R(t)}{R_{ref}} \right)^{N_i} \tag{4.4-60a)*}$$

$$Q_{c,eg} = C_C \; T_C \left(\frac{R(t)}{R_{ref}} \right)^{N_c} \tag{4.4-61a)*}$$

where

R_{ref} = Reference radius at which the autocorrelation times were computed, a commandable parameter

N_r = Exponent to be used to scale the radial gravity noise variance rate, a commandable parameter

N_i = Exponent to be used to scale the in-track gravity noise variance rate, a commandable parameter

N_c = Exponent to be used to scale the cross-track gravity noise variance rate, a commandable parameter

4.4.2.3 Earth Gravity State Noise Model for Geostationary Satellites

GEONS also includes an Earth gravity state noise model for geostationary satellites. This model takes into account the fact that the satellite remains in essentially a constant position with respect to the Earth's surface. For geostationary satellites, the error contribution from errors of omission and commission are negligible. The dominant contribution is in the radial direction arising from the error in the Earth's gravitational constant.

For geostationary satellites, the Earth gravity state noise in RIC coordinates is derived from the following integral:

$$[Q(t_k)]_{RIC,\mu} = \left[\int_{t_k}^{t_{k+1}} \phi(t_{k+1}, t) \; B(t) \mathrm{d}t \right] K \left[\int_{t_k}^{t_{k+1}} B^T(t) \; \phi^T(t_{k+1}, t) \; \mathrm{d}t \right]$$

where

$[Q]_{RIC,\mu}$ = [6 × 6] RIC Earth gravity state noise matrix for geostationary satellites

$[\phi]$ = [6 × 6] RIC state transition matrix given in Equation (4.4-54)

$[B]$ = [6 × 3] RIC matrix of partial derivatives of the RIC coordinates with respect to the velocity vector, given in Equation (4.4-56)

$[K]$ = [3 × 3] RIC Earth gravitational acceleration error matrix given below

$$K = \begin{bmatrix} \dfrac{\sigma_\mu^{\,2}}{R(t)^4} & 0 & 0 \\ 0 & 0 & 0 \\ 0 & 0 & 0 \end{bmatrix}$$

where

σ_μ = error in the Earth's gravitational constant μ_E, with a default value of 2 x 10^7 meters^3/second^2 (note that IERS Technical Note 36, Reference 49, provides the error as 8 x 10^5 meters^3/second^2)

In this case the contribution to the process noise covariance matrix is the following

$$\left[Q_{RIC,\mu}\right] = \begin{bmatrix} Q_\mu \dfrac{\Delta T^4}{4} & 0 & 0 & Q_\mu \dfrac{\Delta T^3}{2} & 0 & 0 \\ 0 & 0 & 0 & 0 & 0 & 0 \\ 0 & 0 & 0 & 0 & 0 & 0 \\ Q_\mu \dfrac{\Delta T^3}{2} & 0 & 0 & Q_\mu \Delta T^2 & 0 & 0 \\ 0 & 0 & 0 & 0 & 0 & 0 \\ 0 & 0 & 0 & 0 & 0 & 0 \end{bmatrix}$$

where

$$Q_\mu = \frac{\sigma_\mu^{\,2}}{R(t)^4} \qquad (4.4\text{-}61b)$$

4.4.3 Time Propagation

When using UDU^T factorization of the state error covariance matrix, $[U]$ and $[D]$ are propagated directly. The state error covariance matrix $[P]$ is not propagated directly but can be reformed from the propagated $[U]$ and $[D]$. Propagation of $[U]$ and $[D]$ still requires the state transition matrix $[\Phi]$ and the state noise matrix $[Q]$, computed as shown in Section 4.4.2. The time propagation of $[U]$ and $[D]$ is shown below. This algorithm was taken from Reference 5. Note the difference between the vector or matrix subscript k, and the time subscript t_i.

Define a [N × 2N] matrix $[Y]$, where N is the dimension of the total estimation state vector, partitioned as follows:

$$[Y] = \left[\Phi\ U(t_i) \quad | \quad G_d\right] \qquad (4.4\text{-}62)^*$$

where:

Φ = [N × N] state transition matrix (see Section 4.4.1)

G_d = upper triangular matrix factor of Q_{i-1}, computed using the covariance factorization algorithm defined in Section 2.2.1

Define a [2N × 2N] state diagonal matrix $[\widetilde{D}]$ as follows:

$$\left[\widetilde{D}\right] = \begin{bmatrix} D(t_i) & 0 \\ 0 & Q_d \end{bmatrix} \tag{4.4-63}*$$

where

$[U(t_i)]$ = $[U]$ at time (t_i)

$[D(t_i)]$ = $[D]$ at time (t_i)

Q_d = diagonal matrix factor of Q_{i-1} computed using the covariance factorization algorithm defined in Section 2.2.1

In the following algorithm sequence, $\overline{a}_j, \overline{a}_k, \overline{c}_k$, and $\overline{d}_k$ each represent N vectors with 2N elements, not [2N × N] matrices; and $c_{k,j}$ and $a_{k,j}$ represent element (j) in vector (k), not matrix element (k, j).

N vectors, each of dimension 2N, are initialized as follows:

$$\left[\overline{a}_1\ \overline{a}_2\ \ldots\ldots\ \overline{a}_N\right] = \left[Y\right]^T \tag{4.4-64}*$$

and iterated on the following relations for k = N, N-1, ..., 1:

$$\overline{c}_k = [\widetilde{D}]\,\overline{a}_k \tag{4.4-65}*$$

Because $[\widetilde{D}]$ is diagonal, $\overline{c}_k$ is computed as shown below:

$$c_{k,j} = \widetilde{D}_{j,j}\ a_{k,j} \qquad j = 1, 2, \ldots, 2N \tag{4.4-66}*$$

$$D_{k,k}(t_{i+1}) = \overline{a}_k^T\ \overline{c}_k \tag{4.4-67}*$$

$$\overline{d}_k = \frac{\overline{c}_k}{D_{k,k}(t_{i+1})} \tag{4.4-68}*$$

$$\left.\begin{aligned} U_{j,k}(t_{i+1}) &= \overline{a}_j^T\ \overline{d}_k \\ \overline{a}_j &\leftarrow \overline{a}_j - U_{j,k}(t_{i+1})\,\overline{a}_k \end{aligned}\right\} \quad j = 1, 2, \ldots, \mathrm{k}-1 \tag{4.4-69}*$$

where ← arrow denotes replacement or writing over.

On the last iteration, for k = 1, only the equations for $c_{k,j}$ and $D_{k,k}$ are computed.

4.5 Spacecraft Maneuver Covariance and Clock Variance Increments

This section discusses the algorithms that are provided for incrementing the process noise covariance during maneuvers and for incrementing the time bias and drift variances during specific time intervals. The uncertainty due to maneuver errors can be modeled by additional process noise active during maneuvers. This process noise can be modeled in multiple ways as described in this section. In all cases the process noise is integrated over the propagation interval, and its effect at the update time can be modeled as an additive increment to the covariance as part of the full covariance propagation. The process noise models in Sections 4.5.1.2 and 4.5.2.2 are variations of a technique commonly referred to as State Noise Compensation (see Section 2.2.3.1.2 of Reference 59).

Section 4.5.1 discusses process noise models that use RIC position and velocity variances or variance rates to model the maneuver uncertainty. Section 4.5.2 provides maneuver process noise models that can be used when planned or measured maneuver accelerations are available in GEONS. Section 4.5.3 discusses the augmentation of the spacecraft state covariance to include the maneuver process noise covariance. Section 4.5.4 discusses the capability for increasing the time bias and drift variances. Note that each of the maneuver process noise models in Sections 4.5.1 and 4.5.2 assume that each propagation interval within a maneuver is small compared to the orbit period, but there is no assumption on the length of the maneuver.

4.5.1 Maneuver Process Noise Models Based on Maneuver Variances and Variance Rates

GEONS V3.0 provides two options for computing additional process noise to accommodate maneuver-associated velocity errors that are assumed to be an uncorrelated random walk with intensity in the orbit-fixed RIC frame. The "legacy RICSNC" maneuver process noise model is defined in terms of RIC position and velocity variances. The new "RICSNC" maneuver process noise model is defined in terms of RIC position and velocity variance rates.

4.5.1.1 Legacy RIC Maneuver Process Noise Model

The "legacy RICSNC" maneuver process noise model uses the following approach:

1. Prior to the execution of a scheduled spacecraft maneuver, uplink the planned maneuver start and stop times and the radial, cross-track, and in-track components of the process noise variances associated with the magnitude of the expected velocity change, referenced to the central body frame.
2. Optionally ignore all measurements received during the planned maneuver.
3. At every GEONS propagation step during the maneuver, transform the commanded RIC position and velocity variances to the mean of J2000.0 coordinate frame. Prior to propagating the state error covariance, add the maneuver position and velocity covariance increments to the $[3 \times 3]$ position and velocity portions of the state error covariance matrix using the procedure provided in Section 4.5.3.

The radial, cross-track and in-track components of the position and velocity maneuver variances are computed externally and uplinked to the spacecraft:

$$\sigma^2_{\Delta R,\, r} = \left(\Delta V_r\ \Delta \mathrm{T}\right)^2 \tag{4.5-1}$$

$$\sigma^2_{\Delta R,\, i} = \left(\Delta V_i\ \Delta \mathrm{T}\right)^2 \tag{4.5-2}$$

$$\sigma^2_{\Delta R,\, c} = \left(\Delta V_c\ \Delta \mathrm{T}\right)^2 \tag{4.5-3}$$

$$\sigma^2_{\Delta V,\, r} = \left(\Delta V_r\right)^2 \tag{4.5-4}$$

$$\sigma^2_{\Delta V,\, i} = \left(\Delta V_i\right)^2 \tag{4.5-5}$$

$$\sigma^2_{\Delta V,\, c} = \left(\Delta V_c\right)^2 \tag{4.5-6}$$

where

$\sigma^2_{\Delta R,r}, \sigma^2_{\Delta R,i}, \sigma^2_{\Delta R,c}$ = RIC components of maneuver position variance with respect to the central body, commanded parameters (meters^2)

$\sigma^2_{\Delta V,r}, \sigma^2_{\Delta V,i}, \sigma^2_{\Delta V,c}$ = RIC components of maneuver velocity variance with respect to the central body, commanded parameters (meters^2/second^2)

$\Delta V_r, \Delta V_i, \Delta V_c$ = RIC components of the planned maneuver velocity change with respect to the central body (meters/second^2)

ΔT = GEONS state propagation time step (seconds), nominally equal to the frequency at which the estimation process is performed

The commanded maneuver position and velocity variances are transformed from RIC coordinates referenced to the central body into Mean of J2000.0 coordinates as shown below:

$$P_T(\Delta R) = [T_{RIC \leftarrow XYZ}]_C^{\,T} \begin{bmatrix} \sigma^2_{\Delta R,\, r} & 0 & 0 \\ 0 & \sigma^2_{\Delta R,\, i} & 0 \\ 0 & 0 & \sigma^2_{\Delta R,\, c} \end{bmatrix} [T_{RIC \leftarrow XYZ}]_C \tag{4.5-7}*$$

$$P_T(\Delta V) = \left[T_{RIC \leftarrow XYZ}\right]_C^{\,T} \begin{bmatrix} \sigma^2_{\Delta V,\, r} & 0 & 0 \\ 0 & \sigma^2_{\Delta V,\, i} & 0 \\ 0 & 0 & \sigma^2_{\Delta V,\, c} \end{bmatrix} \left[T_{RIC \leftarrow XYZ}\right]_C \tag{4.5-8}*$$

where $P_T(\Delta R)$ and $P_T(\Delta V)$ are the [3 × 3] maneuver position and velocity covariances, respectively, in J2000.0 coordinates and the transformation matrix $\left[T_{RIC \leftarrow XYZ}\right]_C$ is defined in Section 3.2.4.

4.5.1.2 RIC Maneuver SNC Process Noise Model

GEONS V3.0 also supports a maneuver process noise model that is based on the state noise compensation model (SNC) defined in Section 2.2.3.1 of Reference 59, which is very similar to the velocity process noise model defined in Section 4.4.2. Reference 59 only includes velocity variance rates, but the model defined below additionally includes position variance rates. The position and velocity submatrix is computed in RIC components with respect to the central body and then transformed into mean of J2000 coordinates as shown below; where the transformation matrix, $[T_{RIC \leftarrow XYZ}]_C$, is computed using the position and velocity in the central body frame at time (t_{i-1}):

$$P_{T_{mag}} = \begin{bmatrix} M^T Q_{ric} M \Delta T + M^T \dot{Q}_{ric} M \frac{\Delta T^3}{3} & M^T \dot{Q}_{ric} M \frac{\Delta T^2}{2} \\ M^T \dot{Q}_{ric} M \frac{\Delta T^2}{2} & M^T \dot{Q}_{ric} M \Delta T \end{bmatrix} \quad \text{(4.5-8a)*}$$

where

$$Q_{ric} = \begin{bmatrix} q_r & 0 & 0 \\ 0 & q_i & 0 \\ 0 & 0 & q_c \end{bmatrix} \quad \text{(4.5-8b)*}$$

$$\dot{Q}_{ric} = \begin{bmatrix} \dot{q}_r & 0 & 0 \\ 0 & \dot{q}_i & 0 \\ 0 & 0 & \dot{q}_c \end{bmatrix} \quad \text{(4.5-8c)*}$$

M = $[T_{RIC \leftarrow XYZ}]_C$

q_r = radial maneuver position noise variance rate (meters^2/second) in the central body frame

q_i = in-track maneuver position noise variance rate (meters^2/second) in the central body frame

q_c = cross-track maneuver position noise variance rate (meters^2/second) in the central body frame

$\dot{q}_r$ = radial maneuver velocity noise variance rate (meters^2/second^3) in the central body frame

$\dot{q}_i$ = in-track maneuver velocity noise variance rate (meters^2/second^3) in the central body frame

$\dot{q}_c$ = cross-track maneuver velocity noise variance rate (meters^2/second^3) in the central body frame

ΔT = $t_i - t_{i-1}$ = time step (seconds)

4.5.2 Maneuver Process Noise Models Using Maneuver Acceleration

GEONS V3.0 provides two options for computing additional process noise to accommodate maneuver errors when the maneuver acceleration is modeled using externally measured or planned accelerations as defined in Sections 4.1.5. The "legacy MANSNC" maneuver process noise model is defined in terms of a fractional error in the maneuver acceleration. The new "MANSNC" maneuver process noise model is defined in terms of a fractional error in the maneuver acceleration magnitude and a fractional error in the maneuver direction.

The following procedure is suitable for maneuvers of any length. The GEONS state error covariance is augmented with the computed maneuver velocity covariance every GEONS propagation step during the maneuver time span as described in Section 4.5.3. Optionally, when this model is used, measurements received during the maneuver timespan are not processed in the GEONS filter.

4.5.2.1 Legacy Maneuver Magnitude Process Noise Model

The "legacy MANSNC" process noise model uses the following approach. The mean of J2000.0 inertial components of the velocity maneuver covariance are computed as follows using the externally measured accelerations:

$$\sigma^2_{\Delta V,X} = \left(\varepsilon_T a_{ext,X} \Delta T\right)^2 \qquad (4.5\text{-}9)^*$$

$$\sigma^2_{\Delta V,Y} = \left(\varepsilon_T a_{ext,Y} \Delta T\right)^2 \qquad (4.5\text{-}10)^*$$

$$\sigma^2_{\Delta V,Z} = \left(\varepsilon_T a_{ext,Z} \Delta T\right)^2 \qquad (4.5\text{-}11)^*$$

where

$\sigma^2_{\Delta V,X}, \sigma^2_{\Delta V,Y}, \sigma^2_{\Delta V,Z}$ = Components of maneuver velocity variance in the mean of J2000 frame (meters^2/second^2)

ε_T = fractional error in modeling the maneuver acceleration, a commanded parameter

$a_{ext,X}, a_{ext,Y}, a_{ext,Z}$ = Components of the maneuver accelerations transformed from the input frame to the mean of J2000 frame (meters/second^2), as described in Section 4.1.5

ΔT= GEONS state propagation time step (seconds)

The velocity maneuver covariance in the mean of J2000.0 frame is as shown below:

$$P_T(\Delta V) = \begin{bmatrix} \sigma^2_{\Delta V,X} & 0 & 0 \\ 0 & \sigma^2_{\Delta V,Y} & 0 \\ 0 & 0 & \sigma^2_{\Delta V,Z} \end{bmatrix} \qquad (4.5\text{-}12)^*$$

The maneuver velocity variances is then added to the [3 × 3] velocity portion of the state error covariance matrix at the start of the propagation time step for which the maneuver acceleration was computed using the procedure discussed in Section 4.5.3, except that the position process noise is not included.

4.5.2.2 Maneuver Magnitude and Direction SNC Process Noise Model

GEONS V3.0 also supports a maneuver process noise model that is based on the state noise compensation model for maneuvers defined in Section 2.2.3.2 of Reference 59 that is computed using the fractional error in the magnitude of the maneuver acceleration and the intensity of the maneuver direction noise. The contribution from the error in the maneuver magnitude error is given by

$$P_{T_{mag}} = \begin{bmatrix} \dot{Q}_{mag}\frac{\Delta T^3}{3} & \dot{Q}_{mag}\frac{\Delta T^2}{2} \\ \dot{Q}_{mag}\frac{\Delta T^2}{2} & \dot{Q}_{mag}\Delta T \end{bmatrix} \tag{4.5-12a)*}$$

where

$$\dot{Q}_{mag}(\Delta V) = \begin{bmatrix} \sigma^2_{\Delta V,X} & 0 & 0 \\ 0 & \sigma^2_{\Delta V,Y} & 0 \\ 0 & 0 & \sigma^2_{\Delta V,Z} \end{bmatrix} \tag{4.5-12b)*}$$

$$\sigma^2_{\Delta V,\,X} = \left(\varepsilon_T \Delta V_{Nom,X}\right)^2 \tag{4.5-12c)*}$$

$$\sigma^2_{\Delta V,\,Y} = \left(\varepsilon_T \Delta V_{Nom,Y}\right)^2 \tag{4.5-12d)*}$$

$$\sigma^2_{\Delta V,\,Z} = \left(\varepsilon_T \Delta V_{Nom,Z}\right)^2 \tag{4.5-12e)*}$$

$$\Delta\bar{V}_{Nom} = \bar{a}_{ext}\Delta T \tag{4.5-12f)*}$$

ε_T = fractional error in modeling the maneuver acceleration, a commanded parameter

The contribution from the maneuver direction error is given by

$$P_{T_{dir}} = \begin{bmatrix} \dot{Q}_{dir}\frac{\Delta T^3}{3} & \dot{Q}_{dir}\frac{\Delta T^2}{2} \\ \dot{Q}_{dir}\frac{\Delta T^2}{2} & \dot{Q}_{dir}\Delta T \end{bmatrix} \tag{4.5-12g)*}$$

where $\Delta\bar{V}^{\times}_{Nom}$ is the 3x3 skew-symmetric cross product matrix

$$\dot{Q}_{dir}(\Delta V) = -q_\theta[\Delta\bar{V}^{\times}_{Nom}]^2 \tag{4.5-12h)*}$$

and $\Delta\bar{V}^{\times}_{Nom}$ is the 3x3 skew-symmetric cross product matrix of $\Delta\bar{V}_{Nom}$

q_θ = intensity of the maneuver direction noise, a commanded parameter

4.5.3 Addition of the Maneuver Covariance to the State Covariance

The state error covariance matrix exists in UDU^T factored form. To modify the state error covariance matrix, it must first be reformed from its [U] and [D] components. After the state covariance matrix is modified, symmetry is forced by averaging off-diagonal elements. The new state error covariance matrix is then factored into new [U] and [D] components. It is simpler to reform and modify the state error covariance matrix, rather than modify the [U] and [D] factors directly. In the navigation flight software, the state error covariance matrix will already be reformed for telemetry purposes. The covariance matrix modifications are summarized below when the legacy models in Section 4.5.1.1 and 4.5.2.1 are used (Note the GEONS 3.0 also uses the following procedure for the new RICSNC and MANSNC models):

1. At the start of the propagation time step, reform the state error covariance matrix from its [U] and [D] factors.
2. Add the maneuver variances $P_T(\Delta X)$ and/or $P_T(\Delta V)$ to the corresponding [3 × 3] position and/or velocity portion of the state error covariance matrix.
3. Force symmetry by averaging off-diagonal elements.
4. Compute new [U] and [D] factors for the state error covariance matrix.
5. Propagate the new [U] and [D] factors.

The covariance matrix modifications are summarized below when the models in Section 4.5.1.2 and 4.5.2.2 are used:

1. Propagate the [U] and [D] factors.
2. At the end of the propagation time step, reform the state error covariance matrix from its [U] and [D] factors.
3. Add the maneuver variances $P_{T_{mag}}$ and/or $P_{T_{dir}}$ to the corresponding [3 × 3] position and/or velocity portion of the state error covariance matrix.
4. Force symmetry by averaging off-diagonal elements.
5. Compute new [U] and [D] factors for the state error covariance matrix.

4.5.4 Addition of the Clock Covariance to the State Covariance

The following approach is available for increasing the time bias and time drift variances during specified time intervals. This capability is provided to support a change in clock behavior such as might occur for a HEO during a time period when clock steering using point solutions is not possible because fewer than four GPS satellite are visible.

1. Prior to the expected change in the clock behavior, uplink the variance increment start and stop times and the time bias and time bias drift process noise variances associated with the magnitude of the expected change in the clock behavior.

2. At every GEONS propagation step during the specified time period, prior to propagating the state error covariance,
    a. Reform the state error covariance matrix from its [U] and [D] factors.
    b. Add the time bias and time drift variance increments to the associated diagonal elements of the state error covariance matrix
    c. Compute new [U] and [D] factors for the state error covariance matrix.
    d. Propagate the new [U] and [D] factors.

4.6 Ground Receiver State Propagation

This section provides equations used for propagating the position, velocity, and covariance of a ground-based GPS receiver. This capability is provided to support ground testing of a GPS receiver.

4.6.1 Ground Receiver State Vector Prediction

The ground receiver is assumed to be located at a fixed position on the surface of the Earth. In which case, the position and velocity are constant in the ECEF frame. To compute the ground receiver state at a future time, t_k, in the mean equator and equinox of J2000.0 frame, given the ground receiver state at the current time, t_{k-1}, in the mean equator and equinox of J2000.0 frame, the following method is used.

The receiver state at the current time is transformed from the mean equator and equinox of J2000.0 to the ECEF frame

$$\bar{r}(t_{k-1})_{ECEF} = B(t_{k-1})R_g(t_{k-1})C(t_{k-1})\bar{R}(t_{k-1})_{J2000} \tag{4.6-1}*$$

$$\dot{\bar{r}}(t_{k-1})_{ECEF} = B(t_{k-1})\left(\frac{d}{dt}\left[R(a_g)\right]\right)_{t=t_{k-1}} C(t_{k-1})\bar{R}(t_{k-1})_{J2000} + B(t_{k-1})R_g(t_{k-1})C(t_{k-1})\dot{\bar{R}}(t_{k-1})_{J2000} \tag{4.6-2}*$$

where the transformation matrices $B(t_{k-1})$, $\left(\frac{d}{dt}\left[R(a_g)\right]\right)_{t=t_{k-1}}$, $C(t_{k-1})$, and $R_g(t_{k-1})$ are defined in Equations (3.2-47),(3.2-33), (3.2-26), (3.2-31), respectively.

The ECEF state vector is then transformed back to the mean equator and equinox of J2000.0 frame at time t_k

$$\bar{R}(t_k)_{J2000} = C^T(t_k)R_g^T(t_k)B^T(t_k)\bar{r}(t_k)_{ECEF} \tag{4.6-3}*$$

$$\dot{\bar{R}}(t_k)_{J2000} = C^T(t_k)\left(\frac{d}{dt}\left[R(a_g)\right]\right)^T_{t=t_k} B^T(t_k)\bar{r}(t_k)_{ECEF} + C^T(t_k)R_g^T(t_k)B^T(t_k)\dot{\bar{r}}(t_k)_{ECEF} \tag{4.6-4}*$$

where

$$\begin{aligned} \bar{r}(t_k)_{ECEF} &= \bar{r}(t_{k-1})_{ECEF} \\ \dot{\bar{r}}(t_k)_{ECEF} &= \dot{\bar{r}}(t_{k-1})_{ECEF} \end{aligned} \tag{4.6-5}*$$

Note that these equations replace those defined for a satellite-based receiver in Sections 4.1 and 4.2.

4.6.2 State Transition Matrix

Computation of state transition matrix for space-based receivers is discussed in Section 4.4.1. For the ground-based user, the position and velocity submatrix of the state transition matrix is identity in the ECEF coordinate frame. Because the solar radiation pressure coefficient and atmospheric drag coefficient corrections are not applicable to this ground-based user, they will be "estimated" using initial coefficient values of zero, near-zero initial variances, and zero process noise variances.

The position and velocity components of state transition matrix for a ground-based receiver in the mean of J2000.0 frame are approximated as follows:

$$\frac{\partial \overline{R}(t_i)_{J2000}}{\partial \overline{R}(t_{i-1})_{J2000}} = C^T(t_i)R_g^T(t_i)B^T(t_i)B(t_{i-1})R_g(t_{i-1})C(t_{i-1})$$

$$\frac{\partial \overline{R}(t_i)_{J2000}}{\partial \dot{\overline{R}}(t_{i-1})_{J2000}} = 0$$

$$\frac{\partial \dot{\overline{R}}(t_i)_{J2000}}{\partial \overline{R}(t_{i-1})_{J2000}} = C^T(t_i)\left(\frac{d}{dt}\left[R(\alpha_g)\right]\right)_{t=t_i}^{T} B^T(t_i)B(t_{i-1})R_g(t_{i-1})C(t_{i-1}) \qquad (4.6\text{-}6)^*$$

$$+ C^T(t_i)R_g^T(t_i)B^T(t_i)B(t_{i-1})\left(\frac{d}{dt}\left[R(\alpha_g)\right]\right)_{t=t_{i-1}} C(t_{i-1})$$

$$\frac{\partial \dot{\overline{R}}(t_i)_{J2000}}{\partial \dot{\overline{R}}(t_{i-1})_{J2000}} = C^T(t_i)R_g^T(t_i)B^T(t_i)B(t_{i-1})R_g(t_{i-1})C(t_{i-1})$$

Note that these partial derivatives are used in Equation (4.4-1) in place those defined for a satellite-based receiver in Equation (4.4-2).

The atmospheric drag correction components are computed as follows

$$\begin{bmatrix} \dfrac{\partial \overline{R}(t_i)}{\partial \Delta C_D(t_{i-1})} \\ \dfrac{\partial \dot{\overline{R}}(t_i)}{\partial \Delta C_D(t_{i-1})} \end{bmatrix} = \begin{bmatrix} 0 \\ 0 \end{bmatrix} \qquad (4.6\text{-}7)^*$$

These partial derivatives are used in Equation (4.4-1) in place those defined for a satellite-based receiver in Equation (4.4-5).

The solar radiation pressure coefficient correction components are computed as follows

$$\begin{bmatrix} \dfrac{\partial \bar{R}(t_i)}{\partial \Delta C_R(t_{i-1})} \\ \dfrac{\partial \dot{\bar{R}}(t_i)}{\partial \Delta C_R(t_{i-1})} \end{bmatrix} = \begin{bmatrix} 0 \\ 0 \end{bmatrix} \tag{4.6-8}*$$

These partial derivatives are used in Equation (4.4-1) in place of those defined for a satellite-based receiver in Equation (4.4-5a).

The remaining partial derivatives are as follows:

$$\frac{\partial \Delta C_D(t_i)}{\partial \Delta C_D(t_{i-1})} = 1 \tag{4.6-9}*$$

$$\frac{\partial \Delta C_R(t_i)}{\partial \Delta C_R(t_{i-1})} = 1 \tag{4.6-10}*$$

$$\frac{\partial \bar{b}_R(t_i)}{\partial \bar{b}_R(t_{i-1})} = \begin{bmatrix} 1 & t_i - t_{i-1} \\ 0 & 1 \end{bmatrix} \tag{4.6-11}*$$

4.6.3 Process Noise Matrix

Computation of the process noise matrix for space-based users is discussed in Section 4.4.2. For the ground-based receiver, the position and velocity submatrix of the process matrix will be computed using nonzero values for other RIC variance rates and zero values for the Earth gravity variance rates in Equations 4.4-32 through 4.4-34. Because the solar radiation pressure coefficient and atmospheric drag coefficient corrections are not applicable to this ground-based user, they will be "estimated" using zero process noise variance rates. All of these variance rates are set via command parameters.

4.7 Moon-Based Receiver State Propagation

This section provides equations used for propagating the position, velocity, and covariance of a Moon-based receiver.

4.7.1 Moon-Based Receiver State Vector Prediction

The moon-based receiver is assumed to be located at a fixed position on the surface of the Moon. In which case, the position and velocity are constant in the Moon-fixed frame. To compute the Moon-based receiver state at a future time, t_k, in the mean equator and equinox of J2000.0 frame, given the receiver state at the current time, t_{k-1}, in the mean equator and equinox of J2000.0 frame, the following method is used.

The receiver state at the propagation start time is transformed from the mean equator and equinox of J2000.0 to Lunar Principal Axis (LPA) frame using the transformation defined in Section 3.2.9 and the fact that the receiver is fixed in the LPA frame

$$\begin{aligned} \bar{r}(t_{k-1})_{LPA} &= T(t_{k-1})_{LPA \leftarrow J2000_{LCI}} \bar{R}(t_{k-1})_{J2000_{LCI}} \\ \dot{\bar{r}}(t_{k-1})_{LPA} &= 0 \end{aligned} \tag{4.7-1}*$$

where

$$\overline{R}(t_{k-1})_{J2000\ _{LCI}} = \overline{R}(t_{k-1})_{J2000\ _{ECI}} - \overline{R}(t_{k-1})_{Moon\ _{ECI}} \tag{4.7-2}*$$

and the transformation matrix $T_{LPA \leftarrow J2000_{LCI}}$ is defined in Equation (3.2-74).

The LPA state vector is then transformed back to the mean equator and equinox of J2000.0 frame at the propagation end time t_k

$$\begin{aligned} \overline{R}(t_k)_{J2000\ _{ECI}} &= \overline{R}(t_k)_{J2000\ _{LCI}} + \overline{R}(t_k)_{Moon\ _{ECI}} \\ \dot{\overline{R}}(t_k)_{J2000\ _{ECI}} &= \dot{\overline{R}}(t_k)_{J2000\ _{LCI}} + \dot{\overline{R}}(t_k)_{Moon\ _{ECI}} \end{aligned} \tag{4.7-3}*$$

where

$$\begin{aligned} \bar{R}(t_k)_{J2000_{LCI}} &= T(t_k)_{2000_{LCI} \leftarrow LPA} \bar{r}(t_{k-1})_{LPA} \\ \dot{\bar{R}}(t_k)_{J2000_{LCI}} &= \dot{T}(t_k)_{2000_{LCI} \leftarrow LPA} \bar{r}(t_{k-1})_{LPA} \end{aligned} \tag{4.7-4}*$$

since

$$\begin{aligned} \bar{r}(t_k)_{LPA} &= \bar{r}(t_{k-1})_{LPA} \\ \dot{\bar{r}}(t_k)_{LPA} &= \dot{\bar{r}}(t_{k-1})_{LPA} = T(t_k)_{2000_{LCI} \leftarrow LPA} 0 \end{aligned} \tag{4.7-5}*$$

and the transformation matrices $T(t_k)_{2000_{LCI} \leftarrow LPA} = \left[T_{LPA \leftarrow J2000_{LCI}}\right]^T$ and $\dot{T}(t_k)_{2000_{LCI} \leftarrow LPA} = \left[\dot{T}_{LPA \leftarrow J2000_{LCI}}\right]^T$ are defined in Equations (3.2-74) and (3.2-91a), respectively.

Note that these equations replace those defined for a satellite-based receiver in Sections 4.1 and 4.2.

4.7.2 State Transition Matrix

Computation of state transition matrix for space-based receivers is discussed in Section 4.4.1. For the Moon-based user, the position and velocity submatrix of the state transition matrix is identity in the LPA coordinate frame. Because the solar radiation pressure coefficient and atmospheric drag coefficient corrections are not applicable to this Moon-based user, they will be "estimated" using initial coefficient values of zero, near-zero initial variances, and zero process noise variances.

The position and velocity components of state transition matrix for a Moon-based receiver in the mean of J2000.0 frame are approximated as follows:

$$\frac{\partial \bar{R}(t_i)_{J2000}}{\partial \bar{R}(t_{i-1})_{J2000}} = T(t_k)_{2000_{LCI} \leftarrow LPA} T(t_{k-1})_{LPA \leftarrow J2000_{LCI}}$$

$$\frac{\partial \bar{R}(t_i)_{J2000}}{\partial \dot{\bar{R}}(t_{i-1})_{J2000}} = 0$$

$$\frac{\partial \dot{\bar{R}}(t_i)_{J2000}}{\partial \bar{R}(t_{i-1})_{J2000}} = \dot{T}(t_k)_{2000_{LCI} \leftarrow LPA} T(t_{k-1})_{LPA \leftarrow J2000_{LCI}}$$

$$\frac{\partial \dot{\bar{R}}(t_i)_{J2000}}{\partial \dot{\bar{R}}(t_{i-1})_{J2000}} = 0 \qquad (4.7\text{-}6)^*$$

Note that these partial derivatives are used in Equation (4.4-1) in place those defined for a satellite-based receiver in Equation (4.4-2).

The atmospheric drag correction components are computed as follows

$$\begin{bmatrix} \dfrac{\partial \overline{R}(t_i)}{\partial \Delta C_D(t_{i-1})} \\ \dfrac{\partial \dot{\overline{R}}(t_i)}{\partial \Delta C_D(t_{i-1})} \end{bmatrix} = \begin{bmatrix} 0 \\ 0 \end{bmatrix} \qquad (4.7\text{-}7)^*$$

These partial derivatives are used in Equation (4.4-1) in place those defined for a satellite-based receiver in Equation (4.4-5).

The solar radiation pressure coefficient correction components are computed as follows

$$\begin{bmatrix} \dfrac{\partial \overline{R}(t_i)}{\partial \Delta C_R(t_{i-1})} \\ \dfrac{\partial \dot{\overline{R}}(t_i)}{\partial \Delta C_R(t_{i-1})} \end{bmatrix} = \begin{bmatrix} 0 \\ 0 \end{bmatrix} \qquad (4.7\text{-}8)^*$$

These partial derivatives are used in Equation (4.4-1) in place of those defined for a satellite-based receiver in Equation (4.4-5a).

The remaining partial derivatives are as follows:

$$\frac{\partial \Delta C_D(t_i)}{\partial \Delta C_D(t_{i-1})} = 1 \qquad (4.7\text{-}9)^*$$

$$\frac{\partial \Delta C_R(t_i)}{\partial \Delta C_R(t_{i-1})} = 1 \qquad (4.7\text{-}10)^*$$

$$\frac{\partial \bar{b}_R(t_i)}{\partial \bar{b}_R(t_{i-1})} = \begin{bmatrix} 1 & t_i - t_{i-1} \\ 0 & 1 \end{bmatrix} \qquad (4.7\text{-}11)^*$$

4.7.3 Process Noise Matrix

Computation of the process noise matrix for space-based users is discussed in Section 4.4.2. For the Moon-based receiver, the position and velocity submatrix of the process matrix will be computed using nonzero values for other RIC variance rates and zero values for the Earth gravity variance rates in Equations 4.4-32 through 4.4-34. Because the solar radiation pressure coefficient and atmospheric drag coefficient corrections are not applicable to this Moon-based user, they cannot be estimated. All of these variance rates are set via command parameters.

Section 5. Measurement Models

This section contains the mathematical specifications for the measurement models used in GEONS. See Section 2.3 for a description of the estimation processing mode options available in GEONS V3.0. Section 5.1 provides an overview of the measurement selection and processing algorithm. Section 5.2 discusses the computation of the GPS SV ephemeris. Sections 5.3 through 5.9 describe the standard GNSS/WAAS measurement, singly differenced GNSS/WAAS measurement, cross-link measurement, Ground Station (GS) measurement, point solution, celestial object measurement, and TDRSS measurement models and associated measurement partial derivatives; respectively.

5.1 Measurement Selection and Processing Overview

Prior to the disabling of Selective Availability (SA) in 2000, the major source of error in the GPS SPS measurements arose from the Selective Availability (SA) corruption applied to the signals so as to limit geometric solutions to approximately 100 meters (two-dimensional, 95 percent of the time). The corruption could be applied via dithering of the GPS SV clocks or corruption of the GPS SV ephemeris data. References 23, 24, and 25 indicate that the impact of SA on pseudorange measurement is approximately 25 to 35 meters (1σ) with an autocorrelation time of approximately 5 minutes. The impact on the Doppler measurement is approximately 0.15 to 0.35 meter per second or approximately 1 hertz. If measurements from a specific SV are sampled at a 5-minute rate, the corruption appears to be white noise.

GEONS' measurement selection algorithm is outlined in Figure 5-1. Measurements are selected and processed based on a minimum measurement sampling interval, which is a commandable parameter for each measurement type. In addition, measurements are not processed during uplinked maneuver time spans. The only GNSS SVs and WAAS GEOs considered valid in this selection process are those for which (1) processing is enabled, (2) up-to-date SV Navigation data is available, (3) SV health is nominal, and (4) SV accuracy is nominal.

Two GNSS SV measurement selection options are available in GEONS. The "cyclic" option cycles through all GPS SVs that are being tracked at (or near) each processing epoch to select measurements from only one valid GNSS SV, based on the minimum SV sampling frequency, which is a commandable parameter nominally equal to 300 seconds. Note that if measurements for a specific SV were selected and subsequently edited in the filter processing, they are still considered to have been selected. The "all-available" option selects all measurements available from valid GPS SVs at each measurement epoch. The "all-available" option is always used to select WAAS GEO, cross-link, GS, point solution, celestial object, and TDRSS measurements.

When multiple satellite states are being estimated, the option is available to process common GPS SV and WAAS GEO measurements either as independent measurements or as singly-differenced measurements. When singly-differenced GNSS and/or WAAS measurement processing is used, the option for "Select Common Transmitters" can be used to select and process only measurements from GNSS SVs and WAAS GEOs that have measurements to both the local and remote receivers. Note that this selection algorithm assumes that when multiple receiver states are estimated simultaneously they will be in sufficiently close formation to see essentially the same set of GNSS

SVs/WAAS GEOs. In conjunction with this option, the “Force Standard on Local” option can be used to also process all local receiver measurements as standard measurements in addition to the singly-differenced processing. Only cross-link measurements from the remote receivers to the local receiver are processed.

If the current measurement update time does not occur during a maneuver time span, select and process GNSS, WAAS GEO, cross-link, GS, point solution, and celestial object measurement(s) for each of the N_S receiver states being estimated:

1 If GNSS measurements are enabled and the elapsed time from the last successful GNSS measurement update is greater than or equal to the minimum GNSS measurement sampling interval, perform the following tests to select and process GNSS measurements for each of the N_S receivers:

1.1 If "All Available" selection is enabled, select and process measurements as follows:

1.1.1 If standard measurement processing is selected, process standard measurements to the local and/or remote receivers from all GNSS SVs that pass the validation tests (i.e. is enabled for processing, has recent navigation data[1], has valid SV health indicator[2] (= 0), and has SV accuracy indicator[3] in acceptable range (≤15) and TASS message integrity flag set to valid for this SV if available)

1.1.2 If singly-differenced measurement processing of pseudorange and/or Doppler is selected and "Select Common Transmitters" option is enabled and

1.1.2.1 If "Force Standard on Local" option is enabled and

1.1.2.1.1 If common measurements from 4 or more GNSS SVs to the local and at least one remote receiver are available, select all GNSS SVs that pass the validation tests. Form and process singly-differenced measurements for the selected GNSS SVs that have common measurements to the local receiver and at least one remote receiver and in addition process standard measurements from all selected GNSS SVs to the local satellite.

1.1.2.1.2 If common measurements from 4 or more GNSS SVs to the local and at least one remote receiver are not available, select all GNSS SVs that pass the validation tests. Form and process singly-differenced measurements for the selected GNSS SVs that have common measurements to the local receiver and at least one remote receiver, process standard measurements for the remaining selected GNSS SVs to the remote satellites, and in addition process standard measurements from all selected GNSS SVs to the local satellite.

1.1.2.2 If "Force Standard on Local" option is disabled and

1.1.2.2.1 If common measurements from 4 or more GNSS SVs to the local and at least one remote receiver are available, form and process only singly-differenced measurements for only the GNSS SVs that pass the validation tests and have measurements to the local receiver and at least one remote receiver.

1.1.2.2.2 If common measurements from 4 or more GNSS SVs to the local and at least one remote receiver are not available, select all GNSS SVs that pass the validation tests. Form and process singly-differenced measurements for the selected GNSS SVs that have measurements to the local receiver and at least one remote receiver and process measurements for the remaining selected GNSS SVs as standard measurements.

Notes:

[1] Determined based on the associated time of epoch (t_{oe}) available in the Broadcast Orbit-3 data record of a RINEX Navigation Data File and in subframes 2/3 of the GNSS Navigation Message. The navigation data is recent if $\left|t - t_{oe}\right| \leq 2$ hours, where t is the measurement time.

[2]Available in the Broadcast Orbit-6 data record of a RINEX Navigation Data File and in word 3 of subframe 1 and page 25 of subframes 4 and 5 of the GNSS Navigation Message

[3]Available in the Broadcast Orbit-6 data record of a RINEX Navigation Data File and in word 3 of subframe 1 of the GNSS Navigation Message

Figure 5-1. Measurement Selection/Processing Algorithm (1 of 3)

1.1.3 If singly-differenced measurement processing of pseudorange and/or Doppler is selected and "Select Common Transmitters is disabled:

1.1.3.1 If "Force Standard on Local" option is enabled, select all GNSS SVs that pass the validation tests. Form and process singly-differenced measurements for the selected GNSS SVs that have common measurements to the local receiver and at least one remote receiver, process standard measurements for the remaining selected GNSS SVs to the remote satellites, and in addition process standard measurements from all selected GNSS SVs to the local satellite.

1.1.3.2 If "Force Standard on Local" option is disabled, select all GNSS SVs that pass the validation tests. Form and process singly-differenced measurements for the selected GNSS SVs that have measurements to the local receiver and at least one remote receiver and process measurements for the remaining selected GNSS SVs as standard measurements.

1.1.4 If singly-differenced measurement processing of carrier phase is selected, form and process singly-differenced carrier phase measurements for only the GNSS SVs that pass the validation tests and have measurements to the local receiver and at least one remote receiver.

1.2 If "Cyclic" selection is enabled, select and process measurements from one GNSS SV (note that cyclic option was removed in GEONS Release 3.0)

1.2.1 If standard measurement processing is selected, select the next GNSS SV that passes the validation tests and cyclic test (i.e. the elapsed time during which this GNSS SV has not been selected for processing is greater than or equal to the minimum sampling frequency for the same GNSS SV). Process standard measurements from the selected GNSS SV to the local and/or remote receivers

1.2.2 If singly-differenced measurement processing is selected and

1.2.2.1 If "Force Standard on Local" option is enabled, select the next GNSS SV that passes the validation test and the cyclic test. If the selected GNSS SV has common measurements to the local receiver and at least one remote receiver, form and process as singly-differenced measurements. In addition process standard measurements from the selected GNSS SV to the local satellite. If the selected GNSS SV does not have common measurements, process standard measurements to the local or remote satellites from the selected GNSS SV.

1.2.2.2 If "Force Standard on Local" option is disabled, select the next GNSS SV that passes the validation tests and the cyclic test. If the selected GNSS SV that has common measurements to the local receiver and at least one remote receiver, form and process singly-differenced measurements from the selected GNSS SV. If the selected GNSS SV does not have common measurements, process standard measurements to the local or remote satellites.

2 If WAAS GEO measurements are enabled and the elapsed time from the last successful WAAS GEO measurement update is greater than or equal to the minimum WAAS GEO measurement sampling interval, perform the following tests to select and process WAAS GEO measurements for each of the N_S receivers:

2.1 If standard measurement processing is selected, select each WAAS GEO that passes the validation tests (i.e. is enabled for processing, has recent navigation data, has valid health indicator, and has acceptable accuracy indicator and process standard measurements from the selected GNSS SVs to the local and/or remote receivers.

2.2 If singly-differenced measurement processing of pseudorange and/or Doppler is selected and "Select Common Transmitters" option is enabled,

2.2.1 If "Force Standard on Local" option is enabled, select all GNSS SVs that pass the validation tests. Form and process singly-differenced measurements for all GNSS SVs that have common measurements to the local receiver and at least one remote receiver and in addition process standard measurements from all selected GNSS SVs to the local satellite.

2.2.2 If "Force Standard on Local" option is disabled, select all GNSS SVs that pass the validation tests and have common measurements to the local receiver and at least one remote receiver. Form and process singly-differenced measurements for the selected GNSS SVs.

Figure 5-1. Measurement Selection/Processing Algorithm (2 of 3)

2.3	If singly-differenced measurement processing of pseudorange and/or Doppler is selected and "Select Common Transmitters" option is disabled,
2.3.1	If "Force Standard on Local" option is enabled, select all GNSS SVs that pass the validation tests. Form and process singly-differenced measurements for all GNSS SVs that have common measurements to the local receiver and at least one remote receiver, process standard measurements from all other selected GNSS SVs to the remote satellites, and in addition process standard measurements from all selected GNSS SVs to the local satellite.
2.3.2	If "Force Standard on Local" option is disabled, select all GNSS SVs that pass the validation tests. Form and process singly-differenced measurements for all GNSS SVs that have common measurements to the local receiver and at least one remote receiver and process standard measurements for all other selected GNSS SVs
2.4	If singly-differenced measurement processing of carrier phase is selected, form and process singly-differenced carrier phase measurements for only the GNSS SVs that pass the validation tests and have measurements to the local receiver and at least one remote receiver.
3	If cross-link measurements are enabled and the elapsed time from the last successful cross-link measurement update is greater than or equal to the minimum cross-link measurement sampling interval, perform the following tests to select and process cross-link measurements to the each receiver:
3.1	Select each transmitting satellite that passes the validation tests (i.e. is enabled for processing, has recent state vector)
3.2	Process measurements from all valid transmitting satellites to the local satellite
4	If ground station measurements are enabled and the elapsed time from the last successful ground station measurement update is greater than or equal to the minimum ground station measurement sampling interval, process most recent ground station measurements within the selection window for each of the N_S receivers
5	If point solution measurements are enabled and the elapsed time from the last successful point solution measurement update is greater than or equal to the minimum point solution measurement sampling interval, process most recent point solution measurements within the selection window for each of the N_S receivers
6	If celestial object measurements are enabled and the elapsed time from the last successful celestial object measurement update is greater than or equal to the minimum celestial object measurement sampling interval, process most recent measurements within the selection window from each enabled celestial object sensor on each of the N_S receivers
7	If TDRSS measurements are enabled and the elapsed time from the last successful TDRSS measurement update is greater than or equal to the minimum TDRSS measurement sampling interval, process most recent measurement within the selection window from each enabled TDRSS satellite for each of the N_S receivers

Figure 5-1. Measurement Selection/Processing Algorithm (3 of 3)

5.2 GPS/Galileo Space Vehicle/WAAS GEO Ephemeris Computation

The transmitting satellite position and velocity are needed to model the GPS/WAAS and Galileo pseudorange and Doppler measurements. The section presents the algorithms for computing the GPS/Galileo SV position and velocity from the broadcast ephemeris message data, which is the primary method used in flight operation. In addition, the transmitting satellite position and velocity vectors can be computed by interpolation on position and velocity vectors equally spaced in time. Note that, if the TDRSS Augmentation Service for Satellites (TASS) supports GPS-like ranging

from the TDRSS GEO transmitters, these transmitters would be handled as WAAS GEOs in GEONS. Section 5.2.4 discusses application of the GPS differential corrections that are broadcast by the TASS. Section 5.2.5 discusses the application of the GPS Improved Clock and Ephemeris (ICE) differential correction parameters, which are provided as part of the GPS Broadcast message in message types 34 or 13 and 14.

5.2.1 GPS/Galileo Broadcast Ephemeris Parameters

Table 5-2 lists the GPS ephemeris parameters that are contained in the broadcast navigation legacy messages (LNAV message parameters listed in Table 20-III in Reference 10). References 10 and 63 provide a detailed description of the GPS and Galileo broadcast ephemeris message parameters, respectively. The definition of the Galileo LNAV ephemeris parameters is the same as for the GPS ephemeris parameters. Note that GEONS 3.0 does not support the modernized CNAV broadcast messages defined in Table 30-I in Reference 10.

Table 5-2. Ephemeris Parameters Contained in the LNAV Broadcast Navigation Message

Parameter	Description	Units
t_{oe}	Ephemeris reference time	Seconds from the beginning of GPS week
M_o	Mean anomaly at reference time (t_{oe})	Radians
Δn	Mean motion correction	Radians per second
e	Eccentricity	Unitless
$\sqrt{A}$	Square-root of the semimajor axis	$\sqrt{\text{meters}}$
Ω_o	Longitude of ascending node at weekly epoch (at t=0, not at t=t_{oe})	Radians
ι_o	Uncorrected orbit inclination at t_{oe}	Radians
ω	Argument of perigee	Radians
$\dot{\Omega}$ (Ω-dot)	***Inertial*** rate of change of right ascension of ascending node	Radians per second
$\dot{\imath}$ ($\imath$-dot)	Rate of orbit inclination	Radians per second
C_{uc}, C_{us}	Argument of latitude corrections due to second harmonic perturbations	Radians
C_{ic}, C_{is}	Inclination corrections due to second harmonic perturbations	Radians
C_{rc}, C_{rs}	Radius corrections due to second harmonic perturbations	Meters
IODE	Age of ephemeris data	–

It should be noted that some parameters in Table 5-1 are given in units different from those used in the original navigation message. Navigation messages telemetered down from the GPS SVs describe $M_0, \Omega_0, \imath_0$, and ω in semicircles (i.e., π radians) and $\Delta n, \dot{\Omega}$, and $\dot{\imath}$ in semicircles/per

second. The value of π to be used to convert from semicircles to radians is 3.1415926535898. The following user algorithm for GPS ephemeris computations use the parameters with units given in Table 5-1, not the ones coming from the navigation message.

5.2.2 User Algorithm for GPS/Galileo SV Antenna Phase Center Position Computation

The GPS SV broadcast ephemeris parameters provide the GPS SV antenna phase center position in the WGS 84 ECEF frame that is consistent with the definition of the ITRF. Section 30.3.3.5.1.1 in Reference 10 states that "The full coordinate transformation for translating to the corresponding ECI SV antenna phase center position may be accomplished in accordance with the computations detailed in Chapter 5 of IERS Technical Note 36: IERS Conventions (2010) and equations for UT1, x_p and y_p as documented in Table 30-VIII. Ongoing WGS 84 re-adjustment at NGA and incorporating the 2010 IERS Conventions, are expected to bring Earth based coordinate agreement to within 2 cm. In the context of the Conventions, the user may as a matter of convenience choose to implement the transformation computations via either the "Celestial Intermediate Origin (CIO) based approach" or the "Equinox based approach"."

The following algorithm for computing the ECEF coordinates of the GPS SV antenna phase center is based on Table 20-IV in Reference 10. The algorithm for computing the ECEF/GTRF Galileo antenna phase center position is identical except that the algorithm must be evaluated using GST times vs the GPS time used for computation of the GPS SV position. The transformation from the ECEF/ITRF to the ECI/GCRF is discussed in Section 3.2.

The semimajor axis and the uncorrected mean motion are given by:

$$A = \left(\sqrt{A}\right)^2 \tag{5.2-1}*$$

$$n_0 = \sqrt{\mu / A^3} \tag{5.2-2}*$$

The signal transmit time is expressed relative to the ephemeris reference time, t_{oe}, as follows:[1]

$$\Delta t_k = t_T - t_{oe} \tag{5.2-3}*$$

Then, the corrected mean motion and the mean anomaly are given by

$$n = n_0 + \Delta n \tag{5.2-4}*$$

[1] The time t_T appearing on the right-hand side of Equation (5.2-3) is GPS system time at the time of signal transmission, i.e., GPS signal receive time corrected for signal transit time. Furthermore, Δt_k shall be the actual total time difference between the time t and the epoch time t_{oe} and must account for beginning or end of week crossovers. This can be achieved as follows: If Δt_k is less than –302400 seconds, then add 604800 seconds to Δt_k; if Δt_k is greater than 302400 seconds, then subtract 604800 seconds from Δt_k. This procedure will guarantee that the magnitude of Δt_k is less than 302400 seconds.

$$M_k = M_0 + n\,\Delta t_k \tag{5.2-5}*$$

If the eccentric anomaly (E_k) is required, it can be obtained using the following Kepler's equation:

$$M_k = E_k - e\sin E_k \tag{5.2-6}*$$

This equation is solved by the following iteration scheme:

$$f\left(E_k^n\right) = E_k^n - e\sin E_k^n - M_k \tag{5.2-7}*$$

$$D^n = 1 - e\cos\left[E_k^n - 0.5 f\left(E_k^n\right)\right] \tag{5.2-8}*$$

$$E_k^{n+1} = E_k^n - \frac{f\left(E_k^n\right)}{D^n} \tag{5.2-9}*$$

where

$$E_k^0 = M_k + e\sin M_k \tag{5.2-10}*$$

The following relations between the true anomaly (ν_k) and the eccentric anomaly will be used to compute the true anomaly from the eccentric anomaly or vice versa:

$$\nu_k = \tan^{-1}\left\{\frac{\sqrt{1-e^2}\,\sin E_k\,/(1-e\cos E_k)}{(\cos E_k - e)/(1-e\cos E_k)}\right\} \tag{5.2-11}*$$

$$E_k = \cos^{-1}\left\{\frac{e+\cos\nu_k}{1+e\cos\nu_k}\right\} \tag{5.2-12}*$$

The argument of latitude is defined as follows:

$$\Phi_k = \nu_k + \omega \tag{5.2-13}*$$

The corrections to the argument of latitude, inclination, and radius due to the second-order harmonic perturbations are computed using the following equations:

$$\delta u_k = C_{us}\sin 2\Phi_k + C_{uc}\cos 2\Phi_k \tag{5.2-14}*$$

$$\delta\imath_k = C_{is}\sin 2\Phi_k + C_{ic}\cos 2\Phi_k \tag{5.2-15}*$$

$$\delta R_k = C_{rs}\sin 2\Phi_k + C_{rc}\cos 2\Phi_k \tag{5.2-16}*$$

Then, the corrected argument of latitude, inclination, and radius are given by

$$u_k = \Phi_k + \delta u_k \tag{5.2-17}*$$

$$R_k = A(1 - e\cos E_k) + \delta R_k \tag{5.2-18}*$$

$$\iota_k = \iota_0 + \delta\iota_k + \dot{\iota}\,\Delta t_k \tag{5.2-19}*$$

Using the orbital parameters computed above, the Cartesian components of the position vector in the orbital plane and ECEF systems can be obtained as follows. The SV position components in the orbital plane coordinates are given by

$$\left.\begin{aligned} X'_k &= R_k \cos u_k \\ Y'_k &= R_k \sin u_k \end{aligned}\right\} \tag{5.2-20}*$$

The corrected longitude of the ascending node is needed to convert these orbital plane components into the ECEF components. The required longitude of ascending node is obtained as follows:

$$\Omega_k = \Omega_0 + (\dot{\Omega} - \omega_e)\,\Delta t_k - \omega_e\, t_{oe} \tag{5.2-21}*$$

Then, the ECEF Cartesian components of the GPS spacecraft position vector are given by

$$x_k = X'_k \cos\Omega_k - Y'_k \sin\Omega_k \cos\iota_k \tag{5.2-22}*$$

$$y_k = X'_k \sin\Omega_k + Y'_k \cos\Omega_k \cos\iota_k \tag{5.2-23}*$$

$$z_k = Y'_k \sin\iota_k \tag{5.2-24}*$$

Note that the following World Geodetic System-84 (WGS-84) values are to be used in the equations given above:

$$\mu = \begin{cases} 3.986005\times10^{14}\ m^3/s^2; & GPS \\ 3.986004418\times10^{14}\ m^3/s^2; & Galileo \end{cases}$$ WGS-84 Earth's gravitational constant

ω_e = $7.2921151467 \times 10^{-5}$ radians/second: WGS-84 value of the Earth's rotation rate

The ECEF components defined above are transformed into the Cartesian components in the mean equator and equinox of J2000.0 coordinate system using the following rotation matrices defined in Section 3.2:

$$\overline{R}_{J2000} = C^T R_g{}^T B^T \overline{r}_{EF} \tag{5.2-25}*$$

where

C = transformation matrix from J2000.0 to true of date coordinate frame

R_g = transformation matrix from true of date to pseudo-Earth-fixed coordinate frame

B = transformation matrix from pseudo-Earth-fixed to ECEF coordinate frame

5.2.3 GPS/Galileo Antenna Phase Center Velocity Computation

The following algorithm for velocity computation is based on the algorithm given in Table 20-IV sheet 3 and sheet 4 in Reference 10. For notational simplicity, the subscript *k* will be dropped from all the expressions given in this section. Equations (5.2-22) through (5.2-24), which compute the position components along the ECEF axes, can be rewritten as follows:

$$\bar{r}_{EF} \equiv \begin{pmatrix} x_{EF} \\ y_{EF} \\ z_{EF} \end{pmatrix} \equiv M\ \bar{R}_2' \tag{5.2-26}$$

where a 3×2 matrix M and a two-dimensional position vector $\bar{R}_2'$ are, respectively, defined as follows:

$$M \equiv \begin{bmatrix} \cos\Omega & -\cos\iota\sin\Omega \\ \sin\Omega & \cos\iota\cos\Omega \\ 0 & \sin\iota \end{bmatrix} \tag{5.2-27}$$

$$\bar{R}_2' \equiv \begin{pmatrix} X' \\ Y' \end{pmatrix} \tag{5.2-28}$$

Rewriting Equation (5.2-25), the mean of J2000.0 (inertial) position vector can be obtained as follows:

$$\bar{R} = C^T R_g^T B^T M\ \bar{R}_2' \tag{5.2-29}$$

It will be assumed that the C and B matrices are time-independent. Then, in Equation (5.2-29), R_g, M and $\bar{R}_2'$ are the only ones that depend on time. Differentiating Equation (5.2-29) with respect to time, the following expression for the J2000.0 velocity vector is obtained:

$$\dot{\bar{R}} = C^T \dot{R}_g^T B^T M\ \bar{R}_2' + C^T R_g^T B^T \dot{M}\ \bar{R}_2' + C^T R_g^T B^T M\ \dot{\bar{R}}_2' \tag{5.2-30}*$$

or equivalently

$$\dot{\bar{R}} = C^T \dot{R}_g^T B^T \bar{r}_{EF} + C^T R_g^T B^T \dot{\bar{r}}_{EF} \tag{5.2-30b}*$$

where

$$\dot{\bar{r}}_{EF} = \dot{M}\ \bar{R}_2' + M\ \dot{\bar{R}}_2' \tag{5.2-30c}*$$

The velocity vector $\dot{\bar{R}}_2'$ represents the spacecraft velocity in the orbit plane coordinate system and is determined by the rate of change in time of the X' and Y' (given by Equation 5.2-20):

$$\dot{X}' = \dot{R}\cos u - R\dot{u}\sin u \tag{5.2-31}*$$

$$\dot{Y}' = \dot{R}\sin u + R\dot{u}\cos u \tag{5.2-32}*$$

where

$$\dot{R} = A\,e\sin E\,\dot{E} + \delta\dot{R} \tag{5.2-33}*$$

$$\delta\dot{R} = 2\dot{\nu}\left[C_{rs}\cos 2(\nu+\omega) - C_{rc}\sin 2(\nu+\omega)\right] \tag{5.2-34}*$$

and

$$\dot{u} = \dot{\nu} + \delta\dot{u} \tag{5.2-35}*$$

$$\delta\dot{u} = 2\dot{\nu}\left[C_{us}\cos 2(\nu+\omega) - C_{uc}\sin 2(\nu+\omega)\right] \tag{5.2-36}*$$

In Equations (5.2-33) through (5.2-36), $\delta\dot{R}$ and $\delta\dot{u}$ denote the time derivatives of δR and δu, respectively. The time derivatives of orbital parameters given above can be obtained from the time derivatives of E (eccentric anomaly) and ν (true anomaly). $\dot{E}$ and $\dot{\nu}$ may be computed as follows:

$$\dot{E} = \frac{n}{(1-e\cos E)} \tag{5.2-37}$$

$$\dot{\nu} = \frac{n}{\sqrt{(1-e^2)}}\,\frac{(1+e\cos\nu)}{(1-e\cos E)} \tag{5.2-38}$$

Using these relations, the terms containing the rates of change of R and u can be computed as follows:

$$\dot{R} = \frac{n\,A}{R}\left[A\,e\sin E + \frac{2}{\sqrt{(1-e^2)}}\,(1+e\cos\nu)\left[C_{rs}\cos 2(\nu+\omega) - C_{rc}\sin 2(\nu+\omega)\right]\right] \tag{5.2-39}*$$

and

$$\begin{aligned} R\dot{u} &= R\dot{\nu}\left[1+2\left(C_{us}\cos 2(\nu+\omega) - C_{uc}\sin 2(\nu+\omega)\right)\right] \\ &= \frac{Rn}{\sqrt{(1-e^2)}}\,\frac{(1+e\cos\nu)}{(1-e\cos E)}\left[1+2\left(C_{us}\cos 2(\nu+\omega) - C_{uc}\sin 2(\nu+\omega)\right)\right] \end{aligned} \tag{5.2-40}*$$

In Equation (5.2-39), the quantity n denotes the mean motion. This completes the computation of $\dot{X}'$ and $\dot{Y}'$ given by Equations (5.2-31) and (5.2-32).

The time derivative of the matrix R_g is given by Equation (3.2-33) in Section 3.2.3.1. From the definition of M given by Equation (5.2-27), the time derivative of M is given by:

$$\dot{M} \equiv -(\dot{\Omega} - \omega_e)\begin{bmatrix} \sin\Omega & \cos\iota\cos\Omega \\ -\cos\Omega & \cos\iota\sin\Omega \\ 0 & 0 \end{bmatrix} + \dot{\iota}_{tot}\begin{bmatrix} 0 & \sin\iota\sin\Omega \\ 0 & -\sin\iota\cos\Omega \\ 0 & \cos\iota \end{bmatrix} \tag{5.2-41}$$

In the above equation, $\dot{\iota}_{tot}$ denotes the time derivative of the inclination and can be computed using the following equation:

$$\dot{\iota}_{tot} = \dot{\iota} + \frac{\mathrm{d}(\delta\iota)}{\mathrm{d}t} \tag{5.2-42}*$$

where

$$\begin{aligned} \frac{\mathrm{d}(\delta\iota)}{\mathrm{d}t} &= 2\dot{\nu}\left(C_{is}\cos 2\Phi - C_{ic}\sin 2\Phi\right) \\ &= \frac{2n}{\sqrt{(1-e^2)}}\frac{(1+e\cos\nu)}{(1-e\cos E)}\left(C_{is}\cos 2\Phi - C_{ic}\sin 2\Phi\right) \end{aligned} \tag{5.2-43}*$$

5.2.4 TASS GPS Differential Corrections

The TDRSS Augmentation Service for Satellites (TASS) will provide precise GPS differential corrections and other ancillary data to enable decimeter level orbit determination accuracy and nanosecond time-transfer accuracy, onboard in real-time. TASS will broadcast its message on the S-band multiple access channel of NASA's TDRSS. Broadcasts will be available from three or more TDRSS satellites, providing global coverage. In addition to the GPS differential corrections, TASS will provide real-time Earth orientation and solar flux information and GPS integrity information (which can be used to screen GPS SV measurements for processing).

When available the TASS differential corrections are added to the ECEF GPS SV position and velocity vectors computed using Equations (5.2-22) through (5.2-24) and (5.2-30c) prior to transforming these vectors to the ECI frame in Equation (5.2-25) and (5.2-30b):

$$\begin{aligned} \bar{r}_{EF}(t)_{Corrected} &= \bar{r}_{EF}(t) + \Delta\bar{r}_{EF}(t_{DC_k}) + \Delta\dot{\bar{r}}_{EF}(t_{DC_k})\left[t - t_{DC_k}\right] \\ \dot{\bar{r}}_{EF}(t)_{Corrected} &= \dot{\bar{r}}_{EF}(t) + \Delta\dot{\bar{r}}_{EF}(t_{DC_k}) + \frac{\Delta\dot{\bar{r}}_{EF}(t_{DC_k}) - \Delta\dot{\bar{r}}_{EF}(t_{DC_{k-1}})}{t_{DC_k} - t_{DC_{k-1}}}\left[t - t_{DC_k}\right] \end{aligned} \tag{5.2-44}$$

where

t_{DC_k} = time tag of TASS differential correction value closest to the request time t

$\Delta\bar{r}_{EF}(t_{DC_k})$ = position differential correction at time t_{DC_k} from the TASS message

$\Delta\dot{\bar{r}}_{EF}(t_{DC_k})$ = rate of change of position differential correction at time t_{DC_k} from the TASS message

5.2.5 GPS Improved Clock and Ephemeris (ICE) Differential Correction Parameters

To enable decimeter level orbit determination in real time, differential correction parameters are provided as part of the GPS Broadcast message in message types 34 or 13 and 14. Section 30.3.3.7 of Reference 10 provides a detailed discussion of these corrections. In addition to the normal quasi-Keplerian elements, A_0, e_n, i_{0-n}, Ω_{o-n}, ω_n and M_{0-n}, discussed in Section 5.2.1, the differential correction parameters listed in Table 5-3 are provided. These parameters apply to the clock and ephemeris data transmitted by other GPS SVs.

Table 5-3. Clock and Ephemeris Differential Correction Parameters Contained in the Broadcast Navigation Message Types 34 or 13 and 14

Parameter	Description	Units
PRN ID	PRN of satellite to which correction applies	
t_{OD}	Reference Time of week of the Differential Correction data relative to the GPS week	Seconds from the beginning of GPS week
δa_{f0}	SV Clock Bias Correction	Seconds
δa_{f1}	SV Clock Drift Correction	Seconds per second
$UDRA$	User Differential Range Accuracy Index	dimensionless
$\Delta\alpha$	Alpha Correction to Ephemeris Parameters	dimensionless
$\Delta\beta$	Beta Correction to Ephemeris Parameters	dimensionless
$\Delta\gamma$	Gamma Correction to Ephemeris Parameters	Radians
Δi	Angle of Inclination Correction	Radians
$\Delta\Omega$	Angle of Right Ascension Correction	Radians
ΔA	Semi-Major Axis Correction	Meters
$UD\dot{R}A$	Change Rate of User Differential Range Accuracy Index	dimensionless

Note that some of the parameters in Table 5-3 are given in units of radians not semicircles (i.e., π radians) as in the raw navigation message. The value of π to be used to convert from semicircles to radians is 3.1415926535898. The following user algorithm for GPS ephemeris computations assume parameters with units listed in Table 5-2.

A set of corrected quasi-Keplerian parameters is computed as follows. First construct a set of initial (uncorrected) elements for SV *n* using the parameters listed in Table 5-1.:

$$A_i = \left(\sqrt{A_n}\right)^2$$

$$e_i = e_n$$

$$i_i = i_{0-n}$$

$$\Omega_i = \Omega_{0-n} \tag{5.2-45}$$

$$\alpha_i = e_n \cos(\omega_n)$$

$$\beta_i = e_n \sin(\omega_n)$$

$$\gamma_i = M_{0-n} + \omega_n$$

The terms α_i, β_i and γ_i form a subset of stabilized ephemeris elements which are corrected as follows:

$$\alpha_c = \alpha_i + \Delta\alpha$$

$$\beta_c = \beta_i + \Delta\beta \tag{5.2-46}$$

$$\gamma_c = \gamma_i + \Delta\gamma$$

The corrected quasi-Keplerian elements are then given by

$$A_c = A_i + \Delta A$$

$$e_c = \left(\alpha_c^2 + \beta_c^2\right)^{1/2}$$

$$i_c = i_i + \Delta i \tag{5.2-47}$$

$$\Omega_c = \Omega_i + \Delta\Omega$$

$$\omega_c = \tan^{-1}(\beta_c / \alpha_c)$$

$$M_{0-c} = \gamma_c - \omega_c + \Delta M_0$$

where

$$\Delta M_0 = -\frac{3\Delta A}{2A_c}\sqrt{\frac{\mu_E}{A_c^3}}[(t_{oe} + 604800 * WN_{oe}) - (t_{OD} + 604800 * WN)] \tag{5.2-48}$$

where WN_{oe} is the week number associated with t_{oe}, the reference time of the broadcast message parameters, and WN is the current week number associated with t_{OD}, the reference time of the differential correction data. The ΔM_0 term in serves to propagate the mean anomaly at the reference time to the epoch time of the navigation message being corrected. The corrections calculated by the fitting process are good at the epoch time of the specific broadcast elements being corrected.

The corrected quasi-Keplerian elements are then used to compute the position and velocity of the GPS SV using equations provided in Sections 5.2.2 and 5.2.3.

5.3 GNSS Pseudorange, Doppler, and Carrier Phase Measurement Models

The computational algorithms for the GNSS C/A code pseudorange, Doppler, and integrated carrier phase measurements are discussed in this section. GNSS sources supported in GEONS are GPS, WAAS, and Galileo. The general form of the measurement model is as follows:

$$Y_k = G\ [\bar{X}(t_k),\ t_k] + \varepsilon \tag{5.3-1}$$

where t_k is the true measurement time, referenced to UTC, and ε is the measurement error. It is assumed that ε has a zero-mean Gaussian distribution with standard deviation σ, which is commandable for each measurement type. The measurement standard deviation is typically determined through analysis of the random component of the measurement error as part of the filter tuning process. GEONS models the GPS measurement standard as a constant value; however, in situations where there is a large variation in the received signal strength, computing the pseudorange measurement standard as a function of the received signal strength can provide a more realistic value of the noise contribution. Section 12.4 provides GPS pseudorange noise model that have been used to simulate weak GPS signals.

For GEONS, the estimation state vector, $\overline{X}(t)$ includes the receiver position vector, $\overline{R}$; velocity vector, $\dot{\overline{R}}$; optional corrections to the atmospheric drag and solar radiation pressure coefficients, ΔC_D and ΔC_R; GNSS receiver bias, b_R; and GNSS receiver bias rate, d_R, for one or more receivers; ionospheric delay scale factor, γ_I; and measurement-dependent biases. In addition, when GNSS pseudorange and Doppler measurements are processed, one pseudorange bias and one Doppler bias can be estimated for each GPS SV, WAAS GEO, and Galileo SV that is tracked. When integrated carrier phase measurements are processed, one integer ambiguity bias is estimated for each GNSS SV-receiver pair. When a ground-based receiver state is estimated, corrections to the drag and solar radiation pressure coefficients are not estimated.

Section 5.3.1 addresses preprocessing of pseudorange measurements obtained from the GNSS receiver. The measurement model for the one-way pseudorange measurements from the GPS SV/WAAS GEO to the user receiver is presented in Section 5.3.2. The one-way Doppler measurement model is defined in Section 5.3.3. The integrated carrier beat phase measurement model is defined in Section 5.3.4. Note that, if the TDRSS Augmentation Service for Satellites (TASS) supports GPS-like ranging from the TDRSS GEO transmitters, these transmitters would be handled as WAAS GEOs in GEONS. Section 5.3.5 discusses the ionospheric correction model using GPS navigation data. Sections 5.3.6 through 5.3.8 present the Galileo pseudorange, Doppler, and integrated carrier phase measurement models, respectively.

5.3.1 Pseudorange Measurement Preprocessing

GEONS processes full pseudorange measurements. This section provides algorithms that can be used to compute the full pseudorange measurement given raw measurement data provided by typical GPS receivers. Section 5.3.1.1 provides an algorithm for computing the full pseudorange given a fractional measurement. Section 5.3.1.2 provides an algorithm for computing the full pseudorange given the transmit time measured by the receiver.

5.3.1.1 Fractional Pseudorange Measurement Preprocessing (not implemented in GEONS)

The preprocessing of fractional GPS/WAAS pseudorange measurements is discussed in this section. Note that the units in which the fractional C/A code is expressed vary with the type of receiver. For the Loral Tensor receiver, the fractional C/A code pseudoranges are given in units of one-sixteenth ($1/16^{th}$) of a code phase chip. The nominal C/A code chipping is 1.023 megahertz, which gives a one-C/A-code chip length of (1/1.023) microseconds. Thus, $1/16^{th}$ of a C/A code chip is given by

$$\gamma \equiv 10^{-6}/(16\times 1.023)] \text{ seconds in time}$$

$$= c\,\gamma \text{ meters in equivalent distance} \tag{5.3-2}$$

where c denotes the speed of light (c = 299792458 meters/second).

The observed fractional pseudoranges given in units of $1/16^{th}$ chip, $\Re'_{obs}$, can be converted into meters as follows:

$$\widetilde{\Re}_{obs}\,(\text{in meters}) = c\,\gamma\,\Re'_{obs}\ \ (\text{in units of } 1/16^{th} \text{ chip}) \tag{5.3-3}$$

Note that the time interval γ is defined in terms of the reference receiver clock. The fractional pseudorange measurement obtained from Equation (5.3-3) does not include the C/A code pseudorange integer ambiguity. This range ambiguity is generally given by an integer times 1 millisecond, which is the repetition interval of C/A code. Let I_{amb} denote this integer ambiguity (in milliseconds), then the observed full preudorange will be given by

$$\Re_{obs}\,(\text{in meters}) = c\,\gamma\,\Re'_{obs}\,(\text{in units of } 1/16^{th} \text{ chip}) + \text{c}\,I_{amb}\times 10^{-3} \tag{5.3-4}$$

where $\Re'_{obs}$ (in units of $1/16^{th}$ chip) and the associated measurement timetag referenced to the GPS system time are provided by the receiver.

If I_{amb} (in milliseconds) is not available from the GPS receiver, it can be computed as follows.

Define q such that

$$q \equiv c \cdot (10^{-3} \text{ seconds}) = 299792.458 \text{ meters} \tag{5.3-5}$$

Then, the *observed* full pseudorange, $\Re_{obs}$, from GPS SV/WAAS GEO j to user receiver n can be expressed as:

$$\left(\Re_{obs}\right)^{n}_{G/W_j} = I_{amb}\cdot q + \widetilde{\Re}_{obs} \tag{5.3-6}$$

where I_{amb} denotes the integer millisecond ambiguity of the pseudorange measurement and $\widetilde{\Re}_{obs}$, whose value lies between zero and $\pm q$, represents the actual fractional pseudorange measurement expressed in meters. The integer ambiguity, I_{amb}, can be obtained from the computed pseudorange [given later in Equation (5.3-20)] based on the predicted user position vector and user clock offset at the time of each measurement processing, as follows:

Define N_c (an integer) and $\widetilde{\Re}$ (a real number between 0 and $\pm q$) as

$$N_c = \left[\frac{\Re}{q} \right]_{INT} \tag{5.3-7}$$

$$\widetilde{\Re} \equiv \Re - N_c \cdot q \tag{5.3-8}$$

where $\Re$ is the computed pseudorange obtained using Equation (5.3-20). In the first expression above, $[\ ]_{INT}$ denotes the integer part of the quotient enclosed by the square brackets. Note that N_c and $\widetilde{\Re}$ obtained from Equations (5.3-7) and (5.3-8) can be both positive or negative depending on the sign of $\Re$. The integer N_c obtained in this manner can, in most cases, be used for I_{amb}, which is needed in Equation (5.3-6) to construct the *observed* full pseudorange. However, there are some cases where this simple replacement may not work due to errors associated with the computed full pseudorange. These exceptions will most likely occur when (1) $\left|\widetilde{\Re}_{obs}\right| \approx q$ and $\left|\widetilde{\Re}\right| \approx 0$ or (2) $\left|\widetilde{\Re}_{obs}\right| \approx 0$ and $\left|\widetilde{\Re}\right| \approx q$. These conditions can be stated in a more quantitative manner as follows:

Case (1): $\quad q - \varepsilon \le \left|\widetilde{\Re}_{obs}\right| < q \quad$ and $\quad 0 \le \left|\widetilde{\Re}\right| \le \varepsilon$

Case (2): $\quad 0 \le \left|\widetilde{\Re}_{obs}\right| \le \varepsilon \quad$ and $\quad q - \varepsilon \le \left|\widetilde{\Re}\right| < q$

where ε denotes an assumed maximum range error magnitude (on the order of 20 kilometers). The measurement diagrams shown in Figure 5-2 illustrate these two cases graphically. The diagrams suggest that the magnitude of I_{amb} for Case (1) should be ($|N_c|-1$), and that for Case (2) should be ($|N_c|+1$). In all other cases, I_{amb} should be equal to N_c. The appropriate values of I_{amb} for these various cases are summarized in Table 5-2.

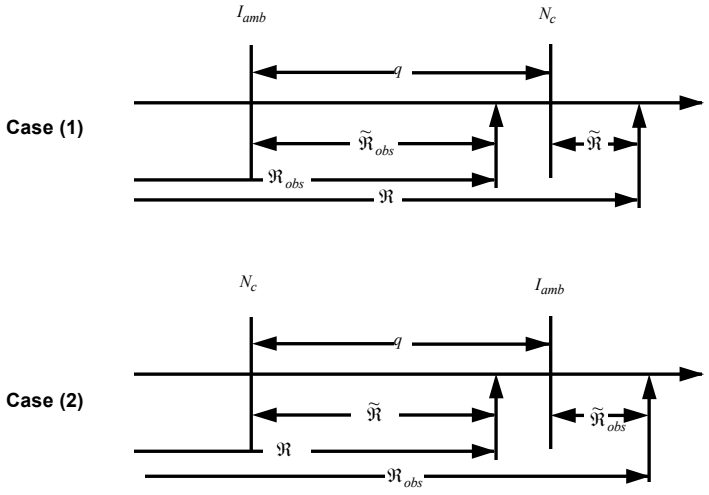

Figure 5-2. Special Cases for Computing the Pseudorange Integer Ambiguity

Table 5-4. Relationship Between I_{amb} and N_c

Sign of $\Re$	Case	I_{amb}
Positive	Case (1)	N_c - 1
	Case (2)	N_c + 1
	All other cases	N_c
Negative	Case (1)	N_c + 1
	Case (2)	N_c - 1
	All other cases	N_c

5.3.1.2 Transmit Time and Carrier Frequency Measurement Preprocessing (not implemented in GEONS)

The preprocessing of raw GPS/WAAS transmit time and carrier frequency measurements is discussed in this section.

Many GPS receivers are built using the Plessey GPS Builder chip set, which performs pseudorange and Doppler measurements at multiples of "TICs" of the processor clock. The measurement times in TICs, N_{TIC} , can be converted to a raw GPS receive time, $t_R^{(RC)}$, as follows:

$$t_R^{(RC)} = t_{R_0}^{(RC)} + \delta t_{NAV} + N_{TIC} * \Delta t_{TIC} \tag{5.3-8b}$$

where

$t_{R_0}^{(RC)}$ = offset of receiver clock at $N_{TIC} = 0$ from GPS time, set at power-on or initialized by command

δt_{NAV} = offset of the current receiver clock from GPS time computed using the Time of Word (TOW) from the GPS navigation message, which can be determined to within ±0.5 second

Δt_{TIC} = time interval per TIC, nominally 0.0999999 seconds

Whenever the receiver is in contact with the GPS constellation, the raw GPS receive time should be within ±0.5 second of GPS system time.

The Plessey GPS Builder chip set provides the following raw measurements:

N_{20} = number of 20 millisecond code epochs

N_1 = number of 1 millisecond code epochs

ϕ_c = number of half chips of code phase

ϕ_{dco} = fractional code digitally controlled oscillator (DCO) phase below one half chip, with resolution of 1/2048 of a chip

N_{dco} = Carrier DCO cycle count in whole cycles between TICs (nominally over 0.0999999 seconds)

The code transmit time (modulo 1 second), $t_T'^{(SC)}$, is constructed as follows from these raw measurements

$$t_T'^{(SC)} = \left[\frac{1}{1000} \left\{ 20N_{20} + N_1 + \frac{\phi_c}{2046} + \frac{\phi_{dco}}{2046 * 1024} - 0.0002443792766 \right\} + 1 \right]_{FRAC} \quad (5.3\text{-}8c)$$

In the expression above, $[\ ]_{FRAC}$ denotes the fractional part of the quotient enclosed by the square brackets.

The observed code time delay, $\Delta\tilde{\tau}$, can then be computed as follows:

$$\Delta\tilde{\tau} = t_R'^{(RC)} - t_T'^{(SC)} \quad (5.3\text{-}8d)^*$$

where the code receive time (modulo 1 second), $t_R'^{(RC)}$, equals the fractional number of seconds in the measured raw receive time, $t_R^{(RC)}$,

$$t_R'^{(RC)} = \left[t_R^{(RC)} \right]_{FRAC} \quad (5.3\text{-}8e)$$

For pseudoranges of less than 150,000 kilometers, the true code time delay will lie between 0 and 0.5 seconds. Assuming that the current raw receiver time estimate is accurate to within 0.5 seconds, $\Delta\tilde{\tau}$ should lie between -0.5 and 0.5 seconds. Therefore if $\Delta\tilde{\tau} > 0.5$, subtract 1 second and if $\Delta\tilde{\tau} < -0.5$ seconds add 1 second.

The full raw pseudorange measurement is then given by

$$\tilde{\Re}_{obs} \text{(in meters)} = c\,\Delta\tilde{\tau} \quad (5.3\text{-}8f)$$

where c denotes the speed of light (c = 299792458 meters/second).

The Doppler measurement is computed as follows from the raw carrier DCO cycle count, N_{dco}

$$F_{obs} = -\left(N_{dco} / \Delta F_N - C_{Nom}\right) R_{dco} \quad (5.3\text{-}8g)$$

where

ΔF_N = Carrier DCO cycle scale factor

C_{Nom} = Nominal carrier DCO

R_{dco} = Carrier DCO resolution

5.3.1.3 Dual-Frequency Pseudorange Preprocessing

If GPS measurements are available simultaneously on more than one frequency (i.e., L2 C or L5 in addition to L1 C/A), the pseudorange measurements are corrected for the group delay effects

using the following relationships defined in Reference 10 (Section 30.3.3.3.1.1.2) and Reference 46 (Sections 20.3.3.3.1.2.2):

$$\Re_{obs} = \begin{cases} \dfrac{\left(\Re_{obs}^{L2C} - \gamma_{12}\Re_{obs}^{L1C/A}\right) + c\left(ISC_j^{L2C} - \gamma_{12}ISC_j^{L1C/A}\right)}{1-\gamma_{12}} - cT_{GD_j}\text{; for L1 - C/A and L2 C} \\ \dfrac{\left(\Re_{obs}^{L5I5} - \gamma_{15}\Re_{obs}^{L1C/A}\right) + c\left(ISC_j^{L5I5} - \gamma_{15}ISC_j^{L1C/A}\right)}{1-\gamma_{15}} - cT_{GD_j}\text{; for L1 - C/A and L5 I5} \\ \dfrac{\left(\Re_{obs}^{L5Q5} - \gamma_{15}\Re_{obs}^{L1C/A}\right) + c\left(ISC_j^{L5Q5} - \gamma_{15}ISC_j^{L1C/A}\right)}{1-\gamma_{15}} - cT_{GD_j}\text{; for L1 - C/A and L5 Q5} \\ \dfrac{\left(\Re_{obs}^{L5I5} - \gamma_{25}\Re_{obs}^{L2C}\right) + c\left(ISC_j^{L5I5} - \gamma_{25}ISC_j^{L2C}\right)}{1-\gamma_{25}} - cT_{GD_j}\text{; for L2 C and L5 I5} \\ \dfrac{\left(\Re_{obs}^{L5Q5} - \gamma_{25}\Re_{obs}^{L2C}\right) + c\left(ISC_j^{L5Q5} - \gamma_{25}ISC_j^{L2C}\right)}{1-\gamma_{25}} - cT_{GD_j}\text{; for L2 C and L5 Q5} \end{cases} \tag{5.3-8h}$$

where

$\Re_{obs}$ = Pseudorange in meters corrected for ionospheric and group delay effects

$\Re_{obs}^{i}$ = Pseudorange in meters measured on the L-band channel indicated by *i*

ISC_j^i = Inter-signal correction for SV *j* for the channel indicated by *i* in seconds; measured values of the mean SV group delay differential between the L1 P(Y)-code and *i* code are provided as message type 30 data (Table 20-IV in Reference 46)

T_{GD_j} = Associated group delay correction for SV_j in seconds, which is available in message type 30

γ_{ij} = Ratio of nominal center frequencies

$$\begin{aligned} \gamma_{12} &= \left(\frac{F_T^{L1}}{F_T^{L2}}\right)^2 = \left(\frac{1575.42}{1227.6}\right)^2 = \left(\frac{77}{60}\right)^2 \\ \gamma_{15} &= \left(\frac{F_T^{L1}}{F_T^{L5}}\right)^2 = \left(\frac{1575.42}{1176.45}\right)^2 = \left(\frac{154}{115}\right)^2 \\ \gamma_{25} &= \left(\frac{F_T^{L2}}{F_T^{L5}}\right)^2 = \left(\frac{1227.6}{1176.45}\right)^2 = \left(\frac{24}{23}\right)^2 \end{aligned} \tag{5.3-8i}$$

If Galileo measurements are available simultaneously on more than one frequency (i.e., E5a or E5b in addition to E1), the pseudorange measurements are corrected for the group delay effects using the following relationships:

$$\Re_{obs} = \begin{cases} \dfrac{\left(\Re_{obs}^{E1} - \gamma_{15a}\Re_{obs}^{E5a}\right) + c\left(1-\gamma_{15a}\right) BGD_j(E1, E5a)}{1-\gamma_{15a}}; \text{ for E1 and E5a} \\ \dfrac{\left(\Re_{obs}^{E1} - \gamma_{15b}\Re_{obs}^{E5b}\right) + c\left(1-\gamma_{15b}\right) BGD_j(E1, E5b)}{1-\gamma_{15b}}; \text{ for E1 and E5b} \end{cases} \tag{5.3-8j}$$

$$\begin{aligned} \gamma_{15a} &= \left(\frac{F_T^{E1}}{F_T^{E5a}}\right)^2 = \left(\frac{1575.42}{1176.45}\right)^2 = \left(\frac{154}{115}\right)^2 \\ \gamma_{15b} &= \left(\frac{F_T^{E1}}{F_T^{E5b}}\right)^2 = \left(\frac{1575.42}{1207.14}\right)^2 = \left(\frac{154}{118}\right)^2 \end{aligned} \tag{5.3-8k}$$

5.3.2 GPS/WAAS Pseudorange Measurement Model and Associated Partial Derivatives

This section provides an expression that can be used to compute the observed pseudorange given by Equation (5.3-3) in terms of the GPS/WAAS and receiver states and the corresponding times. The pseudorange is obtained from the signal transit time interval, which is defined as

$$\Delta\tau \equiv t_R^{(RC)} - t_T^{(SC)} \tag{5.3-9}$$

where $t_R^{(RC)}$ denotes the receive time measured by the receiver clock and $t_T^{(SC)}$ is the transmit time measured by the GPS SV/WAAS GEO clock. The pseudorange $\Re$ is then defined as the speed of light (c) times the time interval $\Delta\tau$ given by Equation (5.3-9):

$$\Re \equiv c\,\Delta\tau \tag{5.3-10}$$

Equation (5.3-9) can be written in terms of the GPS/WAAS system times t_R and t_T corresponding to $t_R^{(RC)}$ and $t_T^{(SC)}$ and the respective clock offset terms δt_R and δt_S as follows:

$$\begin{aligned} \Delta\tau &= (t_R + \delta t_R) - (t_T + \delta t_S) \\ &\equiv \Delta t + (\delta t_R - \delta t_S) \end{aligned} \tag{5.3-11}$$

where

$$\Delta t \equiv t_R - t_T \tag{5.3-12}$$

Some GPS receivers provide the measurement timetag $t_R^{(RC)}$ corrected to within 500 microseconds of t_R. In such cases, the residual receiver clock bias, $\tilde{b}_R(t)$, can be estimated and used in Equation (5.3-19).

The GPS SV/WAAS GEO clock offset term, δt_S, is computed using Equation (3.3-9) and may be assumed to be known.

The definition of the pseudorange defined by Equation (5.3-10) can be written as

$$\Re = c\,\Delta t + c\,(\delta t_R - \delta t_S) \tag{5.3-13}$$

The above equation will be used to compute the pseudorange measurement in terms of the position vectors and clock offset parameters of the GPS SV/WAAS GEO and the receiver.

The time interval Δt appearing in the first term on the right-hand side of Equation (5.3-13) represents the true signal travel time from the GPS SV/WAAS GEO to the receiver. The first term on the right-hand side of Equation (5.3-13) can be expressed as

$$c\Delta t = \rho_{G/W_j}^{n,i} + \delta\rho_{Iono} + \delta\rho_{tropo} + \delta\rho_{et} + \delta\rho_{hw} \tag{5.3-14}$$

with

$$\rho_{G/W_j}^{n,i} = \left|\overline{R}_{A_i}{}^{n}(t_R^n) - \overline{R}_{G/W_j}(t_T)\right| \tag{5.3-15}$$

In the above equation, $\rho_{G/W_j}^{n,i}$ denotes the distance between the position of GPS SV/WAAS GEO j at the signal transmit time t_T and the position of receiver n's i^{th} antenna at the signal receive time t_R. The $\delta\rho_{Iono}$ and $\delta\rho_{tropo}$ terms represent the time delay due to the ionospheric and tropospheric refraction effects, the $\delta\rho_{et}$ term represents the effects of the GPS SV/WAAS GEO ephemeris and time errors (after the δt_S correction is applied), and the $\delta\rho_{hw}$ term represents a possible (receiver and SV) hardware-related delay. In Equation (5.3-15), the position of the transmitting antenna of the GPS SV/WAAS GEO at the time (t_T) of signal transmission is denoted by $\overline{R}_{G/W_j}(t_T)$, and the position of the i^{th} receiving antenna at the time of the signal reception (t_R^n) is denoted by $\overline{R}_{A_i}^{n}(t_R^n)$.

Combining Equations (5.3-13) and (5.3-14) yields the following expression for the pseudorange:

$$\Re_{G/W_j}^{n} \equiv \rho_{G/W_j}^{n,i} + c(\delta t_R^n - \delta t_S) + \delta\rho_{Iono} + \delta\rho_{tropo} + \delta\rho_{et} + \delta\rho_{hw} \tag{5.3-16}$$

The correction terms representing the tropospheric refraction effect and hardware-related delays are not modeled in GEONS. Then, Equation (5.3-16) reduces to the following equation:

$$\Re_{G/W_j}^{n} = \rho_{G/W_j}^{n,i} + c\delta t_R^n + \delta\rho_{et} + \delta\rho_{Iono} - c\delta t_S \tag{5.3-17}$$

with

$$\rho_{G/W_j}^{n,i} = \left|\overline{R}_{A_i}{}^{n}(t_R^n) - \overline{R}_{G/W_j}(t_T)\right| \tag{5.3-18}$$

For a spacecraft-based receiver, the location of the i^{th} receiving antenna with respect to the spacecraft's center of mass can be modeled in terms of constant offsets with respect to the spacecraft body frame $\left[\left(\Delta x_{A_i}^n\right)_B, \left(\Delta y_{A_i}^n\right)_B, \left(\Delta z_{A_i}^n\right)_B\right]$. In this case, the position of the receiving antenna is computed using Equation 3.2-61 in Section 3.2.8.

The computation of ρ using Equation (5.3-18) requires knowledge of the signal transmit time (t_T) given the signal receive time (t_R^n). Note that the equivalent UTC signal receive time will be needed

for the propagation of the user state vector to the signal receive time. The equivalent measurement time with respect to UTC can be computed using the procedure given in Section 3.3.1.

The following Newton-Raphson iterative scheme is used to solve for the actual signal transmit time, t_T, as follows

$$t_{T,m+1} = t_{T,m} + \frac{c\cdot(t_R^n - t_{T,m}) - \left|\bar{R}_{A_i}^n(t_R^n) - \bar{R}_{G/W_j}(t_{T,m})\right|}{c - \left[\hat{u}_m^n \cdot \dot{\bar{R}}_{G/W_j}(t_{T,m})\right]}$$

where

$t_{T,m+1}$ = $(m+1)^{th}$ approximation for t_T

$t_{T,m}$ = m^{th} approximation for t_T

$\hat{u}_m^n$ = m^{th} approximation for the unit vector $\dfrac{\bar{R}_{A_i}^n(t_R^n) - \bar{R}_{G/W_j}(t_{T,m})}{\left|\bar{R}_{A_i}^n(t_R^n) - \bar{R}_{G/W_j}(t_{T,m})\right|}$

$\dot{\bar{R}}_{G/W_j}(t_{T,m})$ = velocity of the transmitting GPS SV/WAAS GEO j at time $t_{T,m}$

t_R^n = signal reception time at the receiver n

Ignoring negligible terms, the above equation reduces to

$$t_{T,m+1} = t_R^n - \frac{\left|\bar{R}_{A_i}^n(t_R^n) - \bar{R}_{G/W_j}(t_{T,m})\right|}{c}$$

The iterative solution of the above equation is started by setting $t_{T,0} = t_R^n$, such that $\bar{R}_{G/W_j}(t_{T,0}) = \bar{R}_{G/W_j}(t_R^n)$. This iterative scheme is continued until the condition $\left|t_{T,m+1} - t_{T,m}\right| \le \varepsilon$ is satisfied, where ε is a small tolerance (nominally equal to 10^{-8} second).

This algorithm requires the knowledge of $\dot{\bar{R}}_{G/W_j}$, the velocity vector of GPS SV/WAAS GEO j (the computation of the velocity vectors was discussed in Section 5.1). Computations of measurements and associated partial derivatives will be performed using state vectors given in the mean of J2000.0 coordinate system.

The residual receiver time offset δt_R is computed as follows:

$$c\delta t_R^n = b_R{}^n(t) \tag{5.3-19}$$

where the computation of $b_R{}^n(t)$ or optionally $\tilde{b}_R{}^n(t)$ is discussed in Section 4.3.

The correction due to the ionospheric refraction in Equation (5.3-17), $\delta\rho_{Iono}$, can be modeled using the algorithm defined in Section 5.3.5 and the ionospheric delay scale factor γ_I can be estimated. Alternatively, measurements with large ionosphere delays can be edited based on the height of the signal path above the Earth. The measurement corrections due to GPS SV ephemeris

errors and time dithering (SA effects) in Equation (5.3-17), $\delta\rho_{et}$, are known to be sizable. Pseudorange biases, $\overline{b}_{\rho}^{G/W_j}$, can also be estimated to absorb the combined effects of the ionospheric and GPS SV/WAAS GEO ephemeris and clock errors. One pseudorange bias is estimated for each GPS SV/WAAS GEO tracked by the local receiver. The last term on the right-hand side of Equation (5.3-17) represents the GPS SV time correction, which is given in Section 3.3.2. Currently, a WAAS GEO time correction is not implemented.

Each receiver timetags its measurements using a receive time based on its own clock, $t_R^{(RC)_n}$. Therefore, when multiple spacecraft states are estimated, the measurement timetags for each spacecraft will generally not be at exactly the same times. The GEONS filter propagates and updates all spacecraft states at a common UTC epoch time, which is determined based on the estimation mode as discussed in Section 2.3. To account for the offset of the true UTC receive time for spacecraft n measurements, $t_R^{UTC_n}$, from the UTC filter state epoch, Equation (5.3-18) is linearized about the current filter state time, t_k:

$$\rho_{G/W_j}^{n,i}(t_R^{UTC_n}) = \rho_{G/W_j}^{n,i}(t_k) - \dot{\rho}_{G/W_j}^{n,i}(t_k)\Delta t_R^n \tag{5.3-19b}$$

where the offset of the true UTC receive time for spacecraft n measurements from the UTC filter state epoch is given by

$$\Delta t_R^n = \left[\left(t_k - t_R^{(RC)_n}\right) + \left(t_R^{(RC)_n} - t_R^{UTC_n}\right)\right] = \left(t_k - t_R^{(RC)_n}\right) + \delta t_R^n = \left(t_k - t_R^{(RC)_n}\right) + \frac{b_R^n(t_k)}{c} \tag{5.3-19c)*}$$

Note that in Release 2.7 and prior releases, Δt_R^n is implemented assuming that $t_k = t_R^{(RC)_n}$; this is corrected in Release 2.8. Under these conditions, Equations (5.3-17) and (5.3-18) can be rewritten as

$$\begin{aligned}\Re_{G/W_j}^n(t_R^{UTC_n}) = {} & \rho_{G/W_j}^{n,i}(t_k) - \dot{\rho}_{G/W_j}^{n,i}(t_k)\Delta t_R^n + b_R{}^n(t_k) - d_R{}^n(t_k)\Delta t_R^n + b_\rho^{G/W_j}(t_k) \\ & + \gamma_I(t_k)\delta\rho_{Iono}^{SF}(t_k) - c\left(\delta t_{S_j} + \delta t_{S_j}^{SF}\right)\end{aligned} \tag{5.3-20)*}$$

$$\rho_{G/W_j}^{n,i}(t_k) = \left|\overline{R}_{A_i}{}^n(t_k) - \overline{R}_{G/W_j}(t_k')\right| \tag{5.3-21)*}$$

$$\dot{\rho}_{G/W_j}^{n,i}(t_k) = \frac{\hat{\rho}_{G/W_j}^{n,i}(t_k)\cdot\left(\dot{\overline{R}}_{A_i}^n(t_k) - \dot{\overline{R}}_{G/W_j}(t_k')\right)}{1 - \hat{\rho}_{G/W_j}^{n,i}(t_k)\cdot\left(\dot{\overline{R}}_{G/W_j}(t_k')/c\right)} \tag{5.3-22)*}$$

In the above equations, the subscript j indicates the j^{th} GPS SV/WAAS GEO. The timetag of the k^{th} measurement, t_k, is equal to the value of the measured receive time, $t_R^{(RC)}$, and t'_k is the signal transmit time, t_T, computed based on t_k. The receiver clock bias $b_R{}^n(t)$ or optionally $\tilde{b}_R{}^n(t)$ is computed using the estimated parameters $b_R{}^n(t_k)$ and $\dot{b}_R{}^n(t_k)$, as defined in Equation 4.3-14a and 4.3-14 of Section 4.3. The term $-\dot{\rho}_{G/W_j}^{n,i}(t_k)\Delta t_R{}^n$ is significant when the receiver time bias or measurement timetag difference is large. The GPS-system pseudorange bias, b_ρ^{G/W_j}, is defined in

Section 4.3. For single frequency measurements, the ionospheric delay correction, $\delta\rho_{Iono}^{SF}$, can be modeled using the algorithm defined in Section 5.3.5, where $\gamma_I(t)$ is the ionospheric delay scale factor, which can be estimated. The last two terms on the right-hand side of Equation (5.3-20) represent the total SV time correction, which is computed using Equations 3.3-10 or 3.3-11 (for single and dual frequency GPS users) and Equation 3.3-12 (only for single frequency GPS users) in Section 3.3.2 evaluated at the signal transmit time t'_k. Currently, a WAAS GEO time correction is not implemented in GEONS. The position and velocity of the receiving antenna are computed using Equation 3.2-61 in Section 3.2.8.

(Equation deleted) (5.3-23)

The matrix (a row vector in this case) of partial derivatives of the pseudorange measurement with respect to the estimation state vector, $\overline{X}(t_k)$, is defined as follows:

$$\left[H(t_k)\right]_{\Re_{G/W\,j}^{n}} \equiv \frac{\partial \Re_{G/W_j}^{n}(t_R^{UTC})}{\partial \overline{X}(t_k)} \tag{5.3-24}$$

The partial derivatives with respect to those parameters that are not explicitly included in the pseudorange measurement equation will be zeros. The following are the only nonzero elements if the state vector consists of absolute states for both the local and remote satellites:

$$\frac{\partial \Re_{G/W_j}^{n}(t_R^{UTC})}{\partial \overline{R}^{n}(t_k)} = \frac{\partial \rho_{G/W_j}^{n,i}(t_k)}{\partial \overline{R}^{n}(t_k)} - \frac{\partial \dot{\rho}_{G/W_j}^{n,i}(t_k)}{\partial \dot{\overline{R}}^{n}(t_k)} \Delta t_R^n \tag{5.3-25}*$$

$$\frac{\partial \Re_{G/W_j}^{n}(t_R^{UTC})}{\partial \dot{\overline{R}}^{n}(t_k)} = -\frac{\partial \dot{\rho}_{G/W_j}^{n,i}(t_k)}{\partial \dot{\overline{R}}^{n}(t_k)} \Delta t_R^n \tag{5.3-26}*$$

$$\frac{\partial \Re_{G/W_j}^{n}(t_R^{UTC})}{\partial \gamma_I(t_k)} = \delta\rho_{Iono}^{SF}(t_k) \tag{5.3-27}*$$

$$\frac{\partial \Re_{G/W_j}^{n}(t_R^{UTC})}{\partial b_R{}^{n}(t_k)} = 1 - \frac{\dot{\rho}_{G/W_j}^{n,i}(t_k)}{c} - \frac{d_R{}^{n}(t_k)}{c} \tag{5.3-28}*$$

$$\frac{\partial \Re_{G/W_j}^{n}(t_R^{UTC})}{\partial d_R{}^{n}(t_k)} = -\Delta t_R^n \tag{5.3-28b}*$$

$$\frac{\partial \Re_{G/W_j}^{n}(t_R^{UTC})}{\partial b_\rho^{G/W_j}(t_k)} = 1 \tag{5.3-28a}*$$

where

$$\frac{\partial \rho^{n,i}_{G/W_j}(t_k)}{\partial \bar{R}^n(t_k)} = \left[\frac{\bar{R}_{A_i}{}^n(t_k) - \bar{R}_{G/W_j}(t_k')}{\rho^{n,i}_{G/W_j}(t_k)}\right]^T = \left(\hat{\rho}^{n,i}_{G/W_j}(t_k)\right)^T \qquad \text{(5.3-28b)*}$$

$$\frac{\partial \dot{\rho}^{n,i}_{G/W_j}(t_k)}{\partial \bar{R}^n(t_k)} \cong \frac{1}{\rho^{n,i}_{G/W_j}(t_k)\left[1 - \hat{\rho}^{n,i}_{G/W_j}(t_k)\cdot\left(\dot{\bar{R}}_{G/W_j}(t_k')/c\right)\right]} \times \left[\left(\dot{\bar{R}}^n(t_k) - \dot{\bar{R}}_{G/W_j}(t_k')\right) - \dot{\rho}^{n,i}_{G/W_j}(t_k)\left(\hat{\rho}^{n,i}_{G/W_j}(t_k) - \frac{\dot{\bar{R}}_{G/W_j}(t_k')}{c}\right)\right]^T \qquad \text{(5.3-28c)*}$$

$$\frac{\partial \dot{\rho}^{n,i}_{G/W_j}(t_k)}{\partial \dot{\bar{R}}^n(t_k)} = \frac{\left(\hat{\rho}^{n,i}_{G/W_j}(t_k)\right)^T}{1 - \hat{\rho}^{n,i}_{G/W_j}(t_k)\cdot\dot{\bar{R}}_{G/W_j}(t_k')/c} \qquad \text{(5.3-28d)*}$$

The superscript T on the right-hand sides of Equations (5.3-28b) through (5.3-28d) denote the transpose, indicating that these partial derivatives are given as row vectors. Equation (5.3-28c) is an approximation in which the dependence of t_k', the argument of $\bar{R}_{G/W}(t_k')$ and $\dot{\bar{R}}_{G/W}(t_k')$, on $\bar{R}(t_k)$ is ignored.

If the state vector includes relative states for the nonlocal satellites, the associated nonzero pseudorange measurement partial derivatives are as follows:

$$\frac{\partial \Re^n_{G/W\,j}(t_R^{UTC})}{\partial \bar{R}^1(t_k)} = \frac{\partial \Re^{\,n}_{G/W\,j}(t_R^{UTC})}{\partial \bar{R}^n(t_k)} \frac{\partial \bar{R}^{\,n}(t_k)}{\partial \bar{R}^1(t_k)} = \frac{\partial \rho^{\,n,i}_{G/W_j}(t_k)}{\partial \bar{R}^n(t_k)} - \frac{\partial \dot{\rho}^{n,i}_{G/W_j}(t_k)}{\partial \bar{R}^n(t_k)} \Delta t_R^n \qquad \text{(5.3-25a)}$$

$$\frac{\partial \Re^n_{G/W\,j}(t_R^{UTC})}{\partial \bar{R}^n_{rel}(t_k)} = \frac{\partial \Re^{\,n}_{G/W\,j}(t_R^{UTC})}{\partial \bar{R}^n(t_k)} \frac{\partial \bar{R}^{\,n}(t_k)}{\partial \bar{R}^n_{rel}(t_k)} = \frac{\partial \rho^{\,n,i}_{G/W_j}(t_k)}{\partial \bar{R}^n(t_k)} - \frac{\partial \dot{\rho}^{n,i}_{G/W_j}(t_k)}{\partial \bar{R}^n(t_k)} \Delta t_R^n;\ n \neq 1 \qquad \text{(5.3-25b)}$$

$$\frac{\partial \Re^n_{G/W_j}(t_R^{UTC})}{\partial \dot{\bar{R}}^1(t_k)} = \frac{\partial \Re^{\,n}_{G/W\,j}(t_R^{UTC})}{\partial \dot{\bar{R}}^n(t_k)} \frac{\partial \dot{\bar{R}}^{\,n}(t_k)}{\partial \dot{\bar{R}}^1(t_k)} = -\frac{\partial \dot{\rho}^{n,i}_{G/W_j}(t_k)}{\partial \dot{\bar{R}}^n(t_k)} \Delta t_R^n \qquad \text{(5.3-26a)*}$$

$$\frac{\partial \Re^n_{G/W_j}(t_R^{UTC})}{\partial \dot{\bar{R}}^n_{rel}(t_k)} = \frac{\partial \Re^{\,n}_{G/W\,j}(t_R^{UTC})}{\partial \dot{\bar{R}}^n(t_k)} \frac{\partial \dot{\bar{R}}^{\,n}(t_k)}{\partial \dot{\bar{R}}^n_{rel}(t_k)} = -\frac{\partial \dot{\rho}^{n,i}_{G/W_j}(t_k)}{\partial \dot{\bar{R}}^n(t_k)} \Delta t_R^n;\ n \neq 1 \qquad \text{(5.3-26b)*}$$

$$\frac{\partial \Re^n_{G/W_j}(t_R^{UTC})}{\partial b_\rho^{G/W_j}(t_k)} = 1 \qquad \text{(5.3-28e)*}$$

$$\frac{\partial \Re^n_{G/W\,j}(t_R^{UTC})}{\partial b_R^1(t_k)} = \frac{\partial \Re^{\,n}_{G/W\,j}(t_R^{UTC})}{\partial b_R^n(t_k)} \frac{\partial b^{\,n}_R(t_k)}{\partial b_R^1(t_k)} = 1 - \frac{\dot{\rho}^{n,i}_{G/W_j}(t_k)}{c} - \frac{d_R}{c} \qquad \text{(5.3-28f)*}$$

$$\frac{\partial \Re^n_{G/W\,j}(t_R^{UTC})}{\partial b^n_{rel}(t_k)} = \frac{\partial \Re^{\,n}_{G/W\,j}(t_R^{UTC})}{\partial b^n_R(t_k)} \frac{\partial b^n_R(t_k)}{\partial b^n_{rel}(t_k)} = 1 - \frac{\dot{\rho}^{n,i}_{G/W_j}(t_k)}{c} - \frac{d_R}{c};\ n \neq 1 \qquad \text{(5.3-28g)*}$$

$$\frac{\partial \Re^n_{G/W_j}(t_R^{UTC})}{\partial \gamma_I(t_k)} = \delta\rho^{SF}_{Iono}(t_k) \qquad \text{(5.3-28h)*}$$

$$\frac{\partial \Re^n_{G/W_j}(t_R^{UTC})}{\partial d_R{}^1(t_k)} = -\Delta t^1_R \qquad \text{(5.3-28i)*}$$

$$\frac{\partial \Re^n_{G/W_j}(t_R^{UTC})}{\partial d_{rel}{}^n(t_k)} = -\Delta t^n_R;\quad n \neq 1 \qquad \text{(5.3-28j)*}$$

5.3.3 GPS/WAAS Doppler Instantaneous Measurement Model and Associated Partial Derivatives

An instantaneous Doppler shift data extracted at the receiver can be defined as

$$F_D(t) = F_R(t) - F_{REF} \qquad \text{(5.3-29)}$$

where $F_R(t)$ is Doppler-shifted receive carrier frequency and F_{REF} is the receiver-generated local reference frequency. When the receiver and the transmitter use the same frequency standards, the receiver-generated reference frequency, F_{REF}, will be equal to the transmit frequency, F_T. For GPS tracking, this is not the case. There will be small difference between the two frequency standards used by the receiver and the transmitter. The frequency difference due to this difference will be interpreted as the receiver reference frequency bias. Even when the two frequency standards are the same, the frequency difference obtained from Equation (5.3-29) does not represent a pure Doppler effect. It will include contributions from non-Doppler sources such as the atmospheric refraction effects, which are not modeled in GEONS.

A procedure to compute the Doppler shift is discussed below. The first term on the right-hand side of Equation (5.3-28), F_R, the instantaneous Doppler shifted carrier frequency observed at the receiver, can be represented by the following equation:

$$F_R = F'_T\left(1 - \frac{\dot{\rho}}{c}\right) + \delta F_{iono} + \delta F_{et} \qquad \text{(5.3-30)}$$

where

F'_T = actual GPS SV/WAAS GEO transmit carrier frequency

$\dot{\rho}$ = time rate of change of the light-time-corrected range from the SV to the receiving antenna ρ [defined in Equation (5.3-22)]

δF_{iono} = frequency perturbation due to the ionospheric refraction effect

δF_{et} = frequency uncertainty due to limited accuracy in F_T and $\dot{\rho}$ due to SA effects

Doppler biases, $\bar{b}_d^{G/W_j}$, can be estimated to absorb the combined effects of the ionospheric and GPS SV/WAAS GEO ephemeris and clock errors. One Doppler bias is estimated for each GPS SV/WAAS GEO tracked by the local receiver.

The second term on the right-hand side of Equation (5.3-29), F_{REF}, the receiver-generated reference frequency, can be written as

$$F_{REF} = F_T + \delta F_{REF} \tag{5.3-31}$$

In Equation (5.3-31), F_T denotes the nominal transmit frequency, which may be different from the actual transmit frequency, F_T', used in Equation (5.3-30). Using Equations (5.3-30) and (5.3-31), Equation (5.3-29) can be written as

$$F_D = F_T^{'}\left(1 - \frac{\dot{\rho}}{c}\right) + b_d^{G/W_j} - (F_T + \delta F_{REF}) \tag{5.3-32}$$

Neglecting the second- and higher-order terms,

$$F_D = -F_T^{'}\frac{\dot{\rho}}{c} + b_d^{G/W_j} + \delta F_T + \delta F_{rel}^{'} - \delta F_{REF} \tag{5.3-33}$$

where δF_T denotes the difference between F_T' and F_T and can be approximated for GPS SVs using the SV clock correction parameters discussed in Section 3.3.2,

$$\delta F_T = F_T\left(\frac{\partial \delta t_{Sj}}{\partial t_{SV}}\right) \cong \delta \dot{t}_{S_j} F_T \tag{5.3-34}$$

The term $\delta F_{rel}'$ on the right-hand side of Equation (5.3-33) represents the relativistic correction to the Doppler measurement. This term can be computed using the following approximate expression:

$$\frac{\delta F_{rel}}{F_T} = \frac{1}{2c^2}\left(\left|\dot{\overline{R}}\right|^2 - \left|\dot{\overline{R}}_{G/W_j}\right|^2\right) + \frac{\mu}{c^2}\left(\frac{1}{\left|\overline{R}\right|} - \frac{1}{\left|\overline{R}_{G/W_j}\right|}\right) \tag{5.3-35}$$

The first term on the right-hand side of this equation is due to the special relativistic effect, and the second term is due to the general relativistic effect.

However, in the case of a GPS SV/WAAS GEO, the transmit frequency is already adjusted to reduce this effect. With such an adjustment in the transmit frequency, almost 100 percent of the relativistic effect is compensated for the receiver located on the ground. However, for Earth-orbiting satellites, the compensation is not as complete. The fractional frequency correction computed using Equation (5.3-35) for a low-Earth satellite is approximately 0.714×10^{-9}. This is equivalent to 1.125 hertz in terms of the L1 carrier frequency (L1 carrier frequency) = 1.57542×10^{9} hertz). According to the GPS frequency plan (Reference 10, Paragraph 3.3.1.1), the amount of the fractional frequency correction (used for all SV transmit frequencies to compensate the relativistic frequency shift for the ground receiver) is 0.44647×10^{-9}. When this correction is applied to a low-Earth satellite, there is a residual relativistic effect amounting to a fractional frequency shift of

approximately 0.269×10^{-9} ($\approx$ 0.42 hertz). The term $\delta F'_{rel}$ on the right-hand side of Equation (5.3-33) represents this residual relativistic effect. The amount of the fractional frequency shift due to the relativistic effect does not change much as long as the GPS SV/WAAS GEO and the user receiver each maintains a relatively constant geocentric radius. The residual relativistic effect for GEONS orbit determination is computed using the following equation:

$$\frac{\delta F'_{rel}}{F_T} = \frac{1}{2c^2}\left(\left|\dot{\overline{R}}\right|^2 - \left|\dot{\overline{R}}_{G/W_j}\right|^2\right) + \frac{\mu}{c^2}\left(\frac{1}{\left|\overline{R}\right|} - \frac{1}{\left|\overline{R}_{G/W_j}\right|}\right) - (\delta F_{rel})_{cor} \tag{5.3-36}$$

where

$(\delta F_{rel})_{cor}$ = fractional frequency correction applied to the GPS SV transmit frequency (0.44647×10^{-9}) or the WAAS GEO transmit frequency (TBD)

The last term on the right-hand side of Equation (5.3-33) represents the receiver frequency bias, which can be expressed in terms of the receiver time bias rate parameter introduced earlier in discussing the pseudorange modeling as follows:

$$\delta F_{REF} \cong \left(\frac{d_R(t)}{c}\right) F_T \tag{5.3-37}$$

Thus, using Equations (5.3-34), (5.3-35), and (5.3-37), Equation (5.3-33) can be rewritten as follows (note that ionospheric refraction and SA effects are not included):

$$\begin{aligned}\left(F_D(t_k)\right)^n_{G/W_j} = F_T\Bigg[&-\frac{\dot{\rho}^{n,i}_{G/W_j}(t_k)}{c} + \delta\dot{t}_{S_j} - \frac{d_R{}^n(t_k)}{c} + \frac{1}{2c^2}\left(\left|\dot{\overline{R}}^n\right|^2 - \left|\dot{\overline{R}}_{G/W_j}\right|^2\right) \\ &+ \frac{\mu}{c^2}\left(\frac{1}{\left|\overline{R}^n\right|} - \frac{1}{\left|\overline{R}_{G/W_j}\right|}\right) - (\delta F_{rel})_{cor}\Bigg] + b_d^{G/W_j}(t_k)\end{aligned} \tag{5.3-38}*$$

In this equation, the subscript j indicates the GPS SV/WAAS GEO number; and the transmit frequency, F_T, is assumed to be known (nominally 1575.42 Mhertz for the L1 carrier, 1227.6 Mhertz for the L2 carrier, and 1176.45 Mhertz for the L5 carrier).

In most GPS receivers, Doppler measurements are obtained by averaging the instantaneous Doppler shift over a short interval of 500 milliseconds centered about the measurement output. Considering the short averaging interval, it is appropriate to use a formulation based on the instantaneous Doppler shift for GEONS. The instantaneous Doppler shift is given by Equation (5.3-38). The instantaneous range-rate ($\dot{\rho}$) that appears on the right-hand side of this equation can be expressed in terms of the position and velocity vectors of the transmitter and the receiver. The expression for the instantaneous range rate ($\dot{\rho}$) is defined by

$$\dot{\rho}(t_k) \equiv \lim_{\Delta t\to 0}\left[\frac{\rho_j(t_k) - \rho_j(t_k - \Delta t)}{\Delta t}\right] \tag{5.3-39}$$

where $\rho(t_k)$ was defined earlier by Equation (5.3-21), which can be equivalently rewritten as

$$\rho_{G/W_j}^{n,i}{}^2(t_k) = \left(\overline{R}_{A_i}^n(t_k) - \overline{R}_{G/W_j}(t_k')\right)\cdot\left(\overline{R}_{A_i}^n(t_k) - \overline{R}_{G/W_j}(t_k')\right) \tag{5.3-40}$$

Note that, in Equation (5.3-40), the transmit time (t_k') is a function of $\rho_{G/W_j}^{n,i}(t_k)$:

$$t_k' = t_k - \frac{\rho_{G/W_j}^{n,i}(t_k)}{c} \tag{5.3-41}$$

Differentiating both sides of Equation (5.3-40) with respect to t_k yields

$$\begin{aligned}\rho_{G/W_j}^{n,i}(t_k)\dot{\rho}_{G/W_j}^{n,i}(t_k) &= \left(\overline{R}_{A_i}^n(t_k) - \overline{R}_{G/W_j}(t_k')\right)\cdot\left[\dot{\overline{R}}_{A_i}^n(t_k) - \dot{\overline{R}}_{G/W_j}(t_k')\left(\frac{dt_k'}{dt_k}\right)\right] \\ &= \left(\overline{R}_{A_i}^n(t_k) - \overline{R}_{G/W_j}(t_k')\right)\cdot\left[\dot{\overline{R}}_{A_i}^n(t_k) - \dot{\overline{R}}_{G/W_j}(t_k')\left(1 - \frac{\dot{\rho}_{G/W_j}^{n,i}(t_k)}{c}\right)\right]\end{aligned} \tag{5.3-42}$$

Using the line-of-sight unit vector, $\hat{\rho}_{G/W_j}^{n,i}(t_k)$, defined by

$$\hat{\rho}_{G/W_j}^{n,i}(t_k) \equiv \frac{\overline{R}_{A_i}^n(t_k) - \overline{R}_{G/W_j}(t_k')}{\rho_{G/W_j}^{n,i}(t_k)} \tag{5.3-43}*$$

Equation (5.3-43) can be rewritten as

$$\dot{\rho}_{G/W_j}^{n,i}(t_k) = \hat{\rho}_{G/W_j}^{n,i}(t_k)\cdot\left[\dot{\overline{R}}_{A_i}^n(t_k) - \dot{\overline{R}}_{G/W_j}(t_k')\left(1 - \frac{\dot{\rho}_{G/W_j}^{n,i}(t_k)}{c}\right)\right] \tag{5.3-44}$$

Solving for $\dot{\rho}_{G/W_j}^{n,i}(t_k)$ from the above equation,

$$\dot{\rho}_{G/W_j}^{n,i}(t_k) = \frac{\hat{\rho}_{G/W_j}^{n,i}(t_k)\cdot\left(\dot{\overline{R}}_{A_i}^n(t_k) - \dot{\overline{R}}_{G/W_j}(t_k')\right)}{1 - \hat{\rho}_{G/W_j}^{n,i}(t_k)\cdot\left(\dot{\overline{R}}_{G/W_j}(t_k')/c\right)} \tag{5.3-45}*$$

The desired instantaneous Doppler shift is obtained using Equations (5.3-38) and (5.3-45), where the position and velocity of the receiving antenna are computed using Equation (3.2-61).

From Equation (5.3-38), the following nonzero partial derivatives of the Doppler shift are obtained if the state vector consists of absolute states for both the local and remote satellites:

$$\frac{\partial\left(F_D(t_k)\right)_{G/W_j}^n}{\partial\overline{R}^n(t_k)} = -\frac{F_T}{c}\left(\frac{\partial\dot{\rho}_{G/W_j}^{n,i}(t_k)}{\partial\overline{R}^n(t_k)}\right);\ \frac{\partial\left(F_D(t_k)\right)_{G/W_j}^n}{\partial\dot{\overline{R}}^n(t_k)} = -\frac{F_T}{c}\left(\frac{\partial\dot{\rho}_{G/W_j}^{n,i}(t_k)}{\partial\dot{\overline{R}}^n(t_k)}\right) \tag{5.3-46}*$$

$$\frac{\partial\left(F_D(t_k)\right)^n_{G/W_j}}{\partial d_R{}^n(t_k)} = -\frac{F_T}{c} \tag{5.3-47)*}$$

$$\frac{\partial\left(F_D(t_k)\right)^n_{G/W_j}}{\partial b_d^{G/W_j}(t_k)} = 1 \tag{5.3-47a)*}$$

The state partial derivatives of $\dot{\rho}_j(t_k)$ on the right-hand side of Equation (5.3-46) can be obtained using the following equations:

$$\begin{aligned}\frac{\partial\dot{\rho}^{n,i}_{G/W_j}(t_k)}{\partial\overline{R}^n(t_k)} \cong & \frac{1}{\rho^{n,i}_{G/W_j}(t_k)\left[1-\hat{\rho}^{n,i}_{G/W_j}(t_k)\cdot\left(\dot{\overline{R}}_{G/W_j}(t_k')/c\right)\right]} \\ & \times\left[\left(\dot{\overline{R}}^n(t_k)-\dot{\overline{R}}_{G/W_j}(t_k')\right)-\dot{\rho}^{n,i}_{G/W_j}(t_k)\left(\hat{\rho}^{n,i}_{G/W_j}(t_k)-\frac{\dot{\overline{R}}_{G/W_j}(t_k')}{c}\right)\right]^T\end{aligned} \tag{5.3-48)*}$$

$$\frac{\partial\dot{\rho}^{n,i}_{G/W_j}(t_k)}{\partial\dot{\overline{R}}^n(t_k)} = \frac{\left(\hat{\rho}^{n,i}_{G/W_j}(t_k)\right)^T}{1-\hat{\rho}^{n,i}_{G/W_j}(t_k)\cdot\left(\dot{\overline{R}}_{G/W_j}(t_k')/c\right)} \tag{5.3-49)*}$$

The superscript T on the right-hand sides of Equations (5.3-48) and (5.3-49) denote the transpose, indicating that these partial derivatives are given as row vectors. Also note that Equation (5.3-48) is an approximation in which the dependence of t_k', the argument of $\overline{R}_{G/W_j}(t_k')$ and $\dot{\overline{R}}_{G/W_j}(t_k')$, on $\overline{R}^n(t_k)$ is ignored.

If the state vector includes relative states for the nonlocal satellites, the associated nonzero Doppler measurement partial derivatives are as follows:

$$\begin{aligned}\frac{\partial\left(F_D(t_k)\right)^n_{G/W_j}}{\partial\overline{R}^1(t_k)} &= -\frac{F_T}{c}\left(\frac{\partial\dot{\rho}^{n,i}_{G/W_j}(t_k)}{\partial\overline{R}^n(t_k)}\right) \\ \frac{\partial\left(F_D(t_k)\right)^n_{G/W_j}}{\partial\dot{\overline{R}}^1(t_k)} &= -\frac{F_T}{c}\left(\frac{\partial\dot{\rho}^{n,i}_{G/W_j}(t_k)}{\partial\dot{\overline{R}}^n(t_k)}\right)\end{aligned} \tag{5.3-46a)}$$

$$\begin{aligned}\frac{\partial\left(F_D(t_k)\right)^n_{G/W_j}}{\partial\overline{R}^n_{rel}(t_k)} &= -\frac{F_T}{c}\left(\frac{\partial\dot{\rho}^{n,i}_{G/W_j}(t_k)}{\partial\overline{R}^n(t_k)}\right);\ n\neq 1 \\ \frac{\partial\left(F_D(t_k)\right)^n_{G/W_j}}{\partial\dot{\overline{R}}^n_{rel}(t_k)} &= -\frac{F_T}{c}\left(\frac{\partial\dot{\rho}^{n,i}_{G/W_j}(t_k)}{\partial\dot{\overline{R}}^n(t_k)}\right);\ n\neq 1\end{aligned} \tag{5.3-46b)}$$

$$\frac{\partial\left(F_D(t_k)\right)^n_{G/W_j}}{\partial d_R{}^1(t_k)} = -\frac{F_T}{c} \qquad \text{(5.3-47b)*}$$

$$\frac{\partial\left(F_D(t_k)\right)^n_{G/W_j}}{\partial d_{R_{rel}}{}^n(t_k)} = -\frac{F_T}{c};\ n \neq 1 \qquad \text{(5.3-47c)*}$$

$$\frac{\partial\left(F_D(t_k)\right)^n_{G/W_j}}{\partial b_d^{G/W_j}(t_k)} = 1 \qquad \text{(5.3-47d)*}$$

5.3.4 GPS/WAAS Integrated Carrier Phase Measurement Model and Associated Partial Derivatives

This section provides an expression that is used to compute the integrated carrier beat phase measurement in terms of the GPS/WAAS and receiver states and the corresponding times. The carrier beat phase measurement is formed in a GPS receiver as the difference between the phase of the local receiver oscillator and the phase of the received carrier signal. The measurement is ambiguous with respect to the number of integer cycles ($N_{\phi_n}^{G/W_j}(t_{acq})$) at the time (t_{acq}) when the signal is first acquired from each GPS SV. At any epoch other than the initial acquisition epoch, the receiver measures the fractional phase difference and the number of integer cycles accumulated since that epoch. Prior to processing in GEONS, the resulting raw integrated carrier beat phase observation (in cycles), $(\phi_{obs})^n_{G/W_j}(t_R^{UTC_n})$, is multiplied by the wavelength of the carrier ($\lambda_C = c/F_T$, where F_T = 1575.42 Mhertz for L1, 1227.6 Mhertz for L2 carrier frequency, and 1176.45 Mhertz for L5) to scale the carrier phase observation to meters:

$$(\Phi_{obs})^n_{G/W_j}(t_R^{UTC_n}) = \lambda_C(\phi_{obs})^n_{G/W_j}(t_R^{UTC_n}) \qquad \text{(5.3-50)}$$

The integrated carrier beat phase measurement (in meters), Φ^n_{G/W_j}, can be modeled as follows:

$$\Phi^n_{G/W_j}(t_R^{UTC_n}) = \rho^{n,i}_{G/W_j}(t_k) - \dot{\rho}^{n,i}_{G/W_j}(t_k)\Delta t_R^n + b_R{}^n(t_k) - \gamma_I(t_k)\delta\rho^{SF}_{Iono}(t_k) + b_{\phi_n}^{G/W_j}(t_k) - c\left(\delta t_{Sj} + \delta t_{S_j}^{SF}\right) \qquad \text{(5.3-51)*}$$

where the offset of the true UTC receive time for spacecraft n measurements from the UTC filter state epoch is given by

$$\Delta t_R^n = \left[\left(t_k - t_R^{(RC)_n}\right) + \left(t_R^{(RC)_n} - t_R^{UTC_n}\right)\right] = \left(t_k - t_R^{(RC)_n}\right) + \delta t_R^n = \left(t_k - t_R^{(RC)_n}\right) + \frac{b_R^n(t_k)}{c} \qquad \text{(5.3-51a)*}$$

Note that in Release 2.7 and prior releases, Δt_R^n is implemented assuming that $t_k = t_R^{(RC)_n}$; this is corrected in Release 2.8.

In the above equations, the superscript *n* indicates the n^{th} receiver, the superscript *i* indicates the i^{th} antenna, and subscript *j* indicates the j^{th} GPS SV/WAAS GEO. The time tag t_k is the measured receive time of the k^{th} measurement, and t'_k is the signal transmission time. The geometrical range

($\rho^{n,i}_{G/W_j}$) and range rate ($\dot{\rho}^{n,i}_{G/W_j}$) are computed as described in Sections 5.3.2 and 5.3.3, respectively. The receiver clock bias, $b_R{}^n(t)$, is in meters. The correction due to the ionospheric refraction, $\delta\rho^{SF}_{Iono}(t_k)$, can be modeled using the algorithm defined in Section 5.3.5 and the ionospheric scale factor, $\gamma_I(t_k)$, can be estimated. The terms δt_{Sj} and $\delta t^{SF}_{S_j}$ are the SV time offset from GPS system time and group delay correction for single-frequency users, defined in Equations (3.3-10) and (3.3-12), respectively. The term $b^{G/W_j}_{\phi_n}(t_k) = \lambda_C N^{G/W_j}_{\phi_n}(t_{acq})$ is the estimated carrier phase bias between GPS SV/WAAS GEO *j* and receiver *n* at the carrier phase acquisition time (t_{acq}), scaled to meters.

The carrier phase bias $b^{G/W_j}_{\phi_n}(t_k)$ is different for each acquisition of a GPS SV/WAAS GEO by a receiver. The carrier phase bias is reinitialized at the start of each new acquisition based on the difference between the predicted pseudorange $\Re^n_{G/W_j}(t_{acq})$ (defined in Equation 5.3-20) and the observed integrated carrier phase at the acquisition time t_{acq}:

$$b^{G/W_j}_{\phi_n}(t_k = t_{acq}) = (\Phi_{obs})^n_{G/W_j}(t_{acq}) - \Phi^n_{G/W_j}(t_{acq}) \qquad (5.3\text{-}52)^*$$

Similarly, the carrier phase bias variance is reinitialized at the start of each new acquisition to the predicted carrier phase residual variance computed as described in Step 3 in Section 2.3.1.

The matrix (a row vector in this case) of partial derivatives of the integrated carrier beat phase measurement with respect to $\overline{X}(t_k)$ is defined as follows:

$$\left[H(t_k)\right]_{\Phi^n_{G/W_j}(t_k)} \equiv \frac{\partial \Phi^n_{G/W_j}(t_k)}{\partial \overline{X}(t_k)} \qquad (5.3\text{-}53)$$

The partial derivatives with respect to those parameters that are not explicitly included in the measurement equation will be zeros. The following are the only nonzero elements if the state vector consists of absolute states for both the local and remote satellites:

$$\frac{\partial \Phi^n_{G/W_j}(t_k)}{\partial \overline{R}^n(t_k)} = \frac{\partial \rho^{n,i}_{G/W_j}(t_k)}{\partial \overline{R}^n(t_k)} - \frac{b^n_R(t_k)}{c}\frac{\partial \dot{\rho}^{n,i}_{G/W_j}(t_k)}{\partial \overline{R}^n(t_k)} \qquad (5.3\text{-}54)^*$$

$$\frac{\partial \Phi^n_{G/W_j}(t_k)}{\partial \dot{\overline{R}}^n(t_k)} = -\frac{b^n_R(t_k)}{c}\frac{\partial \dot{\rho}^{n,i}_{G/W_j}(t_k)}{\partial \dot{\overline{R}}^n(t_k)} \qquad (5.3\text{-}55)^*$$

$$\frac{\partial \Phi^n_{G/W_j}(t_k)}{\partial b_R{}^n(t_k)} = 1 - \frac{\dot{\rho}^{n,i}_{G/W_j}(t_k)}{c} \qquad (5.3\text{-}56)^*$$

$$\frac{\partial \Phi^n_{G/W_j}(t_k)}{\partial b^{G/W_j}_{\phi_n}(t_k)} = 1 \qquad (5.3\text{-}57)^*$$

$$\frac{\partial \Phi^{n}_{G/W_j}(t_k)}{\partial \gamma_I(t_k)} = -\delta\rho^{SF}_{Iono}(t_k) \qquad \text{(5.3-57a)*}$$

where the partial derivatives of the geometrical range ($\rho^{n,i}_{G/W_j}$) and range rate ($\dot{\rho}^{n,i}_{G/W_j}$) are computed as defined in Equations 5.3-28b through 5.3-28d in Section 5.3.2.

If the state vector includes relative states for the nonlocal satellites, the associated nonzero pseudorange measurement partial derivatives are as follows:

$$\frac{\partial \Phi^{n}_{G/W\,j}(t_k)}{\partial \overline{R}^{1}(t_k)} = \frac{\partial \Phi^{\,n}_{G/W\,j}(t_k)}{\partial \overline{R}^{\,n}(t_k)} \frac{\partial \overline{R}^{\,n}(t_k)}{\partial \overline{R}^{1}(t_k)} = \frac{\partial \rho^{\,n,i}_{G/W_j}(t_k)}{\partial \overline{R}^{\,n}(t_k)} - \frac{b^{n}_{R}(t_k)}{c} \frac{\partial \dot{\rho}^{n,i}_{G/W_j}(t_k)}{\partial \overline{R}^{\,n}(t_k)} \qquad \text{(5.3-58)}$$

$$\frac{\partial \Phi^{n}_{G/W\,j}(t_k)}{\partial \overline{R}^{\,n}_{rel}(t_k)} = \frac{\partial \Phi^{\,n}_{G/W\,j}(t_k)}{\partial \overline{R}^{\,n}(t_k)} \frac{\partial \overline{R}^{\,n}(t_k)}{\partial \overline{R}^{\,n}_{rel}(t_k)} = \frac{\partial \rho^{\,n,i}_{G/W_j}(t_k)}{\partial \overline{R}^{\,n}(t_k)} - \frac{b^{n}_{R}(t_k)}{c} \frac{\partial \dot{\rho}^{n,i}_{G/W_j}(t_k)}{\partial \overline{R}^{\,n}(t_k)};\ n \neq 1 \qquad \text{(5.3-59)}$$

$$\frac{\partial \Phi^{n}_{G/W_j}(t_k)}{\partial \dot{\overline{R}}^{1}(t_k)} = \frac{\partial \Phi^{\,n}_{G/W\,j}(t_k)}{\partial \dot{\overline{R}}^{\,n}(t_k)} \frac{\partial \dot{\overline{R}}^{\,n}(t_k)}{\partial \dot{\overline{R}}^{1}(t_k)} = -\frac{b^{n}_{R}(t_k)}{c} \frac{\partial \dot{\rho}^{n,i}_{G/W_j}(t_k)}{\partial \dot{\overline{R}}^{\,n}(t_k)} \qquad \text{(5.3-60)*}$$

$$\frac{\partial \Phi^{n}_{G/W_j}(t_k)}{\partial \dot{\overline{R}}^{\,n}_{rel}(t_k)} = \frac{\partial \Phi^{n}_{G/W\,j}(t_k)}{\partial \dot{\overline{R}}^{\,n}(t_k)} \frac{\partial \dot{\overline{R}}^{\,n}(t_k)}{\partial \dot{\overline{R}}^{\,n}_{rel}(t_k)} = -\frac{b^{n}_{R}(t_k)}{c} \frac{\partial \dot{\rho}^{n,i}_{G/W_j}(t_k)}{\partial \dot{\overline{R}}^{\,n}(t_k)};\ n \neq 1 \qquad \text{(5.3-61)*}$$

$$\frac{\partial \Phi^{n}_{G/W_j}(t_k)}{\partial b^{G/W_j}_{\phi_n}(t_k)} = 1 \qquad \text{(5.3-62)*}$$

$$\frac{\partial \Phi^{n}_{G/W\,j}(t_k)}{\partial b^{1}_{R}(t_k)} = \frac{\partial \Phi^{\,n}_{G/W\,j}(t_k)}{\partial b^{n}_{R}(t_k)} \frac{\partial b^{\,n}_{R}(t_k)}{\partial b^{1}_{R}(t_k)} = 1 - \frac{\dot{\rho}^{n,i}_{G/W_j}(t_k)}{c} \qquad \text{(5.3-63)}$$

$$\frac{\partial \Phi^{n}_{G/W\,j}(t_k)}{\partial b^{n}_{rel}(t_k)} = \frac{\partial \Phi^{\,n}_{G/W\,j}(t_k)}{\partial b^{n}_{R}(t_k)} \frac{\partial b^{n}_{R}(t_k)}{\partial b^{n}_{rel}(t_k)} = 1 - \frac{\dot{\rho}^{n,i}_{G/W_j}(t_k)}{c};\ n \neq 1 \qquad \text{(5.3-64)}$$

$$\frac{\partial \Phi^{n}_{G/W_j}(t_k)}{\partial \gamma_I(t_k)} = -\delta\rho^{SF}_{Iono}(t_k) \qquad \text{(5.3-64a)*}$$

5.3.5 Ionospheric Refraction Delay Using GPS Ionospheric Parameters

This section provides a general model for computing ionospheric pseudorange and carrier phase delays between transmitting and receiving satellites that is appropriate for single frequency GPS receivers. Uncorrected ionospheric delays can be a significant source of error in the absolute position and clock estimates for orbits with a long path through the ionosphere.

This model has the following characteristics:

- Suitable for a wide range of GPS-user geometries including
  - High and low elevation from below the GPS constellation
  - Across the Earth's limb from above the GPS constellation
- Models the overall physical characteristics of the delay, i.e. account for variations in the ionosphere with latitude, longitude, height, and time of day
- Models the value of the delay to within about 50% and include a parameter that can be estimated in real-time to correct the modeled delay
- Suitable for implementation as part of an autonomous navigation system integrated with the flight receiver

This model makes use of the ionospheric parameters provided in page 18 of Subframe 4 of the GPS broadcast navigation message (Reference 35). These parameters model the ionospheric time delay from ground receivers to a GPS space vehicle (SV), based on a model developed by Klobuchar (Reference 36) and validated by Feess and Stephens (Reference 37).

Figure 5-3 illustrates one possible signal path from a GPS SV to a receiver on a user spacecraft. In this example, the user spacecraft (S/C) is located at point S within the ionosphere, points A and B are at the upper limits of the ionosphere in the direction of the signal path, and the signal path segment within the ionosphere is from point S to point B. The ionospheric delay model numerically integrates the delay along the signal path segment within the ionosphere

$$\delta\rho_{Iono}^{SF}(t_k) = \frac{40.3}{f_T^2}\int_{P_0}^{P_N} N_e(\lambda_{P_i}, \phi_{P_i}, h_{P_i}, t_{P_i}^L)ds \quad \text{(meters)} \tag{5.3-65}$$

where f_T is the GPS transmission frequency (1.57542 GHz for the L1 frequency, 1.2276 GHz for L2 frequency, and 1.17645 for L5 frequency), P_0 and P_N are the end points of the signal path segment within the ionosphere, $N_e(\lambda_{P_i}, \phi_{P_i}, h_{P_i}, t_{P_i}^L)$ is the local electron density at a point P_i on the signal path, which is expressed in electrons per cubic meter, and λ_{P_i} and φ_{P_i} are the geodetic longitude and latitude of the subpoint, h_{P_i} is the height of the point above the Earth, and $t_{P_i}^L$ is the local time at the subpoint.

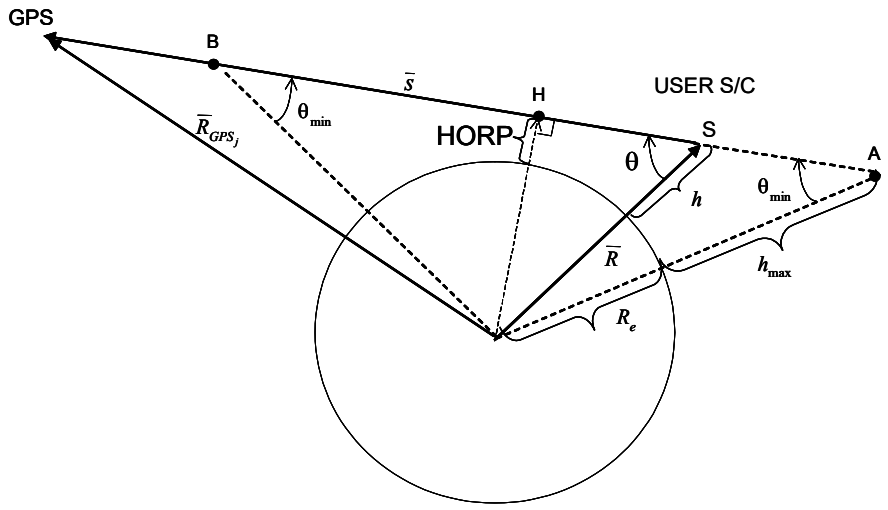

Figure 5-3 Signal Path Geometry

At any point P_i along the signal path segment, $N_e(\lambda_{P_i},\phi_{P_i},h_{P_i},t_{P_i}^L)$ is computed using a modified Chapman profile that relates the local electron density values along the path to $TEC_K(\lambda_{P_i},\phi_{P_i},0,t_{P_i}^L)$, the total vertical electron content computed using the GPS broadcast ionospheric correction parameters.

The Chapman electron density altitude profile relates $N_e(\lambda_{P_i},\phi_{P_i},h_{P_i},t_{P_i}^L)$, the local electron density at a point with altitude h_{P_i}, to $N_m\left(\lambda_{P_i},\phi_{P_i},h_m,t_{P_i}^L\right)$, the maximum electron density at height h_{m},

$$N_e(\lambda_{P_i},\phi_{P_i},h_{P_i},t_{P_i}^L) = N_m\left(\lambda_{P_i},\phi_{P_i},h_m,t_{P_i}^L\right)e^{\left(1-z-e^{-z}\right)} \tag{5.3-66}$$

where

$$z = \frac{h_{P_i} - h_m}{h_s}$$

Typically, h_{m}, the maximum density height, is selected to be 350 kilometers and h_{s}, the ionospheric scale height ≈ 100 to 200 kilometers, which is a commandable parameter.

The value of the maximum density in the Chapman profile $N_m(\lambda_{P_i},\phi_{P_i},h_m,t_{P_i}^L)$ for a point along the ray path segment, is computed by equating $TEC_C(\lambda_i,\phi_i,t_{P_i}^L)$, the total vertical electron content computed based on the Chapman profile, to $TEC_K(\lambda_{P_i},\phi_{P_i},t_{P_i}^L)$, the total vertical electron content computed using the GPS broadcast ionospheric correction parameters.
The total vertical electron content based on a Chapman profile is given by:

$$
\begin{aligned}
TEC_C(\lambda_{P_i},\phi_{P_i},t_{P_i}^L) &= \int_0^\infty N_e(\lambda_{P_i},\phi_{P_i},h,t_{P_i}^L)dh \\
&= N_m(\lambda_{P_i},\phi_{P_i},h_m,t_{P_i}^L)\int_0^\infty \exp(1-z-\exp(-z)dh \\
&= N_m(\lambda_{P_i},\phi_{P_i},h_m,t_{P_i}^L)h_s[\exp(1-\exp(-z))]_{h=0}^{h=\infty} \\
&= N_m(\lambda_{P_i},\varphi_{P_i},h_m,t_{P_i}^L)h_s[e-\exp(1-\exp(h_m/h_s))] \\
&\cong N_m(\lambda_{P_i},\phi_{P_i},h_m,t_{P_i}^L)h_s e \qquad \text{where} \quad e = 2.7182818
\end{aligned}
\tag{5.3-67}
$$

Equating TEC_C to TEC_K gives

$$
N_m\left(\lambda_{P_i},\phi_{P_i},\mathrm{h_m},t_{P_i}^L\right) = \frac{TEC_K(\lambda_{P_i},\phi_{P_i},t_{P_i}^L)}{h_s e} \tag{5.3-68}
$$

The value of $TEC_K(\lambda_{P_i},\phi_{P_i},t_{P_i}^L)$ is computed using Equation (5.3-72), which is provided in Section 5.3.5.1.

The total ionospheric delay (in meters) is computed over the signal path following Equation (5.3-65):

$$
\delta\rho_{Iono}^{SF}(t_k) = \frac{40.3}{f_T^2}\int_A^B \frac{TEC_K(\lambda_{P_i},\phi_{P_i},t_{P_i}^L)}{h_s e}\exp(1-z_{P_i}-\exp(-z_{P_i}))\,\mathrm{ds} \tag{5.3-69}
$$

where the parameter s denotes distance along AB and the altitude of P can be expressed in terms of this parameter (s) and the factor $\gamma_I(t)$ is introduced as an arbitrary overall scale factor, which can be estimated. This integral is obtained using a simple trapezoidal summation rule:

$$
\delta\rho_{Iono}^{SF}(t_k) = \frac{40.3\ \gamma_I(t_k)}{f_T^2 h_s e}\sum_{P_i} TEC_K(\lambda_{P_i},\phi_{P_i},t_{P_i}^L)\exp(1-z_{P_i}-\exp(-z_{P_i}))\Delta s \tag{5.3-70}*
$$

The integration algorithm is described in Section 5.3.5.2. Alternatively, a numerical quadrature rule could be used but was not selected since it was unlikely that the more complex algorithm would improve the overall accuracy of the computation.

5.3.5.1 Algorithm for Computing Total Vertical Electron Content

The GPS single-frequency user ionospheric correction algorithm provides the ionospheric delay for an L1 signal (in seconds) along the path from a user located on the ground at geodetic latitude and longitude λ_U and ϕ_U to a specific GPS SV at an elevation el and azimuth az with respect to the user

$$
T_{Iono}(\lambda_U,\phi_U,t_U^L) \cong \frac{40.3}{cf_{L1}^2\sin el}TEC_K(\lambda_I,\phi_I,t_I^L) \quad \text{(seconds)} \tag{5.3-71}
$$

where λ_I and ϕ_I are the geodetic longitude and latitude of the ionospheric subpoint (i.e. the geographic point where the ray path intersects the mean ionospheric height, chosen to be a vertical height of 350 kilometers) and f_{L1} is the L1 transmission frequency (1.57542 GHz).

If the correction algorithm is evaluated for the case where the GPS SV is directly above the ground location,

$$TEC_K(\lambda_I, \phi_I, t_I^L) \cong \frac{cf_{L1}^2}{40.3} T_{Iono}(\lambda_I, \phi_I, t_I^L) \qquad (5.3\text{-}72)^*$$

The following algorithm is used to compute $T_{Iono}(\lambda_I, \phi_I, t_I^L)$. This algorithm is adapted from References 35 and 38 and simplified for the case where the GPS SV is directly above the ground location. The coefficients α_n and β_n are transmitted in page 18 of Subframe 4 of the GPS navigation message.

1. Compute λ_I and ϕ_I (in semicircles) corresponding to the position vector of P_i expressed in the ECEF frame, $(\bar{r}_{P_i})_{ECEF} = BR_g C(\bar{R}_{P_i})_{J2000}$

$$\lambda_I \cong \frac{\lambda_{P_i}}{\pi} \quad \text{(semicircles)} \qquad (5.3\text{-}73a)^*$$
$$\phi_I \cong \frac{\phi_{P_i}}{\pi}$$

where

$$\lambda_{P_i} = \tan^{-1}\frac{(y_{P_i})_{ECEF}}{(x_{P_i})_{ECEF}}; \quad 0 \le \lambda_{P_i} < 2\pi$$
$$\text{(radians)} \qquad (5.3\text{-}73b)^*$$
$$\phi_{P_i} = \sin^{-1}\frac{(z_{P_i})_{ECEF}}{r_{P_i}}; \quad -\frac{\pi}{2} \le \phi_{P_i} \le \frac{\pi}{2}$$

2. Compute the local time t_I^L at the subionospheric point.

$$t_I^L = 4.32 \times 10^4 \lambda_I + t_k \quad \text{(seconds)} \qquad (5.3\text{-}74)^*$$

where t_k is the current UTC seconds of day. If t_l>86,400, use $t_I^L = t_I^L$ -86400. If t_I^L <0, use $t_I^L = t_I^L$ +86400.

3. Compute the geomagnetic latitude ϕ_m of the subionospheric location

$$\phi_m = \phi_I + 0.064\cos\pi(\lambda_I - 1.617) \quad \text{(semicircles)} \qquad (5.3\text{-}75)^*$$

4. Compute P, the period of the ionospheric time delay

$$P = \begin{cases} \sum_{n=0}^{3} \beta_n (\phi_m)^n, & \text{if } \sum_{n=0}^{3} \beta_n (\phi_m)^n \geq 72000 \\ 72000 & \text{if } \sum_{n=0}^{3} \beta_n (\phi_m)^n < 72000 \end{cases} \quad \text{(seconds)} \qquad (5.3\text{-}76)^*$$

5. Compute x

$$x = \frac{2\pi\left(t_I^L - 50400\right)}{P} \text{ (radians)} \qquad (5.3\text{-}77)^*$$

6. Compute the amplitude A

$$A = \begin{cases} \sum_{n=0}^{3} \alpha_n (\phi_m)^n, & \text{if } \sum_{n=0}^{3} \alpha_n (\phi_m)^n > 0 \\ 0 & \text{if } \sum_{n=0}^{3} \alpha_n (\phi_m)^n \leq 0 \end{cases} \quad \text{(seconds)} \qquad (5.3\text{-}78)^*$$

7. Compute the ionospheric time delay

$$T_{iono}(\lambda_I, \phi_I, t_I^L) = \begin{cases} \left[5\times10^{-9} + A\left(1 - \frac{x^2}{2} + \frac{x^4}{24}\right)\right], & |x| < \pi/2 \\ 5\times10^{-9}, & |x| \geq \pi/2 \end{cases} \quad \text{(seconds)} \qquad (5.3\text{-}79)^*$$

5.3.5.2 Algorithm for Integrating Along the Ray Path

In Figure 5-3, h denotes the altitude of the receiver, and HORP denotes the height of the ray path above the Earth. It is assumed that, above a specified altitude ($h_{\max}$), there are no free electrons that contribute to the ionospheric delays in signal propagation. Thus the ionospheric delay correction is computed only when HORP is less than $h_{\max}$. In Figure 5-3, A and B are two points on the ray path for which the altitudes are equal to $h_{\max}$. The following parameters are used in this computation.

$\overline{R}$ = Position vector of the receiving satellite

$\overline{R}_{GPS_j}$ = Position vector of the transmitting GPS SV

$R = \left|\overline{R}\right|$

$h_{\max}$ = 3000 kilometers, the assumed maximum ionospheric altitude

R_e = mean Earth's radius

$\overline{s} = \overline{R}_{GPS_j} - \overline{R}$, line-of-sight vector from user s/c to GPS

$\hat{s} = \frac{\overline{s}}{s}$, line-of-sight unit vector from user s/c to GPS

$$HORP = \left| \overline{R}_{GPS_j} - \frac{\overline{s}\left(\overline{s} \cdot \overline{R}_{GPS_j}\right)}{s^2} \right| - R_e$$

$R_A = R_e + h_{\max}$, radial distance of point A

$R_B = R_A$, radial distance of point B

$R_H = R_e +$ HORP , radial distance of point H (point with h= HORP)

$\theta = \sin^{-1}\left(\frac{R_H}{R}\right)$, $0 \le \theta < \pi$ radians

$\theta_{\min} = \sin^{-1}\left(\frac{R_H}{R_A}\right)$, $0 \le \theta_{\min} < \pi$ radians

Δs : line integration step size, a commandable parameter

When computing the line integral defined by Equation (5.3-70), the following cases are considered separately.

Case 1: When HORP > hmax , the ionospheric correction is 0

Case 2: When HORP $\le h_{\max}$, and $\theta < \pi/2$

(i) if $h < h_{\max}$, the integration is performed from the user S/C position to B

(ii) if $h \ge h_{\max}$, the integration will be performed from A to B

Case 3: When HORP $\le$ hmax, and $\theta \ge \pi/2$

(iii) if $h < h_{\max}$, the integration will be performed from the user S/C position to B

(iv) if $h \ge h_{\max}$, the ionospheric correction is 0

Thus, there are three cases where the finite ionospheric corrections are computed:

(i) HORP $\le h_{\max}$, $\theta < \pi/2$, and $h < h_{\max}$

In this case, the line integral defined in Equation (5.3-70) is computed by integrating the electron density function from the user S/C position to B. The total distance from the user spacecraft to the point B is given by

$$d = R\cos\theta + R_B \cos\theta_{\min} \qquad (5.3\text{-}80)^*$$

The number of points at which the Chapman electron profile computation is required is computed as follows:

Using $N = [d/\Delta s]_{\text{int}}$ (integer part of the quotient), redefine Δs as

$$\Delta s = d/N \qquad (5.3\text{-}81)^*$$

The $(N+1)$ position vectors needed for the Chapman profile computation are given by:

$$\overline{R}_{P_i} = \overline{R} + (i\Delta s)\hat{s} \ : i = 0, 1, 2, \ldots, N \qquad (5.3\text{-}82)^*$$

Now $\left\{\overline{R}_{P_i}, t\right\}$ is converted into the corresponding geographical latitude, longitude, height, and local solar time: $\left\{\phi_{P_i}, \lambda_{P_i}, h_{P_i}, t_{P_i}^L\right\}$ using Equations (5.3-73) and (5.3-74). The associated altitudes are computed approximately as follows:

$$h_{P_i} = \left|\overline{R}_{P_i}\right| - R_e \tag{5.3-83}*$$

Using $\left\{\phi_{P_i}, \lambda_{P_i}, h_{P_i}, t_{P_i}^L \mid i = 0,1,2,\cdots,N\right\}$, $\Delta\rho_{Iono}(t)$ given by Equation (5.3.70) can be obtained.

(ii) HORP $\leq h_{\max}$, $\theta < \pi/2$, and $h \geq h_{\max}$

In this case, the line integral defined in Equation (5.3.70) will be computed by integrating the electron density function from A to B. The total distance from A to B is given by

$$d = 2R_A \cos\theta_{\min} \tag{5.3-84}*$$

The position vector of the point A is given by:

$$\overline{R}_A = \overline{R} + d_1 \hat{s} \tag{5.3-85}*$$

where

$$d_1 = R\cos\theta - R_A \cos\theta_{\min} \tag{5.3-86}*$$

and the (N +1) position vectors needed for the Chapman profile computation are given by:

$$\overline{R}_{P_i} = \overline{R}_A + (i\Delta s)\hat{s} \ : i = 0, 1, 2, \ldots., N \tag{5.3-87}*$$

The computation of Δs and N, and of the final integral can be performed following the steps given above for case (i)..

(iii) HORP $\leq h_{\max}$, $\theta \geq \pi/2$, and $h < h_{\max}$

In this case, the line integral defined in Equation (5.3.70) is computed by integrating the electron density function from the user S/C position to point B. The total distance from the user S/C to B is given by

$$d = R\cos\theta + R_B \cos\theta_{\min} \tag{5.3-88}*$$

and the rest of the computational steps are similar to those given for case (i).

5.3.6 Galileo Pseudorange Measurement Model and Associated Partial Derivatives

This section provides an expression that is used to compute the observed pseudorange in terms of the Galileo and receiver states and the corresponding times. The pseudorange is obtained from the signal transit time interval, which is defined as

$$\Delta\tau \equiv t_R^{(RC)} - t_T^{(SC)} \tag{5.3.6-1}$$

where $t_R^{(RC)}$ denotes the receive time measured by the receiver clock and $t_T^{(SC)}$ is the transmit time. The pseudorange $\Re$ is then defined as the speed of light (c) times the time interval $\Delta\tau$ given by Equation (5.3.6-1):

$$\Re \equiv c\,\Delta\tau \tag{5.3.6-2}$$

Calculation of the Galileo pseudorange measurement follows the same procedure that is discussed in Section 5.3.2 for the GPS/WAAS pseudorange. The pseudorange measurement equation is as follows:

$$\begin{aligned}\Re_{GAL_j}^{n}(t_{_R}^{UTC_n}) = {} & \rho_{GAL_j}^{n,i}(t_k) - \dot{\rho}_{GAL_j}^{n,i}(t_k)\Delta t_R^n + b_R{}^n(t_k) - d_R{}^n(t_k)\Delta t_R^n + b_\rho^{GAL_j}(t_k) \\ & + \gamma_I(t_k)\delta\rho_{Iono}^{SF}(t_k) - c\left(\delta t_{GAL_j} + \delta t_{GAL_j}^{SF}\right)\end{aligned} \tag{5.3.6-3}*$$

$$\rho_{GAL_j}^{n,i}(t_k) = \left|\bar{R}_{A_i}{}^n(t_k) - \bar{R}_{GAL_j}(t_k')\right| \tag{5.3.6-4}*$$

$$\dot{\rho}_{GAL_j}^{n,i}(t_k) = \frac{\hat{\rho}_{GAL_j}^{n,i}(t_k)\cdot\left(\dot{\bar{R}}_{A_i}^n(t_k) - \dot{\bar{R}}_{GAL_j}(t_k')\right)}{1 - \hat{\rho}_{GAL_j}^{n,i}(t_k)\cdot\left(\dot{\bar{R}}_{GAL_j}(t_k')/c\right)} \tag{5.3.6-5}*$$

In the above equations, the subscript j indicates the j^{th} Galileo SV. The timetag of the k^{th} measurement, t_k, is equal to the value of the measured receive time, $t_R^{(RC)}$, and t'_k is the signal transmit time, t_T, computed based on t_k. The receiver clock bias $b_R{}^n(t)$ is computed using the estimated parameters $b_R{}^n(t_k)$ and $\dot{b}_R{}^n(t_k)$, as defined in Equation 4.3-14a and 4.3-14 of Section 4.3. The term $-\dot{\rho}_{GAL_j}^{n,i}(t_k)\Delta t_R{}^n$ is significant when the receiver time bias or measurement timetag difference is large. The Galileo pseudorange bias, $b_\rho^{GAL_j}$, is defined in Section 4.3. For single frequency measurements, the ionospheric delay correction, $\delta\rho_{Iono}^{SF}$, can be modeled using GPS ionospheric coefficients in the algorithm defined in Section 5.3.5, where $\gamma_I(t)$ is the ionospheric delay scale factor, which can be estimated. The last two terms on the right-hand side of Equation (5.3.6-3) provide the total Galileo satellite time correction, which is defined in Section 3.3.9. This correction is evaluated at the signal transmit time t'_k converted to GST using Equation 3.3.9-2 for both single and dual frequency GPS users and in addition Equation 3.3.9-4

for single frequency GPS users. The position and velocity of the receiving antenna are computed using Equation 3.2-61 in Section 3.2.8.

The matrix (a row vector in this case) of partial derivatives of the pseudorange measurement with respect to the estimation state vector, $\overline{X}(t_k)$, is defined as follows:

$$\left[H(t_k)\right]_{\Re^n_{GAL\,j}} \equiv \frac{\partial \Re^n_{GAL_j}(t_R^{UTC})}{\partial \overline{X}(t_k)} \tag{5.3.6-6}$$

Note that the equations for the partial derivatives of the Galileo pseudorange measurements are the same as for the GPS pseudorange measurements. The partial derivatives with respect to those parameters that are not explicitly included in the pseudorange measurement equation will be zeros. The following are the only nonzero elements if the state vector consists of absolute states for both the local and remote satellites:

$$\frac{\partial \Re^n_{GAL_j}(t_R^{UTC})}{\partial \overline{R}^n(t_k)} = \frac{\partial \rho^{n,i}_{GAL_j}(t_k)}{\partial \overline{R}^n(t_k)} - \frac{\partial \dot{\rho}^{n,i}_{GAL_j}(t_k)}{\partial \overline{R}^n(t_k)} \Delta t_R^n \tag{5.3.6-7}*$$

$$\frac{\partial \Re^n_{GAL_j}(t_R^{UTC})}{\partial \dot{\overline{R}}^n(t_k)} = -\frac{\partial \dot{\rho}^{n,i}_{GAL_j}(t_k)}{\partial \dot{\overline{R}}^n(t_k)} \Delta t_R^n \tag{5.3.6-8}*$$

$$\frac{\partial \Re^n_{GAL_j}(t_R^{UTC})}{\partial \gamma_I(t_k)} = \delta\rho^{SF}_{Iono}(t_k) \tag{5.3.6-9}*$$

$$\frac{\partial \Re^n_{GAL_j}(t_R^{UTC})}{\partial b_R{}^n(t_k)} = 1 - \frac{\dot{\rho}^{n,i}_{GAL_j}(t_k)}{c} - \frac{d_R{}^n(t_k)}{c} \tag{5.3.6-10}*$$

$$\frac{\partial \Re^n_{GAL_j}(t_R^{UTC})}{\partial d_R{}^n(t_k)} = -\Delta t_R^n \tag{5.3.6-11}*$$

$$\frac{\partial \Re^n_{GAL_j}(t_R^{UTC})}{\partial b_\rho^{GAL_j}(t_k)} = 1 \tag{5.3.6-12}*$$

where

$$\frac{\partial \rho^{n,i}_{GAL_j}(t_k)}{\partial \overline{R}^n(t_k)} = \left[\frac{\overline{R}_{A_i}{}^n(t_k) - \overline{R}_{GAL_j}(t'_k)}{\rho^{n,i}_{GAL_j}(t_k)} \right]^T \tag{5.3.6-13}*$$

$$\frac{\partial \dot{\rho}^{n,i}_{GAL_j}(t_k)}{\partial \bar{R}^n(t_k)} \cong \frac{1}{\rho^{n,i}_{GAL_j}(t_k)\left[1-\hat{\rho}^{n,i}_{GAL_j}(t_k)\cdot\left(\dot{\bar{R}}_{GAL_j}(t'_k)/c\right)\right]} \times \left[\left(\dot{\bar{R}}^n(t_k)-\dot{\bar{R}}_{GAL_j}(t'_k)\right)-\dot{\rho}^{n,i}_{GAL_j}(t_k)\left(\hat{\rho}^{n,i}_{GAL_j}(t_k)-\frac{\dot{\bar{R}}_{GAL_j}(t'_k)}{c}\right)\right]^T \quad (5.3.6\text{-}14)^*$$

$$\frac{\partial \dot{\rho}^{n,i}_{GAL_j}(t_k)}{\partial \dot{\bar{R}}^n(t_k)} = \frac{\left(\hat{\rho}^{n,i}_{GAL_j}(t_k)\right)^T}{1-\hat{\rho}^{n,i}_{GAL_j}(t_k)\cdot\left(\dot{\bar{R}}_{GAL_j}(t'_k)/c\right)} \quad (5.3.6\text{-}15)^*$$

The superscript T on the right-hand sides of Equations (5.3.6-13) through (5.3.6-15) denote the transpose, indicating that these partial derivatives are given as row vectors. Equation (5.3.6-14) is an approximation in which the dependence of t'_k, the argument of $\bar{R}_{GAL}(t'_k)$ and $\dot{\bar{R}}_{GAL}(t'_k)$, on $\bar{R}(t_k)$ is ignored.

If the state vector includes relative states for the nonlocal satellites, the associated nonzero pseudorange measurement partial derivatives are as follows:

$$\frac{\partial \Re^n_{GAL\,j}(t^{UTC}_R)}{\partial \bar{R}^1(t_k)} = \frac{\partial \rho^{n,i}_{GAL_j}(t_k)}{\partial \bar{R}^n(t_k)} - \frac{\partial \dot{\rho}^{n,i}_{GAL_j}(t_k)}{\partial \bar{R}^n(t_k)}\Delta t^n_R \quad (5.3.6\text{-}16)$$

$$\frac{\partial \Re^n_{GAL\,j}(t^{UTC}_R)}{\partial \bar{R}^n_{rel}(t_k)} = \frac{\partial \rho^{n,i}_{GAL_j}(t_k)}{\partial \bar{R}^n(t_k)} - \frac{\partial \dot{\rho}^{n,i}_{GAL_j}(t_k)}{\partial \bar{R}^n(t_k)}\Delta \mathrm{t}^n_R;\ n \neq 1 \quad (5.3.6\text{-}17)$$

$$\frac{\partial \Re^n_{GAL_j}(t^{UTC}_R)}{\partial \dot{\bar{R}}^1(t_k)} = -\frac{\partial \dot{\rho}^{n,i}_{GAL_j}(t_k)}{\partial \dot{\bar{R}}^n(t_k)}\Delta t^n_R \quad (5.3.6\text{-}18)^*$$

$$\frac{\partial \Re^n_{GAL_j}(t^{UTC}_R)}{\partial \dot{\bar{R}}^n_{rel}(t_k)} = -\frac{\partial \dot{\rho}^{n,i}_{GAL_j}(t_k)}{\partial \dot{\bar{R}}^n(t_k)}\Delta \mathrm{t}^n_R;\ n \neq 1 \quad (5.3.6\text{-}19)^*$$

$$\frac{\partial \Re^n_{GAL_j}(t^{UTC}_R)}{\partial b^{G/W_j}_{\rho}(t_k)} = 1 \quad (5.3.6\text{-}20)^*$$

$$\frac{\partial \Re^n_{GAL\,j}(t^{UTC}_R)}{\partial b^1_R(t_k)} = 1 - \frac{\dot{\rho}^{n,i}_{GAL_j}(t_k)}{c} - \frac{d_R}{c} \quad (5.3.6\text{-}21)^*$$

$$\frac{\partial \Re^n_{GAL\,j}(t_R^{UTC})}{\partial b^n_{rel}(t_k)} = 1 - \frac{\dot{\rho}^{n,i}_{GAL_j}(t_k)}{c} - \frac{d_R}{c};\ n \neq 1 \qquad (5.3.6\text{-}22)^*$$

$$\frac{\partial \Re^n_{GAL_j}(t_R^{UTC})}{\partial \gamma_I(t_k)} = \delta\rho^{SF}_{Iono}(t_k) \qquad (5.3.6\text{-}23)^*$$

$$\frac{\partial \Re^n_{GAL_j}(t_R^{UTC})}{\partial d_R{}^1(t_k)} = -\Delta t^1_R \qquad (5.3.6\text{-}24)^*$$

$$\frac{\partial \Re^n_{GAL_j}(t_R^{UTC})}{\partial d_{rel}{}^n(t_k)} = -\Delta t^n_R;\quad n \neq 1 \qquad (5.3.6\text{-}25)^*$$

5.3.7 Galileo Instantaneous Doppler Measurement Model and Associated Partial Derivatives

An instantaneous Doppler shift data extracted at the receiver can be defined as

$$F_D(t) = F_R(t) - F_{REF} \qquad (5.3.7\text{-}1)$$

where $F_R(t)$ is Doppler-shifted receive carrier frequency and F_{REF} is the receiver-generated local reference frequency. When the receiver and the transmitter use the same frequency standards, the receiver-generated reference frequency, F_{REF}, will be equal to the transmit frequency, F_T. For Galileo tracking, there will be small difference between the frequency standards used by the receiver and the transmitter. The frequency difference due to this difference is modeled as the receiver reference frequency bias. Even when the two frequency standards are the same, the frequency difference obtained from Equation (5.3.7-1) does not represent a pure Doppler effect since it includes contributions from non-Doppler sources such as the atmospheric refraction effects, which are not modeled in GEONS.

Calculation of the Galileo Doppler measurement follows the same procedure that is discussed in Section 5.3.2 for the GPS/WAAS Doppler. The desired instantaneous Doppler shift is obtained using Equations (5.3.7-2) and (5.3.7-3), where the position and velocity of the receiving antenna are computed using Equation (3.2-61). Note that unlike GPS the Galileo satellite frequency is not adjusted to compensate for the relativistic bias experienced by a receiver located on the ground. This bias is absorbed in the total apparent frequency offset of the satellite clock given by af1 in Equation (3.3.9.2).

$$\left(F_D(t_k)\right)^n_{GAL_j} = F_T\left[-\frac{\dot{\rho}^{n,i}_{GAL_j}(t_k)}{c} + \delta\dot{t}_{GAL_j} - \frac{d_R{}^n(t_k)}{c} + \frac{1}{2c^2}\left(\left|\dot{\bar{R}}^n\right|^2 - \left|\dot{\bar{R}}_{GAL_j}\right|^2\right) + \frac{\mu}{c^2}\left(\frac{1}{\left|\bar{R}^n\right|} - \frac{1}{\left|\bar{R}_{GAL_j}\right|}\right)\right] + b_d^{GAL_j}(t_k) \qquad (5.3.7\text{-}2)^*$$

where

$$\dot{\rho}^{n,i}_{GAL_j}(t_k) = \frac{\hat{\rho}^{n,i}_{GAL_j}(t_k) \cdot \left(\dot{\bar{R}}^n_{A_i}(t_k) - \dot{\bar{R}}_{GAL_j}(t'_k) \right)}{1 - \hat{\rho}^{n,i}_{GAL_j}(t_k) \cdot \left(\dot{\bar{R}}_{GAL_j}(t'_k)/c \right)} \qquad (5.3.7\text{-}3)^*$$

In this equation, the subscript *j* indicates the Galileo SV number; and the transmit frequency, F_T, is assumed to be known (i.e., 1575.42 Mhertz for the E1 carrier, 1176.45 Mhertz for the E5a carrier, and 1207.14 Mhertz for the E5b carrier for the Galileo Open Service). Doppler biases, $\bar{b}_d^{GAL_j}$, can be estimated to absorb the combined effects of the ionospheric and Galileo SV ephemeris and clock errors. One Doppler bias is estimated for each Galileo SV tracked by the local receiver. $\delta\dot{t}_{GAL_j}$ is computed using the Galileo SV clock correction parameters discussed in Section 3.3.9.

Note that the equations for the partial derivatives of the Galileo Doppler measurements are the same as for the GPS Doppler measurements. From Equation (5.3.7-2), the following nonzero partial derivatives of the Doppler shift are obtained if the state vector consists of absolute states for both the local and remote satellites:

$$\frac{\partial \left(F_D(t_k) \right)^n_{GAL_j}}{\partial \bar{R}^n(t_k)} = -\frac{F_T}{c} \left(\frac{\partial \dot{\rho}^{n,i}_{GAL_j}(t_k)}{\partial \bar{R}^n(t_k)} \right); \quad \frac{\partial \left(F_D(t_k) \right)^n_{GAL_j}}{\partial \dot{\bar{R}}^n(t_k)} = -\frac{F_T}{c} \left(\frac{\partial \dot{\rho}^{n,i}_{GAL_j}(t_k)}{\partial \dot{\bar{R}}^n(t_k)} \right) \qquad (5.3.7\text{-}4)^*$$

$$\frac{\partial \left(F_D(t_k) \right)^n_{GAL_j}}{\partial d_R{}^n(t_k)} = -\frac{F_T}{c} \qquad (5.3.7\text{-}5)^*$$

$$\frac{\partial \left(F_D(t_k) \right)^n_{GAL_j}}{\partial b_d^{GAL_j}(t_k)} = 1 \qquad (5.3.7\text{-}6)^*$$

The state partial derivatives of $\dot{\rho}_j(t_k)$ on the right-hand side of Equation (5.3-46) can be obtained using the following equations:

$$\frac{\partial \dot{\rho}^{n,i}_{GAL_j}(t_k)}{\partial \bar{R}^n(t_k)} \cong \frac{1}{\rho^{n,i}_{GAL_j}(t_k) \left[1 - \hat{\rho}^{n,i}_{GAL_j}(t_k) \cdot \left(\dot{\bar{R}}_{GAL_j}(t'_k)/c \right) \right]} \times \left[\left(\dot{\bar{R}}^n(t_k) - \dot{\bar{R}}_{GAL_j}(t'_k) \right) - \dot{\rho}^{n,i}_{GAL_j}(t_k) \left(\hat{\rho}^{n,i}_{GAL_j}(t_k) - \frac{\dot{\bar{R}}_{GAL_j}(t'_k)}{c} \right) \right]^T \qquad (5.3.7\text{-}7)^*$$

$$\frac{\partial \dot{\rho}^{n,i}_{GAL_j}(t_k)}{\partial \dot{\bar{R}}^n(t_k)} = \frac{\left(\hat{\rho}^{n,i}_{GAL_j}(t_k) \right)^T}{1 - \hat{\rho}^{n,i}_{GAL_j}(t_k) \cdot \left(\dot{\bar{R}}_{GAL_j}(t'_k)/c \right)} \qquad (5.3.7\text{-}8)^*$$

The superscript T on the right-hand sides of Equations (5.3.7-7) and (5.3.7-8) denote the transpose, indicating that these partial derivatives are given as row vectors. Also note that Equation (5.3.7-7) is an approximation in which the dependence of t_k', the argument of $\overline{R}_{GAL_j}(t_k')$ and $\dot{\overline{R}}_{GAL_j}(t_k')$, on $\overline{R}^n(t_k)$ is ignored.

If the state vector includes relative states for the nonlocal satellites, the associated nonzero Doppler measurement partial derivatives are as follows:

$$\frac{\partial\left(F_D(t_k)\right)^n_{GAL_j}}{\partial\overline{R}^1(t_k)} = -\frac{F_T}{c}\left(\frac{\partial\dot{\rho}^{n,i}_{GAL_j}(t_k)}{\partial\overline{R}^n(t_k)}\right)$$
$$\frac{\partial\left(F_D(t_k)\right)^n_{GAL_j}}{\partial\dot{\overline{R}}^1(t_k)} = -\frac{F_T}{c}\left(\frac{\partial\dot{\rho}^{n,i}_{GAL_j}(t_k)}{\partial\dot{\overline{R}}^n(t_k)}\right) \tag{5.3.7-9}$$

$$\frac{\partial\left(F_D(t_k)\right)^n_{GAL_j}}{\partial\overline{R}^n_{rel}(t_k)} = -\frac{F_T}{c}\left(\frac{\partial\dot{\rho}^{n,i}_{GAL_j}(t_k)}{\partial\overline{R}^n(t_k)}\right);\ n\neq 1$$
$$\frac{\partial\left(F_D(t_k)\right)^n_{GAL_j}}{\partial\dot{\overline{R}}^n_{rel}(t_k)} = -\frac{F_T}{c}\left(\frac{\partial\dot{\rho}^{n,i}_{GAL_j}(t_k)}{\partial\dot{\overline{R}}^n(t_k)}\right);\ n\neq 1 \tag{5.3.7-10}$$

$$\frac{\partial\left(F_D(t_k)\right)^n_{GAL_j}}{\partial d_R{}^1(t_k)} = -\frac{F_T}{c} \tag{5.3.7-11}*$$

$$\frac{\partial\left(F_D(t_k)\right)^n_{GAL_j}}{\partial d_{R_{rel}}{}^n(t_k)} = -\frac{F_T}{c};\ n\neq 1 \tag{5.3.7-12}*$$

$$\frac{\partial\left(F_D(t_k)\right)^n_{GAL_j}}{\partial b_d^{GAL_j}(t_k)} = 1 \tag{5.3.7-13}*$$

5.3.8 Galileo Integrated Carrier Phase Measurement Model and Associated Partial Derivatives

This section provides an expression that is used to compute the integrated carrier beat phase measurement in terms of the Galileo and receiver states and the corresponding times. The carrier beat phase measurement is formed in a GNSS receiver as the difference between the phase of the local receiver oscillator and the phase of the received carrier signal. The measurement is ambiguous with respect to the number of integer cycles ($N^{GAL_j}_{\varphi_n}(t_{acq})$) at the time (t_{acq}) when the signal is first acquired from each Galileo SV. At any epoch other than the initial acquisition epoch, the receiver measures the fractional phase difference and the number of integer cycles accumulated since that epoch. Prior to processing in GEONS, the resulting raw integrated carrier

beat phase observation (in cycles), $(\varphi_{obs})^{n}_{GAL_j}(t_R^{UTC_n})$, is multiplied by the wavelength of the carrier ($\lambda_C = c/F_T$, where F_T = 1575.42 Mhertz for the E1 carrier, 1176.45 Mhertz for the E5a carrier, and 1207.14 Mhertz for the E5b carrier for the Galileo Open Service) to scale the carrier phase observation to meters:

$$(\Phi_{obs})^{n}_{GAL_j}(t_R^{UTC_n}) = \lambda_C(\varphi_{obs})^{n}_{GAL_j}(t_R^{UTC_n}) \quad (5.3.8\text{-}1)$$

The integrated carrier beat phase measurement (in meters), $\Phi^{n}_{GAL_j}(t_k)$, can be modeled as follows:

$$\Phi^{n}_{GAL_j}(t_R^{UTC_n}) = \rho^{n,i}_{GAL_j}(t_k) - \dot{\rho}^{n,i}_{GAL_j}(t_k)\Delta t^{n}_{R} + b_R{}^{n}(t_k) - \gamma_I(t_k)\delta\rho^{SF}_{Iono}(t_k) + b^{GAL_j}_{\varphi_n}(t_k) - c\left(\delta t_{GALj} + \delta t^{SF}_{GAL_j}\right) \quad (5.3.8\text{-}2)^*$$

where the offset of the true UTC receive time for spacecraft n measurements from the UTC filter state epoch is given by

$$\Delta t^{n}_{R} = \left[\left(t_k - t_R^{(RC)_n}\right) + \left(t_R^{(RC)_n} - t_R^{UTC_n}\right)\right] = \left(t_k - t_R^{(RC)_n}\right) + \delta t^{n}_{R} = \left(t_k - t_R^{(RC)_n}\right) + \frac{b^{n}_{R}(t_k)}{c} \quad (5.3.8\text{-}3)^*$$

Note that in Release 2.7 and prior releases, Δt^{n}_{R} is implemented assuming that $t_k = t_R^{(RC)_n}$; this is corrected in Release 2.8.

In the above equations, the superscript *n* indicates the n^{th} receiver, the superscript *i* indicates the i^{th} antenna, and subscript *j* indicates the j^{th} Galileo satellite. The time tag t_k is the measured receive time of the k^{th} measurement, and t'_k is the signal transmission time. The geometrical range ($\rho^{n,i}_{GAL_j}$) and range rate ($\dot{\rho}^{n,i}_{GAL_j}$) are computed as described in Section 5.3.6. The receiver clock bias, $b_R{}^{n}(t)$, is in meters. The correction due to the ionospheric refraction, $\delta\rho^{SF}_{Iono}(t_k)$, can be modeled using the algorithm defined in Section 5.3.5 and the ionospheric scale factor, $\gamma_I(t_k)$, can be estimated. The terms δt_{GALj} and $\delta t^{SF}_{GAL_j}$ are the Galileo satellite time offset from Galileo system time and group delay correction for single-frequency users, defined in Equations 3.3.9-2 and 3.3.9-4 through 3.3.3-9.5, respectively. The term $b^{GAL_j}_{\varphi_n}(t_k) = \lambda_C N^{GAL_j}_{\varphi_n}(t_{acq})$ is the estimated carrier phase bias between Galileo satellite *j* and receiver *n* at the carrier phase acquisition time (t_{acq}), scaled to meters.

The carrier phase bias $b^{GAL_j}_{\varphi_n}(t_k)$ is different for each acquisition of a Galileo satellite by a receiver. The carrier phase bias is reinitialized at the start of each new acquisition based on the difference between the predicted pseudorange $\Re^{n}_{GAL_j}(t_{acq})$ (defined in Equation 5.3.6-3) and the observed integrated carrier phase at the acquisition time t_{acq}:

$$b^{GAL_j}_{\varphi_n}(t_k = t_{acq}) = (\Phi_{obs})^{n}_{GAL_j}(t_{acq}) - \Phi^{n}_{GAL_j}(t_{acq}) \quad (5.3.8\text{-}4)^*$$

Similarly, the carrier phase bias variance is reinitialized at the start of each new acquisition to the predicted carrier phase residual variance computed as described in Step 3 in Section 2.3.1.

The matrix (a row vector in this case) of partial derivatives of the integrated carrier beat phase measurement with respect to $\bar{X}(t_k)$ is defined as follows:

$$\left[H(t_k)\right]_{\Phi^n_{GAL_j}(t_k)} \equiv \frac{\partial \Phi^n_{GAL_j}(t_k)}{\partial \bar{X}(t_k)} \tag{5.3.8-5}$$

The partial derivatives with respect to those parameters that are not explicitly included in the measurement equation will be zeros. The following are the only nonzero elements if the state vector consists of absolute states for both the local and remote satellites:

$$\frac{\partial \Phi^n_{GAL_j}(t_k)}{\partial \bar{R}^n(t_k)} = \frac{\partial \rho^{n,i}_{GAL_j}(t_k)}{\partial \bar{R}^n(t_k)} - \frac{b^n_R(t_k)}{c}\frac{\partial \dot{\rho}^{n,i}_{GAL_j}(t_k)}{\partial \bar{R}^n(t_k)} \tag{5.3.8-6}*$$

$$\frac{\partial \Phi^n_{GAL_j}(t_k)}{\partial \dot{\bar{R}}^n(t_k)} = -\frac{b^n_R(t_k)}{c}\frac{\partial \dot{\rho}^{n,i}_{GAL_j}(t_k)}{\partial \dot{\bar{R}}^n(t_k)} \tag{5.3.8-7}*$$

$$\frac{\partial \Phi^n_{GAL_j}(t_k)}{\partial b_R{}^n(t_k)} = 1 - \frac{\dot{\rho}^{n,i}_{GAL_j}(t_k)}{c} \tag{5.3.8-8}*$$

$$\frac{\partial \Phi^n_{GAL_j}(t_k)}{\partial b^{GAL_j}_{\varphi_n}(t_k)} = 1 \tag{5.3.8-9}*$$

$$\frac{\partial \Phi^n_{GAL_j}(t_k)}{\partial \gamma_I(t_k)} = -\delta\rho^{SF}_{Iono}(t_k) \tag{5.3.8-10}*$$

where the partial derivatives of the geometrical range ($\rho^{n,i}_{GAL_j}$) and range rate ($\dot{\rho}^{n,i}_{GAL_j}$) are computed as defined in Equations 5.3.6-3 through 5.3.6-5 in Section 5.3.6.

If the state vector includes relative states for the nonlocal satellites, the associated nonzero pseudorange measurement partial derivatives are as follows:

$$\frac{\partial \Phi^n_{GAL\,j}(t_k)}{\partial \bar{R}^1(t_k)} = \frac{\partial \Phi^{\,n}_{GAL\,j}(t_k)}{\partial \bar{R}^n(t_k)}\frac{\partial \bar{R}^{\,n}(t_k)}{\partial \bar{R}^1(t_k)} = \frac{\partial \rho^{\,n,i}_{GAL_j}(t_k)}{\partial \bar{R}^n(t_k)} - \frac{b^n_R(t_k)}{c}\frac{\partial \dot{\rho}^{n,i}_{GAL_j}(t_k)}{\partial \bar{R}^n(t_k)} \tag{5.3.8-11}$$

$$\frac{\partial \Phi^n_{GAL\,j}(t_k)}{\partial \bar{R}^n_{rel}(t_k)} = \frac{\partial \Phi^{\,n}_{GAL\,j}(t_k)}{\partial \bar{R}^n(t_k)}\frac{\partial \bar{R}^{\,n}(t_k)}{\partial \bar{R}^n_{rel}(t_k)} = \frac{\partial \rho^{\,n,i}_{GAL_j}(t_k)}{\partial \bar{R}^n(t_k)} - \frac{b^n_R(t_k)}{c}\frac{\partial \dot{\rho}^{n,i}_{GAL_j}(t_k)}{\partial \bar{R}^n(t_k)};\ n \neq 1 \tag{5.3.8-12}$$

$$\frac{\partial \Phi^n_{GAL_j}(t_k)}{\partial \dot{\bar{R}}^1(t_k)} = \frac{\partial \Phi^{\,n}_{GAL\,j}(t_k)}{\partial \dot{\bar{R}}^n(t_k)}\frac{\partial \dot{\bar{R}}^{\,n}(t_k)}{\partial \dot{\bar{R}}^1(t_k)} = -\frac{b^n_R(t_k)}{c}\frac{\partial \dot{\rho}^{n,i}_{GAL_j}(t_k)}{\partial \dot{\bar{R}}^n(t_k)} \tag{5.3.8-13}*$$

$$\frac{\partial \Phi^{n}_{GAL_j}(t_k)}{\partial \dot{\bar{R}}^{n}_{rel}(t_k)} = \frac{\partial \Phi^{n}_{GAL\,j}(t_k)}{\partial \dot{\bar{R}}^{n}(t_k)} \frac{\partial \dot{\bar{R}}^{n}(t_k)}{\partial \dot{\bar{R}}^{n}_{rel}(t_k)} = -\frac{b^{n}_{R}(t_k)}{c} \frac{\partial \dot{\rho}^{n,i}_{GAL_j}(t_k)}{\partial \dot{\bar{R}}^{n}(t_k)}; n \neq 1 \qquad (5.3.8\text{-}14)^*$$

$$\frac{\partial \Phi^{n}_{GAL_j}(t_k)}{\partial b^{GAL_j}_{\varphi_n}(t_k)} = 1 \qquad (5.3.8\text{-}15)^*$$

$$\frac{\partial \Phi^{n}_{GAL\,j}(t_k)}{\partial b^{1}_{R}(t_k)} = \frac{\partial \Phi^{n}_{GAL\,j}(t_k)}{\partial b^{n}_{R}(t_k)} \frac{\partial b^{n}_{R}(t_k)}{\partial b^{1}_{R}(t_k)} = 1 - \frac{\dot{\rho}^{n,i}_{GAL_j}(t_k)}{c} \qquad (5.3.8\text{-}16)$$

$$\frac{\partial \Phi^{n}_{GAL\,j}(t_k)}{\partial b^{n}_{rel}(t_k)} = \frac{\partial \Phi^{n}_{GAL\,j}(t_k)}{\partial b^{n}_{R}(t_k)} \frac{\partial b^{n}_{R}(t_k)}{\partial b^{n}_{rel}(t_k)} = 1 - \frac{\dot{\rho}^{n,i}_{GAL_j}(t_k)}{c}; n \neq 1 \qquad (5.3.8\text{-}17)$$

$$\frac{\partial \Phi^{n}_{GAL_j}(t_k)}{\partial \gamma_I(t_k)} = -\delta\rho^{SF}_{Iono}(t_k) \qquad (5.3.8\text{-}18)^*$$

5.4 Singly Differenced GPS/WAAS Measurement Models

The computational algorithms for singly differenced GPS/WAAS pseudorange, Doppler, and carrier phase measurements are discussed in this section. The general form of the measurement model is as follows:

$$Y_k = G\ [\bar{X}(t_k),\ t_k] + \varepsilon \tag{5.4-1}$$

where t_k is the true measurement time, referenced to UTC, and ε is the measurement error. It is assumed that ε has a zero-mean Gaussian distribution with standard deviation σ, which is commandable for each measurement type. The measurement standard deviation is typically determined through analysis of the random component of the measurement error as part of the filter tuning process.

For GEONS, the estimation state vector, $\overline{X}(t)$ includes the receiver position vector, $\overline{R}$; velocity vector, $\dot{\overline{R}}$; optional corrections to the drag and solar radiation pressure coefficients, ΔC_D and ΔC_R; GPS receiver time bias, b_R; and GPS receiver bias rate, d_R for one or more receivers. For ground-based receivers, corrections to the drag and solar radiation pressure coefficients are not estimated. There are no measurement biases associated with the singly differenced pseudorange and Doppler measurements. When singly differenced integrated carrier phase measurements are processed, a singly differenced integer ambiguity bias is estimated for each GPS SV/local receiver/remote receiver configuration.

Section 5.4.1 addresses processing of the pseudorange, Doppler, and carrier phase measurements obtained from the GPS receiver to produce the singly differenced measurements. The measurement model for the singly differenced pseudorange measurements is presented in Section 5.4.2. The singly differenced Doppler measurement model is defined in Section 5.4.3. The singly differenced carrier phase measurement model is defined in Section 5.4.4.

5.4.1 Singly Differenced Measurement Preprocessing

The preprocessing of standard GPS/WAAS pseudorange, Doppler, and carrier phase measurements to form the singly differenced measurements is discussed in this section. The singly differenced pseudorange measurements are formed as follows using two pseudorange measurements from the same GPS SV/WAAS GEO measured by GPS receivers on the local receiver (1) and on one nonlocal receiver (n):

$$\left(\Delta\Re_{obs}\right)^{1,n}_{G/W_j} = \left(\Re_{obs}\right)^{1}_{G/W_j} - \left(\Re_{obs}\right)^{n}_{G/W_j} \tag{5.4-2}$$

where

$\left(\Delta\Re_{obs}\right)^{1,n}_{G/W_j}$ = singly differenced pseudorange measurement from the j^{th} GPS SV/WAAS GEO between the local receiver 1 and the n^{th} nonlocal receiver

$\left(\Re_{obs}\right)^{1}_{G/W_j}$ = Full observed pseudorange from the j^{th} GPS SV/WAAS GEO to local receiver 1

$\left(\Re_{obs}\right)^{n}_{G/W_j}$ = Full observed pseudorange from the j^{th} GPS SV/WAAS GEO to the n^{th} nonlocal receiver

The singly differenced Doppler measurements are formed as follows using two Doppler measurements from the same GPS SV/WAAS GEO measured by GPS receivers on the local receiver (1) and on one nonlocal receiver (n):

$$\left(\Delta F_{D_{obs}}\right)^{1,n}_{G/W_j} = \left(F_{D_{obs}}\right)^{1}_{G/W_j} - \left(F_{D_{obs}}\right)^{n}_{G/W_j} \tag{5.4-3}$$

where

$\left(\Delta F_{D_{obs}}\right)^{1,n}_{G/W_j}$ = singly-differenced Doppler measurement from the j^{th} GPS SV/WAAS GEO between the local user receiver 1 and the n^{th} nonlocal receiver

$\left(F_{D_{obs}}\right)^{1}_{G/W_j}$ = Observed Doppler from the j^{th} GPS SV/WAAS GEO to local receiver 1

$\left(F_{D_{obs}}\right)^{n}_{G/W_j}$ = Observed Doppler from the j^{th} GPS SV/WAAS GEO to the n^{th} nonlocal receiver

The singly differenced carrier phase measurements are formed as follows using two carrier phase measurements from the same GPS SV/WAAS GEO measured by GPS receivers on the local receiver (1) and on one nonlocal receiver (n):

$$\left(\Delta\Phi_{obs}\right)^{1,n}_{G/W_j} = \left(\Phi_{obs}\right)^{1}_{G/W_j} - \left(\Phi_{obs}\right)^{n}_{G/W_j} \tag{5.4-3a}$$

where

$\left(\Delta\Phi_{obs}\right)^{1,n}_{G/W_j}$ = singly differenced carrier phase measurement from the j^{th} GPS SV/WAAS GEO between the local receiver 1 and the n^{th} nonlocal receiver

$\left(\Phi_{obs}\right)^{1}_{G/W_j}$ = observed carrier phase from the j^{th} GPS SV/WAAS GEO to local receiver 1 (scaled to meters)

$\left(\Phi_{obs}\right)^{n}_{G/W_j}$ = observed carrier phase from the j^{th} GPS SV/WAAS GEO to the n^{th} nonlocal receiver (scaled to meters)

5.4.2 Singly Differenced GPS/WAAS Pseudorange Measurement Model and Associated Partial Derivatives

This section provides the algorithm used to model the observed singly differenced pseudorange given by Equation (5.4-2) in terms of the GPS/WAAS and receiver states and the corresponding times. The geometric pseudoranges and instantaneous geometric range rates from GPS SV/WAAS GEO j to antenna i on local receiver 1 and antenna m on nonlocal receiver n are defined as follows:

$$\rho^{1,i}_{G/W_j}(t_k) = \left| \overline{R}^1_{A_i}(t_k) - \overline{R}_{G/W_j}(t^1_T) \right| \tag{5.4-4}*$$

$$\rho^{n,m}_{G/W_j}(t_k) = \left| \overline{R}^n_{A_m}(t_k) - \overline{R}_{G/W_j}(t^n_T) \right| \tag{5.4-5}*$$

$$\dot{\rho}^{1,i}_{G/W_j}(t_k) = \frac{\hat{\rho}^{1,i}_{G/W_j}(t_k) \cdot \left(\dot{\overline{R}}^1(t_k) - \dot{\overline{R}}_{G/W_j}(t^1_T) \right)}{1 - \hat{\rho}^{1,i}_{G/W_j}(t_k) \cdot \left(\dot{\overline{R}}_{G/W_j}(t^1_T)/c \right)} \tag{5.4-5a}*$$

$$\dot{\rho}^{n,m}_{G/W_j}(t_k) = \frac{\hat{\rho}^{n,m}_{G/W_j}(t_k) \cdot \left(\dot{\overline{R}}^n(t_k) - \dot{\overline{R}}_{G/W_j}(t^n_T) \right)}{1 - \hat{\rho}^{n,m}_{G/W_j}(t_k) \cdot \left(\dot{\overline{R}}_{G/W_j}(t^n_T)/c \right)} \tag{5.4-5b}*$$

where

t^1_T, t^n_T = Transmission times for signals received at time t_R at receiver 1 and receiver *n*, respectively.

GEONS computes the geometric pseudoranges and instantaneous geometric range rates using the algorithms provided in Sections 5.3.2 and 5.3.3, respectively.

The predicted singly differenced pseudorange measurement is computed as follows

$$\Delta\Re^{1,n}_{G/W_j}(t_k) = \rho^{1,i}_{G/W_j}(t_k) - \dot{\rho}^{1,i}_{G/W_j}(t_k)\Delta t^1_R + b^1_R(t_k) - \left[\rho^{n,m}_{G/W_j}(t_k) - \dot{\rho}^{n,m}_{G/W_j}(t_k)\Delta t^n_R + b^n_R(t_k) \right] \tag{5.4-6}*$$

where the offset of the true UTC receive time for spacecraft n measurements from the UTC filter state epoch is given by

$$\Delta t^n_R = \left[\left(t_k - t^{(RC)_n}_R \right) + \left(t^{(RC)_n}_R - t^{UTC_n}_R \right) \right] = \left(t_k - t^{(RC)_n}_R \right) + \delta t^n_R = \left(t_k - t^{(RC)_n}_R \right) + \frac{b^n_R(t_k)}{c} \tag{5.4-6a}*$$

Note that in Release 2.7 and prior releases, Δt^n_R is implemented assuming that $t_k = t^{(RC)_n}_R$. This is corrected in Release 2.8.

Note that, if the GPS receiver resets the clock bias whenever it exceeds ±0.5 milliseconds, $\tilde{b}^n_R(t_k)$ defined in Equation (4.3-2a) should be used above instead of $b^n_R(t_k)$.

The row vector of partial derivatives of the singly differenced pseudorange measurement with respect to the estimation state vector, $\overline{X}(t_k)$, is defined as follows:

$$\left[H(t_k) \right]_{\Delta\Re^{1,n}_{G/W_j}} \equiv \frac{\partial \Delta\Re^{1,n}_{G/W_j}(t_k)}{\partial \overline{X}(t_k)} \tag{5.4-7}$$

The partial derivatives with respect to those parameters that are not explicitly included in the differenced pseudorange measurement equation will be zeros. The following are the only nonzero partial derivatives if the state vector consists of absolute states for both the local and remote satellites, where $n > 1$:

$$\frac{\partial \Delta\Re^{1,n}_{G/W\,j}(t_k)}{\partial \overline{R}^{1}(t_k)} = \frac{\partial \rho^{\,1,i}_{G/W\,j}(t_k)}{\partial \overline{R}^{1}(t_k)} - \frac{b^1_R(t_k)}{c}\frac{\partial \dot{\rho}^{1,i}_{G/W_j}(t_k)}{\partial \overline{R}^{1}(t_k)} \tag{5.4-8)*}$$

$$\frac{\partial \Delta\Re^{1,n}_{G/W_j}(t_k)}{\partial \dot{\overline{R}}^{1}(t_k)} = -\frac{b^1_R(t_k)}{c}\frac{\partial \dot{\rho}^{1,i}_{G/W_j}(t_k)}{\partial \dot{\overline{R}}^{1}(t_k)} \tag{5.4-8a)*}$$

$$\frac{\partial \Delta\Re^{1,n}_{G/W_j}(t_k)}{\partial \overline{R}^{\,n}(t_k)} = -\frac{\partial \rho^{\,n,m}_{G/W\,j}(t_k)}{\partial \overline{R}^{\,n}(t_k)} + \frac{b^n_R(t_k)}{c}\frac{\partial \dot{\rho}^{n,m}_{G/W_j}(t_k)}{\partial \overline{R}^{\,n}(t_k)} \tag{5.4-9)*}$$

$$\frac{\partial \Delta\Re^{1,n}_{G/W_j}(t_k)}{\partial \dot{\overline{R}}^{\,n}(t_k)} = \frac{b^n_R(t_k)}{c}\frac{\partial \dot{\rho}^{n,m}_{G/W_j}(t_k)}{\partial \dot{\overline{R}}^{\,n}(t_k)} \tag{5.4-9a)*}$$

$$\frac{\partial \Delta\Re^{1,n}_{G/W_j}(t_k)}{\partial b^1_R(t_k)} = 1 - \frac{\dot{\rho}^{1,i}_{G/W_j}(t_k)}{\mathrm{c}} \tag{5.4-10)*}$$

$$\frac{\partial \Delta\Re^{1,n}_{G/W_j}(t_k)}{\partial b^n_R(t_k)} = -1 + \frac{\dot{\rho}^{n,m}_{G/W_j}(t_k)}{\mathrm{c}} \tag{5.4-10a)*}$$

The partial derivatives of the geometric range and range-rate are defined in Equations (5.3-28b) through (5.3-28d).

If the state vector includes relative states for the nonlocal satellites, the associated nonzero pseudorange measurement partial derivatives are as follows, where $n > 1$:

$$\frac{\partial \Delta\Re^{1,n}_{G/W_j}(t_k)}{\partial \overline{R}^{1}(t_k)} = \frac{\partial \rho^{\,1,i}_{G/W\,j}(t_k)}{\partial \overline{R}^{1}(t_k)} - \frac{b^1_R(t_k)}{c}\frac{\partial \dot{\rho}^{1,i}_{G/W_j}(t_k)}{\partial \overline{R}^{1}(t_k)} - \frac{\partial \rho^{\,n,m}_{G/W\,j}(t_k)}{\partial \overline{R}^{\,n}(t_k)} + \frac{b^n_R(t_k)}{c}\frac{\partial \dot{\rho}^{n,m}_{G/W_j}(t_k)}{\partial \overline{R}^{\,n}(t_k)} \tag{5.4-8b}$$

$$\frac{\partial \Delta\Re^{1,n}_{G/W_j}(t_k)}{\partial \dot{\overline{R}}^{1}(t_k)} = -\frac{b^1_R(t_k)}{c}\frac{\partial \dot{\rho}^{1,i}_{G/W_j}(t_k)}{\partial \dot{\overline{R}}^{1}(t_k)} + \frac{b^n_R(t_k)}{c}\frac{\partial \dot{\rho}^{n,m}_{G/W_j}(t_k)}{\partial \dot{\overline{R}}^{\,n}(t_k)} \tag{5.4-8c)*}$$

$$\frac{\partial \Delta\Re^{1,n}_{G/W_j}(t_k)}{\partial \overline{R}^{\,n}_{rel}(t_k)} = -\frac{\partial \rho^{\,n,m}_{G/W\,j}(t_k)}{\partial \overline{R}^{\,n}(t_k)} + \frac{b^n_R(t_k)}{c}\frac{\partial \dot{\rho}^{n,m}_{G/W_j}(t_k)}{\partial \overline{R}^{\,n}(t_k)} \tag{5.4-9b}$$

$$\frac{\partial \Delta\Re^{1,n}_{G/W_j}(t_k)}{\partial \dot{\overline{R}}^{n}_{rel}(t_k)} = \frac{b^n_R(t_k)}{c}\frac{\partial \dot{\rho}^{n,m}_{G/W_j}(t_k)}{\partial \dot{\overline{R}}^{n}(t_k)} \tag{5.4-9c)*}$$

$$\frac{\partial \Delta\Re^{1,n}_{G/W_j}(t_k)}{\partial b^1_R(t_k)} = -\frac{\dot{\rho}^{1,i}_{G/W_j}(t_k)}{c} + \frac{\dot{\rho}^{n,m}_{G/W_j}(t_k)}{c} \tag{5.4-10b)*}$$

$$\frac{\partial \Delta\Re^{1,n}_{G/W_j}(t_k)}{\partial b^n_{rel}(t_k)} = -1 + \frac{\dot{\rho}^{n,m}_{G/W_j}(t_k)}{c} \tag{5.4-10c)*}$$

5.4.3 Singly Differenced GPS/WAAS Doppler Measurement Model and Associated Partial Derivatives

This section provides the algorithm used to model the observed singly differenced Doppler given by Equation (5.4-3) in terms of the GPS/WAAS and receiver states and the corresponding times. The instantaneous geometric range rate from GPS SV/WAAS GEO j to local receiver 1 and nonlocal receiver i are computed as follows using the algorithms provided in Section 5.3.3

$$\dot{\rho}^{1,i}_{G/W_j}(t_k) = \frac{\hat{\rho}^{1,i}_{G/W_j}(t_k)\cdot\left(\dot{\overline{R}}^{1}(t_k) - \dot{\overline{R}}_{G/W_j}(t'_k)\right)}{1 - \hat{\rho}^{1,i}_{G/W_j}(t_k)\cdot\left(\dot{\overline{R}}_{G/W_j}(t'_k)/c\right)} \tag{5.4-11)*}$$

$$\dot{\rho}^{n,m}_{G/W_j}(t_k) = \frac{\hat{\rho}^{n,m}_{G/W_j}(t_k)\cdot\left(\dot{\overline{R}}^{n}(t_k) - \dot{\overline{R}}_{G/W_j}(t'_k)\right)}{1 - \hat{\rho}^{n,m}_{G/W_j}(t_k)\cdot\left(\dot{\overline{R}}_{G/W_j}(t'_k)/c\right)} \tag{5.4-12)*}$$

where the line-of-sight unit vector, $\hat{\rho}^{n,m}_{G/W_j}$, defined by

$$\hat{\rho}^{n,m}_{G/W_j}(t_k) \equiv \frac{\overline{R}^{n}_{A_m}(t_k) - \overline{R}_{G/W_j}(t'_k)}{\rho^{n,m}_{G/W_j}(t_k)} \tag{5.4-13)*}$$

The singly differenced Doppler measurement is then computed as follows

$$\left(\Delta F_D(t_k)\right)^{1,n}_{G/W_j} = -\frac{F_T}{c}\left[\dot{\rho}^{1,i}_{G/W_j}(t_k) + d^1_R(t_k) - \dot{\rho}^{n,m}_{G/W_j}(t_k) - d^n_R(t_k)\right] \tag{5.4-14)*}$$

The computation of the state partial derivatives of the Doppler shift is presented below. The following are the nonzero elements of the vector of measurement partial derivatives if the state vector consists of absolute states for both the local and remote satellites, where $n > 1$:

$$\frac{\partial\left(\Delta F_D(t_k)\right)^{1,n}_{G/W_j}}{\partial \overline{R}^{1}(t_k)} = -\frac{F_T}{c}\left(\frac{\partial \dot{\rho}^{1,i}_{G/W_j}(t_k)}{\partial \overline{R}^{1}(t_k)}\right) \tag{5.4-15)*}$$

$$\frac{\partial\left(\Delta F_D(t_k)\right)_{G/W_j}^{1,n}}{\partial \dot{\overline{R}}^1(t_k)} = -\frac{F_T}{c}\left(\frac{\partial \dot{\rho}_{G/W_j}^{1,i}(t_k)}{\partial \dot{\overline{R}}^1(t_k)}\right) \tag{5.4-15a)*}$$

$$\frac{\partial\left(\Delta F_D(t_k)\right)_{G/W_j}^{1,n}}{\partial \overline{R}^n(t_k)} = \frac{F_T}{c}\left(\frac{\partial \dot{\rho}_{G/W_j}^{n,m}(t_k)}{\partial \overline{R}^n(t_k)}\right) \tag{5.4-16)*}$$

$$\frac{\partial\left(\Delta F_D(t_k)\right)_{G/W_j}^{1,n}}{\partial \dot{\overline{R}}^n(t_k)} = \frac{F_T}{c}\left(\frac{\partial \dot{\rho}_{G/W_j}^{n,m}(t_k)}{\partial \dot{\overline{R}}^n(t_k)}\right) \tag{5.4-16a)*}$$

$$\frac{\partial\left(\Delta F_D(t_k)\right)_{G/W_j}^{1,n}}{\partial d_R^1(t_k)} = -\frac{F_T}{c} \tag{5.4-17)*}$$

$$\frac{\partial\left(\Delta F_D(t_k)\right)_{G/W_j}^{1,n}}{\partial d_R^n(t_k)} = \frac{F_T}{c} \tag{5.4-17a)*}$$

The state partial derivatives of $\dot{\rho}_{G/W_j}^{n,m}(t_k)$ on the right-hand side of Equations (5.4-15) and (5.4-16) are computed using Equations 5.3-28c and 5.3-28d, where $n > 1$.

If the state vector includes relative states for the nonlocal satellites, the associated nonzero Doppler measurement partial derivatives are as follows, where $n > 1$:

$$\frac{\partial\left(\Delta F_D(t_k)\right)_{G/W_j}^{1,n}}{\partial \overline{R}^1(t_k)} = -\frac{F_T}{c}\left(\frac{\partial \dot{\rho}_{G/W_j}^{1,i}(t_k)}{\partial \overline{R}^1(t_k)} - \frac{\partial \dot{\rho}_{G/W_j}^{n,m}(t_k)}{\partial \overline{R}^n(t_k)}\right) \tag{5.4-17b)*}$$

$$\frac{\partial\left(\Delta F_D(t_k)\right)_{G/W_j}^{1,n}}{\partial \dot{\overline{R}}^1(t_k)} = -\frac{F_T}{c}\left(\frac{\partial \dot{\rho}_{G/W_j}^{1,i}(t_k)}{\partial \dot{\overline{R}}^1(t_k)} - \frac{\partial \dot{\rho}_{G/W_j}^{n,m}(t_k)}{\partial \dot{\overline{R}}^n(t_k)}\right) \tag{5.4-17c)*}$$

$$\frac{\partial\left(\Delta F_D(t_k)\right)_{G/W_j}^{1,n}}{\partial \overline{R}_{rel}^n(t_k)} = \frac{F_T}{c}\left(\frac{\partial \dot{\rho}_{G/W_j}^{n,m}(t_k)}{\partial \overline{R}^n(t_k)}\right) \tag{5.4-17d)*}$$

$$\frac{\partial\left(\Delta F_D(t_k)\right)_{G/W_j}^{1,n}}{\partial \dot{\overline{R}}_{rel}^n(t_k)} = \frac{F_T}{c}\left(\frac{\partial \dot{\rho}_{G/W_j}^{n,m}(t_k)}{\partial \dot{\overline{R}}^n(t_k)}\right) \tag{5.4-17e)*}$$

$$\frac{\partial\left(\Delta F_D(t_k)\right)_{G/W_j}^{1,n}}{\partial d_{R_{rel}}^n(t_k)} = \frac{F_T}{c} \tag{5.4-17f)*}$$

5.4.4 Singly Differenced GPS/WAAS Carrier Phase Measurement Model and Associated Partial Derivatives

This section provides the algorithm used to model the observed singly differenced carrier phase given by Equation (5.4-3a) in terms of the GPS/WAAS and receiver states and the corresponding times and defines the associated partial derivatives.

The predicted singly differenced carrier phase measurement is computed as follows

$$\Delta\Phi^{1,n}_{G/W_j}(t_k) = \rho^{1,i}_{G/W_j}(t_k) - \dot{\rho}^{1,i}_{G/W_j}(t_k)\Delta t^1_R + b^1_R(t_k) - \left[\rho^{n,m}_{G/W_j}(t_k) - \dot{\rho}^{n,m}_{G/W_j}(t_k)\Delta t^n_R + b^n_R(t_k)\right] + b^{G/W_j}_{\Delta\phi_{1n}}(t_k) \quad (5.4\text{-}18)^*$$

where the offset of the true UTC receive time for spacecraft n measurements from the UTC filter state epoch is given by

$$\Delta t^n_R = \left[\left(t_k - t^{(RC)_n}_R\right) + \left(t^{(RC)_n}_R - t^{UTC_n}_R\right)\right] = \left(t_k - t^{(RC)_n}_R\right) + \delta t^n_R = \left(t_k - t^{(RC)_n}_R\right) + \frac{b^n_R(t_k)}{c} \quad (5.4\text{-}18a)^*$$

Note that in Release 2.7 and prior releases, Δt^n_R is implemented assuming that $t_k = t^{(RC)_n}_R$. This is corrected in Release 2.8.

Note that, if the GPS receiver resets the clock bias whenever it exceeds ±0.5 milliseconds, $\tilde{b}^n_R(t_k)$ defined in Equation (4.3-2a) should be used above instead of $b^n_R(t_k)$.

The geometric pseudoranges and instantaneous geometric range rates from GPS SV/WAAS GEO j to local receiver 1 ($\rho^{1,i}_{G/W_j}(t_k), \dot{\rho}^{1,i}_{G/W_j}(t_k)$) and nonlocal receiver n ($\rho^{n,m}_{G/W_j}(t_k), \dot{\rho}^{n,m}_{G/W_j}(t_k)$) are defined in Equations (5.4-4) and (5.4-5).

The singly differenced carrier phase bias $b^{G/W_j}_{\Delta\phi_{1n}}(t_k)$ is the estimated difference between the carrier phase bias between GPS SV/WAAS GEO j and receiver 1 and the carrier phase bias between GPS SV/WAAS GEO j and receiver i at the carrier phase acquisition time (t_{acq}), scaled to meters. The singly differenced carrier phase bias is different for each acquisition of a GPS SV/WAAS GEO by a receiver. Therefore, $b^{G/W_j}_{\Delta\phi_{1n}}(t_k)$ is reinitialized at the start of each acquisition based on the difference between the predicted singly differenced pseudorange $\Delta\Re^{1,n}_{G/W_j}(t_{acq})$ (defined in Equation 5.4-6) and the observed singly differenced carrier phase at the acquisition time t_{acq}:

$$b^{G/W_j}_{\Delta\phi_{1n}}(t_k = t_{acq}) = (\Delta\Phi_{obs})^{1,n}_{G/W_j}(t_{acq}) - \Delta\Re^{1,n}_{G/W_j}(t_{acq}) \quad (5.4\text{-}19)^*$$

Similarly, the singly differenced carrier phase bias variance is reinitialized at the start of each new acquisition to the predicted singly differenced carrier phase residual variance computed as described in Step 3 in Section 2.3.1.

The row vector of partial derivatives of the singly differenced carrier phase measurement with respect to the estimation state vector, $\overline{X}(t_k)$, is defined as follows:

$$\left[H(t_k)\right]_{\Delta\Re^{1,n}_{G/W_j}} \equiv \frac{\partial \Delta\Phi^{1,n}_{G/W_j}(t_k)}{\partial \overline{X}(t_k)} \tag{5.4-20}$$

The partial derivatives with respect to those parameters that are not explicitly included in the differenced carrier phase measurement equation will be zeros. The following are the only nonzero partial derivatives if the state vector consists of absolute states for both the local and remote satellites, where $n > 1$:

$$\frac{\partial \Delta\Phi^{1,n}_{G/W_j}(t_k)}{\partial \overline{R}^1(t_k)} = \frac{\partial \rho^{1,i}_{G/W_j}(t_k)}{\partial \overline{R}^1(t_k)} - \frac{b^1_R(t_k)}{c}\frac{\partial \dot{\rho}^{1,i}_{G/W_j}(t_k)}{\partial \overline{R}^1(t_k)} \tag{5.4-21}*$$

$$\frac{\partial \Delta\Phi^{1,n}_{G/W_j}(t_k)}{\partial \dot{\overline{R}}^1(t_k)} = -\frac{b^1_R(t_k)}{c}\frac{\partial \dot{\rho}^{1,i}_{G/W_j}(t_k)}{\partial \dot{\overline{R}}^1(t_k)} \tag{5.4-22}*$$

$$\frac{\partial \Delta\Phi^{1,n}_{G/W_j}(t_k)}{\partial \overline{R}^n(t_k)} = -\frac{\partial \rho^{n,m}_{G/W_j}(t_k)}{\partial \overline{R}^n(t_k)} + \frac{b^n_R(t_k)}{c}\frac{\partial \dot{\rho}^{n,m}_{G/W_j}(t_k)}{\partial \overline{R}^n(t_k)} \tag{5.4-23}*$$

$$\frac{\partial \Delta\Phi^{1,n}_{G/W_j}(t_k)}{\partial \dot{\overline{R}}^n(t_k)} = \frac{b^n_R(t_k)}{c}\frac{\partial \dot{\rho}^{n,m}_{G/W_j}(t_k)}{\partial \dot{\overline{R}}^n(t_k)} \tag{5.4-24}*$$

$$\frac{\partial \Delta\Phi^{1,n}_{G/W_j}(t_k)}{\partial b^1_R(t_k)} = 1 - \frac{\dot{\rho}^{1,i}_{G/W_j}(t_k)}{\mathrm{c}} \tag{5.4-25}*$$

$$\frac{\partial \Delta\Phi^{1,n}_{G/W_j}(t_k)}{\partial b^n_R(t_k)} = -1 + \frac{\dot{\rho}^{n,m}_{G/W_j}(t_k)}{\mathrm{c}} \tag{5.4-26}*$$

$$\frac{\partial \Delta\Phi^{1,n}_{G/W_j}(t_k)}{\partial \Delta b^{G/W_j}_{\phi 1n}(t_k)} = 1 \tag{5.4-27}*$$

The partial derivatives of the geometric range and range-rate are defined in Equations (5.3-28b) through (5.3-28d).

If the state vector includes relative states for the nonlocal satellites, the associated nonzero singly difference carrier phase measurement partial derivatives are as follows, where $n > 1$:

$$\frac{\partial \Delta\Phi^{1,n}_{G/W_j}(t_k)}{\partial \overline{R}^1(t_k)} = \frac{\partial \rho^{1,i}_{G/W_j}(t_k)}{\partial \overline{R}^1(t_k)} - \frac{b^1_R(t_k)}{c}\frac{\partial \dot{\rho}^{1,i}_{G/W_j}(t_k)}{\partial \overline{R}^1(t_k)} - \frac{\partial \rho^{n,m}_{G/W_j}(t_k)}{\partial \overline{R}^n(t_k)} + \frac{b^n_R(t_k)}{c}\frac{\partial \dot{\rho}^{n,m}_{G/W_j}(t_k)}{\partial \overline{R}^n(t_k)} \tag{5.4-28}$$

$$\frac{\partial \Delta\Phi^{1,n}_{G/W_j}(t_k)}{\partial \dot{\bar{R}}^1(t_k)} = -\frac{b^1_R(t_k)}{c}\frac{\partial \dot{\rho}^{1,i}_{G/W_j}(t_k)}{\partial \dot{\bar{R}}^1(t_k)} + \frac{b^n_R(t_k)}{c}\frac{\partial \dot{\rho}^{n,m}_{G/W_j}(t_k)}{\partial \dot{\bar{R}}^n(t_k)} \quad (5.4\text{-}29)^*$$

$$\frac{\partial \Delta\Phi^{1,n}_{G/W_j}(t_k)}{\partial \bar{R}^n_{rel}(t_k)} = -\frac{\partial \rho^{n,m}_{G/W_j}(t_k)}{\partial \bar{R}^n(t_k)} + \frac{b^n_R(t_k)}{c}\frac{\partial \dot{\rho}^{n,m}_{G/W_j}(t_k)}{\partial \bar{R}^n(t_k)} \quad (5.4\text{-}30)$$

$$\frac{\partial \Delta\Phi^{1,n}_{G/W_j}(t_k)}{\partial \dot{\bar{R}}^n_{rel}(t_k)} = \frac{b^n_R(t_k)}{c}\frac{\partial \dot{\rho}^{n,m}_{G/W_j}(t_k)}{\partial \dot{\bar{R}}^n(t_k)} \quad (5.4\text{-}31)^*$$

$$\frac{\partial \Delta\Phi^{1,n}_{G/W_j}(t_k)}{\partial b^1_R(t_k)} = -\frac{\dot{\rho}^{1,i}_{G/W_j}(t_k)}{c} + \frac{\dot{\rho}^{n,m}_{G/W_j}(t_k)}{c} \quad (5.4\text{-}32)^*$$

$$\frac{\partial \Delta\Phi^{1,n}_{G/W_j}(t_k)}{\partial b^n_{rel}(t_k)} = -1 + \frac{\dot{\rho}^{n,m}_{G/W_j}(t_k)}{\mathrm{c}} \quad (5.4\text{-}33)^*$$

$$\frac{\partial \Delta\Phi^{1,n}_{G/W_j}(t_k)}{\partial \Delta b^{G/W_j}_{\phi 1n}(t_k)} = 1 \quad (5.4\text{-}34)^*$$

5.5 Cross-Link Measurement Models

The computational algorithms for the one-way and round-trip cross-link measurement types are discussed in this section. The general form of the measurement model is as follows:

$$Y_k = G\ [\bar{X}(t_k),\ t_k] + \varepsilon \tag{5.5-1}$$

where t_k^{UTC} is the true measurement time, referenced to UTC, and ε is the measurement error.

For GEONS, the estimation state vector, $\overline{X(t)}$ includes the receiver position vector, $\overline{R}$; velocity vector, $\dot{\overline{R}}$; optional corrections to the drag and solar radiation pressure coefficients, ΔC_D and ΔC_R; GPS receiver bias, b_R; and GPS receiver drift, $\dot{d}_R$, for one or more receivers and tracking-system dependent biases. For ground-based receivers, corrections to the drag and solar radiation pressure coefficients are not estimated.

The measurement model for the one-way pseudorange measurements from a remote transmitter to a local receiver is presented in Section 5.5.1. The one-way Doppler measurement model is defined in Section 5.5.2. The round-trip crosslink range and Doppler measurement models are defined in Sections 5.5.3 and 5.5.4, respectively.

5.5.1 One-Way Cross-Link Pseudorange Measurement Model and Associated Partial Derivatives

The one-way cross-link pseudorange is obtained by measuring the signal transit time interval, which is defined as

$$\Delta\tau \equiv t_R^{(RC)} - t_T^{(TC)} \tag{5.5-2}$$

where $t_R^{(RC)}$ denotes the receive time measured by the receiver clock and $t_T^{(TC)}$ is the transmit time measured by the transmitter clock. The cross-link pseudorange $\Re$ is then defined as the speed of light (c) times the time interval $\Delta\tau$ given by Equation (5.5-2):

$$\Re^{CL} \equiv c\,\Delta\tau \tag{5.5-3}$$

Equation (5.5-2) can be written in terms of the true UTC times t_R^{UTC} and t_T^{UTC} corresponding to $t_R^{(RC)}$ and $t_T^{(TC)}$ and the respective receiver clock offset terms δt_R and δt_T as follows:

$$\begin{aligned}\Delta\tau &= (t_R^{UTC} + \delta t_R) - (t_T^{UTC} + \delta t_T) \\ &\equiv \Delta t + (\delta t_R - \delta t_T)\end{aligned} \tag{5.5-4}$$

where

$$\Delta t \equiv t_R^{UTC} - t_T^{UTC} \tag{5.5-5}$$

The definition of the one-way crosslink pseudorange can be written as

$$\Re^{CL1} = c\Delta t + c(\delta t_R - \delta t_T) \tag{5.5-6}$$

The time interval Δt appearing in the first term on the right-hand side of Equation (5.5-6) represents the true signal travel time from the transmitting spacecraft to the receiver. The first term on the right-hand side of Equation (5.5-6) can be expressed as

$$c\Delta t = \rho + \delta\rho_{iono} + \delta\rho_{hw} \tag{5.5-7}$$

with

$$\rho = \left| \overline{R}^R_{A_m}(t_R^{UTC}) - \overline{R}^T_{A_i}(t_T^{UTC}) \right| \tag{5.5-8}$$

In the above equation, ρ denotes the geometric distance between the position of the transmitting satellite's antenna at the true signal transmit time t_T^{UTC} and the position of the receiver's antenna at the true signal receive time t_R^{UTC} . The second term represents the time delay due to ionospheric refraction effects and the third term represents a (receiver and/or transmitter) hardware-related delay. In Equation (5.5-8), the position of the transmitting satellite's antenna (i) at the time of signal transmission is denoted by $\overline{R}^T_{A_i}(t_T^{UTC})$, and the position of the receiving antenna (m) at the time of the signal reception is denoted by $\overline{R}^R_{A_m}(t_R^{UTC})$.

Combining Equations (5.5-6) and (5.5-7), the following expression for the cross-link pseudorange is obtained:

$$\Re^{CL1} = \rho + b_\rho^{CL1} + c\left(\delta t_R - \delta t_T\right) \tag{5.5-9}$$

with

$$\rho = \left| \overline{R}^R_{A_m}(t_R^{UTC}) - \overline{R}^T_{A_i}(t_T^{UTC}) \right| \tag{5.5-10}$$

$$b_\rho^{CL1} = \delta\rho_{iono} + \delta\rho_{hw} \tag{5.5-11}$$

where b_ρ^{CL1} is the cross-link pseudorange bias exclusive of clock bias effects, an optional element of the estimated state vector defined in Section 4.3.

The following Newton-Raphson iterative scheme is used to solve for the signal transmit time, t_T:

$$t_{T,n+1} = t_R - \frac{\left| \overline{R}^R_{A_m}(t_R) - \overline{R}^T_{A_i}(t_{T,n}) \right|}{c} \tag{5.5-12}*$$

where

$t_{T,n+1}$ = $(n+1)^{th}$ approximation for t_T

$t_{T,n}$ = n^{th} approximation for t_T

t_R = signal reception time at the receiving spacecraft

The iterative solution of the above equation is started by setting $t_{T,0} = t_R$, such that $\overline{R}^T(t_{T,0}) = \overline{R}^T(t_R)$.

The position of the transmitter at time $t_{T,n}$ is computed using linear interpolation. This iterative scheme is continued until the condition $\left|t_{T,n+1} - t_{T,n}\right| \le \varepsilon$ is satisfied, where ε is a small tolerance (nominally equal to 10^{-8} second).

Generalizing Equations (5.5-9) through (5.5-10) to a formation of N_S satellites yields

$$\Re_{nj}^{CL1}(t_R^{UTC}) = \rho^{nj}(t_R^{UTC}) + b_{\rho_j}^{CL1}(t_R^{UTC}) + c\left(\delta t_R^n - \delta t_T^j\right); \quad n = 1,..,N_S;\ j = 1,..,N_S;\ j \neq n \quad (5.5\text{-}13)$$

$$\rho^{nj}(t_R^{UTC}) = \left|\overline{R}_{A_m}^n(t_R^{UTC}) - \overline{R}_{A_i}^j(t_T^{UTC})\right|; \quad n = 1,..,N_S;\ j = 1,..,N_S;\ j \neq n \quad (5.5\text{-}14)$$

where satellite *n* is the receiving satellite and satellite *j* is the transmitting satellite. The position of the j transmitting satellites can either be estimated or obtained from an ephemeris message provided via the cross-link communications signal. The cross-link pseudorange bias, $b_{\rho_j}^{CL1}$, is defined in Section 4.3. The position of each cross-link transmitting and receiving antenna is computed using Equation 3.2-61 in Section 3.2.8. In Equation 3.2-61, the position of the receiving satellite is always a component of the estimated state vector and the position of the transmitting satellite can be either a component of the estimated state vector or a state vector that is either propagated or extracted from a ephemeris file (ground processing only). The transmitter and receiver clock offsets are related to the time bias estimates for the transmitting and receiving satellites at t_R^{UTC} as follows:

$$\begin{aligned} c\delta t_R^n &= b_R^n(t_R^{UTC}) \\ c\delta t_T^j &= b_R^j(t_T^{UTC}) = b_R^j(t_R^{UTC}) - d_R^j(t_R^{UTC}) \cdot \Delta t \end{aligned} \quad (5.5\text{-}14a)$$

The receiver timetags each crosslink measurement using the measured receive time, $t_k = t_R^{(RC)}$. To account for the offset of the measured receive time from the true UTC receive time, $t_R^{UTC} = t_k - \delta t_R$, Equation (5.5-14) is linearized about the measured receive time:

$$\rho^{nj}(t_R^{UTC}) = \rho^{nj}(t_k) - \dot{\rho}^{nj}(t_k)\delta t_R \quad (5.5\text{-}14b)$$

where

$$\rho^{nj}(t_k) = \left|\overline{R}_{A_m}^n(t_k) - \overline{R}_{A_i}^j(t_k')\right|; \quad n = 1,..,N_S;\ j = 1,..,N_S;\ j \neq n \quad (5.5\text{-}14c)^*$$

$$\dot{\rho}^{nj}(t_k) = \frac{\hat{\rho}^{nj}(t_k) \cdot \left(\dot{\overline{R}}_{A_m}^n(t_k) - \dot{\overline{R}}_{A_i}^{\ j}(t_k')\right)}{1 - \hat{\rho}^{nj}(t_k) \cdot \left(\dot{\overline{R}}_{A_i}^{\ j}(t_k')/c\right)} \quad (5.5\text{-}14d)^*$$

$$\hat{\rho}^{nj}(t_k) = \frac{\overline{R}^{n}_{A_m}(t_k) - \overline{R}^{j}_{A_i}(t'_k)}{\left|\overline{R}^{n}_{A_m}(t_k) - \overline{R}^{j}_{A_i}(t'_k)\right|} \qquad \text{(5.3-14e)*}$$

where t'_k is the signal transmission time computed based on the measured receive time. The position and velocity of each cross-link transmitting and receiving antenna are computed using Equation 3.2-61 in Section 3.2.8. Using this approximation, Equation (5.5-13) can be rewritten in terms of quantities computed at the measured receive time:

$$\Re^{CL1}_{nj}(t_R^{UTC_n}) \cong \left[\rho^{nj}(t_k) - \dot{\rho}^{nj}(t_k)\Delta t^n_R + b^{CL1}_{\rho_j}(t_k)\right]\left[1 + \frac{d^j_R(t_k)}{c}\right] + b^n_R(t_k) - b^j_R(t_k) + b_2(t_k); \quad n = 1,..,N_S;\ j = 1,..,N_S;\ j \neq n \qquad \text{(5.5-14f)*}$$

where the offset of the true UTC receive time for spacecraft n measurements from the UTC filter state epoch is given by

$$\Delta t^n_R = \left[\left(t_k - t_R^{(RC)_n}\right) + \left(t_R^{(RC)_n} - t_R^{UTC_n}\right)\right] = \left(t_k - t_R^{(RC)_n}\right) + \delta t^n_R = \left(t_k - t_R^{(RC)_n}\right) + \frac{b^n_R(t_k)}{c} \qquad \text{(5.5-14g)*}$$

Note that in Release 2.7 and prior releases, Δt^n_R is implemented assuming that $t_k = t_R^{(RC)_n}$. This is corrected in Release 2.8. The optional cross-link pseudorange bias state, $b^{CL1}_{\rho_j}$, and associated covariance are reset when a programmable time lapse is detected in the provided measurement.

In Equation 5.5-14f, the additional bias term $b_2(t_k)$ is a correction developed in Reference 47 to account for second-order effects that can be significant prior to convergence of the absolute filter states. Optionally, this second-order bias is computed as follows

$$b_2 = \frac{1}{2} trace(D^{nj} P^{rel,nj}_{k,pos});\ 1 \le n \le N_S; 1 \le j \le N_S;\ j \neq n \qquad \text{(5.5-14h)*}$$

The 3x3 relative covariance submatrix of the relative position of satellite n with respect to satellite j is defined as

$$P^{rel,nj}_{k,pos} = E\left(\left[\left(\hat{\overline{R}}^{n}(t_k) - \hat{\overline{R}}^{j}(t_k)\right) - \left(\overline{R}^{n}(t_k) - \overline{R}^{j}(t_k)\right)\right]\left[\left(\hat{\overline{R}}^{n}(t_k) - \hat{\overline{R}}^{j}(t_k)\right) - \left(\overline{R}^{n}(t_k) - \overline{R}^{j}(t_k)\right)\right]^T\right) \qquad \text{(5.5-14i)}$$

If absolute states are being estimated, this submatrix is computed using components of the absolute covariance matrix

$$P^{rel,nj}_{k,pos} = [P]^{nn}_{pos} + [P]^{jj}_{pos} - [P]^{nj}_{pos} - [P]^{jn}_{pos} \qquad \text{(5.5-14j)*}$$

where $[P]^{nj}_{pos}$ is the 3x3 submatrix of the full absolute predicted covariance matrix $[P]$ corresponding to the covariance of the satellite n position and the satellite j position. In the case where satellite j is not being estimated (i.e. its location is provided in a precise ephemeris), $P^{rel,nj}_{k,pos} = [P]^{nn}_{pos}$.

If relative states are being estimated, the $P_{k,pos}^{rel,nj}$ submatrix is computed using components of the relative covariance matrix $\left[P_{rel}\right]$

$$P_{k,pos}^{rel,nj} = \begin{cases} E\left(\left[\left(\hat{\bar{R}}^{n}(t_k)-\bar{R}^{n}(t_k)\right)\right]\left[\left(\hat{\bar{R}}^{n}(t_k)-\bar{R}^{n}(t_k)\right)\right]^{T}\right); \text{ satellite j is not estimated} \\ E\left(\left[\left(\hat{\bar{R}}^{n}(t_k)-\bar{R}^{n}(t_k)\right)-\left(\hat{\bar{R}}^{1}(t_k)-\bar{R}^{1}(t_k)\right)\right]\left[\left(\hat{\bar{R}}^{n}(t_k)-\bar{R}^{n}(t_k)\right)-\left(\hat{\bar{R}}^{1}(t_k)-\bar{R}^{1}(t_k)\right)\right]^{T}\right); \text{ n} \neq 1, \text{j} = 1 \\ E\left(\left[\left(\hat{\bar{R}}^{1}(t_k)-\bar{R}^{1}(t_k)\right)-\left(\hat{\bar{R}}^{j}(t_k)-\bar{R}^{j}(t_k)\right)\right]\left[\left(\hat{\bar{R}}^{1}(t_k)-\bar{R}^{1}(t_k)\right)-\left(\hat{\bar{R}}^{j}(t_k)-\bar{R}^{j}(t_k)\right)\right]^{T}\right); \text{ n} = 1, \text{j} \neq 1 \\ E\left(\left[\left(\hat{\bar{R}}_{rel}^{n}(t_k)-\bar{R}_{rel}^{n}(t_k)\right)-\left(\hat{\bar{R}}_{rel}^{j}(t_k)-\bar{R}_{rel}^{j}(t_k)\right)\right]\left[\left(\hat{\bar{R}}_{rel}^{n}(t_k)-\bar{R}_{rel}^{n}(t_k)\right)-\left(\hat{\bar{R}}_{rel}^{j}(t_k)-\bar{R}_{rel}^{j}(t_k)\right)\right]^{T}\right); \text{ otherwise} \end{cases} \quad \text{(5.5-14k)*}$$

$$= \begin{cases} \left[P_{rel}\right]_{pos}^{nn}; \text{ satellite j is not estimated} \\ \left[P_{rel}\right]_{pos}^{nn}; \text{ n} \neq 1, \text{j} = 1 \\ \left[P_{rel}\right]_{pos}^{jj}; \text{ n} = 1, \text{j} \neq 1 \\ \left[P_{rel}\right]_{pos}^{nn} + \left[P_{rel}\right]_{pos}^{jj} - \left[P_{rel}\right]_{pos}^{nj} - \left[P_{rel}\right]_{pos}^{jn}; \text{ otherwise} \end{cases}$$

where

$$\bar{R}_{rel}^{n}(t_k) = \begin{cases} \bar{R}^{1}(t_k), & n = 1 \\ \bar{R}^{n}(t_k) - \bar{R}^{1}(t_k), & n > 1 \end{cases}$$

and $P_{k,pos_{nj}}^{rel}$ is the 3x3 submatrix of the full **relative** predicted covariance matrix $\left[P_{rel}\right]$ corresponding to the covariance of the satellite n relative position and the satellite j relative position.

The 3x3 D^{nj} matrix is given by

$$D^{nj} = \frac{\partial \hat{\rho}^{nj}}{\partial \bar{R}^{n}} = \frac{1}{\rho^{nj}}\left(I - \hat{\rho}^{nj}\left(\hat{\rho}^{nj}\right)^{T}\right) \quad \text{(5.5-14l)*}$$

where the range vector, geometric range, and range unit vector are given by

$$\bar{\rho}^{nj}(t_k) = \bar{R}_{A_m}^{n}(t_k) - \bar{R}_{A_i}^{j}(t_k') \quad \text{(5.5-14m)}$$

$$\rho^{nj}(t_k) = \left|\bar{\rho}^{nj}(t_k)\right| \quad \text{(5.5-14n)}$$

$$\hat{\rho}^{nj}(t_k) = \frac{\bar{\rho}^{nj}(t_k)}{\rho^{nj}(t_k)} \quad \text{(5.5-14o)}$$

When the second-order correction term $b_2(t_k)$ is included in the predicted measurement, a second-order variance correction term B_k is also included in the cross-link range measurement variance calculation such that

$$V_k = H_k P_k H_k^{T} + R_k + B_k \quad \text{(5.5-14p)*}$$

This is done by augmenting the value of a_0 used to start the recursive computation of V_k discussed in Section 2.3, such that:

$$a_0 = R_k + B_k \tag{5.5-14q)*}$$

where the second order variance term B_k for a cross-link range measurement is given by

$$B_k = \frac{1}{2} trace(D^{nj} P^{rel}_{k,pos_{nj}} D^{nj} P^{rel}_{k,pos_{nj}}) \tag{5.5-14r)*}$$

The matrix (a row vector in this case) of partial derivatives of the pseudorange measurement with respect to the estimation state vector, $\overline{X}(t_k)$, is defined as follows when $\overline{X}(t_k)$ consists of N_S satellite state vectors:

$$\left[H(t_k)\right]_{\Re^{CL}_{nj}} \equiv \frac{\partial \Re^{CL}_{nj}(t_k)}{\partial \overline{X}(t_k)}; \quad n = 1,..,N_S;\ j = 1,..,N_S;\ j \neq n \tag{5.5-15}$$

The following are the nonzero elements of the partial derivative vector when the estimation state vector consists of absolute state vectors for the receiving satellite *n* and the transmitting satellite *j,* omitting terms of $O(\frac{1}{c^2})$ and higher*:*

$$\frac{\partial \Re^{CL1}_{nj}(^{UTC}_{R})}{\partial \overline{R}^{n}(t_k)} = \left[1 + \frac{d^j_R(t_k)}{c}\right] \frac{\partial \rho^{nj}(t_k)}{\partial \overline{R}^{n}(t_k)} - \frac{b^n_R(t_k)}{c} \frac{\partial \dot{\rho}^{nj}(t_k)}{\partial \overline{R}^{n}(t_k)} \tag{5.5-16)*}$$

$$\frac{\partial \Re^{CL1}_{nj}(t^{UTC}_R)}{\partial \dot{\overline{R}}^{n}(t_k)} = -\frac{b^n_R(t_k)}{c} \frac{\partial \dot{\rho}^{nj}(t_k)}{\partial \dot{\overline{R}}^{n}(t_k)} \tag{5.5-16a)*}$$

$$\frac{\partial \Re^{CL1}_{nj}(^{UTC}_{R})}{\partial \overline{R}^{j}(t_k)} = \left[1 + \frac{d^j_R(t_k)}{c}\right] \frac{\partial \rho^{nj}(t_k)}{\partial \overline{R}^{j}(t_k)} - \frac{b^n_R(t_k)}{c} \frac{\partial \dot{\rho}^{nj}(t_k)}{\partial \overline{R}^{j}(t_k)} \tag{5.5-16b)*}$$

$$\frac{\partial \Re^{CL1}_{nj}(t^{UTC}_R)}{\partial \dot{\overline{R}}^{j}(t_k)} = -\frac{b^n_R(t_k)}{c} \frac{\partial \dot{\rho}^{nj}(t_k)}{\partial \dot{\overline{R}}^{j}(t_k)} \tag{5.5-16c)*}$$

$$\frac{\partial \Re^{CL1}_{nj}(t^{UTC}_R)}{\partial b^{CL1}_{\rho_j}(t_k)} = 1 + \frac{d^j_R(t_k)}{c} \tag{5.5-17)*}$$

$$\frac{\partial \Re^{CL1}_{nj}(t^{UTC}_R)}{\partial b^{n}_R(t_k)} = 1 - \frac{\dot{\rho}^{nj}(t_k)}{c} \tag{5.5-17a)*}$$

$$\frac{\partial \Re^{CL1}_{nj}(t^{UTC}_R)}{\partial b^{j}_R(t_k)} = -1 \tag{5.5-17b)*}$$

$$\frac{\partial \Re_{nj}^{CL1}(t_R^{UTC})}{\partial d_R^j(t_k)} = \frac{1}{c}\left[\rho^{nj}(t_k)\right] \tag{5.5-17c)*}$$

where

$$\frac{\partial \rho^{nj}(t_k)}{\partial \overline{R}^n(t_k)} = \hat{\rho}^{nj}(t_k)^T \tag{5.5-17d)*}$$

$$\frac{\partial \dot{\rho}^{nj}(t_k)}{\partial \overline{R}^n(t_k)} = \frac{\left[\left(\dot{\overline{R}}_{A_m}{}^n(t_k) - \dot{\overline{R}}_{A_i}{}^j(t_k')\right) - \dot{\rho}^{nj}(t_k)\left[\hat{\rho}^{nj}(t_k) - \frac{\dot{\overline{R}}_{A_i}{}^j(t_k')}{c}\right]\right]^T}{\rho^{nj}(t_k)\left[1 - \hat{\rho}^{nj}(t_k)\cdot\left(\dot{\overline{R}}_{A_i}{}^j(t_k')/c\right)\right]} \tag{5.5-17e)*}$$

$$\frac{\partial \dot{\rho}^{nj}(t_k)}{\partial \dot{\overline{R}}^n(t_k)} = \frac{\left(\hat{\rho}^{nj}(t_k)\right)^T}{1 - \hat{\rho}^{nj}(t_k)\cdot\left(\dot{\overline{R}}_{A_i}{}^j(t_k')/c\right)} \tag{5.5-17f)*}$$

$$\frac{\partial \rho^{nj}(t_k)}{\partial \overline{R}^j(t_k)} = -\hat{\rho}^{nj}(t_k)^T \tag{5.5-17g)*}$$

$$\frac{\partial \dot{\rho}^{nj}(t_k)}{\partial \overline{R}^j(t_k)} = \frac{-\left[\left(\dot{\overline{R}}_{A_m}{}^n(t_k) - \dot{\overline{R}}_{A_i}{}^j(t_k')\right) - \dot{\rho}^{nj}(t_k)\left[\hat{\rho}^{nj}(t_k) - \frac{\dot{\overline{R}}_{A_i}{}^j(t_k')}{c}\right]\right]^T}{\rho^{nj}(t_k)\left[1 - \hat{\rho}^{nj}(t_k)\cdot\left(\dot{\overline{R}}_{A_i}{}^j(t_k')/c\right)\right]} \tag{5.5-17h)*}$$

$$\frac{\partial \dot{\rho}^{nj}(t_k)}{\partial \dot{\overline{R}}^j(t_k)} = \frac{-\left(\hat{\rho}^{nj}(t_k)\right)^T\left[1 - \dot{\rho}^{nj}(t_k)/c\right]}{\left[1 - \hat{\rho}^{nj}(t_k)\cdot\left(\dot{\overline{R}}_{A_i}{}^j(t_k')/c\right)\right]} \tag{5.5-17i)*}$$

If the estimation state vector consists of an absolute state for the local satellite (1) and relative states for the remote satellites (>1), where *n* and *j* are >1 -- Note that this option is not implemented in GEONS 3.0:

:

$$\begin{aligned} \frac{\partial \Re_{1j}^{CL1}(t_k)}{\partial \overline{R}^1(t_k)} &= 0 \\ \frac{\partial \Re_{1j}^{CL1}(t_k)}{\partial \dot{\overline{R}}^1(t_k)} &= 0 \end{aligned} \quad \text{(omitting terms of O}(\frac{1}{c^2})\text{)} \tag{5.5-17j)*}$$

$$\frac{\partial \Re_{n1}^{CL1}(t_k)}{\partial \overline{R}^1(t_k)} = 0$$
$$\frac{\partial \Re_{n1}^{CL1}(t_k)}{\partial \dot{\overline{R}}^1(t_k)} = 0 \quad \text{(omitting terms of O}(\frac{1}{c^2}) \tag{5.5-17k)*}$$

The following are the nonzero partial derivatives of the one-way crosslink pseudorange measurement, omitting terms of $O(\frac{1}{c^2})$ and higher:

$$\frac{\partial \Re_{nj}^{CL1}(t_R^{UTC})}{\partial \overline{R}_{rel}^n(t_k)} = \frac{\partial \Re_{nj}^{CL1}(t_R^{UTC})}{\partial \overline{R}^n(t_k)} \frac{\partial \overline{R}^n(t_k)}{\partial \overline{R}_{rel}^n(t_k)} = \left[1 + \frac{d_R^j(t_k)}{c}\right] \frac{\partial \rho^{nj}(t_k)}{\partial \overline{R}^n(t_k)} - \frac{b_R^n(t_k)}{c} \frac{\partial \dot{\rho}^{nj}(t_k)}{\partial \overline{R}^n(t_k)}$$
$$\frac{\partial \Re_{nj}^{CL1}(t_R^{UTC})}{\partial \dot{\overline{R}}_{rel}^n(t_k)} = \frac{\partial \Re_{nj}^{CL1}(t_R^{UTC})}{\partial \dot{\overline{R}}^n(t_k)} \frac{\partial \dot{\overline{R}}^n(t_k)}{\partial \dot{\overline{R}}_{rel}^n(t_k)} = -\frac{b_R^n(t_k)}{c} \frac{\partial \dot{\rho}^{nj}(t_k)}{\partial \dot{\overline{R}}^n(t_k)} \quad \text{for } n > 1; j = 1,..., N_S; n \neq j \tag{5.5-17l)*}$$

$$\frac{\partial \Re_{nj}^{CL1}(t_R^{UTC})}{\partial \overline{R}_{rel}^j(t_k)} = \frac{\partial \Re_{nj}^{CL1}(t_R^{UTC})}{\partial \overline{R}^j(t_k)} \frac{\partial \overline{R}^j(t_k)}{\partial \overline{R}_{rel}^j(t_k)} = \left[1 + \frac{d_R^j(t_k)}{c}\right] \frac{\partial \rho^{nj}(t_k)}{\partial \overline{R}^j(t_k)} - \frac{b_R^n(t_k)}{c} \frac{\partial \dot{\rho}^{nj}(t_k)}{\partial \overline{R}^j(t_k)}$$
$$\frac{\partial \Re_{nj}^{CL1}(t_R^{UTC})}{\partial \dot{\overline{R}}_{rel}^j(t_k)} = \frac{\partial \Re_{nj}^{CL1}(t_R^{UTC})}{\partial \dot{\overline{R}}^j(t_k)} \frac{\partial \dot{\overline{R}}^j(t_k)}{\partial \dot{\overline{R}}_{rel}^j(t_k)} = -\frac{b_R^n(t_k)}{c} \frac{\partial \dot{\rho}^{nj}(t_k)}{\partial \dot{\overline{R}}^j(t_k)} \quad \text{for } n = 1,..., N_S; j > 1; n \neq j \tag{5.5-17m)*}$$

$$\frac{\partial \Re_{nj}^{CL1}(t_k)}{\partial b_{\rho_j}^{CL1}(t_k)} = 1 + \frac{d_R^j(t_k)}{c} \quad \text{for } n = 1,..., N_S; j = 1,..., N_S; n \neq j \tag{5.5-17n)*}$$

$$\frac{\partial \Re_{nj}^{CL1}(t_R^{UTC})}{\partial b_R^1(t_k)} = -\frac{\dot{\rho}^{nj}(t_k)}{c} \quad \text{for } n = 1,..., N_S; j = 1,..., N_S; n \neq j \tag{5.5-17o)*}$$

$$\frac{\partial \Re_{nj}^{CL}(t_R^{UTC})}{\partial d_R^1(t_k)} = \frac{1}{c}\left[\rho^{nj}(t_k) + b_{\rho_j}^{CL1}(t_k)\right] \quad \text{for } n = 1,..., N_S; j = 1,..., N_S; n \neq j \tag{5.5-17p)*}$$

$$\frac{\partial \Re_{nj}^{CL1}(t_R^{UTC})}{\partial b_{R_{rel}}^n(t_k)} = 1 - \frac{\dot{\rho}^{nj}(t_k)}{c} \quad \text{for } n > 1; j = 1,..., N_S; n \neq j \tag{5.5-17q)*}$$

$$\frac{\partial \Re_{nj}^{CL1}(t_R^{UTC})}{\partial b_{R_{rel}}^j(t_k)} = -1 \quad \text{for } n = 1,..., N_S; j > 1; n \neq j \tag{5.5-17r)*}$$

$$\frac{\partial \Re_{nj}^{CL}(t_R^{UTC})}{\partial d_{R_{rel}}^j(t_k)} = \frac{1}{c}\left[\rho^{nj}(t_k) + b_{\rho_j}^{CL1}(t_k)\right] \quad \text{for } n = 1,..., N_S; j > 1; n \neq j \tag{5.5-17s)*}$$

Computations of measurements and associated partial derivatives are performed using state vectors given in the mean of J2000.0 coordinate system.

5.5.2 One-Way Cross-Link Averaged Doppler Measurement Model and Associated Partial Derivatives

An instantaneous Doppler shift between transmitting satellite j and receiving satellite n can be defined as

$$F_{D_{nj}}^{CL1}(t) = F_R(t) - F_{REF}(t) \tag{5.5-18}$$

where

$F_R(t)$ = Doppler-shifted cross-link carrier frequency

$F_{REF}(t)$ = receiver-generated local reference frequency

When the receiver and the transmitter use the same frequency standards, the receiver-generated reference frequency, F_{REF}, will be equal to the transmit frequency, F_T. For cross-link tracking, this is not the case. There will be small difference between the two frequency standards used by the receiver and the transmitter.

The procedures to compute the instantaneous (not implemented in Release 2.2) and averaged one-way cross-link Doppler shift are presented below. The first term on the right-hand side of Equation (5.5-18), F_R, the instantaneous Doppler shifted carrier frequency observed at the receiver, can be represented by the following equation:

$$F_R = F_T'\left(1 - \frac{\dot{\rho}^{nj}}{c}\right) + \delta F_{atm} \tag{5.5-19}$$

where

F_T' = true cross-link transmit frequency

$\dot{\rho}^{nj}$ = time rate of change of the light-time-corrected range from transmitting antenna i on satellite j to receiving antenna m on satellite n [defined in Equation (5.5-14d)]

δF_{atm} = frequency perturbation due to the atmospheric refraction effects

The second term on the right-hand side of Equation (5.5-18), $F_{REF}(t)$, the receiver-generated reference frequency, can be written as

$$F_{REF}(t) = F_T + \delta F_{REF} = F_T\left(1 + \frac{d_R^n(t)}{c}\right) \tag{5.5-20}$$

where $d_R^n(t)$ is the receiver's time bias rate. In Equation (5.5-20), F_T denotes the nominal transmit frequency, which may be different from the actual transmit frequency, F_T', used in Equation (5.5-19),

$$F_T'(t) = F_T + \delta F_T = F_T\left(1 + \frac{d_R^j(t)}{c}\right) \tag{5.5-21}$$

where $d_R^j(t)$ is the transmitter's time bias rate. Using Equations (5.5-19) through (5.5-21), Equation (5.5-18) can be written as

$$F_{D_{nj}}^{CL1} = F_T\left(1 + \frac{d_R^j(t)}{c}\right)\left(1 - \frac{\dot{\rho}^{nj}}{c}\right) - F_T\left(1 + \frac{d_R^n(t)}{c}\right) + \delta F_{atm} \tag{5.5-22}$$

Neglecting terms of $O(\frac{1}{c^2})$ and higher, the instantaneous one-way Doppler shift reduces to

$$F_{D_{nj}}^{CL1}(t_k) = -\frac{F_T}{c}\left(\dot{\rho}^{nj}(t) + d_R^n - d_R^j\right) + \delta F_{atm} \tag{5.5-23}$$

In the case of receivers that provide an instantaneous Doppler shift measurement, the instantaneous Doppler shift from antenna i on the jth transmitter to antenna m on the receiving satellite n is modeled as follows:

$$F_{D_{nj}}^{CL1}(t_k) = -\frac{F_T}{c}\left(\dot{\rho}^{nj}(t) + d_R^n - d_R^j\right) + b_{d_j}^{CL1} \tag{5.5-24}$$

where $b_{d_j}^{CL1}$ is the instantaneous one-way cross-link Doppler bias.

In the case of receivers that average the instantaneous Doppler shift over an interval ΔT, nominally equal to 10 seconds, the resulting averaged one-way crosslink Doppler shift measurement from antenna i on the *j*th transmitter to antenna m on the receiving satellite n is modeled as follows:

$$\overline{F_{D_{nj}}^{CL1}(t_k)} = \frac{1}{\Delta T}\int_{t_k-\Delta T}^{t_k}\left[-\frac{F_T}{c}\left(\dot{\rho}^{nj}(t) + d_R^n - d_R^j\right) + \delta F_{atm}\right]\, dt \tag{5.5-25}$$

$$\overline{F_{D_{nj}}^{CL1}(t_k)} = -\frac{F_T}{c}\left(\frac{\Delta\rho^{nj}(t_k)}{\Delta T} + d_R^n - d_R^j\right) + \overline{b_{d_j}^{CL1}(t_k)} \tag{5.5-26}*$$

where

$$\Delta\rho^{nj}(t_k) = \rho^{nj}(t_k) - \rho^{nj}(t_k - \Delta T) \tag{5.5-27}*$$

and $\rho^{nj}(t_k)$, the range between the transmitting and receiving antennas, is defined in Equation (5.5-14c) and the optional one-way cross-link Doppler bias, $\overline{b_{d_j}^{CL1}}$, can be an estimated.

$$\overline{b_{d_{nj}}^{CL1}} \cong b_{d_{nj}}^{CL1} = \delta F_{atm} \tag{5.5-28}$$

The optional cross-link Doppler bias state, $b_{\rho_j}^{CL1}$, and associated covariance are reset when a programmable time lapse is detected in the provided measurement. In the above equations, satellite *n* is the receiving satellite and satellite *j* is the transmitting satellite. The position of the *j* transmitting satellites can either be estimated or obtained from an ephemeris message provided via the cross-link communications signal.

The computation of the nonzero state partial derivatives of the averaged cross-link Doppler shift is presented below. From Equation (5.5-26), the following equations are obtained for the receiving satellite for the case where $\overline{X}(t_k)$ consists of N_S absolute state vectors for both the local (1) and remote satellites:

$$\frac{\partial \overline{F_{D_{nj}}^{CL1}(t_k)}}{\partial \overline{R}^n(t_k)} = -\frac{F_T}{c\Delta T}\left[\hat{\rho}^{nj}(t_k)^T - \hat{\rho}^{nj}(t_k - \Delta T)^T \frac{\partial \overline{R}^n(t_k - \Delta T)}{\partial \overline{R}^n(t_k)}\right] \quad (5.5\text{-}29)^*$$

$$\frac{\partial \overline{F_{D_{nj}}^{CL1}(t_k)}}{\partial \dot{\overline{R}}^n(t_k)} = \frac{F_T}{c\Delta T}\left[\hat{\rho}^{nj}(t_k - \Delta T)^T \frac{\partial \overline{R}^n(t_k - \Delta T)}{\partial \dot{\overline{R}}^n(t_k)}\right] \quad (5.5\text{-}30)^*$$

$$\frac{\partial \overline{F_{D_{nj}}^{CL1}(t_k)}}{\partial \Delta C_D^n(t_k)} = \frac{F_T}{c\Delta T}\left[\hat{\rho}^{nj}(t_k - \Delta T)^T \frac{\partial \overline{R}^n(t_k - \Delta T)}{\partial \Delta C_D^n(t_k)}\right] \quad (5.5\text{-}31)^*$$

$$\frac{\partial \overline{F_{D_{nj}}^{CL1}(t_k)}}{\partial \Delta C_R^n(t_k)} = \frac{F_T}{c\Delta T}\left[\hat{\rho}^{nj}(t_k - \Delta T)^T \frac{\partial \overline{R}^n(t_k - \Delta T)}{\partial \Delta C_R^n(t_k)}\right] \quad (5.5\text{-}32)^*$$

$$\frac{\partial \overline{F_{D_{nj}}^{CL1}(t_k)}}{\partial d_R^n(t_k)} = -\frac{F_T}{c} \quad (5.5\text{-}32a)^*$$

and for the *j* transmitting satellites being estimated, where $j \neq n$

$$\frac{\partial \overline{F_{D_{nj}}^{CL1}(t_k)}}{\partial \overline{R}^j(t_k)} = \frac{F_T}{c\Delta T}\left[\hat{\rho}^{nj}(t_k)^T - \hat{\rho}^{nj}(t_k - \Delta T)^T \frac{\partial \overline{R}^j(t_k - \Delta T)}{\partial \overline{R}^j(t_k)}\right] \quad (5.5\text{-}33)^*$$

$$\frac{\partial \overline{F_{D_{nj}}^{CL1}(t_k)}}{\partial \dot{\overline{R}}^j(t_k)} = -\frac{F_T}{c\Delta T}\left[\hat{\rho}^{nj}(t_k - \Delta T)^T \frac{\partial \overline{R}^j(t_k - \Delta T)}{\partial \dot{\overline{R}}^j(t_k)}\right] \quad (5.5\text{-}34)^*$$

$$\frac{\partial \overline{F_{D_{nj}}^{CL1}(t_k)}}{\partial \Delta C_D^j(t_k)} = -\frac{F_T}{c\Delta T}\left[\hat{\rho}^{nj}(t_k - \Delta T)^T \frac{\partial \overline{R}^j(t_k - \Delta T)}{\partial \Delta C_D^j(t_k)}\right] \quad (5.5\text{-}35)^*$$

$$\frac{\partial \overline{F_{D_{nj}}^{CL1}(t_k)}}{\partial \Delta C_R^j(t_k)} = -\frac{F_T}{c\Delta T}\left[\hat{\rho}^{nj}(t_k - \Delta T)^T \frac{\partial \overline{R}^j(t_k - \Delta T)}{\partial \Delta C_R^j(t_k)}\right] \quad (5.5\text{-}36)^*$$

$$\frac{\partial \overline{F_{D_{nj}}^{CL1}(t_k)}}{\partial b_{d_j}^{CL1}(t_k)} = 1 \quad (5.5\text{-}37)^*$$

$$\frac{\partial \overline{F_{D_{nj}}^{CL1}(t_k)}}{\partial d_R^j(t_k)} = \frac{F_T}{c} \quad (5.5\text{-}37a)^*$$

The partial derivatives of the range in Equations (5.5-29) through (5.6-36) are defined in Equation (5.5-16) in Section 5.5.1. These derivatives are evaluated at the current measurement timetag, t_k, and at the time $t_k - \Delta T$, where ΔT is the Doppler averaging interval. The partial derivatives of the measurement with respect to the atmospheric drag coefficient and solar radiation pressure coefficient corrections in Equations (5.5-31), (5.5-32), (5.5-35) and (5.5-36) are computed only if these state parameters are being estimated.

The matrix of partial derivatives of the position vector at time $t_k - \Delta T$ with respect to the estimation state vector in Equations (5.5-29) through (5.6-34) is related to the components of the state transition matrix defined by Equation (4.4-1a) in Section 4.4.1 as follows

$$\left(\frac{\partial \overline{R}^n(t_k - \Delta T)}{\partial \overline{R}^n(t_k)}\right) = (W)_{i=1,2,3;\, j=1,2,3} \quad (5.5\text{-}38)^*$$

$$\left(\frac{\partial \overline{R}^n(t_k - \Delta T)}{\partial \dot{\overline{R}}^n(t_k)}\right) = (W)_{i=1,2,3;\, j=4,5,6} \quad (5.5\text{-}38a)^*$$

$$\left(\frac{\partial \overline{R}^n(t_k - \Delta T)}{\partial \Delta C_D^n}\right) = (W)_{i=1,2,3;\, j=7} \quad (5.5\text{-}38b)^*$$

$$\left(\frac{\partial \overline{R}^n(t_k - \Delta T)}{\partial \Delta C_R^n}\right) = (W)_{i=1,2,3;\, j=8} \quad (5.5\text{-}38c)^*$$

where

$$W = \begin{bmatrix} \dfrac{\partial \overline{R}^{\,n}(t_k)}{\partial \overline{R}^{\,n}(t_k - \Delta T)} & \dfrac{\partial \overline{R}^{\,n}(t_k)}{\partial \dot{\overline{R}}^{\,n}(t_k - \Delta T)} & \dfrac{\partial \overline{R}^{\,n}(t_k)}{\partial \Delta C_D^n(t_k - \Delta T)} & \dfrac{\partial \overline{R}^{\,n}(t_k)}{\partial \Delta C_R^n(t_k - \Delta T)} \\ \dfrac{\partial \dot{\overline{R}}^{\,n}(t_k)}{\partial \overline{R}^{\,n}(t_k - \Delta T)} & \dfrac{\partial \dot{\overline{R}}^{\,n}(t_k)}{\partial \dot{\overline{R}}^{\,n}(t_k - \Delta T)} & \dfrac{\partial \dot{\overline{R}}^{\,n}(t_k)}{\partial \Delta C_D^n(t_k - \Delta T)} & \dfrac{\partial \dot{\overline{R}}^{\,n}(t_k)}{\partial \Delta C_R^n(t_k - \Delta T)} \\ 0_{1x3} & 0_{1x3} & 1 & 0 \\ 0_{1x3} & 0_{1x3} & 0 & 1 \end{bmatrix}^{-1} \quad \text{(5.5-38d)*}$$

If the atmospheric drag coefficient correction and/or the solar radiation pressure coefficient correction are not estimated, the matrix W does not include the columns associated with these state components.

If the estimation state vector consists of an absolute state for the local satellite (*n, j*=1) and relative states for the remote satellites (*n, j*>1), the following are the nonzero partial derivatives of the crosslink Doppler measurement -- Note that this option is not implemented in GEONS 3.0:

$$\frac{\partial \overline{F_{D_{nj}}^{CL1}(t_k)}}{\partial \overline{R}_{rel}^{n}(t_k)} = -\frac{F_T}{c\Delta T}\left[\hat{\rho}^{nj}(t_k)^T - \hat{\rho}^{nj}(t_k - \Delta T)^T \frac{\partial \overline{R}_{rel}^{n}(t_k - \Delta T)}{\partial \overline{R}_{rel}^{n}(t_k)}\right] \text{for } n > 1; j = 1,..., N_S; n \neq j \quad \text{(5.5-38e)*}$$

$$\frac{\partial \overline{F_{D_{nj}}^{CL1}(t_k)}}{\partial \dot{\overline{R}}_{rel}^{n}(t_k)} = \frac{F_T}{c\Delta T}\left[\hat{\rho}^{nj}(t_k - \Delta T)^T \frac{\partial \overline{R}_{rel}^{n}(t_k - \Delta T)}{\partial \dot{\overline{R}}_{rel}^{n}(t_k)}\right] \text{for } n > 1; j = 1,..., N_S; n \neq j \quad \text{(5.5-38f)*}$$

$$\frac{\partial \overline{F_{D_{nj}}^{CL1}(t_k)}}{\partial \Delta C_{D_{rel}}^{n}(t_k)} = \frac{F_T}{c\Delta T}\left[\hat{\rho}^{nj}(t_k - \Delta T)^T \frac{\partial \overline{R}_{rel}^{j}(t_k - \Delta T)}{\partial \Delta C_{D_{rel}}^{n}(t_k)}\right] \text{for } n > 1; j = 1,..., N_S; n \neq j \quad \text{(5.5-38g)*}$$

$$\frac{\partial \overline{F_{D_{nj}}^{CL1}(t_k)}}{\partial \Delta C_{Rrel}^{n}(t_k)} = \frac{F_T}{c\Delta T}\left[\hat{\rho}^{nj}(t_k - \Delta T)^T \frac{\partial \overline{R}_{rel}^{n}(t_k - \Delta T)}{\partial \Delta C_{Rrel}^{n}(t_k)}\right] \text{for } n > 1; j = 1,..., N_S; n \neq j \quad \text{(5.5-38h)*}$$

$$\frac{\partial \overline{F_{D_{nj}}^{CL1}(t_k)}}{\partial \overline{R}_{rel}^{j}(t_k)} = \frac{F_T}{c\Delta T}\left[\hat{\rho}^{nj}(t_k)^T - \hat{\rho}^{nj}(t_k - \Delta T)^T \frac{\partial \overline{R}_{rel}^{j}(t_k - \Delta T)}{\partial \overline{R}_{rel}^{j}(t_k)}\right] \text{for } n = 1,..., N_S; j > 1; n \neq j \quad \text{(5.5-38i)*}$$

$$\frac{\partial \overline{F_{D_{nj}}^{CL1}(t_k)}}{\partial \dot{\overline{R}}_{rel}^{j}(t_k)} = -\frac{F_T}{c\Delta T}\left[\hat{\rho}^{nj}(t_k - \Delta T)^T \frac{\partial \overline{R}_{rel}^{j}(t_k - \Delta T)}{\partial \dot{\overline{R}}_{rel}^{j}(t_k)}\right] \text{for } n = 1,..., N_S; j > 1; n \neq j \quad \text{(5.5-38j)*}$$

$$\frac{\partial \overline{F_{D_{nj}}^{CL1}(t_k)}}{\partial \Delta C_{D_{rel}}^{j}(t_k)} = -\frac{F_T}{c\Delta T}\left[\hat{\rho}^{nj}(t_k - \Delta T)^T \frac{\partial \overline{R}_{rel}^{j}(t_k - \Delta T)}{\partial \Delta C_{D_{rel}}^{j}(t_k)}\right] \text{for } n = 1,..., N_S; j > 1; n \neq j \quad \text{(5.5-38k)*}$$

$$\frac{\partial \overline{F_{D_{nj}}^{CL1}(t_k)}}{\partial \Delta C_{R_{rel}}^{j}(t_k)} = -\frac{F_T}{c\Delta T}\left[\hat{\rho}^{nj}(t_k - \Delta T)^T \frac{\partial \overline{R}_{rel}^{j}(t_k - \Delta T)}{\partial \Delta C_{R_{rel}}^{j}(t_k)}\right] \text{ for } n = 1,...,N_S;\ j > 1;\ n \neq j \quad (5.5\text{-}38l)^*$$

$$\frac{\partial \overline{F_{D_{nj}}^{CL1}(t_k)}}{\partial b_{d_j}^{CL1}(t_k)} = 1, \text{ for } n = 1,...,N_S;\ j = 1,...,N_S;\ n \neq j \quad (5.5\text{-}38m)^*$$

The partial derivatives of the measurement with respect to the atmospheric drag coefficient and solar radiation pressure coefficient corrections in Equations (5.5-31), (5.5-32), (5.5-35) and (5.5-36) are computed only if these state parameters are being estimated.

The partial derivatives of the relative position vector at the time $t_k - \Delta T$ with respect to the estimated relative state vector components in Equations (5.5-30a) through (5.5-36a) are related to the components of the inverse of the state transition matrix defined by Equation (4.4-1b) in Section 4.4.1 as follows:

$$\left(\frac{\partial \overline{X}_{rel}(t_k - \Delta T)}{\partial \overline{X}_{rel}(t_k)}\right) = \left(\frac{\partial \overline{X}_{rel}(t_k)}{\partial \overline{X}_{rel}(t_{k-1})}\right)^{-1} \quad (5.5\text{-}38n)^*$$

where

$$\overline{X}_{rel} = \begin{bmatrix} \overline{X}^1 \\ \overline{X}_{rel}^2 \\ \vdots \\ \overline{X}_{rel}^{N_S} \\ \overline{B} \end{bmatrix} \quad (5.5\text{-}38o)$$

and

$$\overline{X}_{rel}^{n} = \overline{X}^n - \overline{X}^1 = \begin{bmatrix} \overline{R}^n - \overline{R}^1 \\ \dot{\overline{R}}^n - \dot{\overline{R}}^1 \\ \Delta C_D^n - \Delta C_D^1 \\ \Delta C_R^n - \Delta C_R^1 \\ \overline{b}_R^n - \overline{b}_R^1 \end{bmatrix} = \begin{bmatrix} \overline{R}_{rel}^n \\ \dot{\overline{R}}_{rel}^n \\ \left(\Delta C_D^n\right)_{rel} \\ \left(\Delta C_R^n\right)_{rel} \\ \overline{b}_{rel}^n \end{bmatrix};\ n \neq 1 \quad (5.5\text{-}38p)$$

If the atmospheric drag coefficient correction and/or the solar radiation pressure coefficient correction are not estimated, the state transition matrix does not include the columns associated with these state components.

5.5.3 Two-Way Cross-Link Range Measurement Model and Associated Partial Derivatives

The two-way cross-link range is obtained by measuring the round-trip signal transit time from the source satellite n to target satellite j and back to satellite n. This interval is defined as

$$\Delta\tau \equiv t_R^n - t_T^n \tag{5.5-39}$$

where t_R^n denotes the receive time measured by the receiver clock on satellite n and t_T^n is the transmit time measured by the clock on source satellite n. The two-way cross-link range measurement is defined as one-half of the speed of light (c) times the time interval $\Delta\tau$:

$$\begin{aligned}\Re_{nj}^{CL2}(t_R^{UTC}) \equiv \frac{c}{2}\Delta\tau = \frac{1}{2}\Big[\rho_1^{nj}(t_R^{UTC}) + \rho_2^{nj}(t_R^{UTC}) + b_{\rho_j}^{CL2}(t_R^{UTC})\Big] \\ \times\left[1+\frac{d_R^n(t_R^{UTC})}{c}\right]; \quad n=1,..,N_S;\ j=1,..,N_S;\ j\neq n\end{aligned} \tag{5.5-40}$$

where

$$\rho_1^{nj}(t_R^{UTC}) = \left|\overline{R}_{A_i}^{j}(t_{R_1}^{UTC}) - \overline{R}_{A_m}^{n}(t_{T_1}^{UTC})\right| \tag{5.5-41}$$

$$\rho_2^{nj}(t_R^{UTC}) = \left|\overline{R}_{A_m}^{n}(t_{R_2}^{UTC}) - \overline{R}_{A_i}^{j}(t_{T_2}^{UTC})\right| \tag{5.5-42}$$

and b_ρ^{CL2} is the round-trip cross-link range bias exclusive of clock bias effects, an optional element of the estimated state vector defined in Section 4.3.

Linearizing $\rho_1^{nj}(t_R^{UTC})$ and $\rho_2^{nj}(t_R^{UTC})$ about the measured receive time tag $t_k = t_R^{UTC} + \delta t_R^n$ yields:

$$\begin{aligned}\Re_{nj}^{CL2}(t_R^{UTC_n}) \cong \frac{1}{2}\Big[\rho_1^{nj}(t_k) - \dot\rho_1^{nj}(t_k)\Delta t_R^n + \rho_2^{nj}(t_k) - \dot\rho_2^{nj}(t_k)\Delta t_R^n + b_{\rho_j}^{CL2}(t_k)\Big] \\ \times\left[1+\frac{d_R^n(t_k)}{c}\right] + b_2(t_k); \quad n=1,..,N_S;\ j=1,..,N_S;\ j\neq n\end{aligned} \tag{5.5-43}*$$

where

$$\rho_1^{nj}(t_k) = \left|\overline{R}_{A_i}^{j}(t_k') - \overline{R}_{A_m}^{n}(t_k'')\right| \tag{5.5-44}*$$

$$\rho_2^{nj}(t_k) = \left|\overline{R}_{A_m}^{n}(t_k) - \overline{R}_{A_i}^{j}(t_k')\right| \tag{5.5-45}*$$

$$\hat\rho_1^{nj}(t_k) = \frac{\overline{R}_{A_i}^{j}(t_k') - \overline{R}_{A_m}^{n}(t_k'')}{\rho_1^{nj}(t_k)} \tag{5.5-45a}*$$

$$\hat{\rho}_2^{nj}(t_k) = \frac{\bar{R}_{A_m}^n(t_k) - \bar{R}_{A_i}^j(t_k')}{\rho_2^{nj}(t_k)} \qquad \text{(5.5-45b)*}$$

$$\dot{\rho}_1^{nj}(t_k) = \frac{\hat{\rho}_1^{nj}(t_k) \cdot \left(\dot{\bar{R}}_{A_i}^j(t_k') - \dot{\bar{R}}_{A_m}^n(t_k'')\right)}{1 - \hat{\rho}_1^{nj}(t_k) \cdot \left(\dot{\bar{R}}_{A_m}^n(t_k'')/c\right)} \left(1 - \frac{\dot{\rho}_2^{nj}(t_k)}{c}\right) \qquad \text{(5.5-46)*}$$

$$\dot{\rho}_2^{nj}(t_k) = \frac{\hat{\rho}_2^{nj}(t_k) \cdot \left(\dot{\bar{R}}_{A_m}^n(t_k) - \dot{\bar{R}}_{A_i}^j(t_k')\right)}{1 - \hat{\rho}_2^{nj}(t_k) \cdot \left(\dot{\bar{R}}_{A_i}^j(t_k')/c\right)} \qquad \text{(5.5-47)*}$$

The offset of the true UTC receive time for spacecraft n measurements from the UTC filter state epoch is given by

$$\Delta t_R^n = \left[\left(t_k - t_R^{(RC)_n}\right) + \left(t_R^{(RC)_n} - t_R^{UTC_n}\right)\right] = \left(t_k - t_R^{(RC)_n}\right) + \delta t_R^n = \left(t_k - t_R^{(RC)_n}\right) + \frac{b_R^n(t_k)}{c} \qquad \text{(5.5-47a)*}$$

Note that in Release 2.7 and prior releases, Δt_R^n is implemented assuming that $t_k = t_R^{(RC)_n}$. This is corrected in Release 2.8. The optional cross-link range bias state, $b_{\rho_j}^{CL2}$, and associated covariance are reset when a programmable time lapse is detected in the provided measurement. The optional bias term $b_2(t_k)$, which is a correction developed in Reference 47 to account for second-order effects that can be significant prior to convergence of the absolute filter states, is computed as discussed in Section 5.5.1.

The initial transmission time from satellite n (t_k''), the intermediate receive and transmission times (assumed to be equal) from satellite j (t_k'), and the associated transmitter and receiver positions and velocities are computed using the Newton Ralphson iterative scheme defined in Section 5.5.1 (Equation 5.5-12) to solve for t_k' given t_k and then for t_k'' given t_k'. The position of each cross-link transmitting and receiving antenna is computed using Equation 3.2-61 in Section 3.2.8. In Equation 3.2-61, the position of the satellite *n* is always a component of the estimated state vector and the position of the intermediate satellite *j* can be either a component of the estimated state vector or a state vector that is either propagated or extracted from an ephemeris file (ground processing only).

In Equation 5.5-43, the additional bias term $b_2(t_k)$ is a correction developed in Reference 47 to account for second-order effects that can be significant prior to convergence of the absolute filter states. This second-order bias is computed as defined in Equations 5.5-14g through 5.5-14o in Section 5.5.1. When the optional second-order correction term $b_2(t_k)$ is included in the predicted measurement, a second-order variance correction term B_k is also included in the cross-link range measurement variance calculation such that

$$V_k = H_k P_k H_k^T + R_k + B_k \qquad \text{(5.5-47b)*}$$

The second-order variance correction B_k is computed using Equation 5.5-14r in Section 5.5.1.

The following are the nonzero elements of the partial derivative vector when the estimation state vector consists of absolute state vectors for the receiving satellite *n* and the satellite *j,* omitting terms of $O(\frac{1}{c^2})$ and higher:

$$\frac{\partial \Re_{nj}^{CL2}(t_R^{UTC})}{\partial \bar{R}^n(t_k)} = \frac{1}{2}\left[1+\frac{d_R^n(t_k)}{c}\right]\left[\frac{\partial \rho_1^{nj}(t_k)}{\partial \bar{R}^n(t_k)}+\frac{\partial \rho_2^{nj}(t_k)}{\partial \bar{R}^n(t_k)}\right]-\frac{b_R^n(t_k)}{2c}\left[\frac{\partial \dot{\rho}_1^{nj}(t_k)}{\partial \bar{R}^n(t_k)}+\frac{\partial \dot{\rho}_2^{nj}(t_k)}{\partial \bar{R}^n(t_k)}\right]$$
$$\frac{\partial \Re_{nj}^{CL2}(t_R^{UTC})}{\partial \dot{\bar{R}}^n(t_k)} = -\frac{b_R^n(t_k)}{2c}\left[\frac{\partial \dot{\rho}_1^{nj}(t_k)}{\partial \dot{\bar{R}}^n(t_k)}+\frac{\partial \dot{\rho}_2^{nj}(t_k)}{\partial \dot{\bar{R}}^n(t_k)}\right] \quad (5.5\text{-}48)^*$$

$$\frac{\partial \Re_{nj}^{CL2}(^{UTC}_{R})}{\partial \bar{R}^j(t_k)} = \frac{1}{2}\left[1+\frac{d_R^n(t_k)}{c}\right]\left[\frac{\partial \rho_1^{nj}(t_k)}{\partial \bar{R}^j(t_k)}+\frac{\partial \rho_2^{nj}(t_k)}{\partial \bar{R}^j(t_k)}\right]-\frac{b_R^n(t_k)}{2c}\left[\frac{\partial \dot{\rho}_1^{nj}(t_k)}{\partial \bar{R}^j(t_k)}+\frac{\partial \dot{\rho}_2^{nj}(t_k)}{\partial \bar{R}^j(t_k)}\right]$$
$$\frac{\partial \Re_{nj}^{CL2}(t_R^{UTC})}{\partial \dot{\bar{R}}^j(t_k)} = -\frac{b_R^n(t_k)}{2c}\left[\frac{\partial \dot{\rho}_1^{nj}(t_k)}{\partial \dot{\bar{R}}^j(t_k)}+\frac{\partial \dot{\rho}_2^{nj}(t_k)}{\partial \dot{\bar{R}}^j(t_k)}\right] \quad (5.5\text{-}49)^*$$

$$\frac{\partial \Re_{nj}^{CL2}(t_R^{UTC})}{\partial b_{\rho_j}^{CL2}(t_k)} = \frac{1}{2}\left[1+\frac{d_R^n(t_k)}{c}\right] \quad (5.5\text{-}50)^*$$

$$\frac{\partial \Re_{nj}^{CL2}(t_R^{UTC})}{\partial b_R^n(t_k)} = \frac{1}{2}\left[-\frac{\dot{\rho}_1^{nj}(t_k)}{c}-\frac{\dot{\rho}_2^{nj}(t_k)}{c}\right] \quad (5.5\text{-}51)^*$$

$$\frac{\partial \Re_{nj}^{CL2}(t_R^{UTC})}{\partial b_R^j(t_k)} = 0 \quad (5.5\text{-}52)^*$$

$$\frac{\partial \Re_{nj}^{CL2}(t_R^{UTC})}{\partial d_R^n(t_k)} = \frac{1}{2c}\left[\rho_1^{nj}(t_k)+\rho_2^{nj}(t_k)+b_{\rho_j}^{CL2}(t_k)\right] \quad (5.5\text{-}53)^*$$

$$\frac{\partial \Re_{nj}^{CL2}(t_R^{UTC})}{\partial d_R^j(t_k)} = 0 \quad (5.5\text{-}54)^*$$

where

$$\frac{\partial \rho_1^{nj}(t_k)}{\partial \bar{R}^n(t_k)} = -\hat{\rho}_1^{nj}(t_k)^T \quad (5.5\text{-}55)^*$$

$$\frac{\partial \rho_2^{nj}(t_k)}{\partial \bar{R}^n(t_k)} = \hat{\rho}_2^{nj}(t_k)^T \quad (5.5\text{-}55b)^*$$

$$\frac{\partial \dot{\rho}_1^{nj}(t_k)}{\partial \overline{\dot{R}}^n(t_k)} \cong \frac{-\left[\left(\dot{\overline{R}}_{A_i}^{j}(t'_k) - \dot{\overline{R}}_{A_m}^{n}(t''_k)\right) - \dot{\rho}_1^{nj}(t_k)\left(\hat{\rho}_1^{nj}(t_k) - \dfrac{\dot{\overline{R}}_{A_m}^{n}(t''_k)}{c}\right)\right]^T}{\rho_1^{nj}(t_k)\left[1 - \hat{\rho}_1^{nj}(t_k)\cdot\left(\dot{\overline{R}}_{A_m}^{n}(t''_k)/c\right)\right]}\left(1 - \frac{\dot{\rho}_2^{nj}(t_k)}{c}\right) \qquad (5.5\text{-}56)^*$$

$$-\frac{1}{c}\frac{\hat{\rho}_1^{nj}(t_k)\cdot\left(\dot{\overline{R}}_{A_i}^{j}(t'_k) - \dot{\overline{R}}_{A_m}^{n}(t''_k)\right)}{\left[1 - \hat{\rho}_1^{nj}(t_k)\cdot\left(\dot{\overline{R}}_{A_m}^{n}(t''_k)/c\right)\right]}\frac{\partial \dot{\rho}_2^{nj}(t_k)}{\partial \overline{\dot{R}}^n(t_k)}$$

$$\frac{\partial \dot{\rho}_2^{nj}(t_k)}{\partial \overline{\dot{R}}^n(t_k)} \cong \frac{\left[\left(\dot{\overline{R}}_{A_m}^{n}(t_k) - \dot{\overline{R}}_{A_i}^{j}(t'_k)\right) - \dot{\rho}_2^{nj}(t_k)\left(\hat{\rho}_2^{nj}(t_k) - \dfrac{\dot{\overline{R}}_{A_i}^{j}(t'_k)}{c}\right)\right]^T}{\rho_2^{nj}(t_k)\left[1 - \hat{\rho}_2^{nj}(t_k)\cdot\left(\dot{\overline{R}}_{A_i}^{j}(t'_k)/c\right)\right]} \qquad (5.5\text{-}57)^*$$

$$\frac{\partial \dot{\rho}_1^{nj}(t_k)}{\partial \dot{\overline{R}}^n(t_k)} = \frac{-\left(\hat{\rho}_1^{nj}(t_k)\right)^T\left[1 - \dot{\rho}_1^{nj}(t_k)/c\right]}{\left[1 - \hat{\rho}_1^{nj}(t_k)\cdot\left(\dot{\overline{R}}_{A_m}^{n}(t''_k)/c\right)\right]}\left(1 - \frac{\dot{\rho}_2^{nj}(t_k)}{c}\right) - \frac{1}{c}\frac{\hat{\rho}_1^{nj}(t_k)\cdot\left(\dot{\overline{R}}_{A_i}^{j}(t'_k) - \dot{\overline{R}}_{A_m}^{n}(t''_k)\right)}{\left[1 - \hat{\rho}_1^{nj}(t_k)\cdot\left(\dot{\overline{R}}_{A_m}^{n}(t''_k)/c\right)\right]}\frac{\partial \dot{\rho}_2^{nj}(t_k)}{\partial \dot{\overline{R}}^n(t_k)} \qquad (5.5\text{-}58)^*$$

$$\frac{\partial \dot{\rho}_2^{nj}(t_k)}{\partial \dot{\overline{R}}^n(t_k)} = \frac{\left(\hat{\rho}_2^{nj}(t_k)\right)^T}{1 - \hat{\rho}_2^{nj}(t_k)\cdot\left(\dot{\overline{R}}_{A_i}^{j}(t'_k)/c\right)} \qquad (5.5\text{-}59)^*$$

$$\frac{\partial \rho_1^{nj}(t_k)}{\partial \overline{R}^j(t_k)} = \hat{\rho}_1^{nj}(t_k)^T \qquad (5.5\text{-}60)^*$$

$$\frac{\partial \rho_2^{nj}(t_k)}{\partial \overline{R}^j(t_k)} = -\hat{\rho}_2^{nj}(t_k)^T \qquad (5.5\text{-}61)^*$$

$$\frac{\partial \dot{\rho}_1^{nj}(t_k)}{\partial \overline{\dot{R}}^j(t_k)} \cong \frac{\left[\left(\dot{\overline{R}}_{A_i}^{j}(t'_k) - \dot{\overline{R}}_{A_m}^{n}(t''_k)\right) - \dot{\rho}_1^{nj}(t_k)\left(\hat{\rho}_1^{nj}(t_k) - \dfrac{\dot{\overline{R}}_{A_m}^{n}(t''_k)}{c}\right)\right]^T}{\rho_1^{nj}(t_k)\left[1 - \hat{\rho}_1^{nj}(t_k)\cdot\left(\dot{\overline{R}}_{A_m}^{n}(t''_k)/c\right)\right]}\left(1 - \frac{\dot{\rho}_2^{nj}(t_k)}{c}\right) \qquad (5.5\text{-}62)^*$$

$$-\frac{1}{c}\frac{\hat{\rho}_1^{nj}(t_k)\cdot\left(\dot{\overline{R}}_{A_i}^{j}(t'_k) - \dot{\overline{R}}_{A_m}^{n}(t''_k)\right)}{\left[1 - \hat{\rho}_1^{nj}(t_k)\cdot\left(\dot{\overline{R}}_{A_m}^{n}(t''_k)/c\right)\right]}\frac{\partial \dot{\rho}_2^{nj}(t_k)}{\partial \overline{\dot{R}}^n(t_k)}$$

$$\frac{\partial \dot{\rho}_2^{nj}(t_k)}{\partial \dot{\overline{R}}^{j}(t_k)} \cong -\frac{\left[\left(\dot{\overline{R}}_{A_m}^{n}(t_k)-\dot{\overline{R}}_{A_i}^{j}(t_k')\right)-\dot{\rho}_2^{nj}(t_k)\left(\hat{\rho}_2^{nj}(t_k)-\frac{\dot{\overline{R}}_{A_i}^{j}(t_k')}{c}\right)\right]^T}{\rho_2^{nj}(t_k)\left[1-\hat{\rho}_2^{nj}(t_k)\cdot\left(\dot{\overline{R}}_{A_i}^{j}(t_k')/c\right)\right]} \tag{5.5-63}*$$

$$\frac{\partial \dot{\rho}_1^{nj}(t_k)}{\partial \dot{\overline{R}}^{j}(t_k)} = \frac{\left(\hat{\rho}_1^{nj}(t_k)\right)^T}{1-\hat{\rho}_1^{nj}(t_k)\cdot\left(\dot{\overline{R}}_{A_m}^{n}(t_k'')/c\right)}\left(1-\frac{\dot{\rho}_2^{nj}(t_k)}{c}\right)-\frac{1}{c}\frac{\hat{\rho}_1^{nj}(t_k)\cdot\left(\dot{\overline{R}}_{A_i}^{j}(t_k')-\dot{\overline{R}}_{A_m}^{n}(t_k'')\right)}{\left[1-\hat{\rho}_1^{nj}(t_k)\cdot\left(\dot{\overline{R}}_{A_m}^{n}(t_k'')/c\right)\right]}\frac{\partial \dot{\rho}_2^{nj}(t_k)}{\partial \dot{\overline{R}}^{n}(t_k)} \tag{5.5-64}*$$

$$\frac{\partial \dot{\rho}_2^{nj}(t_k)}{\partial \dot{\overline{R}}^{j}(t_k)} = \frac{-\left(\hat{\rho}_2^{nj}(t_k)\right)^T\left[1-\dot{\rho}_2^{nj}(t_k)/c\right]}{\left[1-\hat{\rho}_2^{nj}(t_k)\cdot\left(\dot{\overline{R}}_{A_i}^{j}(t_k')/c\right)\right]} \tag{5.5-65}*$$

If the estimation state vector consists of an absolute state for the local satellite (1) and relative states for the remote satellites (>1), where *n* and *j* are >1 -- Note that this option is not implemented in GEONS 3.0:

$$\begin{aligned}\frac{\partial \Re_{1j}^{CL2}(t_k)}{\partial \overline{R}^{1}(t_k)} &= 0\\ \frac{\partial \Re_{1j}^{CL2}(t_k)}{\partial \dot{\overline{R}}^{1}(t_k)} &= 0\end{aligned} \quad \text{(omitting terms of } O(\frac{1}{c^2}) \tag{5.5-66}*$$

$$\begin{aligned}\frac{\partial \Re_{n1}^{CL2}(t_k)}{\partial \overline{R}^{1}(t_k)} &= 0\\ \frac{\partial \Re_{n1}^{CL2}(t_k)}{\partial \dot{\overline{R}}^{1}(t_k)} &= 0\end{aligned} \quad \text{(omitting terms of } O(\frac{1}{c^2}) \tag{5.5-67}*$$

$$\frac{\partial \Re_{nj}^{CL2}(t_R^{UTC})}{\partial b_{R_{rel}}^{j}(t_k)} = 0 \quad \text{for } n = 1,\ldots,N_S;\ j>1;\ n \neq j \tag{5.5-68}*$$

The following are the nonzero partial derivatives of the round-trip crosslink range measurement, omitting terms of $O(\frac{1}{c^2})$ and higher

$$\frac{\partial \Re_{nj}^{CL2}(t_R^{UTC})}{\partial \bar{R}_{rel}^{n}(t_k)} = \frac{\partial \Re_{nj}^{CL2}(t_R^{UTC})}{\partial \bar{R}^{n}(t_k)} \frac{\partial \bar{R}^{n}(t_k)}{\partial \bar{R}_{rel}^{n}(t_k)} = \frac{1}{2}\left[1 + \frac{d_R^n(t_k)}{c}\right]\left[\frac{\partial \rho_1^{nj}(t_k)}{\partial \bar{R}^{n}(t_k)} + \frac{\partial \rho_2^{nj}(t_k)}{\partial \bar{R}^{n}(t_k)}\right] - \frac{b_R^n(t_k)}{2c}\left[\frac{\partial \dot{\rho}_1^{nj}(t_k)}{\partial \bar{R}^{n}(t_k)} + \frac{\partial \dot{\rho}_2^{nj}(t_k)}{\partial \bar{R}^{n}(t_k)}\right]$$

$$\frac{\partial \Re_{nj}^{CL2}(t_R^{UTC})}{\partial \dot{\bar{R}}_{rel}^{n}(t_k)} = \frac{\partial \Re_{nj}^{CL2}(t_R^{UTC})}{\partial \dot{\bar{R}}^{n}(t_k)} \frac{\partial \dot{\bar{R}}^{n}(t_k)}{\partial \dot{\bar{R}}_{rel}^{n}(t_k)} = -\frac{b_R^n(t_k)}{2c}\left[\frac{\partial \dot{\rho}_1^{nj}(t_k)}{\partial \dot{\bar{R}}^{n}(t_k)} + \frac{\partial \dot{\rho}_2^{nj}(t_k)}{\partial \dot{\bar{R}}^{n}(t_k)}\right] \quad \text{(5.5-69)*}$$

for $n > 1; j = 1,..., N_S; n \neq j$

$$\frac{\partial \Re_{nj}^{CL2}(t_R^{UTC})}{\partial \bar{R}_{rel}^{j}(t_k)} = \frac{\partial \Re_{nj}^{CL2}(t_R^{UTC})}{\partial \bar{R}^{j}(t_k)} \frac{\partial \bar{R}^{j}(t_k)}{\partial \bar{R}_{rel}^{j}(t_k)} = \frac{1}{2}\left[1 + \frac{d_R^n(t_k)}{c}\right]\left[\frac{\partial \rho_1^{nj}(t_k)}{\partial \bar{R}^{j}(t_k)} + \frac{\partial \rho_2^{nj}(t_k)}{\partial \bar{R}^{j}(t_k)}\right] - \frac{b_R^n(t_k)}{2c}\left[\frac{\partial \dot{\rho}_1^{nj}(t_k)}{\partial \bar{R}^{j}(t_k)} + \frac{\partial \dot{\rho}_2^{nj}(t_k)}{\partial \bar{R}^{j}(t_k)}\right]$$

$$\frac{\partial \Re_{nj}^{CL2}(t_R^{UTC})}{\partial \dot{\bar{R}}_{rel}^{j}(t_k)} = \frac{\partial \Re_{nj}^{CL2}(t_R^{UTC})}{\partial \dot{\bar{R}}^{j}(t_k)} \frac{\partial \dot{\bar{R}}^{j}(t_k)}{\partial \dot{\bar{R}}_{rel}^{j}(t_k)} = -\frac{1}{2}\left[\frac{b_R^n(t_k)}{c}\frac{\partial \dot{\rho}_1^{nj}(t_k)}{\partial \dot{\bar{R}}^{j}(t_k)} + \frac{b_R^n(t_k)}{c}\frac{\partial \dot{\rho}_2^{nj}(t_k)}{\partial \dot{\bar{R}}^{j}(t_k)}\right] \quad \text{(5.5-70)*}$$

for $n = 1,..., N_S; j > 1; n \neq j$

$$\frac{\partial \Re_{nj}^{CL2}(t_k)}{\partial b_{\rho_j}^{CL2}(t_k)} = \frac{1}{2}\left[1 + \frac{d_R^n(t_k)}{c}\right] \quad \text{for } n = 1,..., N_S; j = 1,..., N_S; n \neq j \quad \text{(5.5-71)*}$$

$$\frac{\partial \Re_{nj}^{CL2}(t_R^{UTC})}{\partial b_R^1(t_k)} = \frac{1}{2}\left[-\frac{\dot{\rho}_1^{nj}(t_k)}{c} - \frac{\dot{\rho}_2^{nj}(t_k)}{c}\right] \quad \text{for } n = 1,..., N_S; j = 1,..., N_S; n \neq j \quad \text{(5.5-72)*}$$

$$\frac{\partial \Re_{nj}^{CL2}(t_R^{UTC})}{\partial d_R^1(t_k)} = \frac{1}{2c}\left[\rho_1^{nj}(t_k) + \rho_2^{nj}(t_k) + b_{\rho_j}^{CL2}(t_k)\right] \quad \text{for } n = 1,..., N_S; j = 1,..., N_S; n \neq j \quad \text{(5.5-73)*}$$

$$\frac{\partial \Re_{nj}^{CL2}(t_R^{UTC})}{\partial b_{R_{rel}}^{n}(t_k)} = \frac{1}{2}\left[-\frac{\dot{\rho}_1^{nj}(t_k)}{c} - \frac{\dot{\rho}_2^{nj}(t_k)}{c}\right] \quad \text{for } n > 1; j = 1,..., N_S; n \neq j \quad \text{(5.5-74)*}$$

$$\frac{\partial \Re_{nj}^{CL2}(t_R^{UTC})}{\partial d_{R_{rel}}^{n}(t_k)} = \frac{1}{2c}\left[\rho_1^{nj}(t_k) + \rho_2^{nj}(t_k) + b_{\rho_j}^{CL2}(t_k)\right] \quad \text{for } n = 1,..., N_S; j > 1; n \neq j \quad \text{(5.5-75)*}$$

5.5.4 Two-Way Cross-Link Averaged Doppler Measurement Model and Associated Partial Derivatives

The instantaneous two-way cross-link Doppler is obtained by measuring the round-trip signal frequency shift from source satellite n to target satellite j and back to satellite n.

$$F_{D_{nj}}^{CL2}(t) = F_R(t) - F_{REF}(t) \quad \text{(5.5-76)}$$

where

$F_R(t)$ = Doppler-shifted cross-link carrier frequency

$F_{REF}(t)$ = receiver-generated local reference frequency

For two-way measurements, satellite n generates both the transmitted and local reference frequencies. Therefore, the receiver-generated reference frequency, F_{REF}, will be equal to the true transmit frequency, F'_T.

The first term on the right-hand side of Equation (5.5-76), F_R, the instantaneous Doppler shifted carrier frequency observed at the receiver, can be represented by the following equation:

$$F_R = F'_T\left(1 - \frac{\dot{\rho}_1^{nj} + \dot{\rho}_2^{nj}}{c}\right) + \delta F_{atm} \tag{5.5-77}$$

where

F'_T = true cross-link transmit frequency from satellite n

$\dot{\rho}_1^{nj}$ = time rate of change of the light-time-corrected range from transmitting antenna m on satellite n to receiving antenna i on target satellite j [defined in Equation (5.5-46)]

$\dot{\rho}_2^{nj}$ = time rate of change of the light-time-corrected range from transmitting antenna i on target satellite j to receiving antenna m on satellite n [defined in Equation (5.5-47)]

δF_{atm} = frequency perturbation due to the atmospheric refraction effects

The true transmit frequency, F'_T, is related to the nominal transmit frequency, F_T, as follows

$$F'_T(t) = F_T + \delta F_T = F_T\left(1 + \frac{d_R^n(t)}{c}\right) \tag{5.5-78}$$

Using Equation (5.5-78), Equation (5.5-76) can be written as

$$F_{D_{nj}}^{CL2} = -F_T\left(1 + \frac{d_R^j(t)}{c}\right)\left(\frac{\dot{\rho}_1^{nj} + \dot{\rho}_2^{nj}}{c}\right) + \delta F_{atm} \tag{5.5-79}$$

Neglecting terms of $O(\frac{1}{c^2})$ and higher, the instantaneous two-way Doppler shift reduces to

$$F_{D_{nj}}^{CL2}(t_k) = -\frac{F_T}{c}\left(\dot{\rho}_1^{nj}(t) + \dot{\rho}_2^{nj}(t)\right) + \delta F_{atm} \tag{5.5-80}$$

In the case of receivers that provide an instantaneous Doppler shift measurement, the instantaneous two-way Doppler shift from antenna i on the jth transmitter to antenna m on the receiving satellite n would be modeled as follows -- note that this model is not implemented in GEONS 3.0:

$$F_{D_{nj}}^{CL2}(t_k) = -\frac{F_T}{c}\left(\dot{\rho}_1^{nj}(t) + \dot{\rho}_2^{nj}(t)\right) + b_{d_j}^{CL2} \tag{5.5-81}$$

In the case of receivers that average the instantaneous Doppler shift over an interval ΔT, nominally equal to 10 seconds, the resulting averaged two-way crosslink Doppler shift measurement is modeled as follows:

$$\begin{aligned}\overline{F_{D_{nj}}^{CL2}(t_k)} &= -\frac{F_T}{c}\left(\frac{\Delta\rho_1^{nj}(t_k)+\Delta\rho_2^{nj}(t_k)}{\Delta T}+d_R^n(t_k)-d_R^n(t_k'')\right)+b_d^{CL2}(t_k)\\ &= -\frac{F_T}{c}\left(\frac{\Delta\rho_1^{nj}(t_k)+\Delta\rho_2^{nj}(t_k)}{\Delta T}+\dot{d}_R^n(t_k)(t_k-t_k'')\right)+b_d^{CL2}(t_k)\end{aligned} \quad (5.5\text{-}82)^*$$

where $b_d^{CL2}(t_k)$ is the averaged two-way Doppler measurement bias and

$$\Delta\rho_1^{nj}(t_k)=\rho_1^{nj}(t_k)-\rho_1^{nj}(t_k-\Delta T)$$

$$\Delta\rho_2^{nj}(t_k)=\rho_2^{nj}(t_k)-\rho_2^{nj}(t_k-\Delta T)$$

$$\rho_1^{nj}(t_k)=\left|\bar{R}_{A_i}^{j}(t_k')-\bar{R}_{A_m}^{n}(t_k'')\right| \quad (5.5\text{-}44)^*$$

$$\rho_2^{nj}(t_k)=\left|\bar{R}_{A_m}^{n}(t_k)-\bar{R}_{A_i}^{j}(t_k')\right| \quad (5.5\text{-}45)^*$$

$$\hat{\rho}_1^{nj}(t_k)=\frac{\bar{R}_{A_i}^{j}(t_k')-\bar{R}_{A_m}^{n}(t_k'')}{\rho_1^{nj}(t_k)} \quad (5.5\text{-}45a)^*$$

$$\hat{\rho}_2^{nj}(t_k)=\frac{\bar{R}_{A_m}^{n}(t_k)-\bar{R}_{A_i}^{j}(t_k')}{\rho_2^{nj}(t_k)} \quad (5.5\text{-}45b)^*$$

The optional cross-link Doppler bias state, b_d^{CL2}, and associated covariance are reset when a programmable time lapse is detected in the provided measurement.

For the source satellite *n* for the case where $\bar{X}(t_k)$ consists of N_S absolute state vectors for both the local (1) and remote satellites:

$$\frac{\partial\overline{F_{D_{nj}}^{CL2}(t_k)}}{\partial\bar{R}^n(t_k)}=-\frac{F_T}{c\Delta T}\begin{bmatrix}-\hat{\rho}_1^{nj}(t_k)^T+\hat{\rho}_1^{nj}(t_k-\Delta T)^T\frac{\partial\bar{R}^n(t_k''-\Delta T)}{\partial\bar{R}^n(t_k)}\\ +\hat{\rho}_2^{nj}(t_k)^T-\hat{\rho}_2^{nj}(t_k-\Delta T)^T\frac{\partial\bar{R}^n(t_k-\Delta T)}{\partial\bar{R}^n(t_k)}\end{bmatrix} \quad (5.5\text{-}83)^*$$

$$\frac{\partial\overline{F_{D_{nj}}^{CL2}(t_k)}}{\partial\dot{\bar{R}}^n(t_k)}=\frac{F_T}{c\Delta T}\left[-\hat{\rho}_1^{nj}(t_k-\Delta T)^T\frac{\partial\bar{R}^n(t_k-\Delta T)}{\partial\dot{\bar{R}}^n(t_k)}+\hat{\rho}_2^{nj}(t_k-\Delta T)^T\frac{\partial\bar{R}^n(t_k-\Delta T)}{\partial\dot{\bar{R}}^n(t_k)}\right] \quad (5.5\text{-}84)^*$$

$$\frac{\partial \overline{F_{D_{nj}}^{CL2}(t_k)}}{\partial \Delta C_D^n(t_k)} = \frac{F_T}{c\Delta T}\left[-\hat{\rho}_1^{nj}(t_k - \Delta T)^T \frac{\partial \bar{R}^n(t_k - \Delta T)}{\partial \Delta C_D^n(t_k)} + \hat{\rho}_2^{nj}(t_k - \Delta T)^T \frac{\partial \bar{R}^n(t_k - \Delta T)}{\partial \Delta C_D^n(t_k)} \right] \quad (5.5\text{-}85)^*$$

$$\frac{\partial \overline{F_{D_{nj}}^{CL2}(t_k)}}{\partial \Delta C_R^n(t_k)} = \frac{F_T}{c\Delta T}\left[-\hat{\rho}_1^{nj}(t_k - \Delta T)^T \frac{\partial \bar{R}^n(t_k - \Delta T)}{\partial \Delta C_R^n(t_k)} + \hat{\rho}_2^{nj}(t_k - \Delta T)^T \frac{\partial \bar{R}^n(t_k - \Delta T)}{\partial \Delta C_R^n(t_k)} \right] \quad (5.5\text{-}86)^*$$

$$\frac{\partial \overline{F_{D_{nj}}^{CL2}(t_k)}}{\partial \dot{d}_R^n(t_k)} = -\frac{F_T}{c}\left(t_k - t_k''\right) = -\frac{F_T}{c}\left(\frac{\rho_1^{nj}(t_k) + \rho_2^{nj}(t_k)}{c} \right) \quad (5.5\text{-}87)^*$$

and for the target satellite *j* being estimated, where $j \neq n$

$$\frac{\partial \overline{F_{D_{nj}}^{CL2}(t_k)}}{\partial \bar{R}^j(t_k)} = \frac{F_T}{c\Delta T}\begin{bmatrix} -\hat{\rho}_1^{nj}(t_k)^T + \hat{\rho}_1^{nj}(t_k - \Delta T)^T \dfrac{\partial \bar{R}^j(t_k - \Delta T)}{\partial \bar{R}^j(t_k)} \\ +\hat{\rho}_2^{nj}(t_k)^T - \hat{\rho}_2^{nj}(t_k - \Delta T)^T \dfrac{\partial \bar{R}^j(t_k - \Delta T)}{\partial \bar{R}^j(t_k)} \end{bmatrix} \quad (5.5\text{-}88)^*$$

$$\frac{\partial \overline{F_{D_{nj}}^{CL2}(t_k)}}{\partial \dot{\bar{R}}^j(t_k)} = -\frac{F_T}{c\Delta T}\left[-\hat{\rho}_1^{nj}(t_k - \Delta T)^T \frac{\partial \bar{R}^j(t_k - \Delta T)}{\partial \dot{\bar{R}}^j(t_k)} + \hat{\rho}_2^{nj}(t_k - \Delta T)^T \frac{\partial \bar{R}^j(t_k - \Delta T)}{\partial \dot{\bar{R}}^j(t_k)} \right] \quad (5.5\text{-}89)^*$$

$$\frac{\partial \overline{F_{D_{nj}}^{CL2}(t_k)}}{\partial \Delta C_D^j(t_k)} = -\frac{F_T}{c\Delta T}\left[-\hat{\rho}_1^{nj}(t_k - \Delta T)^T \frac{\partial \bar{R}^j(t_k - \Delta T)}{\partial \Delta C_D^j(t_k)} + \hat{\rho}_2^{nj}(t_k - \Delta T)^T \frac{\partial \bar{R}^j(t_k - \Delta T)}{\partial \Delta C_D^j(t_k)} \right] \quad (5.5\text{-}90)^*$$

$$\frac{\partial \overline{F_{D_{nj}}^{CL2}(t_k)}}{\partial \Delta C_R^j(t_k)} = -\frac{F_T}{c\Delta T}\left[-\hat{\rho}_1^{nj}(t_k - \Delta T)^T \frac{\partial \bar{R}^j(t_k - \Delta T)}{\partial \Delta C_R^j(t_k)} + \hat{\rho}_2^{nj}(t_k - \Delta T)^T \frac{\partial \bar{R}^j(t_k - \Delta T)}{\partial \Delta C_R^j(t_k)} \right] \quad (5.5\text{-}91)^*$$

$$\frac{\partial \overline{F_{D_{nj}}^{CL2}(t_k)}}{\partial b_{d_j}^{CL2}(t_k)} = 1 \quad (5.5\text{-}92)^*$$

The matrix of partial derivatives of the position vector at time $t_k - \Delta T$ with respect to the estimation state vector in the equations above are related to the components of the state transition matrix.

5.6 GS Measurement Models

The computational algorithms for one-way range and Doppler measurements from ground stations to a satellite receiver are discussed in this section. Although a ground station-to-satellite range measurement capability is not currently available, one-way range measurement processing is included in GEONS to support ground processing applications. The general form of the measurement model is as follows:

$$Y_k = G\ [\bar{X}(t_k),\ t_k] + \varepsilon \tag{5.6-1}$$

where t_k is the true measurement time, referenced to UTC, and ε is the measurement error. It is assumed that ε has a zero-mean Gaussian distribution with standard deviation σ, which is commandable for each measurement type. The measurement standard deviation is typically determined through analysis of the random component of the measurement error as part of the filter tuning process.

For GEONS, the estimation state vector, $\overline{X}(t)$ includes the receiver position vector, $\overline{R}$; velocity vector, $\dot{\overline{R}}$; optional corrections to the drag and solar radiation pressure coefficients, ΔC_D and ΔC_R; receiver time bias, b_R; and receiver time bias rate, d_R, for one or more receivers. Optionally, a GS range bias can be estimated. There are no additional measurement bias parameters associated with the GS Doppler measurements.

Section 5.6.1 addresses preprocessing of the raw GS Doppler measurements obtained from either a GS S-band receiver or a transceiver capable of providing integrated Doppler extracted from an forward link signal. The measurement model for the one-way range from the GS to the receiver, which is also used in the computation of the GS Doppler measurement, and associated partial derivatives are presented in Section 5.6.2. The GS one-way forward Doppler measurement model and associated partial derivatives are defined in Section 5.6.3. Section 5.6.4 provides an algorithm for preprocessing round-trip range-rate measurements so that they can be processed as one-way Doppler measurements, which is not appropriate for autonomous navigation but is useful in preflight analysis of the expected performance using the one-way range and Doppler measurements.

5.6.1 Raw GS Doppler Measurement Preprocessing (not implemented in GEONS)

The GS tracking signal path is shown in Figure 5-4. An S-band signal is transmitted from the GS and the Doppler shifted signal is received at the local satellite. One-way GS tracking can be operated using either a fixed radiated carrier frequency (FRCF) with onboard Doppler compensation (OBDC) or a GS frequency sweep to aid signal acquisition. In either case, the nominal RCF after acquisition is 2106.406250 megahertz. Note that the discussion below is based on the Doppler extractor flown as an experiment on the Extreme Ultraviolet Explorer (EUVE) spacecraft.

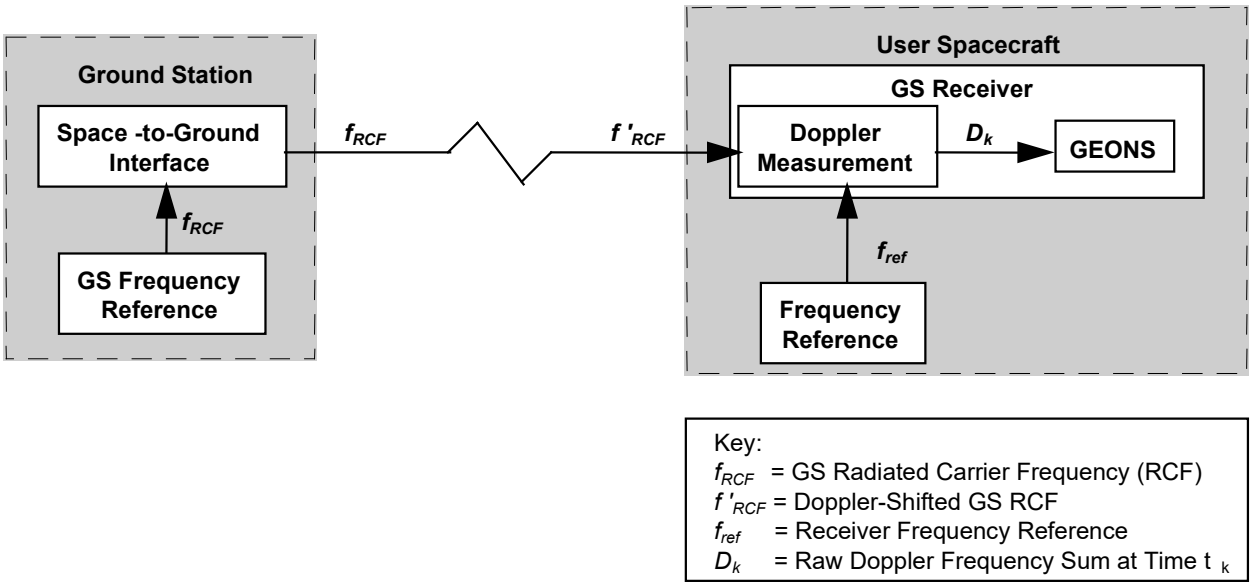

Figure 5-4. GS Forward-Link Signal Path

The GS receiver measures the Doppler shift of the forward-link signal with respect to an internal frequency reference. The Doppler measurement function is accomplished via a software accumulation of a scaled and biased nondestruct Doppler shift to provide a Doppler frequency sum measurement. The stability requirements for this frequency reference are dependent on the accuracy requirements of the user spacecraft. To achieve the highest accuracy, the frequency reference should be stable to 1 part in 10^{12} (1σ) over 10 to 100 seconds, with a drift of less than 1 part in 10^{10} per day (3σ). All timing associated with the Doppler measurement process should be synchronized with the spacecraft's timing reference.

The receiver's raw Doppler measurement output consists of the nondestruct frequency sum, D_k. The raw Doppler frequency sums are available nominally every 1.024 seconds. The navigation software samples the Doppler frequency sums, nominally every 8.192 or 16.384 seconds, checks and corrects the measurements for accumulator rollover, and converts them to the averaged Doppler measurements that are input to GEONS.

The navigation software driver performs the following checks on the receiver's telemetry to validate the sampled Doppler frequency sum measurements:

1. Set a Valid Doppler Frequency Sum indicator if all the following receiver conditions are true:
    a) Carrier Lock
    b) Receiver Lock
    c) STDN Mode
    d) Subcarrier Detect/Lock
    e) Non-Zero Doppler Frequency Sum

f) External Frequency Reference Selected

g) External Frequency Reference Status is healthy

2. Check the cycle slip indicator every 1.024 seconds and set a cycle slip indicator if a cycle slip was detected at any time between successive Doppler frequency sum samples.

3. Check the carrier drop pending indicator every 1.024 seconds and set a carrier drop pending indicator if a carrier drop pending was detected at any time between successive measurement collections, or during the first 1.024 second major cycle after the second Doppler frequency sum.

When two successive valid Doppler frequency sums are available, the navigation software driver differences successive S-band receiver Doppler frequency sums to compute a Doppler frequency sum difference, ΔD_k. If this difference is negative, accumulator rollover has occurred. In this case, the maximum value that the accumulator can hold is added to the difference.

The k^{th} average measured frequency difference measurement between the Doppler-shifted GS radiated carrier frequency (RCF) and the receiver's frequency reference, $\overline{F_D^{GS}(t_k)}_{obs}$, is then computed as follows:

$$\overline{F_D^{GS}(t_k)}_{obs} = \frac{K}{M}\Delta D_k - B_D \tag{5.6-2}$$

where

K = resolution of the receiver's carrier tracking numerically controlled oscillator (NCO) in hertz per bit

M = product of the number of accumulated NCO samples in each Doppler accumulation interval with the number of 1.024-second intervals in the Doppler averaging interval, ΔT; where the the number of accumulated NCO samples in each Doppler accumulation interval may be a function of the command rate

ΔD_k = difference between successive valid Doppler frequency sum samples at times t_k and $t_k - \Delta T$, accounting for the accumulator rollover

ΔT = Doppler averaging interval, typically 8.192 or 16.384 seconds

B_D = constant frequency bias that ensures that each frequency sum is a positive number

The measured average frequency difference is related to the k^{th} average Doppler shift of the actual GS RCF over the Doppler averaging interval, $\overline{f_D(k)}$, as follows:

$$\overline{f_D(k)} = \overline{F_D^{GS}(t_k)}_{obs} - \Delta F_f \tag{5.6-2a}$$

where

ΔF_f = difference between the actual GS RCF, $f_{RCF,}$ and the receiver's S-band Doppler frequency reference, f_{ref}

The navigation software driver performs the following checks to validate the average Doppler frequency difference measurements:

1. Sets an indicator if the Doppler measurement exceeds a ground commandable maximum value.
2. Sets a Valid Doppler Measurement indicator if the following conditions are true:
   a) The number of 1.024 second cycle slip indicators is below a ground commandable threshold, and
   b) The number of 1.024 second carrier drop pending indicators is below a ground commandable threshold, and
   c) The Doppler measurement is less than a ground commandable maximum value.
   d) The Doppler measurement does not span a day boundary.

The first valid average Doppler frequency difference measurement following a time interval without measurements larger than a commandable maximum time interval is considered to be at the start of a new tracking contact.

5.6.2 GS One-Way Forward Range and Associated Partial Derivatives

The timetag associated with the k^{th} measurement is the UTC receive time of the signal at the local receiver as measured with respect to the spacecraft/receiver clock, $t_R^{(RC)}$. In the presence of a spacecraft timing bias, the true measurement receive time is given by

$$t_R^{UTC} = t_R^{(RC)} - \delta t_R \tag{5.6-3}$$

where δt_R is the offset of the receiver's timing reference from UTC, given by

$$\delta t_R = \frac{b_R(t)}{c}$$

The accumulated receiver clock bias, $b_R(t)$, can be estimated using one-way GS range measurements alone or in combination with GNSS measurements.

If the forward-link GS signal is transmitted from GS j at time t_T and received at satellite receiver n at time t_R (equal to the measurement time), the measured pseudorange is given by:

$$\Re_{GS_j}^n(t_R^{UTC}) = c \cdot (t_R - t_T) = \rho_{GS_j}^{n,i}(t_R^{UTC}) + \delta\rho_{atm}(t_T) + b_R(t_R^{UTC}) + b_\rho^{GS_j}(t_R^{UTC}) \tag{5.6-4}$$

In this equation, c is the speed of light, $\delta\rho_{atm}(t_T)$ is the modeled tropospheric delay associated with a signal transmitted at time t_T in meters, $b_\rho^{GS_j}$ is an additional time delay due to hardware

and unmodeled atmospheric signal delays, and $\rho_{GS_j}^{n,i}(t_R^{UTC})$ is the distance traversed by the signal from the GS j to antenna i

$$\rho_{GS_j}^{n,i}(t_R^{UTC}) = \left|\bar{R}_{A_i}^{n}(t_R) - \bar{R}_{GS_j}(t_T)\right| \qquad (5.6\text{-}4a)^*$$

where

$\overline{R}_{GS_j}(t_T)$ = position of the transmitting GS *j* at time t_T

$\overline{R}_{A_i}^{n}(t_R)$ = position of the ith receiving antenna on satellite *n* at time t_R, which is computed using Equation 3.2-61 in Section 3.2.8.

The backward signal-trace method is used to determine time t_T when the signal was transmitted from the GS. This method uses the following Newton-Raphson iterative scheme to solve for the time t_T

$$t_{T,m+1} = t_R - \frac{\left|\overline{R}_{A_i}^{n}(t_R) - \overline{R}_{GS_j}(t_{T,m})\right|}{c} \qquad (5.6\text{-}5)^*$$

where

$t_{T,m+1}$ = $(m+1)^{th}$ approximation for t_T

$t_{T,m}$ = m^{th} approximation for t_T

t_R = signal reception time at the satellite receiver

The iterative solution of Equation (5.6-5) is started by setting

$$t_{T,0} = t_R \qquad (5.6\text{-}6)^*$$

such that

$$\overline{R}_{GS_j}(t_{T,0}) = \overline{R}_{GS_j}(t_R) \qquad (5.6\text{-}7)^*$$

The position vector for the transmitting GS is available in ECEF coordinates and must first be transformed to J2000.0 inertial coordinates using the transformations defined in Sections 3.2.1 through 3.2.3. This iterative scheme is continued until the condition $\left|t_{T,m+1} - t_{T,m}\right| \le \varepsilon$ is satisfied, where ε is a small tolerance (nominally equal to 10^{-8} second). After the GS signal transmit time, t_T, is found, the distance between the local satellite receiver and the GS can be calculated using Equation (5.6-4a).

The tropospheric delay associated with a signal transmitted at time t_T in meters, $\delta\rho_{atm}(t_T)$, is computed using the following empirical formula

$$\delta\rho_{atm}(t_T) = \frac{1.8958\left(\frac{\alpha}{340}\right)}{(0.06483 + \sin E)^{1.4}} \quad (5.6\text{-}8)^*$$

where

α is the monthly surface refractivity index for the GS in parts per million

E is elevation angle from the GS to the spacecraft, which is computed as follows:

$$sin\, E = \frac{\bar{\rho}^n_{GS_j}(t_R^{UTC}) \cdot \bar{R}_{GS_j}(t_T)}{\rho^n_{GS_j}(t_R^{UTC}) \left|\bar{R}_{GS_j}(t_T)\right|} \quad (5.6\text{-}9)^*$$

$$\bar{\rho}^{n,i}_{GS_j}(t_R^{UTC}) = \bar{R}^n_{A_i}(t_R) - \bar{R}_{GS_j}(t_T) \quad (5.6\text{-}10)^*$$

The GEONS filter propagates and updates all spacecraft states at a common UTC filter state epoch t_k.

Note that linearization of the GS PR measurement is not implemented in GEONS 3.0. To account for the offset of the true UTC receive time for spacecraft n measurements from the UTC filter state epoch, Equation (5.6-4) can be linearized about the current filter state time:

$$\rho^{n,i}_{GS_j}(t_R^{UTC_n}) = \rho^{n,i}_{GS_j}(t_k) - \dot{\rho}^{n,i}_{GS_j}(t_k)\Delta t_R^n \quad (5.6.2\text{-}1)$$

where the offset of the true UTC receive time for spacecraft n measurements from the UTC filter state epoch is given by

$$\Delta t_R^n = \left[\left(t_k - t_R^{(RC)_n}\right) + \left(t_R^{(RC)_n} - t_R^{UTC_n}\right)\right] = \left(t_k - t_R^{(RC)_n}\right) + \delta t_R^n = \left(t_k - t_R^{(RC)_n}\right) + \frac{b_R^n(t_k)}{c} \quad (5.6.2\text{-}2)^*$$

Taking this offset into account, Equation (5.6-4) can be rewritten as follows:

$$\Re^n_{GS_j}(t_R^{UTC_n}) = \rho^{n,i}_{GS_j}(t_k) - \dot{\rho}^{n,i}_{GS_j}(t_k)\Delta t_R^n + \delta\rho_{atm}(t_k) + b_R{}^n(t_k) - d_R{}^n(t_k)\Delta t_R^n + b_\rho^{GS_j}(t_k) \quad (5.6.2\text{-}3)^*$$

where

$$\rho^{n,i}_{GS_j}(t_k) = \left|\bar{R}_{A_i}{}^n(t_k) - \bar{R}_{GS_j}(t_k')\right| \quad (5.6.2\text{-}4)^*$$

$$\dot{\rho}^{n,i}_{GS_j}(t_k) = \frac{\hat{\rho}^{n,i}_{GS_j}(t_k) \cdot \left(\dot{\bar{R}}^n_{A_i}(t_k) - \dot{\bar{R}}_{GS_j}(t_k')\right)}{1 - \hat{\rho}^{n,i}_{GS_j}(t_k) \cdot \left(\dot{\bar{R}}_{GS_j}(t_k')/c\right)} \quad (5.6.2\text{-}5)^*$$

In the above equations, the subscript j indicates the j^{th} GS, t_k is the current filter epoch time, and t'_k is the signal transmit time, t_T, computed based on t_k. The receiver clock bias $b_R{}^n(t)$ is computed using the estimated parameters $b_R{}^n(t_k)$ and $\dot{b}_R{}^n(t_k)$ as defined in Equation 4.3-14a and 4.3-14 of Section 4.3. The term $-\dot{\rho}^{n,i}_{GS_j}(t_k)\Delta t_R{}^n$ is significant when the receiver time bias or measurement

timetag difference is large. The GS pseudorange bias, $b_{\rho}^{GS_j}$, is defined in Section 4.3. The position and velocity of the receiving antenna are computed using Equation 3.2-61 in Section 3.2.8.

The following are the nonzero components of the row vector of partial derivatives of the GS range with respect to the components of the estimation state vector, $\overline{X}(t_k)$, consisting of absolute states for the local and nonlocal satellites:

$$\frac{\partial \Re_{GS_j}^n(t_R^{UTC})}{\partial \bar{R}^n(t_k)} = \frac{\partial \rho_{GS_j}^{n,i}(t_k)}{\partial \bar{R}^n(t_k)} - \frac{\partial \dot{\rho}_{GS_j}^{n,i}(t_k)}{\partial \bar{R}^n(t_k)} \Delta t_R^n \qquad (5.6.2\text{-}6)^*$$

$$\frac{\partial \Re_{GS_j}^n(t_R^{UTC})}{\partial \dot{\bar{R}}^n(t_k)} = -\frac{\partial \dot{\rho}_{GS_j}^{n,i}(t_k)}{\partial \dot{\bar{R}}^n(t_k)} \Delta t_R^n \qquad (5.6.2\text{-}7)^*$$

$$\frac{\partial \Re_{GS_j}^n(t_R^{UTC})}{\partial b_{\rho}^{GS_j}(t_R^{UTC})} = 1 \qquad (5.6.2\text{-}8)^*$$

$$\frac{\partial \Re_{GS_j}^n(t_R^{UTC})}{\partial b_R(t_k)} = 1 \qquad (5.6.2\text{-}9)^*$$

$$\frac{\partial \Re_{GS_j}^n(t_R^{UTC})}{\partial d_R{}^n(t_k)} = -\Delta t_R^n \qquad (5.6.2\text{-}10)^*$$

Where

$$\frac{\partial \rho_{GS_j}^{n,i}(t_k)}{\partial \bar{R}^n(t_k)} = \frac{\bar{\rho}_{GS_j}^{n,i}(t_k)^T}{\rho_{GS_j}^{n,i}(t_k)} \qquad (5.6.2\text{-}11)^*$$

$$\frac{\partial \dot{\rho}_{GS_j}^{n,i}(t_k)}{\partial \bar{R}^n(t_k)} \cong \frac{1}{\rho_{GS_j}^{n,i}(t_k)\left[1-\hat{\rho}_{GS_j}^{n,i}(t_k)\cdot\left(\dot{\bar{R}}_{GS_j}(t_k')/c\right)\right]} \left[\left(\dot{\bar{R}}^n(t_k) - \dot{\bar{R}}_{G/W_j}(t_k')\right) - \dot{\rho}_{GS_j}^{n,i}(t_k)\left(\hat{\rho}_{GS_j}^{n,i}(t_k) - \frac{\dot{\bar{R}}_{GS_j}(t_k')}{c}\right)\right]^T \qquad (5.6.2\text{-}12)^*$$

$$\frac{\partial \dot{\rho}_{GS_j}^{n,i}(t_k)}{\partial \dot{\bar{R}}^n(t_k)} = \frac{\left(\hat{\rho}_{GS_j}^{n,i}(t_k)\right)^T}{1-\hat{\rho}_{GS_j}^{n,i}(t_k)\cdot\left(\dot{\bar{R}}_{GS_j}(t_k')/c\right)} \qquad (5.6.2\text{-}13)^*$$

If the estimated state vector includes relative states for the nonlocal satellites, the following are the nonzero components of the row vector of partial derivatives of the GS range with respect to the components of the estimation state vector, $\overline{X}(t_k)$:

$$\frac{\partial \Re_{GS_j}^n(t_R^{UTC})}{\partial \bar{R}^1(t_k)} = \frac{\partial \rho_{GS_j}^{n,i}(t_k)}{\partial \bar{R}^n(t_k)} - \frac{\partial \dot{\rho}_{GS_j}^{n,i}(t_k)}{\partial \bar{R}^n(t_k)} \Delta t_R^n \qquad (5.6.2\text{-}14)^*$$

$$\frac{\partial \Re_{GS_j}^n(t_R^{UTC})}{\partial \bar{R}_{rel}^n(t_k)} = \frac{\partial \rho_{GS_j}^{n,i}(t_k)}{\partial \bar{R}^n(t_k)} - \frac{\partial \dot{\rho}_{GS_j}^{n,i}(t_k)}{\partial \bar{R}^n(t_k)} \Delta t_R^n; n \neq 1 \qquad (5.6.2\text{-}15)^*$$

$$\frac{\partial \Re_{GS_j}^n(t_R^{UTC})}{\partial \dot{\bar{R}}^1(t_k)} = -\frac{\partial \dot{\rho}_{GS_j}^{n,i}(t_k)}{\partial \dot{\bar{R}}^n(t_k)} \Delta t_R^n \qquad (5.6.2\text{-}16)^*$$

$$\frac{\partial \Re^n_{GS_j}(t_R^{UTC})}{\partial \dot{R}^n_{rel}(t_k)} = -\frac{\partial \dot{\rho}^{n,i}_{GS_j}(t_k)}{\partial \dot{R}^n(t_k)} \Delta t_R^n; n \neq 1 \qquad (5.6.2\text{-}17)^*$$

$$\frac{\partial \Re^n_{GS_j}(t_R^{UTC})}{\partial b_R^1(t_k)} = \frac{\partial \Re^n_{GS_j}(t_R^{UTC})}{\partial b_R^n(t_k)} \frac{\partial b_R^n(t_k)}{\partial b_R^1(t_k)} = 1\text{-}\frac{\dot{\rho}^{n,i}_{GS_j}(t_k)}{c} - \frac{d_R^n(t_k)}{c} \qquad (5.6.2\text{-}18)^*$$

$$\frac{\partial \Re^n_{GS_j}(t_R^{UTC})}{\partial b^n_{rel}(t_k)} = \frac{\partial \Re^n_{GS_j}(t_R^{UTC})}{\partial b_R^n(t_k)} \frac{\partial b_R^n(t_k)}{\partial b^n_{rel}(t_k)} = 1\text{-}\frac{\dot{\rho}^{n,i}_{GS_j}(t_k)}{c} - \frac{d_R^n(t_k)}{c};\ n \neq 1 \qquad (5.6.2\text{-}19)^*$$

$$\frac{\partial \Re^n_{GS_j}(t_R^{UTC})}{\partial {d_R}^1(t_k)} = -\Delta t_R^1 \qquad (5.6.2\text{-}20)^*$$

$$\frac{\partial \Re^n_{GS_j}(t_R^{UTC})}{\partial {d_{rel}}^n(t_k)} = -\Delta t_R^n; \quad n \neq 1 \qquad (5.6.2\text{-}21)^*$$

$$\frac{\partial \Re^n_{GS_j}(t_k)}{\partial b_\rho^{GS_j}(t_k)} = 1 \qquad (5.6.2\text{-}22)^*$$

5.6.3 GS One-Way Forward Averaged Doppler Measurement Model and Associated Partial Derivatives

If the transmitting GS is not known, the GS associated with the first measurement in each tracking contact is identified by the process of elimination. All visible GSs are identified using the algorithm provided in Section 7.1 of this document to test the visibility of each GS located in the onboard GS catalog. For each the visible GSs, the GS-to-satellite Doppler measurement is modeled using the model provided below. The GS that produces the smallest measurement residuals is selected as the transmitting station for that contact.

The instantaneous Doppler-shifted RCF received at the spacecraft is equal to

$$f'_{RCF} = f_{RCF}\left(1 - \frac{\dot{\rho}}{c}\right) + \delta F_{atm} + \delta F_{rel} \qquad (5.6\text{-}12)$$

$$f'_{RCF} \cong f_{RCF}\left(1 - \frac{\dot{\rho}}{c}\right) + \delta F_{atm} \qquad (5.6\text{-}12a)$$

where

f'_{RCF} = Doppler-shifted RCF

f_{RCF} = transmitted GS RCF

$\dot{\rho}$ = time rate of change of the light-time-corrected range from the GS to the receiving spacecraft antenna, ρ [defined in Equation (5.6-4)]

δF_{atm} = signal delay due to atmospheric effects

δF_{rel} = signal delay due to relativistic effects

GEONS models the atmospheric correction due to tropospheric refraction near the GS. The corrections for relativistic effects are not applied in the GS measurement model.

The true instantaneous Doppler shift is given by

$$(f_D)_{true} = f'_{RCF} - f_{RCF} \tag{5.6-13}$$

The Doppler shift is measured onboard with respect to the receiver's S-band frequency reference, such that the instantaneous Doppler measurement is given by

$$(f_D)_{ext} = f'_{RCF} - f_{ref}(t) \tag{5.6-14}$$

where

$f_{ref}(t)$ = receiver's S-band frequency reference at time t, nominally equal to 2106.406250 megahetz

Substituting Equation (5.6-12) into Equation (5.6-14), omitting the relativistic corrections, and averaging over the Doppler averaging interval, ΔT, the averaged Doppler measurement from the jth GS to satellite n can be expressed as

$$\left(\overline{F_D(t_k)}\right)^n_{GS_j} = \frac{1}{\Delta T}\int_{t_k-\Delta T}^{t_k}(f_D)^n_{ext}(t)dt \tag{5.6-15}$$

$$\left(\overline{F_D(t_k)}\right)^n_{GS_j} = \frac{1}{\Delta T}\int_{t_k-\Delta T}^{t_k}\left[f_{RCF}\left(1-\frac{\dot{\rho}^{n,i}_{GS_j}}{c}\right)+\delta F_{atm}-f^n_{ref}(t)\right]dt + b_d^{GS_j}(t_k) \tag{5.6-16}$$

$$\left(\overline{F_D(t_k)}\right)^n_{GS_j} = f_{RCF}\left(1-\frac{\Delta\rho^{n,i}_{GS_j}(t_k)}{c\Delta T}-\frac{\Delta\rho_{atm}(t_k)}{c\Delta T}\right)-\overline{f^n_{ref}(t_k)}+b_d^{GS_j}(t_k) \tag{5.6-17}*$$

where

$$\Delta\rho^{n,i}_{GS_j}(t_k) = \rho^{n,i}_{GS_j}(t_k) - \rho^{n,i}_{GS_j}(t_k-\Delta T) \tag{5.6-18}*$$

$$\Delta\rho_{atm}(t_k) = \delta\rho_{atm}(t_k) - \delta\rho_{atm}(t_k-\Delta T) \tag{5.6-19}*$$

The range between transmitting ground station j and receiving antenna i on satellite n, $\rho^{n,i}_{GS_j}(t_k)$, is computed using Equation (5.6-4); $\delta\rho_{atm}(t_k)$ is the tropospheric delay associated with a signal transmitted at time t_k in meters, which is computed using Equation (5.6-8); $b_d^{GS_j}(t_k)$ is the value of the GS Doppler measurement bias in Hertz associated with the *j*th GS; and $\overline{f^n_{ref}(t_k)}$ is the

averaged value of $f^n_{ref}(t_k)$ over the time $t_k - \Delta T$ to t_k. The value of $\overline{f^n_{ref}(t_k)}$ is approximated as follows, neglecting the effects of frequency drift over the averaging interval:

$$\overline{f^n_{ref}(t_k)} \cong f^n_{ref}(t_k) = f_{ref}(t_0)\left[1 + \frac{d^n_R(t_k)}{c}\right] \qquad (5.6\text{-}20)^*$$

where $d^n_R(t_k)$, the receiver time bias rate, is computed using Equation 4.3-19 and $f_{ref}(t_0)$ is the initial value of the S-band Doppler reference frequency, a commanded parameter nominally equal to 2106406250 Hertz.

Note that the measurement model as currently implemented in GEONS assumes that the Doppler averaging interval is equal to the interval between calls to the state estimation task, or equivalently the integration stepsize.

Note that because the Doppler measurement model requires the computation of the range at an earlier time, $\rho^n_{GS_j}(t_k - \Delta T)$, the first Doppler measurement in a contact is rejected if the state vector is not available at that time.

The nonzero components of the row vector of partial derivatives of the GS Doppler measurements with respect to the components of the estimation state vector, $\bar{X}(t_k)$, consisting of absolute states for the local and nonlocal satellites are as follows:

$$\frac{\partial\left(\overline{F_D(t_k)}\right)^n_{GS_j}}{\partial \bar{R}^n(t_k)} = -\frac{f_{RCF}}{c\Delta T}\left[\frac{\partial \rho^{n,i}_{GS_j}(t_k)}{\partial \bar{R}^n(t_k)} - \frac{\partial \rho^{n,i}_{GS_j}(t_k - \Delta T)}{\partial \bar{R}^n(t_k - \Delta T)}\left(\frac{\partial \bar{R}^n(t_k - \Delta T)}{\partial \bar{R}^n(t_k)}\right)\right] \qquad (5.6\text{-}21)^*$$

$$\frac{\partial\left(\overline{F_D(t_k)}\right)^n_{GS_j}}{\partial \dot{\bar{R}}^n(t_k)} = \frac{f_{RCF}}{c\Delta T}\left[\frac{\partial \rho^{n,i}_{GS_j}(t_k - \Delta T)}{\partial \bar{R}^n(t_k - \Delta T)}\left(\frac{\partial \bar{R}^n(t_k - \Delta T)}{\partial \dot{\bar{R}}^n(t_k)}\right)\right] \qquad (5.6\text{-}22)^*$$

$$\frac{\partial\left(\overline{F_D(t_k)}\right)^n_{GS_j}}{\partial \Delta C^n_D(t_k)} = \frac{f_{RCF}}{c\Delta T}\left[\frac{\partial \rho^{n,i}_{GS_j}(t_k - \Delta T)}{\partial \bar{R}^n(t_k - \Delta T)}\left(\frac{\partial \bar{R}^n(t_k - \Delta T)}{\partial \Delta C^n_D(t_k)}\right)\right] \qquad (5.6\text{-}23)^*$$

$$\frac{\partial\left(\overline{F_D(t_k)}\right)^n_{GS_j}}{\partial \Delta C^n_R(t_k)} = \frac{f_{RCF}}{c\Delta T}\left[\frac{\partial \rho^{n,i}_{GS_j}(t_k - \Delta T)}{\partial \bar{R}^n(t_k - \Delta T)}\left(\frac{\partial \bar{R}^n(t_k - \Delta T)}{\partial \Delta C^n_R(t_k)}\right)\right] \qquad (5.6\text{-}24)^*$$

$$\frac{\partial\left(\overline{F_D(t_k)}\right)^n_{GS_j}}{\partial d^n_R(t_k)} = \frac{\partial\left(\overline{F_D(t_k)}\right)^n_{GS_j}}{\partial f^n_{ref}(t_k)}\frac{\partial f^n_{ref}(t_k)}{\partial d^n_R(t_k)} = -\frac{f_{ref}(t_0)}{c} \qquad (5.6\text{-}25)^*$$

$$\frac{\partial\left(\overline{F_D(t_k)}\right)^n_{GS_j}}{\partial b_d^{GS_j}(t_k)} = 1 \qquad \text{(5.6-25b)*}$$

The partial derivatives of the range in Equations (5.6-21) and (5.6-22) are defined in Equation (5.6.2-11) in Section 5.6.2. These derivatives are evaluated at the current measurement timetag, t_k, and at the time $t_k - \Delta T$, where ΔT is the Doppler averaging interval.

The partial derivatives of the position vector at the time $t_k - \Delta T$ with respect to the estimated state vector are related to the components of the state transition submatrix defined by Equation (4.4-1a) in Section 4.4.1 as follows

$$\left(\frac{\partial \overline{R}^n(t_k - \Delta T)}{\partial \overline{R}^n(t_k)}\right) = (W)_{i=1,2,3;\, j=1,2,3} \qquad \text{(5.6-26)*}$$

$$\left(\frac{\partial \overline{R}^n(t_k - \Delta T)}{\partial \dot{\overline{R}}^n(t_k)}\right) = (W)_{i=1,2,3;\, j=4,5,6} \qquad \text{(5.6-27)*}$$

$$\left(\frac{\partial \overline{R}^n(t_k - \Delta T)}{\partial \Delta C_D^n}\right) = (W)_{i=1,2,3;\, j=7} \qquad \text{(5.6-28)*}$$

$$\left(\frac{\partial \overline{R}^n(t_k - \Delta T)}{\partial \Delta C_R^n}\right) = (W)_{i=1,2,3;\, j=8} \qquad \text{(5.6-29)*}$$

where

$$W = \begin{bmatrix} \dfrac{\partial \overline{R}^n(t_k)}{\partial \overline{R}^n(t_k - \Delta T)} & \dfrac{\partial \overline{R}^n(t_k)}{\partial \dot{\overline{R}}^n(t_k - \Delta T)} & \dfrac{\partial \overline{R}^n(t_k)}{\partial \Delta C_D^n(t_k - \Delta T)} & \dfrac{\partial \overline{R}^n(t_k)}{\partial \Delta C_R^n(t_k - \Delta T)} \\ \dfrac{\partial \dot{\overline{R}}^n(t_k)}{\partial \overline{R}^n(t_k - \Delta T)} & \dfrac{\partial \dot{\overline{R}}^n(t_k)}{\partial \dot{\overline{R}}^n(t_k - \Delta T)} & \dfrac{\partial \dot{\overline{R}}^n(t_k)}{\partial \Delta C_D^n(t_k - \Delta T)} & \dfrac{\partial \dot{\overline{R}}^n(t_k)}{\partial \Delta C_R^n(t_k - \Delta T)} \\ 0_{1x3} & 0_{1x3} & 1 & 0 \\ 0_{1x3} & 0_{1x3} & 0 & 1 \end{bmatrix}^{-1} \qquad \text{(5.6-30)*}$$

If the atmospheric drag coefficient correction and/or the solar radiation pressure coefficient correction are not estimated, the matrix W does not include the columns associated with these state components.

If the estimated state vector consists of an absolute state for the local satellite (n=1) and relative states for the nonlocal satellites (n>1), the nonzero partial derivatives of a GS Doppler measurement with respect to the components of the estimation state vector, $\overline{X}(t_k)$, are computed as follows:

$$\frac{\partial\left(\overline{F_D(t_k)}\right)^n_{GS_j}}{\partial \overline{R}^1(t_k)} = -\frac{f_{RCF}}{c\Delta T}\left[\frac{\partial \rho^{n,i}_{GS_j}(t_k)}{\partial \overline{R}^n(t_k)} - \frac{\partial \rho^{n,i}_{GS_j}(t_k-\Delta T)}{\partial \overline{R}^n(t_k-\Delta T)}\left(\frac{\partial \overline{R}^1(t_k-\Delta T)}{\partial \overline{R}^1(t_k)}\right)\right] \quad \text{(5.6-21a)*}$$

$$\frac{\partial\left(\overline{F_D(t_k)}\right)^n_{GS_j}}{\partial \dot{\overline{R}}^1(t_k)} = \frac{f_{RCF}}{c\Delta T}\left[\frac{\partial \rho^{n,i}_{GS_j}(t_k-\Delta T)}{\partial \overline{R}^n(t_k-\Delta T)}\left(\frac{\partial \overline{R}^1(t_k-\Delta T)}{\partial \dot{\overline{R}}^1(t_k)}\right)\right] \quad \text{(5.6-22a)*}$$

$$\frac{\partial\left(\overline{F_D(t_k)}\right)^n_{GS_j}}{\partial \Delta C^1_D(t_k)} = \frac{f_{RCF}}{c\Delta T}\left[\frac{\partial \rho^{n,i}_{GS_j}(t_k-\Delta T)}{\partial \overline{R}^n(t_k-\Delta T)}\left(\frac{\partial \overline{R}^1(t_k-\Delta T)}{\partial \Delta C^1_D(t_k)}\right)\right] \quad \text{(5.6-23a)*}$$

$$\frac{\partial\left(\overline{F_D(t_k)}\right)^n_{GS_j}}{\partial \Delta C^1_R(t_k)} = \frac{f_{RCF}}{c\Delta T}\left[\frac{\partial \rho^{n,i}_{GS_j}(t_k-\Delta T)}{\partial \overline{R}^n(t_k-\Delta T)}\left(\frac{\partial \overline{R}^1(t_k-\Delta T)}{\partial \Delta C^1_R(t_k)}\right)\right] \quad \text{(5.6-24a)*}$$

$$\frac{\partial\left(\overline{F_D(t_k)}\right)^n_{GS_j}}{\partial d^1_R(t_k)} = \frac{\partial\left(\overline{F_D(t_k)}\right)^n_{GS_j}}{\partial f^n_{ref}(t_k)}\frac{\partial f^n_{ref}(t_k)}{\partial d^n_R(t_k)} = -\frac{f_{ref}(t_0)}{c} \quad \text{(5.6-25c)*}$$

$$\frac{\partial\left(\overline{F_D(t_k)}\right)^n_{GS_j}}{\partial \overline{R}^n_{rel}(t_k)} = -\frac{f_{RCF}}{c\Delta T}\left[\frac{\partial \rho^{n,i}_{GS_j}(t_k)}{\partial \overline{R}^n(t_k)} - \frac{\partial \rho^{n,i}_{GS_j}(t_k-\Delta T)}{\partial \overline{R}^n(t_k-\Delta T)}\left(\frac{\partial \overline{R}^n_{rel}(t_k-\Delta T)}{\partial \overline{R}^n_{rel}(t_k)}\right)\right]; n \neq 1 \quad \text{(5.6-21b)*}$$

$$\frac{\partial\left(\overline{F_D(t_k)}\right)^n_{GS_j}}{\partial \dot{\overline{R}}^n_{rel}(t_k)} = \frac{f_{RCF}}{c\Delta T}\left[\frac{\partial \rho^{n,i}_{GS_j}(t_k-\Delta T)}{\partial \overline{R}^n(t_k-\Delta T)}\left(\frac{\partial \overline{R}^n_{rel}(t_k-\Delta T)}{\partial \dot{\overline{R}}^n_{rel}(t_k)}\right)\right]; n \neq 1 \quad \text{(5.6-22b)*}$$

$$\frac{\partial\left(\overline{F_D(t_k)}\right)^n_{GS_j}}{\partial \Delta C^n_{D_{rel}}(t_k)} = \frac{f_{RCF}}{c\Delta T}\left[\frac{\partial \rho^{n,i}_{GS_j}(t_k-\Delta T)}{\partial \overline{R}^n(t_k-\Delta T)}\left(\frac{\partial \overline{R}^n_{rel}(t_k-\Delta T)}{\partial \Delta C^n_{D_{rel}}(t_k)}\right)\right]; n \neq 1 \quad \text{(5.6-23b)*}$$

$$\frac{\partial\left(\overline{F_D(t_k)}\right)^n_{GS_j}}{\partial \Delta C^n_{R_{rel}}(t_k)} = \frac{f_{RCF}}{c\Delta T}\left[\frac{\partial \rho^{n,i}_{GS_j}(t_k-\Delta T)}{\partial \overline{R}^n(t_k-\Delta T)}\left(\frac{\partial \overline{R}^n_{rel}(t_k-\Delta T)}{\partial \Delta C^n_{R_{rel}}(t_k)}\right)\right]; n \neq 1 \quad \text{(5.6-24b)*}$$

$$\frac{\partial\left(\overline{F_D(t_k)}\right)^n_{GS_j}}{\partial d^n_{R\,rel}(t_k)} = \frac{\partial\left(\overline{F_D(t_k)}\right)^n_{GS_j}}{\partial f^n_{ref}(t_k)}\frac{\partial f^n_{ref}(t_k)}{\partial d^n_R(t_k)} = -\frac{f_{ref}(t_0)}{c}; n \neq 1 \quad \text{(5.6-25d)*}$$

$$\frac{\partial\left(\overline{F_D(t_k)}\right)^n_{GS_j}}{\partial b^{GS_j}_d(t_k)} = 1 \quad \text{(5.6-25e)*}$$

The partial derivatives of the range are defined in Equation (5.6.2-11) in Section 5.6.2. These derivatives are evaluated at the current measurement timetag, t_k, and at the time $t_k - \Delta T$, where ΔT is the Doppler averaging interval. The partial derivatives of position vector at the time $t_k - \Delta T$ with respect to the estimated state vector components are related to the components of the inverse of the state transition matrix defined by Equation (4.4-1b) in Section 4.4.1

$$\left(\frac{\partial \overline{X}_{rel}(t_k - \Delta T)}{\partial \overline{X}_{rel}(t_k)}\right) = \left(\frac{\partial \overline{X}_{rel}(t_k)}{\partial \overline{X}_{rel}(t_{k-1})}\right)^{-1} \qquad \text{(5.6-26a)*}$$

where

$$\overline{X}_{rel} = \begin{bmatrix} \overline{X}^1 \\ \overline{X}^2_{rel} \\ \vdots \\ \overline{X}^{NS}_{rel} \\ \overline{B} \end{bmatrix}$$

and

$$\overline{X}^n_{rel} = \overline{X}^n - \overline{X}^1 = \begin{bmatrix} \overline{R}^n - \overline{R}^1 \\ \dot{\overline{R}}^n - \dot{\overline{R}}^1 \\ \Delta C^n_D - \Delta C^1_D \\ \Delta C^n_R - \Delta C^1_R \\ \overline{b}^n_R - \overline{b}^1_R \end{bmatrix} = \begin{bmatrix} \overline{R}^n_{rel} \\ \dot{\overline{R}}^n_{rel} \\ \left(\Delta C^n_D\right)_{rel} \\ \left(\Delta C^n_R\right)_{rel} \\ \overline{b}^n_{rel} \end{bmatrix}; \; n \neq 1$$

5.6.4 GS Round-Trip Range-Rate Measurement Preprocessing (not implemented in GEONS)

Round-trip measurements are not suitable for onboard processing. However, since the capability to measure one-way forward GS Doppler measurements has been implemented on very few spacecraft, the following procedure can be used to preprocess real range-rate measurements so that they can be processed in GEONS using the one-way GS Doppler measurement model given in Section 5.6.3.

The GS round-trip range-rate measurements are accumulated over a Doppler averaging interval, ΔT, equal to 10 seconds. These measurements reflect the total Doppler shift of the signal from the transmitting GS, through the receiving/transmitting satellite, to the receiving GS averaged over the Doppler averaging interval. The real round-trip GS measurements provided by the ground tracking network are timetagged at the receive time of the signal at the GS associated with the end of the averaging interval. For compatibility with the one-way GS Doppler model given in Section 5.6.3, the measurement timetag must be modified to reflect the receive time at the satellite. This

adjustment, which is performed external to GEONS, is computed based on a reference "truth" satellite ephemeris ($\overline{R}_{ref}(t), \dot{\overline{R}}_{ref}(t)$).

The round-trip signal is transmitted from the GS transmitter (node 1) at time t_1, received at the spacecraft receiver (node 2) at time t_2 (equal to t_k), and received at the GS receiver (node 3) at time t_3. The following Newton-Raphson iterative scheme is used to solve for the signal receive/transmission time at the satellite, t_2:

$$t_{2,n+1} = t_3 - \frac{\left|\overline{R}_{GS}(t_3) - \overline{R}_{ref}(t_{2,n})\right|}{c} \tag{5.6-31}$$

where

$t_{2,n+1}$ = $(n+1)^{th}$ approximation for t_2

$t_{2,n}$ = n^{th} approximation for t_2

$\overline{R}_{ref}(t_2)$ = position of the transmitting satellite at time t_2

$\overline{R}_{GS}(t_3)$ = position of the GS at time the reception time t_3

The iterative solution of Equations (5.6-31) is started by setting

$$t_{2,0} = t_3 \tag{5.6-32}$$

$$\overline{R}_{ref}(t_{2,0}) = \overline{R}_{ref}(t_3) \tag{5.6-33}$$

The receiving GS position vector is available in ECEF coordinates and is transformed to J2000.0 inertial coordinates using the transformations defined in Sections 3.2.1 through 3.2.3. This iterative scheme is continued until the condition $\left|t_{1,n+1} - t_{1,n}\right| \le \varepsilon$ is satisfied, where ε is a small tolerance (nominally equal to 10^{-8} second).

5.7 Geometric Point Solution Measurement Models

As an alternative to processing the GPS pseudorange and Doppler measurements discussed in Sections 5.3 and 5.4, the GPS receiver's geometric point solutions can be processed as measurements in GEONS. The geometric point solutions, which are typically available every 0.5 to 1 second, are sampled based on a specified minimum measurement spacing, nominally every 10 seconds. The general form of the measurement model is as follows:

$$Y_k = G\ [\bar{X}(t_k),\ t_k] + \varepsilon \tag{5.7-1}$$

where t_k is the true measurement time, referenced to UTC, and ε is the measurement error. It is assumed that ε has a zero-mean Gaussian distribution with standard deviation σ, which is commandable for each measurement type. The measurement standard deviation is typically determined through analysis of the random component of the measurement error as part of the filter tuning process.

When GEONS processes the point solution measurements, the estimation state vector, $\overline{X}(t)$ includes the receiver position vector, $\overline{R}$; velocity vector, $\dot{\overline{R}}$; corrections to the drag and solar radiation pressure coefficients, ΔC_D and ΔC_R; GPS receiver bias, b_R; and GPS receiver bias rate, d_R for one or more receivers.

Section 5.7.1 addresses preprocessing of the raw geometric point solution measurements obtained from the GPS receiver. The geometric point solution measurement and partial derivative models are presented in Section 5.7.2. Section 5.7.3 provides the measurement update processing algorithm to be used in conjunction with the geometric point solution vector measurements.

5.7.1 Geometric Point Solution Measurement Preprocessing

The measurement model defined in Section 5.7.2 assumes that the raw geometric point solutions consist of the three Cartesian components of the spacecraft position vector referenced to the instantaneous ECEF coordinate frame, $\bar{r}^* = \begin{pmatrix} x^* & y^* & z^* \end{pmatrix}$, and a time bias from GPS time, b^*

$$\bar{p}^* = \left(r^*, b^*\right)$$

with a GPS-referenced receiver time tag, $t_R^{(RC)}$. **Note that if the measurement time tag has been corrected by the receiver to account for the current estimate of the receiver clock's time bias with respect to GPS time, the measurement component *b** should be set to 0.**

5.7.2 Geometric Point Solution Measurement Model and Associated Partial Derivatives

This section provides the algorithm used to model the observed point solution measurements, $\bar{p}^* = \left(r^*, b^*\right)$. The true point solution time t_R is related to the point solution measurement timetag, $t_R^{(RC)}$, as follows:

$$t_R = t_R^{(RC)} - \delta t_R \tag{5.7-2}^*$$

where δt_R is the measurement timetag error, which is related to the residual receiver clock bias, $b_R(t)$, defined in Section 4.3:

$$\delta t_R = \frac{b_R(t)}{c} \tag{5.7-3}*$$

Optionally the current estimate of the measurement timetag error, δt_R, can be used to correct the measurement timetag following Equation (5.7-2). This option is normally exercised when the point solution timetags have not been corrected by the receiver using the point solution time bias estimates.

The geometric point solution measurement model corresponding to the nth spacecraft is computed as follows:

$$\bar{r}^* = \bar{r}^n_{ECEF}(t_k) = BR_g C\bar{R}^n{}_{J2000}(t_k) \tag{5.7-4}*$$

where B, R_g, C are the pseudo-body-fixed to ECEF, True-of-Date to pseudo-body-fixed, and J2000.0 to True-of-Date transformation matrices defined in Section 3.2, respectively, and $\bar{R}^n{}_{J2000}(t_k)$ is the predicted value of the spacecraft position at the UTC-referenced measurement time, t_k, corresponding to the GPS-referenced receiver's measurement time tag, t_R. The GPS time to UTC time conversion algorithm is provided in Section 3.3.1.

The computation of partial derivatives of the geometric point solution measurement model with respect to the estimation state vector, $\bar{X}(t_k)$, is as follows. The matrix of partial derivatives of the geometric point solution measurements with respect to $\bar{X}(t_k)$ is defined as follows:

$$\left[H(t_k)\right]_{\bar{p}^{*n}} = \frac{\partial \bar{p}^{*n}(t_k)}{\partial \bar{X}(t_k)} \tag{5.7-5}$$

The following are the nonzero elements with respect to an estimation state vector consisting of absolute state vector for all satellites:

$$\frac{\partial \bar{r}^{*n}(t_k)}{\partial \bar{R}^n(t_k)} = BR_g C \tag{5.7-6a}*$$

$$\frac{\partial b^{*n}(t_k)}{\partial b^n_R(t_k)} = 1 \tag{5.7-6b}*$$

The following are the nonzero elements with respect to an estimation state vector consisting of an absolute state vector for the local satellite and relative state vectors for all remote satellites:

$$\frac{\partial \bar{r}^{*n}(t_k)}{\partial \bar{R}^1(t_k)} = BR_g C \tag{5.7-6c}*$$

$$\frac{\partial \bar{r}^{*n}(t_k)}{\partial \bar{R}^n_{rel}(t_k)} = BR_g C; \quad n > 1 \tag{5.7-6c)*}$$

$$\frac{\partial b^{*n}(t_k)}{\partial b^n_R(t_k)} = 1 \tag{5.7-6e)*}$$

5.7.3 Measurement Update for Geometric Point Solution Processing

At each valid measurement time, t_k, the measurement update processing is performed successively for each component of the point solution measurement for each of the n spacecraft being estimated. The height of ray path editing test, defined as step 1 in the measurement update procedure presented in Section 2.3.2 is not applicable for this measurement type.

Given the results of the time update (defined in Section 2.3.1), $\hat{\bar{X}}_k(-)$, $U_k(-)$, and $D_k(-)$, compute the updated total state vector, $\hat{\bar{X}}_k(+)$, and the updated state error covariance matrix factors, $U_k(+)$ and $D_k(+)$, successively for the four components of the observed measurement, $\left[\bar{r}^{*n}\right]_i$, $i = 1, 2, 3$; b^{*n}, $i = 4$:

1. Compute the point solution measurement model, $(\bar{r}^n_{ECEF}(t_k), b^n_R)$, and the measurement partial derivative matrix, $H(t_k)$, at time t_k, as defined in Equation 5.7-5. Compute the J2000 to ECEF coordinate rotation matrix, $BR_g C$, only for $i = 1$ and save for use with the $i = 2$ and 3 components.

2. Compute the measurement residual, y^n_k, for the ith measurement component

$$y^n_k = \begin{cases} \left[r^{*n}\right]_i - \left[\bar{r}^n_{ECEF}\right]_i, & i = 1, 2, 3 \\ \left[b^{*n}\right] - \left[b^n_R\right], & i = 4 \end{cases} \tag{5.7-9)*}$$

3. Perform the following n-sigma measurement residual edit test for the ith measurement component before measurement updating the state vector and state error covariance matrix. Compute the predicted measurement residual variance, V_k, using the $\left[U^-\right]$ and $\left[D^-\right]$ factors following the algorithms given in step 3 of Section 2.3.2.

4. Edit the ith measurement component as follows:

   Calculate the sigma ratio

$$D_k = \frac{y_k}{\sqrt{V_k}} \tag{5.7-10)*}$$

If $|D_k| \leq N_\sigma$, accept the *i*th measurement component and continue the measurement update processing. If $|D_k| > N_\sigma$, reject the entire point solution measurement, and the calculation is complete. In these tests, N is a specifiable integer with a default value of 4.

5. Update the state error covariance factors, based on the ith measurement component for spacecraft n following the algorithm given in step 5 of Section 2.3.2.

6. Compute the Kalman gain vector for the *i*th measurement component following step 6 in Section 2.3.2.

7. Update $\hat{\bar{X}}_k(-)$ based on the *i*th measurement component following step 7 in Section 2.3.2.

8. For the i= 1, 2, and 3 components, reset the predicted covariance elements and the predicted estimation state elements as follows and return to step 1 to process the remaining measurement component(s)

$$\left[U^-\right] = \left[U^+\right] \qquad (5.7\text{-}11)^*$$

$$\left[D^-\right] = \left[D^+\right] \qquad (5.7\text{-}12)^*$$

$$\hat{\bar{X}}_k(-) = \hat{\bar{X}}_k(+) \qquad (5.7\text{-}13)^*$$

9. If fault detection is enabled, perform the navigation fault detection tests on the updated state and covariance after the entire point solution measurement is processed, as defined in step 8 of Section 2.3.2.

5.8 Celestial Object Measurement Models

This section contains the mathematical specifications for the celestial object measurement models.

The general form of the measurement model is as follows:

$$Y_k = G\ [\bar{X}(t_k),\ t_k] + \varepsilon \tag{5.8-1}$$

where t_k is the measurement time, referenced to the satellite timing reference, and ε is the measurement error. It is assumed that ε has a zero-mean Gaussian distribution with standard deviation σ, which is commandable for each measurement type. The measurement standard deviation is typically determined through analysis of the random component of the measurement error as part of the filter tuning process. Note that GEONS models the measurement standard deviation as a constant value. However, in situations such as relative range and bearing measurements where there is a large variation in the sensor's measurement noise with relative distance, computing the measurement standard deviation as a function of distance to the target based on calibrated sensor performance can provide a more realistic value of the noise contribution.

The timetag associated with the k^{th} measurement is the sensor measurement time as measured with respect to satellite time, $t_k^{S/C}$. In the presence of a satellite timing bias, the true measurement time is given by

$$t_k = t_k^{S/C} + t_2^B \tag{5.8-2}$$

where t_2^B is the offset of the satellite timing reference from UTC.

For GEONS, the estimation state vector, $\overline{X(t)}$, includes the user satellite position vector, $\overline{R}$; velocity vector, $\dot{\overline{R}}$; receiver time bias and time bias rate, and optional corrections to the solar radiation pressure coefficient, ΔC_R and atmospheric drag coefficient, ΔC_D. When celestial object measurements are processed, the estimation state vector can be augmented to include sensor measurement biases.

Section 5.8.1 describes the satellite attitude models used for three-axis stabilized Sun-pointing and Earth-pointing satellite and for spin-stabilized satellite. Section 5.8.2 provides the models for processing line-of-sight (LOS) measurements to either a celestial object or another satellite and the associated measurement partial derivatives. Section 5.8.3 provides the models for processing planetary sensor measurements for spin-stabilized satellite and the associated measurement partial derivatives. Section 5.8.4 provides the models for the processing measurements of the angular separation of the line-of-sight vectors to two bodies and the associated measurement partial derivatives.

5.8.1 Satellite Models

This section defines the satellite configuration and attitude models used by GEONS to simulate and model celestial object measurements. Sections 5.8.1.1 and 5.8.1.2 provide the models used for three-axis stabilized and spin-stabilized satellite, respectively.

Three-Axis Stabilized Sun-Pointing Satellite

This model is based on the nominal attitude configuration of the Solar and Heliospheric Observatory (SOHO) satellite. Figure 5-5a illustrates the nominal sun-pointing satellite absolute reference frame. The satellite is controlled to maintain the roll, pitch and yaw angles about these axes near zero. The origin of the absolute reference frame is the center of mass of the satellite. The absolute reference frame x_A-axis is aligned with the satellite-to-sun vector, the y_A-axis is perpendicular to the plane that contains the x_A-axis and the normal vector to the ecliptic plane, and the z_A-axis is orthogonal to the x_A-and y_A-axes. The boresight of the sun sensor is assumed to be located along the x_A-axis. The boresight of the star sensor is assumed to be nominally located along the z_A-axis. Figure 5-5b illustrates the relationship of the normal vector to the true ecliptic coordinate frame to the inertial frame. Figure 3-7 illustrates the relationship of the true ecliptic coordinate frame to the inertial Mean of J2000.0 frame.

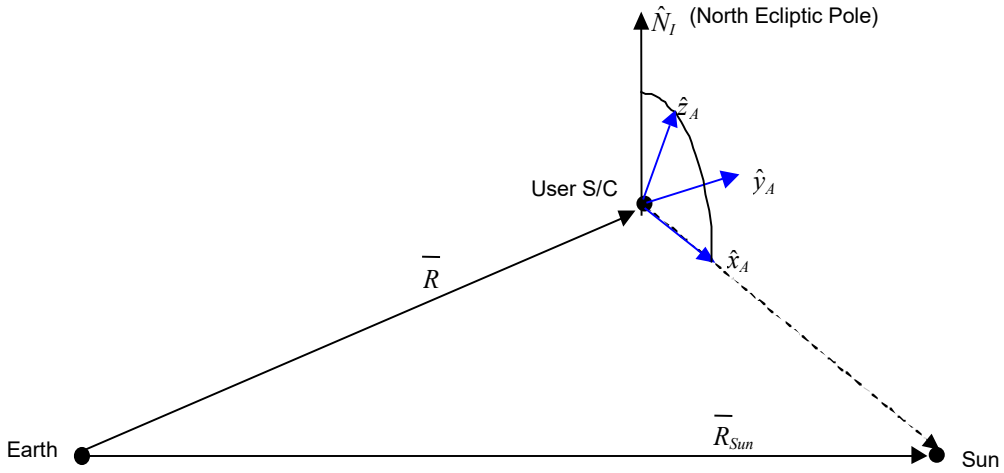

Figure 5-5a. Definition of Sun-Pointing 3-Axis Stabilized Absolute Reference Frame

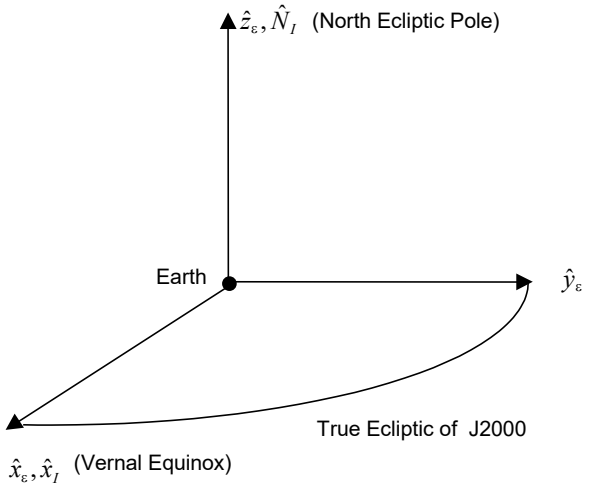

Figure 5-5b. Definition of True Ecliptic Coordinate Frame

The components of the normal vector to the ecliptic in the inertial frame are given as follows:

$$\hat{N}_I^T = (0, -\sin\varepsilon_m, \cos\varepsilon_m) \tag{5.8-4}*$$

where ε_m is the mean obliquity of the ecliptic defined in Equation 3.2-17 in Section 3.2.2.

In this case the absolute reference frame unit vectors referenced to the inertial frame are computed as follows:

$$\begin{aligned} \hat{x}_A &= \frac{\overline{R}_{Sun} - \overline{R}}{\left|\overline{R}_{Sun} - \overline{R}\right|} \\ \hat{y}_A &= -\frac{\hat{x}_A \times \hat{N}_I}{\left|\hat{x}_A \times \hat{N}_I\right|} \\ \hat{z}_A &= \hat{x}_A \times \hat{y}_A \end{aligned} \tag{5.8-5}*$$

The corresponding matrix $M_{AI}(t)$ that transforms from the geocentric inertial frame to the absolute reference frame at time t is given by

$$M_{AI}(t) = \begin{bmatrix} \hat{x}_A^T \\ \hat{y}_A^T \\ \hat{z}_A^T \end{bmatrix} \tag{5.8-6}*$$

The corresponding matrix $A(t)$ that transforms from the absolute reference frame to the satellite body frame at time t is given by

$$A(t) = \begin{bmatrix} \cos\theta\cos\psi & \cos\theta\sin\psi & -\sin\theta \\ -\cos\phi\sin\psi + \sin\phi\sin\theta\cos\psi & \cos\phi\cos\psi + \sin\phi\sin\theta\sin\psi & \sin\phi\cos\theta \\ \sin\phi\sin\psi + \cos\phi\sin\theta\cos\psi & -\sin\phi\cos\psi + \cos\phi\sin\theta\sin\psi & \cos\phi\cos\theta \end{bmatrix} \quad (5.8\text{-}7)^*$$

where

ϕ, θ, ψ = satellite body roll, pitch, and yaw angles at time t with respect to the x_A, y_A, and z_A axes, respectively, corresponding to the 3-2-1 sequence of Euler angle rotations used for SOHO

or equivalently

$$A(t) = \begin{bmatrix} q_1^2 - q_2^2 - q_3^2 + q_4^2 & 2(q_1 q_2 + q_3 q_4) & 2(q_1 q_3 - q_2 q_4) \\ 2(q_1 q_2 - q_3 q_4) & -q_1^2 + q_2^2 - q_3^2 + q_4^2 & 2(q_2 q_3 + q_1 q_4) \\ 2(q_1 q_3 + q_2 q_4) & 2(q_2 q_3 - q_1 q_4) & -q_1^2 - q_2^2 + q_3^2 + q_4^2 \end{bmatrix} \quad (5.8\text{-}8)^*$$

where

q_1, q_2, q_3, q_4 = quaternions or Euler symmetric parameters defining the orientation of the satellite body at time t with respect to the x_A, y_A, and z_A axes

The capability is available to input an attitude history file into GEONS. Operationally, this attitude information could be provided by an onboard attitude estimator operating in parallel with the GEONS orbit estimator or by an advanced star tracking system that provides the attitude quaternion directly.

5.8.1.2 Spin-Stabilized Satellite

This model is based on the nominal attitude configuration of the Polar Plasma Laboratory (Polar) satellite. Figure 5-6 illustrates the nominal spinning satellite reference frame. The satellite spins at a rate ω about the satellite spin axis, nominally parallel to the geometric axis of the satellite, +Z axis. The orientation of the spin-axis with respect to the inertial frame is expressed as follows:

$$\hat{A} = \begin{bmatrix} \cos\alpha\ \cos\delta \\ \sin\alpha\ \cos\delta \\ \sin\delta \end{bmatrix} \quad (5.8\text{-}9)^*$$

where

$\hat{A}$ = unit vector along the spacecraft spin axis, referenced to the geocentric inertial frame

α = the right ascension of the spin axis

δ = declination of the spin axis

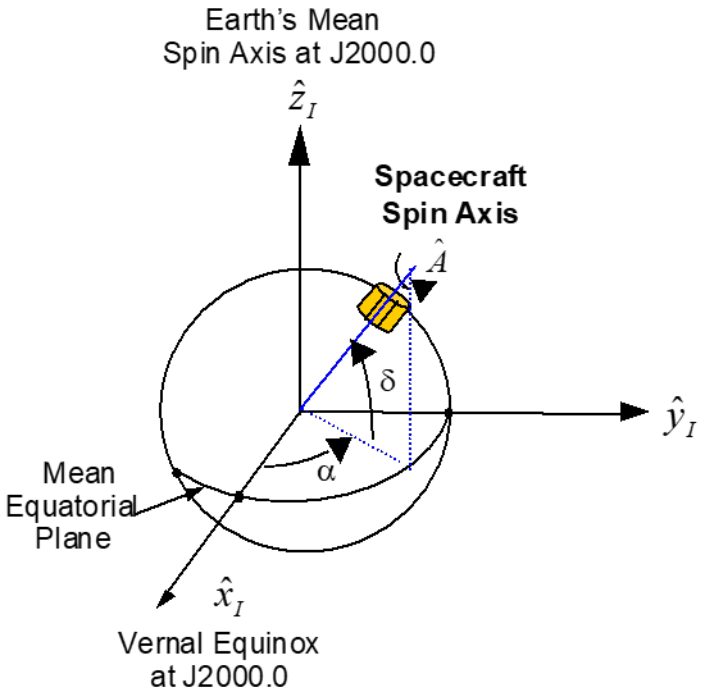

Figure 5-6. Definition of Spin-Stabilized Attitude Reference Frame

5.8.1.3 Three-Axis Stabilized Earth-Pointing Satellite (not implemented in GEONS)

This model is based on the nominal attitude configuration for an Earth-pointing satellite. The satellite is controlled to maintain the roll, pitch and yaw angles about the orbital coordinate system (OCS) axes near zero. The origin of the OCS is the center of mass of the satellite. The OCS z_o-axis points to the center of the Earth, the y_o-axis is aligned with the negative orbit normal, and the x_o-axis is orthogonal to the y_o-and z_o-axes.

The OCS axes referenced to the inertial frame are computed as follows.

$$\begin{aligned} \hat{x}_O &= \hat{y}_O \times \hat{z}_O \\ \hat{y}_O &= -\frac{\overline{R} \times \dot{\overline{R}}}{\left|\overline{R} \times \dot{\overline{R}}\right|} \\ \hat{z}_O &= \frac{-\overline{R}}{\left|\overline{R}\right|} \end{aligned} \qquad (5.8\text{-}10)^*$$

The corresponding matrix $M_{OI}(t)$ that transforms from the geocentric inertial frame to the OCS frame at time t is given by

$$M_{OI}(t) = \begin{bmatrix} \hat{x}_O{}^T \\ \hat{y}_O{}^T \\ \hat{z}_O{}^T \end{bmatrix} \qquad (5.8\text{-}11)^*$$

The corresponding matrix $A(t)$ that transforms from the OCS frame to the satellite body frame at time t is given by

$$A(t) = \begin{bmatrix} \cos p \cos y - \sin r \sin p \sin y & \cos p \sin y + \sin r \sin p \cos y & -\sin p \cos r \\ -\cos r \sin y & \cos r \cos y & \sin r \\ \sin p \cos y + \cos p \sin r \sin y & \sin p \sin y - \cos p \sin r \cos y & \cos r \cos p \end{bmatrix} \quad (5.8\text{-}12)^*$$

where

r, p, y = satellite body roll, pitch, and yaw angles at time t with respect to the x_o, y_o, and z_o axes, respectively, corresponding to the 3-1-2 sequence of Euler angle rotations typically used for 3-axis stabilized satellites

or equivalently

$$A(t) = \begin{bmatrix} q_1^2 - q_2^2 - q_3^2 + q_4^2 & 2(q_1 q_2 + q_3 q_4) & 2(q_1 q_3 - q_2 q_4) \\ 2(q_1 q_2 - q_3 q_4) & -q_1^2 + q_2^2 - q_3^2 + q_4^2 & 2(q_2 q_3 + q_1 q_4) \\ 2(q_1 q_3 + q_2 q_4) & 2(q_2 q_3 - q_1 q_4) & -q_1^2 - q_2^2 + q_3^2 + q_4^2 \end{bmatrix} \quad (5.8\text{-}13)^*$$

where

q_1, q_2, q_3, q_4 = quaternions or Euler symmetric parameters defining the orientation of the satellite body at time t with respect to the x_o, y_o, and z_o axes

5.8.2 Celestial Object and Intersatellite Measurements For a Three-Axis Stabilized Satellite

This section presents measurement models that are appropriate for visual and infrared cameras and digital Sun sensors. These models are not appropriate for the scanning horizon sensors and static Earth sensors typically flown on Earth-orbiting, three-axis-stabilized satellite; these models are provided in Sections 5.8.2.4 and 5.8.2.5, respectively. Section 5.8.2.1 provides models for line-of-sight measurements to a celestial body or another satellite. Section 5.8.2.1 provides models for bearing measurements to another satellite and Section 5.8.2.3 provides models for bearing measurements to a celestial body and landmarks located on that body.

5.8.2.1 Line-of-Sight Measurements for a Three-Axis Stabilized Satellite

This measurement model is appropriate for the type of sensor typically flown on a three-axis stabilized satellite where the celestial object (CO) is a point source, e.g. a digital Sun sensor. This model is also appropriate for intersatellite LOS measurements, such as those described in Reference 29 that are derived from an optical sensor combined with specific light sources (i.e. beacons).

This model was used to process measurements from the Adcole fine pointing sun sensors (FPSS) on the SOHO satellite. Similar sensors have flown on the Solar Maximum Mission (SMM) and Upper Atmosphere Research Satellite (UARS) satellite. Figure 5-7 illustrates the geometry of the SOHO FPSS measurements.

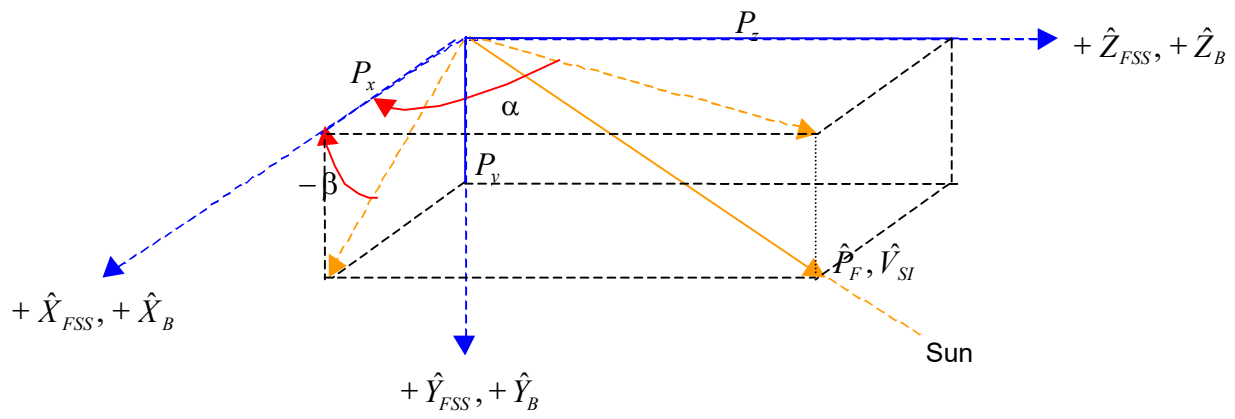

Figure 5-7. SOHO Fine Pointing Sun Sensor Measurements

The raw sensor measurements are the pitch and yaw angles of the LOS unit vector from the satellite to the CO (Sun, Moon, or planet) or another satellite, with respect to the sensor frame of reference. These angles are equivalent to the projection angles of the LOS vector onto the FSS X-Z and X-Y planes, respectively. These angles are related to the satellite-to-CO LOS unit vector components as follows

$$\begin{aligned} \alpha &= \arctan(P_z / P_x) \\ \beta &= \arctan(-P_y / P_x) \end{aligned} \tag{5.8-14}$$

where

α = pitch angle measurement in radians

β = yaw angle measurement in radians

$\hat{P}_S^k = (P_x, P_y, P_z)$ = components of the sensor k-to-CO or sensor k-to target-satellite unit vector in the sensor k frame (e.g. $\hat{X}_{FSS,}\ \hat{Y}_{FSS,}\ \hat{Z}_{FSS}$, as defined in Figure 5-7)

Equation 5.8-14 is used external to GEONS to convert the raw angle measurements to components of the sensor k-to-CO or sensor k-to target-satellite LOS unit vector in the sensor k frame, $\hat{P}_S^k$. The observed LOS measurement unit vector is then transformed to the imaging satellite body frame, applying corrections for calibrated misalignments between the sensor and satellite body frames

$$\left(\hat{P}_B^k\right)_{obs} = M_{SB}^{k\ T} \hat{P}_S^k \tag{5.8-14b}$$

where

M_{SB}^k = transformation matrix from the imaging satellite body frame, $\hat{X}_{B,}\ \hat{Y}_{B,}\ \hat{Z}_B$, to the sensor k frame

For the SOHO satellite, the FSS frame, $\hat{X}_{FSS,}\ \hat{Y}_{FSS,}\ \hat{Z}_{FSS}$, is nominally aligned (i.e. except for sensor misalignments) with the satellite body frame, $\hat{X}_{B,}\ \hat{Y}_{B,}\ \hat{Z}_{B}$.

GEONS uses the following equation to model the components of the LOS unit vector to the CO from sensor k on imaging satellite j in the body frame:

$$\hat{P}_B^k = \frac{M_{BI}^j\ \hat{V}_I^{k,P} + \Delta\hat{P}_B^k + \bar{b}_P^k}{\left| M_{BI}^j\ \hat{V}_I^{k,P} + \Delta\hat{P}_B^k + \bar{b}_P^k \right|} \qquad (5.8\text{-}15)^*$$

where

M_{BI}^j = rotation matrix from the geocentric inertial to the satellite j body frame, $\hat{X}_B^j, \hat{Y}_B^j, \hat{Z}_B^j$, equal to the attitude matrix defined in Section 3.2.8.1

$\hat{V}_I^{k,P}$ = Sensor k-to-CO LOS unit vector, referenced to the geocentric inertial frame (J2000.0)

$\Delta\hat{P}_B^k$ = calibrated line-of-sight measurement biases for sensor k (an input to the orbit estimation process)

$\bar{b}_P^k$ = estimated line-of-sight measurement biases for sensor k

GEONS uses the following equation to model the components of the intersatellite LOS measurement in the body frame from sensor k on imaging satellite j to a beacon on target satellite n:

$$\hat{P}_B^k = \frac{M_{BI}^j\ \hat{V}_I^{k,m} + \Delta\hat{P}_B^k + \bar{b}_P^k}{\left| M_{BI}^j\ \hat{V}_I^{k,m} + \Delta\hat{P}_B^k + \bar{b}_P^k \right|} \qquad (5.8\text{-}15a)^*$$

where

M_{BI}^j = rotation matrix from the geocentric inertial to the satellite j body frame, $\hat{X}_B^j, \hat{Y}_B^j, \hat{Z}_B^j$

$\hat{V}_I^{k,m}$ = LOS unit vector from sensor k on satellite j to beacon m on satellite n, referenced to the geocentric inertial frame (J2000.0)

$\Delta\hat{P}_B^k$ = calibrated line-of-sight measurement biases for sensor k (an input to the orbit estimation process)

$\bar{b}_P^k$ = estimated line-of-sight measurement biases for sensor k

The rotation matrix M_{BI}^j, which is provided by an onboard attitude determination process, is the product of the following two rotations

$$M_{BI}^j = A^j(t)\ M_{AI}^j \qquad (5.8\text{-}15b)$$

where

$A^j(t)$ = rotation matrix from the absolute reference frame, $\hat{x}_A, \hat{y}_A, \hat{z}_A$ to the satellite body frame, $\hat{X}_B^j, \hat{Y}_B^j, \hat{Z}_B^j$, at time t, as defined in Equations 5.8-7 and 5.8-8.

$M_{AI}^{\ j}$ = transformation matrix from the geocentric inertial to absolute reference frame, $\hat{x}_A^j, \hat{y}_A^j, \hat{z}_A^j$, such as that given by Equation (5.8-6) for the SOHO satellite

For the SOHO satellite, the satellite attitude is controlled to maintain the $\hat{X}_B$ axis in alignment with the absolute reference frame $\hat{x}_A$ axis defined in Equation (5.8-5).

The predicted inertial LOS unit vector from sensor k on satellite j to the CO P is computed as follows

$$\hat{V}_I^{k,P} \cong \frac{\overline{R}_I^P - \overline{R}_I^j}{\left|\overline{R}_I^P - \overline{R}_I^j\right|}; \quad \textit{ignoring offsets of sensor image center} \qquad \text{(5.8-15c)*}$$

where

$\overline{R}_I^j$ = position vector of satellite j, referenced to the geocentric inertial frame (J2000.0)

$\overline{R}_I^P$ = Position vector of the CO P referenced to the geocentric inertial frame (J2000.0)

The Earth is at the origin of the geocentric reference frame. The inertial position vectors for the Sun, Moon, and other planets are computed using the planetary ephemeris algorithms given in Section 4.1.1.

The predicted inertial LOS unit vector from the image center of sensor k on satellite j to beacon m on satellite n is computed as follows

$$\hat{V}_I^{k,m} = \frac{\overline{R}_I^{n,m} - \overline{R}_I^{j,k}}{\left|\overline{R}_I^{n,m} - \overline{R}_I^{j,k}\right|} \qquad \text{(5.8-15d)*}$$

where

$\overline{R}_I^{j,k}$ = position vector of the image center of sensor k on satellite j, referenced to the geocentric inertial frame (J2000.0), which is computed as follows, given the locations of the image center in the satellite body frame $\left(\Delta x_I^{j,k}, \Delta y_I^{j,k}, \Delta z_I^{j,k}\right)$

$$\overline{R}_I^{j,k} = \overline{R}^j + \left(M_{BI}^{\ j}\right)^T \begin{bmatrix} \Delta x_I^{j,k} \\ \Delta y_I^{j,k} \\ \Delta z_I^{j,k} \end{bmatrix} \qquad \text{(5.8-15e)*}$$

$\overline{R}_I^{n,m}$ = position vector of beacon m on satellite n, referenced to the geocentric inertial frame (J2000.0), which is computed as follows, given the locations of the beacon in the satellite body frame $\left(\Delta x_I^{n,m}, \Delta y_I^{n,m}, \Delta z_I^{n,m}\right)$

$$\overline{R}_I^{n,m} = \overline{R}^n + \left(M_{BI}^n\right)^T \begin{bmatrix} \Delta x_I^{n,m} \\ \Delta y_I^{n,m} \\ \Delta z_I^{n,m} \end{bmatrix} \tag{5.8-15f}*$$

The CO's position as viewed from the satellite, $\overline{R}^P - \overline{R}^j$, is not its true position. Equation 5.8-15c can be modified to account for planetary aberration. For the case of Sun sensor measurements, the following is the apparent satellite-to-Sun unit vector in the geocentric inertial frame (Reference 28):

$$\hat{V}_I^P = \frac{\left(\overline{R}_I^S - \overline{R}_I^j\right) + \tau\left(-\dot{\overline{R}}_I^S + \dot{\overline{R}}_I^j\right)}{\left|\overline{R}_I^S - \overline{R}_I^j + \tau\left(-\dot{\overline{R}}_I^S + \dot{\overline{R}}_I^j\right)\right|} \tag{5.8-15g}$$

where

$\overline{R}_I^S$ = Position vector of the Sun referenced to the geocentric inertial frame (J2000.0)

$-\dot{\overline{R}}_I^S = -\left[\dfrac{\overline{R}_I^S(t+\delta t) - \overline{R}_I^S(t)}{\delta t}\right]$, instantaneous velocity of the Earth relative to the Sun, where $\delta t = 1$ second

$\dot{\overline{R}}_I^j$ = instantaneous velocity of the satellite relative to the Earth

$$\tau = \frac{1}{c}\left|\frac{\overline{R}_I^S}{R_I^S} - \frac{\overline{R}_I^j}{R_I^j}\right|$$

c = speed of light

Note that this correction is not currently implemented in GEONS for Sun sensor measurement processing.

If the estimation state vector consists of only absolute state vectors, the nonzero components of the row vector of partial derivatives of the ith component of CO LOS vector measurement by sensor k on satellite j, ignoring aberration effects, are equal to the ith row of the matrix of partial derivatives computed as follows:

$$\left[\frac{\partial \hat{P}_B^k}{\partial \overline{R}^j}\right]_i = \left[M_{BI}^j \frac{\partial\left(\hat{V}_I^{k,P}\right)}{\partial \overline{R}^j}\right]_i; \quad i = 1,2,3 \tag{5.8-16}*$$

$$\frac{\partial\left(\hat{P}_B^k\right)_i}{\partial\left(b_P^k\right)_i} = 1; \qquad i = 1,2,3 \qquad \text{(5.8-16a)*}$$

where

$$\frac{\partial \hat{V}_I^{k,P}}{\partial \overline{R}^j} = \frac{1}{\left|\overline{R}^P - \overline{R}^j\right|}\left[-I_{3x3} + \hat{V}_I^{k,P}\hat{V}_I^{k,P^T}\right] \qquad \text{(5.8-16b)*}$$

If the estimation state vector consists of the absolute state vector for the local satellite and relative state vectors for nonlocal satellites, the nonzero components of the row vector of partial derivatives of the ith component of the CO LOS vector measurement by sensor k on satellite j, ignoring aberration effects, are equal to the ith row of the matrix of partial derivatives computed as follows:

$$\left[\frac{\partial \hat{P}_B^k}{\partial \overline{R}^1}\right]_i = \left[M_{BI}^j \frac{\partial \hat{V}_I^{k,P}}{\partial \overline{R}^j}\right]_i; \quad i = 1,2,3 \qquad \text{(5.8-16c)*}$$

$$\left[\frac{\partial \hat{P}_B^k}{\partial \overline{R}_{rel}^j}\right]_i = \left[M_{BI}^j \frac{\partial \hat{V}_I^{k,P}}{\partial \overline{R}^j}\right]_i; \quad i = 1,2,3;\ j > 1 \qquad \text{(5.8-16d)*}$$

$$\frac{\partial\left(\hat{P}_B^k\right)_i}{\partial\left(b_P^k\right)_i} = 1; \qquad i = 1,2,3 \qquad \text{(5.8-16e)*}$$

If the estimation state vector consists of only absolute state vectors, the nonzero components of the row vector of partial derivatives of the ith component of the intersatellite LOS vector measurement from sensor k on satellite j to beacon m on satellite n are equal to the ith row of the matrix of partial derivatives computed as follows:

$$\left[\frac{\partial \hat{P}_B^k}{\partial \overline{R}^j}\right]_i = \left[M_{BI}^j \frac{\partial \hat{V}_I^{k,m}}{\partial \overline{R}^j}\right]_i; \quad i = 1,2,3 \qquad \text{(5.8-16f)*}$$

$$\left[\frac{\partial \hat{P}_B^k}{\partial \overline{R}^n}\right]_i = \left[M_{BI}^j \frac{\partial \hat{V}_I^{k,m}}{\partial \overline{R}^n}\right]_i; \quad i = 1,2,3 \qquad \text{(5.8-16g)*}$$

$$\frac{\partial\left(\hat{P}_B^k\right)_i}{\partial\left(b_P^k\right)_i} = 1; \qquad i = 1,2,3 \qquad \text{(5.8-16h)*}$$

where

$$\frac{\partial \hat{V}_I^{j,m}}{\partial \overline{R}^j} = \frac{1}{\left|\overline{R}_I^{n,m} - \overline{R}_I^{j,k}\right|}\left[-I_{3x3} + \hat{V}_I^{k,m}\hat{V}_I^{k,m^T}\right] \qquad \text{(5.8-16i)*}$$

$$\frac{\partial \hat{\bar{V}}_I^{j,m}}{\partial \bar{R}^n} = \frac{-1}{\left|\bar{R}_I^{n,m} - \bar{R}_I^{j,k}\right|}\left[-I_{3x3} + \hat{V}_I^{k,m}\hat{V}_I^{k,m^T}\right] \qquad \text{(5.8-16j)*}$$

If the estimation state vector consists of the absolute state vector for the local satellite and relative state vectors for nonlocal satellites,

$$\left[\frac{\partial \hat{P}_B^k}{\partial \bar{R}^1}\right]_i = \left[M_{BI}^j \frac{\partial \hat{V}_I^{k,m}}{\partial \bar{R}^j}\right]_i + \left[M_{BI}^j \frac{\partial \hat{V}_I^{k,m}}{\partial \bar{R}^n}\right]_i = 0; \quad \text{i} = 1,2,3 \qquad \text{(5.8-16k)*}$$

The nonzero components of the row vector of partial derivatives of the ith component of the intersatellite LOS vector measurement from sensor k on satellite j to beacon m on satellite n are equal to the ith row of the matrix of partial derivatives computed as follows:

$$\left[\frac{\partial \hat{P}_B^k}{\partial \bar{R}_{rel}^j}\right]_i = \left[M_{BI}^j \frac{\partial \hat{V}_I^{k,m}}{\partial \bar{R}^j}\right]_i; \quad \text{i} = 1,2,3; \text{j} > 1 \qquad \text{(5.8-16l)*}$$

$$\left[\frac{\partial \hat{P}_B^k}{\partial \bar{R}_{rel}^n}\right]_i = \left[M_{BI}^j \frac{\partial \hat{V}_I^{k,m}}{\partial \bar{R}^n}\right]_i; \quad \text{i} = 1,2,3; \text{n} > 1 \qquad \text{(5.8-16m)*}$$

$$\frac{\partial\left(\hat{P}_B^k\right)_i}{\partial\left(b_P^k\right)_i} = 1; \qquad \text{i} = 1,2,3 \qquad \text{(5.8-16n)*}$$

5.8.2.2 Intersatellite Bearing Measurements

The following intersatellite model assumes that the sensor provides dimensionless bearing measurements $\left(x_S^{k,j}, y_S^{k,j}\right)_{obs}$, derived from the line-of-sight vector from a sensor on the imaging satellite to the centroid (or center of mass) of the target satellite, measured with respect to the sensor frame, with distortion corrections applied.

The predicted bearing measurements from sensor k on the imaging satellite i to the target location j on the target satellite at measurement time t_R are defined as follows

$$\begin{bmatrix} x_S^{k,j}(t_R) \\ y_S^{k,j}(t_R) \end{bmatrix} = \frac{1}{Z_S^{k,j}(t_R)}\begin{bmatrix} X_S^{k,j}(t_R) \\ Y_S^{k,j}(t_R) \end{bmatrix} + \begin{bmatrix} \Delta x_S^k + b_x^k(t_R) \\ \Delta y_S^k + b_y^k(t_R) \end{bmatrix} \qquad \text{(5.8.2.2-1)*}$$

where

$x_S^{k,j}, y_S^{k,j}$ = predicted bearing measurements from sensor k on the imaging satellite (i.e. chaser) to the target location j on the target satellite with respect to the sensor frame

$\Delta x_S^k, \Delta y_S^k$ = calibrated bearing measurement bias corrections for sensor k in the sensor frame (optional input to the orbit estimation process

b_x^k, b_y^k = estimated bearing measurement biases for sensor k

$X_S^{k,j}, Y_S^{k,j}, Z_S^{k,j}$ = components of the sensor-to-target vector, $\overline{P}_S^{k,j}$, from sensor k to target location j with respect to the sensor frame

The sensor k-to-target j position vector with respect to the sensor frame, $\overline{P}_S^{k,j}$, is computed by rotating the sensor-to-target position vector in the imaging satellite body frame, $\overline{P}_B^{k,j}$, to the sensor body frame

$$\begin{bmatrix} X_S^{k,j}(t_k) \\ Y_S^{k,j}(t_k) \\ Z_S^{k,j}(t_k) \end{bmatrix} = \overline{P}_S^{k,j} = M_{SB}^k \overline{P}_B^{k,j} \qquad (5.8.2.2\text{-}2)^*$$

where

M_{SB}^k = rotation matrix from the imaging satellite body frame to the sensor k frame, computed using sensor quaternions (updated periodically via commands if thermal and other effects have changed the attitude of the sensor with respect to the body frame of the spacecraft).

$\overline{P}_B^{k,j}$ = sensor k-to-target j position vector in the body frame of satellite i given by

$$\overline{P}_B^{k,j} = M_{BI}^i \, \overline{P}_I^{k,j} \qquad (5.8.2.2\text{-}3)^*$$

M_{BI}^i = rotation matrix from the inertial frame to the satellite i body frame, computed using the attitude quaternions provided as input from an external subsystem (or file)

$\overline{P}_I^{k,j}$ = sensor k-to-target j position vector, referenced to the inertial frame, which is computed as follows

$$\overline{P}_I^{k,j} = \overline{R}_I^j + \left(M_{BI}^j\right)^T \Delta\overline{R}_B^j - [\overline{R}_I^i + \left(M_{BI}^i\right)^T \Delta\overline{R}_B^k] \qquad (5.8.2.2\text{-}4)^*$$

$\overline{R}_I^j$ = predicted position vector of the target satellite j at the measurement time, referenced to the inertial frame (components of the estimated state vector)

M_{BI}^j = rotation matrix from the inertial frame to the target satellite j body frame, computed using the attitude quaternions (an input to the orbit estimation process)

$\Delta\overline{R}_B^j$ = coordinates of the target location j with respect to the target satellite body frame (an input to the orbit estimation process)

$\overline{R}_I^i$ = predicted position vector of imaging satellite i at the measurement time, referenced to the inertial frame (components of the estimated state vector)

$\Delta\bar{R}_B^k$ = coordinates of the sensor k image center with respect to the imaging satellite body frame (an input to the orbit estimation process)

If the estimation state vector consists of only absolute state vectors, the partial derivatives of the $\left(x_S^{k,j}, y_S^{k,j}\right)$ bearing measurements from sensor k on satellite i to the target j with respect to the chaser satellite i and target satellite j position vectors are computed as follows:

$$\begin{bmatrix} \frac{\partial x_S^{k,j}(t_R)}{\partial \bar{R}^i(t_k)} \\ \frac{\partial y_S^{k,j}(t_R)}{\partial \bar{R}^i(t_k)} \end{bmatrix} = \frac{1}{Z_S^{k,j}(t_k)} \begin{bmatrix} \frac{\partial X_S^{k,j}(t_k)}{\partial \bar{R}^i(t_k)} \\ \frac{\partial Y_S^{k,j}(t_k)}{\partial \bar{R}^i(t_k)} \end{bmatrix} - \frac{1}{\left(Z_S^{k,j}(t_k)\right)^2} \frac{\partial\left(Z_S^{k,j}(t_k)\right)}{\partial \bar{R}^i(t_k)} \begin{bmatrix} X_S^{k,j}(t_k) \\ Y_S^{k,j}(t_k) \end{bmatrix} \qquad (5.8.2.2\text{-}5)$$

Which reduces to

$$\begin{aligned} \frac{\partial x_S^{k,j}(t_R)}{\partial \bar{R}^i(t_k)} &= -\begin{bmatrix} \frac{1}{\left(Z_S^{k,j}(t_k)\right)} & 0 & \frac{-X_S^{k,j}(t_k)}{\left(Z_S^{k,j}(t_k)\right)^2} \end{bmatrix} M_{SB}^k M_{BI}^i \\ \frac{\partial y_S^{k,j}(t_R)}{\partial \bar{R}^i(t_k)} &= -\begin{bmatrix} 0 & \frac{1}{\left(Z_S^{k,j}(t_k)\right)} & \frac{-Y_S^{k,j}(t_k)}{\left(Z_S^{k,j}(t_k)\right)^2} \end{bmatrix} M_{SB}^k M_{BI}^i \end{aligned} \qquad (5.8.2.2\text{-}6)^*$$

Similarly

$$\begin{aligned} \frac{\partial x_S^{k,j}(t_R)}{\partial \bar{R}^j(t_k)} &= \begin{bmatrix} \frac{1}{\left(Z_S^{k,j}(t_k)\right)} & 0 & \frac{-X_S^{k,j}(t_k)}{\left(Z_S^{k,j}(t_k)\right)^2} \end{bmatrix} M_{SB}^k M_{BI}^i \\ \frac{\partial y_S^{k,j}(t_R)}{\partial \bar{R}^j(t_k)} &= \begin{bmatrix} 0 & \frac{1}{\left(Z_S^{k,j}(t_k)\right)} & \frac{-Y_S^{k,j}(t_k)}{\left(Z_S^{k,j}(t_k)\right)^2} \end{bmatrix} M_{SB}^k M_{BI}^i \end{aligned} \qquad (5.8.2.2\text{-}7)^*$$

If the estimation state vector consists of the absolute state vector for the local satellite and relative state vectors for nonlocal satellites, the partial derivatives of the $\left(x_S^{k,j}, y_S^{k,j}\right)$ bearing measurements from sensor k on satellite i to the target location j with respect to the position of reference satellite 1 and non-local satellites i and/or j are computed as follows:

$$\begin{bmatrix} \frac{\partial x_S^{k,j}}{\partial \bar{R}^1} \\ \frac{\partial y_S^{k,j}}{\partial \bar{R}^1} \end{bmatrix} = \begin{bmatrix} \frac{\partial x_S^{k,j}}{\partial \bar{R}^i} + \frac{\partial x_S^{k,j}}{\partial \bar{R}^j} \\ \frac{\partial y_S^{k,j}}{\partial \bar{R}^i} + \frac{\partial y_S^{k,j}}{\partial \bar{R}^j} \end{bmatrix} = \begin{bmatrix} 0 & 0 & 0 \\ 0 & 0 & 0 \end{bmatrix} \qquad (5.8.2.2\text{-}8)^*$$

And the non-zero partial derivatives are as follows:

$$\begin{bmatrix} \frac{\partial x_S^{k,j}}{\partial \bar{R}_{rel}^i} \\ \frac{\partial y_S^{k,j}}{\partial \bar{R}_{rel}^i} \end{bmatrix} = \begin{bmatrix} \frac{\partial x_S^{k,j}}{\partial \bar{R}^i} \\ \frac{\partial y_S^{k,j}}{\partial \bar{R}^i} \end{bmatrix}; \quad i > 1,\ j > 0, i \neq j \qquad (5.8.2.2\text{-}9)^*$$

$$\begin{bmatrix} \frac{\partial x_S^{k,j}}{\partial \bar{R}_{rel}^j} \\ \frac{\partial y_S^{k,j}}{\partial \bar{R}_{rel}^j} \end{bmatrix} = \begin{bmatrix} \frac{\partial x_S^{k,j}}{\partial \bar{R}^j} \\ \frac{\partial y_S^{k,j}}{\partial \bar{R}^j} \end{bmatrix}; \quad j > 1,\ i > 0, i \neq j \qquad (5.8.2.2\text{-}10)^*$$

Partial derivatives of the $\left(x_S^{k,j}, y_S^{k,j}\right)$ bearing measurements with respect to the bearing measurement biases for sensor k, b_x^k, b_y^k, are computed as follows:

$$\begin{bmatrix} \frac{\partial x_S^{k,j}}{\partial b_x^k} \\ \frac{\partial y_S^{k,j}}{\partial b_y^k} \end{bmatrix} = \begin{bmatrix} 1 \\ 1 \end{bmatrix} \qquad (5.8.2.2\text{-}13)^*$$

5.8.2.3 Landmark/Celestial Object Bearing Measurements

The following model assumes that the sensor *k* provides dimensionless bearing measurements $\left(x_S^{k,L}, y_S^{k,L}\right)_{obs}$, computed from the line-of-sight vector from a sensor on the imaging satellite to a landmark on/centroid of a celestial body measured with respect to the sensor frame, with distortion corrections applied. Note that in the following discussion, a bearing measurement to the centroid of a celestial body is treated as a landmark located at the centroid of the target body.

The predicted bearing measurements from sensor k on the imaging satellite i to landmark L on the target body at the measurement time t_R is defined as follows

$$\begin{bmatrix} x_S^{k,L}(t_R) \\ y_S^{k,L}(t_R) \end{bmatrix} = \frac{1}{Z_S^{k,L}(t_R)} \begin{bmatrix} X_S^{k,L}(t_R) \\ Y_S^{k,L}(t_R) \end{bmatrix} + \begin{bmatrix} \Delta x_S^k + b_x^k(t_R) \\ \Delta y_S^k + b_y^k(t_R) \end{bmatrix} \qquad (5.8.2.3\text{-}1)^*$$

where

$x_S^{k,L}, y_S^{k,L}$ = predicted bearing measurements from sensor k on the imaging satellite to landmark L on the target body with respect to the sensor frame

$X_S^{k,L}, Y_S^{k,L}, Z_S^{k,L}$ = components of the sensor-to-landmark vector, $\bar{P}_S^{k,L}$, from sensor k to landmark L with respect to the sensor frame

$\Delta x_S^k, \Delta y_S^k$ = calibrated bearing measurement biases for sensor k (an input to the orbit estimation process). Note this input would not be required if totally accounted for in measurement pre-processing.

b_x^k, b_y^k = estimated bearing measurement biases for sensor k

The sensor k-to-landmark position vector with respect to the sensor frame, $\overline{P}_S^{k,L}$, is computed by rotating the sensor-to-landmark position vector in the satellite body frame, $\overline{P}_B^{k,L}$, to the sensor body frame

$$\overline{P}_S^{k,L} = M_{SB}^k \overline{P}_B^{k,L} \qquad (5.8.2.3\text{-}2)^*$$

where

M_{SB}^k = rotation matrix from the satellite body frame to sensor k frame, computed using sensor quaternion periodically updated via commands

$\overline{P}_B^{k,L}$ = sensor-to-landmark vector measured by sensor k on satellite i in the body frame (where i=1 for single-satellite asteroid missions) given by

$$\overline{P}_B^{k,L} = M_{BI}^i \ \overline{P}_I^{k,L} \qquad (5.8.2.3\text{-}3)^*$$

M_{BI}^i = rotation matrix from the inertial to the satellite i body frame, computed using the attitude quaternion provided as input from an external subsystem (or file)

$\overline{P}_I^{k,L}$ = Sensor k-to-landmark L position vector, referenced to the inertial frame, which is computed as follows

$$\overline{P}_I^{k,L} = \overline{R}_I^L - [\overline{R}_I^i + \left(M_{BI}^i\right)^T \Delta \overline{R}_B^k] \qquad (5.8.2.3\text{-}4)^*$$

$\overline{R}_I^L$ = Position vector of landmark L referenced to the inertial frame given by

$$\overline{R}_I^L = \overline{R}_I^T + \left(M_{TI}\right)^T \overline{r}_T^L \qquad (5.8.2.3\text{-}5)^*$$

$\overline{R}_I^i$ = predicted position vector of satellite i at the measurement time, referenced to the inertial frame (components of the estimated state vector)

$\Delta \overline{R}_B^k$ = coordinates of the sensor k image center with respect to the satellite body frame (an input to the orbit estimation process)

$\overline{R}_I^T$ = Center of mass (COM) position vector of the target body on which the landmarks are located, referenced to the inertial frame. This position is either computed based on a planetary ephemeris available in GEONS or an externally-provided ephemeris for a body such as an asteroid.

M_{TI} = rotation matrix from the target-centered inertial (TCI) frame to the target body frame (TBF), computed using the cartographic coordinates of the body consisting of the orientation (i.e. right ascension and declination of date) of the axis of rotation (north pole) and the location and rotation rate of the prime meridian of the object with respect to the inertial ICRF.

$\bar{r}_T^L$ = coordinates of landmark L referenced to the target body frame. This position vector is provided along with the measurements.

The measurement model for the $\left(x_S^{k,T}, y_S^{k,T}\right)$ bearing measurements of the target body centroid with respect to the sensor k frame is the same as the model for the $\left(x_S^{k,L}, y_S^{k,L}\right)$ bearing measurements of landmark locations on the target body except that the "landmark" is the COM of the target body.

If the estimation state vector consists of only absolute state vectors, the partial derivatives of the $\left(x_S^{k,L}, y_S^{k,L}\right)$ bearing measurements from sensor k on satellite i to Landmark on the target body, with respect to the position of satellite i are computed as follows:

$$\begin{bmatrix} \frac{\partial x_S^{k,L}}{\partial \bar{R}^i} \\ \frac{\partial y_S^{k,L}}{\partial \bar{R}^i} \end{bmatrix} = \frac{1}{Z_S^{k,L}} \begin{bmatrix} \frac{\partial X_S^{k,L}}{\partial \bar{R}^i} \\ \frac{\partial Y_S^{k,L}}{\partial \bar{R}^i} \end{bmatrix} - \frac{1}{\left(Z_S^{k,L}\right)^2} \frac{\partial \left(Z_S^{k,L}\right)}{\partial \bar{R}^i} \begin{bmatrix} X_S^{k,L} \\ Y_S^{k,L} \end{bmatrix} \tag{5.8.2.3-6}$$

Which reduces to the following

$$\left[\frac{\partial x_S^{k,L}(t_R)}{\partial \bar{R}^i(t_k)}\right]^T = -\left[M_{SB}^k M_{BI}^i\right]^T \begin{bmatrix} \frac{1}{\left(Z_S^{k,L}(t_k)\right)} \\ 0 \\ \frac{-X_S^{k,L}(t_k)}{\left(Z_S^{k,L}(t_k)\right)^2} \end{bmatrix}$$

$$\left[\frac{\partial y_S^{k,L}(t_R)}{\partial \bar{R}^i(t_k)}\right]^T = -\left[M_{SB}^k M_{BI}^i\right]^T \begin{bmatrix} 0 \\ \frac{1}{\left(Z_S^{k,L}(t_k)\right)} \\ \frac{-Y_S^{k,j}(t_k)}{\left(Z_S^{k,L}(t_k)\right)^2} \end{bmatrix} \tag{5.8.2.3-7}*$$

If the estimation state vector consists of the absolute state vector for the local satellite and relative state vectors for nonlocal satellites, the partial derivatives of the $\left(x_S^{k,L}, y_S^{k,L}\right)$ bearing measurements from sensor k on satellite i to Landmark L with respect to the position of satellite i are computed as follows:

$$\begin{bmatrix} \dfrac{\partial x_S^{k,L}}{\partial \bar{R}^1} \\ \dfrac{\partial y_S^{k,L}}{\partial \bar{R}^1} \end{bmatrix} = \begin{bmatrix} \dfrac{\partial x_S^{k,L}}{\partial \bar{R}^i} \\ \dfrac{\partial y_S^{k,L}}{\partial \bar{R}^i} \end{bmatrix} \qquad (5.8.2.3\text{-}8)^*$$

$$\begin{bmatrix} \dfrac{\partial x_S^{k,L}}{\partial \bar{R}_{rel}^i} \\ \dfrac{\partial y_S^{k,L}}{\partial \bar{R}_{rel}^i} \end{bmatrix} = \begin{bmatrix} \dfrac{\partial x_S^{k,L}}{\partial \bar{R}^i} \\ \dfrac{\partial y_S^{k,L}}{\partial \bar{R}^i} \end{bmatrix}; \quad i > 1 \qquad (5.8.2.3\text{-}9)^*$$

Partial derivatives of the $\left(x_S^{k,L}, y_S^{k,L}\right)$ bearing measurements with respect to the bearing measurement biases for sensor k, b_x^k, b_y^k, are computed as follows:

$$\begin{bmatrix} \dfrac{\partial x_S^{k,L}}{\partial b_x^k} \\ \dfrac{\partial y_S^{k,L}}{\partial b_y^k} \end{bmatrix} = \begin{bmatrix} 1 \\ 1 \end{bmatrix} \qquad (5.8.2.3\text{-}10)^*$$

5.8.2.4 Camera Range Measurement

The camera range model assumes that sensor *k* provides a 1D range measurement $\left(\rho^{k,x}\right)_{obs}$ to some 3D point of interest *x* attached to a target body with known location in the inertial frame. The target body can be a celestial object or another satellite state that is being estimated. Note that in the following discussion, a range measurement to the centroid of a celestial body is treated as a point of interest located at the centroid of the target body.

The predicted range measurement from the camera sensor center *k* on the imaging satellite *i* to point of interest *x* on the target body *T* at measurement time t_R is computed as follows

$$\rho^{k,x}(t_R) = \left|\bar{P}_I^{k,x}(t_R)\right| + \Delta\rho^k + b_\rho^k(t_R) \qquad (5.8.2.4\text{-}1)^*$$

where

$\bar{P}_I^{k,x}$ = vector from camera sensor *k* to point of interest *x*, referenced to the inertial frame

$\Delta\rho^k$ = calibrated range measurement bias for sensor k (an input to the orbit estimation process). Note this input would not be required if totally accounted for in measurement pre-processing.

b_ρ^k = estimated range measurement bias for sensor k

The following equation is used to compute the components of the camera sensor-to-point of interest vector measured by sensor k on satellite i in the inertial frame, (where *i*=1 for single-satellite asteroid missions):

$$\overline{P}_I^{k,x}(t_R) = \overline{R}_I^x(t_R) - \left[\overline{R}_I^i(t_R) + \left(M_{BI}^i \right)^T \Delta \overline{R}_B^k \right] \qquad (5.8.2.4\text{-}2)^*$$

where

$\overline{R}_I^x$ = vector from the inertial frame origin to point *x* at the measurement time, referenced to the inertial frame, given by

$$\overline{R}_I^x = \overline{R}_I^T + M_{IT} \overline{r}_T^x \qquad (5.8.2.4\text{-}3)^*$$

$\overline{R}_I^T$ = position vector of the origin of the target body frame on which the point *x* is located, referenced to the inertial frame. This position is computed based on a planetary ephemeris available in GEONS, an externally-provided ephemeris for a target body such as an asteroid, or predicted state of a second satellite *j*

M_{IT} = rotation matrix from the target body frame (TBF) to the inertial frame

$\overline{r}_T^x$ = coordinates of the point of interest *x* in the target body frame. This position vector is provided along with the measurements.

$\overline{R}_I^i$ = vector from the inertial frame origin to origin of the imaging satellite i body frame at the measurement time, referenced to the inertial frame (components of the predicted satellite state vector)

M_{BI}^i = rotation matrix from the inertial to the imaging satellite *i* body frame, computed using the attitude quaternion provided as input from an external subsystem (or file)

$\Delta \overline{R}_B^k$ = vector from the origin of the imaging satellite i body frame to the camera sensor k image center, referenced to the satellite body frame (input to the orbit estimation process)

If the estimation state vector consists of only absolute state vectors, the only non-zero partial derivatives of the camera range measurement from sensor *k* on satellite *i* to the point of interest on the target body are with respect to the inertial position of imaging satellite *i*, computed as follows, ignoring the linearization correction

$$\frac{\partial \rho^{k,x}(t_k)}{\partial \overline{R}_I^i(t_k)} = \frac{\partial \rho^{k,x}(t_k)}{\partial \overline{P}_I^{k,x}(t_k)} \frac{\partial \overline{P}_I^{k,x}(t_k)}{\partial \overline{R}_I^i(t_k)} = -\left[\frac{\overline{P}_I^{k,x}(t_k)}{\left| \overline{P}_I^{k,x}(t_k) \right|} \right]^T \qquad (5.8.2.4\text{-}4)^*$$

Similarly, if the target body is another satellite *j* that is being estimated:

$$\frac{\partial \rho^{k,x}(t_k)}{\partial \bar{R}_I^j(t_k)} = \frac{\partial \rho^{k,x}(t_k)}{\partial \bar{P}_I^{k,x}(t_k)} \frac{\partial \bar{P}_I^{k,x}(t_k)}{\partial \bar{R}_I^j(t_k)} = \left[\frac{\bar{P}_I^{k,x}(t_k)}{\left| \bar{P}_I^{k,x}(t_k) \right|} \right]^T \quad (5.8.2.4\text{-}5)^*$$

If the estimation state vector consists of the absolute state vector for the local satellite (i=1) or target satellite (j=1) and relative state vectors for nonlocal satellites,

$$\frac{\partial \rho^{k,x}(t_k)}{\partial \bar{R}_I^1(t_k)} = \frac{\partial \rho^{k,x}(t_k)}{\partial \bar{R}_I^i(t_k)}; \quad \text{if target body state is not estimated} \quad (5.8.2\text{-}4.6)^*$$

$$\frac{\partial \rho^{k,x}(t_k)}{\partial \bar{R}_I^1(t_k)} = \frac{\partial \rho^{k,x}(t_k)}{\partial \bar{R}_I^i(t_k)} + \frac{\partial \rho^{k,x}(t_k)}{\partial \bar{R}_I^j(t_k)} = 0; \quad \text{if target body state j is estimated} \quad (5.8.2\text{-}4.7)^*$$

The following are the nonzero partial derivatives of the range measurement for the relative state vectors:

$$\frac{\partial \rho^{k,x}(t_k)}{\partial \bar{R}_{rel,I}^i(t_k)} = \frac{\partial \rho^{k,x}(t_k)}{\partial \bar{R}_I^i(t_k)} = -\left[\frac{\bar{P}_I^{k,x}(t_k)}{\left| \bar{P}_I^{k,x}(t_k) \right|} \right]^T; \quad i > 1 \quad (5.8.2.4\text{-}8)^*$$

Similarly, if the target body is another satellite *j* that is being estimated:

$$\frac{\partial \rho^{k,x}(t_k)}{\partial \bar{R}_{rel,I}^j(t_k)} = \frac{\partial \rho^{k,x}(t_k)}{\partial \bar{R}_I^j(t_k)} = \left[\frac{\bar{P}_I^{k,x}(t_k)}{\left| \bar{P}_I^{k,x}(t_k) \right|} \right]^T; \quad j > 1 \quad (5.8.2.4\text{-}9)^*$$

The partial derivative of the camera range with respect to the range measurement bias for sensor k, b_ρ^k, is computed as follows:

$$\frac{\partial \rho^{k,x}}{\partial b_\rho^k} = 1 \quad (5.8.2.4\text{-}10)^*$$

5.8.3 Planetary Sensor Measurement Models for Spin-Stabilized Satellite

This section presents models used to process CO sensor measurements for spin-stabilized satellite.

5.8.3.1 Sun Angle Measurements from a Spinning Satellite

This model is appropriate for the Sun sensor assemblies (SSAs) flown on spinning satellites such as WIND and POLAR. The SSA measures the angle between the Sun sensor-to-Sun LOS unit vector and the satellite spin axis when the sun is in the measurement plane, i.e. the plane containing the spin axis and a vector normal to the sensor. Figure 5-8 illustrates the measurement geometry.

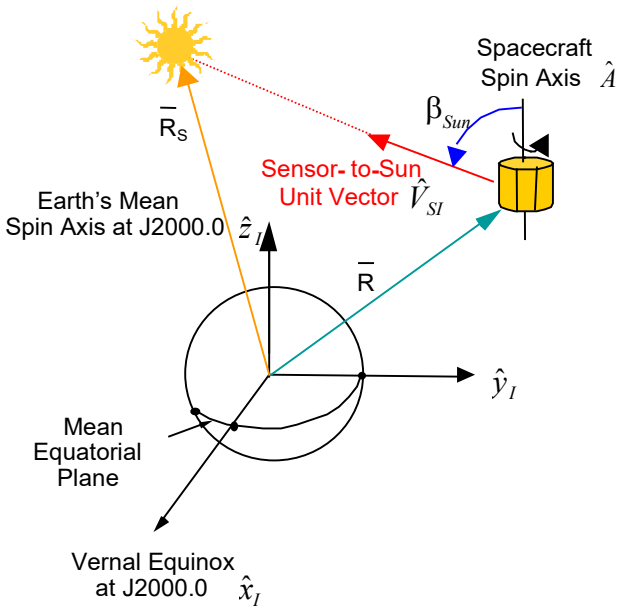

Figure 5-8. Sun Angle Measurement Geometry

The SSA generates a command eye pulse (CEP) when the Sun is in the measurement plane. The time of the CEP, t_{CEP}, provides the measurement timetag. The accuracy of the sun angle measurement is nominally ±0.10 degree. The sun angle is related to the satellite-to-Sun LOS unit vector components as follows

$$\beta^k_{Sun} = \arccos(\hat{V}^j_{SI} \cdot \hat{A}^j) + \Delta\beta^k_{Sun} + b^k{}_{\beta Sun} \qquad (5.8\text{-}17)^*$$

where

β^k_{Sun} = sun angle measurement in radians from sensor k on satellite j

$\hat{V}^j_{SI}$ = satellite-to-Sun line-of-sight (LOS) unit vector at t_{CEP}, referenced to the geocentric inertial frame (J2000.0)

$\hat{A}^j$ = unit vector along the satellite j spin axis at t_{CEP}, referenced to the geocentric inertial frame (J2000.0) (input to this process)

$\Delta\beta^k_{Sun}$ = calibrated sun angle measurement bias for sensor k in radians (an input to the orbit estimation process)

$b^k_{\beta Sun}$ = estimated sun angle measurement bias for sensor k in radians

The predicted inertial LOS unit vector from satellite j to the Sun is computed as follows

$$\hat{V}^j_{SI} = \frac{\bar{R}_S(t_{CEP}) - \bar{R}^j(t_{CEP})}{\left|\bar{R}_S(t_{CEP}) - \bar{R}^j(t_{CEP})\right|} \qquad (5.8\text{-}18)^*$$

where

$\overline{R}^{\,j}(t_{CEP})$ = satellite j position vector at t_{CEP}, referenced to the geocentric inertial frame (J2000.0)

$\overline{R}_S(t_{\ CEP})$ = Position vector of the Sun at t_{CEP} referenced to the geocentric inertial frame (J2000.0)

The inertial position vector for the Sun is computed using the analytic algorithms for the solar positions given in Section 4.1.2.

If the estimation state vector consists of only absolute state vectors, the nonzero components of the row vector of partial derivatives are computed as follows for measurements associated with sun sensors on satellite j:

$$\frac{\partial \beta^k_{Sun}}{\partial \overline{R}^{\,j}(t_{CEP})} = -\frac{1}{\sqrt{1-(\hat{V}^j_{SI}\cdot\hat{A}^j)^2}}\left[\left(\frac{\partial \hat{V}^j_{SI}}{\partial \overline{R}^{\,j}(t_{CEP})}\right)^T \hat{A}^j\right]^T \qquad (5.8\text{-}19)^*$$

$$\frac{\partial \beta^k_{Sun}}{\partial b^k_{\beta_{Sun}}} = 1 \qquad (5.8\text{-}19a)^*$$

where

$$\frac{\partial \hat{V}^j_{SI}}{\partial \overline{R}^{\,j}(t_{CEP})} = \frac{1}{\left|\overline{R}_S(t_{CEP}) - \overline{R}^{\,j}(t_{CEP})\right|}\left[-I_{3x3} + \hat{V}^j_{SI}\hat{V}^{j\,T}_{SI}\right] \qquad (5.8\text{-}20)^*$$

If the estimation state vector consists of the absolute state vector for the local satellite and relative state vectors for nonlocal satellites, the nonzero components of the row vector of partial derivatives are computed as follows for measurements associated with sun sensors on satellite j:

$$\frac{\partial \beta^k_{Sun}}{\partial \overline{R}^{1}(t_{CEP})} = -\frac{1}{\sqrt{1-(\hat{V}^j_{SI}\cdot\hat{A}^j)^2}}\left[\left(\frac{\partial \hat{V}^j_{SI}}{\partial \overline{R}^{\,j}(t_{CEP})}\right)^T \hat{A}^j\right]^T \qquad (5.8\text{-}20a)^*$$

$$\frac{\partial \beta^k_{Sun}}{\partial \overline{R}^{\,j}_{rel}(t_{CEP})} = -\frac{1}{\sqrt{1-(\hat{V}^j_{SI}\cdot\hat{A}^j)^2}}\left[\left(\frac{\partial \hat{V}^j_{SI}}{\partial \overline{R}^{\,j}(t_{CEP})}\right)^T \hat{A}^j\right]^T; \quad j>1 \qquad (5.8\text{-}20b)^*$$

$$\frac{\partial \beta^k_{Sun}}{\partial b^k_{\beta_{Sun}}} = 1 \qquad (5.8\text{-}20c)^*$$

5.8.3.2 Horizon Scanning Measurements from a Spinning Satellite

This model is appropriate for horizon sensor assemblies (HSAs) flown on spinning satellites such as the Barnes HSAs flown on WIND and POLAR. Figure 5-9 illustrates the measurement

geometry. The accuracy of the Earth horizon sensor measurement is nominally 0.1 degree. However, this accuracy is degraded by fluctuations in the Earth's horizon radiance that produce errors of about 10 kilometers in the measurement of the horizon.

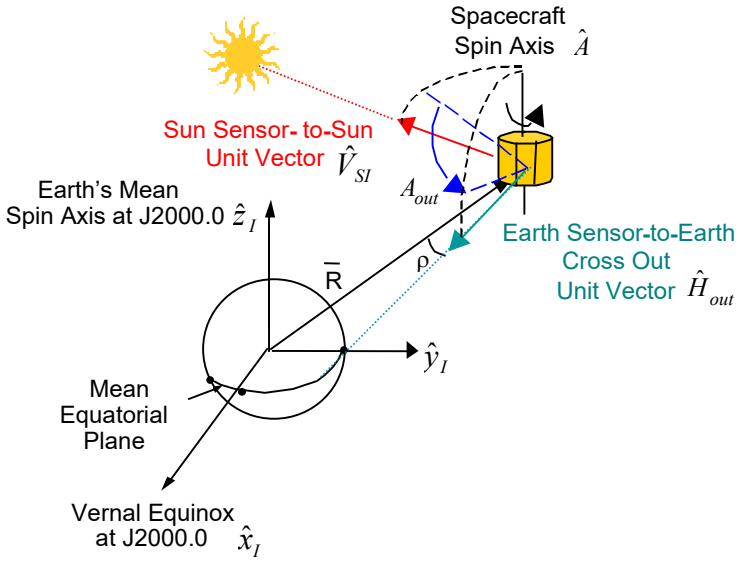

Figure 5-9. Earth-Out Crossing Measurement Geometry

The horizon sensor measures the elapsed time from the Sun sensor's CEP at t_{CEP} to the Earth-in pulse at t_{in} and the elapsed time from the Sun sensor's CEP at t_{CEP} to the Earth-out pulse at t_{out}. Each of these measurements is processed independently in the estimation processing. These times are computed as follows, where horizon sensor k and Sun sensor m are on satellite j

$$\Delta t_{in}^{k,m} = t_{in}^{k} - t_{CEP}^{m} = \frac{1}{\omega^{j}}\left(A_{in}^{j} - \phi^{k,m} + 2\pi n\right) - \delta t_{in}^{k,m} + b_{\Delta t_{in}}^{k,m}$$

$$\Delta t_{out}^{k,m} = t_{out}^{k} - t_{CEP}^{m} = \frac{1}{\omega^{j}}\left(A_{out}^{j} - \phi^{k,m} + 2\pi n\right) - \delta t_{out}^{k,m} + b_{\Delta t_{out}}^{k,m} \qquad (5.8\text{-}21)^{*}$$

where

$\Delta t_{in}^{k,m}, \Delta t_{out}^{k,m}$ = elapsed time in seconds from the CEP from Sun sensor m to the Earth-in/-out pulse from horizon sensor k, normalized to a value between 0 and one spin period

ω^{j} = satellite j spin rate in radians per second (an input from the attitude determination process)

A_{in}^{j}, A_{out}^{j} = dihedral angle on satellite j from the plane containing the spin axis and the satellite-to-Sun vector and the plane containing the spin axis and the satellite-to-Earth-cross-in/out point in radians

$\phi^{k,m}, \phi^{k,m}$ = nominal azimuth from the Sun sensor *m* to the Earth sensor *k* in radians (an input sensor configuration parameter)

n = integer number of revolutions such that $0 \le \left(A_{in}^{j} - \phi_{in}^{k,m} + 2\pi n\right) \le 2\pi$:

$$n = \begin{cases} -1, & \text{if } \left(A_{in}^{j} - \phi_{in}^{k,m}\right) > 2\pi \\ 0, & \text{if } 0 \le \left(A_{in}^{j} - \phi_{in}^{k,m}\right) \le 2\pi \\ +1, & \text{if } \left(A_{in}^{j} - \phi_{in}^{k,m}\right) < 0 \end{cases} \qquad \text{(5.8-21b)*}$$

$\delta t_{in}^{k,m}, \delta t_{out}^{k,m}$ = calibrated measurement biases between the Sun sensor *m* and the Earth sensor *k* at Earth-cross-in/-out in seconds

$b_{\Delta t_{in}}^{k,m}, b_{\Delta t_{out}}^{k,m}$ = estimated measurement biases between the Sun sensor *m* and the Earth sensor *k* at Earth-cross-in/-out in seconds

The dihedral angles A_{in}^{j}, A_{out}^{j} are computed as follows

$$\begin{aligned} A_{in}^{j} &= \arctan 2\left[N_{in}^{j}, D_{in}^{j}\right] \\ A_{out}^{j} &= \arctan 2\left[N_{out}^{j}, D_{out}^{j}\right] \end{aligned} \qquad \text{(5.8-22)*}$$

where

$$\begin{aligned} N_{in}^{j} &= \hat{A}^{j} \cdot (\hat{V}_{SI}^{j} \times \hat{H}_{in}^{j}), \quad D_{in}^{j} = \hat{H}_{in}^{j} \cdot \hat{V}_{SI}^{j} - (\hat{V}_{SI}^{j} \cdot \hat{A}^{j})(\hat{H}_{in}^{j} \cdot \hat{A}^{j}) \\ N_{out}^{j} &= \hat{A}^{j} \cdot (\hat{V}_{SI}^{j} \times \hat{H}_{out}^{j}), \quad D_{out}^{j} = \hat{H}_{out}^{j} \cdot \hat{V}_{SI}^{j} - (\hat{V}_{SI}^{j} \cdot \hat{A}^{j})(\hat{H}_{out}^{j} \cdot \hat{A}^{j}) \end{aligned} \qquad \text{(5.8-23)*}$$

$\hat{V}_{SI}^{j}$ = Satellite-to-Sun line-of-sight (LOS) unit vector at t_{CEP}, referenced to the geocentric inertial frame (J2000.0), computed as in Equation 5.8-18

$\hat{A}^{j}$ = unit vector along the satellite j spin axis at t_{CEP}, referenced to the geocentric inertial frame (J2000.0) (input to this process)

$\hat{H}_{in}^{j}, \hat{H}_{out}^{j}$ = unit vector from the satellite j to the Earth cross-in/-out point at $t_{in/out}$, referenced to the geocentric inertial frame (J2000.0)

The components of $\hat{H}_{in}^{j}$ / $\hat{H}_{out}^{j}$ are derived based on the following relationships, illustrated in Figure 5-10:

$$
\begin{aligned}
\hat{H}_{in}^{j} \cdot \hat{A}^{j}(t_{CEP}) &= \cos(\gamma_S^k) \\
\hat{H}_{in}^{j} \cdot \hat{E}^{j}(t_{in}) &= \cos(\rho_{in}) \\
\hat{H}_{in}^{j} \cdot \hat{H}_{in}^{j} &= 1 \\
\hat{H}_{out}^{j} \cdot \hat{A}^{j}(t_{CEP}) &= \cos(\gamma_S^k) \\
\hat{H}_{out}^{j} \cdot \hat{E}^{j}(t_{out}) &= \cos(\rho_{out}) \\
\hat{H}_{out}^{j} \cdot \hat{H}_{out}^{j} &= 1
\end{aligned}
\qquad (5.8\text{-}24)
$$

where

γ_S^k = measured HSA k mounting angle with respect to the spin axis

ρ_{in}, ρ_{out} = Earth angular radius at the crossing point

$\hat{E}^{j}(t_{in}), \hat{E}^{j}(t_{out})$ = unit vector from satellite j to the center of the Earth at $t_{in/out}$, referenced to the geocentric inertial frame (J2000.0)

$$
\begin{aligned}
\hat{E}^{j}(t_{in}) &= -\frac{\overline{R}^{j}(t_{in})}{\left|\overline{R}^{j}(t_{in})\right|} \\
\hat{E}^{j}(t_{out}) &= -\frac{\overline{R}^{j}(t_{out})}{\left|\overline{R}^{j}(t_{out})\right|}
\end{aligned}
\qquad (5.8\text{-}25)^*
$$

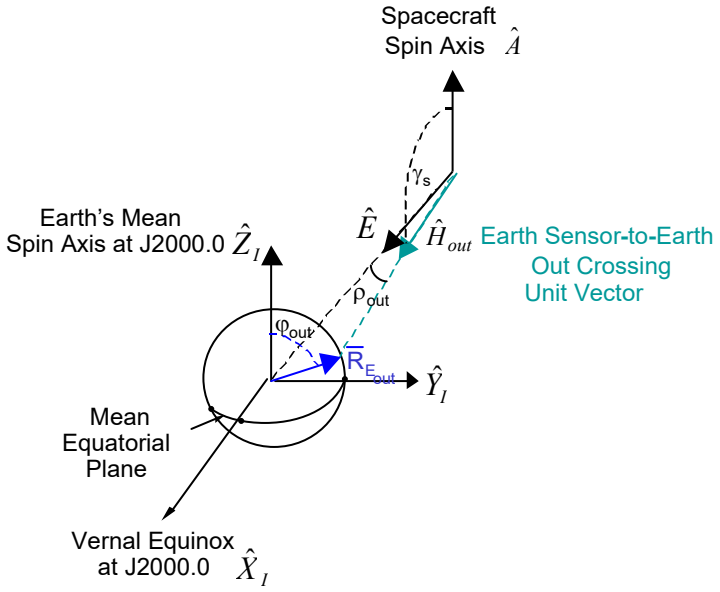

Figure 5-10. Earth/Out Measurement Geometry

The corresponding partial derivative matrices: $\frac{\partial \hat{H}^{j}_{in}}{\partial \overline{R}^{j}(t_{in})}$ and $\frac{\partial \hat{H}^{j}_{out}}{\partial \overline{R}^{j}(t_{out})}$ satisfy the following system of equations

$$\left(\frac{\partial \hat{H}}{\partial \overline{R}^{j}}\right)^{T} \hat{A}^{j} = 0 \tag{5.8-26}$$

$$\left(\frac{\partial \hat{H}}{\partial \overline{R}^{j}}\right)^{T} \hat{E}^{j} = -\left(\frac{\partial \hat{E}^{j}}{\partial \overline{R}^{j}}\right)^{T} \hat{H} + \left(\frac{\partial \cos(\rho)}{\partial \overline{R}^{j}}\right)^{T} \tag{5.8-26a}$$

$$\left(\frac{\partial \hat{H}}{\partial \overline{R}^{j}}\right)^{T} \hat{H} = 0 \tag{5.8-26b}$$

Necessary conditions for Equation 5.8-24 to admit two unique solutions, $\hat{H}_1$ and $\hat{H}_2$, is that the two vectors $\hat{A}^{j}$ and $\hat{R}^{j}$ are independent, that is $\hat{A}^{j} \times \hat{R}^{j} \neq 0$. The following procedure is used to compute these solutions.

The first set of solutions for $\hat{H}_1$ and $\hat{H}_2$ is computed using $\hat{R}^{j}(t_{in/out} \cong t_{CEP})$, $\hat{A}^{j}(t_{CEP})$, and

$$\rho_{in/out} \cong \rho_{N} = \arcsin\left[\frac{R_N + h_N}{\left|R^{j}\right|}\right] \tag{5.8-27}*$$

where

R_N = Earth spherical radius, equal to 6371.38 kilometers

h_N = nominal carbon dioxide height, 38 kilometers

in the following:

$$\hat{\mathrm{H}}_1 = a\hat{A} + b\hat{E} + c\hat{W} \tag{5.8-28}*$$

$$\hat{\mathrm{H}}_2 = a\hat{A} + b\hat{E} - c\hat{W} \tag{5.8-28b}*$$

$$\hat{W} = \frac{\hat{A}^{j} \times \hat{E}^{j}}{\left|\hat{A}^{j} \times \hat{E}^{j}\right|} \tag{5.8-28c}*$$

$$a = \frac{\cos(\gamma_s^{k}) - \hat{A}^{j} \cdot \hat{E}^{j} \cos(\rho_{in/out})}{1 - (\hat{A}^{j} \cdot \hat{E}^{j})^{2}} \tag{5.8-28d}*$$

$$b = \frac{\cos(\rho_{in/out}) - \hat{A}^j \cdot \hat{E}^j \cos(\gamma_s^k)}{1 - (\hat{A}^j \cdot \hat{E}^j)^2} \tag{5.8-28e}*$$

$$c = \sqrt{1 - a^2 - b^2 - 2ab\hat{A}^j \cdot \hat{E}^j} \tag{5.8-28f}*$$

If the value of c in Equation (5.8-28) is imaginary, the measurement is discarded as invalid. To identify which solution to Equation (5.8-28) corresponds to $\hat{H}^j_{in/out}$, the dihedral angle (*more precisely, the rotational angle for the spinning satellite*) Θ from the $\hat{A} \times \hat{H}_1$ plane to the $\hat{A} \times \hat{H}_2$ plane is computed as follows:

$$\begin{aligned} &\Theta = \arctan 2\left[\hat{A} \cdot \left(\hat{H}_1 \times \hat{H}_2\right),\ \left(\hat{H}_1 \cdot \hat{H}_2\right) - \left(\hat{A} \cdot \hat{H}_1\right)\left(\hat{A}_1 \cdot \hat{H}_2\right)\right] \\ &\text{if } \Theta \le 0, \Theta = \Theta + 2\pi \end{aligned} \tag{5.8-29}*$$

If $\Theta < \pi$, $\hat{H}_{in} = \hat{H}_1$ and $\hat{H}_{out} = \hat{H}_2$. If $\Theta \ge \pi$, $\hat{H}_{in} = \hat{H}_2$ and $\hat{H}_{out} = \hat{H}_1$.

Next updated Earth cross-in/out times are computed as $t_{in/out} = t_{CEP} + \Delta t_{in/out}$, where $\Delta t_{in/out}$ is computed using the initial $\hat{H}_{in/out}$ solutions to compute the dihedral angles $A_{in/out}$ in Equation (5.8-21). Then two sets of updated values for $\hat{H}_1$ and $\hat{H}_2$ are computed using $\overline{R}^n$ evaluated at $t_{in} = t_{CEP} + \Delta t_{in}$ and $t_{out} = t_{CEP} + \Delta t_{out}$ to compute $\hat{E}(t_{in})$ and $\hat{E}(t_{out})$ and correcting ρ_{in} and ρ_{out} to account for the Earth's oblateness. The updated values for $\overline{R}^j(t_{in})$ and $\overline{R}^j(t_{out})$ are approximated as follows:

$$\begin{aligned} \overline{R}^j(t_{in}) &\cong \overline{R}^j(t_{CEP}) + \Delta t_{in}^{k,m}\ \dot{\overline{R}}^j(t_{CEP}) \\ \overline{R}^j(t_{out}) &\cong \overline{R}^j(t_{CEP}) + \Delta t_{out}^{k,m}\ \dot{\overline{R}}^j(t_{CEP}) \end{aligned} \tag{5.8-30}*$$

The corrected Earth angular radii are computed as follows

$$\rho_{in/out} = \arcsin\left[\frac{R_{E_{in/out}} + h_N}{\left|R^j\right|}\right] \tag{5.8-31}*$$

where

$$R_{E_{in/out}} = \frac{R_e(1 - f_E)}{\sqrt{(1 - f_E)^2 + (2f_E - f_E^2)\sin^2 \varphi_{in/out}}} \tag{5.8-32}*$$

$$\sin \varphi_{in/out} = (\hat{R}_{E\,in/out})_Z \tag{5.8-32a}*$$

$$\hat{R}_{E\,in/out} = \frac{\hat{H}^j_{in/out} \cos \rho_N + \hat{R}^j}{\sin \rho_N} \tag{5.8-32b}*$$

R_e = Earth's equatorial radius, 6378.1363 kilometers

f_E = Earth's flattening coefficient, equal to 1/298.257

$R_{E\,in/out}$ = magnitude of the vector from the center of the Earth to the Earth in/out crossing point

$\hat{R}_{E\,in/out}$ = unit vector from the center of the Earth to the Earth in/out crossing point expressed in the inertial frame

$(\hat{R}_{E\,in/out})_z$ = z-component of unit vector from the center of the Earth to the Earth in/out crossing point

$\hat{H}^j_{in/out}$ = unit vector from the satellite j to the Earth in/out crossing point based in initial solution of Equation (5.8-28)

The test given in Equation (5.8-29) is then used to determine which of the two solutions at t_{in} corresponds to $\hat{H}^j_{in}$ and which of the two solutions at t_{out} corresponds to $\hat{H}^j_{out}$. Updated values for the measurements are then computed using the updated $\hat{H}^j_{in}$ and $\hat{H}^j_{out}$ solutions to compute the dihedral angles $A^j_{in/out}$ in Equation (5.8-21).

If the estimation state vector consists of only absolute state vectors, the nonzero components of the row vector of partial derivatives associated with the Earth crossing sensors on satellite *j* are computed as follows. Note that in the partial derivative computations, the value of the satellite position vector at t_{CEP} is used.

$$\frac{\partial \Delta t^{k,m}_{in}}{\partial \overline{R}^j(t_{CEP})} = \frac{1}{\omega^j}\frac{\partial A^j_{in}}{\partial \overline{R}^j(t_{CEP})} \qquad (5.8\text{-}33)^*$$

$$\frac{\partial \Delta t^{k,m}_{in}}{\partial b^{k,m}_{\Delta t\ in}} = 1 \qquad (5.8\text{-}33a)^*$$

$$\frac{\partial \Delta t^{k,m}_{out}}{\partial \overline{R}^j(t_{CEP})} = \frac{1}{\omega^j}\frac{\partial A^j_{out}}{\partial \overline{R}^j(t_{CEP})} \qquad (5.8\text{-}33b)^*$$

$$\frac{\partial \Delta t^{k,m}_{out}}{\partial b^{k,m}_{\Delta t\ out}} = 1 \qquad (5.8\text{-}33c)^*$$

where

$$\frac{\partial A_{in}^{j}}{\partial \overline{R}^{j}} = \frac{1}{1+\left(\frac{N_{in}^{j}}{D_{in}^{j}}\right)^{2}}\left[\frac{1}{D_{in}^{j}}\frac{\partial N_{in}^{j}}{\partial \overline{R}^{j}} - \frac{N_{in}^{j}}{\left(D_{in}^{j}\right)^{2}}\frac{\partial D_{in}^{j}}{\partial \overline{R}^{j}}\right] \tag{5.8-34)*}$$

$$\frac{\partial A_{out}^{j}}{\partial \overline{R}^{j}} = \frac{1}{1+\left(\frac{N_{out}^{j}}{D_{out}^{j}}\right)^{2}}\left[\frac{1}{D_{out}^{j}}\frac{\partial N_{out}^{j}}{\partial \overline{R}^{j}} - \frac{N_{out}^{j}}{\left(D_{out}^{j}\right)^{2}}\frac{\partial D_{out}^{j}}{\partial \overline{R}^{j}}\right] \tag{5.8-34a)*}$$

$$\frac{\partial N_{in}^{j}}{\partial \overline{R}^{j}} = \left(\frac{\partial \hat{V}_{SI}^{j}}{\partial \overline{R}^{j}}\right)^{T}\left(\hat{H}_{in}^{j} \times \hat{A}^{j}\right) + \left(\frac{\partial \hat{H}_{in}^{j}}{\partial \overline{R}^{j}}\right)^{T}\left(\hat{A}^{j} \times \hat{V}_{SI}^{j}\right) \tag{5.8-34b)*}$$

$$\frac{\partial D_{in}^{j}}{\partial \overline{R}^{j}} = \left(\frac{\partial \hat{H}_{in}^{j}}{\partial \overline{R}^{j}}\right)^{T}\hat{V}_{SI}^{j} + \left(\frac{\partial \hat{V}_{SI}^{j}}{\partial \overline{R}^{j}}\right)^{T}\hat{H}_{in}^{j} - \left(\hat{H}_{in}^{j} \cdot \hat{A}^{j}\right)\left(\frac{\partial \hat{V}_{SI}^{j}}{\partial \overline{R}^{j}}\right)^{T}\hat{A}^{j} - \left(\hat{V}_{SI}^{j} \cdot \hat{A}^{j}\right)\left(\frac{\partial \hat{H}_{in}^{j}}{\partial \overline{R}^{j}}\right)^{T}\hat{A}^{j} \tag{5.8-34c)*}$$

$$\frac{\partial N_{out}^{j}}{\partial \overline{R}^{j}} = \left(\frac{\partial \hat{V}_{SI}^{j}}{\partial \overline{R}^{j}}\right)^{T}\left(\hat{H}_{out}^{j} \times \hat{A}^{j}\right) + \left(\frac{\partial \hat{H}_{out}^{j}}{\partial \overline{R}^{j}}\right)^{T}\left(\hat{A}^{j} \times \hat{V}_{SI}^{j}\right) \tag{5.8-35)*}$$

$$\frac{\partial D_{out}^{j}}{\partial \overline{R}^{j}} = \left(\frac{\partial \hat{H}_{out}^{j}}{\partial \overline{R}^{j}}\right)^{T}\hat{V}_{SI}^{j} + \left(\frac{\partial \hat{V}_{SI}^{j}}{\partial \overline{R}^{j}}\right)^{T}\hat{H}_{out}^{j} - \left(\hat{H}_{out}^{j} \cdot \hat{A}^{j}\right)\left(\frac{\partial \hat{V}_{SI}^{j}}{\partial \overline{R}^{j}}\right)^{T}\hat{A}^{j} - \left(\hat{V}_{SI}^{j} \cdot \hat{A}^{j}\right)\left(\frac{\partial \hat{H}_{out}^{j}}{\partial \overline{R}^{j}}\right)^{T}\hat{A}^{j} \tag{5.8-35a)*}$$

$$\frac{\partial \hat{V}_{SI}^{j}}{\partial \overline{R}^{j}} = \frac{1}{\left|\overline{R}_{S} - \overline{R}^{j}\right|}\left[-I_{3x3} + \hat{V}_{SI}^{j}\hat{V}_{SI}^{jT}\right] \tag{5.8-36)*}$$

Finally let

$$\frac{\partial \hat{H}_{in}^{j}}{\partial \overline{R}^{j}} = \left(\frac{\partial \hat{H}_{in}^{j}}{\partial X}, \frac{\partial \hat{H}_{in}^{j}}{\partial Y}, \frac{\partial \hat{H}_{in}^{j}}{\partial Z}\right) \tag{5.8-37)*}$$

$$\left(\kappa_{inX}, \kappa_{inY}, \kappa_{inZ}\right)^{T} = \frac{1}{R^{j}}\left(\hat{R}^{j}\hat{R}^{jT} - I_{3x3}\right)\hat{H}_{in}^{j} \tag{5.8-37a)*}$$

$$\eta = R_N + h_N \tag{5.8-37b)*}$$

Solving the system of equations (5.8-26) yields

$$\frac{\partial \hat{H}^{j}_{in}}{\partial X} = \left[\frac{\eta^2 X + \kappa_{inX} \left(R^{j\,2} - \eta^2\right)^{1/2} R^{j\,3}}{\left(\hat{R}^{j} \cdot \left(\hat{A}^{j} \times \hat{H}^{j}_{in}\right)\right) \left(R^{j\,2} - \eta^2\right)^{1/2} R^{j\,3}} \right] \hat{A}^{j} \times \hat{H}^{j}_{in}$$

$$\frac{\partial \hat{H}^{j}_{in}}{\partial Y} = \left[\frac{\eta^2 Y + \kappa_{inY} \left(R^{j\,2} - \eta^2\right)^{1/2} R^{j\,3}}{\left(\hat{R}^{j} \cdot \left(\hat{A}^{j} \times \hat{H}^{j}_{in}\right)\right) \left(R^{j\,2} - \eta^2\right)^{1/2} R^{j\,3}} \right] \hat{A}^{j} \times \hat{H}^{j}_{in} \qquad (5.8\text{-}38)^*$$

$$\frac{\partial \hat{H}^{j}_{in}}{\partial Z} = \left[\frac{\eta^2 Z + \kappa_{inZ} \left(R^{j\,2} - \eta^2\right)^{1/2} R^{j\,3}}{\left(\hat{R}^{j} \cdot \left(\hat{A}^{j} \times \hat{H}^{j}_{in}\right)\right) \left(R^{j\,2} - \eta^2\right)^{1/2} R^{j\,3}} \right] \hat{A}^{j} \times \hat{H}^{j}_{in}$$

Similarly let

$$\frac{\partial \hat{H}^{j}_{out}}{\partial \overline{R}^{j}} = \left(\frac{\partial \hat{H}^{j}_{out}}{\partial X}, \frac{\partial \hat{H}^{j}_{out}}{\partial Y}, \frac{\partial \hat{H}^{j}_{out}}{\partial Z} \right) \qquad (5.8\text{-}39)^*$$

$$\left(\kappa_{outX}, \kappa_{outY}, \kappa_{outZ}\right)^{T} = \frac{1}{R^{j}} \left(\hat{R}^{j} \hat{R}^{j\,T} - I_{3x3}\right) \hat{H}^{j}_{out} \qquad (5.8\text{-}39a)^*$$

then

$$\frac{\partial \hat{H}^{j}_{out}}{\partial X} = \left[\frac{\eta^2 X + \kappa_{outX} \left(R^{j\,2} - \eta^2\right)^{1/2} R^{j\,3}}{\left(\hat{R}_{U} \cdot \left(\hat{A}^{j} \times \hat{H}^{j}_{out}\right)\right) \left(R^{j\,2} - \eta^2\right)^{1/2} R^{j\,3}} \right] \hat{A}^{j} \times \hat{H}^{j}_{out}$$

$$\frac{\partial \hat{H}^{j}_{out}}{\partial Y} = \left[\frac{\eta^2 Y + \kappa_{outY} \left(R^{j\,2} - \eta^2\right)^{1/2} R^{j\,3}}{\left(\hat{R}_{U} \cdot \left(\hat{A}^{j} \times \hat{H}^{j}_{out}\right)\right) \left(R^{j\,2} - \eta^2\right)^{1/2} R^{j\,3}} \right] \hat{A}^{j} \times \hat{H}^{j}_{out} \qquad (5.8\text{-}40)^*$$

$$\frac{\partial \hat{H}^{j}_{out}}{\partial Z} = \left[\frac{\eta^2 Z + \kappa_{outZ} \left(R^{j\,2} - \eta^2\right)^{1/2} R^{j\,3}}{\left(\hat{R}_{U} \cdot \left(\hat{A}^{j} \times \hat{H}^{j}_{out}\right)\right) \left(R^{j\,2} - \eta^2\right)^{1/2} R^{j\,3}} \right] \hat{A}^{j} \times \hat{H}^{j}_{out}$$

If the estimation state vector consists of the absolute state vector for the local satellite and relative state vectors for nonlocal satellites, the nonzero components of the row vector of measurement partial derivatives associated with the Earth crossing sensors *k* and *m* on satellite *j* are computed as follows:

$$\frac{\partial \Delta t^{k,m}_{in}}{\partial \overline{R}^{1}(t_{CEP})} = \frac{1}{\omega^{j}} \frac{\partial A^{j}_{in}}{\partial \overline{R}^{j}(t_{CEP})} \qquad (5.8\text{-}40a)^*$$

$$\frac{\partial \Delta t^{k,m}_{in}}{\partial \overline{R}^{j}_{rel}(t_{CEP})} = \frac{1}{\omega^{j}} \frac{\partial A^{j}_{in}}{\partial \overline{R}^{j}(t_{CEP})}; \quad j > 1 \qquad (5.8\text{-}40b)^*$$

$$\frac{\partial \Delta t_{in}^{k,m}}{\partial b_{\Delta t\ in}^{k,m}} = 1 \qquad \text{(5.8-40c)*}$$

$$\frac{\partial \Delta t_{out}^{k,m}}{\partial \bar{R}^1(t_{CEP})} = \frac{1}{\omega^j} \frac{\partial A_{out}^{j}}{\partial \bar{R}^j(t_{CEP})} \qquad \text{(5.8-40d)*}$$

$$\frac{\partial \Delta t_{out}^{k,m}}{\partial \bar{R}_{rel}^{j}(t_{CEP})} = \frac{1}{\omega^j} \frac{\partial A_{out}^{j}}{\partial \bar{R}^j(t_{CEP})}; \quad j > 1 \qquad \text{(5.8-40e)*}$$

$$\frac{\partial \Delta t_{out}^{k,m}}{\partial b_{\Delta t\ out}^{k,m}} = 1 \qquad \text{(5.8-40f)*}$$

5.8.4 Pseudoangle Measurements

In Reference 30, Battin describes an approach for computing a celestial position fix based on the measurement of the angular distance between a planet and a star or two planets. Because typical satellite star and planetary sensors do not provide direct measures of this angular separation, Battin's method has been adapted to use the angle between simultaneously measured LOS unit vectors to the planet and star or two planets. (Note that if simultaneous measurements are not available one of the measurements will be interpolated to the time of the other measurement.)

The advantage of this method is that the resultant pseudoangle measurements eliminate the need for direct input of the attitude matrix, A(t). Disadvantages of this method are that it requires simultaneous measurements and that it requires the processing of star sensor measurements, which requires access to an onboard star catalog. In addition, it should be noted that in the future advanced star sensor systems will output the attitude quaternion directly rather than the individual LOS vectors to the stars.

5.8.4.1 Pseudoangle Measurement Preprocessing (not implemented in GEONS)

The pseudoangle measurement is the cosine of the angle between the LOS unit vectors to a planet and a star. It is formed as follows from the LOS measurements to the planet and star or another planet, after rotating them to the common satellite body frame:

$$D_{Ps}^{k,m} = (\hat{P}_B^k) \bullet (\hat{w}_{sB}^j) \qquad \text{(5.8-41)*}$$

where

$\hat{P}_B$ = LOS measurement from planet sensor k on satellite j, referenced to the satellite body frame

$\hat{w}_{sB}^j$ = LOS measurement from star sensor m on satellite j to the sth star, referenced to the satellite body frame

If the raw planet/star measurements are the pitch and yaw angle measurements in the sensor frame (typical for a sun sensor), the components of the measured LOS unit vector to the planet/star in the sensor frame can be computed by inverting Equation (5.8-14) and then rotated to the satellite body frame using Equation (5.8-14b). If the raw planet/star measurements are the y_S and z_S coordinates of the LOS unit vector to each planet/star with respect to the sensor focal frame (typical for a star tracker), the components of the measured LOS unit vector to the planet/star in the sensor frame can be computed as follows

$$\begin{aligned} w_{Sx}^{j} &= (1+\tan^2\Omega_y+\tan^2\Omega_z)^{-1/2} \\ w_{Sy}^{j} &= -w_{Sx}^{j}\tan\Omega_y \\ w_{Sz}^{j} &= -w_{Sx}^{j}\tan\Omega_z \end{aligned} \tag{5.8-42}$$

where the star angles, Ω_y, Ω_z, are related to the sensor y_S and z_S coordinates as follows

$$\begin{aligned} \Omega_y &= \frac{y_s}{n_{pixels\_per\_degree} n_{C\_units\_per\_pixel}} \\ \Omega_z &= \frac{z_s}{n_{pixels\_per\_degree} n_{C\_units\_per\_pixel}} \end{aligned} \tag{5.8-43}$$

where

Ω_y, Ω_z = star angles in the star sensor y_S and z_S directions

$n_{pixels\_per\_degree}$ = number of pixels corresponding to one degree

$n_{C\_units\_per\_pixel}$ = number of subpixels in a pixel

and then rotated from the sensor frame to the satellite body frame using Equation (5.8-14b). Similarly the pseudoangle measurement between the LOS unit vectors to two near bodies (e.g. the sun and Mars) is formed as follows:

$$D_{P_1P_2}^{k,m} = (\hat{P}_B^k) \bullet (\hat{P}_B^m) \tag{5.8-44}$$

where

$\hat{P}_B^k$ = LOS measurement from planet sensor k, referenced to the satellite body frame

5.8.4.2 Pseudoangle Measurement Model and Partial Derivatives

Because the angle between the LOS vectors is independent of the coordinate frame in which the vectors are expressed, the following relationship is used to compute the predicted planet-to-star measurement:

$$D_{Ps}^{k,m} = \hat{V}_{PI}^{j} \bullet \hat{w}_{sI}^{j} + \Delta D_{Ps}^{k} + b_{D_{Ps}}^{k,m} = (\hat{w}_{sI}^{j})^T \hat{V}_{PI}^{j} + \Delta D_{Ps}^{k,m} + b_{D_{Ps}}^{k,m} \tag{5.8-45}*$$

where

$\hat{V}_{PI}^{j}$ = LOS unit vector from satellite j to the planet, referenced to the inertial geocentric frame

$\hat{w}_{sI}^{j}$ = LOS unit vector from satellite j to the sth star, referenced to the inertial geocentric frame (which is identified by the star tracker and provided along with the pseudoangle measurement)

$\Delta D_{Ps}^{k,m}$ = calibrated residual pseudoangle measurement bias between planet sensor k and star tracker m on satellite j (unitless) (an input to the orbit estimation processing)

$b_{DPs}^{k,m}$ = estimated residual pseudoangle measurement bias between for planet sensor k and star tracker m on satellite j (unitless)

If the estimation state vector consists of only absolute state vectors, the nonzero components of the row vector of partial derivatives for planet-to-star pseudoangle measurements associated with sensors on satellite *j* are computed as follows:

$$\frac{\partial D_{Ps}^{k,m}}{\partial \overline{R}^{j}} = (\hat{w}_{sI}^{j})^{T} \frac{\partial \hat{V}_{PI}^{j}}{\partial \overline{R}^{j}} = (\hat{w}_{sI}^{j})^{T} \left(\frac{-I_{3x3} + \hat{V}_{PI}^{j} \hat{V}_{PI}^{j\,T}}{\left| \overline{R}_{P} - \overline{R}^{j} \right|} \right) = \frac{-(\hat{w}_{sI}^{j})^{T} + (\hat{w}_{sI}^{j})^{T} \hat{V}_{PI}^{j} \hat{V}_{PI}^{j\,T}}{\left| \overline{R}_{P} - \overline{R}^{j} \right|} \qquad (5.8\text{-}46)^{*}$$

$$\frac{\partial D_{Ps}^{k,m}}{\partial b_{DPs}^{k,m}} = 1 \qquad (5.8\text{-}46a)^{*}$$

If the estimation state vector consists of the absolute state vector for the local satellite and relative state vectors for nonlocal satellites, the nonzero components of the row vector of measurement partial derivatives for planet-to-star pseudoangle measurements associated with sensors on satellite *j* are computed as follows:

$$\frac{\partial D_{Ps}^{k,m}}{\partial \overline{R}^{1}} = (\hat{w}_{sI}^{j})^{T} \frac{\partial \hat{V}_{PI}^{j}}{\partial \overline{R}^{j}} = (\hat{w}_{sI}^{j})^{T} \left(\frac{-I_{3x3} + \hat{V}_{PI}^{j} \hat{V}_{PI}^{j\,T}}{\left| \overline{R}_{P} - \overline{R}^{j} \right|} \right) = \frac{-(\hat{w}_{sI}^{j})^{T} + (\hat{w}_{sI}^{j})^{T} \hat{V}_{PI}^{j} \hat{V}_{PI}^{j\,T}}{\left| \overline{R}_{P} - \overline{R}^{j} \right|} \qquad (5.8\text{-}46b)^{*}$$

$$\frac{\partial D_{Ps}^{k,m}}{\partial \overline{R}_{rel}^{j}} = (\hat{w}_{sI}^{j})^{T} \frac{\partial \hat{V}_{PI}^{j}}{\partial \overline{R}^{j}} = \frac{-(\hat{w}_{sI}^{j})^{T} + (\hat{w}_{sI}^{j})^{T} \hat{V}_{PI}^{j} \hat{V}_{PI}^{j\,T}}{\left| \overline{R}_{P} - \overline{R}^{j} \right|}; \quad j > 1 \qquad (5.8\text{-}46c)^{*}$$

$$\frac{\partial D_{Ps}^{k,m}}{\partial b_{DPs}^{k,m}} = 1 \qquad (5.8\text{-}46d)^{*}$$

Similarly the pseudoangle measurement between the LOS unit vectors to two near bodies (e.g. the sun and Mars) is modeled as follows:

$$D_{P_1P_2}^{k,m} = \hat{V}_{P_1I}^{\ j} \bullet \hat{V}_{P_2I}^{j} + \Delta D_{P_1P_2}^{k,m} + b_{D_{P_1P_2}}^{k,m} = \hat{V}_{P_2I}^{j\ T} \hat{V}_{P_1I}^{j} + \Delta D_{P_1P_2}^{k,m} + b_{D_{P_1P_2}}^{k,m} \quad (5.8\text{-}47)^*$$

If the estimation state vector consists of only absolute state vectors, the nonzero components of the row vector of associated measurement partial derivatives are computed as follows:

$$\frac{\partial D_{P_1P_2}^{k,m}}{\partial \overline{R}^{j}} = \hat{V}_{P_1I}^{T} \frac{\partial \hat{V}_{P_2I}^{j}}{\partial \overline{R}^{j}} + \hat{V}_{P_2I}^{T} \frac{\partial \hat{V}_{P_1I}^{j}}{\partial \overline{R}^{j}} = \frac{-\hat{V}_{P_1I}^{j\ T} + \hat{V}_{P_1I}^{j\ T} \hat{V}_{P_2I}^{j} \hat{V}_{P_2I}^{j\ T}}{\left|\overline{R}_{P_2} - \overline{R}^{j}\right|} + \frac{-\hat{V}_{P_2I}^{j\ T} + \hat{V}_{P_2I}^{j\ T} \hat{V}_{P_1I}^{j} \hat{V}_{P_1I}^{j\ T}}{\left|\overline{R}_{P_1} - \overline{R}^{j}\right|} \quad (5.8\text{-}48)^*$$

$$\frac{\partial D_{P_1P_2}^{k,m}}{\partial b_{D_{P_1P_2}}^{k,m}} = 1 \quad (5.8\text{-}48a)^*$$

If the estimation state vector consists of the absolute state vector for the local satellite and relative state vectors for nonlocal satellites, the nonzero components of the row vector of partial derivatives for pseudoangle measurements between the LOS unit vectors to two near bodies associated with sensors on satellite *j* are computed as follows:

$$\frac{\partial D_{P_1P_2}^{k,m}}{\partial \overline{R}^{1}} = \hat{V}_{P_1I}^{T} \frac{\partial \hat{V}_{P_2I}^{j}}{\partial \overline{R}^{j}} + \hat{V}_{P_2I}^{T} \frac{\partial \hat{V}_{P_1I}^{j}}{\partial \overline{R}^{j}} = \frac{-\hat{V}_{P_1I}^{j\ T} + \hat{V}_{P_1I}^{j\ T} \hat{V}_{P_2I}^{j} \hat{V}_{P_2I}^{j\ T}}{\left|\overline{R}_{P_2} - \overline{R}^{j}\right|} + \frac{-\hat{V}_{P_2I}^{j\ T} + \hat{V}_{P_2I}^{j\ T} \hat{V}_{P_1I}^{j} \hat{V}_{P_1I}^{j\ T}}{\left|\overline{R}_{P_1} - \overline{R}^{j}\right|} \quad (5.8\text{-}48b)^*$$

$$\frac{\partial D_{P_1P_2}^{k,m}}{\partial \overline{R}_{rel}^{j}} = \hat{V}_{P_1I}^{T} \frac{\partial \hat{V}_{P_2I}^{j}}{\partial \overline{R}^{j}} + \hat{V}_{P_2I}^{T} \frac{\partial \hat{V}_{P_1I}^{j}}{\partial \overline{R}^{j}} = \frac{-\hat{V}_{P_1I}^{j\ T} + \hat{V}_{P_1I}^{j\ T} \hat{V}_{P_2I}^{j} \hat{V}_{P_2I}^{j\ T}}{\left|\overline{R}_{P_2} - \overline{R}^{j}\right|} + \frac{-\hat{V}_{P_2I}^{j\ T} + \hat{V}_{P_2I}^{j\ T} \hat{V}_{P_1I}^{j} \hat{V}_{P_1I}^{j\ T}}{\left|\overline{R}_{P_1} - \overline{R}^{j}\right|};\ j > 1 \quad (5.8\text{-}48c)^*$$

$$\frac{\partial D_{P_1P_2}^{k,m}}{\partial b_{D_{P_1P_2}}^{k,m}} = 1 \quad (5.8\text{-}48d)^*$$

5.9 TDRSS Measurement Models

The computational algorithms for one-way TDRSS Doppler measurements are discussed in this section. The general form of the measurement model is as follows:

$$Y_k = G\ [\bar{X}(t_k),\ t_k] + \varepsilon \tag{5.9-1}$$

where t_k is the true measurement time, referenced to UTC, and ε is the measurement error. It is assumed that ε has a zero-mean Gaussian distribution with standard deviation σ, which is commandable for each measurement type. The measurement standard deviation is typically determined through analysis of the random component of the measurement error as part of the filter tuning process. For GEONS, the estimation state vector, $\overline{X}(t)$ includes the receiver position vector, $\overline{R}$; velocity vector, $\dot{\overline{R}}$; optional corrections to the drag and solar radiation pressure coefficients, ΔC_D and ΔC_R; receiver time bias, b_R; receiver time bias rate, d_R, for one or more receivers; and measurement-dependent biases. The Tracking and Data Relay Satellite (TDRS) state vectors are propagated in the navigation filter.

Section 5.9.1 addresses preprocessing of the raw TDRSS Doppler measurements obtained from a TDRSS S-band receiver onboard the spacecraft. The model for the one-way forward link range from the TDRSS Ground Terminal (TGT) to the TDRS to the local satellite receiver, which is used in the computation of the TDRSS Doppler measurement, is presented in Section 5.9.2. The TDRSS one-way forward Doppler measurement model and associated partial derivatives are defined in Section 5.9.3. Section 5.9.4 provides the measurement model and associated partial derivatives for TDRSS differenced one-way Doppler (DOWD) measurements, which are appropriate for ground processing using GEONS.

5.9.1 Raw TDRSS Doppler Measurement Preprocessing (not implemented in GEONS)

The TDRSS tracking signal path is shown in Figure 5-11. A K-band signal is transmitted from an antenna at the TGT to the space-to-ground link (SGL) antenna on a TDRS. The TDRS translates the signal to the required transmit frequency by converting to S-band and removing a pilot frequency. The S-band signal is then transmitted from either the TDRS multiple access (MA) antenna system or a single-access (SA) antenna to the user satellite. One-way TDRSS tracking is operated using a fixed radiated carrier frequency (FRCF) with onboard Doppler compensation (OBDC). The nominal RCF is 2106.406250 megahertz.

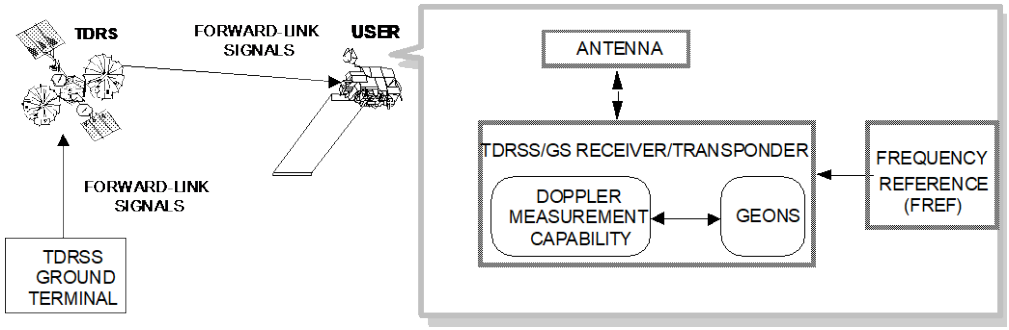

Figure 5-11. TDRSS Forward-Link Signal Path

The user satellite can have more than one TDRSS receiver/transponder, often with one tied to an omnidirectional antenna and one tied to a single-access antenna. The receiver on the user satellite extracts the Doppler frequency by differencing the incoming frequency with the S-band reference frequency. The Doppler measurement function is accomplished via a software accumulation of a scaled and biased nondestruct Doppler shift to provide a Doppler frequency sum measurement. The receiver's raw Doppler measurement output consists of the nondestruct frequency sum. The raw Doppler frequency sums are available nominally every 1.024 seconds. The navigation software samples the Doppler frequency sums, nominally every 8.192 or 16.384 seconds, validates and corrects the measurements for accumulator rollover, and converts them to the averaged Doppler measurements that are input to GEONS. Section 20.9 in Reference 3 describes the measurement validation and conversion processing that was implemented for the TDRSS Doppler extraction capability on the Terra spacecraft.

5.9.2 TDRSS Pseudorange and Associated Partial Derivatives

The timetag associated with the k^{th} measurement is the UTC receive time of the signal at the local receiver as measured with respect to the spacecraft/receiver clock, $t_R^{(RC)}$. In the presence of a spacecraft timing bias, the true measurement time is given by

$$t_k = t_R^{(RC)} - \delta t_R \tag{5.9-2}$$

where δt_R is the offset of the receiver's timing reference from UTC, given by

$$\delta t_R = \frac{b_R(t_k)}{c} \tag{5.9-3}$$

If the receiver time offset, δt_R, is larger than 1 millisecond, it should be used to correct the measurement receiver time tag as shown in Equation 5.9-2. The accumulated receiver clock bias, $b_R(t)$, can be estimated if GPS/WAAS measurements are processed in GEONS in addition to TDRSS Doppler measurement data. However, if only TDRSS Doppler measurements are processed, the receiver time offset correction is not observable and would have to be provided by another satellite subsystem.

TDRSS tracking does not provide a measurement of the TGT-to-TDRS-to-satellite pseudorange; however, the TGT-to-TDRS-to-satellite range is computed as part of the Doppler measurement model. The backward signal-trace method is used to determine when the signal was transmitted from the TGT and the TDRS. After the actual transmit times are determined, the range between the TGT and the TDRS and the TDRS and local satellite receiver are computed.

If the forward-link signal is transmitted from an antenna at the TGT at time t_{T_1}, received by the SGL antenna on TDRS *p* and transmitted from MA or SA antenna *q* on TDRS *p* at time t_{T_2}, and received at antenna *i* on satellite *n* at time t_R (equal to t_k), the distance traversed by the signal is given by the range, $\rho_{TDRS_p}^{n,i}$:

$$\rho_{TDRS_p}^{n,i} = c \cdot (t_R - t_{T_2}) + c \cdot (t_{T_2} - t_{T_1}) = \left| \overline{R}_{A_i}^{n}(t_R) - \overline{R}_{TDRS_{p,q}}(t_{T_2}) \right| + \left| \overline{R}_{TDRS_{p,\mathrm{SGL}}}(t_{T_2}) - \overline{R}_{TGT_p}(t_{T_1}) \right| \qquad (5.9\text{-}4)^*$$

where

c = speed of light

$\overline{R}_{A_i}^{n}(t_R)$ = position of antenna i on receiving satellite n at time t_R , which is computed using Equation 3.2-61 in Section 3.2.8

$\overline{R}_{TDRS_{p,q}}(t_{T_2})$ = position of transmitting MA or SA antenna q on TDRS p at time t_{T_2} (currently the TDRS antenna offsets are not modeled in GEONS)

$\overline{R}_{TDRS_{p,\mathrm{SGL}}}(t_{T_2})$ = position of receiving SGL antenna on TDRS p at time t_{T_2} (currently the TDRS antenna offsets are not modeled in GEONS)

$\overline{R}_{TGT_p}(t_{T_1})$ = position of the transmitting ground antenna associated with TDRS p at the TGT at time t_{T_1}

The transponder delay on the TDRS or the user satellite is not modeled.

The Newton-Raphson iterative scheme is used to solve for the actual signal transmit time, t_{T_2}, as follows

$$t_{T_2,m+1} = t_R - \frac{\left| \overline{R}_{A_i}^{n}(t_R) - \overline{R}_{TDRS_{p,q}}(t_{T_2,m}) \right|}{c} \qquad (5.9\text{-}5)^*$$

where

$t_{T,m+1}$ = $(m+1)^{th}$ approximation for t_T

$t_{T,m}$ = m^{th} approximation for t_T

t_R = signal reception time at the satellite receiver

The iterative solution of Equation (5.9-5) is started by setting

$$t_{T_2,0} = t_R \qquad (5.9\text{-}6)^*$$

such that

$$\overline{R}_{TDRS_{p,q}}(t_{T_2,0}) = \overline{R}_{TDRS_{p,q}}(t_R) \qquad (5.9\text{-}7)^*$$

The TDRS state vector is propagated to the time $t_R = t_k$ using a Runge-Kutta integrator and the full acceleration model. The TDRS positions at the updated transmission times are computed as follows

$$\overline{R}_{TDRS_{p,q}}(t_{T_2,m}) = \overline{R}_{TDRS_{p,q}}(t_R) - \Delta t_m \dot{\overline{R}}_{TDRS_{p,q}}(t_R) \qquad (5.9\text{-}8)^*$$

where

$$\Delta t_m = t_R - t_{T_2,m} \tag{5.9-9}*$$

This iterative scheme is continued until the condition $\left|t_{T,m+1} - t_{T,m}\right| \le \varepsilon$ is satisfied, where ε is a small tolerance (nominally equal to 10^{-8} second). The TGT transmission time t_{T_1} is then computed using the same iterative scheme to solve:

$$t_{T_1,m+1} = t_{T_2} - \frac{\left|\overline{R}_{TDRS_{p,\mathrm{SGL}}}(t_{T_2}) - \overline{R}_{TGT_p}(t_{T_1,m})\right|}{c} \tag{5.9-10}*$$

After the signal transmission times are found, the distance between the local satellite receiver and the TDRS and the TDRS and the associated TGT antenna are calculated using Equation (5.9-4). The position and velocity vectors for the TGT antennas are available in ECEF coordinates and must be transformed to J2000.0 inertial coordinates using the transformations defined in Sections 3.2.1 through 3.2.3.

If the estimation state vector consists of absolute states for the local and remote satellites, the following are the nonzero partial derivatives of the range with respect to the components of the estimation state vector, $\overline{X}(t_k)$, where $\overline{R}^n(t_k)$ is the receiving satellite state vector:

$$\frac{\partial \rho^{n,i}_{TDRS_p}(t_k)}{\partial \overline{R}^n(t_k)} = \frac{\partial \rho^{n,i}_{TDRS_p}(t_k)}{\partial \overline{R}^n(t_R)} = \frac{\overline{R}^n_{A_i}(t_R) - \overline{R}_{TDRS_{p,q}}(t_{T_2})}{\left|\overline{R}^n_{A_i}(t_R) - \overline{R}_{TDRS_{p,q}}(t_{T_2})\right|} \tag{5.9-11}*$$

If the estimation state vector includes relative states for the remote satellites, the following are the nonzero partial derivatives of the range with respect to the components of the estimation state vector, $\overline{X}(t_k)$:

$$\frac{\partial \rho^{n,i}_{TDRS_p}(t_k)}{\partial \overline{R}^1(t_k)} = \frac{\partial \rho^{n,i}_{TDRS_{p,}}(t_k)}{\partial \overline{R}^n(t_R)} \frac{\partial \overline{R}^n(t_R)}{\partial \overline{R}^1(t_R)} = \frac{\overline{R}^n_{A_i}(t_R) - \overline{R}_{TDRS_{p,q}}(t_{T_2})}{\left|\overline{R}^n_{A_i}(t_R) - \overline{R}_{TDRS_{p,q}}(t_{T_2})\right|} \tag{5.9-12}*$$

$$\frac{\partial \rho^{n,i}_{TDRS_p}(t_k)}{\partial \overline{R}^n_{rel}(t_k)} = \frac{\partial \rho^{n,i}_{TDRS_p}(t_k)}{\partial \overline{R}^n(t_R)} \frac{\partial \overline{R}^n(t_R)}{\partial \overline{R}^n_{rel}(t_R)} = \frac{\overline{R}^n_{A_i}(t_R) - \overline{R}_{TDRS_{p,q}}(t_{T_2})}{\left|\overline{R}^n_{A_i}(t_R) - \overline{R}_{TDRS_{p,q}}(t_{T_2})\right|}; \quad n \ne 1 \tag{5.9-13}*$$

5.9.3 TDRSS Forward-Link Averaged Doppler Measurement Model and Associated Partial Derivatives

The TDRS associated with the first valid measurement in each tracking contact is identified by the process of elimination. All visible TDRSs are identified using the HORP test defined in Section 7.4 of this document. For each the visible TDRS, the TGT-to-TDRS-to-satellite Doppler

measurement is modeled using the model provided below. The TDRS that produces the smallest measurement residual is selected as the transmitting TDRS for that contact.

The instantaneous Doppler-shifted RCF received at the spacecraft is equal to

$$f'_{RCF} = f_{RCF}\left(1 - \frac{\dot{\rho}}{c}\right) + \delta F_{atm} + \delta F_{rel} \tag{5.9-14}$$

where

f'_{RCF} = Doppler-shifted RCF

f_{RCF} = transmitted TDRSS RCF, a commandable parameter, nominally equal to 2106406250 Hertz

$\dot{\rho}$ = time rate of change of the light-time-corrected range from the TGT to the TDRS to the spacecraft receiver, $\rho^{n,i}_{TDRS_j}$ [defined in Equation (5.9-4)]

δF_{atm} = signal delay due to atmospheric effects

δF_{rel} = signal delay due to relativistic effects

GEONS does not apply corrections for atmospheric and relativistic effects in the TDRS measurement model.

$$f'_{RCF} \cong f_{RCF}\left(1 - \frac{\dot{\rho}}{c}\right) \tag{5.9-15}$$

The true instantaneous Doppler shift is given by

$$(f_D)_{true} = f'_{RCF} - f_{RCF} \tag{5.9-16}$$

The Doppler shift is measured onboard with respect to the receiver's S-band frequency reference, such that the instantaneous Doppler measurement is given by

$$(f_D)_{ext} = f'_{RCF} - f_{ref}(t) \tag{5.9-17}$$

where

$f_{ref}(t)$ = receiver's S-band frequency reference at time t, nominally equal to 2106.406250 megahetz

Substituting Equation (5.9-15) into Equation (5.9-17) and averaging over the Doppler averaging interval, ΔT, the averaged Doppler measurement can be expressed as

$$\left(\overline{F_D(t_k)}\right)^{n,i}_{TDRS_p} = \frac{1}{\Delta T}\int_{t_k-\Delta T}^{t_k} (f_D)^n_{ext}(t)dt \tag{5.9-18}$$

$$\left(\overline{F_D(t_k)}\right)^{n,i}_{TDRS_p} = \frac{1}{\Delta T}\int_{t_k-\Delta T}^{t_k}\left[f_{RCF}\left(1-\frac{\dot{\rho}^{n,i}_{TDRS_p}}{c}\right)-f^n_{ref}(t)\right]dt + b_d^{TDRS_p}(t_k) \tag{5.9-19}$$

$$\left(\overline{F_D(t_k)}\right)^{n,i}_{TDRS_p} = f_{RCF}\left(1-\frac{\Delta\rho^{n,i}_{TDRS_p}(t_k)}{c\Delta T}\right)-\overline{f^n_{ref}(t_k)} + b_d^{TDRS_p}(t_k) \tag{5.9-20}*$$

where

$$\Delta\rho^{n,i}_{TDRS_p}(t_k) = \rho^{n,i}_{TDRS_p}(t_k) - \rho^{n,i}_{TDRS_p}(t_k-\Delta T) \tag{5.9-21}*$$

and $b_d^{TDRS_p}(t_k)$ is the current value of the Doppler bias associated with TDRS *p* in Hertz and $\overline{f^n_{ref}(t_k)}$ is the averaged value of $f^n_{ref}(t_k)$ over the time $t_k - \Delta T$ to t_k. This value is approximated as follows, neglecting the effects of frequency drift over the averaging interval:

$$\overline{f^n_{ref}(t_k)} \cong f^n_{ref}(t_k) = f_{ref}(t_0)\left[1+\frac{d^n_R(t_k)}{c}\right] \tag{5.9-22}*$$

where $d^n_R(t_k)$, the receiver time bias rate, is computed using Equation 4.3-19 and $f_{ref}(t_0)$ is the initial value of the S-band Doppler reference frequency, a commanded parameter nominally equal to 2106406250 Hertz.

Note that the measurement model as currently implemented in GEONS assumes that the Doppler averaging interval is equal to the interval between calls to the state estimation task, or equivalently the integration stepsize.

Note that because the Doppler measurement model requires the computation of the range at an earlier time, $\rho(t_k - \Delta T)$, the range is computed at the time of the first Doppler measurement in a contact but the measurement update is not performed. In addition, the measurement update process is not performed for the first Doppler measurement following the uplink of a new TDRS vector because the discontinuity in the TDRS state will produce a large Doppler residual.

If the estimation state vector consists of absolute states for the local and remote satellites, the nonzero partial derivatives of the Doppler measurements with respect to the components of the estimation state vector, $\overline{X}(t_k)$, for the receiving satellite *n* are computed as follows:

$$\frac{\partial\left(\overline{F_D(t_k)}\right)^{n,i}_{TDRS_p}}{\partial\overline{R}^n(t_k)} = -\frac{f_{RCF}}{c\Delta T}\left[\frac{\partial\rho^{n,i}_{TDRS_p}(t_k)}{\partial\overline{R}^n(t_k)} - \frac{\partial\rho^{n,i}_{TDRS_p}(t_k-\Delta T)}{\partial\overline{R}^n(t_k-\Delta T)}\left(\frac{\partial\overline{R}^n(t_k-\Delta T)}{\partial\overline{R}^n(t_k)}\right)\right] \tag{5.9-23}*$$

$$\frac{\partial\left(\overline{F_D(t_k)}\right)^{n,i}_{TDRS_p}}{\partial\dot{\overline{R}}^n(t_k)} = \frac{f_{RCF}}{c\Delta T}\left[\frac{\partial\rho^{n,i}_{TDRS_p}(t_k-\Delta T)}{\partial\overline{R}^n(t_k-\Delta T)}\left(\frac{\partial\overline{R}^n(t_k-\Delta T)}{\partial\dot{\overline{R}}^n(t_k)}\right)\right] \tag{5.9-24}*$$

$$\frac{\partial\left(\overline{F_D(t_k)}\right)^{n,i}_{TDRS_p}}{\partial \Delta C_D^n(t_k)} = \frac{f_{RCF}}{c\Delta T}\left[\frac{\partial \rho^{n,i}_{TDRS_p}(t_k-\Delta T)}{\partial \overline{R}^n(t_k-\Delta T)}\left(\frac{\partial \overline{R}^n(t_k-\Delta T)}{\partial \Delta C_D^n(t_k)}\right)\right] \tag{5.9-25}*$$

$$\frac{\partial\left(\overline{F_D(t_k)}\right)^{n,i}_{TDRS_p}}{\partial \Delta C_R^n(t_k)} = \frac{f_{RCF}}{c\Delta T}\left[\frac{\partial \rho^{n,i}_{TDRS_p}(t_k-\Delta T)}{\partial \overline{R}^n(t_k-\Delta T)}\left(\frac{\partial \overline{R}^n(t_k-\Delta T)}{\partial \Delta C_R^n(t_k)}\right)\right] \tag{5.9-26}*$$

$$\frac{\partial\left(\overline{F_D(t_k)}\right)^{n,i}_{TDRS_p}}{\partial d_R^n(t_k)} = \frac{\partial\left(\overline{F_D(t_k)}\right)^{n,i}_{TDRS_p}}{\partial f_{ref}^n(t_k)}\frac{\partial f_{ref}^n(t_k)}{\partial d_R^n(t_k)} = -\frac{f_{ref}(t_0)}{c} \tag{5.9-27}*$$

$$\frac{\partial\left(\overline{F_D(t_k)}\right)^{n,i}_{TDRS_p}}{\partial b_d^{TDRS_p}(t_k)} = 1 \tag{5.9-28}*$$

The partial derivatives of the range in Equations (5.9-23) through (5.9-26) are defined in Equation (5.9-11) in Section 5.9.2. These derivatives are evaluated at the current measurement timetag, t_k, and at the time $t_k - \Delta T$, where ΔT is the Doppler averaging interval.

The matrix of partial derivatives of position in Equations (5.9-23) through (5.9-26) is related to the components of the state transition matrix defined by Equation (4.4-1a) in Section 4.4.1 as follows

$$\left(\frac{\partial \overline{R}^n(t_k-\Delta T)}{\partial \overline{R}^n(t_k)}\right) = (W)_{i=1,2,3;\,j=1,2,3} \tag{5.9-31}*$$

$$\left(\frac{\partial \overline{R}^n(t_k-\Delta T)}{\partial \dot{\overline{R}}^n(t_k)}\right) = (W)_{i=1,2,3;\,j=4,5,6} \tag{5.9-32}*$$

$$\left(\frac{\partial \overline{R}^n(t_k-\Delta T)}{\partial \Delta C_D^n}\right) = (W)_{i=1,2,3;\,j=7} \tag{5.9-33}*$$

$$\left(\frac{\partial \overline{R}^n(t_k-\Delta T)}{\partial \Delta C_R^n}\right) = (W)_{i=1,2,3;\,j=8} \tag{5.9-34}*$$

where

$$W = \begin{bmatrix} \dfrac{\partial \overline{R}^{\,n}(t_k)}{\partial \overline{R}^{\,n}(t_k - \Delta T)} & \dfrac{\partial \overline{R}^{\,n}(t_k)}{\partial \dot{\overline{R}}^{\,n}(t_k - \Delta T)} & \dfrac{\partial \overline{R}^{\,n}(t_k)}{\partial \Delta C_D^n(t_k - \Delta T)} & \dfrac{\partial \overline{R}^{\,n}(t_k)}{\partial \Delta C_R^n(t_k - \Delta T)} \\ \dfrac{\partial \dot{\overline{R}}^{\,n}(t_k)}{\partial \overline{R}^{\,n}(t_k - \Delta T)} & \dfrac{\partial \dot{\overline{R}}^{\,n}(t_k)}{\partial \dot{\overline{R}}^{\,n}(t_k - \Delta T)} & \dfrac{\partial \dot{\overline{R}}^{\,n}(t_k)}{\partial \Delta C_D^n(t_k - \Delta T)} & \dfrac{\partial \dot{\overline{R}}^{\,n}(t_k)}{\partial \Delta C_R^n(t_k - \Delta T)} \\ 0_{1x3} & 0_{1x3} & 1 & 0 \\ 0_{1x3} & 0_{1x3} & 0 & 1 \end{bmatrix}^{-1} \quad \text{(5.9-35)*}$$

If the atmospheric drag coefficient correction and/or the solar radiation pressure coefficient correction are not estimated, the matrix W does not include the columns associated with these state components.

If the estimation state vector includes the relative states for the remote satellites (n≠1), the nonzero partial derivatives of the Doppler measurements with respect to the components of the estimation state vector, $\overline{X}(t_k)$, for the receiving satellite *n* are computed as follows:

$$\frac{\partial\left(\overline{F_D(t_k)}\right)^{n,i}_{TDRS_p}}{\partial \overline{R}^1(t_k)} = -\frac{f_{RCF}}{c\Delta T}\left[\frac{\partial \rho^{\,n,i}_{TDRS_p}(t_k)}{\partial \overline{R}^n(t_k)} - \frac{\partial \rho^{\,n,i}_{TDRS_p}(t_k - \Delta T)}{\partial \overline{R}^n(t_k - \Delta T)}\left(\frac{\partial \overline{R}^1(t_k - \Delta T)}{\partial \overline{R}^1(t_k)}\right)\right] \quad \text{(5.9-36)*}$$

$$\frac{\partial\left(\overline{F_D(t_k)}\right)^{n,i}_{TDRS_p}}{\partial \overline{R}^n_{rel}(t_k)} = -\frac{f_{RCF}}{c\Delta T}\left[\frac{\partial \rho^{\,n,i}_{TDRS_p}(t_k)}{\partial \overline{R}^n(t_k)} - \frac{\partial \rho^{\,n,i}_{TDRS_p}(t_k - \Delta T)}{\partial \overline{R}^n(t_k - \Delta T)}\left(\frac{\partial \overline{R}^n_{rel}(t_k - \Delta T)}{\partial \overline{R}^n_{rel}(t_k)}\right)\right] \quad n \neq 1 \quad \text{(5.9-36a)*}$$

$$\frac{\partial\left(\overline{F_D(t_k)}\right)^{n,i}_{TDRS_p}}{\partial \dot{\overline{R}}^1(t_k)} = \frac{f_{RCF}}{c\Delta T}\left[\frac{\partial \rho^{\,n,i}_{TDRS_p}(t_k - \Delta T)}{\partial \overline{R}^n(t_k - \Delta T)}\left(\frac{\partial \overline{R}^1(t_k - \Delta T)}{\partial \dot{\overline{R}}^1(t_k)}\right)\right] \quad \text{(5.9-37)*}$$

$$\frac{\partial\left(\overline{F_D(t_k)}\right)^{n,i}_{TDRS_p}}{\partial \dot{\overline{R}}^n_{rel}(t_k)} = \frac{f_{RCF}}{c\Delta T}\left[\frac{\partial \rho^{\,n,i}_{TDRS_p}(t_k - \Delta T)}{\partial \overline{R}^n(t_k - \Delta T)}\left(\frac{\partial \overline{R}^n_{rel}(t_k - \Delta T)}{\partial \dot{\overline{R}}^n_{rel}(t_k)}\right)\right] \quad n \neq 1 \quad \text{(5.9-37a)*}$$

$$\frac{\partial\left(\overline{F_D(t_k)}\right)^{n,i}_{TDRS_p}}{\partial \Delta C^1_D(t_k)} = \frac{f_{RCF}}{c\Delta T}\left[\frac{\partial \rho^{\,n,i}_{TDRS_p}(t_k - \Delta T)}{\partial \overline{R}^n(t_k - \Delta T)}\left(\frac{\partial \overline{R}^1(t_k - \Delta T)}{\partial \Delta C^1_D(t_k)}\right)\right] \quad \text{(5.9-38)*}$$

$$\frac{\partial\left(\overline{F_D(t_k)}\right)^{n,i}_{TDRS_p}}{\partial \Delta C^n_{D_{rel}}(t_k)} = \frac{f_{RCF}}{c\Delta T}\left[\frac{\partial \rho^{\,n,i}_{TDRS_p}(t_k - \Delta T)}{\partial \overline{R}^n(t_k - \Delta T)}\left(\frac{\partial \overline{R}^n_{rel}(t_k - \Delta T)}{\partial \Delta C^n_{D_{rel}}(t_k)}\right)\right] \quad n \neq 1 \quad \text{(5.9-38a)*}$$

$$\frac{\partial\left(\overline{F_D(t_k)}\right)^{n,i}_{TDRS_p}}{\partial \Delta C^1_R(t_k)} = \frac{f_{RCF}}{c\Delta T}\left[\frac{\partial \rho^{\,n,i}_{TDRS_p}(t_k - \Delta T)}{\partial \overline{R}^n(t_k - \Delta T)}\left(\frac{\partial \overline{R}^1(t_k - \Delta T)}{\partial \Delta C^1_R(t_k)}\right)\right] \quad \text{(5.9-39)*}$$

$$\frac{\partial\left(\overline{F_D(t_k)}\right)^{n,i}_{TDRS_p}}{\partial \Delta C^n_{R_{rel}}(t_k)} = \frac{f_{RCF}}{c\Delta T}\left[\frac{\partial \rho^{\,n,i}_{TDRS_p}(t_k - \Delta T)}{\partial \overline{R}^n(t_k - \Delta T)}\left(\frac{\partial \overline{R}^n(t_k - \Delta T)}{\partial \Delta C^n_{R_{rel}}(t_k)}\right)\right] \quad n \neq 1 \quad \text{(5.9-39a)*}$$

$$\frac{\partial\left(\overline{F_D(t_k)}\right)^{n,i}_{TDRS_p}}{\partial d^1_R(t_k)} = \frac{\partial\left(\overline{F_D(t_k)}\right)^{n,i}_{TDRS_p}}{\partial f^n_{ref}(t_k)} \frac{\partial f^n_{ref}(t_k)}{\partial d^n_R(t_k)} = -\frac{f_{ref}(t_0)}{c} \tag{5.9-40}*$$

$$\frac{\partial\left(\overline{F_D(t_k)}\right)^{n,i}_{TDRS_p}}{\partial d^n_{R_{rel}}(t_k)} = \frac{\partial\left(\overline{F_D(t_k)}\right)^{n,i}_{TDRS_p}}{\partial f^n_{ref}(t_k)} \frac{\partial f^n_{ref}(t_k)}{\partial d^n_{R_{rel}}(t_k)} = -\frac{f_{ref}(t_0)}{c} \quad n \neq 1 \tag{5.9-40a}*$$

$$\frac{\partial\left(\overline{F_D(t_k)}\right)^{n,i}_{TDRS_p}}{\partial b_d^{TDRS_p}(t_k)} = 1 \tag{5.9-41}*$$

The partial derivatives of the range are defined in Equations (5.9-12) and (5.9-13). The partial derivatives of position vector at the time $t_k - \Delta T$ with respect to the estimated state vector components are related to the components of the inverse of the state transition matrix defined by Equation (4.4-1b) in Section 4.4.1

$$\left(\frac{\partial \overline{X}_{rel}(t_k - \Delta T)}{\partial \overline{X}_{rel}(t_k)}\right) = \left(\frac{\partial \overline{X}_{rel}(t_k)}{\partial \overline{X}_{rel}(t_{k-1})}\right)^{-1} \tag{5.9-42}*$$

where

$$\overline{X}_{rel} = \begin{bmatrix} \overline{X}^1 \\ \overline{X}^2_{rel} \\ \vdots \\ \overline{X}^{N_S}_{rel} \\ \overline{B} \end{bmatrix}$$

and

$$\overline{X}^n_{rel} = \overline{X}^n - \overline{X}^1 = \begin{bmatrix} \overline{R}^n - \overline{R}^1 \\ \dot{\overline{R}}^n - \dot{\overline{R}}^1 \\ \Delta C^n_D - \Delta C^1_D \\ \Delta C^n_R - \Delta C^1_R \\ \overline{b}^n_R - \overline{b}^1_R \end{bmatrix} = \begin{bmatrix} \overline{R}^n_{rel} \\ \dot{\overline{R}}^n_{rel} \\ \left(\Delta C^n_D\right)_{rel} \\ \left(\Delta C^n_R\right)_{rel} \\ \overline{b}^n_{rel} \end{bmatrix} ; n \neq 1$$

5.9.4 TDRSS Differenced One-Way Doppler (DOWD) Measurement Model and Associated Partial Derivatives

The DOWD measurements are suitable for ground processing. With a wide-beam antenna system, the one-way return signal generated from the user spacecraft can be received by more than one TDRS. By differencing the one-way return Doppler measurements, most of the spacecraft

oscillator's frequency bias is cancelled. The following discussion is based on the description provided in Section 7.3 and Appendix A.8 of the *Goddard Trajectory Determination System (GTDS) Mathematical Theory* (Ref. 27).

The observed DOWD measurements are formed by differencing averaged (nondestruct) one-way return Doppler measurements from the transmitting antenna i on spacecraft n via two different return-link TDRS (p and q) to the TGT that are measured at time T_R.

$$\Delta\left(\overline{F_{D_{obs}}(t_R)}\right)^{n,i}_{TDRS_{p-q}} = \left(\overline{F_{D_{obs}}(t_R)}\right)^{n,i}_{TDRS_p} - \left(\overline{F_{D_{obs}}(t_R)}\right)^{n,i}_{TDRS_q} \qquad (5.9.4\text{-}1)^*$$

The corresponding DOWD measurements are modeled as follows

$$\Delta\left(\overline{F_D(t_R)}\right)^{n,i}_{TDRS_{p-q}} = \left(\overline{F_D(t_R)}\right)^{n,i}_{TDRS_p} - \left(\overline{F_D(t_R)}\right)^{n,i}_{TDRS_q} + \Delta b_d^{TDRS_{p-q}} \qquad (5.9.4\text{-}2)^*$$

where $\left(\overline{F_D(t_R)}\right)^{n,i}_{TDRS_p}$ is the one-way return link Doppler shift via TDRS p averaged over the Doppler count interval ΔT from T_R - ΔT to T_R and $\Delta b_d^{TDRS_{p-q}}$ is a DOWD measurement bias. Calculation of $\left(\overline{F_D(t_R)}\right)^{n,i}_{TDRS_p}$ and $\left(\overline{F_D(t_R)}\right)^{n,i}_{TDRS_q}$ is discussed below.

In the case of TDRS return link tracking, the Doppler shifted signal is made of two components. The long-trip path component, which is transmitted at time T_1 from the user spacecraft, received/retransmitted at time T_2 at the TDRS, and measured at time T_R at the TGT, is given by

$$\left(\rho^{n,i}_{TDRS_p}\right)_l(t_R) = \left|\bar{R}_{TDRS_p}(t_{T_2}) - \bar{R}^n_{A_i}(t_{T_1})\right| + \left|\bar{R}_{TGT}(t_R) - \bar{R}_{TDRS_p}(t_{T_2})\right| \qquad (5.9.4\text{-}3)^*$$

where the signal transmission times T_2 and T_1 and associated state vectors are computed via backward tracing using the Newton-Raphson iterative procedure described in Section 5.9.2.

The phase of the Doppler signal is maintained by transmitting a coherent pilot-tone frequency to the return-link TDRS. This short-trip path component, which is transmitted at time T_3 from the TGT, received/retransmitted at time T_4 at the TDRS, and received at time T_R at the TGT, is given by

$$(\rho^{n,i}_{TDRS_p})_s(t_R) = \left|\bar{R}_{TDRS_p}(t_{T_4}) - \bar{R}_{TGT}(t_{T_3})\right| + \left|\bar{R}_{TGT}(t_R) - \bar{R}_{TDRS_p}(t_{T_4})\right| \qquad (5.9.4\text{-}4)^*$$

where the times T_4 and T_3 and associated state vectors are computed using the Newton-Raphson iterative procedure described in Section 5.9.2.

The two Doppler-shifted frequencies are mixed in the transponder of the return link TDRS according to a fixed ratio to produce the observed Doppler shift. The resulting Doppler shift averaged over the Doppler count interval ΔT is modeled as follows:

$$\left(\overline{F_D(t_R)}\right)^{n,i}_{TDRS_p} = -\frac{1}{c\Delta T}\left(A\left(\Delta\rho^{n,i}_{TDRS_p}\right)_l(t_R) + B\left(\Delta\rho^{n,i}_{TDRS_p}\right)_s(t_R)\right) \qquad (5.9.4\text{-}5)^*$$

where

$$\left(\Delta\rho^{n,i}_{TDRS_p}(t_R)\right)_l = \left(\rho^{n,i}_{TDRS_p}(t_R)\right)_l - \left(\rho^{n,i}_{TDRS_p}(t_R - \Delta T)\right)_l \quad (5.9.4\text{-}6)^*$$

$$\left(\Delta\rho^{n,i}_{TDRS_p}(t_R)\right)_s = \left(\rho^{n,i}_{TDRS_p}(t_R)\right)_s - \left(\rho^{n,i}_{TDRS_p}(t_R - \Delta T)\right)_s \quad (5.9.4\text{-}7)^*$$

In this equation A is the effective transmit frequency from the user provided with the tracking data and B is the pilot-tone frequency translation from the return-link TDRS. The values of the pilot-tone frequency translation depend on both the return-link service type and the frequency band of the link. Table ANX-1 in Reference 77 lists the values of the translation frequency for each service type associated with the TDRSS ground terminals prior to the Space Network Ground Segment Sustainment (SGSS) changes and after SGSS.

The partial derivative of a DOWD measurement with respect any solve-for parameter, s, can be written as follows

$$\frac{\partial\Delta\left(\overline{F_D(t_R)}\right)^{n,i}_{TDRS_{p-q}}}{\partial s} = \frac{\partial\left(\overline{F_D(t_R)}\right)^{n,i}_{TDRS_p}}{\partial s} - \frac{\partial\left(\overline{F_D(t_R)}\right)^{n,i}_{TDRS_q}}{\partial s} \quad (5.9.4\text{-}8)^*$$

Calculation of $\frac{\partial\left(\overline{F_D(t_R)}\right)^{n,i}_{TDRS_p}}{\partial s}$ and $\frac{\partial\left(\overline{F_D(t_R)}\right)^{n,i}_{TDRS_q}}{\partial s}$ is discussed below.

The non-zero partial derivatives of a DOWD measurement with respect to the components of the estimation state vector are computed as follows for TDRS *p* and similarly for TDRS *q*. Note that the partial derivatives of the short range with respect to the user satellite state vector are zero and the partial derivatives with respect to the user spacecraft time bias parameters are not computed because they would cancel out when differenced. In addition, the GEONS estimation state vector does not include the TDRS state vectors or TDRS transponder delays.

$$\frac{\partial\left(\overline{F_D(t_R)}\right)^{n,i}_{TDRS_p}}{\partial\bar{R}^n(t_R)} = -\frac{A}{c\Delta T}\left(\frac{\partial\left(\rho^{n,i}_{TDRS_p}\right)_l(t_R)}{\partial\bar{R}^n(t_R)} - \frac{\partial\left(\rho^{n,i}_{TDRS_p}\right)_l(t_R - \Delta T)}{\partial\bar{R}^n(t_R - \Delta T)}\left(\frac{\partial\bar{R}^n(t_R - \Delta T)}{\partial\bar{R}^n(t_R)}\right)\right) \quad (5.9.4\text{-}9)^*$$

$$\frac{\partial\left(\overline{F_D(t_R)}\right)^{n,i}_{TDRS_p}}{\partial\dot{\bar{R}}^n(t_R)} = \frac{A}{c\Delta T}\left(\frac{\partial\left(\rho^{n,i}_{TDRS_p}\right)_l(t_R - \Delta T)}{\partial\bar{R}^n(t_R - \Delta T)}\right)\left(\frac{\partial\bar{R}^n(t_R - \Delta T)}{\partial\dot{\bar{R}}^n(t_R)}\right) \quad (5.9.4\text{-}10)^*$$

$$\frac{\partial\left(\overline{F_D(t_R)}\right)^{n,i}_{TDRS_p}}{\partial\Delta C^n_D(t_R)} = \frac{A}{c\Delta T}\left(\frac{\partial\left(\rho^{n,i}_{TDRS_p}\right)_l(t_R - \Delta T)}{\partial\bar{R}^n(t_R - \Delta T)}\right)\left(\frac{\partial\bar{R}^n(t_R - \Delta T)}{\partial\Delta C^n_D(t_R)}\right) \quad (5.9.4\text{-}11)^*$$

$$\frac{\partial\left(\overline{F_D(t_R)}\right)^{n,i}_{TDRS_p}}{\partial\Delta C^n_R(t_R)} = \frac{A}{c\Delta T}\left(\frac{\partial\left(\rho^{n,i}_{TDRS_p}\right)_l(t_R - \Delta T)}{\partial\bar{R}^n(t_R - \Delta T)}\right)\left(\frac{\partial\bar{R}^n(t_R - \Delta T)}{\partial\Delta C^n_R(t_R)}\right) \quad (5.9.4\text{-}12)^*$$

and

$$\frac{\partial\Delta\left(\overline{F_D(t_R)}\right)^{n,i}_{TDRS_{p-q}}}{\partial\Delta b_d^{TDRS_{p-q}}\left(t_R\right)}=1 \qquad (5.9.4\text{-}13)^*$$

The partial derivatives of the long range in Equations (5.9.4-9) through (5.9.4-12) are computed as follows where these derivatives are evaluated for T_R equal to the current measurement timetag, t_R, and at the time $t_R-\Delta T$.

$$\frac{\partial\left(\rho^{\,n,i}_{TDRS_p}\right)_l(t_R)}{\partial\overline{R}^n(t_R)}=-\frac{\overline{R}_{TDRS_p}(t_{T_2})-\overline{R}^n_{A_i}(t_{T_1})}{\left|\overline{R}_{TDRS_{p,q}}(t_{T_2})-\overline{R}^n_{A_i}(t_{T_1})\right|}\left(\frac{\partial\overline{R}^n(t_{T_1})}{\partial\overline{R}^n(t_R)}\right) \qquad (5.9\text{-}14)^*$$

$$\frac{\partial\left(\rho^{\,n,i}_{TDRS_p}\right)_l(t_R-\Delta T)}{\partial\overline{R}^n(t_R-\Delta T)}=-\frac{\overline{R}_{TDRS_p}(t_{T_2}-\Delta T)-\overline{R}^n_{A_i}(t_{T_1}-\Delta T)}{\left|\overline{R}_{TDRS_{p,q}}(t_{T_2}-\Delta T)-\overline{R}^n_{A_i}(t_{T_1}-\Delta T)\right|}\left(\frac{\partial\overline{R}^n(t_{T_1}-\Delta T)}{\partial\overline{R}^n(t_R-\Delta T)}\right) \qquad (5.9\text{-}15)^*$$

Note that in the calculation of measurement partial derivative, the partial derivative $\frac{\partial\overline{R}^n(t_{T_1})}{\partial\overline{R}^n(t_R)}$ will be small and likely can be ignored. The matrix of partial derivative of position in Equations (5.9.4-9) through (5.9.4-12) are relative to the components of the state transition matrix as defined previously in Equations (5.9-31) through (5.9-35) in Section 5.9.2.

5.10 X-Ray Pulsar Navigation Measurement Models

X-ray observations of celestial sources can provide useful navigation information for spacecraft in a range of applications from Low-Earth Orbit (LEO) to interplanetary and even interstellar space. X-ray emitting pulsars, which are neutron stars whose X-ray emission is modulated at the rotational period of the star, are a source of such information. A subset of pulsars, the millisecond pulsars, are highly stable clocks, with long-term stability comparable to laboratory atomic clocks. The X-ray navigation (XNAV) concept implemented in GEONS uses X-ray observations of such pulsars. For these pulsars, a physical model with a handful of parameters can predict the arrival time of pulses to microsecond accuracy over months or years. A measurement of the difference between the measured arrival time of a pulse at a spacecraft and the predicted arrival time according to an onboard navigation solution can provide an error signal that can be used to measure the location of the spacecraft in a manner similar to GPS.

X-ray pulsar measurement models were implemented in GEONS to support the Station Explorer for X-ray Timing and Navigation Technology (SEXTANT) technology demonstration on the Neutron-star Interior Composition Explorer (NICER) mission. References 60 and 61 provide additional details about the implementation of the X-ray pulsar measurement models and associated simulation structure for the SEXTANT demonstration.

The general form of the pulsar measurement model is as follows:

$$Y_k = G\ [\bar{X}(t_k),\ t_k] + \varepsilon \tag{5.10-1}$$

where t_k is the true measurement time, referenced to UTC, and ε is the measurement error. It is assumed that ε has a zero-mean Gaussian distribution with standard deviation σ, which is commandable for each measurement type. The measurement standard deviation is typically determined through analysis of the random component of the measurement error as part of the filter tuning process.

When GEONS processes the x-ray pulsar navigation measurements, the estimation state vector, $\overline{X}(t)$ includes the receiver position vector, $\overline{R}$; velocity vector, $\dot{\overline{R}}$; receiver time bias, b_R; and receiver time bias rate, d_R, per pulsar phase bias, $\delta\varphi$, and corrections to the drag and solar radiation pressure coefficients, ΔC_D and ΔC_R; for one or more spacecraft.

Section 5.10.1 addresses preprocessing of the raw measurements. The x-ray pulsar measurement and partial derivative models are presented in Section 5.10.2.

5.10.1 X-Ray Pulsar Navigation Measurement Preprocessing

The key measurable for an XNAV detector are the pulse arrival times determined from a set of detected X-ray photons. For the SEXTANT demonstration, preprocessing consists of collecting photon events, identifying the source pulsar, and buffering photon events from the X-ray Timing Instrument until a target accumulated observation time from a single pulsar is met. The photon events are then batch processed using a Maximum Likelihood (ML) estimation algorithm to produce single pulsar phase and frequency measurements. A detailed description of the associated algorithms is provided in Sections 3 and 7 of the SEXTANT ADD (REF 73).

5.10.2 X-Ray Pulsar Navigation Measurement Model and Associated Partial Derivatives

This section provides the algorithms used to model the observed X-ray pulsar phase and frequency measurements. A pulsar almanac, which consists of a list of pulsars, with their associated timing models, X-ray light-curve templates, count rate estimates, and energy distributions, and associated raw data, is maintained in the ground system. The SEXTANT ground system relies on the Tempo2 pulsar timing software for the generation of timing models by fitting parameterized models to measured radio and X-ray pulse time-of-arrival data and for generating the piecewise polynomial approximations to the full timing models that are used for efficient onboard processing.

The pulsar pulse phase observed at the detector on the spacecraft at time t_k, $\phi(t_k)$, is modeled as

$$\varphi(t_k) = \varphi_{REF}\left(t_A\right) + \delta\varphi \tag{5.10-2}*$$

where $\phi_{REF}(t_A)$ is the phase evolution at a hypothetical reference observatory, t_A is the arrival time of the pulse wavefront at a hypothetical reference observatory, and $\delta\varphi$ is a constant per pulsar phase bias. The delayed arrival time at the reference observatory is given by

$$t_A = t_k - \frac{b_R(t)}{c} + \tau(t_k) \tag{5.10-3}*$$

where t_k is the arrival time of the pulse wavefront at the spacecraft detector, b_R is the receiver time bias, and $\tau(t)$ is the light propagation time of the pulse wavefront moving from the detector to the reference observatory.

For a geocentric reference observatory, the model for the light propagation time from the detector to the reference observatory is the first order approximation

$$\tau(t_k) \cong \frac{\hat{n} \cdot \overline{R}(t_k - \frac{b_R(t)}{c})}{c} \tag{5.10-4}*$$

where $\hat{n}$ is the pulsar direction unit vector and $\overline{R}$ is the spacecraft position in a coordinate frame centered at the reference observatory. For the geocentric reference observatory, GEONS evaluates the phase model, as referenced to Universal Coordinated Time (UTC), at the reference observatory and accounts for the Romer, or geometric, delay. In this case, the relative parallax and solar system Shapiro delays, etc., are negligible.

For a SSB reference observatory, additional terms are needed to meet high accuracy timing requirements. These terms include timing parallax, orbital parallax, Shapiro delays due to Sun and planets, which are discussed in References 60 and 61. For the SSB reference observatory, GEONS transforms the spacecraft state to barycentric coordinates and time and evaluates the phase model, as referenced to barycentric time, accounting for parallax, Romer delay, and Solar Shapiro delay.

The frequency measurement model is determined by differentiating Eq. (5.10-2), with respect to time leading to

$$f(t_k) = \dot{\varphi}(t_k) = \dot{\varphi}_{REF}\left(t_A\right)\left[1 - \frac{d_R(t)}{c} + \frac{\hat{n}\cdot\dot{\bar{R}}(t_k)}{c}\right] \tag{5.10-5}*$$

The SEXTANT flight software relies on the pulsar timing software TEMPO2 (REF 73) to provide a model for phase evolution at a hypothetical reference observatory. TEMPO2 models are least-squares fits to radio observatory data of the form

$$\phi_{REF}(t) = p\big(t - \Delta(t)\big) \tag{5.10-6}*$$

where p is a quadratic or cubic polynomial shifted by timing correction $\Delta(t)$ that includes terms for Romer, Einstein, and Shapiro, and binary delays. TEMPO2 also provides piecewise polynomial approximations to the full timing model $\varphi_{REF}(t)$, which are used by the SEXTANT flight software to compute the phase and frequency at the arrival time at the reference observatory:

$$\phi_{REF}(t_A) = \phi_{REF}(t_0) + \dot{\phi}_{REF}(t_0)\left[t_A - t_0\right] + \ddot{\phi}_{REF}(t_0)\frac{\left[t_A - t_0\right]^2}{2} \tag{5.10-7}*$$

$$\dot{\phi}_{REF}(t_A) = \dot{\phi}_{REF}(t_0) + \ddot{\phi}_{REF}(t_0)\left[t_A - t_0\right] \tag{5.10-8}*$$

$$\ddot{\phi}_{REF}(t_A) = \ddot{\phi}_{REF}(t_0) \tag{5.10-9}*$$

The following are the nonzero partial derivatives of the X-ray pulse measurements with respect to the estimation state vector, $\bar{X}(t_k)$, consisting of absolute state vector for all satellites and the constant phase bias:

$$\frac{\partial\phi^n(t_k)}{\partial\bar{R}^n(t_k)} = \frac{\partial\phi^n_{REF}(t_A)}{\partial\tau^n(t_k)}\frac{\partial\tau^n(t_k)}{\partial\bar{R}^n(t_k)} = \dot{\phi}^n_{REF}\left(t_A\right)\left[\frac{\hat{n}^T}{c}\right] \tag{5.10-10}*$$

$$\frac{\partial\varphi^n(t_k)}{\partial b^n_R(t_k)} = -\frac{\dot{\varphi}^n_{REF}\left(t_A\right)}{c} \tag{5.10-11}*$$

$$\frac{\partial\varphi^n(t_k)}{\partial\delta\varphi} = 1 \tag{5.10-12}*$$

$$\frac{\partial f^n(t_k)}{\partial\bar{R}^n(t_k)} = \frac{\partial\dot{\varphi}^n_{REF}(t_A)}{\partial\tau^n(t_k)}\frac{\partial\tau^n(t_k)}{\partial\bar{R}^n(t_k)} = \ddot{\varphi}^n_{REF}\left(t_A\right)\left[\frac{\hat{n}^T}{c}\right]\left[1 - \frac{d^n_R(t_k)}{c} + \frac{\hat{n}\cdot\dot{\bar{R}}^n(t_k)}{c}\right] \tag{5.10-13}*$$

$$\frac{\partial f^n(t_k)}{\partial\dot{\bar{R}}^n(t_k)} = \frac{\partial\dot{\phi}^n_{REF}(t_A)}{\partial\tau^n(t_k)}\frac{\partial\tau^n(t_k)}{\partial\dot{\bar{R}}^n(t_k)} = \dot{\phi}^n_{REF}\left(t_A\right)\left[\frac{\hat{n}^T}{c}\right] \tag{5.10-14}*$$

$$\frac{\partial f^n(t_k)}{\partial b_R^n(t_k)} = -\frac{\ddot{\varphi}_{REF}^n\left(t_A\right)}{c}\left[1 - \frac{d_R^n(t_k)}{c} + \frac{\hat{n}\cdot\dot{\bar{R}}^n(t_k)}{c}\right] \qquad (5.10\text{-}15)^*$$

$$\frac{\partial f^n(t_k)}{\partial d_R^n(t_k)} = -\frac{\dot{\varphi}_{REF}^n\left(t_A\right)}{c} \qquad (5.10\text{-}16)^*$$

5.11 Two-Leg GPS Pseudorange Measurement Model

This section provides the computational algorithms for one-way range measurements transmitted by a GPS SV, received and retransmitted by a relay satellite, and received by a ground station. These measurements are referred to as "Two-Leg GPS" pseudorange measurements in GEONS. The general form of the measurement model is as follows:

$$Y_k = G\ [\bar{X}(t_k),\ t_k] + \varepsilon \tag{5.11-1}$$

where t_k is the true measurement time, referenced to UTC, and ε is the measurement error. It is assumed that ε has a zero-mean Gaussian distribution with standard deviation σ, which is commandable for each measurement type. The measurement standard deviation is typically determined through analysis of the random component of the measurement error as part of the filter tuning process.

For GEONS, the associated estimation state vector, $\overline{X}(t)$ includes the receiver position vector, $\overline{R}$; velocity vector, $\dot{\overline{R}}$; optional corrections to the drag and solar radiation pressure coefficients, ΔC_D and ΔC_R; receiver time bias, b_R; and receiver time bias rate, d_R, for one or more receivers. There are no two-leg GPS measurement bias parameters in the estimation state vector.

Note that the timetag for the two-leg GPS pseudorange should be the signal reception time measured at the GS. However, in the current implementation of the two-leg GPS pseudorange measurement model, the timetag associated with the k^{th} measurement is the UTC receive time of the signal at the local receiver as measured with respect to the spacecraft/receiver clock, $t_R^{(RC)}$. This is a simplification made for a preliminary implementation to evaluate expected performance.

Assuming that the forward-link L-band signal is transmitted from GPS SV j at time t_T , received at the local receiver n at time t_k, retransmitted with delay Δt_{2G} due to signal processing on the relay satellite, and received at GS m at time t_{GS} with delay Δt_{GS}, the two-leg GPS pseudorange is modeled as follows:

$$\begin{aligned}\Re^n_{2G_{j,m}}(t_k) = c\cdot(t_{GS} - t_T) = \rho^{n,i}_{GS_m}(t_k) + \rho^{n,i}_{G/W_j}(t_k) + b_R{}^n(t_k) - d_R{}^n(t_k)\Delta t^n_R \\ + \delta\rho_{atm}(t_T) + c\left(\Delta t_{2G} + \Delta t_{GS_m}\right) - c\left(\delta t_{S_j} + \delta t^{SF}_{S_j}\right)\end{aligned} \tag{5.11-2}*$$

$$\rho^{n,i}_{GS_m}(t_k) = \left|\overline{R}_{GS_m}(t_{GS}) - \overline{R}^n_{A_i}(t_k)\right| \tag{5.11-3}*$$

$$\rho^{n,i}_{G/W_j}(t_k) = \left|\overline{R}_{A_i}{}^n(t_k) - \overline{R}_{G/W_j}(t_T)\right| \tag{5.11-4}*$$

In the above equations, the subscript j indicates the j^{th} GPS SV and the subscript m indicates the m^{th} GS. The timetag of the k^{th} measurement, t_k, is equal to the value of the receive time, $t_R^{(RC)}$ at the local receiver. In the presence of a spacecraft timing bias, the true receive time on the relay satellite is given by

$$t_k = t_R^{(RC)} - \delta t_R \tag{5.11-5}$$

where δt_R is the offset of the receiver's timing reference from UTC, given by

$$\delta t_R = \frac{b_R(t_k)}{c}$$

$\rho_{GS_m}^{n,i}(t_k)$ is the distance traversed by the signal from antenna *i* on the relay satellite to GS *m* where

$\overline{R}_{GS_m}(t_{GS})$ = position of the receiving GS *m* at time t_{GS}. The position vector of the transmitting GS is transformed from ECEF coordinates to J2000.0 inertial coordinates at the time t_{GS} using the transformations defined in Sections 3.2.1 through 3.2.3.

$\overline{R}_{A_i}^{n}(t_k)$ = position of the *i*th receiving antenna on relay satellite *n* at time t_k, which is computed using Equation 3.2-61 in Section 3.2.8.

In the current preliminary implementation, this signal receive time on the relay satellite is assumed to be known; however, actual two-leg GPS measurements would be timetagged with the time of reception at the ground station and the time of signal transmission from the relay would be computed using the Newton Raphson iterative scheme defined for the spacecraft-to-GS segment in Section 5.6.4.

$\rho_{G/W_j}^{n,i}$ denotes the distance between the position of the j^{th} GPS SV at the signal transmit time t_T and the position of receiver *n*'s i^{th} antenna at the signal receive time t_k where

$\overline{R}_{G/W_j}(t_T)$ = position of the the transmitting GPS SV *j* at the transmission time t_T, which is computed based on t_k using the Newton-Raphson iterative scheme defined in Section 5.3.3.

The receiver clock bias $b_R{}^n(t)$ is computed using the estimated parameters $b_R{}^n(t_k)$ and $\dot{b}_R{}^n(t_k)$, as defined in Equation 4.3-14a and 4.3-14 of Section 4.3.

The atmospheric delay, $\delta\rho_{atm}(t_T)$, is not currently implemented. The last two terms on the right-hand side of Equation (5.11-3) represent the total SV time correction, which is computed using Equations 3.3-10 or 3.3-11 (for single and dual frequency GPS users) and Equation 3.3-12 (only for single frequency GPS users) in Section 3.3.2 evaluated at the signal transmit time t_T.

Note that the linearization correction to account for the offset of the true UTC receive time from the UTC filter state epoch, e.g. see Equation 5.3-19b and 5.3-19c, is not implemented for the two-leg GPS measurements.

The matrix (a row vector in this case) of partial derivatives of the pseudorange measurement with respect to the estimation state vector, $\overline{X}(t_k)$, is defined as follows:

$$\left[H(t_k)\right]_{\Re_{G/W_j}^n} \equiv \frac{\partial \Re_{2G_{j,m}}^n(t_k)}{\partial \overline{X}(t_k)} \tag{5.11-6}$$

The partial derivatives with respect to those parameters that are not explicitly included in the pseudorange measurement equation will be zeros. The following are the only nonzero elements if the state vector consists of absolute states for both the local and remote satellites:

$$\frac{\partial \Re^{n}_{2G_{j,m}}(t_k)}{\partial \overline{R}^{n}(t_k)} = \frac{\partial \rho^{n,i}_{G/W_j}(t_k)}{\partial \overline{R}^{n}(t_k)} + \frac{\partial \rho^{n,i}_{GS_{mj}}(t_k)}{\partial \overline{R}^{n}(t_k)} \tag{5.11-7}*$$

$$\frac{\partial \Re^{n}_{2G_{j,m}}(t_k)}{\partial b_R{}^{n}(t_k)} = 1 - \frac{d_R{}^{n}(t_k)}{c} \tag{5.11-8}*$$

$$\frac{\partial \Re^{n}_{2G_{j,m}}(t_k)}{\partial d_R{}^{n}(t_k)} = -\Delta t^{n}_{R} \tag{5.11-9}*$$

where

$$\frac{\partial \rho^{n,i}_{G/W_j}(t_k)}{\partial \overline{R}^{n}(t_k)} = \left[\frac{\overline{R}_{A_i}{}^{n}(t_k) - \overline{R}_{G/W_j}(t_T)}{\rho^{n,i}_{G/W_j}(t_k)} \right]^{T} \tag{5.11-10}*$$

$$\frac{\partial \rho^{n,i}_{GS_m}(t_k)}{\partial \overline{R}^{n}(t_k)} = \left[\frac{\overline{R}_{GS_m}(t_{GS}) - \overline{R}_{A_i}{}^{n}(t_k)}{\rho^{n,i}_{GS_m}(t_k)} \right]^{T} \tag{5.11-11}*$$

The superscript T on the right-hand sides of Equations (5.3-28b) through (5.3-28d) denote the transpose, indicating that these partial derivatives are given as row vectors.

Section 6. Real-Time State Propagation

The GEONS real-time state propagation function takes the near-real-time output of the GEONS filter and propagates it forward to a requested time. Figure 6-1 illustrates the relationship between the GEONS filter and real-time prediction processes for a filter execution frequency of 10 seconds.

Section 6.1 defines the algorithm used to propagate the user position and velocity filter estimates to real-time. Section 6.2 provides the simplified acceleration model used in the real-time propagation.

6.1 Real-Time Propagation Algorithm

The real-time propagation algorithm is defined as follows:

Sequence: Shown in Table 6-1 for a filter execution frequency of 10 seconds

Integrator: 4th-order Runge-Kutta defined in Section 4.2

Accelerations included: Central body point mass and Earth J_2 zonal harmonic when the central body is the Earth

where

$\bar{R}_C$ and $\dot{\bar{R}}_C$ = user position and velocity vector in the central-body mean of J2000.0 coordinate frame

$\bar{R}_C$ and $\dot{\bar{R}}_C$ = real-time user position and velocity vectors in the central-body mean of J2000.0 coordinate frame

6.2 Real-Time Propagation Acceleration Model

For real-time propagation, the spacecraft acceleration, $\bar{a}$, includes the following components:

- Gravitational acceleration (point-mass contribution) due to the central-body mass ($\overline{a_C}$)
- Gravitational acceleration due to the oblateness of the Earth's gravitational potential, if the Earth is the central body ($\bar{a}_{J_2}$)

The acceleration, $\bar{a}$, is expressed in terms of these components as

$$\bar{a} = \begin{cases} \bar{a}_E + \bar{a}_{J_2}; & \text{central body} = \text{Earth} \\ \bar{a}_C; & \text{central body} \neq \text{Earth} \end{cases} \qquad (6.2\text{-}1)^*$$

The central body point mass acceleration is computed as follows

$$\bar{a}_C = -\frac{\mu_C \bar{R}_C}{R_C^{\,3}} \qquad (6.2\text{-}2)^*$$

where

μ_C = gravitational constant of the central body

Section 4.1.2 of this document discusses the computation of the complete nonspherical gravitational acceleration. The acceleration due to the oblateness of the Earth's gravitational potential is obtained by including only the effects due to the $\widetilde{C}_2^0$ term in the computation. In this case, the TOD components of the acceleration vector, defined in Equations (4.1-55) through (4.1-57), reduce to the following:

$$\ddot{x}_{NS} = \left(\frac{1}{r} \frac{\partial \psi_{J_2}}{\partial r} - \frac{z}{r^2 \sqrt{x^2 + y^2}} \frac{\partial \psi_{J_2}}{\partial \phi} \right) x \tag{6.2-3}*$$

$$\ddot{y}_{NS} = \left(\frac{1}{r} \frac{\partial \psi_{J_2}}{\partial r} - \frac{z}{r^2 \sqrt{x^2 + y^2}} \frac{\partial \psi_{J_2}}{\partial \phi} \right) y \tag{6.2-4}*$$

$$\ddot{z}_{NS} = \left(\frac{1}{r} \frac{\partial \psi_{J_2}}{\partial r} \right) z + \frac{\sqrt{x^2 + y^2}}{r^2} \frac{\partial \psi_{J_2}}{\partial \phi} \tag{6.2-5}*$$

The partial derivatives of the oblateness portion of the Earth's potential with respect to r and ϕ are given by

$$\frac{\partial \psi_{J_2}}{\partial r} = -\frac{3}{2} \frac{\mu_E}{r^2} \left(\frac{R_e}{r} \right)^2 C_2^0 \left[3 \sin^2 \phi - 1 \right] \tag{6.2-6}*$$

$$\frac{\partial \psi_{J_2}}{\partial \phi} = 3 \frac{\mu_E}{r} \left(\frac{R_e}{r} \right)^2 C_2^0 \cos \phi \sin \phi \tag{6.2-7}*$$

where

$$\sin \phi = \frac{z}{r} \tag{6.2-8}*$$

$$\cos \phi = \frac{\sqrt{x^2 + y^2}}{r} \tag{6.2-9}*$$

The TOD components of the Earth's J2 acceleration are then transformed to the mean of J2000.0 reference frame using Equation (4.1-39).

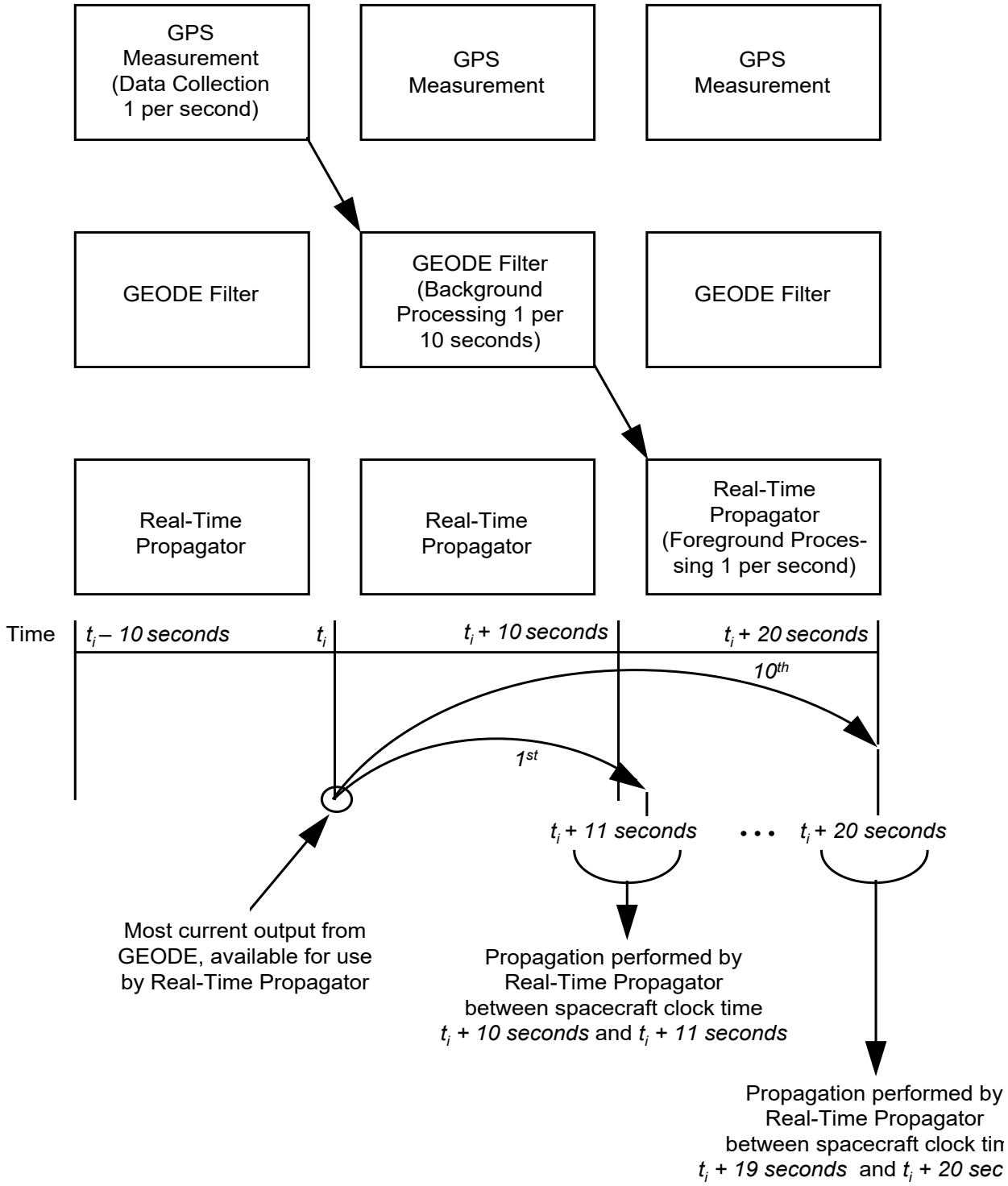

Figure 6-1. GEONS Real-Time Interface Sequence

Table 6-1. Real-Time State Propagation Sequence

Current Spacecraft Time	Action	System Component*
t_i	GPS measurement	GPS Receiver
t_i + 1 second to t_i + 10 seconds	Propagate: $\overline{R}_{i-1}(+)$ to $\overline{R}_i(-)$ $\dot{\overline{R}}_{i-1}(+)$ to $\dot{\overline{R}}_i(-)$ If GPS measurement is selected, process measurement and update state: $\overline{R}_i(-) \rightarrow \overline{R}_i(+)$ $\dot{\overline{R}}_i(-) \rightarrow \dot{\overline{R}}_i(+)$	GEONS Filter
t_i + 10 seconds to t_i + 11 seconds	Propagate: $\overline{R}_i(+)$ to $\widetilde{R}(t_i + 11 \text{ seconds})$ $\dot{\overline{R}}_i(+)$ to $\dot{\widetilde{R}}(t_i + 11 \text{ seconds})$	GEONS Real-Time State Propagator
t_i + 11 seconds to t_i + 12 seconds	Propagate: $\widetilde{R}(t_i + 11 \text{ seconds})$ to $\widetilde{R}(t_i + 12 \text{ seconds})$ $\dot{\widetilde{R}}(t_i + 11 \text{ seconds})$ to $\dot{\widetilde{R}}(t_i + 12 \text{ seconds})$	GEONS Real-Time State Propagator
• • •	• • •	GEONS Real-Time State Propagator
t_i + 19 seconds to t_i + 20 seconds	Propagate: $\widetilde{R}(t_i + 19 \text{ seconds})$ to $\widetilde{R}(t_i + 20 \text{ seconds})$ $\dot{\widetilde{R}}(t_i + 19 \text{ seconds})$ to $\dot{\widetilde{R}}(t_i + 20 \text{ seconds})$	GEONS Real-Time State Propagator

*For illustration purposes, the GEONS Filter sequence shows only position and velocity vector propagation and update; it does not show the propagation and update of other state vector elements and the state error covariance matrix.

Section 7. Doppler Compensation Prediction

This section provides the algorithms used in computing the predicted Doppler shift and creating the associated frequency control word (FCW).

Onboard Doppler Compensation (OBDC) involves calculating the predicted frequency shift of the forward-link GS or TDRSS signal due to user spacecraft dynamics. By offsetting the receiver's center frequency appropriately, the Doppler shift due to user spacecraft dynamics can be compensated to assist user acquisition of the GS or TDRSS signal. Assuming fixed radiated carrier frequency (RCF) operation, OBDC can be performed autonomously by the user spacecraft.

GEONS computes FCWs for all GSs or TDRSs visible to the spacecraft at the next real-time state output time, nominally as part of the real-time state prediction function, which is typically executed every 1.0 or 1.024 seconds. GEONS outputs these FCWs ordered in terms of increasing GS/TDRS-to-satellite range. Selection of the FCW to send to the receiver would be performed by a receiver control function in the spacecraft primary computer. If FCWs are needed at a higher rate than every 1.0 or 1.024 seconds for the receiver to achieve carrier lock, the spacecraft's receiver control function could use a linear interpolator to compute intermediate values. Section 7.1 discusses the algorithm used to identify the visible GSs. Sections 7.2 and 7.3 present the algorithms used to compute the GS and TDRSS FCWs, respectively.

7.1 GS Visibility Test

GEONS identifies which GS(s) are visible at time t using the following procedure.

The instantaneous line-of-sight vector from the satellite to each GS in the GEONS GS catalog is computed as follows:

$$\bar{\rho}^{i} = \bar{R}(t) - \bar{R}^{i}_{GS}(t) \qquad (7.1\text{-}1)^{*}$$

where

$\bar{R}(t)$ = position vector of the satellite at time t, referenced to the Mean of J2000. inertial reference frame

$\bar{R}^{i}_{GS}(t)$ = position of the i^{th} GS at time t, referenced to the Mean of J2000. inertial reference frame

The position vectors for each GS are available in ECEF coordinates. The GS position vector is transformed from the ECEF frame to the J2000.0 reference frame using the transformations defined in Sections 3.2.1 through 3.2.3.

Visibility is determined based on whether the elevation angle, E, of the line-of-sight vector with respect to the local horizon is greater than a minimum elevation angle, $E_{\min_{vis}}$. Figure 7-1 illustrates a visible (A) and not visible (B) case. The GS is visible if the following is true:

$$\sin E > \sin E_{\min_{vis}} \tag{7.1-2}*$$

where $E_{\min_{vis}}$ is a commandable minimum elevation angle within the 0 to +90 degrees range, $E_{\min_{vis}}$ and E are positive above the local horizon and negative below the horizon, and

$$\sin E = \frac{\overline{\rho}^{i} \cdot \overline{R}^{i}_{GS}(t)}{\left|\overline{\rho}^{i}\right|\left|\overline{R}^{i}_{GS}(t)\right|} \tag{7.1-3}*$$

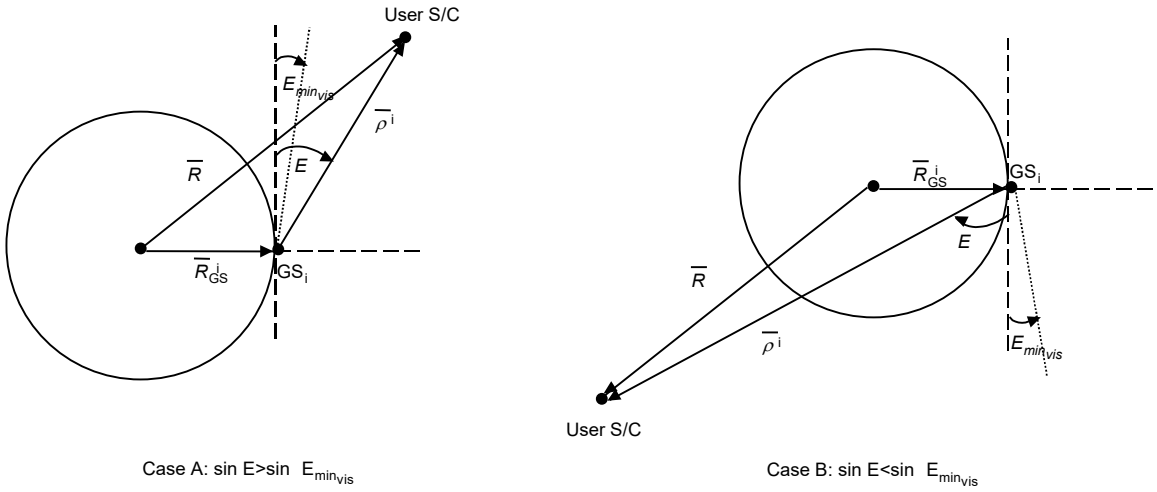

Figure 7-1. Line-of-Sight Visibility Cases

7.2 GS FCW Computation

FCWs are computed for all GSs that pass the visibility test defined in Section 7.1. If no GS passes the visibility test, a zero FCW is output.

The following algorithm is used to compute the predicted instantaneous frequency offset of the GS's Doppler-shifted RCF with respect to the receiver's frequency reference:

$$f_D(t) = \left[1 - \frac{\left[\dot{\overline{R}} - \dot{\overline{R}}_{GS}\right] \cdot \left[\overline{R} - \overline{R}_{GS}\right]}{c\left|\overline{R} - \overline{R}_{GS}\right|}\right] f_{RCF} - f_{ref}(t) \tag{7.2-1}*$$

where

$f_D(t)$ = predicted frequency shift at time t in Hertz

$\overline{R}$ = satellite position vector at time t

$\dot{\overline{R}}$ = satellite velocity vector at time t

$\overline{R}_{GS}$ = ground station position vector at time t

$\dot{\overline{R}}_{GS}$ = ground station velocity vector at time t

c = speed of light

f_{RCF} = GS radiated carrier frequency in Hertz (a commanded parameter nominally equal to 2106406250 Hertz)

$f_{ref}(t)$ = Doppler frequency reference at time t [defined in Equation (5.6-20)]

The formula for computing the frequency control words is then given by

$$FCW = \frac{f_D(t)}{f_{res}} \qquad (7.2\text{-}2)^*$$

where

f_{res} = frequency resolution of the receiver FCW in hertz per bit (a commanded parameter)

For input the receiver, the interface driver must convert the FCW to the appropriate serial command format.

The receiver uses the FCW to adjust its receive frequency. The receiver frequency will be offset by this FCW according to the following equation:

$$f_{out} = F_{CF} + (FCW \times f_{res}) = F_{CF} + f_D(t) \qquad (7.2\text{-}3)$$

where

f_{out} = receiver output frequency

F_{CF} = receiver's assigned center frequency, nominally equal to 2106.406250 megahertz

f_{res} = frequency resolution of the receiver FCW, in Hertz per bit

GEONS outputs these FCWs and the associated GS identifiers ordered in terms of increasing GS-to-satellite range, $\left|\overline{\rho}^i\right|$, where the line-of-sight vector $\overline{\rho}^i$ is defined by Equation (7.1-1).

7.3 TDRSS FCW Computation

FCWs are computed for all TDRSs that pass the visibility test defined in Section 7.4. If no TDRS passes the visibility test, a zero FCW is output.

The following algorithm is used to compute the predicted instantaneous frequency offset of the TDRS's Doppler-shifted RCF with respect to the receiver's frequency reference:

$$f_D(t) = f_{RCF}\left[1 - \frac{\left[\dot{\overline{R}}^i - \dot{\overline{R}}_{TDRS_j}\right]\cdot\left[\overline{R}^i - \overline{R}_{TDRS_j}\right]}{\left|\overline{R}^i - \overline{R}_{TDRS_j}\right|c} + \frac{\left[\dot{\overline{R}}_{TDRS_j} - \dot{\overline{R}}_{TGT_j}\right]\cdot\left[\overline{R}_{TDRS_j} - \overline{R}_{TGT_j}\right]}{\left|\overline{R}_{TDRS_j} - \overline{R}_{TGT_j}\right|c}\right] - f_{ref}(t) \quad (7.3\text{-}1)^*$$

where

$f_D(t)$ = predicted frequency shift at time t in Hertz

$\overline{R}^i$ = receiving satellite i position vector at time t

$\dot{\overline{R}}^i$ = receiving satellite i velocity vector at time t

$\overline{R}_{TDRS_j}$ = TDRS j position vector at time t

$\dot{\overline{R}}_{TDRS_j}$ = TDRS j velocity vector at time t

$\overline{R}_{TGT_j}$ = position vector of TGT ground antenna associated with TDRS j at time t

$\dot{\overline{R}}_{TGT_j}$ = velocity vector of TGT ground antenna associated with TDRS j at time t

c = speed of light (meters per second)

f_{RCF} = TDRS radiated carrier frequency in Hertz (a commanded parameter nominally equal to 2106406250 Hertz)

$f_{ref}(t)$ = Doppler frequency reference at time t in Hertz [defined in Equation (5.9-22)]

The formula for computing the frequency control words is then given by

$$FCW = \frac{f_D(t)}{f_{res}} \quad (7.3\text{-}2)^*$$

where

f_{res} = frequency resolution of the receiver FCW in hertz per bit (a commanded parameter)

For input the receiver, the interface driver must convert the FCW to the appropriate serial command format.

The receiver uses the FCW to adjust its receive frequency. The receiver frequency will be offset by this FCW according to the following equation:

$$f_{out} = F_{CF} + (FCW \times f_{res}) = F_{CF} + f_D(t) \tag{7.3-3}$$

where

f_{out} = receiver output frequency

F_{CF} = receiver's assigned center frequency, nominally equal to 2106.406250 megahertz

f_{res} = frequency resolution of the receiver FCW, in Hertz per bit

GEONS outputs these FCWs and the associated TDRS identifiers ordered in terms of increasing TDRS-to-satellite range.

7.4 TDRS Visibility Test

GEONS identifies which TDRS(s) are visible at time t using the following procedure for each TDRS.

a. Verify that the TDRS is not occulted by the Earth. Compute the distance

$$d = |\bar{d}| = \left| \bar{R}_{TDRS_j} - \frac{\bar{x}\left(\bar{x} \cdot \bar{R}_{TDRS_j}\right)}{x^2} \right| \tag{7.4-1}*$$

where

$$\bar{x} = \bar{R} - \bar{R}_{TDRS_j} \tag{7.4-2}*$$

and

$\bar{R}_{TDRS_j}$ = TDRS j position vector at the measurement time

$\bar{R}$ = receiver position vector at the measurement time

x = magnitude of $\bar{x}$

The TDRS is not occulted if $d \geq R_e$ [case (a) in Figure 7-2], where R_e equals the mean equatorial radius of the Earth.

If $d < R_e$ [case (b) in Figure 7-2], compute

$$\delta = x' - \sqrt{(R_e)^2 - d^2} \tag{7.4-3}*$$

where

.

$$x' = \left| \frac{\bar{x} \cdot \bar{R}_{TDRS_j}}{x} \right| \qquad (7.4\text{-}4)^*$$

If $x \leq \delta$, the TDRS is not occulted. Otherwise, the TDRS is not visible.

b. Verify that the signal path is within the TDRS antenna field of view. For each TDRS, compute the angle

$$\beta = \cos^{-1}\left(\frac{\bar{x}}{x} \cdot \frac{\bar{R}_{TDRS_j}}{R_{TDRS_j}} \right) \qquad (7.4\text{-}2)^*$$

If $\beta \leq \beta_{max}$, the TDRS is visible, where β_{max} is a commandable parameter. For multiple access users, the field of view is ±13 degrees with respect to the nadir vector. For single-access users, the field of view is ±22.5 degrees East-West and ±31 degrees North-South.

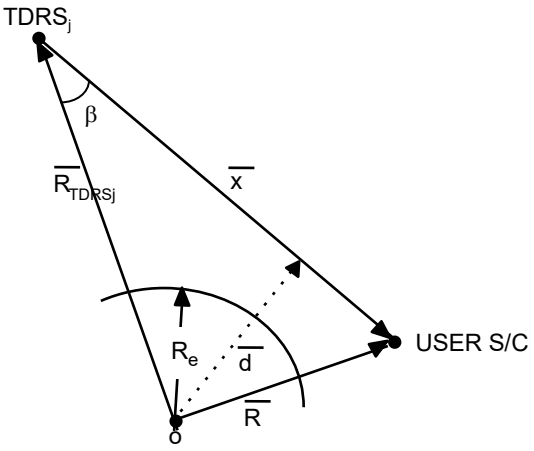

a. $d \geq R_e$

RAY PATH IS ABOVE
THE EARTH

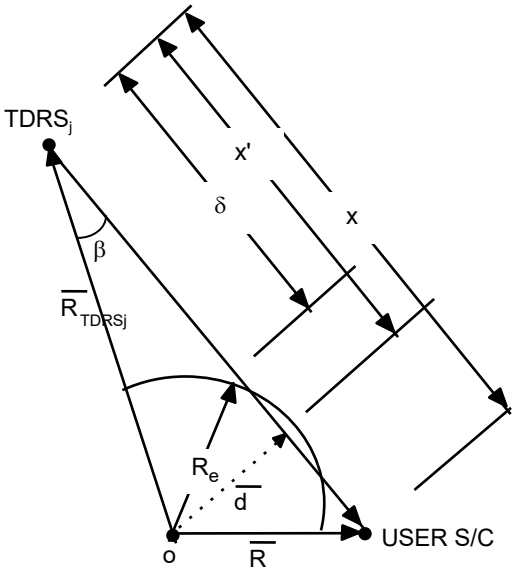

b. $d < R_e$

RAY PATH PASSES THROUGH
THE EARTH

Figure 7-2. TDRS Visibility

Section 8. Averaged Orbital Element Ephemeris

As part of the GEONS fault detection process, the difference between the estimated state vector and a comparison state vector is computed and tested against a commanded tolerance to detect degradation in GEONS performance prior to filter divergence. In addition, this comparison state vector can be used for (re)initialization of the GEONS state estimation process. This section provides an averaged ephemeris method that can be used to provide a comparison state vector if another source (e.g. GPS point solutions) is not available.

Section 8.1 describes the overall procedure for computing the averaged state vector. The algorithm for computing the reference averaged equinoctial elements and equinoctial element rates is given in Section 8.2. The transformations between equinoctial elements and spacecraft position and velocity are defined in Section 8.3.

8.1 Computation of the Averaged State Vector

The averaged state vector is computed using a set of reference averaged equinoctial elements and equinoctial element rates. The reference averaged equinoctial elements and equinoctial element rates can be computed using state vectors from two orbital periods previous to the current period, as presented in Section 8.2. Alternatively, reference averaged equinoctial elements and equinoctial element rates could be uplinked to the spacecraft. The equinoctial system, defined is Section 8.3.1, was selected because all of its elements are slowly varying for any orbital eccentricity and inclination.

The averaged state vector at the request time, t_c, is computed as follows

a. Compute the averaged equinoctial elements at the request time, t_c, as follows

$$\overline{\overline{E}(t_c)} = \overline{\overline{E}_{ref}^{-2}} + \overline{\dot{\overline{E}}_{ref}^{-2}}\ \Delta t \qquad (8.1\text{-}1)^*$$

where

$\overline{\overline{E}(t_c)}$ = vector of averaged equinoctial elements $(\bar{a}, \bar{h}, \bar{k}, \bar{p}, \bar{q}, \bar{\lambda})$ evaluated at the request time t_c

$\overline{\overline{E}_{ref}^{-2}}$ = vector of reference averaged equinoctial elements associated with the reference time t_{ref}^{-2}

$\overline{\dot{\overline{E}}_{ref}^{-2}}$ = vector of reference averaged equinoctial element rates associated with the reference time t_{ref}^{-2}

t_{ref}^{-2} = reference time for the reference averaged equinoctial elements computed over the next-to-last orbital period

Δt = $t_c - t_{ref}^{-2}$

b. Compute the averaged state vector by converting the averaged equinoctial elements at the request time to position and velocity using the transformation provided in Section 8.3.2.

8.2 Computation of Reference Averaged Equinoctial Elements and Rates

Reference averaged equinoctial elements are computed over each successive spacecraft orbital period as follows:

$$\overline{(E_i)^0_{ref}} = \frac{1}{N+1}\sum_{n=0}^{N} E_i(t_0 + n\delta t),\ \ i = 1, 5$$
$$\overline{(E_6)^0_{ref}} = \lambda(t_{ref}) \qquad (8.2\text{-}1)^*$$

where

$\overline{\overline{E}^0_{ref}}$ = reference averaged equinoctial element vector $(\bar{a}, \bar{h}, \bar{k}, \bar{p}, \bar{q}, \bar{\lambda})$ associated with the current reference time t_{ref}

t_{ref} = reference time for new set of reference averaged equinoctial elements, equal to the center of the averaging interval

t_0 = time of the first point in the current summation interval

$E_i(t)$ = component of osculating equinoctial element vector at time t obtained from the osculating position and velocity vectors $(\overline{R}(t), \dot{\overline{R}}(t))$ using the transformation given in Section 8.3.3

N = number of osculating equinoctial element sets included in the summation

δt = time interval between successive osculating equinoctial elements included in the summation, a commanded parameter typically 1.0 or 1.024 seconds

The value of N is chosen so that the average is performed over one spacecraft orbital period, *P*, to within <1.024 seconds:

$$N = 2\left(\text{int}\left[\frac{P + \delta t}{2\,\delta t}\right]\right) \qquad (8.2\text{-}2)^*$$

where

$$P = 2\pi\sqrt{\frac{(\overline{a_{ref}^{-1}})^3}{\mu_E}} \qquad (8.2\text{-}3)^*$$

and

μ_E = gravitational constant of the Earth

$\overline{a_{ref}^{-1}}$ = reference averaged semimajor axis associated with previous set of the reference averaged equinoctial elements

The averaged equinoctial element rates for the semimajor axis, a, and mean longitude, λ, are computed as follows using the averaged semimajor and mean longitude computed over the current and previous orbital periods

$$\begin{aligned}\overline{\dot{a}_{ref}^{0}} &= \frac{1}{t_{ref} - t_{ref}^{-1}}\left[\overline{a_{ref}^{0}} - \overline{a_{ref}^{-1}}\right] \\ \overline{\dot{\lambda}_{ref}^{0}} &= \frac{1}{t_{ref} - t_{ref}^{-1}}\left[\overline{\lambda_{ref}^{0}} - \overline{\lambda_{ref}^{-1}} + 2\pi\right]\end{aligned} \qquad (8.2\text{-}4)^*$$

The rates for the remaining reference averaged equinoctial elements are assumed to be zero.

To minimize the amount of data that must be stored onboard, the summation in Equation (8.2-1) is accumulated incrementally. Note that the algorithm must be restarted following a spacecraft maneuver. The algorithm is as follows:

For $n = 0$, first execution:

a. Set the initial value of t_0 equal to the current osculating state vector time tag

b. Convert the predicted osculating position and velocity at time t_0 to equinoctial elements using the transformation in Section 8.3.3, and initialize the summation for elements 1 through 5

$$SUM_i = E_i(t_0)$$

c. Compute N and t_{ref}

$$P = 2\pi\sqrt{\frac{a^3(t_0)}{\mu_E}}$$

$$N = 2\left(\text{int}\left[\frac{P + \delta t}{2\,\delta t}\right]\right)$$

$$t_{ref} = t_0 + \frac{N\delta t}{2}$$

For $0<n<N$:

Convert the predicted osculating position and velocity at time $t_0 + n\delta t$ to equinoctial elements and continue to accumulate the summation for elements 1 through 5:

$$SUM_i = SUM_i + E_i(t_0 + n\delta t)$$

For $n=N$:

a. Convert the predicted osculating position and velocity at time $t_0 + N\delta t$ to equinoctial elements

b. Complete the summation for elements 1 through 5

$$SUM_i = SUM_i + E_i(t_0 + N\delta t)$$

c. Compute the reference averaged equinoctial elements using Equation (8.2-1)

$$\overline{(E_i)^0_{ref}} = \frac{1}{N+1} SUM_i, \quad i = 1, 5$$
$$\overline{(E_6)^0_{ref}} = \lambda(t_{ref})$$

d. If this is the first time reference averaged equinoctial elements are computed, set

$$\overline{\dot{a}^0_{ref}} = 0$$
$$\overline{\dot{\lambda}^0_{ref}} = \frac{2\pi}{N\delta t}$$

Otherwise, compute the reference averaged equinoctial element rates using Equation (8.2-4):

$$\overline{\dot{a}^0_{ref}} = \frac{1}{t_{ref} - t^{-1}_{ref}} \left[\overline{a^0_{ref}} - \overline{a^{-1}_{ref}} \right]$$
$$\overline{\dot{\lambda}^0_{ref}} = \frac{1}{t_{ref} - t^{-1}_{ref}} \left[\overline{\lambda^0_{ref}} - \overline{\lambda^{-1}_{ref}} + 2\pi \right]$$

e. If this is not the first time that reference averaged equinoctial elements and equinoctial element rates have been computed, update the saved values for the reference averaged equinoctial elements and equinoctial element rates for the next-to-last orbital period

$$\overline{\overline{E}^{-1}_{ref}} \rightarrow \overline{\overline{E}^{-2}_{ref}}$$
$$\overline{\dot{\overline{E}}^{-1}_{ref}} \rightarrow \overline{\dot{\overline{E}}^{-2}_{ref}}$$
$$t^{-1}_{ref} \rightarrow t^{-2}_{ref}$$

Update the saved values for the reference averaged equinoctial elements and equinoctial element rates for the last orbital periods

$$\overline{\overline{E}_{ref}^{0}} \rightarrow \overline{\overline{E}_{ref}^{-1}}$$

$$\overline{\dot{\overline{E}}_{ref}^{0}} \rightarrow \overline{\dot{\overline{E}}_{ref}^{-1}}$$

$$t_{ref} \rightarrow t_{ref}^{-1}$$

f. Compute N for the next orbital period average using Equations (8.2-2) and (8.2-3),

$$P = 2\pi\sqrt{\frac{\overline{\overline{(a_{ref}^{-1})^3}}}{\mu_E}}$$

$$N = 2\left(\text{int}\left[\frac{P + \delta t}{2\,\delta t}\right]\right)$$

g. Update the value of t_{ref} for the next orbital period where t_0 is the first time point in the next averaging interval, equal to the last point in the last averaging interval

$$t_{ref} = t_0 + \frac{N\delta t}{2}$$

h. Initialize the summation for $n = 0$, $i = 1$ through 5 for the next orbital period average

$$SUM_i = E_i(t_0)$$

Note that only the current value of N and the reference averaged equinoctial elements and rates over the previous two orbital periods must be saved onboard.

8.3 Equinoctial Element Transformations

This section provides the algorithms used to transform between the equinoctial elements and position and velocity. Section 8.3.1 provides a definition of the equinoctial elements. Section 8.3.2 discusses the transformation from equinoctial elements to Cartesian coordinates and Section 8.3.3 discusses the transformation from Cartesian coordinates to equinoctial elements.

8.3.1 Definition of Equinoctial Elements

The equinoctial elements are defined as follows:

a = semimajor axis

h = projection of the eccentricity vector $\bar{e}$ on the $\hat{y}_{ep}$ axis

k = projection of the eccentricity vector $\bar{e}$ on the $\hat{x}_{ep}$ axis

p = projection of the nodal vector $\overline{N}$ on the $\hat{y}_{ep}$ axis

q = projection of the nodal vector $\overline{N}$ on the $\hat{x}_{ep}$ axis

λ = mean longitude

where

$\overline{e}$ = eccentricity vector pointing in the direction of the $\hat{x}_p$ axis (perifocus) and having a magnitude equal to the orbital eccentricity

$\overline{N}$ = nodal vector pointing in the direction of the ascending node and having a magnitude equal to $\tan(i/2)^j$, where i denotes the orbital inclination and j=+1 for direct orbits and -1 for retrograde orbits

The equinoctial system, which is denoted by x_{ep}, y_{ep}, and z_{ep}, has its $\hat{x}_{ep}$ axis (principal direction) directed toward the "origin of longitudes." The "origin of longitudes" lies in the plane of the orbit and is displaced by the angle Ω from the ascending node $\overline{N}$, where Ω is the right ascension of the ascending node. Unit vectors along the coordinate directions, x_{ep}, y_{ep}, and z_{ep}, are denoted by $\hat{f}$, $\hat{g}$, and $\hat{w}$, respectively. The equinoctial system is illustrated in Figure 8-1. In this figure, $\hat{x}$, $\hat{y}$, and $\hat{z}$ indicate the inertial coordinate frame.

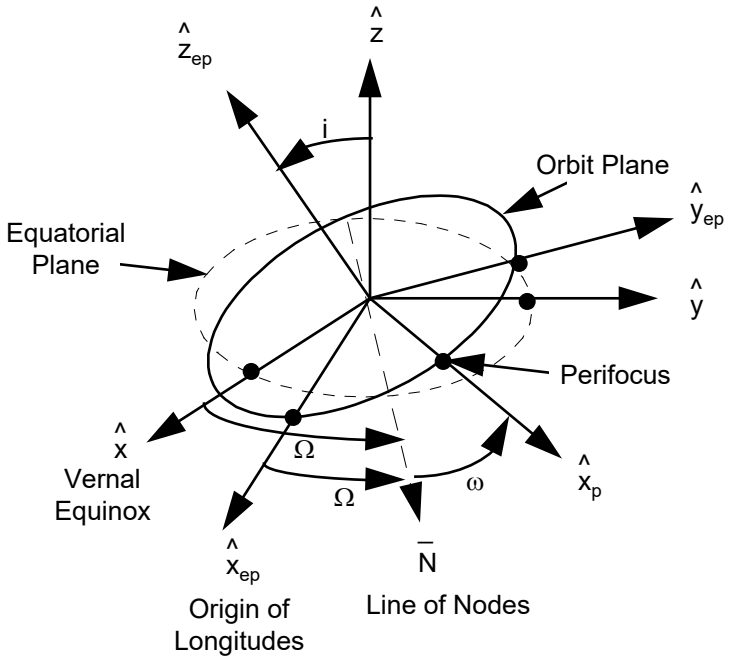

Figure 8-1. Equinoctial Coordinate System

8.3.2 Transformation From Equinoctial Elements to Cartesian Coordinates

Conversion from equinoctial elements, $\overline{E}(t) = (a, h, k, p, q, \lambda)$, to inertial Cartesian coordinates, $\overline{R}(t)$ and $\dot{\overline{R}}(t)$, is performed in the following manner. First, the generalized Kepler equation for the equinoctial elements,

$$\lambda = F + h\cos F - k\sin F \tag{8.3-1}*$$

is solved for the eccentric longitude F, which is the sum of the eccentric anomaly, the argument of perigee, and the right ascension of the ascending node.

This equation is solved by the following iteration scheme:

$$f(F_n) = F_n + h\cos F_n - k\sin F_n - \lambda \tag{8.3-2}*$$

$$D_n = 1 - h\sin\left[F_n - 0.5f(F_n)\right] - k\cos\left[F_n - 0.5f(F_n)\right] \tag{8.3-3}*$$

$$F_{n+1} = F_n - \frac{f(F_n)}{D_n} \tag{8.3-4}*$$

where

$$F_0 = \lambda - h\cos\lambda + k\sin\lambda \tag{8.3-5}*$$

Next, the position and velocity coordinates in the equinoctial coordinate system (x_{ep}, y_{ep}, z_{ep}) are obtained as follows for the direct and retrograde cases:

$$X_1 = a\left[(1 - h^2\beta)\cos F + hk\beta\sin F - k\right] \tag{8.3-6}*$$

$$Y_1 = a\left[(1 - k^2\beta)\sin F + hk\beta\cos F - h\right] \tag{8.3-7}*$$

$$\dot{X}_1 = \frac{na^2}{R}\left[hh\beta\cos F - (1 - h^2\beta)\sin F\right] \tag{8.3-8}*$$

$$\dot{Y}_1 = \frac{na^2}{R}\left[(1 - k^2\beta)\cos F - hk\beta\sin F\right] \tag{8.3-9}*$$

where

$$\beta = \frac{1}{1 + \sqrt{1 - h^2 - k^2}} \tag{8.3-10}*$$

The transformation from the equinoctial system to the inertial Cartesian system is given by

$$\overline{R} = X_1 \hat{f} + Y_1 \hat{g} \tag{8.3-11}*$$

$$\dot{\overline{R}} = \dot{X}_1 \hat{f} + \dot{Y}_1 \hat{g} \tag{8.3-12}*$$

where $\hat{f}$ and $\hat{g}$ are unit vectors directed along the $\hat{x}_{ep}$ and $\hat{y}_{ep}$ axes, respectively. These vectors in inertial Cartesian coordinates are as follows:

$$\left[\hat{f} \quad \hat{g} \quad \hat{w}\right] = \frac{1}{1+p^2+q^2}\begin{bmatrix} 1-p^2+q^2 & 2pqj & 2p \\ 2pq & (1+p^2-q^2)j & -2q \\ -2pj & 2q & (1-p^2-q^2)j \end{bmatrix} \tag{8.3-13}*$$

where

j = 1 for direct orbits ($0 \le i < 90$ degrees)

j = -1 for retrograde orbits ($90 < i \le 180$ degrees)

In the GEONS, the operational choice of direct or retrograde elements is an input option.

8.3.3 Transformation From Cartesian Coordinates to Equinoctial Elements

Conversion from inertial Cartesian coordinates, $\overline{R}(t)$ and $\dot{\overline{R}}(t)$, to equinoctial elements, $\overline{E}(t)$ = (a, h, k, p, q, λ), is performed in the following manner. The semimajor axis is computed as follows:

$$a = \left[\frac{2}{R} - \frac{\left|\dot{\overline{R}}\right|^2}{\mu_E}\right]^{-1} \tag{8.3-14}*$$

where μ_E is the gravitational constant of the Earth.

The mean motion is given by

$$n = \sqrt{\frac{\mu_E}{a^3}} \tag{8.3-15}*$$

and the eccentricity vector is given by

$$\overline{e} = -\frac{\overline{R}}{R} - \frac{(\overline{R} \times \dot{\overline{R}}) \times \dot{\overline{R}}}{\mu_E} = \frac{1}{\mu_E}\left[\left(\dot{R}^2 - \frac{\mu_E}{R}\right)\overline{R} - \left(\overline{R} \cdot \dot{\overline{R}}\right)\dot{\overline{R}}\right] \tag{8.3-16}*$$

The unit vector $\hat{w}$ is defined as

$$\hat{w} = \frac{\overline{R} \times \dot{\overline{R}}}{\left| \overline{R} \times \dot{\overline{R}} \right|} \tag{8.3-17}*$$

The unit vectors $\hat{f}$ and $\hat{g}$ can then be computed as follows:

$$\hat{f} = \left[1 - \frac{w_x^2}{1 + w_z j} \quad -\frac{w_x w_y}{1 + w_z j} \quad -w_x j \right] \tag{8.3-18}*$$

$$\hat{g} = \hat{w} \times \hat{f} \tag{8.3-19}*$$

The equinoctial elements *h*, *k*, *p*, and *q* are then given by

$$h = \overline{e} \cdot \hat{g} \tag{8.3-20}*$$

$$k = \overline{e} \cdot \hat{f} \tag{8.3-21}*$$

$$p = \frac{w_x}{1 + w_z j} \tag{8.3-22}*$$

$$q = -\frac{w_y}{1 + w_z j} \tag{8.3-23}*$$

The mean longitude is computed using the generalized Kepler equation

$$\lambda = F + h\cos F - k\sin F \tag{8.3-24}*$$

where

$$F = \tan^{-1}\left(\frac{\sin F}{\cos F} \right) \tag{8.3-25}*$$

with

$$\cos F = k + \frac{(1 - k^2\beta)X_1 - hk\beta Y_1}{a\sqrt{1 - h^2 - k^2}} \tag{8.3-26}*$$

$$\sin F = h + \frac{(1 - h^2\beta)Y_1 - hk\beta X_1}{a\sqrt{1 - h^2 - k^2}} \tag{8.3-27}*$$

and

$$\beta = \frac{1}{1 + \sqrt{1 - h^2 - k^2}} \tag{8.3-28}*$$

Finally, the position and velocity coordinates, relative to the equinoctial coordinate system, are given by

$$X_1 = \overline{R} \cdot \hat{f} \tag{8.3-29}*$$

$$Y_1 = \overline{R} \cdot \hat{g} \tag{8.3-30}*$$

8.3.4 Transformation From Keplerian Elements to Equinoctial Elements

Conversion from the classical Keplerian elements, $(a, e, i, \Omega, \omega, M)$, to equinoctial elements, $\overline{E}(t) = (a, h, k, p, q, \lambda)$, is performed in the following manner:

$$\begin{aligned} a &= a \\ h &= e \sin(\omega + \Omega j) \\ k &= e \cos(\omega + \Omega j) \\ p &= \left(\tan\left(\frac{i}{2}\right) \right)^j \sin\Omega \\ q &= \left(\tan\left(\frac{i}{2}\right) \right)^j \cos\Omega \\ \lambda &= M + \omega + \Omega j \end{aligned} \tag{8.3-31}*$$

where

j = 1 for direct orbits ($0 \le i < 90$ degrees)

j = -1 for retrograde orbits ($90 < i \le 180$ degrees)

In the GEONS, the operational choice of direct or retrograde elements is an input option.

At the time of perigee passage, τ_p, $M = 0$ and $\lambda = \omega + \Omega$.

Section 9. Orbit Control Algorithms

This section provides a generic maneuver targeting algorithm that can be used to compute a change in velocity needed to reach a desired target orbit, i.e. to compute a direct transfer orbit maneuver. This algorithm is appropriate for computing intercept maneuvers (employing a single impulsive burn) and rendezvous maneuvers (employing two impulsive burns). One specific application for this capability is the computation of rendezvous maneuvers that will return a satellite to its correct location in a formation. This section also includes more advanced formation control algorithms developed by GSFC personnel.

Section 9.1 discusses the generic maneuver targeting algorithm. Section 9.2 presents the advanced formation control algorithms.

9.1 Generic Maneuver Targeting Algorithm

Figure 9-1 illustrates the geometry of the two maneuvers associated with the rendezvous problem. The intercept problem requires only the first of these maneuvers. Given two position vectors [the satellite location at the desired maneuver start time, $t_0, \left(\overline{R}(t_0)\right)$ and the target trajectory location $\left(\overline{R}_T(t_f)\right)$ at the desired maneuver end time, t_f], the Lambert targeting algorithm gives the initial velocity $\left(\dot{\overline{R}}_{trans}(t_0)\right)$ that will generate the transfer trajectory connecting the two positions $\left(\overline{R}(t_0) \text{and } \overline{R}_T(t_f)\right)$.

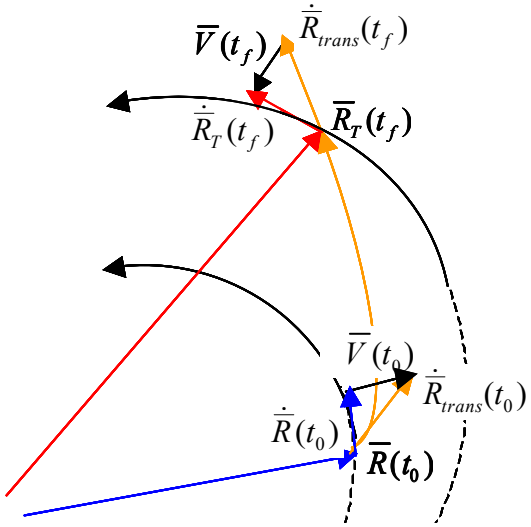

Figure 9-1 Geometry of Rendezvous Targeting Problem

Since the Lambert problem is defined in a two-body (i.e. the satellite and the central-body) environment and the optimum time of flight is not known, the targeting algorithm is performed iteratively to compute both the $\Delta\overline{V}(t_0)$ required for the initial insertion into the transfer

trajectory and the $\Delta\overline{V}(t_f)$ required for insertion into the target trajectory from the transfer trajectory. Figure 9-2 provides an overview of the Lambert targeting algorithm implemented in GEONS.

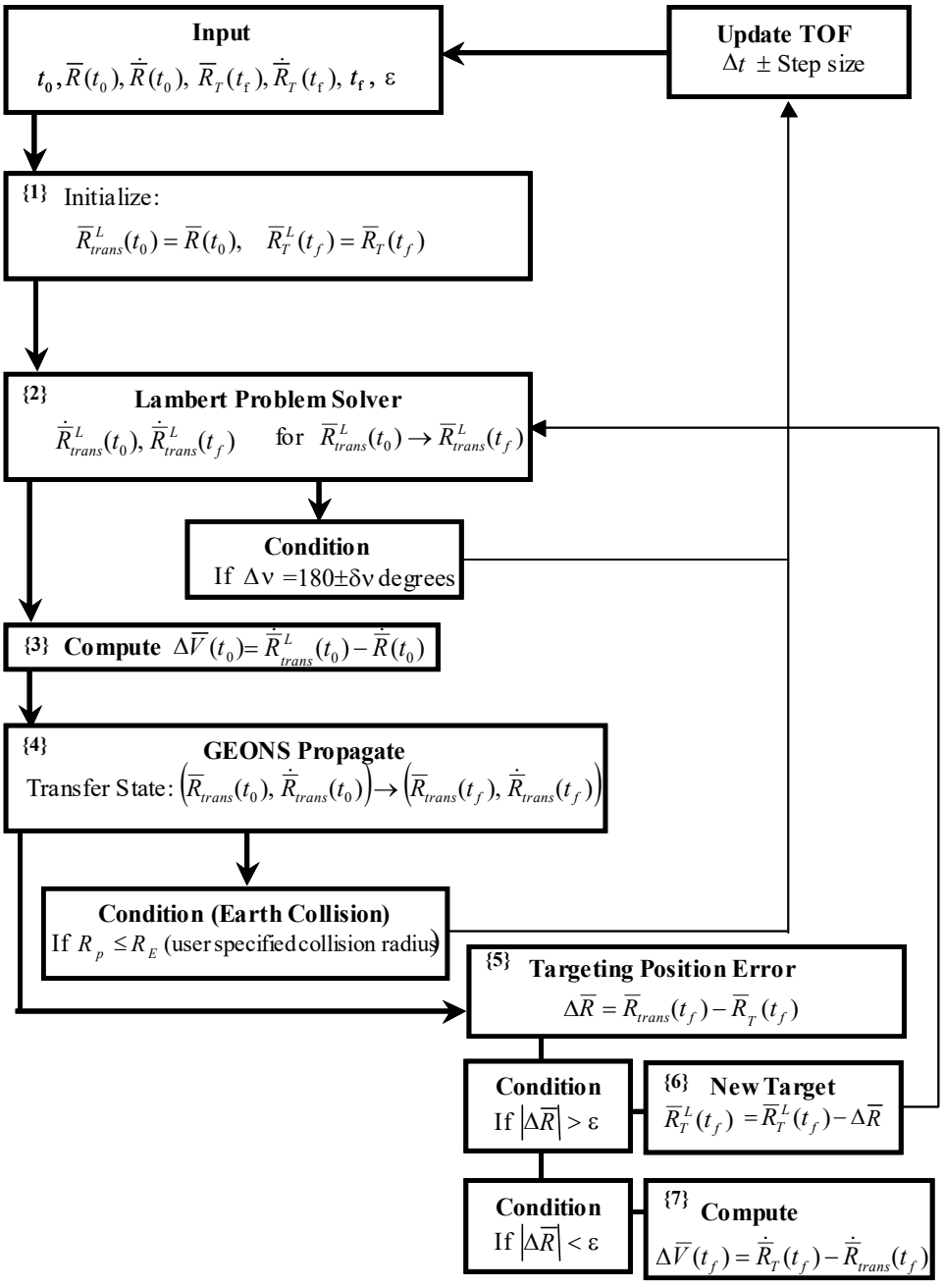

Figure 9-2 Overview of the Lambert Targeting Algorithm

Because the solution method presented in Section 9.1.1 uses classical f and g functions to represent the two-body transfer trajectory, the Lambert problem must be solved in the central-body coordinate frame. If the central body is not the Earth, the current GEONS ECI state vector must be transformed to the central-body frame as discussed in Section 3.2.11. The details of the targeting algorithm are as follows, with inputs $t_0, \overline{R}(t_0), \dot{\overline{R}}(t_0)$, and $t_f, \overline{R}_T(t_f), \dot{\overline{R}}_T(t_f)$ referenced to the central-body frame and the convergence tolerance ε:

1. Initialize $\overline{R}^L_{trans}(t_0) = \overline{R}(t_0)$, $\overline{R}^L_T(t_f) = \overline{R}_T(t_f)$.
2. Solve the Lambert problem in the central-body frame to determine the initial and final velocity ($\dot{\overline{R}}^L_{trans}(t_0), \dot{\overline{R}}^L_{trans}(t_f)$) of the transfer trajectory from the satellite position at t_0 ($\overline{R}^L_{trans}(t_0)$) to the target position at time t_f ($\overline{R}^L_{trans}(t_f) = \overline{R}^L_T(t_f)$). The solution method is provided in Section 9.1.1. If a solution cannot be computed (e.g. $\Delta\nu = 180 \pm \delta\nu$ degrees or initial and target orbits are normal), exit this procedure.
3. Compute the change in velocity required for the initial insertion into the transfer trajectory $\Delta\overline{V}(t_0) = \dot{\overline{R}}^L_{trans}(t_0) - \dot{\overline{R}}(t_0)$.
4. Propagate the transfer trajectory state from the maneuver time $\left(\overline{R}_{trans}(t_0) = \overline{R}(t_0), \dot{\overline{R}}_{trans}(t_0) = \dot{\overline{R}}^L_{trans}(t_0)\right)$ to the desired target orbit insertion time, $t_f = t_0 + \Delta t$ to obtain $\left(\overline{R}_{trans}(t_f), \dot{\overline{R}}_{trans}(t_f)\right)$. Determine if the transfer trajectory will impact the central body using the procedure defined in Section 9.1.3. If collision occurs, exit this procedure.
5. Compute the targeting position error: $\Delta\overline{R} = \overline{R}_{trans}(t_f) - \overline{R}_T(t_f)$
6. If $\left|\Delta\overline{R}\right| > \varepsilon$, adjust the Lambert target position to $\overline{R}^L_T(t_f) = \overline{R}^L_T(t_f) - \Delta\overline{R}$ and repeat the process starting at step 2. Figure 9-3 illustrates this iterative process. Exit if the maximum number of iterations is exceeded.
7. If $\left|\Delta\overline{R}\right| < \varepsilon$, compute the change in velocity required for insertion into the target trajectory from the transfer trajectory $\Delta\overline{V}(t_f) = \dot{\overline{R}}_T(t_f) - \dot{\overline{R}}_{trans}(t_f)$.

A series of calculations using different times of flight is needed to determine the time of flight that requires the minimum $\Delta\overline{V}(t_0)$. In general, the $\Delta\overline{V}(t_0)$ is larger if the time of flight is longer than one satellite orbit.

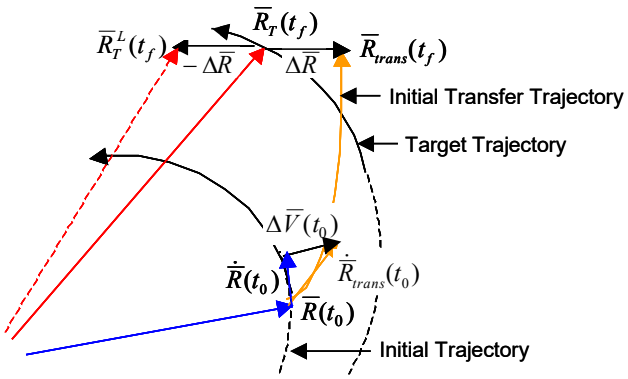

Figure 9-3 First Iteration of the Lambert Targeting Problem

9.1.1 Solution to Lambert's Problem

In Lambert's problem, two position vectors and the time of flight between them are known but the orbit between the endpoints is not known. Many different solutions to this problem have been developed. Section 6.7 of Reference 31 provides a detailed discussion of several solution methods.

The solution method presented in this section, uses classical f and g functions expressed in terms of universal variables to represent the two-body transfer trajectory between the two position vectors. Consequently, the solution must be computed in the central-body coordinate frame. The f and g functions can be used as follows to propagate a satellite state vector using two-body dynamics:

$$\begin{aligned}\bar{R}(t) &= f\bar{R}(t_0) + g\dot{\bar{R}}(t_0)\\ \dot{\bar{R}}(t) &= \dot{f}\bar{R}(t_0) + \dot{g}\dot{\bar{R}}(t_0)\end{aligned} \tag{9.1-1}$$

Computation of the f and g functions is discussed in Section 9.1.2.

The following algorithm is used to solve the Lambert problem to determine the velocity ($\dot{\bar{R}}^L_{trans}(t_0), \dot{\bar{R}}^L_{trans}(t_f)$) of the transfer trajectory given the satellite position and velocity at t_0 ($\bar{R}^L_{trans}(t_0) = \bar{R}(t_0)$ and $\dot{\bar{R}}(t_0)$), the time of flight (Δt), and the target position at time $t_f = t_0 + \Delta t$ ($\bar{R}^L_{trans}(t_f)$). Two distinct solutions exist corresponding to (1) the short way for which the change in true anomaly (ν) <180 degrees (for which $t_m = 1$ below) and (2) the long way for which the change in true anomaly ($\Delta\nu$) >180 degrees (for which $t_m = -1$ below). The special case of $\Delta\nu$ =180 degrees cannot be solved using this method.

1. Determine value for t_m that will require the minimum velocity change. The short way should be used when the normal vector to the initial orbit plane, $\bar{N}_0$, and the normal vector to the transfer orbit plane, $\bar{N}_{trans}$, are in the same direction. The long way should be used when the normal vectors are in the opposite directions:

$$
\begin{aligned}
&\overline{N}_0 = \overline{R}^L_{trans}(t_0) \times \dot{\overline{R}}(t_0) \\
&\overline{N}_{trans} = \overline{R}^L_{trans}(t_0) \times \overline{R}^L_{trans}(t_f) \\
&\text{If } \overline{N}_0 \cdot \overline{N}_{trans} > 0, \text{use short way } (t_m = 1) \\
&\text{If } \overline{N}_0 \cdot \overline{N}_{trans} < 0, \text{use long way } (t_m = -1) \\
&\text{If } \overline{N}_0 \cdot \overline{N}_{trans} = 0, \text{solution cannot be computed because the orbits are normal}
\end{aligned}
\tag{9.1-2}
$$

2. Use the universal variable approach provided in Section 9.3 to compute the functions $f, g, \text{and } \dot{g}$ for the transfer trajectory from $\overline{R}^L_{trans}(t_0)$ to $\overline{R}^L_{trans}(t_0 + \Delta t) = \overline{R}^L_{trans}(t_f)$, for the selected value of t_m and Δt.

3. Compute the velocity of the transfer trajectory at times t_0 and t_f

$$
\begin{aligned}
\dot{\overline{R}}^L_{trans}(t_0) &= \frac{\overline{R}^L_{trans}(t_f) - f\overline{R}^L_{trans}(t_0)}{g} \\
\dot{\overline{R}}^L_{trans}(t_f) &= \frac{\dot{g}\overline{R}^L_{trans}(t_f) - \overline{R}^L_{trans}(t_0)}{g}
\end{aligned}
\tag{9.1-3}
$$

9.1.2 Computation of f and g Functions

Using f and g functions, the transfer trajectory state vector at time t_f can be expressed in terms of the transfer trajectory at time t_0 as follows:

$$
\begin{aligned}
\overline{R}^L_{trans}(t_f) &= f\overline{R}^L_{trans}(t_0) + g\dot{\overline{R}}^L_{trans}(t_0) \\
\dot{\overline{R}}^L_{trans}(t_f) &= \dot{f}\overline{R}^L_{trans}(t_0) + \dot{g}\dot{\overline{R}}^L_{trans}(t_0)
\end{aligned}
\tag{9.1-4}
$$

Several different representations for the f and g functions are available. Section 4.3.1 of Reference 31 and Sections 4.5, 4.6 and 9.7 in Reference 32 discuss these functions in detail. The universal-variable formulation was selected because it provides a single set of equations for all the conic sections.

Reference 31 shows that, for the case when the change is the true anomaly $\Delta\upsilon$ is known (as it is in the Lambert problem), the f and g functions can be expressed as follows

$$
\begin{aligned}
f &= 1 - \frac{y_n}{R_0} \\
\dot{f} &= \frac{\sqrt{\mu_C y_n}\,(-R_f - R_0 + y_n)}{R_f R_0 A} \\
g &= A\sqrt{\frac{y_n}{\mu_C}} \\
\dot{g} &= 1 - \frac{y_n}{R_f}
\end{aligned}
\tag{9.1-5}
$$

where μ_C is the gravitational constant of the central body and

$$
\begin{aligned}
R_0 &= \left|\overline{R}^L_{trans}(t_0)\right| \\
R_f &= \left|\overline{R}^L_{trans}(t_f)\right|
\end{aligned}
\tag{9.1-6}
$$

The value of A is determined as follows for either the short or long way:

$$
A = t_m \sqrt{R_f R_0 (1 + \cos(\Delta\nu))}
\tag{9.1-7}
$$

where

$$
\cos(\Delta\nu) = \frac{\overline{R}^L_{trans}(t_0) \cdot \overline{R}^L_{trans}(t_f)}{R_0 R_f}
\tag{9.1-8}
$$

For the special case A=0.0 (i.e. $\Delta\nu = 180 \pm \delta\nu$ degrees), there is no solution using this method.

The value of the remaining variable in Equation 9.1-5 (y_n), depends on the value of the variable ψ that corresponds to the specified change in time, Δt. The value of ψ is determined iteratively using the following bisection technique, which is more robust than the Newton-Ralphson scheme for a wider range of orbits. This technique is performed by bounding the correct value of ψ and picking a trial value of ψ that halfway between these bounds. Subsequent iterations successively readjust the upper and lower bounds until the interval is tight enough to locate the correct value of ψ.

The details of the algorithm are as follows with inputs $\overline{R}^L_{trans}(t_0)$ and $\overline{R}^L_{trans}(t_0 + \Delta t) = \overline{R}^L_{trans}(t_f)$ referenced to the central-body frame, t_m and Δt:

1. Determine the value of A as follows

$$
\begin{aligned}
R_0 &= \left|\overline{R}^L_{trans}(t_0)\right| \\
R_f &= \left|\overline{R}^L_{trans}(t_0 + \Delta t)\right|
\end{aligned}
$$

$$\cos(\Delta\nu) = \frac{\overline{R}^{L}_{trans}(t_0) \cdot \overline{R}^{L}_{trans}(t_0 + \Delta t)}{R_0 R_f}$$

$$A = t_m \sqrt{R_f R_0 \left(1 + \cos(\Delta\nu)\right)}$$

If $\Delta\nu = 180 \pm \delta\nu$ degrees, exit the procedure; solution cannot be computed.

2. Set the initial values for the square of the change in the eccentric anomaly, (appropriate for single revolution solutions, adjust initial bounds to solve for multiple revolution cases) and c_2, and c_3:

$$\psi_{up} = 4\pi^2 \text{ (radians)}^2$$
$$\psi_{low} = -4\pi^2 \text{ (radians)}^2$$
$$\psi_n = 0.0$$
$$c_2 = \frac{1}{2}$$
$$c_3 = \frac{1}{6}$$

3. Solve for the value of ψ_n that corresponds to the desired time of flight Δt using the following iteration bisection technique:

a.) Compute y_n

$$y_n = R_0 + R_f + \frac{A\left(\psi_n c_3 - 1\right)}{\sqrt{c_2}}$$

If $A > 0.0$ and $y_n < 0.0$, readjust ψ_{low} as follows until $y_n > 0.0$

$$\psi_{low} = \psi_{low} - \pi^2$$
$$\psi_n = \frac{\psi_{low} + \psi_{up}}{2}$$
$$y_n = R_0 + R_f + \frac{A\left(\psi_n c_3 - 1\right)}{\sqrt{c_2}}$$

b.) Compute $\chi_0 = \sqrt{\frac{y_n}{c_2}}$

c.) Compute the current time of flight based on the current values for y_n, χ_0, c_3 and μ_C (gravitational constant of the central body in meters^3/second^2)

$$\Delta t_n = \frac{\chi_0^3 c_3 + A\sqrt{y_n}}{\sqrt{\mu_C}}$$

d.) Compare the current time of flight to the desired time of flight

If $\left|\Delta t_n - \Delta t\right| \le 10^{-6}$, iteration has converged, proceed to step 4

If $\left|\Delta t_n - \Delta t\right| > 10^{-6}$,

Adjust ψ_n as follows

If $\Delta t_n \le \Delta t$, reset $\psi_{low} = \psi_n$

If $\Delta t_n > \Delta t$, reset $\psi_{up} = \psi_n$

$$\psi_{n+1} = \frac{\psi_{low} + \psi_{up}}{2}$$

$$\psi_n = \psi_{n+1}$$

Recompute c_2 and c_3 as follows

If $\psi_n > 10^{-6}$, (elliptical case)

$$c_2 = \frac{1 - \cos\sqrt{\psi_n}}{\psi_n}$$

$$c_3 = \frac{\sqrt{\psi_n} - \sin\sqrt{\psi_n}}{\sqrt{(\psi_n)^3}}$$

If $\psi_n < -10^{-6}$, (hyperbolic case)

$$c_2 = \frac{1 - \cosh\sqrt{-\psi_n}}{\psi_n}$$

$$c_3 = \frac{\sinh\sqrt{-\psi_n} - \sqrt{-\psi_n}}{\sqrt{(-\psi_n)^3}}$$

Otherwise, (parabolic case)

$$c_2 = \frac{1}{2}$$

$$c_3 = \frac{1}{6}$$

and repeat iteration procedure starting at step 3a.

4. Compute the f and g functions using Equation 9.1-5.

9.1.3 Central Body Collision Detection Algorithm

One of the most important factors that determine if a trajectory solution obtained for Lambert's Problem is usable is that the transfer trajectory does not intersect the central body. The standard method of calculating a collision involves determining the flight-path angle and the radius of perigee (R_p). For computational efficiency, the flight-path angle will not be calculated; instead

an examination of the behavior of the transfer trajectory between apogee and perigee will be used to determine a possible collision. The algorithm listed below uses a series of dot products of the position and velocity vectors to check if it is necessary to compute the R_p to determine if the transfer trajectory intersects the central body. Section 7.7 of Reference 32 provides the detailed discussion of the collision detection algorithm listed below.

The parameters of interest are the following, expressed in the central body frame:

$$\left\{\overline{R}_{trans}(t_0), \dot{\overline{R}}_{trans}(t_0), \overline{R}_{trans}(t_f), \dot{\overline{R}}_{trans}(t_f), R_p\right\}$$

The flight-path angle is the angular separation between the velocity vector and the local horizontal plane. The sign of the flight-path angle is positive when the trajectory travels from perigee to apogee and negative from apogee to perigee. The change in sign will be analyzed using the dot products of the position and velocity at the start and end of the transfer trajectory (maneuver period). The sign at the start and end of the transfer are used to determine if the transfer orbit's perigee occurred during the maneuver. The central body collision detection algorithm is given below.

1. Compute the dot product of the satellite position vector $\overline{R}_{trans}(t_0) = \overline{R}(t_0)$ and the velocity vector $\dot{\overline{R}}_{trans}(t_0)$ at the start of the transfer trajectory:

$$\overline{R}_{trans}(t_0) \cdot \dot{\overline{R}}_{trans}(t_0)$$

2. Compute the dot product of the satellite position vector $\overline{R}_{trans}(t_f)$ and the velocity vector $\dot{\overline{R}}_{trans}(t_f)$ at the end of the transfer trajectory (end of the maneuver):

$$\overline{R}_{trans}(t_f) \cdot \dot{\overline{R}}_{trans}(t_f)$$

3. Determine if perigee occurs during the transfer and if the R_p should be calculated.

   a) If $\left.\begin{array}{l} \overline{R}_{trans}(t_0) \cdot \dot{\overline{R}}_{trans}(t_0) \\ \overline{R}_{trans}(t_f) \cdot \dot{\overline{R}}_{trans}(t_f) \end{array}\right\}$ *Both Positive or Negative*

   perigee passage does not occur and collision is not possible.

   b) If $\left.\begin{array}{l} \overline{R}_{trans}(t_0) \cdot \dot{\overline{R}}_{trans}(t_0) < 0 \text{ (satellite is headed towards perigee)} \\ \overline{R}_{trans}(t_f) \cdot \dot{\overline{R}}_{trans}(t_f) > 0 \text{ (satellite is headed towards apogee)} \end{array}\right\}$

   collision is possible and the following collision test is performed:

   Compute $R_p = a(1-e)$

   where

$$a = \left(\frac{2}{\left| \overline{R}_{trans}(t_0) \right|} - \frac{\left| \dot{\overline{R}}_{trans}(t_0) \right|^2}{\mu_C} \right)^{-1}$$

$$e = \sqrt{\frac{a - p}{a}}$$

$$p = \frac{h^2{}_{trans}}{\mu_C}$$

$$h_{trans} = \left| \overline{R}_{trans}(t_0) \times \dot{\overline{R}}_{trans}(t_0) \right|$$

If $R_p \le R_C$(a user specified collision radius), collision occurs on the transfer trajectory.

9.2 Formation Control Algorithms

The GEONS software provides generic interfaces to support integration with user-provided orbit and formation control software.

Section 10. Cold-Start Initialization Algorithm

In low-Earth orbit (LEO), GEONS can be initialized using a point solution – i.e. an instantaneous solution for position, velocity, and receiver time bias based on four or more simultaneous GPS pseudorange and Doppler measurements. Point solutions are available from most GPS space receivers. This is not the case in high-Earth orbits or highly elliptical orbits, where there are rarely, if ever, sufficient satellites visible to compute a point solution. In these situations, a different initialization approach is required.

This section presents a robust method, developed by the Colorado Center for Astrodynamics Research (CCAR), that can be used to provide a satellite state vector for initialization/reinitialization of GEONS, when four or more simultaneous GPS measurements are not available. This method processes a batch of pseudorange and/or Doppler measurements collected over an orbital arc to compute an initial state estimate. This algorithm assumes knowledge of nominal orbital elements, (e.g. a, e, i, ω, Ω) and performs a search on the mean longitude ($\lambda_{initial}$) to estimate the host satellite position within the orbit and the approximate receiver clock bias and bias rate. Reference 33 discusses the development of this method and presents the results of a simulation using this method, which includes large orbital uncertainties and measurement errors.

10.1 Algorithm Overview

This method, which is based on an orbital element representation, uses the constraints of orbital dynamics to narrow the range of possible initial conditions. The angular orientation of the orbit (inclination, node, and argument of perigee), and the orbital energy are constrained by the launch; whereas the position of the spacecraft within the orbital plane is poorly known. The standard injection errors associated with the orbital elements can be estimated based on the launch vehicle design and history.

In this initialization method, the spacecraft state vector is represented using the equinoctial orbital elements (a, h, k, p, q, λ), which are defined in Section 8.3.1 of this document. These elements are closely related to the classical orbital elements (a, e, i, Ω, ω, M), but are better suited for handling circular, equatorial orbits. The first five elements, which define the geometry of the orbit, are held fixed, e.g. equal to the nominal post-launch orbit insertion values. The final parameter, the mean longitude (λ), defines the position of the spacecraft within the orbit. This value is not well known ahead of time. So, the goal of the initialization process is to determine the correct value of λ at the requested filter initialization time, $t_{initial}$, and to compute the associated initial position and velocity estimates.

This method assumes that the onboard GPS receiver acquires and tracks as many satellites as possible using a cold start or blind search technique. The receiver is assumed to form both pseudorange and Doppler measurements and to collect the broadcast GPS satellite ephemeris data from all visible satellites at intervals of 1 minute or smaller.

Time onboard the spacecraft is assumed to be known to within 1 second after acquisition and tracking of the first GPS satellite. The stability of the clock is assumed to be on the order of 1 part in 10^{10}. In this case, the large receiver clock bias will dominate the pseudorange residuals. However, by comparing residuals for different satellites, a reliable initial bias value can be computed using these measurements. If measurements from only one satellite are available, it is not always possible to isolate the correct starting point in the orbit if there is a large receiver clock bias.

The algorithm assumes knowledge of the orbital elements, $(a, e, i, \Omega, \omega)$, and performs a search to estimate the remaining unknown – the location within the orbit, characterized by the mean longitude at the initialization time, $\lambda_{initial}$. To process all the measurements in the batch, the nominal spacecraft orbital elements are used to predict the spacecraft position and velocity at each of the measurement times. The expected pseudorange and/or Doppler measurements are computed using the spacecraft position and velocity predictions and the GPS satellite positions computed from the broadcast ephemerides. These are compared to the actual measurements from the receiver and the residuals for the entire data arc are accumulated.

The characteristics of the measurement residuals for the batch indicate which value of $\lambda_{initial}$ is best. For PR measurements without clock biases and for Doppler measurements, the root-mean-square (RMS) of the residuals is unambiguously smallest for the correct position within the orbital plane. In the presence of a large clock bias, there is an offset in the pseudorange residuals that prevents the use of a simple RMS evaluation. When measurements are available from more than one GPS SV within the batch, the correct $\lambda_{initial}$ can be identified by the minimum standard deviation of the measurement residuals. The value of $\lambda_{initial}$ that minimizes the residual standard deviation locates the correct host vehicle position within the orbit. The mean of the pseudorange residuals for this $\lambda_{initial}$ provides a coarse estimate of the receiver clock bias. The mean of the Doppler residuals for this $\lambda_{initial}$ provides a coarse estimate of the receiver clock bias rate. The position and velocity estimates can then be produced at the initialization time based upon the nominal orbital elements and the best $\lambda_{initial}$.

The algorithm starts with a coarse search in increments of the mean longitude, $\Delta\lambda$, for the value $\lambda_{initial}$ that provides the minimum residual standard deviation. This search provides an initial estimate for $\lambda_{initial}^{\min}$ and brackets the search region in which the minimum occurs. The location of the minimum is then refined using the Golden Section Search method. The accuracy of the solution is ultimately limited by the uncertainty in the nominal elements. The results presented in Reference 33 indicate that the search space is well defined for measurement data arcs of 100 minutes or longer eliminating the possibility of searching in a false null region. For initialization near perigee, data arcs as short as 10 minutes are adequate.

When the best $\lambda_{initial}^{\min}$ is found, the position and velocity at the requested initialization time are computed based on the nominal elements and $\lambda_{initial}^{\min}$. An initial estimate of the receiver clock bias is provided by the mean of the pseudorange residuals associated with the minimum residual standard deviation. An initial estimate of the receiver clock bias rate is provided by the mean of the Doppler residuals associated with the minimum residual standard deviation. The initial covariance matrix can be computed from the launch uncertainties.

10.2 Initialization Algorithm Summary

The following steps summarize the algorithm used to successively refine the estimate for the best $\lambda_{initial}$ ($\lambda_{initial}^{\min}$) and to compute an initial satellite position and velocity at the requested initialization time based on the assumed nominal orbital elements and the computed $\lambda_{initial}^{\min}$. This algorithm requires the following input values, in addition to the Broadcast ephemeris associated with each GPS SV tracked during the measurement data arc:

$a, e, i, \Omega, \omega =$ nominal classical orbital elements

$[\rho_{obs}(t_m), f_{obs}(t_m), t_m] =$ batch of M observed pseudorange and/or Doppler measurements, nominally at 1-minute intervals

$t_{initial} =$ initialization time (equal to batch end time)

$b_R^0 =$ initial value of the receiver time bias in meters, nominally equal to 0

$d_R^0 =$ initial value of the receiver time bias rate in meters per second, nominally equal to 0

$\Delta\lambda =$ size of increment in λ, nominally 0.2π radians

1. Convert the nominal classical orbit elements (a, e, i, Ω, ω) to equinoctial elements (a, h, k, p, q) using the algorithm defined in Section 8.3.4 of this document.
2. Use the coarse search algorithm defined in Section 10.3 with a search region of $\lambda_{initial}^{s} = 0$ to $\lambda_{initial}^{f} = 2\pi$, in increments of $\Delta\lambda$ to obtain an initial estimate for the $\lambda_{initial}^{\min}$, the receiver clock bias, b_R, and the receiver clock bias rate, d_R, and to bracket the search region.
3. Refine the estimate for $\lambda_{initial}^{\min}$ using the Golden Section Search method described in Section 10.4, applying the receiver bias and bias rate estimates computed in step 2, narrowing the search region to $\lambda_{initial}^{\min}$ (from step 2) $\pm$ $0.5\,\Delta\lambda$. Compute update to the receiver clock bias, b_R, and the receiver clock bias rate, d_R, using the best $\lambda_{initial}^{\min}$.
4. Use the transformation defined in Section 8.3.3 to convert the element set $a, h, k, p, q, \lambda_{initial}^{\min}$ to obtain the position and velocity at the initialization time, $t_{initial}$.

10.3 Coarse Search Algorithm

This algorithm is used to bracket the region in which the best value $\lambda_{initial}^{\min}$ occurs. The search algorithm consists of the following steps, given the following input values, in addition to the Broadcast ephemeris associated with each GPS SV tracked during the measurement data arc:

$a, h, k, p, q =$ nominal equinoctial orbital elements

$t_{initial} =$ initialization time

$[\rho_{obs}(t_m), f_{obs}(t_m), t_m]$ = batch of M observed pseudorange and/or Doppler measurements, nominally at 1-minute intervals

$\lambda^s_{initial}$ = starting value for $\lambda_{initial}$ search (radians)

$\lambda^f_{initial}$ = ending value for $\lambda_{initial}$ search (radians)

$\Delta\lambda$ = size of increment in λ (radians)

b_R = current value of the receiver time bias (meters)

d_R = current value of the receiver time bias rate (meters per second)

1. For each $\lambda_{initial}(i) = \lambda^s_{initial} + i\Delta\lambda$, $i = 0, 1, \ldots$, while $\lambda_{initial}(i) \le \lambda^f_{initial}$

   a. At each measurement time, t_m, in the batch:

      i). Compute the value of the mean longitude at the measurement time t_m,

$$\lambda_m = \lambda_{initial}(i) + \sqrt{\frac{\mu_E}{a^3}}(t_m - t_{initial}) \qquad (10.3\text{-}1)^*$$

      Using the algorithm defined in Section 8.3.2, convert the equinoctial elements $(a, h, k, p, q, \lambda_m)$ to obtain the position and velocity vectors at t_m, $\overline{R}(t_m), \dot{\overline{R}}(t_m)$.

      ii). Compute predicted measurements for all visible GPS SVs at time t_m, using the following equations:

$$\text{For pseudorange: } \Re^n_{G/W_j}(t_m) = \rho^n_{G/W_j}(t_m) + b_R - c\left(\delta t_{Sj}\right)_{L1} \qquad (10.3\text{-}2)^*$$

$$\text{For Doppler: } \left(F_D(t_m)\right)^n_{G/W_j} = F_T\left[-\frac{\dot{\rho}^n_{G/W_j}(t_m)}{c} + a_{1j} - \frac{{d_R}^n}{c} + \frac{1}{2c^2}\left(\left|\dot{\overline{R}}^n\right|^2 - \left|\dot{\overline{R}}_{G/W_j}\right|^2\right) + \frac{\mu}{c^2}\left(\frac{1}{\left|\overline{R}^n\right|} - \frac{1}{\left|\overline{R}_{G/W_j}\right|}\right) - (\delta F_{rel})_{cor}\right] \qquad (10.3\text{-}3)^*$$

      The terms $\rho^n_{G/W_j}(t_m), \left(\delta t_{Sj}\right)_{L1}, F_T, \dot{\rho}^n_{G/W_j}(t_m), \dot{\overline{R}}_{G/W_j}, (\delta F_{rel})_{cor}$ are defined in Sections 5.3.2 and 5.3.3 of this document.

      iii). Compute measurement residuals for all visible GPS SVs.

$$\text{For Pseudorange: } \Delta\rho_j(t_m) = \rho_{obs_j}(t_m) - \Re^n_{G/W_j}(t_m)$$

$$\text{For Doppler: } \Delta f_j(t_m) = f_{obs_j}(t_m) - \left(F_D(t_m)\right)^n_{G/W_j}$$

iv). Accumulate the sum of the residuals and the sum of the squares of the residuals over the measurements in the batch.

For Pseudorange :

$$\sum_{n=1}^{m}\left(\Delta\rho(t_n)\right)=\sum_{n=1}^{m-1}\left(\Delta\rho(t_n)\right)+\sum_{j}\left(\Delta\rho_j(t_m)\right)$$

$$\sum_{n=1}^{m}\left(\Delta\rho(t_n)\right)^2=\sum_{n=1}^{m-1}\left(\Delta\rho(t_n)\right)^2+\sum_{j}\left(\Delta\rho_j(t_m)\right)^2$$

For Doppler :

$$\sum_{n=1}^{m}\left(\Delta f(t_n)\right)=\sum_{n=1}^{m-1}\left(\Delta f(t_n)\right)+\sum_{j}\left(\Delta f_j(t_m)\right)$$

$$\sum_{n=1}^{m}\left(\Delta f(t_n)\right)^2=\sum_{n=1}^{m-1}\left(\Delta f(t_n)\right)^2+\sum_{j}\left(\Delta f_j(t_m)\right)^2$$

b. Compute the the mean value, mean squared value, and standard deviation of the measurement residuals over the batch

For Pseudorange :

$$E\left[\Delta\rho(\lambda_{initial}(i))\right]=\frac{1}{M}\sum_{n=1}^{M}\left(\Delta\rho(t_n)\right)$$

$$E\left[\left(\Delta\rho(\lambda_{initial}(i))\right)^2\right]=\frac{1}{M}\sum_{n=1}^{M}\left(\Delta\rho(t_n)\right)^2$$

$$\sigma_\rho(\lambda_{initial}(i))=\sqrt{E\left[\left(\Delta\rho(\lambda_{initial}(i))\right)^2\right]-E\left[\Delta\rho(\lambda_{initial}(i))\right]^2}$$

For Doppler :

$$E\left[\Delta f(\lambda_{initial}(i))\right]=\frac{1}{M}\sum_{n=1}^{M}\left(\Delta f(t_n)\right)$$

$$E\left[\left(\Delta f(\lambda_{initial}(i))\right)^2\right]=\frac{1}{M}\sum_{n=1}^{M}\left(\Delta f(t_n)\right)^2$$

$$\sigma_f(\lambda_{initial}(i))=\sqrt{E\left[\left(\Delta f(\lambda_{initial}(i))\right)^2\right]-E\left[\Delta f(\lambda_{initial}(i))\right]^2}$$

2. Determine the best $\lambda_{initial}^{\min}$ as the value that produces the smallest pseudorange residual standard deviations if pseudorange measurements are available or otherwise the value that produces the smallest Doppler residual standard deviations.

3. Set time bias error flag if there are measurements from only one GPS SV. Otherwise, compute the receiver clock bias and clock bias rate corrections as the mean of the pseudorange and Doppler residuals, respectively, for the best $\lambda_{initial}^{\min}$.

$$\Delta b_R = E\left[\Delta\rho(\lambda_{initial}^{\min})\right]$$
$$\Delta d_R = -\frac{c}{F_T} E\left[\Delta f(\lambda_{initial}^{\min})\right]$$

and update the current value of the receiver clock bias and clock bias rate

$$b_R = b_R + \Delta b_R$$
$$d_R = d_R + \Delta d_R$$

10.4 Golden Section Search for Minimum

The Golden Section Search method can be used to find the location of a minimum when the minimum has been bracketed. A minimum is known to be bracketed in the interval (a, c) if there is a triplet of points, a<b<c, such that $f(b) < f(a)$ and $f(b) < f(c)$. The following description is based on that provided in Reference 34. The Golden Section Search method is analogous to the bisection method, which is used to search for the root of a function.

The search method consists of choosing a new point x, either between a and b or between b and c, evaluating $f(x)$, and then selecting a new bracketing triple of points. For example, if b<x<c is selected and $f(b) < f(x)$, the new bracketing triplet of points is (a, b, x). Otherwise, if $f(b) > f(x)$, the new bracketing triplet of points is (b, x, c). The middle point of the new triplet is the abscissa whose ordinate is the best minimum achieved so far. The process of bracketing is continued until the distance between the two outer points of the triplet is tolerably small.

In this application, the search is performed to find the value of $\lambda_{initial}^{\min}$ that minimizes the standard deviation of the measurement residuals. The search method consists of the following steps, given the following input values, in addition to the Broadcast ephemeris associated with each GPS SV tracked during the measurement data arc:

$a, h, k, p, q =$ nominal equinoctial orbital elements

$t_{initial} =$ initialization time

$[\rho_{obs}(t_m), f_{obs}(t_m), t_m] =$ batch of M observed pseudorange or Doppler measurements, nominally at 1-minute intervals

$\lambda_{initial}^{\min} =$ initial best estimate for $\lambda_{initial}$ that minimizes standard deviation of the measurement residuals (radians)

$\Delta\lambda =$ size of increment in λ (radians)

$b_R =$ current value of the receiver time bias (meters)

$d_R =$ current value of the receiver time bias rate (meters per second)

$\varepsilon =$ convergence tolerance, nominally equal to 10^{-7}

$I_{\max}^{Golden} =$ maximum number of iterations, nominally equal to 50

R= 0.61803 39887 49894

C= (1-R)= 0.38196 60112 50105

1. Set the initial values for the search as follows:

$$\lambda_{initial}(0) = \lambda_{initial}^{\min} - \Delta\lambda/2$$
$$\lambda_{initial}(3) = \lambda_{initial}^{\min} + \Delta\lambda/2$$
$$\lambda_{initial}(1) = \lambda_{initial}^{\min} - C\left(\lambda_{initial}^{\min} - \lambda_{initial}(0)\right)$$
$$\lambda_{initial}(2) = \lambda_{initial}^{\min}$$

2. Evaluate the residual standard deviation functions $f(\lambda_{initial}(1))$ and $f(\lambda_{initial}(2))$, where $f(\lambda_{initial}(i)) = \sigma_\rho(\lambda_{initial}(i))$ for pseudorange measurements or $f(\lambda_{initial}(i)) = \sigma_f(\lambda_{initial}(i))$ for Doppler measurements, using the following algorithm:

   a. At each measurement time, t_m, in the batch:

      i). Compute the value of the mean longitude at the measurement time t_m,

$$\lambda_m = \lambda_{initial}(i) + \sqrt{\frac{\mu_E}{a^3}}\left(t_m - t_{initial}\right) \qquad (10.4\text{-}1)^*$$

      Using the algorithm defined in Section 8.3.2, convert the equinoctial elements $(a, h, k, p, q, \lambda_m)$ to obtain the position and velocity vectors at t_m, $\bar{R}(t_m), \dot{\bar{R}}(t_m)$.

      ii). Compute predicted measurements for all visible GPS SVs at time t_m, using the following equations:

$$\text{For Pseudorange}: \Re^n_{G/W_j}(t_m) = \rho^n_{G/W_j}(t_m) + b_R - c\left(\delta t_{Sj}\right)_{L1} \qquad (10.4\text{-}2)^*$$

$$\text{For Doppler}: \left(F_D(t_m)\right)^n_{G/W_j} = F_T\left[-\frac{\dot{\rho}^n_{G/W_j}(t_m)}{c} + a_{1j} - \frac{\dot{d}_R{}^n}{c} + \frac{1}{2c^2}\left(\left|\dot{\bar{R}}^n\right|^2 - \left|\dot{\bar{R}}_{G/W_j}\right|^2\right) + \frac{\mu}{c^2}\left(\frac{1}{\left|\bar{R}^n\right|} - \frac{1}{\left|\bar{R}_{G/W_j}\right|}\right) - (\delta F_{rel})_{cor}\right] \qquad (10.4\text{-}3)^*$$

      The terms $\rho^n_{G/W_j}(t_m), \left(\delta t_{Sj}\right)_{L1}, F_T, \dot{\rho}^n_{G/W_j}(t_m), \dot{\bar{R}}_{G/W_j}, (\delta F_{rel})_{cor}$ are defined in Sections 5.3.2 and 5.3.3 of this document.

      iii). Compute measurement residuals for all visible GPS SVs.

$$\text{For Pseudorange}: \Delta\rho_j(t_m) = \rho_{obs_j}(t_m) - \Re^n_{G/W_j}(t_m)$$

$$\text{For Doppler}: \Delta f_j(t_m) = f_{obs_j}(t_m) - \left(F_D(t_m)\right)^n_{G/W_j}$$

iv). Accumulate the sum of the residuals and the sum of the squares of the residuals over the measurements in the batch.

For Pseudorange :

$$\sum_{n=1}^{m}\left(\Delta\rho(t_n)\right) = \sum_{n=1}^{m-1}\left(\Delta\rho(t_n)\right) + \sum_j\left(\Delta\rho_j(t_m)\right)$$

$$\sum_{n=1}^{m}\left(\Delta\rho(t_n)\right)^2 = \sum_{n=1}^{m-1}\left(\Delta\rho(t_n)\right)^2 + \sum_j\left(\Delta\rho_j(t_m)\right)^2$$

For Doppler :

$$\sum_{n=1}^{m}\left(\Delta f(t_n)\right) = \sum_{n=1}^{m-1}\left(\Delta f(t_n)\right) + \sum_j\left(\Delta f_j(t_m)\right)$$

$$\sum_{n=1}^{m}\left(\Delta f(t_n)\right)^2 = \sum_{n=1}^{m-1}\left(\Delta f(t_n)\right)^2 + \sum_j\left(\Delta f_j(t_m)\right)^2$$

b. Compute the the mean value, mean squared value, and standard deviation of the measurement residuals over the batch

For Pseudorange :

$$E\left[\Delta\rho(\lambda_{initial}(i))\right] = \frac{1}{M}\sum_{n=1}^{M}\left(\Delta\rho(t_n)\right)$$

$$E\left[\left(\Delta\rho(\lambda_{initial}(i))\right)^2\right] = \frac{1}{M}\sum_{n=1}^{M}\left(\Delta\rho(t_n)\right)^2$$

$$\sigma_\rho(\lambda_{initial}(i)) = \sqrt{E\left[\left(\Delta\rho(\lambda_{initial}(i))\right)^2\right] - E\left[\Delta\rho(\lambda_{initial}(i))\right]^2}$$

For Doppler :

$$E\left[\Delta f(\lambda_{initial}(i))\right] = \frac{1}{M}\sum_{n=1}^{M}\left(\Delta f(t_n)\right)$$

$$E\left[\left(\Delta f(\lambda_{initial}(i))\right)^2\right] = \frac{1}{M}\sum_{n=1}^{M}\left(\Delta f(t_n)\right)^2$$

$$\sigma_f(\lambda_{initial}(i)) = \sqrt{E\left[\left(\Delta f(\lambda_{initial}(i))\right)^2\right] - E\left[\Delta f(\lambda_{initial}(i))\right]^2}$$

3. Perform iterative search until the distance between the two outer points is tolerably small. Use $f(\lambda_{initial}(i)) = \sigma_p(\lambda_{initial}(i))$ if pseudorange measurements are available and $f(\lambda_{initial}(i)) = \sigma_f(\lambda_{initial}(i))$ if only Doppler measurements are available.

Do until $\left|\lambda_{initial}(3) - \lambda_{initial}(0)\right| < \varepsilon\left[\left|\lambda_{initial}(1)\right| + \left|\lambda_{initial}(2)\right|\right]$,

If $f(\lambda_{initial}(2)) < f(\lambda_{initial}(1))$,

$$\lambda_{initial}(0) = \lambda_{initial}(1)$$
$$\lambda_{initial}(1) = \lambda_{initial}(2)$$
$$\lambda_{initial}(2) = R * \lambda_{initial}(1) + C * \lambda_{initial}(3)$$
$$f(\lambda_{initial}(1)) = f(\lambda_{initial}(2))$$
$$\text{Compute } f(\lambda_{initial}(2)) = \begin{cases} \sigma_\rho(\lambda_{initial}(2)) & \text{for pseudorange measurements} \\ \sigma_f(\lambda_{initial}(2)) & \text{for Doppler measurements} \end{cases} \text{ as in Step 2}$$

else

$$\lambda_{initial}(3) = \lambda_{initial}(2)$$
$$\lambda_{initial}(2) = \lambda_{initial}(1)$$
$$\lambda_{initial}(1) = R * \lambda_{initial}(2) + C * \lambda_{initial}(0)$$
$$f(\lambda_{initial}(2)) = f(\lambda_{initial}(1))$$
$$\text{Compute } f(\lambda_{initial}(1)) = \begin{cases} \sigma_\rho(\lambda_{initial}(1)) & \text{for pseudorange measurements} \\ \sigma_f(\lambda_{initial}(1)) & \text{for Doppler measurements} \end{cases} \text{ as in Step 2}$$

4. If $f(\lambda_{initial}(1)) < f(\lambda_{initial}(2))$, $\lambda_{initial}^{\min} = \lambda_{initial}(1)$

   else $\lambda_{initial}^{\min} = \lambda_{initial}(2)$

5. Set time bias error flag if there are measurements from only one GPS SV. Otherwise, compute the receiver clock bias and clock bias rate corrections as the mean of the pseudorange and Doppler residuals, respectively, for the best $\lambda_{initial}^{\min}$.

$$\Delta b_R = E\left[\Delta\rho(\lambda_{initial}^{\min})\right]$$
$$\Delta d_R = -\frac{c}{F_T} E\left[\Delta f(\lambda_{initial}^{\min})\right]$$

and update the current value of the receiver clock bias and clock bias rate

$$b_R = b_R + \Delta b_R$$
$$d_R = d_R + \Delta d_R$$

Section 11. Attitude Estimation Algorithms

The explicit form for the attitude EKF algorithms is based on the Multiplicative EKF (MEKF) defined in Reference 39. The attitude state estimation algorithm incorporates the attitude determination method using non-aligned antenna presented in Reference 40, which uses an extended Kalman filter to process GPS signal-to-noise ratio (SNR) and GPS double-difference carrier phase measurements. These algorithms have been demonstrated to provide attitude estimates in the 0.5 degree range. Section 11.1 defines the estimation state, Section 11.2 defines the state error covariance, Section 11.3 describes the state estimation processing flow, Section 11.4 discusses attitude state and covariance propagation, Section 11.5 provides the measurement models, and Section 11.6 provides an attitude state initialization procedure. These algorithms are not currently implemented but could be implemented in a future GEONS release.

11.1 Attitude Estimation State Vector

The attitude estimation problem determines the rotation that a body has experienced to take it from its nominal orientation to its current orientation, measured in the external reference frame. The attitude estimation algorithm estimates an attitude state vector, $\bar{x}_A$, for each spacecraft being estimated. The spacecraft attitude is parameterized using a unit quaternion to represent the rotation from the Mean of J2000.0 inertial reference frame to the body frame.

The unit quaternion has a three-vector part ($\bar{q}_V$) and a scalar part (q_4):

$$\bar{\bar{q}} = \begin{bmatrix} \bar{q}_V \\ q_4 \end{bmatrix} = \begin{bmatrix} \hat{e}\sin(\theta/2) \\ \cos(\theta/2) \end{bmatrix} \tag{11.1-1}$$

where $\bar{e}$ is the Euler axis of rotation and θ is the Euler angle of rotation.

The components of the attitude quaternion are also referred to as Euler symmetric parameters. The column vector of Euler symmetric parameters is a special case of the more general quaternion. For the Euler symmetric parameters, the inverse quaternion is equal to the conjugate quaternion:

$$\left(\bar{\bar{q}}\right)^{-1} = \begin{bmatrix} -\bar{q}_V \\ q_4 \end{bmatrix} \tag{11.1-2}$$

The transformation of a vector from the inertial reference frame to the spacecraft body frame is performed as follows using the attitude matrix $A_{B\leftarrow XYZ}\left(\bar{\bar{q}}\right)$

$$\left[\bar{V}\right]_B = A_{B\leftarrow XYZ}\left(\bar{\bar{q}}\right)\left[\bar{V}\right]_{XYZ} \tag{11.1-3}$$

where

$$A_{B\leftarrow XYZ}\left(\overline{\overline{q}}\right)=\left(q_4^2-\left|\overline{q}_V\right|^2\right)I_{3\times 3}-2q_4\left[\overline{q}_V\times\right]+2\overline{q}_V\overline{q}_V{}^T \tag{11.1-4}$$

and

$$\left[\overline{q}_V\times\right]\equiv\begin{bmatrix}0 & -q_3 & q_2\\ q_3 & 0 & -q_1\\ -q_2 & q_1 & 0\end{bmatrix} \tag{11.1-5}$$

or equivalently

$$A_{B\leftarrow XYZ}\left(\overline{\overline{q}}\right)=\begin{bmatrix}q_1^2-q_2^2-q_3^2+q_4^2 & 2(q_1q_2+q_3q_4) & 2(q_1q_3-q_2q_4)\\ 2(q_1q_2-q_3q_4) & -q_1^2+q_2^2-q_3^2+q_4^2 & 2(q_2q_3+q_1q_4)\\ 2(q_1q_3+q_2q_4) & 2(q_2q_3-q_1q_4) & -q_1^2-q_2^2+q_3^2+q_4^2\end{bmatrix} \tag{11.1-6}$$

The following quaternion multiplication convention is used

$$\overline{\overline{p}}\otimes\overline{\overline{q}}\equiv\begin{bmatrix}p_4\overline{q}_V+q_4\overline{p}_V-\overline{p}_V\times\overline{q}_V\\ p_4q_4-\overline{p}_V\cdot\overline{q}_V\end{bmatrix} \tag{11.1-7}$$

such that $A(\overline{\overline{p}})A(\overline{\overline{q}})=A(\overline{\overline{p}}\otimes\overline{\overline{q}})$.

The MEKF represents the true attitude as the quaternion product

$$\overline{\overline{q}}(t)=\delta\overline{\overline{q}}(\overline{\alpha}(t))\otimes\overline{\overline{q}}_{ref}(t) \tag{11.1-8}$$

where $\overline{\overline{q}}_{ref}(t)$ is the current best estimate of the true attitude unit quaternion, $\delta\overline{\overline{q}}(\overline{\alpha}(t))$ is a unit quaternion representing the rotation from $\overline{\overline{q}}_{ref}(t)$ to the true attitude $\overline{\overline{q}}(t)$. Following Reference 39, $\delta\overline{\overline{q}}(\overline{\alpha}(t))$ is parameterized such that

$$\delta\overline{\overline{q}}(\overline{\alpha}(t))=\left(1+\frac{\alpha^2}{4}\right)^{-1/2}\begin{bmatrix}\frac{\overline{\alpha}(t)}{2}\\ 1\end{bmatrix} \tag{11.1-9}$$

where $\overline{\alpha}(t)$ is a three-component representation of the attitude error in the body frame

$$\overline{\alpha}(t)=\frac{2\delta\overline{q}_V}{\delta q_4} \tag{11.1-10}$$

and $\frac{\overline{\alpha}(t)}{2}$ is commonly referred to as the Gibbs vector. The associated attitude matrices are approximated as follows

$$A(\delta\bar{\bar{q}}(\bar{\alpha}(t))) \cong I_{3\times3} - [\bar{\alpha}\times] - \frac{1}{2}\left(\alpha^2 I_{3\times3} - \bar{\alpha}\bar{\alpha}^T\right), \text{ to } 2^{\text{nd}} \text{ order in } \alpha \tag{11.1-11}$$

$$\begin{aligned} A(\bar{\bar{q}}(t)) &= A(\delta\bar{\bar{q}}(\bar{\alpha}(t)) \otimes \bar{\bar{q}}_{ref}(t)) = A(\delta\bar{\bar{q}}(\bar{\alpha}(t)))A(\bar{\bar{q}}_{ref}(t)) \\ &\cong \left(I_{3\times3} - [\bar{\alpha}\times]\right)A(\bar{\bar{q}}_{ref}(t)), \text{ to first order in } \alpha \end{aligned} \tag{11.1-12}$$

The nine component attitude state vector estimate for each spacecraft is defined as

$$\hat{\bar{x}}_A(t) = \begin{bmatrix} \hat{\bar{\alpha}}(t) \\ \Delta\hat{\bar{b}}_\omega(t) \\ \Delta\hat{\bar{s}}_{cal}(t) \end{bmatrix} \tag{11.1-13}$$

where $\Delta\hat{\bar{b}}_\omega(t)$ is a vector of estimated attitude rate errors. In the case where gyro measurements are used to compute the reference angular rate vector $\left(\bar{\omega}_{ref}(t)\right)$, $\Delta\hat{\bar{b}}_\omega(t)$ is the estimated error in the gyro drift vector. Otherwise, $\Delta\hat{\bar{b}}_\omega(t)$ is the estimated error in the angular velocity vector. Optionally, $\Delta\hat{\bar{s}}_{cal}(t)$ can be estimated, which is a vector of errors in the antenna gain calibration coefficients.

11.2 Attitude State Error Covariance Matrix

The attitude state error covariance at time t_k is defined as follows:

$$[P_A] = \begin{bmatrix} \sigma_1^2 & C_{1,2}\sigma_1\sigma_2 & \cdots & C_{1,N}\sigma_1\sigma_N \\ C_{2,1}\sigma_1\sigma_2 & \sigma_2^2 & \cdots & \cdot \\ \cdot & \cdot & \cdots & \cdot \\ \cdot & \cdot & \cdots & \cdot \\ \cdot & \cdot & \cdots & \cdot \\ \cdot & \cdot & \cdots & \cdot \\ \cdot & \cdot & \cdots & \cdot \\ \cdot & \cdot & \cdots & \cdot \\ C_{N,1}\sigma_1\sigma_N & \cdot & \cdots & \sigma_N^2 \end{bmatrix} \tag{11.2-1}$$

where

$[P_A]$ = [N × N] attitude error covariance matrix, where N equals 9

σ_i = standard deviation of the estimate of attitude state vector element i

σ_i^2 = variance of the estimate of state vector element i

$C_{i,j} = C_{j,i}$ = correlation coefficient for elements i and j, absolute value < 1

The state error covariance is initialized or reinitialized using command parameters. The initial covariance matrix is diagonal: the initial state error variances σ_i^2 are used directly in Equation 11.2-1 to form $[P_A]$ with $C_{i,i} = 1$ and off-diagonal $C_{i,j} = 0$. The covariance for individual state vector elements can be reinitialized by resetting the associated diagonal elements in the full covariance matrix to their initial values and the associated off-diagonal elements to zero. Whenever the attitude covariance is initialized or reinitialized, it is factored into components $[U_A]$ and $[D_A]$ as discussed in Section 2.2.1.

11.3 Attitude Estimation Algorithm

The EKF algorithm consists of the following three major processes:

1. **Attitude State Initialization.** This process consists of computing an initial estimate for the attitude states.
2. **Time Update**. This process consists of propagating the attitude state estimate and state error covariance from the time of the previous $(k-1)^{th}$ measurement to the time of the current $(k)^{th}$ measurement.
3. **Measurement Update**. This process consists of correcting the attitude state and covariance to include the effects of the current measurement.

These steps are described below.

11.3.1 Attitude State Initialization

At the time of the first SNR measurement, compute an initial attitude state using the algorithm provided in Section 11.6.

11.3.2 Time Update Process

The time update is performed at each time t_i, where t_i is either the time of the next valid measurement t_k or an intermediate time if the time between measurements is greater than the maximum integration step size

$$t_i = \begin{cases} t_k & ; t_k - t_{k-1} \le \delta t_{max} \\ t_{i-1} + \delta t_{max} & ; t_k - t_{k-1} > \delta t_{max} \end{cases} \qquad (11.3\text{-}1)^*$$

where δt_{max} is equal to the maximum state vector integration step size.

Given the estimated total attitude state vector at the previous measurement time (t_{k-1}) $\hat{\bar{x}}_{A_{k-1}}(+)$; associated state variables $\hat{\bar{\bar{q}}}_{ref_{k-1}}(+)$, $\hat{\bar{\omega}}_{ref_{k-1}}(+)$, $\hat{\bar{s}}_{cal_{k-1}}(+)$, and $\hat{\bar{b}}_{\omega_{k-1}}(+)$,; the state error covariance factors, $U_{A_{k-1}}(+)$ and $D_{A_{k-1}}(+)$; and a measurement at time t_k denoted by Y_k, the following steps are performed:

1. Compute the predicted attitude reference quaternion $\hat{\bar{\bar{q}}}_{ref_i}(-)$, reference angular velocity vector $\hat{\bar{\omega}}_{ref_i}(-)$, gyro bias vector $\hat{\bar{b}}_{\omega_i}(-)$, antenna gain calibration vector $\hat{\bar{s}}_{cal_i}(-)$, and the attitude state vector, $\hat{\bar{x}}_{A_i}(-)$, at the time t_i using the attitude state prediction algorithms that are defined in Section 11.4.

2 Compute the attitude state transition matrix ϕ_{A_i} and attitude process noise matrix Q_{A_i} using the algorithms defined in Section 11.4.

3. Propagate the attitude state error covariance matrix factors to the time t_i to obtain $U_{A_i}(-)$ and $D_{A_i}(-)$ using the attitude covariance propagation algorithm defined in Section 4.4.3.

   If $t_i < t_k$, set $U_{A_i}(+)=U_{A_i}(-)$, $D_{A_i}(+)=D_{A_i}(-)$, $\hat{\bar{x}}_{A_i}(+)=\hat{\bar{x}}_{A_i}(-)$, $\hat{\bar{\bar{q}}}_{ref_i}(+)=\hat{\bar{\bar{q}}}_{ref_i}(-)$, $\hat{\bar{\omega}}_{ref_i}(+)=\hat{\bar{\omega}}_{ref_i}(-)$, $\hat{\bar{b}}_{\omega_i}(+)=\hat{\bar{b}}_{\omega_i}(-)$, and $\hat{\bar{s}}_{cal_i}(+)=\hat{\bar{s}}_{cal_i}(-)$ and repeat the time update until $t_i = t_k$.

11.3.3 Measurement Update

The measurement update is performed separately for each measurement at each valid measurement time, t_k. Note that implementation of the measurement update using the hybrid batch EKF algorithm defined in Section 2.3.2.4 should be considered for processing of multiple measurements occurring during the same update time span.

If resolution of the carrier phase integers has not been successful, all SNR measurements at t_k are processed before the double-difference carrier phase (DDCP) measurements are processed. If resolution of the carrier phase integers has been successful, the SNR measurements are not processed to estimate the attitude state but are optionally processed to compute SNR calibration coefficients as discussed in Section 11.5.2.

Given the results of the time update, $\hat{\bar{x}}_{A_k}(-)$, $\hat{\bar{\bar{q}}}_{ref_k}(-)$, $\hat{\bar{\omega}}_{ref_k}(-)$, $\hat{\bar{b}}_{\omega_k}(-)$, $\hat{\bar{s}}_{cal_k}(-)$, $U_{A_k}(-)$, and $D_{A_k}(-)$ as well as the measurement variance, R_k, compute the updated total attitude state vector and related parameters, $\hat{\bar{x}}_{A_k}(+)$, $\hat{\bar{\bar{q}}}_{ref_k}(+)$, $\hat{\bar{\omega}}_{ref_k}(+)$, $\hat{\bar{b}}_{\omega_k}(+)$, and $\hat{\bar{s}}_{cal_k}(+)$ and updated state error covariance matrix factors $U_{A_k}(+)$ and $D_{A_k}(+)$, according to the following steps:

1. Compute the predicted measurement, $\hat{Y}_k$, the measurement residuals, y_k, and the measurement partial derivatives, H_k, at time t_k from

$$\hat{Y}_k = G\left[\hat{\bar{x}}_{A_k}(-),\, t_k\right] \tag{11.3-2}*$$

$$y_k = Y_k - \hat{Y}_k \tag{11.3-3}*$$

$$H_k = \left[\frac{\partial G}{\partial \bar{x}_A}\right]_{\bar{x}_A = \hat{\bar{x}}_{A_k}(-)} \tag{11.3-4}*$$

where Y_k is the actual scalar measurement. If the DDCP integer resolution is not currently successful, the measurement model equation, G, and associated partial derivatives, H, for SNR measurements are given in Section 11.5.1. If the DDCP integer resolution is currently successful, the SNR measurements can be optionally processed to estimate the antenna gain calibration coefficients using the formulas for G and H, provided in Section 11.5.2. The DDCP measurements are processed using the formulas for G and H provided in Section 11.5.3.

2. Perform the following n-sigma measurement residual edit test before updating the state vector and state error covariance matrix. The predicted measurement residual variance is computed using the U and D factors. The following algorithms were taken from References 7 and 8:

$$\bar{f} = (U^-)^T H^T \tag{11.3-5}*$$

$$v_j = D^-_{j,j} f_j \;; \quad j = 1,2,\ldots,N \tag{11.3-6}*$$

$$a_0 = R_k \tag{11.3-7}*$$

where

U^- = $U_{A_k}(-)$

D^- = the diagonal matrix $D_{A_k}(-)$

H = 1 × N measurement partial derivative matrix

R_k = measurement variance, a commanded parameter, specific to each measurement type

Then, for j = 1, 2, ..., N, compute

$$a_j = a_{j-1} + f_j\, v_j \tag{11.3-8}*$$

The predicted measurement residual variance, V_k is then computed as

$$V_k = a_{\mathrm{N}} \tag{11.3-9}*$$

4. Edit the measurement as follows:

Calculate the sigma ratio

$$S_k = \frac{y_k}{\sqrt{V_k}} \qquad (11.3\text{-}10)^*$$

If $|S_k| \le N_\sigma$, accept the measurement and continue the measurement update. If $|S_k| > N_\sigma$, reject the measurement, and exit the measurement update procedure. In these tests, N_σ is a specifiable number with a default value of 4.

5. Update the state error covariance factors for j =1, 2, ..., N, as follows:

$$D_{j,j}^{+} = D_{j,j}^{-} a_{j-1} / a_j \qquad (11.3\text{-}11)^*$$

$$b_j \leftarrow v_j \qquad (11.3\text{-}12)^*$$

$$p_j = -f_j / a_{j-1} \qquad (11.3\text{-}13)^*$$

$$\left.\begin{aligned} U_{i,j}^{+} &= U_{i,j}^{-} + b_i p_j \\ b_i &\leftarrow b_i + U_{i,j}^{-} v_j \end{aligned}\right\} \quad i = 1,2,\ldots,j-1 \qquad (11.3\text{-}14)^*$$

where *a, f,* and *v* are already available from the measurement residual variance computation and

$\leftarrow$ arrow = replacement or "writing over"

$U^{-} = U_{A_k}(-)$

$U^{+} = U_{A_k}(+)$

$D^{-} = D_{A_k}(-)$

$D^{+} = D_{A_k}(+)$

The state error covariance matrix $P_{A_k}(+)$ is computed from its measurement updated *U* and *D* factors:

$$P_{A_k}(+) = U_{A_k}(+) D_{A_k}(+) U_{A_k}^{T}(+) P_{A_k}(+) \qquad (11.3\text{-}15)^*$$

6. Compute the Kalman gain vector

$$\overline{K}_k = \overline{b} / V_k \qquad (11.3\text{-}16)^*$$

where $\overline{K}_k$ is the $[N \times 1]$ Kalman gain vector and the components of $\overline{b}$ are defined in Equation (11.3-14)

7. Update $\hat{\overline{x}}_{A_k}$

$$\hat{\bar{x}}_{A_k}(+)=\hat{\bar{x}}_{A_k}(-)+\bar{K}_k y_k \qquad (11.3\text{-}17)^*$$

and reset the reference attitude quaternion and the reference angular velocity vector

$$\hat{\bar{\bar{q}}}_{ref_k}(+) = \delta\bar{\bar{q}}(\hat{\bar{\alpha}}(+)) \otimes \hat{\bar{\bar{q}}}_{ref_k}(-) \qquad (11.3\text{-}18)^*$$

$$\hat{\bar{\omega}}_{ref_k}(+) = \hat{\bar{\omega}}_{ref_k}(-) - \Delta\hat{\bar{b}}_{\omega_k}(+) \qquad (11.3\text{-}19)^*$$

If gyro measurements are used to model the angular velocity, reset the gyro drift

$$\hat{\bar{b}}_{\omega_k}(+) = \hat{\bar{b}}_{\omega_k}(-) + \Delta\hat{\bar{b}}_{\omega_k}(+) \qquad (11.3\text{-}20)^*$$

If antenna gain calibration coefficients are being estimated, reset the calibration coefficient vector

$$\hat{\bar{s}}_{cal_k}(+) = \hat{\bar{s}}_{cal_k}(-) + \Delta\hat{\bar{s}}_{cal_k}(+) \qquad (11.3\text{-}21)^*$$

Note that in the case of DDCP measurements, these are saved as temporary updates.

8. After processing the double-difference carrier phase measurements for all GPS SVs and all spacecraft antenna baselines at time t_k, perform the integer resolution check described in Section 11.5.4 to detect incorrect assignment of the integer ambiguity. If the test is passed, the final state and covariance updates computed at time t_k are permanently applied.

11.4 Attitude State and Covariance Propagation Algorithms

Reference Quaternion Propagation

The predicted value of the reference quaternion is computed by integrating the following equation

$$\begin{aligned}\dot{\bar{\bar{q}}}_{ref}(t) &= \frac{1}{2}\begin{bmatrix}\bar{\omega}_{ref}(t)\\ 0\end{bmatrix} \otimes \bar{\bar{q}}_{ref}(t) \\ &= \frac{1}{2}\Omega\left(\bar{\omega}_{ref}(t)\right)\bar{\bar{q}}_{ref}(t)\end{aligned} \qquad (11.4\text{-}1)$$

where $\bar{\omega}_{ref}(t)$ is the best estimate of angular velocity of the reference attitude in the body frame and

$$\Omega(\bar{\omega}) \equiv \begin{bmatrix}-[\bar{\omega}\times] & \bar{\omega}\\ -\bar{\omega}^T & 0\end{bmatrix} \qquad (11.4\text{-}2)$$

Assuming that the angular velocity is nearly constant over the integration interval, Equation (11.4-1) can be analytically integrated to obtain:

$$\bar{\bar{q}}_{ref_i}(-) = \exp\left[\frac{1}{2}\Omega(\hat{\bar{\omega}}_{ref_i}(-))\Delta t_i\right] \quad \bar{\bar{q}}_{ref_{i-1}}(+) \tag{11.4-3}*$$

where, $\Delta t_i = t_i - t_{i-1}$ and following Equation C-79 in Reference 41,

$$\exp\left[\frac{1}{2}\Omega(\hat{\bar{\omega}}_{ref}(-))\Delta t\right] = I_{4\times4}\cos\left(\frac{1}{2}\omega_{ref}\Delta t\right) + \frac{1}{\omega_{ref}}\Omega(\bar{\omega}_{ref})\sin\left(\frac{1}{2}\omega_{ref}\Delta t\right)$$

$$= \begin{bmatrix} \cos\left(\frac{1}{2}\omega_{ref}\Delta t\right) & \frac{\omega_3}{\omega_{ref}}\sin\left(\frac{1}{2}\omega_{ref}\Delta t\right) & \frac{-\omega_2}{\omega_{ref}}\sin\left(\frac{1}{2}\omega_{ref}\Delta t\right) & \frac{\omega_1}{\omega_{ref}}\sin\left(\frac{1}{2}\omega_{ref}\Delta t\right) \\ \frac{-\omega_3}{\omega_{ref}}\sin\left(\frac{1}{2}\omega_{ref}\Delta t\right) & \cos\left(\frac{1}{2}\omega_{ref}\Delta t\right) & \frac{\omega_1}{\omega_{ref}}\sin\left(\frac{1}{2}\omega_{ref}\Delta t\right) & \frac{\omega_2}{\omega_{ref}}\sin\left(\frac{1}{2}\omega_{ref}\Delta t\right) \\ \frac{\omega_2}{\omega_{ref}}\sin\left(\frac{1}{2}\omega_{ref}\Delta t\right) & \frac{-\omega_1}{\omega_{ref}}\sin\left(\frac{1}{2}\omega_{ref}\Delta t\right) & \cos\left(\frac{1}{2}\omega_{ref}\Delta t\right) & \frac{\omega_3}{\omega_{ref}}\sin\left(\frac{1}{2}\omega_{ref}\Delta t\right) \\ \frac{-\omega_1}{\omega_{ref}}\sin\left(\frac{1}{2}\omega_{ref}\Delta t\right) & \frac{-\omega_2}{\omega_{ref}}\sin\left(\frac{1}{2}\omega_{ref}\Delta t\right) & \frac{-\omega_3}{\omega_{ref}}\sin\left(\frac{1}{2}\omega_{ref}\Delta t\right) & \cos\left(\frac{1}{2}\omega_{ref}\Delta t\right) \end{bmatrix} \tag{11.4-4}*$$

where $\omega_{ref} = \left|\hat{\bar{\omega}}_{ref}(-)\right|$ and $\omega_1, \omega_2, \omega_3$ are the components of $\hat{\bar{\omega}}_{ref}(-)$.

Reference Angular Velocity Propagation Using Gyro Measurements

In the case where a set of gyros provides angular rate measurements in the body frame $(\bar{\omega}_{gyro}(t))$, the true angular velocity is defined as

$$\bar{\omega}(t_i) = \bar{\omega}_{gyro}(t_i) - \bar{b}_{\omega}(t_i) - \bar{\eta}_b(t_i) \tag{11.4-5}$$

where $\bar{\eta}_b(t_i)$ is a zero-mean white noise process with standard deviation σ_b for all components. The predicted angular velocity expressed in the body frame is computed as follows

$$\hat{\bar{\omega}}_{ref_i}(-) = \bar{\omega}_{gyro}(t_i) - \hat{\bar{b}}_{\omega_i}(-) \tag{11.4-6}*$$

where $\hat{\bar{b}}_{\omega_i}(-)$ is the predicted value of the gyro drift.

Gyro Drift Vector Propagation

The state equation for the true gyro drift is defined as

$$\dot{\bar{b}}_w(t_i) = \bar{\eta}_{\dot{b}}(t_i) \tag{11.4-7}$$

where $\bar{\eta}_{\dot{b}}(t_i)$ is a zero-mean white noise process with standard deviation $\sigma_{\dot{b}}$ for all components. A random walk model is used to model the gyro drift rate noise; therefore, the gyro drift is constant over the propagation interval

$$\hat{\bar{b}}_{\omega_i}(-) = \hat{\bar{b}}_{\omega_{i-1}}(+) \tag{11.4-8}*$$

Reference Angular Velocity Propagation Without Gyro Measurements

Alternatively, if a set of gyros is not used to provide the angular rates, $\hat{\bar{\omega}}_{ref_i}(-)$ is computed by numerically integrating Euler's equations using the fourth-order Runge-Kutta integrator defined in Section 4.2:

$$I\,\dot{\bar{\omega}} = -\bar{\omega} \times (I\,\bar{\omega}) + \bar{T} \tag{11.4-9}*$$

where I is the moment of inertial tensor expressed in the body frame (commanded parameters). $\bar{T}$ is the sum of external torques expressed in the body frame. In GEONS,

$$\bar{T} = \bar{T}_{GG} + \bar{T}_{external} \tag{11.4-10}*$$

where $\bar{T}_{GG}$ is the gravity gradient torque and additional external torques $\bar{T}_{external}$ can be provided via command input. The gravity gradient torque is modeled as follows

$$\bar{T}_{GG} = \frac{3\mu_E}{R^3}\left[\hat{r}_B \times \left(I \cdot \hat{r}_B\right)\right] \tag{11.4-11}*$$

where $R = \left|\bar{R}(t_k)\right|$, the magnitude of the spacecraft position vector. The unit vector $\hat{r}_B$ along the spacecraft position vector expressed in the body frame is computed by

$$\hat{r}_B = \frac{\bar{r}_B(t_k)}{R} = \frac{A(\hat{\bar{\bar{q}}}_{ref_k}(-))\bar{R}(t_k)}{R} \tag{11.4-12}*$$

Antenna Calibration Coefficient Vector Propagation

The predicted antenna gain calibration coefficient vector propagates as a constant:

$$\hat{\bar{s}}_{cal_i}(-) = \hat{\bar{s}}_{cal_{i-1}}(+) \tag{11.4-13}*$$

Attitude State Vector Propagation

The state equations for the attitude error vector, attitude rate errors, and antenna gain coefficient errors are as follows

$$\dot{\bar{\alpha}}(t_i) = -\bar{\omega}_{ref}(t_i) \times \bar{\alpha}(t_i) - \Delta\bar{b}_{\omega} - \bar{\eta}_b \tag{11.4-14}$$

$$\Delta\dot{\bar{b}}_w(t_i) = \bar{\eta}_{\dot{b}}(t_i) \tag{11.4-15}$$

$$\Delta\bar{s}_{cal}(t_i) = \bar{\eta}_s(t_i) \tag{11.4-16}$$

where $\bar{\eta}_b(t_i)$, $\bar{\eta}_{\dot{b}}(t_i)$, and $\bar{\eta}_s(t_i)$ are zero-mean white noise processes with standard deviations σ_b, $\sigma_{\dot{b}}$, and σ_s for all components, respectively. Since the attitude state vector estimates $\hat{\bar{x}}_A(t)$ are used to reset the values of $\bar{q}_{ref_i}(+)$, $\hat{\bar{\omega}}_{ref_i}(+)$, $\hat{\bar{b}}_{\omega_i}(+)$, and $\hat{\bar{s}}_{cal_i}(+)$ in step 7 of the measurement update process, the predicted values for the attitude state vector components are identically zero:

$$\hat{\bar{x}}_{A_i}(-) = \begin{bmatrix} \hat{\bar{\alpha}}_i(-) \\ \Delta\hat{\bar{b}}_{\omega_i}(-) \\ \Delta\hat{\bar{s}}_{cal_i}(-) \end{bmatrix} = \begin{bmatrix} 0 \\ 0 \\ 0 \end{bmatrix} \tag{11.4-17}*$$

Attitude State Transition Matrix

The attitude state transition matrix is obtained by analytically integrating the following state equation

$$\frac{d\hat{\bar{x}}_A(t_i)}{dt} = \frac{d}{dt}\begin{bmatrix} \hat{\bar{\alpha}}_i \\ \Delta\hat{\bar{b}}_{\omega_i} \\ \Delta\hat{\bar{s}}_{cal_i} \end{bmatrix} = \begin{bmatrix} \left[-\hat{\bar{\omega}}_{ref}\times\right] & -I_{3\times3} & 0_{3\times3} \\ 0_{3\times3} & 0_{3\times3} & 0_{3\times3} \\ 0_{3\times3} & 0_{3\times3} & 0_{3\times3} \end{bmatrix}\begin{bmatrix} \hat{\bar{\alpha}}_i \\ \Delta\hat{\bar{b}}_{\omega_i} \\ \Delta\hat{\bar{s}}_{cal_i} \end{bmatrix} \tag{11.4-18}$$

assuming that the angular velocity is nearly constant over the integration interval, to obtain

$$\hat{\bar{x}}_{A_i}(-) = \exp\left(F\,\Delta t_i\right)\,\hat{\bar{x}}_{A_{i-1}}(+) \tag{11.4-19}$$

where

$$F = \begin{bmatrix} \left[-\hat{\bar{\omega}}_{ref}\times\right] & -I_{3\times3} & 0_{3\times3} \\ 0_{3\times3} & 0_{3\times3} & 0_{3\times3} \\ 0_{3\times3} & 0_{3\times3} & 0_{3\times3} \end{bmatrix} \tag{11.4-20}$$

Taking the partial derivatives of Equation (11.4-19) yields

$$\phi_{A_i} = \frac{\partial \overline{x}_A^n(t_i)^T}{\partial \overline{x}_A^n(t_{i-1})} = \exp\left(F\,\Delta t_i\right) = \begin{bmatrix} \exp\left(\left[-\hat{\overline{\omega}}_{ref} \times\right]\Delta t_i\right) & -\psi_i & 0_{3\times3} \\ 0_{3\times3} & I_{3\times3} & 0_{3\times3} \\ 0_{3\times3} & 0_{3\times3} & I_{3\times3} \end{bmatrix} \qquad (11.4\text{-}21)^*$$

where $\hat{\overline{\omega}}_{ref} = \hat{\overline{\omega}}_{ref_i}(-)$, $\omega_{ref} = \left|\hat{\overline{\omega}}_{ref}(-)\right|$, and

$$\psi_i = I\Delta t_i + \left[-\hat{\overline{\omega}}_{ref} \times\right]\left(1 - \cos(\omega_{ref}\Delta t_i)\right)/\,\omega_{ref}^2 + \left[\hat{\overline{\omega}}_{ref} \times\right]^2\left(\omega_{ref}\Delta t_i - \sin(\omega_{ref}\Delta t_i)\right)/\,\omega_{ref}^3 \qquad (11.4\text{-}22)^*$$

Attitude Process Noise Matrix

The attitude process noise matrix, Q_{A_i}, is given by

$$Q_{A_i} = \int_{t_{k-1}}^{t_k} \phi_{A_i} G(\tau) Q(\tau) G^T(\tau) {\phi_{A_i}}^T d\tau \qquad (11.4\text{-}23)$$

where

$$G(\tau) = \begin{bmatrix} -I_{3\times3} & 0_{3\times3} & 0_{3\times3} \\ 0_{3\times3} & I_{3\times3} & 0_{3\times3} \\ 0_{3\times3} & 0_{3\times3} & I_{3\times3} \end{bmatrix} \qquad (11.4\text{-}24)$$

$$Q(\tau) = \begin{bmatrix} \sigma_b^2 I_{3\times3} & 0_{3\times3} & 0_{3\times3} \\ 0_{3\times3} & \sigma_{\dot{b}}^2 I_{3\times3} & 0_{3\times3} \\ 0_{3\times3} & 0_{3\times3} & \sigma_s^2 I_{3\times3} \end{bmatrix} \qquad (11.4\text{-}25)$$

Which yields

$$Q_{A_i} = \begin{bmatrix} \sigma_b^2 \Delta t_i I_{3\times3} + \sigma_{\dot{b}}^2 \Delta t_i \psi_i {\psi_i}^T & -\sigma_{\dot{b}}^2 \Delta t_i \psi_i & 0_{3\times3} \\ -\sigma_{\dot{b}}^2 \Delta t_i {\psi_i}^T & \sigma_{\dot{b}}^2 \Delta t_i I_{3\times3} & 0_{3\times3} \\ 0_{3\times3} & 0_{3\times3} & \sigma_s^2 \Delta t_i I_{3\times3} \end{bmatrix} \qquad (11.4\text{-}26)^*$$

11.5 Attitude Measurement Models

The attitude estimator processes both SNR and double-differenced GPS carrier phase measurements.

11.5.1 SNR Measurement Model and Partial Derivatives

The GPS SNR measurement is a measurement of the signal strength of a received GPS signal, which is also referred to as the antenna gain. Assuming that the antenna's gain pattern is known and is invariant in the spacecraft body frame, the received signal strength is dependent on the relationship between the direction of the antenna boresight vector, which is constant in the body frame, and the line-of-sight vector to the receiving antenna to the GPS SV transmitter. The observed SNR measurements (SNR) are either scaled by an uplinked value for the maximum SNR ($SNR_{\max}$) or used in the antenna calibration equation to form a measurement that is consistent with the cosine of the elevation angle of the transmitting GPS SV with respect to the receiving antenna boresight vector:

$$Y_k = \begin{cases} s_0 + s_1 SNR + s_2 SNR^2, \text{ if self - calibration coefficients are available} \\ \dfrac{SNR}{SNR_{\max}}, \text{otherwise} \end{cases} \qquad (11.5\text{-}1)^*$$

where (s_0, s_1, s_2) are components of the antenna gain calibration coefficient vector $\bar{s}_{cal}$, which can be commanded or optionally computed using the self-calibration algorithm defined in Section 11.5.2.

The predicted SNR measurement for antenna p on satellite n is computed as follows:

$$\hat{Y}_k = \hat{S}^{n,p}_{G_j}(t_k) = \left[\bar{B}^{n,p}\right]_B \cdot \left[\hat{u}^n_{G_j}(\hat{\bar{\bar{q}}}_{ref_k}(-))\right]_B \qquad (11.5\text{-}2)^*$$

where

$\left[\bar{B}^{n,p}\right]_B$ = Boresight unit vector for antenna p on satellite n expressed in the body frame (commanded values)

$\left[\hat{u}^n_{G_j}(\hat{\bar{\bar{q}}}_{ref_k}(-))\right]_B$ = Line-of-sight unit vector from receiving satellite n to the GPS transmitter j expressed in the body frame

The line-of-sight vector in the body frame is computed as follows using the predicted value of the quaternion at the measurement time:

$$\left[\hat{u}^n_{G_j}(\hat{\bar{\bar{q}}}_{ref_k}(-))\right]_B = A(\hat{\bar{\bar{q}}}_{ref_k}(-))\left[\hat{u}^n_{G_j}(t_k)\right]_{XYZ} \qquad (11.5\text{-}3)^*$$

where the line-of-sight vector in the inertial reference frame is given by:

$$\left[\hat{u}^n_{G_j}(t_k)\right]_{XYZ} = \frac{\bar{R}_{G_j}(t_T) - \bar{R}(t_R)}{\left|\bar{R}_{G_j}(t_T) - \bar{R}(t_R)\right|} \qquad (11.5\text{-}4)^*$$

In Equation (11.5-4), the position of the transmitting antenna of the GPS SV at the time (t_T) of signal transmission is denoted by $\overline{R}_{G_j}(t_T)$, and the position of the receiver pon satellite n at the time of the signal reception (t_R) is denoted by $\overline{R}(t_R)$.

Similarly, the observed SNR measurement for antenna p on satellite n can be expressed as follows in terms of the true quaternion $\overline{\overline{q}}(t_k)$

$$Y_k = S_{G_j}^{n,p}(t_k) = \left[\overline{B}^{n,p}\right]_B \cdot \left[\hat{u}_{G_j}^n(\overline{\overline{q}}(t_k))\right]_B \tag{11.5-5}$$

where the true line-of-sight vector can be expressed by

$$\begin{aligned}\left[\hat{u}_{G_j}^n(\overline{\overline{q}}(t_k))\right]_B &= A_{B\leftarrow XYZ}(\overline{\overline{\hat{q}}})\left[\hat{u}_{G_j}^n(t_k)\right]_{XYZ} \\ &= A(\delta\overline{\overline{q}}(\overline{\alpha}(t))A(\overline{\overline{\hat{q}}}_{ref_k}(-))\left[\hat{u}_{G_j}^n(t_k)\right]_{XYZ} \\ &= A(\delta\overline{\overline{q}}(\overline{\alpha}(t))\left[\hat{u}_{G_j}^n(\overline{\overline{\hat{q}}}_{ref_k}(-))\right]_B\end{aligned} \tag{11.5-6}$$

Expanding Equation 11.5-5 to first order in $\overline{\alpha}$ about the predicted reference yields:

$$\begin{aligned}Y_k &= \left[\overline{B}^{n,p}\right]_B \cdot (I_{3\times 3} - [\overline{\alpha}\times])\left[\hat{u}_{G_j}^n(\overline{\overline{\hat{q}}}_{ref_k}(-))\right]_B \\ &= \left[\overline{B}^{n,p}\right]_B \cdot \left[\hat{u}_{G_j}^n(\overline{\overline{\hat{q}}}_{ref_k}(-))\right]_B + \left[\overline{B}^{n,p}\right]_B \cdot \left[\left[\hat{u}_{G_j}^n(\overline{\overline{\hat{q}}}_{ref_k}(-))\right]_B \times\right]\overline{\alpha}\end{aligned} \tag{11.5-7}$$

The associated measurement partial derivatives are as follows:

$$H_k = \left(\frac{\partial S_{G_j}^{n,p}(t_k)}{\partial \overline{x}_A^n}\right) = \left[\left[\overline{B}^{n,p}\right]_B \cdot \left[\left[\hat{u}_{G_j}^n(\overline{\overline{\hat{q}}}_{ref_k}(-))\right]_B \times\right] \quad 0_{1\times 3} \quad 0_{1\times 3}\right] \tag{11.5-8}*$$

Note that when the SNR measurements are processed to determine the spacecraft attitude error, the antenna gain calibration vector is not estimated (i.e. the associated measurement partial derivations are set to 0).

11.5.2 Self Calibration Using SNR Measurements

The SNR method of attitude determination works best when a calibration of the receiving antenna gain pattern is available. Therefore, when the DDCP integer resolution is successful, antenna self-calibration is optionally performed using the SNR measurements. The self-calibration is performed by using the estimated attitude state and calibrating the SNR map as if the estimated attitude state is error-free. The coefficients $\overline{s}_{cal} = \begin{bmatrix} s_0 & s_1 & s_2 \end{bmatrix}^T$ of a third-degree polynomial are fit to the calibration data. This calibration model assumes that all GPS SV transmitting antennas have

similar characteristics and all receiving antennas on a given spacecraft have similar gain patterns that are symmetric around the boresight. After the calibration coefficient covariance falls below a specified value, the calibration polynomial is available for use in Equation 11.5-1 to process SNR measurements for attitude state estimation in the event that the carrier phase integer resolution procedure fails and carrier phase measurement updates are not performed.

The calibration polynomial is fit to the dot product between the line-of-sight unit vector and the antenna boresight unit vector. The "observed" measurement is given by

$$Y_k = \left[\overline{B}^{n,p}\right]_B \cdot \left[\hat{u}^n_{G_j}(\bar{\bar{\hat{q}}}_{ref_k}(-)\right]_B \qquad (11.5\text{-}9)^*$$

The line-of-sight unit vector is computed using Equations 11.5-3 and 11.5-4 using the predicted quaternion estimate obtained from processing DDCP measurements. The predicted measurement is given by

$$\hat{Y}_k = s_0 + s_1(SNR) + s_2(SNR)^2 \qquad (11.5\text{-}10)^*$$

with the following non-zero measurement partial derivatives

$$H_k = \left(\frac{\partial \hat{Y}_k}{\partial \overline{s}^n_{cal}}\right) = \begin{bmatrix} 1 & SNR & SNR^2 \end{bmatrix} \qquad (11.5\text{-}11)^*$$

11.5.3 GPS Double-Difference Carrier Phase Measurement Model and Partial Derivatives

The GPS single and double-difference carrier phase measurements are dependent on the relative position of two antennas in the reference frame. Since the relative position of the two antennas is known in the body frame, these measurements can be used to determine the spacecraft attitude.

The difference in the distance from GPS transmitter i to antennas p and q on satellite n is given by

$$\Delta\rho^{n,p,q}_{G_i}(t_k) = \rho^{n,p}_{G_i}(t_k) - \rho^{n,q}_{G_i}(t_k) = \left[\overline{b}^{n,p,q}_A\right]_B \cdot \left[\hat{u}^n_{G_i}(\bar{\bar{q}}(t_k))\right]_B \text{ (meters)} \qquad (11.5\text{-}12)$$

where $\left[\overline{b}^{n,p,q}_A\right]_B$ is the antenna baseline vector connecting antennas p and q in the body frame (in meters).

The fractional carrier phase received at each antenna is measured. The difference in the fractional carrier phase measurements from GPS transmitter i measured by antennas p and q on satellite n is given by

$$\begin{aligned}\Delta\Phi^{n,p,q}_{G_i}(t_k) &= \Phi^{n,p}_{G_i}(t_k) - \Phi^{n,q}_{G_i}(t_k) \\ &= \left[\overline{b}^{n,p,q}_A\right]_B \cdot \left[\hat{u}^n_{G_j}(\bar{\bar{q}}(t_k))\right]_B - \Delta b^{G_i}_{\phi_{p,q}}\lambda_{carrier} + \Delta\Phi^{G_i}_{RHCP_{p,q}} + \beta^n_{p,q}\end{aligned} \text{ (meters)} \qquad (11.5\text{-}13)$$

where

$\Delta b_{\phi_{p,q}}^{G_i}$ =Difference in the integer ambiguities between antennas p and q

$\Delta\Phi_{RHCP_{p,q}}^{G_i}$ =Difference in the phase due to the polarization of the incoming signal for antennas p and q

$\beta_{p,q}^{n}$ =Difference in the line biases between antennas p and q, which is due to the electrical line length from the antenna phase center to the point interior to the receiver where the measurement is actually made

The dot products in Equations 11.5-12 and 11.5-13 are independent of the coordinate frame used to express the vectors. For the GEONS implementation, the computations are performed in the Body frame. The antenna baseline vector connecting antenna p and antenna q is computed as follows in terms of the known antenna offsets in the body frame:

$$\left[\bar{b}_A^{n,p,q}\right]_B = \left(\left[\bar{r}^{\,n}_{A_p}\right]_B - \left[\bar{r}^{\,n}_{A_q}\right]_B\right) \quad \text{(meters)} \tag{11.5-14}$$

where

$$\left[\bar{r}^{\,n}_{A_p}\right]_B = \begin{bmatrix} \left(\Delta x^n_{A_m}\right)_B \\ \left(\Delta y^n_{A_m}\right)_B \\ \left(\Delta z^n_{A_m}\right)_B \end{bmatrix} \tag{11.5-15}*$$

where $\left[\left(\Delta x^n_{A_m}\right)_B \quad \left(\Delta y^n_{A_m}\right)_B \quad \left(\Delta z^n_{A_m}\right)_B\right]$ are the coordinates of the antenna in the body frame, which are commanded parameters.

For convenience, the antenna baselines are defined with respect to antenna 1 such that

$$\left[\bar{b}_A^{n,p,1}\right]_B = \left(\left[\bar{r}_{A_p}\right]_B - \left[\bar{r}_{A_1}\right]_B\right),\ p = 2,..,N_{antennas\,/\,satellite} \tag{11.5-16}*$$

where, for convenience, antenna 1 is selected to be the closest to zenith pointing. The line-of-sight unit vector is computed using Equations 11.5-3 and 11.5-4. Following the approach presented in Reference 42, the polarization phase correction $\Delta\Phi_{RHCP_{p,q}}^{G_i}$ is computed as follows

$$\Delta\Phi_{RHCP_{p,q}}^{G_i} = \Phi_{RHCP_p}^{G_i}(t_k) - \Phi_{RHCP_q}^{G_i}(t_k) \tag{11.5-17}*$$

where

$$\Phi_{RHCP_p}^{G_i}(t_k) = \frac{\lambda_{carrier}}{2\pi}\left[\arctan\left(\frac{T_{21} + eT_{12}}{T_{11} - eT_{22}}\right)\right] \quad \text{(in meters)} \tag{11.5-18}*$$

where e is the ellipticity of the E-field vector and T_{ij} are components of the GPS transmitter to receiving antenna rotation matrix $T_{A_p \leftarrow TR}$, where

$$T_{A_p \leftarrow TR} = \left(T_{XYZ \leftarrow B} T_{B \leftarrow A_P}\right)^T T_{XYZ \leftarrow TR} \tag{11.5-19}*$$

The rotation matrix from the body frame to the inertial frame $T_{XYZ \leftarrow B}$, is computed as follows in terms of the attitude matrix.

$$T_{XYZ \leftarrow B} = A^T_{B \leftarrow XYZ}\left(\bar{\bar{\hat{q}}}_{ref_k}(-)\right) \tag{11.5-20}*$$

The rotation from the receiving antenna frame to the body frame, $T_{B \leftarrow A_P}$, is computed as follows

$$T_{B \leftarrow A_P} = \begin{bmatrix} \hat{x}_B \cdot \hat{x}_{A_p} & \hat{x}_B \cdot \hat{y}_{A_p} & \hat{x}_B \cdot \hat{z}_{A_p} \\ \hat{y}_B \cdot \hat{x}_{A_p} & \hat{y}_B \cdot \hat{y}_{A_p} & \hat{y}_B \cdot \hat{z}_{A_p} \\ \hat{z}_B \cdot \hat{x}_{A_p} & \hat{z}_B \cdot \hat{y}_{A_p} & \hat{z}_B \cdot \hat{z}_{A_p} \end{bmatrix} \tag{11.5-21}*$$

For a distant transmitter such as GPS, the transmitter to receiver line-of-sight vector is the same for all receiving antennas and the transmitter to Mean of J2000.0 inertial rotation matrix can be written as

$$T_{XYZ \leftarrow TR} = \begin{bmatrix} \dfrac{\sqrt{\left(\bar{\rho}^n_{G_j}\right)^2_y + \left(\bar{\rho}^n_{G_j}\right)^2_z}}{\left|\bar{\rho}^n_{G_j}\right|} & 0 & \dfrac{\left(\bar{\rho}^n_{G_j}\right)_x}{\left|\bar{\rho}^n_{G_j}\right|} \\ \dfrac{-\left(\bar{\rho}^n_{G_j}\right)_x \left(\bar{\rho}^n_{G_j}\right)_y}{\left|\bar{\rho}^n_{G_j}\right| \sqrt{\left(\bar{\rho}^n_{G_j}\right)^2_y + \left(\bar{\rho}^n_{G_j}\right)^2_z}} & \dfrac{\left(\bar{\rho}^n_{G_j}\right)_z}{\sqrt{\left(\bar{\rho}^n_{G_j}\right)^2_y + \left(\bar{\rho}^n_{G_j}\right)^2_z}} & \dfrac{\left(\bar{\rho}^n_{G_j}\right)_y}{\left|\bar{\rho}^n_{G_j}\right|} \\ \dfrac{-\left(\bar{\rho}^n_{G_j}\right)_x \left(\bar{\rho}^n_{G_j}\right)_z}{\left|\bar{\rho}^n_{G_j}\right| \sqrt{\left(\bar{\rho}^n_{G_j}\right)^2_y + \left(\bar{\rho}^n_{G_j}\right)^2_z}} & \dfrac{-\left(\bar{\rho}^n_{G_j}\right)_y}{\sqrt{\left(\bar{\rho}^n_{G_j}\right)^2_y + \left(\bar{\rho}^n_{G_j}\right)^2_z}} & \dfrac{\left(\bar{\rho}^n_{G_j}\right)_z}{\left|\bar{\rho}^n_{G_j}\right|} \end{bmatrix} \tag{11.5-22}*$$

where

$$\bar{\rho}^n_{G_j} = \bar{R}^n(t^n_R) - \bar{R}_{G_j}(t_T) \tag{11.5-23}*$$

The DDCP measurement is formed to remove the line bias contribution. The predicted DDCP measurement is computed as follows:

$$\begin{aligned} \hat{Y}_k &= \nabla\Delta\Phi^{n,p,1}_{G_{i,j}}(t_k) = \Delta\Phi^{n,p,1}_{G_i}(t_k) - \Delta\Phi^{n,p,1}_{G_j}(t_k) \\ &= \left[\bar{b}^{n,p,1}_A\right]_B \cdot \left(\left[\hat{u}^n_{G_i}\left(\bar{\bar{q}}_{ref_k}(-)\right)\right]_B - \left[\hat{u}^n_{G_j}\left(\bar{\bar{q}}_{ref_k}(-)\right)\right]_B\right) - I^{n,p,1}_{G_{i,j}}(t_k)\lambda_{\text{Carrier}} + \nabla\Delta\Phi^{n,p,1}_{RHCP_{i,j}}(t_k) \end{aligned} \quad \text{(meters)} \tag{11.5-24}*$$

where the GPS SV j is the designated Master PRN (selected as the first GPS SV for which carrier phase measurements are input at a given time). The double-difference integer ambiguity is defined as follows

$$I_{G_{i,j}}^{n,p,1}(t_k) = \left(\Delta b_{\phi_{p,1}}^{G_i} - \Delta b_{\phi_{p,1}}^{G_j}\right) \qquad (11.5\text{-}25)^*$$

and computed as discussed in Section 11.5.4. The GPS SV to spacecraft line-of-sight vector in the body frame is computed as in equation 11.5-3.

If the residual $y_k = \left(Y_k - \hat{Y}_k\right) \geq y_{\max}$, the measurement is edited. Otherwise, the associated measurement partial derivatives are computed by taking the partial derivative of the true measurement model, given by

$$\begin{aligned} Y_k &= \left[\bar{b}_A^{n,p,1}\right]_B \cdot \left(I_{3\times 3} - [\bar{a}\times]\right)\left(\left[\hat{u}_{G_i}^n(\bar{\bar{q}}_{ref_k}(-))\right]_B - \left[\hat{u}_{G_j}^n(\bar{\bar{q}}_{ref_k}(-))\right]_B\right) \\ &= \left[\bar{b}_A^{n,p,1}\right]_B \cdot \left(\left[\hat{u}_{G_i}^n(\bar{\bar{q}}_{ref_k}(-))\right]_B - \left[\hat{u}_{G_j}^n(\bar{\bar{q}}_{ref_k}(-))\right]_B\right) + \left[\bar{b}_A^{n,p,1}\right]_B \cdot \left[\left(\left[\hat{u}_{G_i}^n(\bar{\bar{q}}_{ref_k}(-))\right]_B - \left[\hat{u}_{G_j}^n(\bar{\bar{q}}_{ref_k}(-))\right]_B\right)\times\right]\bar{\alpha} \end{aligned} \qquad (11.5\text{-}26)^*$$

to obtain

$$H_k = \left(\frac{\nabla\Delta\Phi_{G_{i,j}}^{n,p,q}(t_k)}{\partial\bar{x}_A^n}\right) = \left[\left[\bar{B}^{n,p}\right]_B \cdot \left[\left(\left[\hat{u}_{G_i}^n(\bar{\bar{q}}_{ref_k}(-))\right]_B - \left[\hat{u}_{G_j}^n(\bar{\bar{q}}_{ref_k}(-))\right]_B\right)\times\right] \quad 0_{1\times 3} \quad 0_{1\times 3}\right] \qquad (11.5\text{-}27)^*$$

11.5.4 Double-Differenced Carrier Phase Integer Resolution and Residual Check

If the initial estimate of the attitude is sufficiently accurate, the double-difference integers $I_{G_{i,j}}^{n,p,1}(t_k)$ in Equation 11.5-24 can be resolved simply by assignment by rounding the measurement residual to the nearest integer:

$$I_{G_{i,j}}^{n,p,1}(t_k) = \left[\frac{Y_k - \nabla\Delta\Phi_{G_{i,j}}^{n,p,1}(t_k)}{\lambda_{\text{Carrier}}}\right]_{\text{Rounded to nearest integer}} \qquad (11.5\text{-}34)^*$$

In order to assure that the attitude estimate is sufficiently accurate, an initial integer resolution procedure is performed at each measurement epoch. After all carrier phase measurements for that epoch are processed, the measurement residuals are recomputed for all antenna baselines and all GPS SVs using the most recent attitude state estimate. These residual differences are tested against a threshold and the residual standard deviation computed for all residuals that fall below the threshold. If enough of these residuals fall below the threshold and the residual standard deviation is below a specified tolerance, the a priori estimate is assumed to be accurate and the integers are assigned. The state and covariance updates are applied only if the test is passed.

The algorithm continues to check the residuals at each measurement epoch. In the event that the residuals increase above a specified threshold, an error flag is set. If this occurs at successive measurement epochs, the algorithm will assume that the incorrect integers were assigned, the measurement update will not be performed and the SNR measurement processing will be resumed until the resolution is successful again.

11.6 Attitude State Initialization

The following procedure is used to obtain an initial attitude state. When the first SNR measurements are available, the measurement from antenna 1 (defined to be the closest to zenith pointing) and GPS SV with the highest SNR measurement is selected. The algorithm assumes that the current spacecraft attitude is such that this antenna's boresight vector is aligned with the known line-of sight vector from the spacecraft to the transmitting GPS SV. Using this approach, this initial estimate should be within one hemisphere of truth and typically within a cone of 20 to 30 degrees of truth.

The line-of-sight vector to the GPS SV with the highest SNR measurement is computed

$$\left[\hat{u}^n_{G_j}(t_k)\right]_{XYZ} = \frac{\overline{R}_{G_j}(t_T) - \overline{R}^n(t^n_R)}{\left|\overline{R}_{G_j}(t_T) - \overline{R}^n(t^n_R)\right|} \tag{11.6-1}*$$

Assuming that the antenna boresight vector $\overline{B}^{n,p}$ is currently aligned with $\hat{u}^n_{G_j}(t_k)$, the quaternion associated with the rotation from the nominal boresight orientation along the zenith vector $\hat{\zeta}$ to the current orientation is computed in terms of the Euler angle of rotation θ

$$\theta = \arccos\left(\left[\hat{u}^n_{G_j}(t_k)\right] \cdot \hat{\zeta}\right) \tag{11.6-3}$$

and the Euler axis of rotation

$$\overline{e} = \frac{\hat{u}^n_{G_j}(t_k) \times \hat{\zeta}}{\left|\hat{u}^n_{G_j}(t_k) \times \hat{\zeta}\right|} \tag{11.6-4}$$

The zenith vector points along $+\hat{R}$, which is known from the spacecraft ephemeris. Using Equation (11.1-1) to obtain $\overline{\overline{q}}^{\,init}$, the initial attitude is

$$A^{init}_{B \leftarrow XYZ} = T_{B \leftarrow A_p} T^{init}_{A_p \leftarrow XYZ} \tag{11.6-5}*$$

where

$$T^{init}_{A_p \leftarrow XYZ} = A\left(\overline{\overline{q}}^{\,init}\right) \tag{11.6-6}*$$

and $T_{B \leftarrow A_p}$ is computed as in Equation (11.5-21). Implicit in this initialization is an arbitrary rotation around the boresight vector, which needs to be corrected on the first few filter updates.

Section 12. GPS/Galileo Measurement Simulation

This section presents the specifications for the simulation of GPS and Galileo measurements. Figure 12-1 illustrates the top-level simulation algorithm.

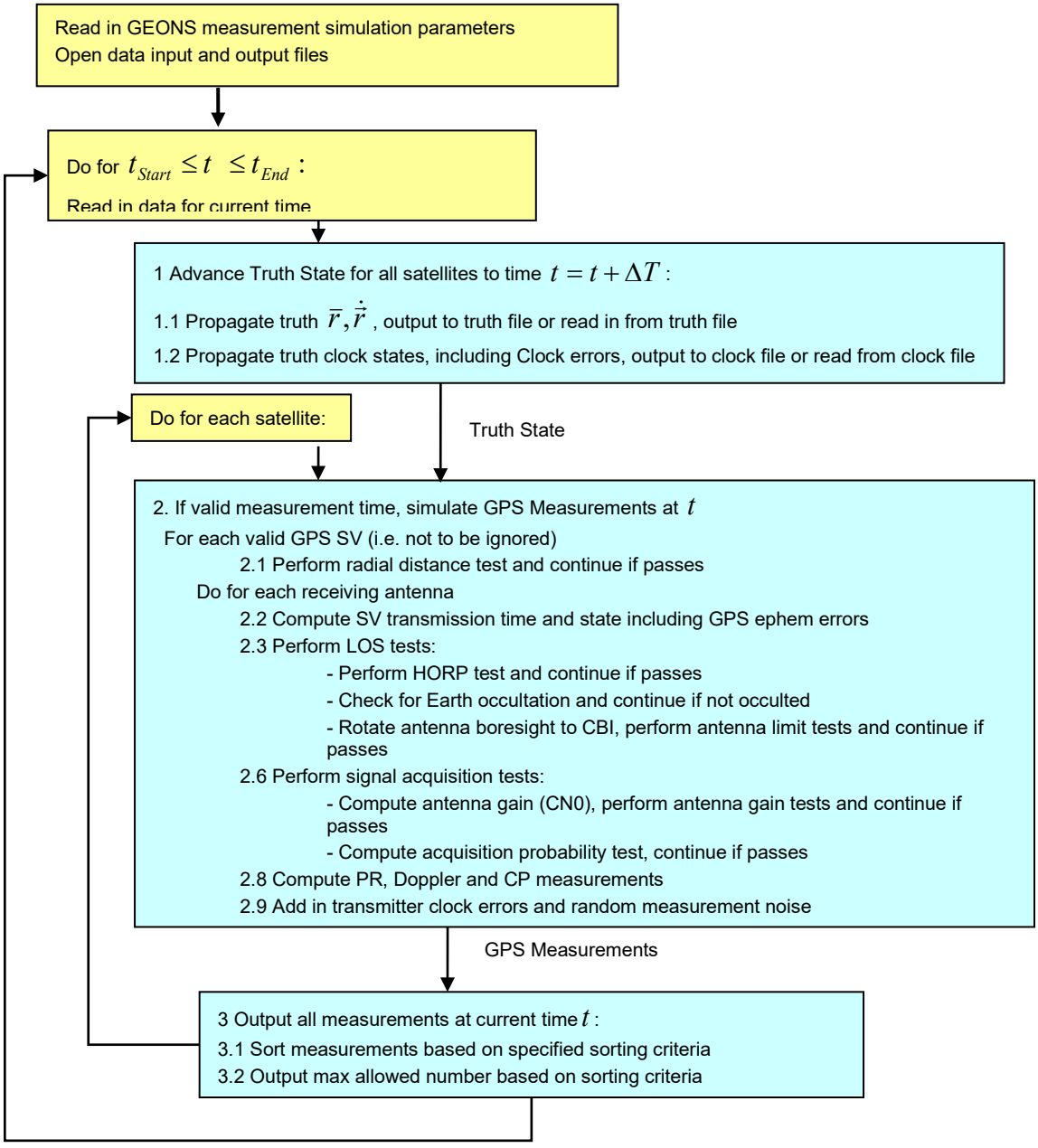

Figure 12-1 Measurement Simulation Algorithm

Section 12.1 defines the measurement simulation models. Section 12.2 defines the receiver clock error model. Section 12.3 defines the transmitter ephemeris and clock error models. Section 12.4 defines the measurement noise model. Section 12.5 defines the measurement validity tests.

12.1 GPS and Galileo Measurement Simulation Models

This section defines the simulation models for GPS and Galileo pseudorange, Doppler and carrier phase measurements.

12.1.1 GNSS Pseudorange Simulation

The GPS/WAAS and Galileo PR measurements are computed at the true UTC receive time, t_R^{UTC}, following the specifications provided in Sections 5.3.2 and 5.3.7, respectively, with the addition of random measurement noise and transmitter ephemeris and transmission time errors as follows:

$$\Re_{G/W_j}^{n}(t_k^n) = \rho_{G/W_j}^{n,i}(t_R^{UTC}) + b_R{}^n(t_R^{UTC}) + b_\rho^{G/W_j}(t_R^{UTC}) + \gamma_I(t_R^{UTC})\delta\rho_{Iono}^{SF}(t_k) - c\left(\delta t_{S_j} + \delta t_{S_j}^{SF}\right) - c\Delta t_{S_j} + \sigma_\rho^{G/W}(t_R^{UTC}) \quad (12.1.1\text{-}1)^*$$

$$\rho_{G/W_j}^{n,i}(t_R^{UTC}) = \left|\overline{R}_{A_i}{}^n(t_R^{UTC}) - \overline{R}_{G/W_j}(t_T^{UTC})\right| \quad (12.1.1\text{-}2)^*$$

In the above equations, the subscript *j* indicates the *j*th GPS SV/WAAS GEO. The timetag of the k^{th} measurement, t_k^n, is equal to the value of the measured receive time, $t_R^{(RC)_n} = t_R^{UTC} + b_R^n(t_R^{UTC})/c$, and t_T^{UTC} is the true signal transmit time computed by solving the light time equation starting with t_R^{UTC}. GPS SV ephemeris errors, which are computed as discussed in Section 12.3, are included in the computation of the transmitter position $\overline{R}_{G/W_j}(t_T^{UTC})$ and velocity $\dot{\overline{R}}_{G/W_j}(t_T^{UTC})$ vectors. The receiver time bias $b_R{}^n(t)$ is computed using the simulated time bias parameters $b_R{}^n(t_R^{UTC})$, $d_R{}^n(t_R^{UTC})$, and $\dot{d}_R{}^n(t_R^{UTC})$, as defined in Section 12.2. The GPS-system pseudorange bias, b_ρ^{G/W_j}, is defined in Section 4.3. For single frequency measurements, the ionospheric delay correction, $\delta\rho_{Iono}^{SF}$, can be modeled using the algorithm defined in Section 5.3.5, where $\gamma_I(t)$ is the ionospheric delay scale factor. The terms $-c\left(\delta t_{S_j} + \delta t_{S_j}^{SF}\right)$ represent the total SV time correction, which is computed using Equation 3.3-10 or 3.3-11 (for single and dual frequency GPS users) and Equation 3.3-12 (only for single frequency GPS users) in Section 3.3.2 evaluated at the signal transmit time (t_T^{UTC}). The transmitting GPS time error $\Delta t_{S_i}(t)$ is computed using ICE data parameters as defined in Equation 3.3-10c in Section 3.3. The term $\sigma_\rho^{G/W}(t_k)$ is the random measurement noise, which is computed as discussed in Section 12.4. The position and velocity of the receiving antenna are computed using Equation 3.2-61 in Section 3.2.8.

Simulation of Galileo pseudorange measurements follows the same procedure that is discussed above for the GPS/WAAS pseudorange, with the exception that the total SV time corrections are computed as defined in Section 3.3.9 and ICE time errors are not included.

12.1.2 GNSS Instantaneous Doppler Simulation

The GPS instantaneous Doppler measurements are computed following the specifications provided in Section 5.3.3 with the addition of random measurement noise and transmitter ephemeris and transmission time errors as follows:

$$\left(F_D(t_k^n)\right)_{G/W_j}^n = F_T\left[-\frac{\dot{\rho}_{G/W_j}^{n,i}(t_R^{UTC})}{c} + \delta\dot{t}_{S_j} - \frac{d_R{}^n(t_R^{UTC})}{c} + \frac{1}{2c^2}\left(\left|\dot{\overline{R}}^n\right|^2 - \left|\dot{\overline{R}}_{G/W_j}\right|^2\right)\right. \\ \left. + \frac{\mu}{c^2}\left(\frac{1}{\left|\overline{R}^n\right|} - \frac{1}{\left|\overline{R}_{G/W_j}\right|}\right) - (\delta F_{rel})_{cor}\right] + b_d^{G/W_j}(t_R^{UTC}) + \sigma_d^{G/W}(t_R^{UTC}) \quad (12.1.2\text{-}1)^*$$

In this equation, the subscript j indicates the GPS SV/WAAS GEO number; and the transmit frequency, F_T, is assumed to be known (nominally 1575.42 Mhertz for the L1 carrier, 1227.6 Mhertz for the L2 carrier, and 1176.45 Mhertz for the L5 carrier). GPS ephemeris errors, which are computed as discussed in Section 12.3, are included in the computation of the transmitter position $\overline{R}_{G/W_j}(t_T^{UTC})$ and velocity $\dot{\overline{R}}_{G/W_j}(t_T^{UTC})$ vectors. The term $\sigma_d^{G/W}(t_R^{UTC})$ is the random measurement noise, which is computed as discussed in Section 12.4.

Simulation of Galileo Doppler measurements follows the same procedure that is discussed above for the GPS/WAAS Doppler, with the exception that the associated Galileo transmission frequency is used, $\delta\dot{t}_{GAL_j}$ is computed using the Galileo SV clock correction parameters discussed in Section 3.3.9, and $(\delta F_{rel})_{cor}$ is not included.

12.1.3 GNSS Carrier Phase Simulation

The carrier beat phase measurement is formed in a GPS receiver as the difference between the phase of the local receiver oscillator and the phase of the received carrier signal. The measurement is ambiguous with respect to the number of integer cycles ($N_{\phi_n}^{G/W_j}(t_{acq})$) at the time ($t_{acq}$) when the signal is first acquired from each GPS SV. At any epoch other than the initial acquisition epoch, the receiver measures the fractional phase difference and the number of integer cycles accumulated since that epoch.

The GPS integrated carrier beat phase measurements (in meters), Φ_{G/W_j}^n, are computed following the specifications provided in Section 5.3.4 with the addition of random measurement noise and GPS ephemeris and transmission time errors as follows:

$$\Phi_{G/W_j}^n(t_k^n) = \rho_{G/W_j}^{n,i}(t_R^{UTC}) + b_R{}^n(t_R^{UTC}) - \gamma_I(t_k)\delta\rho_{Iono}^{SF}(t_R^{UTC}) + b_{\phi_n}^{G/W_j}(t_R^{UTC}) \\ - c\left(\delta t_{Sj} + \delta t_{S_j}^{SF}\right) - c\Delta t_{Sj} + \sigma_{\phi_n}^{G/W_j}(t_R^{UTC}) \quad (12.1.3\text{-}1)^*$$

In the above equations, the superscript *n* indicates the n^{th} receiver, the superscript *i* indicates the i^{th} antenna, and subscript *j* indicates the j^{th} GPS SV/WAAS GEO. The time tag t_k^n is the measured receive time of the k^{th} measurement, and t_T^{UTC} is the true signal transmission time. The geometrical range ($\rho_{G/W_j}^{n,i}$) and range rate ($\dot{\rho}_{G/W_j}^{n,i}$) are computed as described in Sections 5.3.2 and 5.3.3, respectively. The receiver time bias, $b_R{}^n(t)$, is in meters. The correction due to the ionospheric refraction, $\delta\rho_{Iono}^{SF}(t_R^{UTC})$, can be modeled using the algorithm defined in Section 5.3.5. The terms δt_{Sj} and $\delta t_{S_j}^{SF}$ are the SV time offset from GPS system time and group delay correction for single-frequency users, defined in Equations (3.3-10) and (3.3-12), respectively. The transmitting GPS time error $\Delta t_{S_i}(t)$ is computed using ICE data parameters as defined in Equation 3.3-10c in Section 3.3. The term $\sigma_\phi^{G/W}(t_R^{UTC})$ is the random measurement noise, which is computed as discussed in Section 12.4.

The raw integrated carrier beat phase observation (in cycles), $(\phi_{obs})_{G/W_j}^n(t_R^{UTC_n})$, is computed by dividing by the wavelength of the carrier ($\lambda_C = c/F_T$, where F_T = 1575.42 Mhertz for L1, 1227.6 Mhertz for L2 carrier frequency, and 1176.45 Mhertz for L5) to convert the carrier phase observation from meters to cycles and optionally adding the carrier phase integer ambiguity:

$$(\phi_{obs})_{G/W_j}^n(t_R^{UTC_n}) = (\Phi_{obs})_{G/W_j}^n(t_R^{UTC_n})/\lambda_C - N_{\phi_n}^{G/W_j}(t_{acq}) \qquad (12.1.3\text{-}2)$$

where the term $N_{\phi_n}^{G/W_j}(t_{acq})$ is the carrier phase integer ambiguity between GPS SV/WAAS GEO *j* and receiver *n* at the carrier phase acquisition time (t_{acq}), in cycles, which is computed as follows:

$$N_{\phi_n}^{G/W_j}(t_{acq}) = N_{lower}^{G/W_j} + \left(N_{upper}^{G/W_j} - N_{lower}^{G/W_j}\right)\varepsilon \qquad (12.1.3\text{-}3)$$

where N_{lower}^{G/W_j} and N_{upper}^{G/W_j} are the lower and upper bounds set by the user and ε is a uniform random number between [0,1]. The integer ambiguity $N_{\phi_n}^{G/W_j}(t_R^{UTC})$ is different for each acquisition of a GPS or Galileo SV/WAAS GEO by a receiver and is therefore reinitialized at the start of each new acquisition and held constant for that acquisition.

Simulation of Galileo Carrier Phase measurements follows the same procedure that is discussed above for the GPS/WAAS Carrier Phase, with the exception that the total SV time corrections are computed as defined in Section 3.3.9 and ICE time errors are not included.

12.2 Receiver Clock Error Model Simulation

The receiver clock error model can include the effects of clock noise in addition to acceleration effects due to the presence of a constant acceleration, frequency aging, and temperature changes

that are associated with eclipses. The effect of aging on the receiver's frequency reference is modeled by including a time bias acceleration term that is equal to derivative of the normalized frequency aging function

$$\frac{f_r(t_i)}{f_r(t_0)} = 1 + b_1 \ln[\frac{(t_i - t_0)}{b_2} + 1] \tag{12.2-1}$$

$$\dot{d}_R^{aging}(t_i) = \frac{c}{f_r(t_0)} \frac{df_r(t_i)}{dt} = \frac{cb_1}{[t_i - t_0] + b_2} \tag{12.2-2}$$

The coefficients b_1 and b_2 are determined by fitting the normalized frequency aging function to empirical data to characterize the magnitude and effective rate of decay.

The effect of frequency variations that occur before/during/after eclipses can be modeled by including a time bias acceleration term for specific time intervals, which is equal to the a sinusoidal variation, with amplitude equal to b_3 and period equal to the duration of the variation (in seconds)

$$\dot{d}_R^{event}(t_i) = \begin{cases} c\, b_3 \cos\left(\dfrac{2\pi\left(t_i - t_{start}^{event}\right)}{t_{end}^{event} - t_{start}^{event}} \right); \text{if } t_{start}^{event} < t_i \le t_{end}^{event} \\ 0; \text{otherwise} \end{cases} \tag{12.2-3}$$

where b_3, t_{start}^{event}, and t_{end}^{event} are input parameters for each event to be modeled.

Frequency variations that occur due to the effect of the Earth's magnetic field on a spinning spacecraft can be modeled by including a clock bias acceleration term when the spacecraft is near the Earth, which is equal to a sinusoidal variation with amplitude equal to b_4 (in seconds/seconds^2), period equal to the spin period, P_{Spin}, (in seconds), maximum radius $R_{\max}^{mag}$ (in meters), and t_{start} equal to the start time of the simulation.

$$\dot{d}_R^{mag}(t_i) = \begin{cases} cb_4 \cos\left(\dfrac{2\pi\left(t_i - t_{start}\right)}{P_{Spin}} \right); \text{if } R^n \le R_{\max}^{mag} \\ 0; \text{otherwise} \end{cases} \tag{12.2-4}$$

In addition, the drift of the satellite clock versus a clock at rest on the surface of the Earth due to relativity (meters/second) $\Delta d_{R_{\text{Rel}}}^n(t)$ is given by

$$\Delta d_{R_{\text{Rel}}}^n(t) = c\left(-\frac{1}{c^2}\left(\frac{\mu_E}{R_S^n} + \frac{\left(\dot{R}_S^n\right)^2}{2} \right) + 6.96929\text{x}10^{-10} \right) \text{ (m/s)} \tag{12.2-4a)*}$$

The full clock propagation is performed sequentially as follows:

$$\begin{bmatrix} b_R(t_{i+1}) \\ d_R(t_{i+1}) \\ \dot{d}_R(t_{i+1}) \end{bmatrix} = \begin{bmatrix} 1 & \Delta T & \frac{\Delta T^2}{2} \\ 0 & 1 & \Delta T \\ 0 & 0 & 1 \end{bmatrix} \begin{bmatrix} b_R(t_i) \\ d_R(t_i) \\ \dot{d}_R(t_i) \end{bmatrix} + \begin{bmatrix} \Delta d^n_{R_{\text{Rel}}}(t_{i+1})\Delta T \\ 0 \\ \Delta \dot{d}^{aging}_R(t_{i+1}) + \Delta \dot{d}^{event}_R(t_{i+1}) + \Delta \dot{d}^{mag}_R(t_{i+1}) \end{bmatrix} + Q \begin{bmatrix} \varepsilon_1 \\ \varepsilon_2 \\ \varepsilon_3 \end{bmatrix} \quad (12.2\text{-}5)$$

where

$$\begin{aligned} \Delta \dot{d}^{aging}_R(t_{i+1}) &= \dot{d}^{aging}_R(t_{i+1}) - \dot{d}^{aging}_R(t_i) \\ \Delta \dot{d}^{event}_R(t_{i+1}) &= \dot{d}^{event}_R(t_{i+1}) - \dot{d}^{event}_R(t_i) \\ \Delta \dot{d}^{mag}_R(t_{i+1}) &= \dot{d}^{mag}_R(t_{i+1}) - \dot{d}^{mag}_R(t_i) \end{aligned} \quad (12.2\text{-}6)$$

and ΔT is the clock prediction step size in seconds. The values ε_1, ε_2, and ε_3 are normally distributed deviates with zero mean and unit variance, which are initialized with different random number seeds. The parameters q_1, q_2, and q_3 are process noise variances rates associated with frequency white noise, frequency random walk, and frequency random run, respectively.

For the correlated clock error model, the components of the matrix Q are defined such that QQ^T is equal to the full clock covariance matrix:

$$QQ^T = c^2 \begin{bmatrix} q_1\Delta T + q_2\frac{\Delta T^3}{3} + q_3\frac{\Delta T^5}{20} & q_2\frac{\Delta T^2}{2} + q_3\frac{\Delta T^4}{8} & q_3\frac{\Delta T^3}{6} \\ q_2\frac{\Delta T^2}{2} + q_3\frac{\Delta T^4}{8} & q_2\Delta T + q_3\frac{\Delta T^3}{3} & q_3\frac{\Delta T^2}{2} \\ q_3\frac{\Delta T^3}{6} & q_3\frac{\Delta T^2}{2} & q_3\Delta T \end{bmatrix} \quad (12.2\text{-}7)$$

where Q is the upper right triangular matrix given by

$$Q = \begin{bmatrix} \sigma_{11} & \sigma_{12} & \sigma_{13} \\ 0 & \sigma_{22} & \sigma_{23} \\ 0 & 0 & \sigma_{33} \end{bmatrix} = \begin{bmatrix} \sqrt{\dot{Q}_{b_R}\Delta T + \dot{Q}_{d_R}\frac{\Delta T^3}{12} + \dot{Q}_{\dot{d}_R}\frac{\Delta T^5}{720}} & \sqrt{\dot{Q}_{d_R}\Delta T + \dot{Q}_{\dot{d}_R}\frac{\Delta T^3}{12}}\frac{\Delta T}{2} & \sqrt{\dot{Q}_{\dot{d}_R}\Delta T}\frac{\Delta T^2}{6} \\ 0 & \sqrt{\dot{Q}_{d_R}\Delta T + \dot{Q}_{\dot{d}_R}\frac{\Delta T^3}{12}} & \sqrt{\dot{Q}_{\dot{d}_R}\Delta T}\frac{\Delta T}{2} \\ 0 & 0 & \sqrt{\dot{Q}_{\dot{d}_R}\Delta T} \end{bmatrix} \quad (12.2\text{-}8)$$

where

$\dot{Q}_{b_R} = c^2 q_1$ =Receiver time bias process noise variance rate (meters^2/second)

$\dot{Q}_{d_R} = c^2 q_2$ =Receiver time bias rate process noise variance rate (meters^2/second^3)

$\dot{Q}_{\dot{d}_R} = c^2 q_3$ =Receiver time bias acceleration process noise variance rate (meters^2/second^5)

The bias and rate terms are initialized at the start of the simulation by:

$$\begin{aligned} b_R(t_0) &= b_R^{(0)} \\ d_R(t_0) &= d_R^{(0)} \\ \dot{d}_R(t_0) &= \dot{d}_R^{(0)} \end{aligned} \tag{12.2-9}$$

where the *(0)* superscript denotes the initial clock bias, drift, and acceleration values provided by the user.

The values used to model the performance of the receiver clock are based on the associated Hadamard variances. The GEONS Ground MATLAB Simulation (GGMS) tool suite has been configured to model an Oven Controlled Crystal Oscillator (OCXO), an MMS-like Ultra-Stable Oscillator (USO), a Spectratime Rubidium Atomic Frequency Standard (RAFS) (REF 66), and a Deep Space Atomic Clock (DSAC) (REF 67). The clock simulation model given above is the same model used for the GPS clocks in the GPS Master Control Segment as described in REF 65. In that reference the authors show that the Hadamard deviation produced by this model is given by

$$\sigma_H^2(\tau) = (10/3)q_0\tau^{-2} + q_1\tau^{-1} + (1/6)q_2\tau + (11/120)q_3\tau^3$$

where the q-parameters are the variances of the driving white noises processes. The q-parameters for simulating the clock are obtained by fitting this model to typical performance data for the associated oscillator as shown in Figure 12-2. Table 12-1 lists the Hadamard deviations used to simulate the performance of different quality clocks.

Table 12-1. Hadamard Deviations Used in Clock Models

	q_0	q_1	q_2	q_3
OCXO	0	1.87e-23	1.50e-23	0.0
USO	0	1.11e-24	1.11e-25	1.11e-35
RAFS	0	3.70e-24	1.87e-33	7.56e-59
DSAC	0	4.23e-26	6.19e-38	2.24e-61

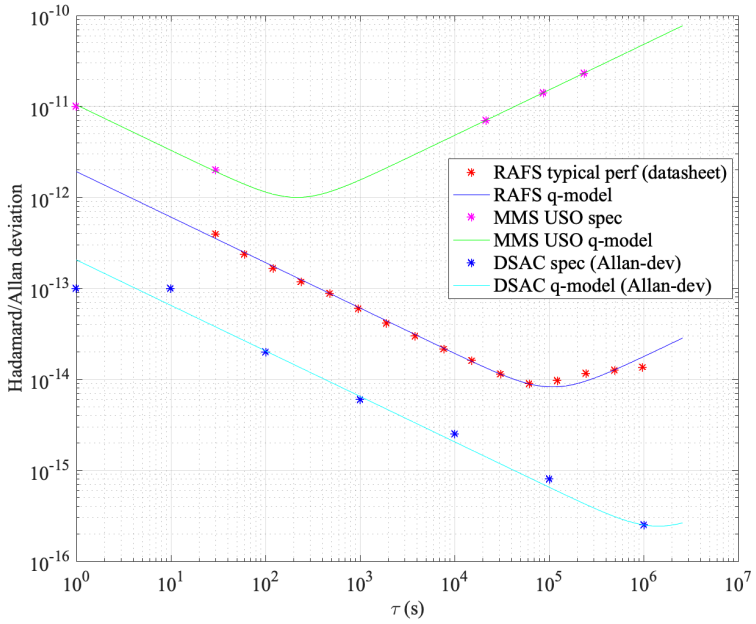

Figure 12-2. Parameter Fits to Typical Oscillator Performance Data

12.3 Transmitter Ephemeris and Clock Error Model

Ephemeris and clock errors can be added to the transmitter ephemeris and clock offsets that are computed based on the broadcast ephemeris files as discussed in Section 5.2. These errors, which can be specified in either the ECEF or RIC frames, are computed using the following model

$$e(t) = A(0) + \sum_{i=1}^{N}\left[A(2i-1)\cos\left(\frac{2\pi}{T_i}t\right) + A(2i)\sin\left(\frac{2\pi}{T_i}t\right)\right]$$

where t is the elapsed time from the start of the simulation, N is the number of periods, T_i is the length of each period, and the $A(i)$ error vector components are model parameters for each of the position and clock bias error components. The user can set the model parameters as desired.

The recommended approach is to define model parameters to capture observed characteristic periods of 24, 12 and 8 hours and correlations based on differences between historical broadcast and precise ephemerides. Correlations can be modeled using a "Components of Variance" model (e.g., Louis Scharf, "Statistical Signal Processing: Detection, Estimation, and Time Series Analysis", Addison Wesley, 1991). In this approach, the (RIC or ECEF broadcast minus precise) errors are assumed to follow the linear model above with random 'A' parameters that have a zero-mean Gaussian distribution with covariance S. Under these assumptions, the linear least squares estimate of 'A' is also zero-mean Gaussian with covariance S. Therefore, S can be estimated from a sequence of such least squares estimates over non-overlapping segments of (e.g., 1-day) of historical broadcast minus precise data and used for sampling 'A' for simulation.

This approach was used to compute coefficients to model the typical GPS RIC ephemeris and clock errors. These coefficients are implemented in the GGMS to simulate GPS RIC ephemeris

and clock errors. Figure 12-3 shows an example of GPS ephemeris and clock errors generated by the model, which are randomized from run to run.

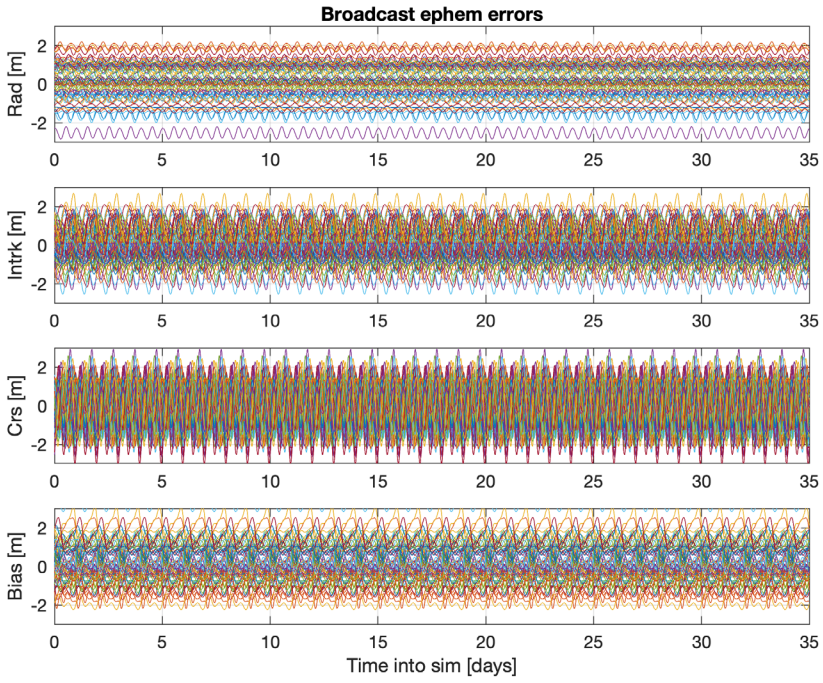

Figure 12-3. Typical Simulated GPS Ephemeris and Clock Errors

12.4 Measurement Noise Model

The measurement noise sigma for each GPS or Galileo transmitter is modeled based on the acquired signal strength of the observation using a simple step-function noise model or using a more realistic noise model based on thermal noise theory.

12.4.1 Step-Function Measurement Noise Model

For antenna gains above the J+1 cut-off value and below the J cut-off value, the $\sigma_M(J)$ noise sigma is used.

The measurement noise sigma is determined as follows:

For $J=1$, J_{Total} values, where J_{Total} is the total number of noise segments specified as input, determine the measurement noise sigma ($\sigma_M(J)$) associated with the $CN0_k$, which is computed as described in Section 12.5.6:

For J=1, if $C\mathrm{N0}_{\mathrm{Max}}^{noise}(2) < CN0_k$,

$$\sigma_{\rho}^{G/W}(CN0_k) = \sigma_{\rho}^{G/W}(1)$$
$$\sigma_{d}^{G/W}(CN0_k) = \sigma_{d}^{G/W}(1)$$
$$\sigma_{\phi}^{G/W}(CN0_k) = \sigma_{\phi}^{G/W}(1)$$

For J=2, J_{Total}-*1,* if $C\mathrm{N0}_{\mathrm{Max}}^{noise}(J+1) < CN0_k \le C\mathrm{N0}_{\mathrm{Max}}^{noise}(J)$,

$$\sigma_{\rho}^{G/W}(CN0_k) = \sigma_{\rho}^{G/W}(J)$$
$$\sigma_{d}^{G/W}(CN0_k) = \sigma_{d}^{G/W}(J)$$
$$\sigma_{\phi}^{G/W}(CN0_k) = \sigma_{\phi}^{G/W}(J)$$

For J= J_{Total}, if $CN0_k \le C\mathrm{N0}_{\mathrm{Max}}^{noise}(J_{Total})$,

$$\sigma_{\rho}^{G/W}(CN0_k) = \sigma_{\rho}^{G/W}(J_{Total})$$
$$\sigma_{d}^{G/W}(CN0_k) = \sigma_{d}^{G/W}(J_{Total})$$
$$\sigma_{\phi}^{G/W}(CN0_k) = \sigma_{\phi}^{G/W}(J_{Total})$$

The measurement noise contribution is then computed as

$$\varepsilon_1\sigma_{\rho}^{G/W}(CN0_k), \varepsilon_2\sigma_{d}^{G/W}(CN0_k), \varepsilon_3\sigma_{\phi}^{G/W}(CN0_k),$$

where the values ε_1, ε_2, and ε_3 are normally distributed deviates with zero mean and unit variance, which are initialized with different random number seeds and are independent for each satellite.

12.4.2 Pseudorange Measurement Noise Model Based on Thermal Noise Theory
(currently implemented in the GEONS Ground MATLAB Simulation (GGMS tools)

This simulated noise model incorporates a multi-step additive random error model based on standard GPS thermal noise theory, e.g. Equation 14.72 in REF 68. For Lunar simulations where there can be a large variation in the acquired signal strength, a 20-step model was implemented with 2 dB per step with 2x margin. In this model, the following equation is used to compute the PR standard deviation in meters for the segment of the model associated with the measured value of C/N_0:

$$\sigma_{\rho}^{G/W}(CN0\ ) = SF_{CN0} * \sigma_{\rho}^{G/W}(CN0_k)$$

where SF_{CN0} is a scale factor multiplier with suggested typical value ranges provided below

$$\sigma_{\rho}^{G/W}(CN0_k) = cT_C \left[\frac{B_{dll} * d_{dll}}{2 * CN0_k}\left(1 + \frac{2}{(2 - d_{dll})T_{\mathrm{int}} * CN0_k}\right)\right]^{1/2}$$

$CN0_k$ = minimum value in segment k closest to CN0

T_C = code chip period in seconds; equal to 1/1.023e6 seconds for C/A code

B_{dll} = Delay-locked loop (DLL) bandwidth in Hz; typically ≤1.0 Hz when carrier aiding is used, otherwise 5-10 Hz

d_{dll} = early-late DLL spacing in units of code chips; typically ≤ 1

T_{int} = Predetection integration time in seconds; value depends on code tracked but typically ranges from 1 ms for strong signals to 20 ms for weak signals

12.5 Measurement Validity Editing

This section defines the measurement validity tests that are associated with GPS measurement simulation.

12.5.1 Radial Distance Editing

The measurement is included only if the spacecraft radial distance is within the specified minimum and maximum limits.

$$R_{\min} \le \left|\overline{R}^n(t)\right| \le R_{\text{Max}} \tag{12.5-1}$$

12.5.2 HORP and Earth Occultation Editing

The measurement is included only if it does not fail the HORP editing test, which is defined in Section 2.3.2.1. The Earth occultation test is identical to the HORP test performed with a HORP value =0. The HORP test will not be passed if the transmitter is occulted by the Earth so an additional test is not required.

12.5.3`Antenna Limit Tests

The antenna boresight angle is computed based on the orientation of the antenna's boresight vector. The orientation of the receiving antenna's boresight vector can be specified in the following body frames: (1) orbit plane (RIC), (2) VBN, (3) ecliptic, and (4) attitude-based. The orientation of the transmitting antenna's boresight vector is assumed to be in the radial direction in the orbit plane (RIC) reference frame.

The measurement is included only if the receiving antenna boresight angle is within the specified minimum and maximum limits

$$\theta_{R,bore_{\min}} \le \theta_{R,bore}(t_k) \le \theta_{R,bore_{\text{Max}}} \tag{12.5.3-1}$$

where the receiver's boresight angle is defined as the angle between the receiver-to-transmitter line-of-sight vector, $\hat{u}_{los}$, and the receiver's boresight vector, $\hat{u}^{XYZ}_{R,bore}$.

$$\theta_{R,bore} = \cos^{-1}\left(\hat{u}_{los} \cdot \hat{u}^{XYZ}_{R,bore}\right)$$
$$\hat{u}_{los} = \frac{\overline{R}^{n}(t_k) - \overline{R}_{G/W_j}(t_k)}{\left|\overline{R}^{n}(t_k) - \overline{R}_{G/W_j}(t_k)\right|} \quad (12.5.3\text{-}2)$$

The receiver's boresight vector in the inertial frame is computed by rotating the receiver's boresight vector from its reference body frame to the inertial frame:

$$\hat{u}^{XYZ}_{R,bore} = T_{J2000 \leftarrow B}\hat{u}^{B}_{R,bore} \quad (12.5.3\text{-}3)$$

The measurement is included only if the transmitting antenna boresight angle is within the specified minimum and maximum limits

$$\theta_{t,bore_{\min}} \le \theta_{t,bore}(t_k) \le \theta_{t,bore_{\max}} \quad (12.5.3\text{-}4)$$

where the transmitter's boresight angle is defined as the angle between the receiver-to-transmitter line-of-sight vector and the transmitter's boresight vector rotated to the inertial frame:

$$\theta_{t,bore} = \cos^{-1}\left(\hat{u}_{los} \cdot \hat{u}^{XYZ}_{t,bore}\right) \quad (12.5.3\text{-}5)$$

12.5.4 Receiving Antenna Signal-to-Noise Ratio Calculation

The receiving antenna signal-to-noise ratio (C/N_0) in dB-Hertz, is given by:

$$C/N_0 = \left(EIRP + A_t\right) + \left(G_r + A_r\right) + 20\log\left(\frac{1}{4\pi\left|\overline{\rho}_r(t)\right|}\frac{c}{F_T}\right) + A_e + A_s - 10\log\left(T_s\right) + 228.6 \quad (12.5.4\text{-}1)$$

where *EIRP* is the effective isotropic radiated power of the transmitting antenna (specified as input), A_t is the signal attenuation due to the transmitting antenna pattern (computed based on the transmitting antenna model file), G_r is the receiver's antenna gain in the maximum gain direction (specified as input), A_r is the signal attenuation due to the receiving antenna pattern (computed based on the receiving antenna pattern file), F_T is the transmission frequency in Hertz (specified as input), $\left|\overline{\rho}_r(t)\right|$ is the transmitter to receiver range, A_e is the signal attenuation from the troposphere (not included), A_s is system losses (specified as input), and T_s is the receiving antenna system noise temperature in degree Kelvin (specified as input). REF 64 discusses calibration of the GPS link parameters used in Equation 12.5.4-1 with respect to GPS signal strengths acquired on-orbit by the Navigator receiver in the MMS Phase 2B orbit.

For lunar simulation analysis, the GGMS can include the effect of the nominal solar maximum Sun (excluding solar radio burst events) on the receiver system noise temperature. Since the beamwidth of the antenna is much larger than the total angle subtended by the Sun (approximately 0.5 degrees), we compute the effective antenna area, A_e, assuming a constant gain toward the Sun, where G_{sun} is computed as the receive gain toward the direction of the center of the Sun,

$$A_e = G_{sun}\lambda_{L1}^2 / (4\pi) \quad (12.5.4\text{-}1)$$

The effective area is multiplied by the solar flux, S_{sun}, approximated using the typical average value during solar maximum of 150 Solar Flux Units (SFU) near GPS frequencies (e.g., solar cycle flux plot at standard monitored frequency of 1415MHz can be seen in [REF 71]) or S_{sun}=150x10^{-22} W/m^2/Hz. We also account for a factor of ½ due to the fact that the solar emissions are unpolarized and the GPS antenna is (right hand) circularly polarized. Thus, we get an increment due to the Sun to the system noise temperature of

$$T_{sun} = 0.5 A_e S_{sun} / k \quad (12.5.4\text{-}2)$$

with *k* the Boltzmann constant. This term is then used to increment the system noise temperature from its nominal value as the simulation progresses. The C/N$_0$ loss due to the Sun is given by

$$L_{sun} \le 10\log_{10}\left[\left(T_{sys} + T_{sun}\right) / T_{sys}\right] \quad (12.5.4\text{-}3)$$

For example, for a ~0.5m parabolic dish receive antenna operating near Earth, with peak gain toward the Sun, the effect is limited to less than about 2 dB. With a higher gain antenna or lower base noise system noise, this effect would be larger. During transient Solar Radio Burst events, the solar flux, and resulting impact, can be much, much larger, but we do not model such events.

The antenna gain pattern files provide the signal attenuation for a specific type of transmitting or receiving antenna. The GPS measurement simulation process currently supports both one- and two-dimensional antenna pattern models. The one-dimensional (1D) antenna gain pattern, which is a function of only the elevation with respect to the antenna boresight direction, does not have any azimuthal dependence. The 1D attenuation pattern is given in tabular form. The attenuation at a particular boresight angle is computed using a cubic spline interpolator. The default GPS 1D transmitting antenna patterns are normalized such that the attenuation is zero at the edge-of-Earth boresight angle. The two-dimensional (2D) antenna gain pattern is a csv file containing a Naz x Nel array of gain values where Naz = number of azimuth values and Nel = number of elevation values. The gain at a particular azimuth and elevation with respect to the antenna boresight direction is computed by linear interpolation.

Section 12.5.8 describes the high-fidelity GPS sidelobe link antenna model currently available in the GGMS. Section 12.5.9 discusses receiving antenna models.

12.5.5 Antenna Gain Limit Tests

The measurement is included only if the antenna gain (CN0) is within the specified minimum and maximum limits.

$$C\mathrm{N0}_{\mathrm{Min}}^{acq} \le CN0_k \le C\mathrm{N0}_{\mathrm{Max}}^{\mathrm{acq}} \quad (12.5.5\text{-}1)$$

Where $C\mathrm{N0}_{\mathrm{Max}}^{\mathrm{acq}} = C\mathrm{N0}_{\mathrm{Max}}^{\mathrm{acq}}(1)$ defined in Section 12.5.6.

The measurement is included only if the relative antenna gain with respect to the strongest acquired signal is within the specified range ($\Delta CN0_{\text{Max}}^{acq}$):

$$\max(CN0_i) - \Delta CN0_{\text{Max}}^{\text{acq}} \le CN0_k \le \max(CN0_i) \qquad (12.5.5\text{-}2)$$

12.5.6 GPS Signal Acquisition Probability Calculation and Tracking Test

The acquisition probability is computed based on the probability associated with the signal-to-noise ratio (CN0) level and the delay time between attempted acquisitions. The acquisition probability random seed value and the probability of GPS acquisition segments/values and wait times before trying reacquisition are specified as input:

The algorithm is as follows:

1. If the GPS SV is already being tracked, continue tracking.
2. If the GPS SV is not currently being tracked, perform the new acquisition probability test

    a. Determine the wait time (Δt_{wait}) and probability of acquisition ($P_a(CN0)$) associated with the CN0 computed as described in Section 12.5.4, starting with the $J=1$, J_{Total} values, where J_{Total} is the total number of acquisition segments specified as input:

    If $\quad CN0_{\text{Max}}^{acq}(J+1) < CN0_k \le CN0_{\text{Max}}^{acq}(J)$

$$\begin{aligned} P_a(CN0_k) &= P_a(J) \\ \Delta t_{wait} &= \Delta t_a(J) \end{aligned} \qquad (12.5.6\text{-}1)$$

    Else if $CN0_{\text{Min}}^{acq} \le CN0_k \le CN0_{\text{Max}}^{acq}(J_{Total})$

$$\begin{aligned} P_a(CN0_k) &= P_a(J_{Total}) \\ \Delta t_{wait} &= \Delta t_a(J_{Total}) \end{aligned} \qquad (12.5.6\text{-}2)$$

    b. If elapsed time since last acquisition attempt is $< \Delta t_{wait}$, exit process

    c. Else if elapsed time since last acquisition attempt is $\ge \Delta t_{wait}$,

        i. Set time of last acquisition attempt =current time

        ii. Call random number generator (rand) to return a uniform random number between 0 and 1 (rand) starting with the input seed value iacqseed

        iii. Determine acquisition: signal is acquired if rand $\le P_a(CN0)$

Where

$CN0_{\text{Min}}^{acq}$ = Minimum CN0 value that can be acquired

$CN0^{acq}_{\text{Max}}(J)$ = Maximum CN0 value at which acquisition probability for segment J applies

$P_a(J)$ = Probability value when CN0 value is associated with segment J

$\Delta t_a(J)$ = Delay before trying reacquisition (in seconds) when CN0 value is associated with segment J

12.5.7 Time Interval Editing (currently not implemented in GEONS)

The measurement is included only if the measurement time within the specified time intervals.

12.5.8 Transmitter Antenna Models

The GPS signal simulation model available in the GGMS includes a high-fidelity GPS sidelobe link model based on in-orbit measured transmit patterns from the GPS-ACE project [REF 69]. The mainlobe portion of each transmit pattern is drawn from the best available data for each block and merged with the sidelobes measured by GPS ACE. The Block IIA and IIF mainlobes are modeled using a best-estimate of the average gain and shape of the Block IIF mainlobe. Block IIR and IIRM transmit patterns are modeled on a per-SV basis using data released by Lockheed Martin [REF 75]. Block III mainlobes are modeled by averaging the public IIRM mainlobe data, as it is assumed the Block III mainlobe structure and gain is closely related to that of the IIRM antennas.

This GGMS simulation model also incorporates the International GNSS System (IGS) GPS yaw model. Based on the calibration analysis, the per-block GPS transmit power and a few receiver parameters were adjusted to provide a good match between simulated and MMS-2B GPS measurements in terms of signal-to-noise ratio (C/N_0), number of signals tracked, tracking arcs and filter residuals. Figure 12-4 compares the EIRP based on GPS per block ACE Patterns and a Conservative Gal E1 Antenna Gain Model for Galileo transmissions.

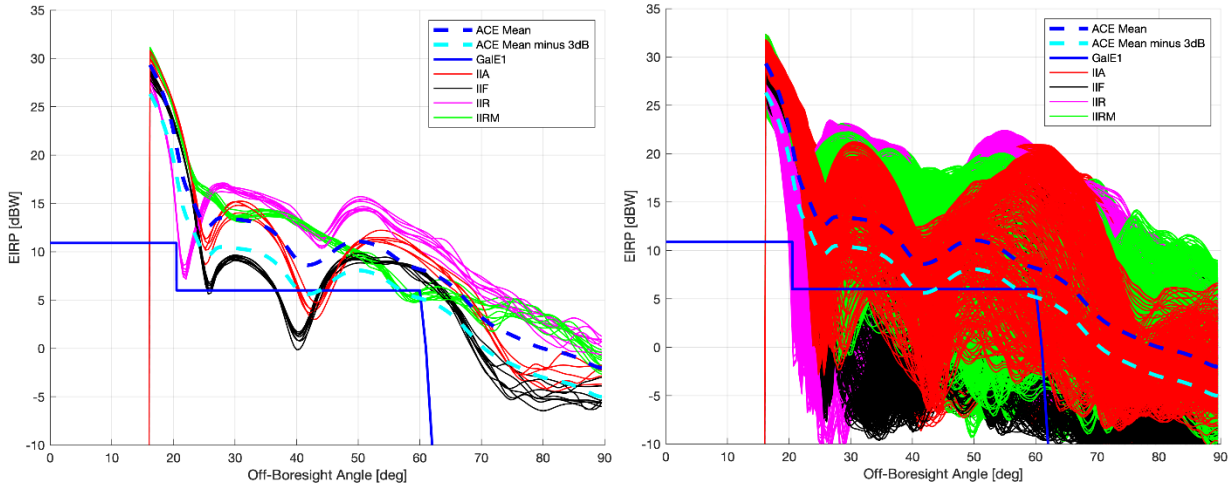

Figure 12-4. Comparison of EIRP based on GPS ACE Patterns and Conservative Gal E1 Antenna Gain Model. Left plot shows per-SV patterns averaged over azimuth. Right plot shows all azimuth cuts

12.5.9 Receiving Antenna Models

In general, the receiving antenna gain pattern must be tailored to the specific user antenna configuration. The GGMS includes receiving gain pattern files for the following types of antennas:

- Parabolic lunar high-gain antenna
- Patch antenna
- Omni-directional antenna

Abbreviations and Acronyms

C/A	Coarse Acquisition
CDRS	Command and Data Reception System
CM	center of mass
CPU	central processing unit
DSN	Deep Space Network
ECEF	Earth-centered Earth-fixed
EKF	Extended Kalman Filter
EOS	Earth Observing System
EP	Explorer Platform
ET	ephemeris time
ERFA	Essential Routines for Fundamental Astronomy
EUVE	Extreme Ultraviolet Explorer
FDD	Flight Dynamics Division
GCRF	Geocentric Celestial Reference Frame
GEONS	GPS Enhanced Orbit Determination Experiment
GHA	Greenwich hour angle
GNSS	Global Navigation Satellite Systems
GPS	Global Positioning System
GPST	GPS time system
GSFC	Goddard Space Flight Center
HORP	height of ray path
HSI	Hyperspectral Imager
IAT	International Atomic Time
ICRF	International Celestial Reference Frame
IERS	International Earth Rotation Service
ITRF	International Terrestrial Reference Frame
JD	Julian date
JGM	Joint Gravity Model

MIPS	million instructions per second
MJD	modified Julian date
NASA	National Aeronautics and Space Administration
Nav.	navigation
RAM	random-access memory
RIC	radial, in-track, cross-track
ROM	read-only memory
RPU	receiver/processor unit
SA	Selective Availability
S/C	spacecraft
sec	second
SOFA	Standards Of Fundamental Astronomy
SPS	Standard Positioning Service
SV	space vehicle
TDB	barycentric dynamical time
TDRSS	Tracking and Data Relay Satellite System
TOD	true equator and equinox of date
TONS	TDRSS Onboard Navigation System
TT	Terrestrial Time
UCB	Ultraviolet Cosmic Background
USNO	United States Naval Observatory
UTC	coordinated universal time
UT1	universal time corrected for polar motion
WGS	World Geodetic System

References

1. GSFC Code 590, *Goddard Enhanced Onboard Navigation System (GEONS) Software Requirements Matrix, Release 3.0,* David Gaylor, July 2023

2. Goddard Space Flight Center, 552-FDD-91/039R0UD0, *TDRSS Onboard Navigation System (TONS) Experiment Ground Support System System Description*, W. Steger (CSC) et al., prepared by Computer Sciences Corporation, July 1992

3. Lockheed Martin Missiles and Space, Document No. 20045510C, *Software Requirements Specification Flight Software - Navigation CSCI for EOS-AM Spacecraft (SD-110a),* J. R. Herberg, June 3, 1997

4. a.i. solution, Inc., FDSS-23-0035, *Global Positioning System (GPS) Enhanced Onboard Navigation System (GEONS) Mathematical Specifications, Release 2.17*, A. Long et al., November 28, 2012

5. G. J. Bierman, *Factorization Methods for Discrete Sequential Estimation*, New York: Academic Press, Inc., 1977

6. P. S. Maybeck, *Stochastic Models, Estimation, and Control,* Volume 1. New York: Academic Press, Inc., 1979

7. Computer Sciences Corporation, CSC/SD-89/6148, J2000.0 *Coordinate Conversion Software Mathematical Background and System Description (Revision 1),* M. Regardie, S. Devlin, and J. Roitz, September 1989

8. Nautical Almanac Office, U.S. Naval Observatory and H. M. Nautical Almanac Office*, The Astronomical Almanac for 1984.* Washington, D.C.: U.S. Government Printing Office, and London: Her Majesty's Stationary Office, 1983

9. B. Hofmann-Wellenhof et al., *GPS Theory and Practice, Third Revised Edition.* New York: Springer-Verlag, 1994

10. GPS Enterprise Space & Missile Systems Center, IS-GPS-200*,* Revision M*, Navstar GPS Space Segment/Navigation User Segment Interfaces,* prepared by SAIC, 13 April 2021

11. T. C. Van Flandern and K. F. Pulkkinen, "Low-Precision Formulae for Planetary Positions," *The Astrophysical Journal Supplement Series,* 41, November 1979, pp. 391–411

12. Martin-Marietta Corporation Astro-Space Division, Interoffice Memo, GN&C-362, EOS-GN&C-300, *Two Methods for Obtaining Solar Ephemeris Accuracies to Better Than 10 Arc Seconds for EOS-AM,* October 6, 1993

13. I. Harris and W. Priester, "Time-Dependent Structure of the Upper Atmosphere," *Journal of Atmospheric Sciences,* July 1952, vol. 19, no. 4 (also issued as NASA/GSFC document TN-D-1443)

14. Goddard Space Flight Center, TN-D-144*, Theoretical Models for the Solar Cycle Variation of the Upper Atmosphere,* I. Harris and W. Priester, August 1962

15. I. Harris and W. Priester, "Atmospheric Structure and Its Variations in the Region Form 120 to 80 KM," *COSPAR International Reference Atmosphere (CIRA) 1965, Space Research IV.* Amsterdam: North Holland Publishing Company, 1965

16. Computer Sciences Corporation, CSC/TM-84/6865, *Analytic Representation of the Harris-Priester Atmospheric Density Model in the 110- to 2000-Kilometers Region,* T. Mo and T. Lee, October 1984

17. TRW Corporation, JSC-20688, 85-TM-18, *Kalman Filtering Techniques*, W. H. Lear, September 1985

18. J. Wright, "Sequential Orbit Determination With Auto-Correlated Gravity Modeling Errors," *Journal of Guidance and Control,* vol. 4, 1981, p. 304

19. Applied Technology Associates, Inc*., Simultaneous Orbit Determination With Physical Connectedness,* September 1988

20. R. Gersten et al., "Statistical Properties of Orbit Perturbations Induced by the Earth's Anomalous Gravity," *Journal of Spacecraft,* vol. 4, 1967, p. 1145

21. Kurt Brock et al., "GPS Attitude and Orbit Determination for Space," *ION GPS-94 Proceedings*, ION GPS-94 Conference, Salt Lake City, Utah, September 20–23, 1994

22. Clark Cohen, *Attitude Determination Using GPS*, PhD Dissertation, Department of Aeronautics and Astronautics, Stanford University, December 1992

23. Michael Braasch, "A Signal Model for GPS," *NAVIGATION: Journal of the Institute of Navigation*, vol. 37, no. 4, Winter 1990-91

24. Kurt Feigl et al., "A Scheme for Reducing the Effect of Selective Availability on Precise Geodetic Measurements from the Global Positioning System," *Geophysical Research Letters*, vol. 18, no. 7, July 1991, pages 1289-1292

25. Roger Hart, Goddard Space Flight Center, private communication, March 1995

26. http://www.moshier.net, December 22, 2004

27. Goddard Space Flight Center, FDD/552-89/001, Goddard Trajectory Determination System (GTDS) Mathematical Theory, Revision 1, A. C. Long, et. al, prepared by Computer Sciences Corporation, July 1989, Section 6.2.1

28. Computer Sciences Corporation, CSC/TR-93/6057R1UD0, *Multimission Three-Axis Stabilized Spacecraft (MTASS) Flight Dynamics Support System (FDSS) Mathematical Background,* M. Lambertson and J. Keat. June 1994

29. J. Keat et al, "Earth Horizon Modeling and Application to Static Earth Sensors on TRMM Spacecraft," *Proceedings of the 1995 Flight Mechanics/Estimation Theory Symposium*, May 16-18, 1995

30. M. Challa and G. Natanson, "Recent Developments in Earth Oblateness Modeling For Attitude Determination," *Proceedings of the 14th International Symposium on Space Flight Dynamics*, Iguassu Falls, Brazil, February 8-12, 1999

31. D. Vallado, *Fundamentals of Astrodynamics and Applications*, McGraw Hill, Space Technology Series, New York, 1997

32. R. Battin, *An Introduction to the Mathematics and Methods of Astrodynamics*, American Institute of Aeronautics and Astronautics, New York, 1987

33. E. Speed and P. Axelrad, "Initialization Algorithm Using Orbital Elements," Colorado Center for Astrodynamics Research, September 3, 2001

34. William Press et al., *Numerical Recipes in FORTRAN, The Art of Scientific Computing,* Chapter 10, Cambridge University Press, 1992

35. ARINC Research Corporation, ICD-GPS-200C, *Navstar GPS Space Segment/Navigation User Interfaces,* April 12, 2000

36. J. Klobuchar, "Ionospheric Time-Delay Algorithm for Single-Frequency GPS Users," IEEE Transactions on Aerospace and Electronic Systems, Vol. AES-23, No. 3 , May 1987

37. W. Feess, and S. Stephens, "Evaluation of GPS Ionospheric Time-Delay Model," IEEE Transactions on Aerospace and Electronic Systems, Vol. AES-23, No. 3 , May 1987

38. J. A. Klobuchar, "Ionospheric Effects on GPS," *Global Positioning System: Theory and Applications.* Springer Verlag, Heidelberg, 2nd edition, 1996, p. 513

39. F. L. Markley, *Attitude Estimation or Quaternion Estimation?,* The Journal of the Astronautical Sciences, Vol. 52, Nos. 1 and 2, January—June 2004

40. J. D. Madsen, *Robust Spacecraft Attitude Determination Using Global Positioning System Receivers*, Ph. D Dissertation, The University of Texas at Austin, May 2003

41. J. R. Wertz, *Spacecraft Attitude Determination and Control*, D. Reidel Publishing Company, 1973, Appendix C

42. J. C. Adams and J. P. How, "GPS Attitude Determination for Spinning Spacecraft with Non-aligned Antenna Arrays," Proceedings of the Institute of Navigation National Technical Meeting, Long Beach, CA, January 1998

43. Davies, M. E. et al., "Report of the IAU/IAG/COSPAR Working Group on Cartographic Coordinates and Rotational Elements of the Planets and Satellites: 1994," *Celestial Mechanics and Dynamical Astronomy* 53, pp.127-148

44. A. S. Konopliv et al., "Recent Gravity Models as a Result of the Lunar Prospector Mission," *Icarus* 150, pp. 1-18, 2001

45. J. Williams, Letter to Merton Davies, October 25, 1994

46. GPS Enterprise Space and Missile Systems Center, IS-GPS-705, Revision H*, Navstar GPS Space Segment/User Segment L5 Interfaces,* prepared by SAIC, 23 March 2021

47. P. J. Huxel, *Navigation Algorithms and Observability Analysis for Formation Flying Missions*, Ph. D. Dissertation, University of Texas at Austin, May 2006

48. P. K. Seidelmann et al., "Report of the IAU/IAG/COSPAR Working Group on Cartographic Coordinates and Rotational Elements of the Planets and Satellites: 2000," *Celestial Mechanics and Dynamical Astronomy* 82, pp.83-110, 2002

49. G. Petit and B. Luzum, editors, *IERS Conventions (2010)*, IERS Technical Note No. 36, International Earth Rotation and Reference Systems Service, 2010

50. P. K. Seidelmann, editor, *Explanatory Supplement to the Astronomical Almanac*, University Science Books, 1992

51. E. M. Standish, "JPL Planetary and Lunar Ephemeris, Export Information", December 6, 2005, http://iau-comm4.jpl.nasa.gov/README

52. J. R. Carpenter and K. Berry, AAS 07-359, "Artificial Damping for Stable Long-Term Orbital Covariance Propagation," AAS/AIAA Astrodynamics Specialists Conference, Mackinac Island, Michigan, August 19-23, 2007

53. J. R. Carpenter and T. Lee, "A Stable Clock Error Model Using Coupled First and Second-Order Gauss-Markov Processes," presented at the AAS/AIAA Space Flight Mechanics Meeting, Galveston, Texas, January 27-31, 2008

54. A. Milani et al., Non-gravitational Perturbations and Satellite Geodesy, Adam Hilger, 1987

55. T. Kubo-oka and A. Sengoku, "Solar Radiation Pressure Model for the Relay Satellite of SELENE," *Earth Planets Space*, Vol. 51, 1999, pp 979-986

56. E. Baylis Shanks, "Solutions of Differential Equations by Evaluations of Functions," *Mathematics of Computation*, Vol. 20, No. 93 (Jan., 1966), pp 21-38

57. Neil Ashby, "Relativity in the Global Positioning System," http://relativity.livingreviews.org/open?pubNo=lrr-2003-1&page=articlese3.html, *Living Reviews in Relativity,* Vol 6 (2003)

58. Goddard Space Flight Center, Code 596, SEXTANT-SPEC-ADD-001, *Station Explorer for X-ray Timing and Navigation Technology (SEXTANT) Algorithm Description Document (ADD)*, Luke Winternitz, et al., July 7, 2016

59. NASA, NASA/TP-2018-219822, *Navigation Filter Best Practices,* Edited by J. Russell Carpenter and Christopher N. D'Souza, April 2018

60. Winternitz, L.M.B., Hassouneh, M.A., Mitchell, J.W., Valdez, J.E., Price, S.R., Semper, S.R., Yu, W.H., Ray, P.S., Wood, K.S., Arzoumanian, Z., and Gendreau, K.C., "X-ray pulsar navigation algorithms and testbed for SEXTANT," 2015 IEEE Aerospace Conference, March 2015

61. Winternitz, L.M.B., Mitchell, J.W., Hassouneh, M.A., Valdez, J.E., Price, S.R., Semper, S.R., Yu, W.H., Ray, P.S., Wood, K.S., Arzoumanian, Z., and Gendreau, K.C., "SEXTANT X-ray Pulsar Navigation Demonstration: Flight System and Test Results," 2016 IEEE Aerospace Conference, March 2016

62. AIAA, ANSI/AIAA S-131-2010, Astrodynamics -- *Propagation Specifications, Technical Definitions, and Recommended Practices, American National Standard*, August 2010

63. European Union*, European GNSS (Galileo) Open Service Signal-in-Space Interface Control Document,* Issue 1.3, December 2016

64. Luke B. Winternitz, William A. Bamford, Anne C. Long, Munther Hassouneh, *GPS Based Autonomous Navigation Study for the Lunar Gateway.* 42nd Annual American

Astronautical Society (AAS) Guidance, Navigation, and Control Conference; February 01, 2019 - February 06, 2019; Breckenridge, CO; United States

65. Steven T. Hutsell, Wilson G. Reid, Lt Jeffrey D. Crum, Lt H. Shawn Mobbs, and James A. Buisson. "Operational Use of the Hadamard Variance in GPS", In *Proceedings of the 28th Annual Precise Time and Time Interval Systems and Applications Meeting/Proceedings of the Institute of Navigation GNSS+*, pages 201–214, December 1996
66. Spectratime RAFS datasheet, *https://www.spectratime.com/uploads/documents/ispace/iSpace_RAFS_Spec.pdf*
67. Tjoelker et. al., *Mercury Ion Clock for a NASA Technology Demonstration Mission,* IEEE Transactions on Ultrasonics, Ferroelectrics, and Frequency Control, vol. 63, no. 7, July 2016
68. Jong-Hoon Won, Thomas Pany. "Signal Processing, Chapter 14 in Springer Handbook of Global Navigation Satellite Systems," Peter J.G. Teunissen, Oliver Montenbruck (Eds.) Springer, 2017.
69. J. Donaldson, J. Parker, M. Moreau, D. Highsmith, and P. Martzen, *Characterization of On-Orbit GPS Transmit Antenna Patterns for Space Users*, Proceedings of the Institute of Navigation GNSS+; 24-28 Sep. 2018; Miami, FL.
70. Goddard Space Flight Center, NASA TN D-6681, *Relativistic Time Corrections for Apollo 12 and Apollo 13,* John E. Lavery, August 1972.
71. Helen E. Coffey and Edward H. Erwin, "Online Solar Databases at NGDC – RSTN Solar Radio Databases". 2004. Retrieved online Sept. 2020 at url: http://lasp.colorado.edu/sdo/meetings/session_1_2_3/posters/session2/2_13P_Coffey.pdf.
72. "Orbit Determination Toolbox (ODTBX) 6.5," url: https://opensource.gsfc.nasa.gov/projects/ODTBX/, January 2017.
73. Goddard Space Flight Center, SEXTANT-SPEC-ADD-001, Rev E, Luke Winternitz, et al., *Station Explorer for X-ray Timing and Navigation Technology (SEXTANT) Algorithm Description Document (ADD)*, January 26, 2021
74. G. B. Hobbs, R. T. Edwards, and R. N. Manchester. TEMPO2, a new pulsar-timing package - i. an overview. *Monthly Notices of the Royal Astronomical Society*, 369:655{672, June 2006. ISSN 0035-8711. doi: 10.1111/j.1365-2966.2006.10302.x.
75. https://www.navcen.uscg.gov/?pageName=antennapanels, February 1, 2021.
76. GSFC Code 590, "Goddard Enhanced Onboard Navigation System (GEONS) Software Design Document", David Gaylor, July 2023
77. Goddard Space Flight Center, *Annex, 23 April 21, 2010 to Second TDRSS Ground Terminal (STGT) Description of Observation Measurement and Modeling, Vector Processing Ground rules, and FDF Support Procedures*, Updated 20 November, 2019, 5 April 2020, and 16 October, 2020, to Address Space Network Ground Segment Sustainment (SGSS) Changes